ISSN 1948-5204 (online)

World Journal of *Gastrointestinal Oncology*

World J Gastrointest Oncol 2023 June 15; 15(6): 911-1104

Published by Baishideng Publishing Group Inc

World Journal of Gastrointestinal Oncology

Contents

Monthly Volume 15 Number 6 June 15, 2023

REVIEW

MINIREVIEWS

ORIGINAL ARTICLE

Basic Study

Clinical and Translational Research

World Journal of Gastrointestinal Oncology

Monthly Volume 15 Number 6 June 15, 2023

Contents

NAME OF JOURNAL
World Journal of Gastrointestinal Oncology

ISSN
ISSN 1948-5204 (online)

LAUNCH DATE
February 15, 2009

FREQUENCY
Monthly

EDITORS-IN-CHIEF
Monjur Ahmed, Florin Burada

EDITORIAL BOARD MEMBERS
https://www.wjgnet.com/1948-5204/editorialboard.htm

PUBLICATION DATE
June 15, 2023

INSTRUCTIONS TO AUTHORS
https://www.wjgnet.com/bpg/gerinfo/204

GUIDELINES FOR ETHICS DOCUMENTS
https://www.wjgnet.com/bpg/GerInfo/287

GUIDELINES FOR NON-NATIVE SPEAKERS OF ENGLISH
https://www.wjgnet.com/bpg/gerinfo/240

PUBLICATION ETHICS
https://www.wjgnet.com/bpg/GerInfo/288

PUBLICATION MISCONDUCT
https://www.wjgnet.com/bpg/gerinfo/208

ARTICLE PROCESSING CHARGE
https://www.wjgnet.com/bpg/gerinfo/242

STEPS FOR SUBMITTING MANUSCRIPTS
https://www.wjgnet.com/bpg/GerInfo/239

ONLINE SUBMISSION
https://www.f6publishing.com

World Journal of Gastrointestinal Oncology

Submit a Manuscript: https://www.f6publishing.com

World J Gastrointest Oncol 2023 June 15; 15(6): 911-924

DOI: 10.4251/wjgo.v15.i6.911

ISSN 1948-5204 (online)

REVIEW

Role of neoadjuvant therapy for nonmetastatic pancreatic cancer: Current evidence and future perspectives

Gianluca Cassese, Ho-Seong Han, Yoo-Seok Yoon, Jun Suh Lee, Boram Lee, Antonio Cubisino, Fabrizio Panaro, Roberto Ivan Troisi

Specialty type: Surgery

Provenance and peer review: Invited article; Externally peer reviewed.

Peer-review model: Single blind

Peer-review report's scientific quality classification

Grade A (Excellent): 0
Grade B (Very good): 0
Grade C (Good): C, C, C
Grade D (Fair): D
Grade E (Poor): 0

P-Reviewer: Dambrauskas Z, Lithuania; Takemura N, Japan; Yu CZ, China

Received: December 28, 2022
Peer-review started: December 28, 2022
First decision: February 16, 2023
Revised: February 17, 2023
Accepted: April 24, 2023
Article in press: April 24, 2023
Published online: June 15, 2023

Gianluca Cassese, Roberto Ivan Troisi, Department of Clinical Medicine and Surgery, Division of Minimally Invasive HPB Surgery and Transplantation Service, Federico II University Hospital, Naples 80131, Italy

Ho-Seong Han, Yoo-Seok Yoon, Jun Suh Lee, Boram Lee, Department of Surgery, Seoul National University College of Medicine, Seongnam 13620, Gyeonggi-do, South Korea

Antonio Cubisino, Department of HPB Surgery and Transplantation, Beaujon Hospital, Clichy 92110, France

Fabrizio Panaro, Department of Digestive Surgery and Liver Transplantation, CHU Montpellier, Montpellier 34100, France

Corresponding author: Ho-Seong Han, MD, Professor, Department of Surgery, Seoul National University College of Medicine, 166 Gumi-ro, Bundang-gu, Seongnam 13620, Gyeonggi-do, South Korea. hanhs@snubh.org

Abstract

Pancreatic adenocarcinoma (PDAC) is one of the most common and lethal human cancers worldwide. Surgery followed by adjuvant chemotherapy offers the best chance of a long-term survival for patients with PDAC, although only approximately 20% of the patients have resectable tumors when diagnosed. Neoadjuvant chemotherapy (NACT) is recommended for borderline resectable pancreatic cancer. Several studies have investigated the role of NACT in treating resectable tumors based on the recent advances in PDAC biology, as NACT provides the potential benefit of selecting patients with favorable tumor biology and controls potential micro-metastases in high-risk patients with resectable PDAC. In such challenging cases, new potential tools, such as ct-DNA and molecular targeted therapy, are emerging as novel therapeutic options that may improve old paradigms. This review aims to summarize the current evidence regarding the role of NACT in treating non-metastatic pancreatic cancer while focusing on future perspectives in light of recent evidence.

Key Words: Pancreatic cancer; Pancreatic duct adenocarcinoma; Neoadjuvant chemotherapy; Borderline resectable; Locally advanced pancreatic cancer

Core Tip: Pancreatic adenocarcinoma (PDAC) is one of the most common and lethal human cancers worldwide; yet patients diagnosed with it still have a poor prognosis. Multimodal therapy is one of the most promising treatment options that increase the overall survival. Neoadjuvant chemotherapy (NACT) is recommended for treating borderline resectable PDAC. While recent studies have tried to explore the role of NACT in treating resectable and locally advanced PDAC, novel therapeutic modalities, such as ct-DNA and molecular targeted therapy, may guide both treatment and monitoring during the disease course to improve prognosis.

Citation: Cassese G, Han HS, Yoon YS, Lee JS, Lee B, Cubisino A, Panaro F, Troisi RI. Role of neoadjuvant therapy for nonmetastatic pancreatic cancer: Current evidence and future perspectives. *World J Gastrointest Oncol* 2023; 15(6): 911-924
URL: https://www.wjgnet.com/1948-5204/full/v15/i6/911.htm
DOI: https://dx.doi.org/10.4251/wjgo.v15.i6.911

INTRODUCTION

Pancreatic duct adenocarcinoma (PDAC) is the fourth most common cause of cancer-related deaths worldwide, with a continuously increasing incidence that will likely bring it to the second place in the upcoming decades[1]. The standard treatment of PDAC has always been surgical resection, which in combination with medical chemotherapy (CT) results in the best survival outcomes[2]. Actual real-world data shows a 5-year overall survival (OS) rate of approximately 20% in patients who have undergone resection (rising from less than 5% in 2011), while it is less than 1% in patients who have not (as it was 10 years ago)[3]. However, less than 15% of the patients have resectable tumors when diagnosed, whereas approximately 60% are diagnosed with metastatic tumors and/or have a poor performance status that precludes them from undergoing surgery[4,5]. Furthermore, international multicenter studies based on nationwide registries across Europe and the United States showed that a high percentage of patients with early PDAC were not required for surgical resection, with consequently high variations in the overall resection rates, from 13.2% to 68.7%[6]. Patient age and institutional volumes of pancreatic resections were associated with stage-adjusted resection rates and, more importantly, with postoperative morbidity, mortality, and long-term survival[7-10].

Large cohort studies have reported that approximately 20% of patients who underwent resection experience recurrence within 6 mo and 40% experience recurrence within the postoperative first year, even in cases of margin-free (R0) resection[11]. Such evidence suggests the different biological nature of PDAC, which is now regarded as a systemic disease, from the nature of its early stages. Therefore, surgery cannot allow a total tumor clearance, as a multimodal treatment approach is required. Surgical-related morbidity and mortality may even lead to a delay in the initiation of adjuvant therapy in time in up to one-third of the patients[12].

Based on the anatomical criteria (mainly the extension of the tumor to major locoregional vessels), non-metastatic PDAC was divided in 2006 by the National Comprehensive Cancer Network (NCCN) into resectable (R-PDAC), borderline resectable (BR-PDAC), and non-resectable (UR-PDAC)[13]. A deeper knowledge of the biological and clinical evolution of PDAC has led to a review of its definition, which also includes biological and clinical criteria[14]. Current guidelines recommend an upfront surgery for R-PDAC and neoadjuvant chemotherapy (NACT) for BR-PDAC, combined with modified 5-fluorouracil, leucovorin, irinotecan, and oxaliplatin (FOLFIRINOX) and Gemcitabine + Capecitabine as preferred regimens[15]. NACT is not recommended for UR-PDAC and metastatic PDAC (M-PDAC); however, the latest chemotherapy protocols have shown encouraging results. This allows a higher proportion of patients with locally advanced (LA) and metastatic tumors to gain an opportunity to undergo surgery, with conversion surgery rates ranging from 0% to 40% for LA and from 4% to 9% for M- PDAC[16-18].

Including PDAC in the indications of NACT has gained a great interest. Theoretically, NACT can treat occult non-detected micrometastases in the early stages of macroscopically resectable tumors in a timely manner and can also reduce the size or stage of the tumor, thus ensuring a better surgical control and higher R0 rates. Moreover, it can help in selecting the patients that best fit for surgical resection, exempting non-responders from an unnecessary procedure of ineluctable poor oncological outcomes and relatively high morbidity rates. Finally, it may provide a multimodal treatment option for all patients, owing to its early administration in patients with a better performance status, without any postoperative dropout caused by surgery-related complications. NACT also improves the extent of local tumor control; however, to date, only one randomized prospective trial has failed to show a significant improvement in OS[19].

This review aims to show the actual evidence supporting the wide use of NACT in treating PDAC, while focusing on the possible challenges and future perspectives.

ROLE OF NACT IN TREATING RESECTABLE TUMORS

The recommended treatment for R-PDAC is an upfront surgery followed by adjuvant chemotherapy (AC). The benefits of AC regarding the survival outcomes have been demonstrated in several trials. Particularly, the first milestones were represented by the ESPAC1 and ESPAC3 trials that showed an improved OS after AC with 5-fluorouracil combined with leucovorin and gemcitabine, respectively[20, 21]. The Prodige randomized controlled trial revealed surprising outcomes when FOLFIRINOX were used as the AC regimen when compared to the outcomes of the previous standard of care based on gemcitabine (median OS of 53.5 *vs* 35.5 mo, respectively; $P = 0.001$)[22]. Moreover, well-differentiated tumors, young age, lower-staged tumors, large-volume institutions, and complete treatment were associated with a better OS, while early relapse was a negative prognostic factor.

Several trials have investigated the role of NACT in treating R-PDAC (Table 1). As early as in 2006, the first single-arm phase II trial investigating the safety of NACT (gemcitabine plus radiation) in treating R-PDAC was published by Talamonti *et al*[23]. Similarly, Heinrich *et al*[24] published a phase II single-arm trial enrolling 28 patients receiving NACT. It showed an 89%-resectability after the administration of gemcitabine plus cisplatin regimen that has an acceptable tolerability. However, many double-arm randomized controlled trials (RCT) comparing NACT and upfront surgery failed to reach any significant conclusions. Finally, the Dutch PREOPANC trial recently reported significant long-term outcomes after comparing neoadjuvant radio-chemotherapy (gemcitabine plus radiotherapy) with upfront surgery. The study enrolled 246 patients with R-PDAC of a diameter of more than 2 cm or BR-PDAC. After a median follow-up of 59 mo, the median OS was 15.7 mo in the radio-chemotherapy group *vs* 14.3 mo in the upfront surgery group, with a 5-year OS of 20.5% and 6.5%, respectively ($P = 0.025$)[25]. However, this study had some important drawbacks. First, the enrolled patients underwent a monoregimen AC, which was the standard approach in Netherlands when PREOPANC was initiated; however, it has now been replaced with combination chemotherapy, which is superior. Furthermore, the use of chemo-radiation in either adjuvant or neoadjuvant settings is not supported by other randomized studies[21,26]. Indeed, the recent A021501 phase II trial reported better results for neoadjuvant FOLFIRINOX than the results of chemoradiation in treating BR-PDAC according to both R0 resection rate (57% *vs* 33%, respectively) and 18-month OS (66.7% *vs* 47.3%, respectively)[27]. Similarly, the ESPAC-5F study showed inferior results for chemo-radiotherapy when compared to the results of FOLFIRINOX and gemcitabine combined with capecitabine[28]. Therefore, chemoradiation in the neoadjuvant setting could be more harmful than CT alone; thus, it should not be recommended. Finally, the PREOPANC study enrolled patients with both BR-PDAC and R-PDAC. The results were confounding as they were superior in the subgroup of BR-PDAC, while the hazard ratio (HR) for R-PDAC was not statistically significant: 0.79 [95% confidence interval (CI): 0.54-1.16, $P = 0.23$].

Perri *et al*[29] conducted a retrospective study with a propensity-score matching that focused on 485 patients with R-PDAC. He compared the preoperative use of FOLFIRINOX *vs* gemcitabine combined with NAB-paclitaxel (GA). The FOLFIRINOX cohort had higher rates of radiologic partial response (19% *vs* 6%; $P < 0.01$), as well as higher resection rates (29% *vs* 18%; $P = 0.02$), and patients who underwent R0 resection had significantly better median OS (55 *vs* 17 mo; $P < 0.001$). However, few months later the SWOG-S1505 phase II trial showed similar median OS durations for FOLFIRINOX and GA (23.2 *vs* 23.6 mo, respectively), with survival results similar to those reported for upfront surgery [30].

Regarding the postoperative outcomes of patients with resected tumors who received NACT, a large study on 3748 patients has showed no differences in postoperative complications and mortality, despite the high number of vascular resections in the NACT cohort[31]. Furthermore, the multivariable analysis showed a low likelihood of pancreatic fistula after receiving NACT (OR 0.67, $P < 0.001$). Similar results were published by Cools *et al*[31], even for older patients, with higher rates of major complications after undergoing upfront surgery than the rates after receiving NACT (38% *vs* 24%; $P = 0.06$) and a higher Comprehensive Complication Index (20.9 *vs* 20; $P = 0.03$, respectively).

In conclusion, the use of NACT in treating R-PDAC remains inconclusive despite the encouraging results. The aforementioned theoretical benefits have been applied to other gastrointestinal malignancies, such as esophageal cancer. However, some drawbacks of the wide use of NACT persist, such as the possible delay of surgical resection, possibly due to the complications of CT, or the progression of the disease due to nonresponding to treatment. A negative association of patients' malnutrition with NACT and its outcomes has also been proposed. However, previous studies have showed that, despite the worsening status of nutritional laboratory markers and the poor prognostic nutrition index after receiving NACT, the incidence of postoperative complications, length of hospital stay, and time to postoperative adjuvant therapy initiation is not significantly affected when compared to the incidence of complications after upfront surgery[32]. Finally, a positive biopsy is required to initiate NACT; however, it is not always easy to obtain due to the low cellularity of PDAC and its retroperitoneal anatomical position (close to major vessels)

We are looking forward to the results of several ongoing trials evaluating the role of different NACT regimens such as NEPAFOX and NorPACT-1 and investigating FOLFIRINOX *vs* upfront surgery or NEOPAC focusing on gemcitabine plus oxaliplatin *vs* upfront surgery, as they may lead to significant clinical implications.

Table 1 Trials investigating the role of neoadjuvant chemotherapy for resectable pancreatic adenocarcinoma

Ref.	Study type	Treatment	No. of patients	Resection rate (%)	Median OS (mo)
Talamonti *et al*[23], 2006	Single arm, phase II	Gem + RT	22	85	26[1]
Evans *et al*[113], 2008	Single arm, phase II	Gem + RT	86	74	22
Heinrich *et al*[24], 2008	Single arm, phase II	Gem or Cis	28	89	27
Varadhachary *et al*[114], 2008	Single arm, phase II	Gem/Cis	90	58	19
O'Reilly *et al*[115], 2014	Single arm, phase II	GemOx	38	71	27
Golcher *et al*[116], 2015	Randomized, double arm, phase II	Gem/Cis + RT *vs* upfront surgery	66	19 *vs* 23	17.4 *vs* 14.4 (P = 0.96)
Okano *et al*[117], 2017	Single arm, phase II	S1 + RT	33	96[2]	NA
Motoi *et al*[118], 2019	Randomized, double arm, phase II/III	GemS1 *vs* upfront surgery	364	NA	37
Versteijne *et al*[25], 2022	Randomized, double arm, phase III	Gem + RT *vs* upfront surgery	246	NA	15.7 *vs* 14.3[2]

[1]Calculated only in resected patients.
[2]Cumulative results for both resectable- and borderline resectable- pancreatic adenocarcinoma.
Gem: Gemcitabine; Ox: Oxaliplatin; Cis: Cisplatin; RT: Radiotherapy; OS: Overall survival; NA: Not available.

ROLE OF NACT IN TREATING BORDERLINE-RESECTABLE TUMORS

BR-PDAC was defined by the International Association of Pancreatology based on anatomical, biological, and clinical criteria[13]. From an anatomical point of view, BR-PDAC is defined as a lesion with a high risk for margin-positive resection (R1, R2) due to its proximity to the main vessels. In particular, BR-PDAC is considered in the following cases: any contact of ≥ 180° with the portal vein or superior mesenteric vein (SMV), any contact with the inferior vein cava, and/or any contact of < 180° with a major artery. It should be noted that unlike the definitions based on the NCCN guidelines, this definition does not include the extension to any jejunal branches of the SMV, mainly because of the wide anatomical variability[14]. From a biological point of view, the definition of BR-PDAC includes high levels of cancer antigen 19.9 (CA 19.9 > 500 U/mL), as well as positive lymph nodes on a PET-computed tomography scan, because of the high risk of early metastatic progression[33,34]. Indeed, a recent study by Hata *et al*[33] showed that both serum and peritoneal levels of CA 19.9 are independent prognostic factors of OS. The clinical definition of BR-PDAC is based on the performance status of the patient; an Eastern Cooperative Oncology Group (ECOG) score of more than two was shown to be associated with a high risk of distant metastases (up to 30%)[35]. Biological and clinical criteria also apply when R0 surgery is considered technically achievable.

Current guidelines have a consensus on the effectiveness of NACT as the first-line therapeutic strategy for BR-PDAC. High quality evidence including the results of the recent four-arm randomized phase II trial ESPAC-5F28 supports these recommendations. Patients with BR-PDAC were randomized to receive upfront surgery *vs* NACT (with two different arms, FOLFIRINOX or GA) *vs* chemoradiotherapy, followed by surgery and AC. There were no differences in the R0/R1 resection rate, which was the primary endpoint (44% *vs* 41% after NACT, P = 0.668), or in the number of patients able to undergo adjuvant therapy. However, the 1-year OS was significantly improved after receiving NACT (77% *vs* 42%, respectively; HR = 0.28; P < 0.001), with the FOLFIRINOX arm showing the best results (1-year OS 84% *vs* 79% after GA and 64% after chemoradiotherapy) at the cost of a higher, but manageable, toxicity. Regarding the best NACT regimen, initially, both gemcitabine and capecitabine were chosen because of their application in the metastatic setting. Indeed, gemcitabine has shown a great success in the treatment of PDAC, which was actually considered chemo-resistant prior to its introduction[36,37]. Later on, the good results of FOLFIRINOX and GA in the metastatic and adjuvant settings encouraged their use in combination with the existing NACT regimens. This promoted very encouraging oncological outcomes[22,38]. Recently, Macedo *et al*[39] showed a comparable effectiveness of FOLFIRINOX and GA in a retrospective study comprising 274 consecutive patients. They reported no differences regarding both median OS (37.3 *vs* 31.9 mo) and R0 resection rate (82.8% *vs* 81.8%). Both FOLFIRINOX and GA are the regimens of choice for NACT in treating BR-PDAC when patient conditions are acceptable. Moreover, the multidisciplinary team agrees with these findings.

The additional value of radiotherapy in the neoadjuvant setting of BR-PDAC remains a matter of debate. The largest number of RCTs, such as the aforementioned ESPAC-1 trial, failed to prove its

superiority regarding survival outcomes, which led the European guidelines to not recommend its use [40]. Simultaneously, neoadjuvant chemoradiotherapy is still commonly used in the United States[14]. Indeed, new radiotherapy modalities, such as intraoperative radiotherapy following NACT, have been introduced. A study by Chapman *et al*[41] showed a rather good tolerability; however, compared to NACT followed by surgery alone (26.6 *vs* 35.1 mo; $P > 0.05$), there was no significant advantage in survival outcomes as well as the additional cost of an increased hospital stay (4 *vs* 3.5 d). Newer techniques to minimize the dose directed at the radiosensitive tissues in the abdomen, including stereotactic body radiation therapy and intensity-modulated radiation therapy, are increasingly used in neoadjuvant settings for patients with BR/LA-PDAC[41]. However, there is still limited evidence regarding the supposed advantage of receiving NACT alone.

Traditionally, for non-metastatic tumors, NACT aims to shrink the tumor to facilitate R0 surgery. However, for BR-PDAC, several studies showed improved outcomes after receiving NACT, even in the case of radiologically stable tumors[42,43]. This may be attributed to an additional selective role of NACT, in which it helps in selecting the best candidates for surgery as biologically aggressive tumors progress despite treatment[44]. This biological selection plays an important role in improving the outcomes of pancreatectomies with arterial resections. In the past, many reports have shown poor outcomes of arterial resections [borderline resectable tumors with arterial invasion (BR-A)], supporting the stance that the risks largely outweigh the benefits[45,46]. However, in the era of modern NACT regimens for treating BR-PDAC, an increasing number of studies have shown better outcomes of surgical resections than those of medical therapy alone. The most recent series by Loos *et al*[47] showed encouraging results of 385 consecutive patients undergoing pancreatectomies with associated arterial resection or periadventitial dissection, with a median OS of 20.1 mo, while the five-year OS was 12.5%. The reported in-hospital mortality rate was 8.8%; however, it significantly decreased to 4.8% ($P = 0.005$), showing a learning curve of 15 procedures for pancreatic surgeons with sufficient preexisting experience. In contrast, a recent meta-analysis showed an increased risk of mortality and complications compared to those of standard non-arterial resections (HR 4.09, $P < 0.001$). Therefore, the real risks and benefits of NACT followed by surgery for treating BR-PDAC with arterial involvement remain unclear; thus, well-planned clinical trials should be carried to evaluate its efficacy.

CONVERSION SURGERY AND CHEMOTHERAPY FOR TREATING UNRESECTABLE NON-METASTATIC TUMORS

UR-PDAC is divided into UR-M (metastatic) when there are distant metastases, and UR-LA (locally advanced) when there is a venous involvement nontechnically amenable to reconstruction or a contact of ≥ 180° with the superior mesenteric artery (SMA) or celiac artery or an arterial involvement of the first jejunal branch of the SMA[13,14]. In these cases, even if arterial resection is technically feasible, it has a poor prognosis due to the high rate of local recurrence and systemic progression[48,49]. Patients with UR-LA are candidates for medical therapy, which is classically considered as a palliative solution. However, as early as in 2010, a systematic review reported encouraging outcomes in patients initially classified as having an unresectable tumor and then underwent conversion surgery after CT[50]. Although the regimens were based only on 5-florouracil or gemcitabine, the median OS after conversion surgery was 20 mo, which is comparable to the median OS after upfront surgery which was 23 mo. Many studies followed the first encouraging series, including different CT regimens with or without a radiation therapy, and all reported encouraging results of conversion surgery. However, all studies revealed a high heterogeneity regarding not only the CT protocols, but also the definition of BR-PDAC and UR-PDAC. Data from a meta-analysis including 653 patients with locally advanced PDAC from 21 observational studies showed a median resection rate after FOLFIRINOX-based CT of 26%, with a high variability in median OS, ranging from 10.0 to 32.7 mo, as well as a high heterogeneity among the studies ($I^2 = 61\%$), with different definitions of "locally advanced" PDAC. Recently, a retrospective study enrolling 279 consecutive patients receiving FOLFIRINOX for defined UR-LA-PDAC reported interesting results in a definite setting[51]. After at least four cycles of CT, a partial response (PR) was observed in 34.1% of the patients, and stable disease (SD) in 51.4% of the patients. Fifty patients underwent surgical exploration and 47 (16.8%) underwent curative-intent surgery. The median survival after conversion surgery was 56 mo compared to that of those who did not undergo resection which was only 21 mo ($P < 0.001$). After multivariate analysis, curative-intent surgery was the most important prognostic factor (HR 0.260; $P < 0.001$). Similarly, the Heidelberg group reported a higher resection rate after treatment with FOLFIRINOX than it was after treatment with GA or other regimens (61% *vs* 46% *vs* 52%, respectively; $P = 0.026$) from a retrospective analysis of 575 consecutive patients who underwent conversion surgery after CT[52]. Median OS was higher when conversion surgery was feasible (15.3 *vs* 8.5 mo, $P < 0.0001$), independent from the CT regimen (16.0 mo after FOLFIRINOX *vs* 16.5 mo after gemcitabine and 14.5 mo for others; $P = 0.085$). In a multivariable analysis, a FOLFIRINOX-based regimen was independently associated with better survival outcomes. Importantly, both these studies only included UR-PDAC and not borderline-resectable tumors. Regarding the role of the CT regimen used, a study from Johns Hopkins University reported that 28% of the patients with UR-LA-PDAC

underwent surgical exploration after CT, with a total of 20% of the patients being able to undergo a curative-intent surgery[53]. Of these patients, 60% received a FOLFIRINOX regimen and 19% received gemcitabine. Therefore, the CT regimen could significantly influence the outcomes of UR-LA-PDAC. However, it must be noted that patients who did not undergo resection had a lower ECOG-performance status, higher CA 19-9 Levels, and larger tumors on cross-sectional imaging.

All published studies had many shortcomings, such as having a retrospective study design and the absence of an intention-to-treat (ITT) analysis. Recently, the Verona group published an interesting prospective study with an ITT analysis of NACT followed by a conversion surgery. A cohort of 680 patients was analyzed, including 29.3% with BR-PDAC and 60.7% with UR-LA-PDAC. After clinical, radiological, and biochemical evaluations, 23.9% of the patients underwent surgical exploration, with an overall rate of subsequent resections of 15.1%, accounting for 24.1% of BR-PDAC and 9% of UR-LA-PDAC cases. The independent predictors of resection were age, BR-PDAC, chemotherapy completion, radiologic response, and biochemical response. The median OS for the entire cohort was 12.8 mo with completion of chemotherapy, complementary radiation therapy, and resection, which were found to be associated with improved survival outcomes. Interestingly, in the subgroup analysis, the median OS of patients with UR-LA-PDAC undergoing conversion surgery was 41.8 mo, and no pretreatment and posttreatment factors were associated with survival after pancreatectomy[54].

Post-CT prediction of resectability remains a major challenge that is difficult to standardize since it largely depends on the experiences, skills, and preferences of surgeons, oncologists, and radiologists. A recent multicenter study showed an interinstitutional agreement below 50% when dealing with both resectability evaluation and treatment allocation in BR-PDAC and UR-LA-PDAC[55]. A clear radiological post-CT response is difficult to detect on conventional contrast-enhanced computed tomography scan, with a low correlation between radiological findings and subsequent surgical resection rates[56,57]. Dholakia *et al*[57] reported a series of 50 consecutive LA patients receiving NACT followed by surgery in 58% of cases, although the tumor volume and degree of tumor vessel involvement were not significantly reduced after receiving NACT. Therefore, many authors have suggested that every patient undergoing CT for BR-PDAC or UR-LA-PDAC should undergo surgical exploration, and much debate remains about this argument. Rangelova *et al*[58] suggested a routine surgical exploration in every case of non-progressed LA tumor, regardless of the level of CA 19-9 and the type and dose of the CT regimen. Similarly, the Heidelberg group recommends surgical exploration in every case of SD or PR and suitable performance status, while patients with progressive or worsened clinical conditions must continue systemic treatment[59]. Moreover, the same authors suggested the usefulness of an artery-first approach during surgical exploration to rule out eventual unresectability [60]. In the case of curative-intent resection, more radical surgical procedures, such as systematic mesopancreas dissection and the TRIANGLE approach, have been proposed to achieve higher rates of R0 resections; however, more evidence is needed to support such surgical strategies[61,62]. Finally, some conversion surgeries have been reported to have a high risk for early recurrence (up to 30% within the first 6 mo.) However, the risk factors for early recurrence remain unclear[63].

The multidisciplinary decision process after receiving NACT should consider radiological findings, as well as clinical and biological factors. A strong effort should be made to standardize evaluation and management in this setting, as well as to identify prognostic factors for adequate response and early recurrence. Similarly, larger prospective studies on ITT have aimed to establish objective selection criteria for conversion surgery.

Finally, another interesting argument is the possibility of undergoing conversion surgery after CT for patients with oligo-metastatic UR-M-PDAC. Many authors have proposed the feasibility of such an approach, with improved outcomes when compared to the outcomes of CT alone; however, risk factors and appropriate indications remain unclear[64,65]. A recent study by the Verona Pancreas Institute showed very interesting results of 52 consecutive UR-M-PDAC patients who initially only had liver metastases and underwent conversion surgery[66]. FOLFIRINOX was the most commonly used chemotherapy regimen (63.5%). The median OS of the initial diagnosis was 37.2 mo, while the disease-free survival (DFS) of pancreatectomy was 16.5 mo. Multivariate analysis revealed that vascular resection, operative time, prognostic nutrition index, and neutrophil-to-lymphocyte ratio were associated with OS. A phase III trial comparing the simultaneous resection of the primary tumor and liver metastases after conversion chemotherapy *vs* standard CT in liver-only UR-M-PDAC is currently carried and will likely provide more insights (NCT03398291)[67].

FUTURE PERSPECTIVES

Role of circulating DNA in treating non-metastatic pancreatic cancer

The preoperative determination of resectability is an unresolved issue since the most common sites of metastases are the liver or peritoneum, where sub-centimeter implants may be difficult to detect radiographically[68]. Previous studies have shown that even laparoscopic exploration can miss up to 30% of occult metastases[69]. Similarly, an elevated CA 19-9 Level is a predictor of occult metastases; however, this can also be impaired by a relatively high rate (47%) of false negative results[70]. Several

studies have investigated the possible role of circulating tumor DNA (ct-DNA). Indeed, ct-DNA is a promising new tool for the assessment of many gastrointestinal tumors, despite not being routinely used[71,72]. Patients with R-PDAC have lower levels of ct-DNA, as well as a lower number of genetic mutations in ct-DNA than the levels in patients with UR-PDAC[73,74]. ct-DNA is a reliable and easy-to-use tool for detecting tumoral mutations, such as mutations in the *KRAS* gene, which can be mutated in up to 90% of PDAC patients[75]. *KRAS* mutations are more common in patients with distant metastases than in patients with non-metastatic PDAC (58.9% *vs* 18.2%, respectively)[76], with the association with worse survival outcomes independent of the tumor[77-80]. Furthermore, since ct-DNA has shown higher concordance with metastatic lesions than with primitive tumors, the detection of such mutations may theoretically indicate the presence of occult metastases[73]. However, further studies are required to confirm this hypothesis.

A negative preoperative ct-DNA liquid test was reported to be associated with a low rate of early recurrence (4.6% within 6 mo)[75]. Similarly, non-detectable preoperative ct-DNA was associated with a higher rate of R0 resection with negative lymph nodes than the rate for patients with positive results (80% *vs* 38%)[81]. Furthermore, negative results of preoperative ct-DNA were associated with a better DFS even for patients undergoing R0 resection, suggesting a prognostic role independent of the subsequent surgery[82].

The combination of radiological staging with ct-DNA analysis may optimize the prognostic stratification of non-metastatic tumors, resulting in an additional tool that may aid in deciding whether to undergo surgery, which has high rates of morbidity, or to administer medical therapy[83,84].

Molecular targeted therapy

Genetic mutations are currently considered important, not only for diagnostic and prognostic purposes, but also as targets for molecular targeted therapy in many gastrointestinal cancers[85-87]. Both next-generation sequencing and ct-DNA may be useful tools for identifying such genetic alterations in a non-invasive manner.

To date, three kinds of targets have been investigated for PDAC: oncogenes, tumor suppressors, and caretaker genes[88]. *KRAS* is commonly involved in PDAC carcinogenesis, and its upregulation is considered a potential target of PDAC therapy. Thus, irreversible tyrosine kinase inhibitors may be considered a viable strategy; however, the first studies investigating the possible benefit of cetuximab did not show positive results (median OS 6.3 *vs* 5.9 mo, P = 0.23)[89]. Subsequently, newer epidermal growth factor receptor (EGFR) inhibitors have been tested: Nimotuzumab in combination with gemcitabine improved the OS of patients with both UR-LA-PDAC or UR-M-PDAC in a phase II trial (median OS 8.6 *vs* 6.0 mo, P = 0.03), with better outcomes in the KRAS wild-type subgroup (median OS 11.6 *vs* 5.6 mo, P = 0.03)[90]. In contrast, the EGFR inhibitor, vandetanib, has not shown any efficacy, while a clinical trial investigating the efficacy of afatinib is currently carried (NCT02451553)[91]. There are likely resistance mechanisms in PDAC cells that circumvent EGFR inhibition. Indeed, the additional inhibition of *C-RAF*, together with *KRAS*, led to complete tumor regression in murine PDAC models and human patient-derived xenografts[92]. Further trials are now investigating the possibility of inactivating both oncogenes and downstream crosstalk pathways.

Another frequent mutation in PDAC affects the *CDKN2A* gene, with an estimated frequency of approximately 60%, affecting the tumor suppression pathway that involves the proteins CD4/6 and p53 [93,94]. Ribociclib and palbociclib are newly developed drugs acting on CDK4/6. They have shown encouraging results in many preclinical models of PDAC, as well as for other solid cancers, with promising ongoing clinical trials (NCT02501902)[95-100]. Similarly, the SMAD4/TGF-β pathway can be mutated in 40% of PDAC93 cases. The TGF-β inhibitor, galunisertib, showed encouraging results in both preclinical investigations and phase I/II trials in combination with gemcitabine (estimated HR = 0.796) [101-103]. Moreover, *BRCA* is a well-known caretaker gene whose mutations are involved in many human solid tumors, including PDAC, with a frequency of approximately 6%-7%[104-106]. Newly developed PARP inhibitors have shown significant efficacy in treating other *BRCA* mutant solid tumors [107]. Olaparib was recently tested in a prospective phase III trial (the POLO trial, Pancreas Cancer Olaparib, NCT02184195) to evaluate its efficacy in patients with BRCA-mutant metastatic PDAC[108]. The PFS was increased in the olaparib group (7.4 *vs* 3.8 months, HR = 0.53, P = 0.004), at the cost of higher rates of adverse effects. The median OS did not significantly improve, although the trial is ongoing. In light of these encouraging results, further well-designed trials involving PARP inhibitors in BRCA-mutated PDAC are required.

Finally, chimeric antigen receptor T cells (CAR-T) are another therapeutic option for oncologic immunotherapy based on the reprogramming of autologous T cells from patients against tumoral antigens[109]. CAR-T has already been proven to be effective in treating blood tumors, with some drugs already approved by the FDA[110]. Subsequently, CAR-T cells were engineered and tested against possible targets in PDAC models. A phase II trial is testing CAR-T therapy against the mutant KRAS G12D that had previously shown a reduced response to other immunotherapies (NCT01174121)[111]. Furthermore, HER2/ERBB2 is considered a potential target in this setting, even if it is expressed less frequently (NCT01935843)[112].

Despite being promising, these strategies have not yet produced any significant clinical benefit and have not yet been investigated in the neoadjuvant setting. However, for traditional CT, the regimens were taken from the adjuvant and systemic protocols, suggesting possible future developments in molecular-targeted NACT. This tool may be added to existing protocols for nonmetastatic PDAC in cases of non-responsiveness to other regimens, as well as to obtain an improved response. Therefore, further studies are warranted.

CONCLUSION

Despite the encouraging results of the most recent NACT regimens for treating BR-PDAC, the current evidence supporting their use for R-PDAC remains inconclusive. We are looking forward to the results from several ongoing trials evaluating the role of different NACT regimens such as NEPAFOX and NorPACT-1 and investigating FOLFIRINOX *vs* upfront surgery or NEOPAC focusing on gemcitabine plus oxaliplatin *vs* upfront surgery, as they may have important clinical implications.

In the subset of BR-PDAC with arterial involvement, the benefits of NACT followed by surgery remain unclear; thus, well-planned clinical trials should be carried out to evaluate its efficacy.

Regarding UR-LA-PDAC, a strong effort should be made to standardize evaluation and management, as well as to identify prognostic factors for adequate response and early recurrence. Larger prospective studies on ITT aimed to establish objective selection criteria for conversion surgery. The multidisciplinary decision process after receiving NACT should consider radiological findings, as well as clinical and biological factors. Similarly, encouraging results suggest that also patients with oligo-metastatic UR-M-PDAC should undergo conversion surgery after CT. However, risk factors and appropriate indications remain unclear. Although the road towards protocol standardization remains lengthy and tedious, it is necessary to ensure treatment success and improve overall clinical outcomes.

FOOTNOTES

Author contributions: Cassese G, Han HS, Yoon YS, and Troisi RI were responsible for the conception of the study, its draft, and final review of the manuscript; Lee B and Cubisino A were responsible for administrative support; Lee JS, and Panaro F were responsible for the final editing and review of the manuscript.

Conflict-of-interest statement: The authors declare that they have no conflict of interest.

Country/Territory of origin: South Korea

ORCID number: Gianluca Cassese 0000-0001-9185-2054; Ho-Seong Han 0000-0001-9659-1260; Jun Suh Lee 0000-0001-9487-9826; Fabrizio Panaro 0000-0001-8200-4969; Roberto Ivan Troisi 0000-0001-6280-810X.

S-Editor: Yan JP
L-Editor: A
P-Editor: Yu HG

REFERENCES

1 **Sung H**, Ferlay J, Siegel RL, Laversanne M, Soerjomataram I, Jemal A, Bray F. Global Cancer Statistics 2020: GLOBOCAN Estimates of Incidence and Mortality Worldwide for 36 Cancers in 185 Countries. *CA Cancer J Clin* 2021; **71**: 209-249 [PMID: 33538338 DOI: 10.3322/caac.21660]

2 **Kleeff J**, Korc M, Apte M, La Vecchia C, Johnson CD, Biankin AV, Neale RE, Tempero M, Tuveson DA, Hruban RH, Neoptolemos JP. Pancreatic cancer. *Nat Rev Dis Primers* 2016; **2**: 16022 [PMID: 27158978 DOI: 10.1038/nrdp.2016.22]

3 **Bengtsson A**, Andersson R, Ansari D. The actual 5-year survivors of pancreatic ductal adenocarcinoma based on real-world data. *Sci Rep* 2020; **10**: 16425 [PMID: 33009477 DOI: 10.1038/s41598-020-73525-y]

4 **Lee DH**, Jang JY, Kang JS, Kim JR, Han Y, Kim E, Kwon W, Kim SW. Recent treatment patterns and survival outcomes in pancreatic cancer according to clinical stage based on single-center large-cohort data. *Ann Hepatobiliary Pancreat Surg* 2018; **22**: 386-396 [PMID: 30588531 DOI: 10.14701/ahbps.2018.22.4.386]

5 **Shin DW**, Lee JC, Kim J, Woo SM, Lee WJ, Han SS, Park SJ, Choi KS, Cha HS, Yoon YS, Han HS, Hong EK, Hwang JH. Validation of the American Joint Committee on Cancer 8th edition staging system for the pancreatic ductal

adenocarcinoma. *Eur J Surg Oncol* 2019; **45**: 2159-2165 [PMID: 31202572 DOI: 10.1016/j.ejso.2019.06.002]

6 **Huang L**, Jansen L, Balavarca Y, Molina-Montes E, Babaei M, van der Geest L, Lemmens V, Van Eycken L, De Schutter H, Johannesen TB, Fristrup CW, Mortensen MB, Primic-Žakelj M, Zadnik V, Becker N, Hackert T, Mägi M, Cassetti T, Sassatelli R, Grützmann R, Merkel S, Gonçalves AF, Bento MJ, Hegyi P, Lakatos G, Szentesi A, Moreau M, van de Velde T, Broeks A, Sant M, Minicozzi P, Mazzaferro V, Real FX, Carrato A, Molero X, Besselink MG, Malats N, Büchler MW, Schrotz-King P, Brenner H. Resection of pancreatic cancer in Europe and USA: an international large-scale study highlighting large variations. *Gut* 2019; **68**: 130-139 [PMID: 29158237 DOI: 10.1136/gutjnl-2017-314828]

7 **He W**, Zhao H, Chan W, Lopez D, Shroff RT, Giordano SH. Underuse of surgical resection among elderly patients with early-stage pancreatic cancer. *Surgery* 2015; **158**: 1226-1234 [PMID: 26138347 DOI: 10.1016/j.surg.2015.04.031]

8 **Gooiker GA**, Lemmens VE, Besselink MG, Busch OR, Bonsing BA, Molenaar IQ, Tollenaar RA, de Hingh IH, Wouters MW. Impact of centralization of pancreatic cancer surgery on resection rates and survival. *Br J Surg* 2014; **101**: 1000-1005 [PMID: 24844590 DOI: 10.1002/bjs.9468]

9 **Krautz C**, Nimptsch U, Weber GF, Mansky T, Grützmann R. Effect of Hospital Volume on In-hospital Morbidity and Mortality Following Pancreatic Surgery in Germany. *Ann Surg* 2018; **267**: 411-417 [PMID: 28379871 DOI: 10.1097/SLA.0000000000002248]

10 **Lidsky ME**, Sun Z, Nussbaum DP, Adam MA, Speicher PJ, Blazer DG 3rd. Going the Extra Mile: Improved Survival for Pancreatic Cancer Patients Traveling to High-volume Centers. *Ann Surg* 2017; **266**: 333-338 [PMID: 27429020 DOI: 10.1097/SLA.0000000000001924]

11 **Groot VP**, Gemenetzis G, Blair AB, Rivero-Soto RJ, Yu J, Javed AA, Burkhart RA, Rinkes IHMB, Molenaar IQ, Cameron JL, Weiss MJ, Wolfgang CL, He J. Defining and Predicting Early Recurrence in 957 Patients With Resected Pancreatic Ductal Adenocarcinoma. *Ann Surg* 2019; **269**: 1154-1162 [PMID: 31082915 DOI: 10.1097/SLA.0000000000002734]

12 **Mackay TM**, Smits FJ, Roos D, Bonsing BA, Bosscha K, Busch OR, Creemers GJ, van Dam RM, van Eijck CHJ, Gerhards MF, de Groot JWB, Groot Koerkamp B, Haj Mohammad N, van der Harst E, de Hingh IHJT, Homs MYV, Kazemier G, Liem MSL, de Meijer VE, Molenaar IQ, Nieuwenhuijs VB, van Santvoort HC, van der Schelling GP, Stommel MWJ, Ten Tije AJ, de Vos-Geelen J, Wit F, Wilmink JW, van Laarhoven HWM, Besselink MG; Dutch Pancreatic Cancer Group. The risk of not receiving adjuvant chemotherapy after resection of pancreatic ductal adenocarcinoma: a nationwide analysis. *HPB (Oxford)* 2020; **22**: 233-240 [PMID: 31439478 DOI: 10.1016/j.hpb.2019.06.019]

13 **Isaji S**, Mizuno S, Windsor JA, Bassi C, Fernández-Del Castillo C, Hackert T, Hayasaki A, Katz MHG, Kim SW, Kishiwada M, Kitagawa H, Michalski CW, Wolfgang CL. International consensus on definition and criteria of borderline resectable pancreatic ductal adenocarcinoma 2017. *Pancreatology* 2018; **18**: 2-11 [PMID: 29191513 DOI: 10.1016/j.pan.2017.11.011]

14 **Tempero MA**, Malafa MP, Al-Hawary M, Behrman SW, Benson AB, Cardin DB, Chiorean EG, Chung V, Czito B, Del Chiaro M, Dillhoff M, Donahue TR, Dotan E, Ferrone CR, Fountzilas C, Hardacre J, Hawkins WG, Klute K, Ko AH, Kunstman JW, LoConte N, Lowy AM, Moravek C, Nakakura EK, Narang AK, Obando J, Polanco PM, Reddy S, Reyngold M, Scaife C, Shen J, Vollmer C, Wolff RA, Wolpin BM, Lynn B, George GV. Pancreatic Adenocarcinoma, Version 2.2021, NCCN Clinical Practice Guidelines in Oncology. *J Natl Compr Canc Netw* 2021; **19**: 439-457 [PMID: 33845462 DOI: 10.6004/jnccn.2021.0017]

15 **Okusaka T**, Nakamura M, Yoshida M, Kitano M, Uesaka K, Ito Y, Furuse J, Hanada K, Okazaki K; Committee for Revision of Clinical Guidelines for Pancreatic Cancer of the Japan Pancreas Society. Clinical Practice Guidelines for Pancreatic Cancer 2019 From the Japan Pancreas Society: A Synopsis. *Pancreas* 2020; **49**: 326-335 [PMID: 32132516 DOI: 10.1097/MPA.0000000000001513]

16 **Suker M**, Beumer BR, Sadot E, Marthey L, Faris JE, Mellon EA, El-Rayes BF, Wang-Gillam A, Lacy J, Hosein PJ, Moorcraft SY, Conroy T, Hohla F, Allen P, Taieb J, Hong TS, Shridhar R, Chau I, van Eijck CH, Koerkamp BG. FOLFIRINOX for locally advanced pancreatic cancer: a systematic review and patient-level meta-analysis. *Lancet Oncol* 2016; **17**: 801-810 [PMID: 27160474 DOI: 10.1016/S1470-2045(16)00172-8]

17 **Crippa S**, Cirocchi R, Weiss MJ, Partelli S, Reni M, Wolfgang CL, Hackert T, Falconi M. A systematic review of surgical resection of liver-only synchronous metastases from pancreatic cancer in the era of multiagent chemotherapy. *Updates Surg* 2020; **72**: 39-45 [PMID: 31997233 DOI: 10.1007/s13304-020-00710-z]

18 **Hank T**, Klaiber U, Hinz U, Schütte D, Leonhardt CS, Bergmann F, Hackert T, Jäger D, Büchler MW, Strobel O. Oncological Outcome of Conversion Surgery After Preoperative Chemotherapy for Metastatic Pancreatic Cancer. *Ann Surg* 2022; **277**: e1089-e1098 [PMID: 35758505 DOI: 10.1097/SLA.0000000000005481]

19 **Springfeld C**, Neoptolemos JP. The role of neoadjuvant therapy for resectable pancreatic cancer remains uncertain. *Nat Rev Clin Oncol* 2022; **19**: 285-286 [PMID: 35194164 DOI: 10.1038/s41571-022-00612-6]

20 **Neoptolemos JP**, Kerr DJ, Beger H, Link K, Pederzoli P, Bassi C, Dervenis C, Fernandez-Cruz L, Laçaine F, Friess H, Büchler M. ESPAC-1 trial progress report: the European randomized adjuvant study comparing radiochemotherapy, 6 months chemotherapy and combination therapy versus observation in pancreatic cancer. *Digestion* 1997; **58**: 570-577 [PMID: 9438604 DOI: 10.1159/000201503]

21 **Neoptolemos JP**, Moore MJ, Cox TF, Valle JW, Palmer DH, McDonald AC, Carter R, Tebbutt NC, Dervenis C, Smith D, Glimelius B, Charnley RM, Lacaine F, Scarfe AG, Middleton MR, Anthoney A, Ghaneh P, Halloran CM, Lerch MM, Oláh A, Rawcliffe CL, Verbeke CS, Campbell F, Büchler MW; European Study Group for Pancreatic Cancer. Effect of adjuvant chemotherapy with fluorouracil plus folinic acid or gemcitabine vs observation on survival in patients with resected periampullary adenocarcinoma: the ESPAC-3 periampullary cancer randomized trial. *JAMA* 2012; **308**: 147-156 [PMID: 22782416 DOI: 10.1001/jama.2012.7352]

22 **Conroy T**, Hammel P, Hebbar M, Ben Abdelghani M, Wei AC, Raoul JL, Choné L, Francois E, Artru P, Biagi JJ, Lecomte T, Assenat E, Faroux R, Ychou M, Volet J, Sauvanet A, Breysacher G, Di Fiore F, Cripps C, Kavan P, Texereau P, Bouhier-Leporrier K, Khemissa-Akouz F, Legoux JL, Juzyna B, Gourgou S, O'Callaghan CJ, Jouffroy-Zeller C, Rat P, Malka D, Castan F, Bachet JB; Canadian Cancer Trials Group and the Unicancer-GI–PRODIGE Group. FOLFIRINOX or

Gemcitabine as Adjuvant Therapy for Pancreatic Cancer. *N Engl J Med* 2018; **379**: 2395-2406 [PMID: 30575490 DOI: 10.1056/NEJMoa1809775]

23 **Talamonti MS**, Small W Jr, Mulcahy MF, Wayne JD, Attaluri V, Colletti LM, Zalupski MM, Hoffman JP, Freedman GM, Kinsella TJ, Philip PA, McGinn CJ. A multi-institutional phase II trial of preoperative full-dose gemcitabine and concurrent radiation for patients with potentially resectable pancreatic carcinoma. *Ann Surg Oncol* 2006; **13**: 150-158 [PMID: 16418882 DOI: 10.1245/ASO.2006.03.039]

24 **Heinrich S**, Pestalozzi BC, Schäfer M, Weber A, Bauerfeind P, Knuth A, Clavien PA. Prospective phase II trial of neoadjuvant chemotherapy with gemcitabine and cisplatin for resectable adenocarcinoma of the pancreatic head. *J Clin Oncol* 2008; **26**: 2526-2531 [PMID: 18487569 DOI: 10.1200/JCO.2007.15.5556]

25 **Versteijne E**, van Dam JL, Suker M, Janssen QP, Groothuis K, Akkermans-Vogelaar JM, Besselink MG, Bonsing BA, Buijsen J, Busch OR, Creemers GM, van Dam RM, Eskens FALM, Festen S, de Groot JWB, Groot Koerkamp B, de Hingh IH, Homs MYV, van Hooft JE, Kerver ED, Luelmo SAC, Neelis KJ, Nuyttens J, Paardekooper GMRM, Patijn GA, van der Sangen MJC, de Vos-Geelen J, Wilmink JW, Zwinderman AH, Punt CJ, van Tienhoven G, van Eijck CHJ; Dutch Pancreatic Cancer Group. Neoadjuvant Chemoradiotherapy Versus Upfront Surgery for Resectable and Borderline Resectable Pancreatic Cancer: Long-Term Results of the Dutch Randomized PREOPANC Trial. *J Clin Oncol* 2022; **40**: 1220-1230 [PMID: 35084987 DOI: 10.1200/JCO.21.02233]

26 **Neoptolemos JP**, Stocken DD, Friess H, Bassi C, Dunn JA, Hickey H, Beger H, Fernandez-Cruz L, Dervenis C, Lacaine F, Falconi M, Pederzoli P, Pap A, Spooner D, Kerr DJ, Büchler MW; European Study Group for Pancreatic Cancer. A randomized trial of chemoradiotherapy and chemotherapy after resection of pancreatic cancer. *N Engl J Med* 2004; **350**: 1200-1210 [PMID: 15028824 DOI: 10.1056/NEJMoa032295]

27 **Katz MHG**, Shi Q, Meyers J, Herman JM, Chuong M, Wolpin BM, Ahmad S, Marsh R, Schwartz L, Behr S, Frankel WL, Collisson E, Leenstra J, Williams TM, Vaccaro G, Venook A, Meyerhardt JA, O'Reilly EM. Efficacy of Preoperative mFOLFIRINOX vs mFOLFIRINOX Plus Hypofractionated Radiotherapy for Borderline Resectable Adenocarcinoma of the Pancreas: The A021501 Phase 2 Randomized Clinical Trial. *JAMA Oncol* 2022; **8**: 1263-1270 [PMID: 35834226 DOI: 10.1001/jamaoncol.2022.2319]

28 **Ghaneh P**, Palmer D, Cicconi S, Jackson R, Halloran CM, Rawcliffe C, Sripadam R, Mukherjee S, Soonawalla Z, Wadsley J, Al-Mukhtar A, Dickson E, Graham J, Jiao L, Wasan HS, Tait IS, Prachalias A, Ross P, Valle JW, O'Reilly DA, Al-Sarireh B, Gwynne S, Ahmed I, Connolly K, Yim KL, Cunningham D, Armstrong T, Archer C, Roberts K, Ma YT, Springfeld C, Tjaden C, Hackert T, Büchler MW, Neoptolemos JP; European Study Group for Pancreatic Cancer. Immediate surgery compared with short-course neoadjuvant gemcitabine plus capecitabine, FOLFIRINOX, or chemoradiotherapy in patients with borderline resectable pancreatic cancer (ESPAC5): a four-arm, multicentre, randomised, phase 2 trial. *Lancet Gastroenterol Hepatol* 2023; **8**: 157-168 [PMID: 36521500 DOI: 10.1016/S2468-1253(22)00348-X]

29 **Perri G**, Prakash L, Qiao W, Varadhachary GR, Wolff R, Fogelman D, Overman M, Pant S, Javle M, Koay EJ, Herman J, Kim M, Ikoma N, Tzeng CW, Lee JE, Katz MHG. Response and Survival Associated With First-line FOLFIRINOX vs Gemcitabine and nab-Paclitaxel Chemotherapy for Localized Pancreatic Ductal Adenocarcinoma. *JAMA Surg* 2020; **155**: 832-839 [PMID: 32667641 DOI: 10.1001/jamasurg.2020.2286]

30 **Ahmad SA**, Duong M, Sohal DPS, Gandhi NS, Beg MS, Wang-Gillam A, Wade JL 3rd, Chiorean EG, Guthrie KA, Lowy AM, Philip PA, Hochster HS. Surgical Outcome Results From SWOG S1505: A Randomized Clinical Trial of mFOLFIRINOX Versus Gemcitabine/Nab-paclitaxel for Perioperative Treatment of Resectable Pancreatic Ductal Adenocarcinoma. *Ann Surg* 2020; **272**: 481-486 [PMID: 32740235 DOI: 10.1097/SLA.0000000000004155]

31 **Cools KS**, Sanoff HK, Kim HJ, Yeh JJ, Stitzenberg KB. Impact of neoadjuvant therapy on postoperative outcomes after pancreaticoduodenectomy. *J Surg Oncol* 2018; **118**: 455-462 [PMID: 30114330 DOI: 10.1002/jso.25183]

32 **Tashiro M**, Yamada S, Sonohara F, Takami H, Suenaga M, Hayashi M, Niwa Y, Tanaka C, Kobayashi D, Nakayama G, Koike M, Fujiwara M, Fujii T, Kodera Y. Clinical Impact of Neoadjuvant Therapy on Nutritional Status in Pancreatic Cancer. *Ann Surg Oncol* 2018; **25**: 3365-3371 [PMID: 30097739 DOI: 10.1245/s10434-018-6699-8]

33 **Hata T**, Chiba K, Mizuma M, Masuda K, Ohtsuka H, Nakagawa K, Morikawa T, Hayashi H, Motoi F, Unno M. Levels of tumor markers CEA/CA 19-9 in serum and peritoneal lavage predict postoperative recurrence in patients with pancreatic cancer. *Ann Gastroenterol Surg* 2022; **6**: 862-872 [PMID: 36338582 DOI: 10.1002/ags3.12597]

34 **Hallemeier CL**, Botros M, Corsini MM, Haddock MG, Gunderson LL, Miller RC. Preoperative CA 19-9 level is an important prognostic factor in patients with pancreatic adenocarcinoma treated with surgical resection and adjuvant concurrent chemoradiotherapy. *Am J Clin Oncol* 2011; **34**: 567-572 [PMID: 21150564 DOI: 10.1097/COC.0b013e3181f946fc]

35 **Tzeng CW**, Fleming JB, Lee JE, Xiao L, Pisters PW, Vauthey JN, Abdalla EK, Wolff RA, Varadhachary GR, Fogelman DR, Crane CH, Balachandran A, Katz MH. Defined clinical classifications are associated with outcome of patients with anatomically resectable pancreatic adenocarcinoma treated with neoadjuvant therapy. *Ann Surg Oncol* 2012; **19**: 2045-2053 [PMID: 22258816 DOI: 10.1245/s10434-011-2211-4]

36 **Carmichael J**, Fink U, Russell RC, Spittle MF, Harris AL, Spiessi G, Blatter J. Phase II study of gemcitabine in patients with advanced pancreatic cancer. *Br J Cancer* 1996; **73**: 101-105 [PMID: 8554969 DOI: 10.1038/bjc.1996.18]

37 **Rothenberg ML**, Moore MJ, Cripps MC, Andersen JS, Portenoy RK, Burris HA 3rd, Green MR, Tarassoff PG, Brown TD, Casper ES, Storniolo AM, Von Hoff DD. A phase II trial of gemcitabine in patients with 5-FU-refractory pancreas cancer. *Ann Oncol* 1996; **7**: 347-353 [PMID: 8805925 DOI: 10.1093/oxfordjournals.annonc.a010600]

38 **Conroy T**, Castan F, Lopez A, Turpin A, Ben Abdelghani M, Wei AC, Mitry E, Biagi JJ, Evesque L, Artru P, Lecomte T, Assenat E, Bauguion L, Ychou M, Bouché O, Monard L, Lambert A, Hammel P; Canadian Cancer Trials Group and the Unicancer-GI–PRODIGE Group. Five-Year Outcomes of FOLFIRINOX vs Gemcitabine as Adjuvant Therapy for Pancreatic Cancer: A Randomized Clinical Trial. *JAMA Oncol* 2022; **8**: 1571-1578 [PMID: 36048453 DOI: 10.1001/jamaoncol.2022.3829]

39 **Macedo FI**, Ryon E, Maithel SK, Lee RM, Kooby DA, Fields RC, Hawkins WG, Williams G, Maduekwe U, Kim HJ, Ahmad SA, Patel SH, Abbott DE, Schwartz P, Weber SM, Scoggins CR, Martin RCG, Dudeja V, Franceschi D,

Livingstone AS, Merchant NB. Survival Outcomes Associated With Clinical and Pathological Response Following Neoadjuvant FOLFIRINOX or Gemcitabine/Nab-Paclitaxel Chemotherapy in Resected Pancreatic Cancer. *Ann Surg* 2019; **270**: 400-413 [PMID: 31283563 DOI: 10.1097/SLA.0000000000003468]

40 **Ducreux M**, Cuhna AS, Caramella C, Hollebecque A, Burtin P, Goéré D, Seufferlein T, Haustermans K, Van Laethem JL, Conroy T, Arnold D; ESMO Guidelines Committee. Cancer of the pancreas: ESMO Clinical Practice Guidelines for diagnosis, treatment and follow-up. *Ann Oncol* 2015; **26** Suppl 5: v56-v68 [PMID: 26314780 DOI: 10.1093/annonc/mdv295]

41 **Chapman BC**, Gleisner A, Rigg D, Meguid C, Goodman K, Brauer B, Gajdos C, Schulick RD, Edil BH, McCarter MD. Perioperative outcomes and survival following neoadjuvant stereotactic body radiation therapy (SBRT) versus intensity-modulated radiation therapy (IMRT) in pancreatic adenocarcinoma. *J Surg Oncol* 2018; **117**: 1073-1083 [PMID: 29448308 DOI: 10.1002/jso.25004]

42 **Ferrone CR**, Marchegiani G, Hong TS, Ryan DP, Deshpande V, McDonnell EI, Sabbatino F, Santos DD, Allen JN, Blaszkowsky LS, Clark JW, Faris JE, Goyal L, Kwak EL, Murphy JE, Ting DT, Wo JY, Zhu AX, Warshaw AL, Lillemoe KD, Fernández-del Castillo C. Radiological and surgical implications of neoadjuvant treatment with FOLFIRINOX for locally advanced and borderline resectable pancreatic cancer. *Ann Surg* 2015; **261**: 12-17 [PMID: 25599322 DOI: 10.1097/SLA.0000000000000867]

43 **Wagner M**, Antunes C, Pietrasz D, Cassinotto C, Zappa M, Sa Cunha A, Lucidarme O, Bachet JB. CT evaluation after neoadjuvant FOLFIRINOX chemotherapy for borderline and locally advanced pancreatic adenocarcinoma. *Eur Radiol* 2017; **27**: 3104-3116 [PMID: 27896469 DOI: 10.1007/s00330-016-4632-8]

44 **Wu YHA**, Oba A, Lin R, Watanabe S, Meguid C, Schulick RD, Del Chiaro M. Selecting surgical candidates with locally advanced pancreatic cancer: a review for modern pancreatology. *J Gastrointest Oncol* 2021; **12**: 2475-2483 [PMID: 34790408 DOI: 10.21037/jgo-21-119]

45 **Ouaissi M**, Hubert C, Verhelst R, Astarci P, Sempoux C, Jouret-Mourin A, Loundou A, Gigot JF; Multidisciplary HPB Group of Center of Cancer. Vascular reconstruction during pancreatoduodenectomy for ductal adenocarcinoma of the pancreas improves resectability but does not achieve cure. *World J Surg* 2010; **34**: 2648-2661 [PMID: 20607257 DOI: 10.1007/s00268-010-0699-6]

46 **Bockhorn M**, Burdelski C, Bogoevski D, Sgourakis G, Yekebas EF, Izbicki JR. Arterial en bloc resection for pancreatic carcinoma. *Br J Surg* 2011; **98**: 86-92 [PMID: 21136564 DOI: 10.1002/bjs.7270]

47 **Loos M**, Kester T, Klaiber U, Mihaljevic AL, Mehrabi A, Müller-Stich BM, Diener MK, Schneider MA, Berchtold C, Hinz U, Feisst M, Strobel O, Hackert T, Büchler MW. Arterial Resection in Pancreatic Cancer Surgery: Effective After a Learning Curve. *Ann Surg* 2022; **275**: 759-768 [PMID: 33055587 DOI: 10.1097/SLA.0000000000004054]

48 **Mollberg N**, Rahbari NN, Koch M, Hartwig W, Hoeger Y, Büchler MW, Weitz J. Arterial resection during pancreatectomy for pancreatic cancer: a systematic review and meta-analysis. *Ann Surg* 2011; **254**: 882-893 [PMID: 22064622 DOI: 10.1097/SLA.0b013e31823ac299]

49 **Jegatheeswaran S**, Baltatzis M, Jamdar S, Siriwardena AK. Superior mesenteric artery (SMA) resection during pancreatectomy for malignant disease of the pancreas: a systematic review. *HPB (Oxford)* 2017; **19**: 483-490 [PMID: 28410913 DOI: 10.1016/j.hpb.2017.02.437]

50 **Gillen S**, Schuster T, Meyer Zum Büschenfelde C, Friess H, Kleeff J. Preoperative/neoadjuvant therapy in pancreatic cancer: a systematic review and meta-analysis of response and resection percentages. *PLoS Med* 2010; **7**: e1000267 [PMID: 20422030 DOI: 10.1371/journal.pmed.1000267]

51 **Lee M**, Kang JS, Kim H, Kwon W, Lee SH, Ryu JK, Kim YT, Oh DY, Chie EK, Jang JY. Impact of conversion surgery on survival in locally advanced pancreatic cancer patients treated with FOLFIRINOX chemotherapy. *J Hepatobiliary Pancreat Sci* 2023; **30**: 111-121 [PMID: 34581022 DOI: 10.1002/jhbp.1050]

52 **Hackert T**, Sachsenmaier M, Hinz U, Schneider L, Michalski CW, Springfeld C, Strobel O, Jäger D, Ulrich A, Büchler MW. Locally Advanced Pancreatic Cancer: Neoadjuvant Therapy With Folfirinox Results in Resectability in 60% of the Patients. *Ann Surg* 2016; **264**: 457-463 [PMID: 27355262 DOI: 10.1097/SLA.0000000000001850]

53 **Gemenetzis G**, Groot VP, Blair AB, Laheru DA, Zheng L, Narang AK, Fishman EK, Hruban RH, Yu J, Burkhart RA, Cameron JL, Weiss MJ, Wolfgang CL, He J. Survival in Locally Advanced Pancreatic Cancer After Neoadjuvant Therapy and Surgical Resection. *Ann Surg* 2019; **270**: 340-347 [PMID: 29596120 DOI: 10.1097/SLA.0000000000002753]

54 **Maggino L**, Malleo G, Marchegiani G, Viviani E, Nessi C, Ciprani D, Esposito A, Landoni L, Casetti L, Tuveri M, Paiella S, Casciani F, Sereni E, Binco A, Bonamini D, Secchettin E, Auriemma A, Merz V, Simionato F, Zecchetto C, D'Onofrio M, Melisi D, Bassi C, Salvia R. Outcomes of Primary Chemotherapy for Borderline Resectable and Locally Advanced Pancreatic Ductal Adenocarcinoma. *JAMA Surg* 2019; **154**: 932-942 [PMID: 31339530 DOI: 10.1001/jamasurg.2019.2277]

55 **Kirkegård J**, Aahlin EK, Al-Saiddi M, Bratlie SO, Coolsen M, de Haas RJ, den Dulk M, Fristrup C, Harrison EM, Mortensen MB, Nijkamp MW, Persson J, Søreide JA, Wigmore SJ, Wik T, Mortensen FV. Multicentre study of multidisciplinary team assessment of pancreatic cancer resectability and treatment allocation. *Br J Surg* 2019; **106**: 756-764 [PMID: 30830974 DOI: 10.1002/bjs.11093]

56 **Dudeja V**, Greeno EW, Walker SP, Jensen EH. Neoadjuvant chemoradiotherapy for locally advanced pancreas cancer rarely leads to radiological evidence of tumour regression. *HPB (Oxford)* 2013; **15**: 661-667 [PMID: 23458352 DOI: 10.1111/hpb.12015]

57 **Dholakia AS**, Hacker-Prietz A, Wild AT, Raman SP, Wood LD, Huang P, Laheru DA, Zheng L, De Jesus-Acosta A, Le DT, Schulick R, Edil B, Ellsworth S, Pawlik TM, Iacobuzio-Donahue CA, Hruban RH, Cameron JL, Fishman EK, Wolfgang CL, Herman JM. Resection of borderline resectable pancreatic cancer after neoadjuvant chemoradiation does not depend on improved radiographic appearance of tumor-vessel relationships. *J Radiat Oncol* 2013; **2**: 413-425 [PMID: 25755849 DOI: 10.1007/s13566-013-0115-6]

58 **Rangelova E**, Wefer A, Persson S, Valente R, Tanaka K, Orsini N, Segersvärd R, Arnelo U, Del Chiaro M. Surgery Improves Survival After Neoadjuvant Therapy for Borderline and Locally Advanced Pancreatic Cancer: A Single Institution Experience. *Ann Surg* 2021; **273**: 579-586 [PMID: 30946073 DOI: 10.1097/SLA.0000000000003301]

59 **Klaiber U**, Hackert T. Conversion Surgery for Pancreatic Cancer-The Impact of Neoadjuvant Treatment. *Front Oncol* 2019; **9**: 1501 [PMID: 31993372 DOI: 10.3389/fonc.2019.01501]

60 **Weitz J**, Rahbari N, Koch M, Büchler MW. The "artery first" approach for resection of pancreatic head cancer. *J Am Coll Surg* 2010; **210**: e1-e4 [PMID: 20113929 DOI: 10.1016/j.jamcollsurg.2009.10.019]

61 **Inoue Y**, Saiura A, Yoshioka R, Ono Y, Takahashi M, Arita J, Takahashi Y, Koga R. Pancreatoduodenectomy With Systematic Mesopancreas Dissection Using a Supracolic Anterior Artery-first Approach. *Ann Surg* 2015; **262**: 1092-1101 [PMID: 25587814 DOI: 10.1097/SLA.0000000000001065]

62 **Hackert T**, Strobel O, Michalski CW, Mihaljevic AL, Mehrabi A, Müller-Stich B, Berchtold C, Ulrich A, Büchler MW. The TRIANGLE operation - radical surgery after neoadjuvant treatment for advanced pancreatic cancer: a single arm observational study. *HPB (Oxford)* 2017; **19**: 1001-1007 [PMID: 28838632 DOI: 10.1016/j.hpb.2017.07.007]

63 **Satoi S**, Yamaue H, Kato K, Takahashi S, Hirono S, Takeda S, Eguchi H, Sho M, Wada K, Shinchi H, Kwon AH, Hirano S, Kinoshita T, Nakao A, Nagano H, Nakajima Y, Sano K, Miyazaki M, Takada T. Role of adjuvant surgery for patients with initially unresectable pancreatic cancer with a long-term favorable response to non-surgical anti-cancer treatments: results of a project study for pancreatic surgery by the Japanese Society of Hepato-Biliary-Pancreatic Surgery. *J Hepatobiliary Pancreat Sci* 2013; **20**: 590-600 [PMID: 23660962 DOI: 10.1007/s00534-013-0616-0]

64 **Su BB**, Bai DS, Yu JQ, Zhang C, Jin SJ, Zhou BH, Jiang GQ. Can Patients with Pancreatic Cancer and Liver Metastases Obtain Survival Benefit from Surgery? A Population-Based Study. *J Cancer* 2021; **12**: 539-552 [PMID: 33391450 DOI: 10.7150/jca.51218]

65 **De Simoni O**, Scarpa M, Tonello M, Pilati P, Tolin F, Spolverato Y, Gruppo M. Oligometastatic Pancreatic Cancer to the Liver in the Era of Neoadjuvant Chemotherapy: Which Role for Conversion Surgery? A Systematic Review and Meta-Analysis. *Cancers (Basel)* 2020; **12** [PMID: 33213022 DOI: 10.3390/cancers12113402]

66 **Frigerio I**, Malleo G, de Pastena M, Deiro G, Surci N, Scopelliti F, Esposito A, Regi P, Giardino A, Allegrini V, Bassi C, Girelli R, Salvia R, Butturini G. Prognostic Factors After Pancreatectomy for Pancreatic Cancer Initially Metastatic to the Liver. *Ann Surg Oncol* 2022; **29**: 8503-8510 [PMID: 35976466 DOI: 10.1245/s10434-022-12385-4]

67 **Wei M**, Shi S, Hua J, Xu J, Yu X; Chinese Study Group for Pancreatic Cancer (CSPAC). Simultaneous resection of the primary tumour and liver metastases after conversion chemotherapy versus standard therapy in pancreatic cancer with liver oligometastasis: protocol of a multicentre, prospective, randomised phase III control trial (CSPAC-1). *BMJ Open* 2019; **9**: e033452 [PMID: 31818843 DOI: 10.1136/bmjopen-2019-033452]

68 **Jacobson RA**, Munding E, Hayden DM, Levy M, Kuzel TM, Pappas SG, Masood A. Evolving Clinical Utility of Liquid Biopsy in Gastrointestinal Cancers. *Cancers (Basel)* 2019; **11** [PMID: 31412682 DOI: 10.3390/cancers11081164]

69 **Fong ZV**, Alvino DML, Fernández-Del Castillo C, Mehtsun WT, Pergolini I, Warshaw AL, Chang DC, Lillemoe KD, Ferrone CR. Reappraisal of Staging Laparoscopy for Patients with Pancreatic Adenocarcinoma: A Contemporary Analysis of 1001 Patients. *Ann Surg Oncol* 2017; **24**: 3203-3211 [PMID: 28718038 DOI: 10.1245/s10434-017-5973-5]

70 **Sugiura T**, Uesaka K, Kanemoto H, Mizuno T, Sasaki K, Furukawa H, Matsunaga K, Maeda A. Serum CA19-9 is a significant predictor among preoperative parameters for early recurrence after resection of pancreatic adenocarcinoma. *J Gastrointest Surg* 2012; **16**: 977-985 [PMID: 22411488 DOI: 10.1007/s11605-012-1859-9]

71 **Saini A**, Pershad Y, Albadawi H, Kuo M, Alzubaidi S, Naidu S, Knuttinen MG, Oklu R. Liquid Biopsy in Gastrointestinal Cancers. *Diagnostics (Basel)* 2018; **8** [PMID: 30380690 DOI: 10.3390/diagnostics8040075]

72 **Cassese G**, Han HS, Yoon YS, Lee JS, Cho JY, Lee HW, Lee B, Troisi RI. Preoperative Assessment and Perioperative Management of Resectable Gallbladder Cancer in the Era of Precision Medicine and Novel Technologies: State of the Art and Future Perspectives. *Diagnostics (Basel)* 2022; **12** [PMID: 35885535 DOI: 10.3390/diagnostics12071630]

73 **Brychta N**, Krahn T, von Ahsen O. Detection of KRAS Mutations in Circulating Tumor DNA by Digital PCR in Early Stages of Pancreatic Cancer. *Clin Chem* 2016; **62**: 1482-1491 [PMID: 27591291 DOI: 10.1373/clinchem.2016.257469]

74 **Patel H**, Okamura R, Fanta P, Patel C, Lanman RB, Raymond VM, Kato S, Kurzrock R. Clinical correlates of blood-derived circulating tumor DNA in pancreatic cancer. *J Hematol Oncol* 2019; **12**: 130 [PMID: 31801585 DOI: 10.1186/s13045-019-0824-4]

75 **Almoguera C**, Shibata D, Forrester K, Martin J, Arnheim N, Perucho M. Most human carcinomas of the exocrine pancreas contain mutant c-K-ras genes. *Cell* 1988; **53**: 549-554 [PMID: 2453289 DOI: 10.1016/0092-8674(88)90571-5]

76 **Takai E**, Totoki Y, Nakamura H, Morizane C, Nara S, Hama N, Suzuki M, Furukawa E, Kato M, Hayashi H, Kohno T, Ueno H, Shimada K, Okusaka T, Nakagama H, Shibata T, Yachida S. Clinical utility of circulating tumor DNA for molecular assessment in pancreatic cancer. *Sci Rep* 2015; **5**: 18425 [PMID: 26669280 DOI: 10.1038/srep18425]

77 **Singh N**, Gupta S, Pandey RM, Chauhan SS, Saraya A. High levels of cell-free circulating nucleic acids in pancreatic cancer are associated with vascular encasement, metastasis and poor survival. *Cancer Invest* 2015; **33**: 78-85 [PMID: 25647443 DOI: 10.3109/07357907.2014.1001894]

78 **Buscail E**, Maulat C, Muscari F, Chiche L, Cordelier P, Dabernat S, Alix-Panabières C, Buscail L. Liquid Biopsy Approach for Pancreatic Ductal Adenocarcinoma. *Cancers (Basel)* 2019; **11** [PMID: 31248203 DOI: 10.3390/cancers11060852]

79 **Ako S**, Nouso K, Kinugasa H, Dohi C, Matushita H, Mizukawa S, Muro S, Akimoto Y, Uchida D, Tomoda T, Matsumoto K, Horiguchi S, Tsutsumi K, Kato H, Okada H. Utility of serum DNA as a marker for KRAS mutations in pancreatic cancer tissue. *Pancreatology* 2017; **17**: 285-290 [PMID: 28139399 DOI: 10.1016/j.pan.2016.12.011]

80 **Kim MK**, Woo SM, Park B, Yoon KA, Kim YH, Joo J, Lee WJ, Han SS, Park SJ, Kong SY. Prognostic Implications of Multiplex Detection of KRAS Mutations in Cell-Free DNA from Patients with Pancreatic Ductal Adenocarcinoma. *Clin Chem* 2018; **64**: 726-734 [PMID: 29352043 DOI: 10.1373/clinchem.2017.283721]

81 **McDuff SGR**, Hardiman KM, Ulintz PJ, Parikh AR, Zheng H, Kim DW, Lennerz JK, Hazar-Rethinam M, Van Seventer EE, Fetter IJ, Nadres B, Eyler CE, Ryan DP, Weekes CD, Clark JW, Cusack JC, Goyal L, Zhu AX, Wo JY, Blaszkowsky LS, Allen J, Corcoran RB, Hong TS. Circulating Tumor DNA Predicts Pathologic and Clinical Outcomes Following Neoadjuvant Chemoradiation and Surgery for Patients With Locally Advanced Rectal Cancer. *JCO Precis Oncol* 2021; **5** [PMID: 34250394 DOI: 10.1200/PO.20.00220]

82 **Lee B**, Lipton L, Cohen J, Tie J, Javed AA, Li L, Goldstein D, Burge M, Cooray P, Nagrial A, Tebbutt NC, Thomson B,

Nikfarjam M, Harris M, Haydon A, Lawrence B, Tai DWM, Simons K, Lennon AM, Wolfgang CL, Tomasetti C, Papadopoulos N, Kinzler KW, Vogelstein B, Gibbs P. Circulating tumor DNA as a potential marker of adjuvant chemotherapy benefit following surgery for localized pancreatic cancer. *Ann Oncol* 2019; **30**: 1472-1478 [PMID: 31250894 DOI: 10.1093/annonc/mdz200]

83 **Rollin N**, Cassese G, Pineton DE Chambrun G, Serrand C, Navarro F, Blanc P, Panaro F, Valats JC. An easy-to-use score to predict clinically relevant postoperative pancreatic fistula after distal pancreatectomy. *Minerva Surg* 2022; **77**: 354-359 [PMID: 34693675 DOI: 10.23736/S2724-5691.21.09001-8]

84 **Grunvald MW**, Jacobson RA, Kuzel TM, Pappas SG, Masood A. Current Status of Circulating Tumor DNA Liquid Biopsy in Pancreatic Cancer. *Int J Mol Sci* 2020; **21** [PMID: 33081107 DOI: 10.3390/ijms21207651]

85 **Xie YH**, Chen YX, Fang JY. Comprehensive review of targeted therapy for colorectal cancer. *Signal Transduct Target Ther* 2020; **5**: 22 [PMID: 32296018 DOI: 10.1038/s41392-020-0116-z]

86 **Cassese G**, Han HS, Lee B, Lee HW, Cho JY, Panaro F, Troisi RI. Immunotherapy for hepatocellular carcinoma: A promising therapeutic option for advanced disease. *World J Hepatol* 2022; **14**: 1862-1874 [PMID: 36340753 DOI: 10.4254/wjh.v14.i10.1862]

87 **Xu W**, Yang Z, Lu N. Molecular targeted therapy for the treatment of gastric cancer. *J Exp Clin Cancer Res* 2016; **35**: 1 [PMID: 26728266 DOI: 10.1186/s13046-015-0276-9]

88 **Qian Y**, Gong Y, Fan Z, Luo G, Huang Q, Deng S, Cheng H, Jin K, Ni Q, Yu X, Liu C. Molecular alterations and targeted therapy in pancreatic ductal adenocarcinoma. *J Hematol Oncol* 2020; **13**: 130 [PMID: 33008426 DOI: 10.1186/s13045-020-00958-3]

89 **Philip PA**, Benedetti J, Corless CL, Wong R, O'Reilly EM, Flynn PJ, Rowland KM, Atkins JN, Mirtsching BC, Rivkin SE, Khorana AA, Goldman B, Fenoglio-Preiser CM, Abbruzzese JL, Blanke CD. Phase III study comparing gemcitabine plus cetuximab versus gemcitabine in patients with advanced pancreatic adenocarcinoma: Southwest Oncology Group-directed intergroup trial S0205. *J Clin Oncol* 2010; **28**: 3605-3610 [PMID: 20606093 DOI: 10.1200/JCO.2009.25.7550]

90 **Schultheis B**, Reuter D, Ebert MP, Siveke J, Kerkhoff A, Berdel WE, Hofheinz R, Behringer DM, Schmidt WE, Goker E, De Dosso S, Kneba M, Yalcin S, Overkamp F, Schlegel F, Dommach M, Rohrberg R, Steinmetz T, Bulitta M, Strumberg D. Gemcitabine combined with the monoclonal antibody nimotuzumab is an active first-line regimen in KRAS wildtype patients with locally advanced or metastatic pancreatic cancer: a multicenter, randomized phase IIb study. *Ann Oncol* 2017; **28**: 2429-2435 [PMID: 28961832 DOI: 10.1093/annonc/mdx343]

91 **Middleton G**, Palmer DH, Greenhalf W, Ghaneh P, Jackson R, Cox T, Evans A, Shaw VE, Wadsley J, Valle JW, Propper D, Wasan H, Falk S, Cunningham D, Coxon F, Ross P, Madhusudan S, Wadd N, Corrie P, Hickish T, Costello E, Campbell F, Rawcliffe C, Neoptolemos JP. Vandetanib plus gemcitabine versus placebo plus gemcitabine in locally advanced or metastatic pancreatic carcinoma (ViP): a prospective, randomised, double-blind, multicentre phase 2 trial. *Lancet Oncol* 2017; **18**: 486-499 [PMID: 28259610 DOI: 10.1016/S1470-2045(17)30084-0]

92 **Blasco MT**, Navas C, Martín-Serrano G, Graña-Castro O, Lechuga CG, Martín-Díaz L, Djurec M, Li J, Morales-Cacho L, Esteban-Burgos L, Perales-Patón J, Bousquet-Mur E, Castellano E, Jacob HKC, Cabras L, Musteanu M, Drosten M, Ortega S, Mulero F, Sainz B Jr, Dusetti N, Iovanna J, Sánchez-Bueno F, Hidalgo M, Khiabanian H, Rabadán R, Al-Shahrour F, Guerra C, Barbacid M. Complete Regression of Advanced Pancreatic Ductal Adenocarcinomas upon Combined Inhibition of EGFR and C-RAF. *Cancer Cell* 2019; **35**: 573-587.e6 [PMID: 30975481 DOI: 10.1016/j.ccell.2019.03.002]

93 **Knudsen ES**, O'Reilly EM, Brody JR, Witkiewicz AK. Genetic Diversity of Pancreatic Ductal Adenocarcinoma and Opportunities for Precision Medicine. *Gastroenterology* 2016; **150**: 48-63 [PMID: 26385075 DOI: 10.1053/j.gastro.2015.08.056]

94 **Qian ZR**, Rubinson DA, Nowak JA, Morales-Oyarvide V, Dunne RF, Kozak MM, Welch MW, Brais LK, Da Silva A, Li T, Li W, Masuda A, Yang J, Shi Y, Gu M, Masugi Y, Bui J, Zellers CL, Yuan C, Babic A, Khalaf N, Aguirre A, Ng K, Miksad RA, Bullock AJ, Chang DT, Tseng JF, Clancy TE, Linehan DC, Findeis-Hosey JJ, Doyle LA, Thorner AR, Ducar M, Wollison B, Laing A, Hahn WC, Meyerson M, Fuchs CS, Ogino S, Hornick JL, Hezel AF, Koong AC, Wolpin BM. Association of Alterations in Main Driver Genes With Outcomes of Patients With Resected Pancreatic Ductal Adenocarcinoma. *JAMA Oncol* 2018; **4**: e173420 [PMID: 29098284 DOI: 10.1001/jamaoncol.2017.3420]

95 **Cristofanilli M**, Rugo HS, Im SA, Slamon DJ, Harbeck N, Bondarenko I, Masuda N, Colleoni M, DeMichele A, Loi S, Iwata H, O'Leary B, André F, Loibl S, Bananis E, Liu Y, Huang X, Kim S, Lechuga Frean MJ, Turner NC. Overall Survival with Palbociclib and Fulvestrant in Women with HR+/HER2- ABC: Updated Exploratory Analyses of PALOMA-3, a Double-blind, Phase III Randomized Study. *Clin Cancer Res* 2022; **28**: 3433-3442 [PMID: 35552673 DOI: 10.1158/1078-0432.CCR-22-0305]

96 **Dickson MA**, Schwartz GK, Keohan ML, D'Angelo SP, Gounder MM, Chi P, Antonescu CR, Landa J, Qin LX, Crago AM, Singer S, Koff A, Tap WD. Progression-Free Survival Among Patients With Well-Differentiated or Dedifferentiated Liposarcoma Treated With CDK4 Inhibitor Palbociclib: A Phase 2 Clinical Trial. *JAMA Oncol* 2016; **2**: 937-940 [PMID: 27124835 DOI: 10.1001/jamaoncol.2016.0264]

97 **Heilmann AM**, Perera RM, Ecker V, Nicolay BN, Bardeesy N, Benes CH, Dyson NJ. CDK4/6 and IGF1 receptor inhibitors synergize to suppress the growth of p16INK4A-deficient pancreatic cancers. *Cancer Res* 2014; **74**: 3947-3958 [PMID: 24986516 DOI: 10.1158/0008-5472.CAN-13-2923]

98 **Rencuzogulları O**, Yerlikaya PO, Gürkan AÇ, Arısan ED, Telci D. Palbociclib, a selective CDK4/6 inhibitor, restricts cell survival and epithelial-mesenchymal transition in Panc-1 and MiaPaCa-2 pancreatic cancer cells. *J Cell Biochem* 2020; **121**: 508-523 [PMID: 31264276 DOI: 10.1002/jcb.29249]

99 **Sherr CJ**. A New Cell-Cycle Target in Cancer - Inhibiting Cyclin D-Dependent Kinases 4 and 6. *N Engl J Med* 2016; **375**: 1920-1923 [PMID: 27959598 DOI: 10.1056/NEJMp1612343]

100 **Chou A**, Froio D, Nagrial AM, Parkin A, Murphy KJ, Chin VT, Wohl D, Steinmann A, Stark R, Drury A, Walters SN, Vennin C, Burgess A, Pinese M, Chantrill LA, Cowley MJ, Molloy TJ; Australian Pancreatic Cancer Genome Initiative (APGI), Waddell N, Johns A, Grimmond SM, Chang DK, Biankin AV, Sansom OJ, Morton JP, Grey ST, Cox TR, Turchini J, Samra J, Clarke SJ, Timpson P, Gill AJ, Pajic M. Tailored first-line and second-line CDK4-targeting treatment

combinations in mouse models of pancreatic cancer. *Gut* 2018; **67**: 2142-2155 [PMID: 29080858 DOI: 10.1136/gutjnl-2017-315144]

101 **Shi L**, Sheng J, Wang M, Luo H, Zhu J, Zhang B, Liu Z, Yang X. Combination Therapy of TGF-β Blockade and Commensal-derived Probiotics Provides Enhanced Antitumor Immune Response and Tumor Suppression. *Theranostics* 2019; **9**: 4115-4129 [PMID: 31281535 DOI: 10.7150/thno.35131]

102 **Gueorguieva I**, Tabernero J, Melisi D, Macarulla T, Merz V, Waterhouse TH, Miles C, Lahn MM, Cleverly A, Benhadji KA. Population pharmacokinetics and exposure-overall survival analysis of the transforming growth factor-β inhibitor galunisertib in patients with pancreatic cancer. *Cancer Chemother Pharmacol* 2019; **84**: 1003-1015 [PMID: 31482224 DOI: 10.1007/s00280-019-03931-1]

103 **Melisi D**, Garcia-Carbonero R, Macarulla T, Pezet D, Deplanque G, Fuchs M, Trojan J, Kozloff M, Simionato F, Cleverly A, Smith C, Wang S, Man M, Driscoll KE, Estrem ST, Lahn MMF, Benhadji KA, Tabernero J. TGFβ receptor inhibitor galunisertib is linked to inflammation- and remodeling-related proteins in patients with pancreatic cancer. *Cancer Chemother Pharmacol* 2019; **83**: 975-991 [PMID: 30887178 DOI: 10.1007/s00280-019-03807-4]

104 **Mersch J**, Jackson MA, Park M, Nebgen D, Peterson SK, Singletary C, Arun BK, Litton JK. Cancers associated with BRCA1 and BRCA2 mutations other than breast and ovarian. *Cancer* 2015; **121**: 269-275 [PMID: 25224030 DOI: 10.1002/cncr.29041]

105 **Ghiorzo P**. Genetic predisposition to pancreatic cancer. *World J Gastroenterol* 2014; **20**: 10778-10789 [PMID: 25152581 DOI: 10.3748/wjg.v20.i31.10778]

106 **Holter S**, Borgida A, Dodd A, Grant R, Semotiuk K, Hedley D, Dhani N, Narod S, Akbari M, Moore M, Gallinger S. Germline BRCA Mutations in a Large Clinic-Based Cohort of Patients With Pancreatic Adenocarcinoma. *J Clin Oncol* 2015; **33**: 3124-3129 [PMID: 25940717 DOI: 10.1200/JCO.2014.59.7401]

107 **Kaufman B**, Shapira-Frommer R, Schmutzler RK, Audeh MW, Friedlander M, Balmaña J, Mitchell G, Fried G, Stemmer SM, Hubert A, Rosengarten O, Steiner M, Loman N, Bowen K, Fielding A, Domchek SM. Olaparib monotherapy in patients with advanced cancer and a germline BRCA1/2 mutation. *J Clin Oncol* 2015; **33**: 244-250 [PMID: 25366685 DOI: 10.1200/JCO.2014.56.2728]

108 Olaparib for Metastatic Breast Cancer in Patients with a Germline BRCA Mutation. *N Engl J Med* 2017; **377**: 1700 [PMID: 28792849 DOI: 10.1056/NEJMx170012]

109 **Sterner RC**, Sterner RM. CAR-T cell therapy: current limitations and potential strategies. *Blood Cancer J* 2021; **11**: 69 [PMID: 33824268 DOI: 10.1038/s41408-021-00459-7]

110 **Kochenderfer JN**, Dudley ME, Kassim SH, Somerville RP, Carpenter RO, Stetler-Stevenson M, Yang JC, Phan GQ, Hughes MS, Sherry RM, Raffeld M, Feldman S, Lu L, Li YF, Ngo LT, Goy A, Feldman T, Spaner DE, Wang ML, Chen CC, Kranick SM, Nath A, Nathan DA, Morton KE, Toomey MA, Rosenberg SA. Chemotherapy-refractory diffuse large B-cell lymphoma and indolent B-cell malignancies can be effectively treated with autologous T cells expressing an anti-CD19 chimeric antigen receptor. *J Clin Oncol* 2015; **33**: 540-549 [PMID: 25154820 DOI: 10.1200/JCO.2014.56.2025]

111 **Rosenberg SA**, Tran E, Robbins PF. T-Cell Transfer Therapy Targeting Mutant KRAS. *N Engl J Med* 2017; **376**: e11 [PMID: 28199803 DOI: 10.1056/NEJMc1616637]

112 **Feng K**, Liu Y, Guo Y, Qiu J, Wu Z, Dai H, Yang Q, Wang Y, Han W. Phase I study of chimeric antigen receptor modified T cells in treating HER2-positive advanced biliary tract cancers and pancreatic cancers. *Protein Cell* 2018; **9**: 838-847 [PMID: 28710747 DOI: 10.1007/s13238-017-0440-4]

113 **Evans DB**, Varadhachary GR, Crane CH, Sun CC, Lee JE, Pisters PW, Vauthey JN, Wang H, Cleary KR, Staerkel GA, Charnsangavej C, Lano EA, Ho L, Lenzi R, Abbruzzese JL, Wolff RA. Preoperative gemcitabine-based chemoradiation for patients with resectable adenocarcinoma of the pancreatic head. *J Clin Oncol* 2008; **26**: 3496-3502 [PMID: 18640930 DOI: 10.1200/JCO.2007.15.8634]

114 **Varadhachary GR**, Wolff RA, Crane CH, Sun CC, Lee JE, Pisters PW, Vauthey JN, Abdalla E, Wang H, Staerkel GA, Lee JH, Ross WA, Tamm EP, Bhosale PR, Krishnan S, Das P, Ho L, Xiong H, Abbruzzese JL, Evans DB. Preoperative gemcitabine and cisplatin followed by gemcitabine-based chemoradiation for resectable adenocarcinoma of the pancreatic head. *J Clin Oncol* 2008; **26**: 3487-3495 [PMID: 18640929 DOI: 10.1200/JCO.2007.15.8642]

115 **O'Reilly EM**, Perelshteyn A, Jarnagin WR, Schattner M, Gerdes H, Capanu M, Tang LH, LaValle J, Winston C, DeMatteo RP, D'Angelica M, Kurtz RC, Abou-Alfa GK, Klimstra DS, Lowery MA, Brennan MF, Coit DG, Reidy DL, Kingham TP, Allen PJ. A single-arm, nonrandomized phase II trial of neoadjuvant gemcitabine and oxaliplatin in patients with resectable pancreas adenocarcinoma. *Ann Surg* 2014; **260**: 142-148 [PMID: 24901360 DOI: 10.1097/SLA.0000000000000251]

116 **Golcher H**, Brunner TB, Witzigmann H, Marti L, Bechstein WO, Bruns C, Jungnickel H, Schreiber S, Grabenbauer GG, Meyer T, Merkel S, Fietkau R, Hohenberger W. Neoadjuvant chemoradiation therapy with gemcitabine/cisplatin and surgery versus immediate surgery in resectable pancreatic cancer: results of the first prospective randomized phase II trial. *Strahlenther Onkol* 2015; **191**: 7-16 [PMID: 25252602 DOI: 10.1007/s00066-014-0737-7]

117 **Okano K**, Suto H, Oshima M, Maeda E, Yamamoto N, Kakinoki K, Kamada H, Masaki T, Takahashi S, Shibata T, Suzuki Y. A Prospective Phase II Trial of Neoadjuvant S-1 with Concurrent Hypofractionated Radiotherapy in Patients with Resectable and Borderline Resectable Pancreatic Ductal Adenocarcinoma. *Ann Surg Oncol* 2017; **24**: 2777-2784 [PMID: 28608121 DOI: 10.1245/s10434-017-5921-4]

118 **Motoi F**, Kosuge T, Ueno H, Yamaue H, Satoi S, Sho M, Honda G, Matsumoto I, Wada K, Furuse J, Matsuyama Y, Unno M; Study Group of Preoperative Therapy for Pancreatic Cancer (Prep) and Japanese Study Group of Adjuvant Therapy for Pancreatic cancer (JSAP). Randomized phase II/III trial of neoadjuvant chemotherapy with gemcitabine and S-1 versus upfront surgery for resectable pancreatic cancer (Prep-02/JSAP05). *Jpn J Clin Oncol* 2019; **49**: 190-194 [PMID: 30608598 DOI: 10.1093/jjco/hyy190]

World Journal of Gastrointestinal Oncology

Submit a Manuscript: https://www.f6publishing.com

World J Gastrointest Oncol 2023 June 15; 15(6): 925-942

DOI: 10.4251/wjgo.v15.i6.925

ISSN 1948-5204 (online)

REVIEW

Pancreatic cancer, autoimmune or chronic pancreatitis, beyond tissue diagnosis: Collateral imaging and clinical characteristics may differentiate them

Ana I Tornel-Avelar, Jose Antonio Velarde Ruiz-Velasco, Mario Pelaez-Luna

Specialty type: Gastroenterology and hepatology

Provenance and peer review: Invited article; Externally peer reviewed.

Peer-review model: Single blind

Peer-review report's scientific quality classification
Grade A (Excellent): 0
Grade B (Very good): B
Grade C (Good): C, C, C
Grade D (Fair): 0
Grade E (Poor): 0

P-Reviewer: Liu C, China; Solimando AG, Italy; Tan CL, China

Received: February 20, 2023
Peer-review started: February 20, 2023
First decision: April 2, 2023
Revised: April 21, 2023
Accepted: April 28, 2023
Article in press: April 28, 2023
Published online: June 15, 2023

Ana I Tornel-Avelar, Jose Antonio Velarde Ruiz-Velasco, Department of Gastroenterology, Hospital Civil of Guadalajara "Fray Antonio Alcalde", Guadalajara 44340, Jalisco, Mexico

Mario Pelaez-Luna, Research Division School of Medicine/Department of Gastroenterology, Universidad Nacional Autonoma de México/National Institute of Medical Sciences and Nutrition "Salvador Zubiran", Tlalpan 14000, Mexico City, Mexico

Corresponding author: Mario Pelaez-Luna, MD, Associate Professor of Medicine, Research Division School of Medicine/Department of Gastroenterology, Universidad Nacional Autonoma de México/National Institute of Medical Sciences and Nutrition "Salvador Zubiran", 15 Vasco de Quiroga, Belisario Domínguez Sección XVI, Tlalpan 14000, Mexico City, Mexico. mariopl@prodigy.net.mx

Abstract

Pancreatic ductal adenocarcinoma (PDAC) is one of the most lethal malignancies and is developing into the 2nd leading cause of cancer-related death. Often, the clinical and radiological presentation of PDAC may be mirrored by other inflammatory pancreatic masses, such as autoimmune pancreatitis (AIP) and mass-forming chronic pancreatitis (MFCP), making its diagnosis challenging. Differentiating AIP and MFCP from PDAC is vital due to significant therapeutic and prognostic implications. Current diagnostic criteria and tools allow the precise differentiation of benign from malignant masses; however, the diagnostic accuracy is imperfect. Major pancreatic resections have been performed in AIP cases under initial suspicion of PDAC after a diagnostic approach failed to provide an accurate diagnosis. It is not unusual that after a thorough diagnostic evaluation, the clinician is confronted with a pancreatic mass with uncertain diagnosis. In those cases, a re-evaluation must be entertained, preferably by an experienced multispecialty team including radiologists, pathologists, gastroenterologists, and surgeons, looking for disease-specific clinical, imaging, and histological hallmarks or collateral evidence that could favor a specific diagnosis. Our aim is to describe current diagnostic limitations that hinder our ability to reach an accurate diagnosis among AIP, PDAC, and MFCP and to highlight those disease-specific clinical, radiological, serological, and histological characteristics that could support the presence of any of these three disorders when facing a pancreatic mass with uncertain diagnosis after an initial diagnostic approach has been unsuccessful.

Key Words: Pancreas cancer; Chronic pancreatitis; Autoimmune pancreatitis; Pancreas mass; Endoscopic ultrasound; Diagnosis

Core Tip: This article describes the flaws and hurdles of current diagnostic tools as well as disease specific imaging, serological and histological characteristics that play a significant role in the differentiation of focal autoimmune pancreatitis, mass-forming chronic pancreatitis and pancreatic ductal adenocarcinoma.

Citation: Tornel-Avelar AI, Velarde Ruiz-Velasco JA, Pelaez-Luna M. Pancreatic cancer, autoimmune or chronic pancreatitis, beyond tissue diagnosis: Collateral imaging and clinical characteristics may differentiate them. *World J Gastrointest Oncol* 2023; 15(6): 925-942
URL: https://www.wjgnet.com/1948-5204/full/v15/i6/925.htm
DOI: https://dx.doi.org/10.4251/wjgo.v15.i6.925

INTRODUCTION

Pancreatic ductal adenocarcinoma (PDAC) is one of the most lethal malignancies; its incidence almost matches its fatality rate and continues to increase. PDAC is on track to becoming the 2nd leading cause of cancer-related death. It affects both sexes equally, and its 5-year survival rate is less than 10%[1,2]. Although novel chemotherapy schemes increase its prognosis, surgery seems to be the only treatment that offers better survival rates[3-5]. Such a dismal picture prompts an accurate and early diagnosis of PDAC that may offer better outcomes.

In most cases, the diagnosis of PDAC offers no difficulty; however, different benign conditions, such as inflammatory masses [chronic pancreatitis (CP) and autoimmune pancreatitis (AIP)] as well as other malignant conditions with different treatments and prognoses (*e.g.*, metastases, islet cell tumors, complex cystic lesions, pancreatoblastoma, pancreatic lymphoma, *etc.*) often resemble its clinical, biochemical, and imaging appearance, posing a diagnostic challenge[6].

The most common inflammatory conditions that present as a pancreatic mass include mass-forming CP (MFCP), which accounts for 10%-30% of all cases of CP, and focal AIP, which is a variant of the classic diffusely enlarged pancreas that has been widely described. Focal AIP accounts for 28%-41% of all AIP cases[7,8].

The ability to differentiate among these masses (PDAC, MFCP, and AIP) remains a challenge, as most of the time the clinical picture is confusing, and gross imaging features seem to be similar, which hinders accurate diagnosis and may result in unnecessary surgery regardless of their benign or malignant nature.

Differential diagnosis requires considerable expertise and the use of a myriad of diagnostic tools that include computed tomography (CT), which remains the most available and cost-effective technique to evaluate the pancreas. However, considering that up to 5% to 10% of all pancreatic neoplasms present a contrast enhancement pattern similar to the rest of the pancreatic parenchyma and that its diagnostic accuracy for small lesions decreases significantly, the use of other imaging techniques is often necessary.

Magnetic resonance imaging (MRI) offers a more accurate evaluation of the pancreatic parenchyma; it is able to visualize up to 5% to 10% of the issoatenuated pancreatic masses seen in CT scans, and is capable of revealing lesions smaller than 2 cm in size[9].

Endoscopic ultrasound (EUS) is another valuable tool; it provides high-resolution images of the pancreas, nearby organs, and vascularity and is capable of detecting small lesions and providing information on potential vascular and adjacent organ involvement. A significant drawback is that it remains operator-dependent, which accounts for its variable diagnostic accuracy.

The advent of new techniques such as dynamic MRI, which calculates and evaluates perfusion parameters, may increase the diagnostic yield and provide relevant information regarding chemo-sensitivity to standard and antiangiogenic therapies for PDAC. Perfusion CT, dual-energy CT, and MRI elastography diagnostic performances are encouraging. Pending further research, they seem to produce relevant information that would improve our current capacities to differentiate distinct malignant and benign pancreatic masses[1].

In addition to the former imaging techniques, serologic markers, histologic examination, and in some cases, therapeutic trials (*e.g.*, steroid trial for presumed AIP) can and have been entertained.

Although international consensuses and criteria on the definition, diagnosis, and treatment of AIP and CP have been developed and disease-specific characteristics and available diagnostic tools usually allow precise differentiation of AIP, CP, and PDAC or at least differentiation of a benign lesion from a malignant lesion, their diagnostic accuracy is imperfect. In a significant number of cases, regardless of a

multidisciplinary approach involving access to high notch technology and clinical expertise, an accurate diagnosis of a pancreatic mass remains elusive, and major pancreatic resections in benign conditions such as AIP are still being performed. Some surgical series have reported that focal AIP has been diagnosed in up to 2% of surgical specimens from patients who underwent surgery for presumed PDAC.

Some groups advise that any resectable pancreatic mass should undergo surgery even if a thorough diagnostic evaluation has failed to prove the presence of malignancy. It should not be overlooked that although pancreatic surgery mortality rates in expert hands range from 1%-2%, comorbidity rates, especially those related to a Whipple procedure, are considerable (40%-50%).

Every effort leading to a prompt and accurate diagnosis to avoid surgical delays of a resectable PDAC that can rapidly become nonresectable as well as efforts to avoid unnecessary surgery and its related complications should be considered[1,3].

DIAGNOSTIC TOOLS-CLASSIC CHARACTERISTICS AND FLAWS

Pancreatic cancer

PDAC's clinical picture consisting of abdominal pain, jaundice, weight loss, *etc*., is usually shared by AIP and MFCP among other conditions, and although diagnostic suspicion could increase based on imaging and serum characteristics, these are not exclusive to PDAC, and pathology confirmation remains mandatory.

Carbohydrate antigen 19-9 antigen

Serum carbohydrate antigen 19-9 (Ca 19-9) sensitivity is low. Increased levels (> 37 U/mL) are not exclusive to pancreatic cancer, and they may occur in biliary and other gastrointestinal carcinomas (*i.e*., neuroendocrine tumors of the pancreas, cholangiocarcinoma, or hepatocarcinoma). Expert guidelines do not recommend it as a screening tool for pancreatic cancer, but it is helpful in patient's follow-up and, in some cases, in the selection of potential surgical candidates with an otherwise resectable appearing mass [10].

Ca 19-9 serum levels may increase in benign conditions such as acute and CP, liver cirrhosis, cholangitis, and cholelithiasis[11]. Up to 27% of focal AIP cases mimicking PDAC present with increased levels of Ca 19-9, but usually in numbers < 100 U/mL. Ca 19-9 is not a sensitive or a specific method that could help to distinguish malignant from benign processes[12].

Abdominal US

The role of conventional surface US seems to be limited to the initial evaluation of jaundice. It may identify features suggestive of pancreatic cancer, such as the presence of a hypoechogenic mass in the pancreatic head and dilation of the pancreatic and biliary ducts. However, an accurate and complete assessment of the pancreas, specifically the body and tail, is frequently limited due to the interposition of intestinal loops and gas. The sensitivity and accuracy of abdominal US to assess the pancreas depends on the operator's experience, the patient's body constitution and the location and burden of the disease. Its diagnostic accuracy ranges between 50% and 90% for detecting pancreatic cancer[13].

CT

Contrast-enhanced CT (CECT) has 90% sensitivity, 87% specificity, and 89% accuracy in diagnosing pancreatic cancer and is considered the best method to evaluate the pancreas and pancreatic masses. Its main limitation is its low sensitivity for early lesions and tumors smaller than 2 cm[14] since they usually appear isoattenuating in relation to the surrounding pancreatic parenchyma[15,16].

PDAC usually presents as a poorly defined and spiculated hypoattenuating mass with distal atrophy of the gland. After contrast media administration, it persists as a hypoattenuating mass with respect to the rest of the parenchyma, but in late stages, it shows heterogeneous peripheral enhancement, although atypical forms of AIP and MFCP may share the same characteristics[17].

As will be discussed later, specific and some subtle changes in structure and contrast dynamics may help in the differential.

Magnetic resonance

Some studies consider MRI a superior test compared to CT in characterizing pancreatic masses[18] and delineating the pancreatic ductal system. MRI has become the diagnostic alternative to endoscopic pancreatic cholangiopancreatography. The sensitivity, specificity, and accuracy of MRI for diagnosing pancreatic cancer have been reported to be 93%, 89%, and 90%, respectively[19,20].

PDAC and MFCP appear hypointense on fat-suppressed T1 sequences[21], whereas they have a variable appearance on T2-weighted images (Figure 1)[22], as well as on diffusion-weighted images (DWI)[23]. For example, on the diffusion sequence, pancreatic masses show increased signal intensity relative to the normal pancreatic parenchyma and appear hypointense on the apparent diffusion

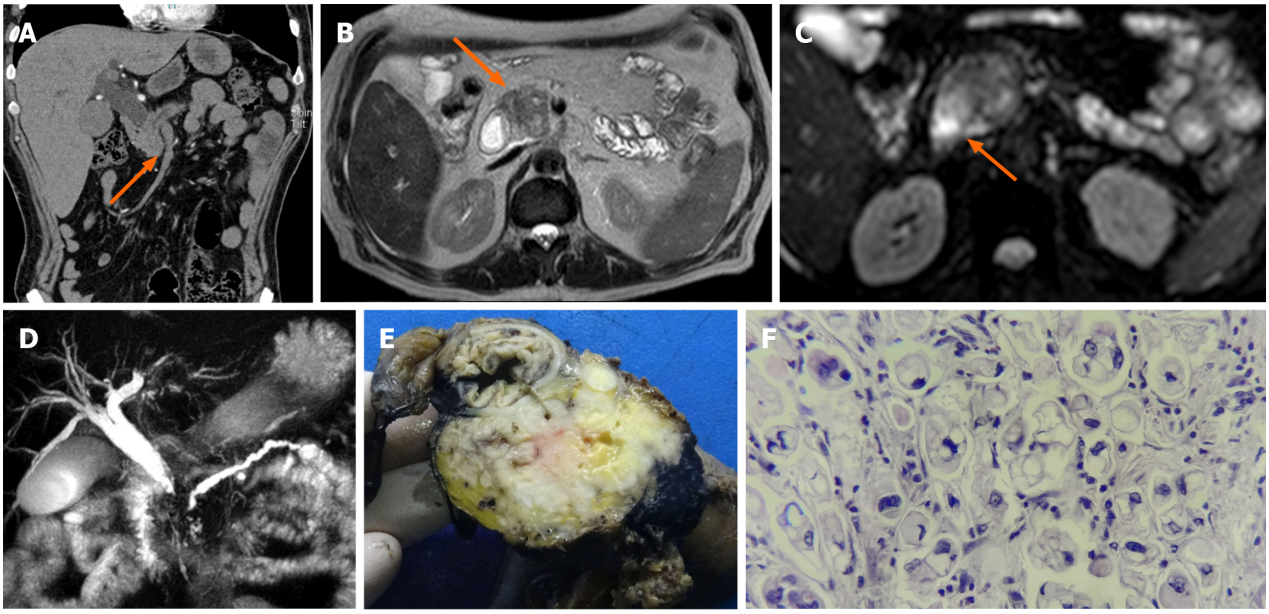

DOI: 10.4251/wjgo.v15.i6.925 **Copyright** ©The Author(s) 2023.

Figure 1 A 62-year-old male patient with a history of abdominal pain and jaundice. A: Contrast-enhanced abdominal tomography shows a poorly enhanced hypocaptured lesion (orange arrow); B: Magnetic resonance imaging (MRI) in the T2 sequence shows a hypointense lesion (orange arrow); C: MRI in the diffusion sequence shows a lesion with restriction (orange arrow); D: In magnetic resonance cholangiopancreatography, the double duct sign is evident; E: Macroscopic specimen of the head of the pancreas in which there is a whitish mass; F: Slides report poorly differentiated pancreatic ductal adenocarcinoma of the pancreas with high-grade signet ring cells with perineural infiltration and invasion of the duodenum and ampulla of Vater.

coefficient (ADC)[24]. However, DWI may not be able to conclusively discriminate an inflammatory mass from a neoplastic solid lesion, as both present similar values in this modality[24,25].

When PDAC appears isointense, MRI can show indirect signs that suggest malignancy, such as gland atrophy and dilatation of the main pancreatic duct (usually > 4 mm)[26,27]. In contrast, in MFCP, the pancreatic duct is dilated to a lesser degree and usually coexists with lengthy and irregular ductal stenosis. In PDAC, duct dilation is uniform, comprising the total length of the upstream duct, and the ductal stenoses are associated or next to the mass (this can also be seen on CECT)[28,29]. Widening of the space between the pancreas, common bile duct (CBD), and duodenal lumen is another sign that is frequently observed in MFCP and not in PDAC[29].

All these characteristics can be observed in atypical forms of AIP and MFCP, making the distinction among them based on noncontrast MRI difficult. Reports on the differentiating capacity of dynamic contrast-enhanced MRI have reported high sensitivity, specificity, and diagnostic accuracy rates[30].

EUS

Since the diagnostic gold standard of PDAC, MFCP, and AIP is histology, EUS has become a valuable tool in the evaluation of pancreatic masses. EUS provides high-resolution images and allows us to obtain a tissue sample. Compared to abdominal US, CECT, and positron emission tomography (PET/CT) in the recognition of early pancreatic tumors, early-stage CP (Figure 2), loco-regional staging of PDAC, and deciding the best site for biopsy, EUS has a better performance[31,32].

For the detection of lesions smaller than 3 cm, EUS has a diagnostic sensitivity of 99% compared to 55% for CECT. It also has a high negative predictive value for ruling out pancreatic cancer[32].

EUS elastography and contrast-enhanced endoscopic US, although still not widely available, are rapidly growing techniques that have demonstrated to be able to characterize and differentiate pancreatic masses based on their stiffness and sonographic contrast dynamics, with promising results and ongoing research and development[33].

Considering all these caveats of imaging techniques, histology still stands as the diagnostic gold standard of pancreatic masses. EUS-guided biopsy has become the method of choice for obtaining pancreatic tissue, with 90% sensitivity and 96% specificity, a complication rate less than 0.8% and a reduced risk of seeding and dissemination[34].

However, its diagnostic yield depends on the quality of the sample, the selected site of puncture, and the interpretation of the results[31]. A 15% to 59% rate of inconclusive diagnoses resulting from the initial EUS-FNA has been reported[35-38].

Repeated EUS biopsy is an accepted strategy in patients with a suspicious pancreatic mass and inconclusive diagnosis after a first diagnostic approach that included a biopsy. The cumulative yield after repeat EUS-FNA for definite PDAC has been reported to be approximately 16%[39].

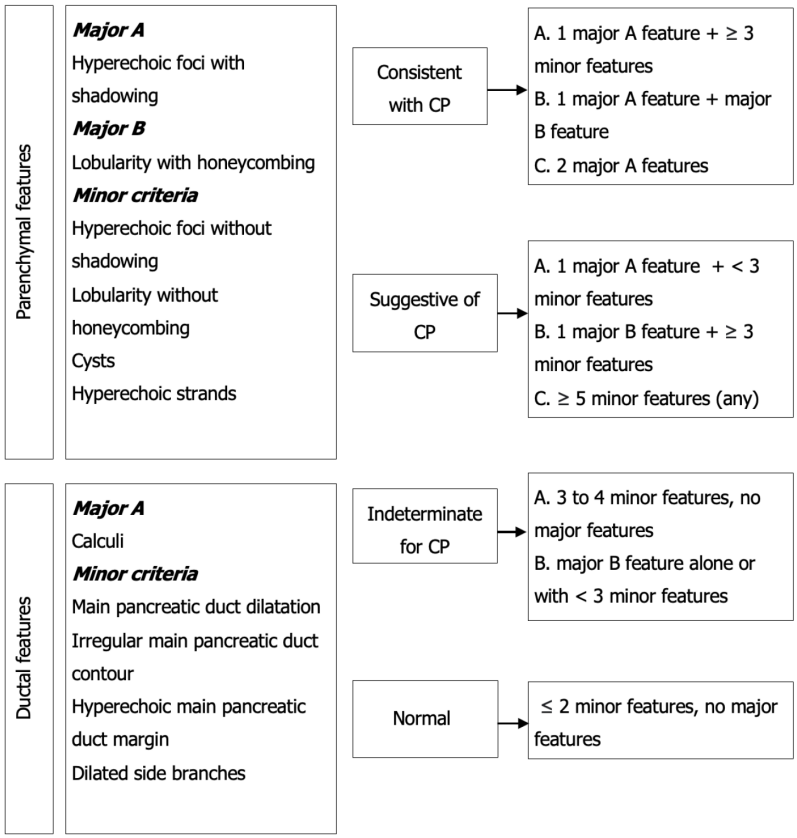

DOI: 10.4251/wjgo.v15.i6.925

Figure 2 Rosemont classification for chronic pancreatitis.

The atypical neoplastic glands of PDAC are usually embedded in a dense stroma (desmoplastic tumors). Biopsy's limited diagnostic yield can be explained by PDAC's associated desmoplastic reaction, which increases the chance of obtaining fibrotic tissue instead of cancer cells; since AIP and MFCP are rich in fibrotic tissue and inflammatory infiltrate, their presence does not rule out malignancy or confirm a benign inflammatory mass[40,41]. Other factors that may affect the diagnostic accuracy of EUS-guided biopsies include operator- and technique-related factors and extent of tumor necrosis.

Since a negative biopsy does not confidently rule out malignancy, if clinical suspicion is high enough, a biopsy should be repeated or if the mass is potentially resectable, surgery must be entertained.

CHRONIC PANCREATITIS

CP is a pathologic fibro-inflammatory syndrome of the pancreas in individuals with genetic, environmental, and/or other risk factors who develop persistent pathologic responses to parenchymal injury or stress[42].

Common features of established and advanced CP include pancreatic atrophy, fibrosis, pain syndromes, duct distortion, calcifications, pancreatic exocrine dysfunction, pancreatic endocrine dysfunction, and dysplasia[8,43]; up to 10% to 30% of cases may present as MFCP[44].

The incidence of PDAC is much higher than that in the general population (several genetic risk factors have been described as well as modifiable and nonmodifiable host factors), with almost 2% to 4% of patients with CP developing PDAC within ten years or more of diagnosis. The presence of a pancreatic mass in patients with CP represents a diagnostic challenge, with significant therapeutic and prognostic implications[4,5,8,45].

Discerning between PDCA and MFCP solely on clinical grounds is challenging; both may present as a pancreatic mass with recurrent abdominal pain, jaundice, weight loss, and pancreatic insufficiencies (exocrine and/or endocrine)[8].

Abdominal ultrasound

Abdominal US does not discern among pancreatic cancer, AIP, and MFCP since all 3 may display similar imaging characteristics. Despite AIP having specific features such as diffuse enlargement of the pancreas, decreased echogenicity, and narrowing of the pancreatic duct due to compression of the

affected parenchyma, the aforementioned technical limitations of abdominal US play a significant role in decreasing its diagnostic yield, especially in focal and atypical forms of AIP[46].

On the other hand, if intraparenchymal calcifications, heterogenicity with hyperechogenicity of the parenchyma, dilatation of the main pancreatic duct, and irregularity of the pancreatic contour can be identified, MFCP is to be suspected. However, some studies have reported that parenchymal calcifications can occur in other pancreatic disorders, such as intraductal papillary mucinous neoplasms (IPMN), with a 20% reported incidence. The calcification pattern in IPMN is indistinguishable from that in CP; calcifications can be found in the pancreatic duct, parenchyma, or diffusely scattered throughout the gland. Punctate calcification was the most common pattern (87%), followed by coarse calcification (33%).

Abdominal US has 67% sensitivity and 90% specificity for the diagnosis of established CP[47].

CECT

Contrast-enhanced imaging may discriminate among the different etiologies of a pancreatic mass[37]. A mass related to MFCP and AIP exhibits homogeneous enhancement similar to the rest of the pancreatic parenchyma, with the opposite occurring in PDAC, which shows poor enhancement in all phases along with poorly delimited margins[33]. These features can be secondary to a marked desmoplastic reaction, low vascularity, and the presence of necrosis and mucin in PDAC[48]. Unfortunately, in advanced stages of CP, MFCP pancreatic parenchyma presents significant fibrosis that modifies the enhancement pattern, especially during the arterial phase, although in some cases, the venous phase is preserved and may help in distinguishing MFCP from PDAC. For the diagnosis of CP, CECT has 75% sensitivity and 91% specificity[49].

Endoscopic retrograde cholangiopancreatography

Once considered the gold standard for assessing the pancreatic duct, EUS has been replaced by magnetic resonance cholangiopancreatography (MRCP) and EUS[50], and its current role is almost exclusively therapeutic.

Histology

Histologic examination is paramount when facing pancreatic masses. CP exhibits a fibrotic pattern that may resemble the one observed in PDAC-related desmoplasia; thus, the presence of chronic inflammatory infiltrate in pancreatic tissue does not rule out PDAC.

Biopsies may not always add to the differential between AIP and CP since the latter might also show lymphocytic and plasma cell infiltrate, as well as macrophage infiltrate and areas of interlobular fibrosis extending into the ductal structures that are also observed in type 1 and 2 AIP.

In CP, acinar and islet cells are usually spliced by fibrous tissue, and the ducts may contain protein plugs that can become calcified. Nevertheless, these features are often seen in elderly patients without CP, especially in those with diabetes mellitus[51].

Repeated biopsy should always be entertained as it improves the diagnostic yield. Mitchell *et al*[39] demonstrated that repeat FNA yields an altered diagnosis in 71% of patients. This is similar to other studies that showed that a second EUS-FNA alters the initial diagnosis in up to 63% to 82% of cases[36-38,52].

AUTOIMMUNE PANCREATITIS

AIP is classified into type 1 and 2 AIP that may present as an acute or chronic form. Type 1 AIP is a manifestation of systemic IgG4-related disease (IgG4-RD), a systemic condition that can affect almost every organ but has a predilection for the pancreas and biliary tract[53,54].

Both types of AIP can mimic PDAC both in imaging appearance and clinical presentation. AIP can present with painless obstructive jaundice in up to 70% of cases as well as with abdominal pain and weight loss in up to 30%[55].

In late stages, if left untreated or if treatment is delayed, AIP can result in CP and present with exocrine pancreatic insufficiency and diabetes mellitus. Thus, MFCP can either be a primary disorder or a complication of AIP[53,56,57].

Criteria for diagnosis are based on imaging, serological, histological, and therapeutic response parameters[1,58].

International Consensus Diagnostic Criteria (ICDC) for type 1 and 2 AIP consider both typical and atypical presentations. The ICDC diagnostic yield for type 1 is high, with a reported sensitivity of 89%-95%, specificity of 100%, and accuracy of 94%. Biopsy is seldom needed since serum and imaging characteristics along with other organ involvement frequently provide enough diagnostic evidence.

Atypical forms of IgG4-related pancreatitis as well as type 2 AIP might require tissue acquisition. In both, but especially in type 2 AIP, collateral information from serum and other organ involvement is missing in most cases (only 25% of type 2 AIP may have concurrent inflammatory bowel disease), making biopsy almost mandatory since pancreatic cancer cannot confidently be ruled out[59-61].

Immunoglobulin IgG4

IgG4 remains a good marker for the diagnosis of IgG4-RD[62], but increased levels can also occur in CP and other benign conditions as well as in up to 10% to 15% of PDAC, but levels are usually less than twice the upper limit of normal[63], which is considered the ideal cut off point to diagnose or differentiate IgG4-RD AIP from other non-IgG4-related diseases with a specificity of 92.6%. IgG4 levels are of no utility in ruling in or out the possibility of type 2 AIP[63,64].

Autoantibodies

Autoantibodies (Abs), including anti-nuclear Ab, anti-Ro/SSA, anti-La/SSB, anti-neutrophil cytoplasmic Ab, anti-lactoferrin Ab, anti-carbonic anhydrase II, anti-plasminogen-binding protein Ab, anti-inhibitor of pancreatic trypsin secretion Ab, anti-DNA, anti-Sm, anti-RNP, and cryoglobulins, are neither sensitive nor specific[65] and lack diagnostic value since they do not differentiate AIP from MFCP or PDAC. In some cases, they may increase the possibility of type 2 AIP[65-67].

Imaging

On imaging, AIP may present as either diffuse, focal, or multifocal pancreas enlargement resembling MFCP and PDAC[68,69].

Abdominal US and contrast-enhanced US

As discussed before, abdominal US does not have any diagnostic value other than being the initial tool to assess jaundice. Although significantly limited with regard to the extension of the pancreas that it can visualize, it can show a hypoechoic mass associated with hyperechoic foci and stranding as well as parenchymal heterogeneity but is unable to differentiate a benign from a malignant mass.

Contrast-enhanced US might provide more information in this regard, but again, the extension of the gland that can be examined as well as technical, operator-, and patient-related factors limit its diagnostic yield.

CT

Abdominal CT allows visualization of the full extension of the pancreas and better characterization of any abnormality.

The classic form or level 1 evidence of AIP according to the ICDC is a diffusely enlarged pancreas with an increased anteroposterior diameter and smooth edges ("sausage pancreas") and is usually accompanied by a hypodense halo or pseudocapsule surrounding the pancreas[1].

Ductwise, the level 1 evidence consists of an irregular and stenotic pancreatic main duct[70-72]. When contrast media is applied, in the early phase, a hypodense mass is usually observed, and in the late phase, it will become isodense. Although a similar behavior is observed in PDAC, AIP usually presents late enhancement in the venous phase.

Up to 30% of the time, AIP presents as a focal mass that is indistinguishable from MFCP and PDAC[6,73]. In PDAC, the pancreatic duct usually has smooth contours, with a short stenosis or abrupt amputation at the tumor site; when located at the head of the pancreas, it may also affect the CBD, and a double duct sign [dilated CBD and main pancreatic duct (MPD)] can be observed.

Vascular involvement is often observed in late stages of PDAC, but AIP may have a similar picture when it presents with retroperitoneal fibrosis affecting local vasculature[61].

Collateral information may aid in the differential diagnosis; the presence of pancreatic calcifications and cysts might suggest MFCP or late phases of AIP, while other organ involvement may suggest AIP [74,75].

Overall, CECT has 59% [95% confidence interval (CI), 41%-75%] sensitivity and 99% (95%CI: 88%-100%) specificity to differentiate AIP from PDAC[76].

Extrapancreatic abnormalities such as renal involvement with bilateral patchy lesions and lymph node or parotid gland involvement are associated with IgG4 systemic disease[74,75].

MRI

On MRI, AIP's diffuse or focal enlargement of the pancreas is observed as a hypointense gland in the T1 sequence and hyperintense in the T2 sequence; however, this is similar to how PDAC is observed.

Additionally, both AIP and PDAC show a similar diffusion restriction pattern on DWI, appearing as a hyperintense gland, but unlike PDAC, AIP shows greater hypointensity in ADC.

A hypointense peripheral pancreatic halo in both sequences[77] and extensive irregular stenosis (≥ 3 mm in length) in the affected pancreatic segment without upstream ductal dilation suggest AIP[26,78,79]. The presence of multiple stenoses has been reported in up to 61.5% of cases with AIP[26] (Figure 3). The penetrating duct sign (which is better observed during MRCP with secretin) in the affected area also favors AIP over PDAC[80,81]. MRI diagnostic yield has a low sensitivity (28.6%-44.4%) but high specificity (100%)[82].

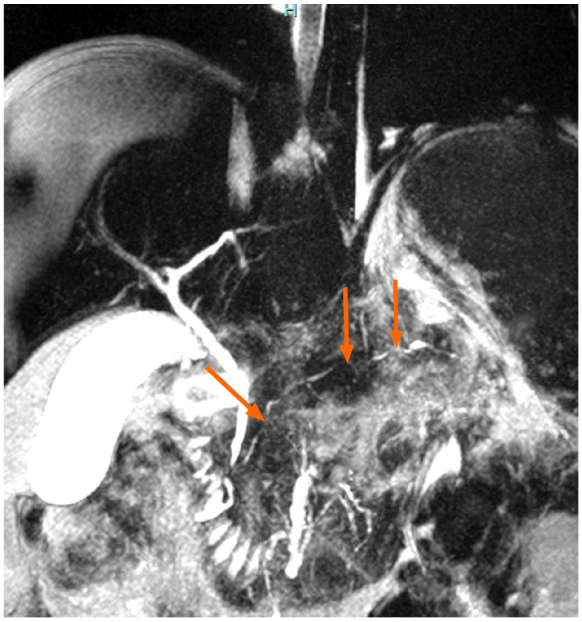

DOI: 10.4251/wjgo.v15.i6.925

Figure 3 A 38-year-old man was diagnosed with autoimmune pancreatitis. The magnetic resonance cholangiopancreatography shows a pancreatic duct with multiple stenoses (orange arrow) without upstream dilation.

Histology

Frequently, after exhaustive diagnostic work-up, atypical forms of IgG4 RD AIP and type 2 AIP remain undiagnosed, and biopsy is needed, which may confirm the diagnosis or distinguish them from MFCP and PDAC.

Histologic findings of AIP differ depending on whether it is type 1 or type 2. IgG4-related AIP (type 1 AIP) is characterized by T-lymphocyte infiltration, lymphoplasmacytic infiltrate with IgG4-positive plasma cells (IgG4+), storiform fibrosis, and obliterative phlebitis[78]. It has been reported that > 40% of IgG+ plasma cells and > 10 IgG4+ plasma cells per high power field (HPF) for puncture specimens or > 50 IgG4+ HPF cells for surgical specimens are present in most AIP type 1[83].

Type 2 AIP histology shows a granulocytic epithelial lesion[22,82], neutrophil and lymphocyte infiltrate and different extents of fibrosis. The pancreatic duct is narrowed by periductal fibrosis and lymphoplasmacytic infiltration, but the ductal epithelium is usually preserved[70] (Figure 4).

PDAC can also show infiltration by IgG4+ plasma cells, but to a lesser extent and unlike AIP, it does not present storiform fibrosis or obliterative phlebitis. When EUS-guided biopsy is unavailable, endoscopic biopsy of the ampulla of Vater may show a lymphoplasmacytic infiltrate with IgG4-positive plasma cells, placing it as a good surrogate in the diagnosis of type 1 AIP[84].

NEW IMAGING TECHNIQUES IN THE PANCREAS

Some recently developed techniques might improve our capability to differentiate benign from malignant pancreatic masses.

Perfusion CT

This is a modality that seems to differentiate between MFCP and PDAC. Yadav *et al*[85] and Aslan *et al*[86] assessed the characteristics of histology-proven PDAC and MFCP on perfusion CT. Blood flow (BF) and blood volume (BV) were the best parameters that differentiated both entities from each other. Although both MFCP and PDAC presented low values in BF and BV compared with normal pancreatic parenchyma, the lowest values were more frequent in PDCA. A cut off value of 19 mL/100 mL/min for BF had 92% sensitivity and 68% specificity to differentiate PDAC from MFCP, and for a value of 5 mL/100 mL in BV, the reported sensitivity and specificity were 100% and 73%, respectively.

These results are encouraging, but they still need to be replicated and validated in larger studies.

Dual-energy CT and low-voltage tube

These techniques have become the modality of choice for pancreatic cancer imaging and have shown good performance in detecting < 2 cm or isoattenuating lesions.

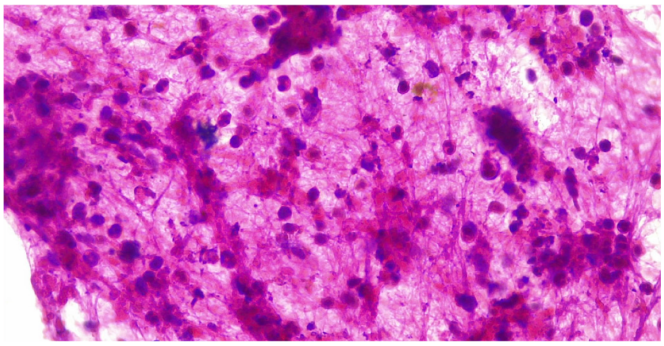

Figure 4 Endoscopic ultrasound guided fine needle biopsy of a type 2 autoimmune pancreatitis. Specimens shows dense lymphocyte infiltrate with scattered neutrophils. Citation: Pelaez-Luna M, Soriano-Rios A, Lira-Treviño AC, Uscanga-Domínguez L. Steroid-responsive pancreatitides. *World J Clin Cases* 2020; 8: 3411-3430. Published by Baishideng Publishing Group Inc[60] (Supplementary material).

These methods allow a more precise characterization of the solid or cystic nature/components of a given pancreatic lesion as well as a better visualization of the pancreatic duct and surrounding vascularity[14,85,86].

Low voltage generated images increase the probability of detecting a hypodense lesion embedded in the normal pancreatic parenchyma compared with those obtained with high voltage equipment, and such distinction becomes more evident during the portal contrasted phase[87]. Low voltage CT has higher sensitivity in diagnosing PDCA compared to high voltage imaging using iodine contrast[86,87].

PET/CT

It has limited and low diagnostic yield when discriminating between benign inflammatory masses and malignant ones[5,87].

MRI elastography

By assessing and comparing the tissue rigidity related to either an inflammatory process or a malignant process, this new tool has a high diagnostic accuracy for differentiating PDAC from AIP but still requires further study.

Shi *et al*[88] reported differences in tissue stiffness in AIP, PDAC, and healthy volunteers. AIP cases showed higher stiffness values [2.67 kPa (2.24-3.56 kPa) than healthy pancreas 1.24 kPa (1.18-1.24 kPa)] but significantly lower stiffness values than PDAC [3.78 kPa (3.22-5.11 kPa)] ($P < 0.05$).

EUS elastography

Either qualitative or quantitative, it might discriminate benign from malignant masses based on their particular stiffness rates. A distortion ratio cutoff point > 10 or a value < 50 in the distortion histogram suggests malignancy[89-91] (Figure 5).

Giovannini *et al*[92] reported EUS elastography findings in 121 cases with pancreatic masses. The sensitivity, specificity, positive predictive value, and negative predictive value for differentiating benign and malignant pancreatic masses were 92.3%, 80.0%, 93.3%, and 77.4%, respectively.

Diagnosing based solely on these parameters is still far from possible; currently, these technological advances have helped in selecting the biopsy site, identifying viable tissue and avoiding necrotic areas within the mass.

LIQUID BIOPSY

Liquid biopsy identifies circulating tumoral DNA, microRNA, and cells. It has been shown to be feasible and efficient in diagnosing different malignant neoplasms at early stages (*e.g.*, lung, breast, colon and liver cancer). It has also been suggested that it could be a reliable confirmatory test and possibly replace the need for tissue biopsy[93]. Information on pancreatic cancer is scarce but promising; it could aid in diagnosis and provide information related to potential therapeutic targets as well as prognosis[94-98].

Its reported sensitivity and specificity in diagnosing PDAC range between 33%-100% and 27%-81%, respectively[94]. Liquid biopsy could also be applied in the study and diagnosis of benign conditions such as AIP and CP.

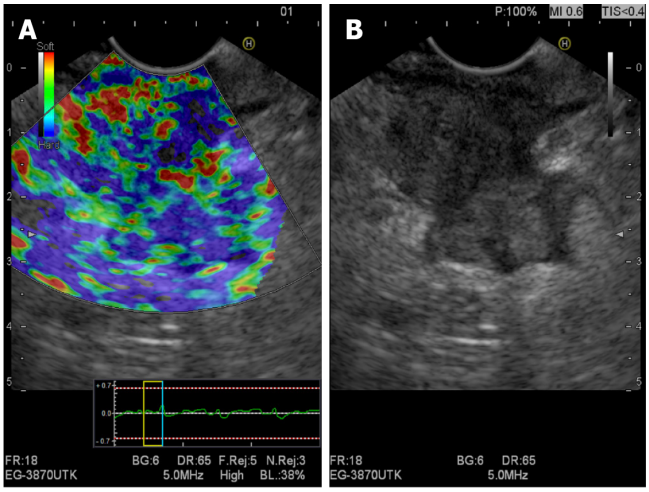

DOI: 10.4251/wjgo.v15.i6.925 **Copyright** ©The Author(s) 2023.

Figure 5 Evaluation of a pancreatic adenocarcinoma using qualitative endoscopic ultrasound elastography. A: Elastography showing a heterogeneous stiff pattern (stiffer areas are shown in blue); B: Linear array endoscopic ultrasound (B-mode) imaging of the same pancreatic mass.

AUXILIARY INFORMATION THAT MAY DIFFERENTIATE PANCREATIC MASSES

Clinical picture

Attention to specific clinical and imaging details that might be disease specific can be highly valuable during the diagnostic work-up of a pancreatic mass (Figure 6).

PDAC can present with migratory thrombophlebitis, acute pancreatitis, hypoglycemia, and hypercalcemia; although DM related to the exocrine pancreas has distinct clinical characteristics that differentiate it from type 1 and 2-DM, it may not be an easy task to differentiate that related to PDCA from that associated with CP[44].

MFCP may show signs of longstanding overt or subclinical exocrine dysfunction in the form of steatorrhea, malnutrition, and vitamin deficiencies. Although no single serum marker is available for CP diagnosis, nutritional serum markers have been used to adjust the pancreatic enzyme supplementation dose, and in some cases, those markers may help in the diagnosis of early CP[99].

We previously reported that age of presentation, history of abdominal pain, acute pancreatitis, presence of other autoimmune diseases, pancreatic duct caliber and other clinical and imaging characteristics might help to differentiate benign from malignant masses[67].

After comparing the clinical and imaging characteristics of resected focal type 2 AIP, CP, and PDAC, the characteristics that favored a benign over a malignant mass were abdominal pain (OR 0.18; 95%CI: 0.07-0.55; $P < 0.001$) and a history of acute pancreatitis (OR 0.48; 95%CI: 0.01-0.16; $P = 0.002$).

In favor of PDAC were obstructive jaundice (OR 28.5; 95%CI: 8.18-79.49; $P < 0.0001$) and main pancreatic duct dilation (OR 5.21; 95%CI: 1.93-14.62; $P < 0.001$). Patients with PDAC were also older than nonmalignant patients ($P < 0.001$).

In the same group of patients, comparing AIP *vs* non-AIP cases (PC and PDAC), abdominal pain (OR 8.75; 95%CI: 1.83-41.75; $P = 0.002$), history of acute pancreatitis (OR 10.28; 95%CI: 3.29-32.12; $P = 0.001$), concurrent autoimmune disease (OR 20; 95%CI: 4.38-91.28; $P = 0.006$) and lack of main pancreatic duct dilation (OR 9.30; 95%CI: 3.05-28.69; $P < 0.0001$). AIP cases were younger ($P < 0.001$).

Imaging characteristics

Features such as mass morphology, pancreatic calcification distribution, presence of duct-penetrating sign, duct stenosis, pancreatic or bile duct wall thickness, and contrast uptake are some disease-specific characteristics that can help to differentiate PDAC, AIP, and MFCP (Table 1).

Pancreatic duct morphology

CT and MRI allow the visualization and assessment of the main pancreatic duct and bile duct morphology, diameter, and other characteristics that can be disrupted by the presence of a pancreatic mass[100].

Although CP and PDAC may be associated with duct stenosis as well as upstream ductal irregularity and dilation, the presence of calcifications, the characteristics of the stenosis, and other extrapancreatic and clinical features can differentiate benign from malignant conditions.

In MFCP, the pancreatic duct lateral branches are usually dilated and deformed, which in MRCP is called the "chain of lakes"[101]. In PDAC, dilation of the MPD is usually more prominent as a result of abrupt narrowing caused by the centrifugal ductal growth pattern of the cancer cells, which is usually

Table 1 Radiological differences in pancreatic masses

Imaging studio	AIP	MFCP	PDAC
Ultrasound			
Conventional	Hypoechoic	Hypoechoic	Hypoechoic
CEUS/CE-EUS	Homogeneous enhancement	Homogeneous enhancement	No enhancement
Eltasography by EUS	Predominantly blue heterogeneous pattern	Heterogeneous pattern with a predominance of green color and blue stippling	Heterogeneous pattern with a predominance of blue color and green stippling
CT			
Simple	Hypodense; peripheral halo	Hypodense Intraparenchymal calcifications or within the pancreatic duct	Hypodense; parenchymal atrophy
Contrasted	Hyperattenuation (compared to the spleen) in the portal venous phase; presence of extrapancreatic involvement	Heterogeneous hyperattenuation; absence of extrapancreatic involvement	No enhancement; vascular invasion
Perfusion		Low BF and BV values compared to normal pancreatic parenchyma but higher than PDAC	Low BF and BV values compared to MFCP
Dual-energy			Appears as a hypodense mass in low voltage imaging (especially during portal phase); in the iodine mapping the mass shows enhancement
MRI			
T1	Hypointense; hypointense peripheral halo	Hypointense	Hypointense
T2	Hyperintense; hypointense peripheral halo	Hyperintense: Early stage; hypointense: Advanced stage	Hyper/hypointense
DWI	Hyperintense	Hyperintense	Hyperintense
ADC	Higher hypointensity than MFCP and PDAC	Hypointense	Hypointense
Elastography	Higher stiffness compared to normal parenchyma but lesser compared to PDAC; multiple scattered lesions		Higher stiffness compared to AIP; single, isolated nodular lesions

ADC: Apparent diffusion coefficient; AIP: Autoimmune pancreatitis; BF: Blood flow; BV: Blood volume; CEUS: Contrast-enhanced ultrasound; CE-EUS: Contrast-enhanced endoscopic ultrasound; EUS: Endoscopic ultrasound; CT: Computed tomography; DWI: Diffusion sequence; MFCP: Mass-forming chronic pancreatitis; PDAC: Pancreatic ductal adenocarcinoma; MRI: Magnetic resonance.

followed by significant atrophy of the pancreatic parenchyma.

In AIP, it is typical to observe stenotic areas without prestenotic dilation[83], although few cases of focal AIP may present upstream dilation of the main pancreatic duct. This is called the "icicle sign" (the MPD could penetrate the mass without complete occlusion, and the pancreatic duct stenosis may taper within the mass), which is caused by periductal fibrosis causing extrinsic compression and ductal narrowing in the affected part of the pancreas. This sign has a specificity of up to 95% and an accuracy of 88% for diagnosing AIP[102,103].

We found that in the presence of a pancreatic mass in the head of the pancreas, the absence of dilation of the main pancreatic duct favors the diagnosis of AIP with a sensitivity of 31% but a specificity of 81% (OR 9.30; 95%CI: 3.05-28.69; $P < 0.0001$)[67].

Double duct sign

The CBD and the MPD converge at the major papilla, and any mass located at the head of the pancreas may compress or engulf either or both, causing subsequent prestenotic ductal dilatation. The radiological image of dilatation of both ductal systems is referred to as the double duct sign[76]. Although not pathognomonic of PDAC, it has been reported to be present in up to 80% of cases. It can be present but less frequently in AIP and MFCP[3].

MFCP showing a double duct sign can show ductal strictures alternated with dilated areas, producing a beaded appearance, although in some cases, the pancreatic duct may be dilated through its entire extension.

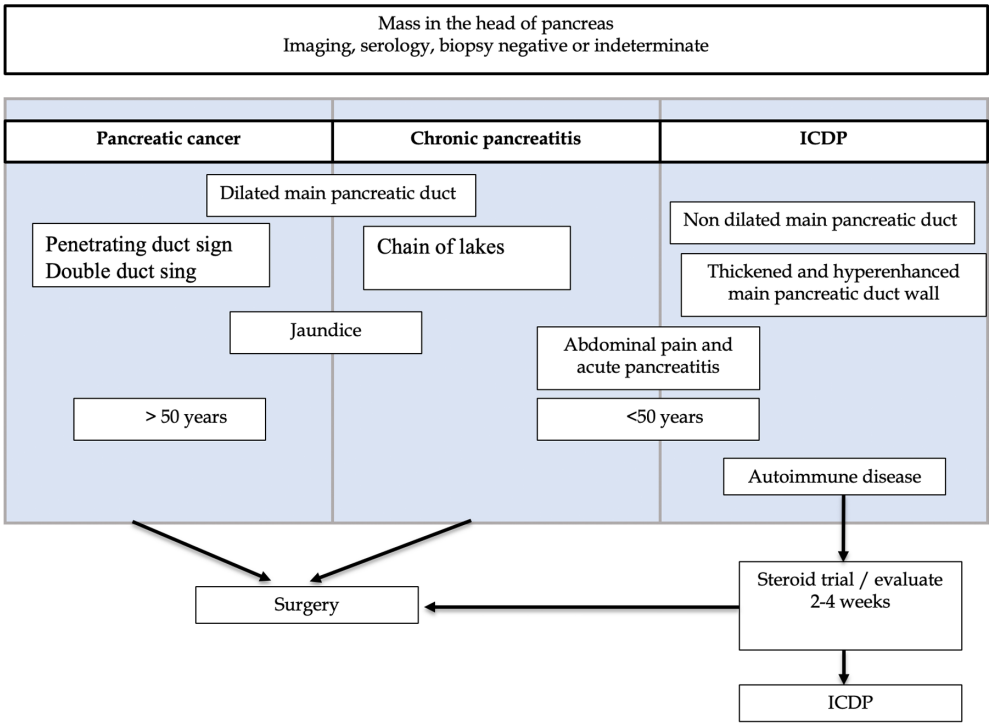

Figure 6 Differences in pancreatic masses. IDCP: Idiopathic duct-centric pancreatitis. Citation: Peláez-Luna M, Medina-Campos C, Uscanga-Domínuez L, Hernandez-Calleros J, Chan-Nuñez C, Negrete E, Angeles A. A Nondilated Main Pancreatic Duct Predicts Type 2 Autoimmune Pancreatitis: Comparative Study of Resected Pancreatic Head Masses. *Digestion* 2020; 101: 137-143. Published by Karger Publishers[67] (Supplementary material).

In AIP, the pancreatic duct caliber is usually normal, with few cases presenting slight dilation. The ductal stenosis length (either biliary or pancreatic) tends to be longer in MFCP and AIP and shorter or punctual in PDCA[75].

Duct-penetrating sign

This sign is defined as a nonobstructed, nonstenotic, or normal-appearing MPD running into a pancreatic mass and is usually seen on MRCP images[100-103]. This sign has a sensitivity of 85% and specificity of 96% to discern an inflammatory pancreatic mass (MFCP and AIP) from PDAC[80].

The pathophysiological basis of the duct-penetrating sign is that the dense fibrotic infiltrate of the PDAC causes an abrupt and complete narrowing of the duct, whereas in inflammatory pancreatic masses, the narrowing is subtle and tends to taper down, and the duct can still be visualized in the affected area in the MRPC[3].

Calcification distribution

Parenchymal calcifications are not unique to CP; they can be present in PDAC and some cystic neoplasms of the pancreas, such as neuroendocrine tumors, serous cystadenoma, and intraductal papillary mucinous neoplasm.

Diffuse parenchymal calcifications with ductal calcifications, parenchymal atrophy, and cystic lesions are specific to CP[86]. In PDAC, calcifications are usually neither diffuse nor intraductal.

The presence of calcifications may not completely rule out or confirm a malignant or benign mass, since long-standing CP cases may develop PDAC. In such a clinical scenario, should a prior CT image be available, a change in the calcification distribution as a result of a new mass displacing them may be observed, which in turn may favor the presence of PDAC in a patient with preexisting CP.

Blood vessels

A pancreatic mass with blood vessel involvement is not unique to malignancies. Although advanced stages of PDAC present with soft tissue involving the celiac trunk and the superior mesenteric and splenic vessels, similar findings can be found in chronic inflammatory processes such as retroperitoneal fibrosis that can be associated with IgG4 systemic disease[62,75].

Pancreatic and biliary duct walls

Some studies have looked for imaging surrogates to differentiate AIP from PDAC and MFCP, highlighting the diagnostic potential of perfusion CT scans as well as EUS.

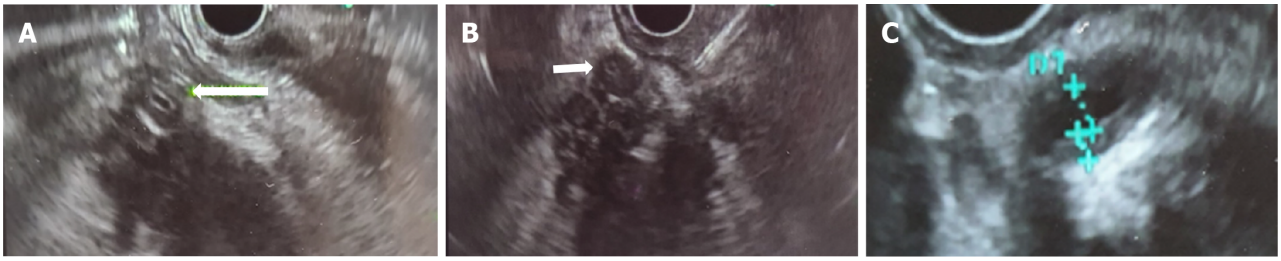

Figure 7 Ductal wall thickening (biliary/pancreatic) in 2 cases of type 2 autoimmune pancreatitis. A: Hypoechoic mass in the head of the pancreas, arrow shows common bile duct (CBD) with hypoechoic symmetrical wall thickening in a histology confirmed type 2 autoimmune pancreatitis (AIP); B. Fine needle biopsy of a hypoechoic mass in the head of the pancreas. Arrow shows CBD with hypoechoic symmetrical wall thickening in the same case of a histology confirmed type 2 AIP; C: Homogeneous, symmetric main pancreatic duct wall thickening in other case of with histology confirmed type 2 AIP. Citation: Pelaez-Luna M, Soriano-Rios A, Lira-Treviño AC, Uscanga-Domínguez L. Steroid-responsive pancreatitides. *World J Clin Cases* 2020; 8: 3411-3430. Published by Baishideng Publishing Group Inc[60] (Supplementary material).

In addition to the classical imaging features of AIP and PDAC, long pancreatic duct stenosis without upstream dilation, subtle bile, and/or pancreatic abnormalities can be of significant aid.

The presence of irregular narrowing of the main pancreatic duct in association with duct wall thickening during EUS has a diagnostic accuracy for type 1 AIP of 98.3%. Hyperechoic parietal thickening is also more frequent in AIP (93%) than in PDAC or CP (23%) (Figure 7).

On CT/MRI, diffuse and homogeneous ductal wall hyperenhancement is present in 47% of AIP and 22% of PDAC cases and has been reported to be highly predictive of AIP[104-107].

STEROID TRIAL

As has been explained throughout this review, the differential diagnosis between focal pattern AIP and PDAC is extremely difficult since the clinical picture, imaging, and serological methods may provide questionable results[71,77-79].

Although some of the clinical and imaging diagnostic difficulties can be overcome with a biopsy; AIP, MFCP, and PDAC can share similar histological findings[108], and the associated inflammation or fibrosis, sampling error, bloody aspirates, and errors in cytologic interpretation may provide equivocal results.

Some have suggested that in highly selected cases with diagnostic uncertainty after a thorough diagnostic approach in experienced centers, a systemic steroid trial may be beneficial[26,74,76,77,109].

On average, a 2- to 4-wk interval is needed to evaluate the response with a radiological study (CECT or MRI) since the clinical response is not a reliable parameter. It is important to keep in mind that patients with pancreatic cancer may show improvement due to the reduction in peritumoral inflammation, which can create confusion[108,109]. There is usually significant radiological improvement in all cases of AIP[77], while the absence of response rules out AIP[26].

Even after a thorough diagnostic approach, up to 5% of resected masses under suspicion of malignancy are benign. Uncertain pancreatic masses require a multidisciplinary approach, preferably in referral centers, by highly experienced specialists (radiologist, gastroenterologist, surgeons, and pathologists).

CONCLUSION

Due to the distinctive therapeutic and prognostic features of AIP, MFCP, and PDAC, a precise diagnosis is of the utmost relevance. The initial approach to a pancreatic mass must include a detailed clinical exam exploring relevant personal, non-personal and family history, exposure to risk factors, blood tests including IgG4 and Ca19-9 levels, and high-quality imaging (CECT). In uncertain cases after an initial approach, MRI, EUS and tissue examination may provide auxiliary concluding diagnostic information. Newer imaging and molecular techniques are promising tools, but further research is still needed. Currently, in the differential diagnosis of uncertain pancreatic masses, all available collateral clinical, imaging, and histological information remains the cornerstone for an accurate diagnosis.

FOOTNOTES

Author contributions: Tornel-Avelar AI and Velarde-Ruiz Velasco JA performed literature research and drafted the

manuscript, and elaborated some tables and figures; Pelaez-Luna M designed the study, performed literature research, elaborated some figures, drafted the manuscript, performed critical review, and editing of final version; and all authors have read and approve the final manuscript.

Conflict-of-interest statement: None of the authors has any financial relationship or conflict of interest to disclose.

Country/Territory of origin: Mexico

ORCID number: Ana I Tornel-Avelar 0000-0003-0865-0596; Jose Antonio Velarde Ruiz-Velasco 0000-0002-6568-7048; Mario Pelaez-Luna 0000-0002-9100-9304.

Corresponding Author's Membership in Professional Societies: American College of Gastroenterology; American Gastroenterological Association; American Society for Gastrointestinal Endoscopy; Asociación Mexicana de Gastroenterología; American Pancreatic Association, International Association of Pancreatology

S-Editor: Chen YL
L-Editor: A
P-Editor: Zhang XD

REFERENCES

1 **Poddighe D**. Autoimmune pancreatitis and pancreatic cancer: Epidemiological aspects and immunological considerations. *World J Gastroenterol* 2021; **27**: 3825-3836 [PMID: 34321847 DOI: 10.3748/wjg.v27.i25.3825]
2 **Sung H**, Ferlay J, Siegel RL, Laversanne M, Soerjomataram I, Jemal A, Bray F. Global Cancer Statistics 2020: GLOBOCAN Estimates of Incidence and Mortality Worldwide for 36 Cancers in 185 Countries. *CA Cancer J Clin* 2021; **71**: 209-249 [PMID: 33538338 DOI: 10.3322/caac.21660]
3 **Wolske KM**, Ponnatapura J, Kolokythas O, Burke LMB, Tappouni R, Lalwani N. Chronic Pancreatitis or Pancreatic Tumor? *Radiographics* 2019; **39**: 1965-1982 [PMID: 31584860 DOI: 10.1148/rg.2019190011]
4 **McGuigan A**, Kelly P, Turkington RC, Jones C, Coleman HG, McCain RS. Pancreatic cancer: A review of clinical diagnosis, epidemiology, treatment and outcomes. *World J Gastroenterol* 2018; **24**: 4846-4861 [PMID: 30487695 DOI: 10.3748/wjg.v24.i43.4846].]
5 **Becker AE**, Hernandez YG, Frucht H, Lucas AL. Pancreatic ductal adenocarcinoma: risk factors, screening, and early detection. *World J Gastroenterol* 2014; **20**: 11182-11198 [PMID: 25170203 DOI: 10.3748/wjg.v20.i32.11182]
6 **Tokar JL**, Walia R. Diagnostic evaluation of solid pancreatic masses. *Curr Gastroenterol Rep* 2013; **15**: 347 [PMID: 23996593 DOI: 10.1007/s11894-013-0347-z]
7 **Sugumar A**, Chari ST. Distinguishing pancreatic cancer from autoimmune pancreatitis: a comparison of two strategies. *Clin Gastroenterol Hepatol* 2009; **7**: S59-S62 [PMID: 19896101 DOI: 10.1016/j.cgh.2009.07.034]
8 **Elsherif SB**, Virarkar M, Javadi S, Ibarra-Rovira JJ, Tamm EP, Bhosale PR. Pancreatitis and PDAC: association and differentiation. *Abdom Radiol (NY)* 2020; **45**: 1324-1337 [PMID: 31705251 DOI: 10.1007/s00261-019-02292-w]
9 **Akisik MF**, Sandrasegaran K, Bu G, Lin C, Hutchins GD, Chiorean EG. Pancreatic cancer: utility of dynamic contrast-enhanced MR imaging in assessment of antiangiogenic therapy. *Radiology* 2010; **256**: 441-449 [PMID: 20515976 DOI: 10.1148/radiol.10091733]
10 **Safi F**, Beger HG, Bittner R, Büchler M, Krautzberger W. CA 19-9 and pancreatic adenocarcinoma. *Cancer* 1986; **57**: 779-783 [PMID: 3455839 DOI: 10.1002/1097-0142(19860215)57:4<779::aid-cncr2820570417>3.0.co;2-c]
11 **Ballehaninna UK**, Chamberlain RS. The clinical utility of serum CA 19-9 in the diagnosis, prognosis and management of pancreatic adenocarcinoma: An evidence based appraisal. *J Gastrointest Oncol* 2012; **3**: 105-119 [PMID: 22811878 DOI: 10.3978/j.issn.2078-6891.2011.021]
12 **Ghazale A**, Chari ST, Smyrk TC, Levy MJ, Topazian MD, Takahashi N, Clain JE, Pearson RK, Pelaez-Luna M, Petersen BT, Vege SS, Farnell MB. Value of serum IgG4 in the diagnosis of autoimmune pancreatitis and in distinguishing it from pancreatic cancer. *Am J Gastroenterol* 2007; **102**: 1646-1653 [PMID: 17555461 DOI: 10.1111/j.1572-0241.2007.01264.x]
13 **Lee ES**, Lee JM. Imaging diagnosis of pancreatic cancer: a state-of-the-art review. *World J Gastroenterol* 2014; **20**: 7864-7877 [PMID: 24976723 DOI: 10.3748/wjg.v20.i24.7864]
14 **Yoon SH**, Lee JM, Cho JY, Lee KB, Kim JE, Moon SK, Kim SJ, Baek JH, Kim SH, Lee JY, Han JK, Choi BI. Small (≤ 20 mm) pancreatic adenocarcinomas: analysis of enhancement patterns and secondary signs with multiphasic multidetector CT. *Radiology* 2011; **259**: 442-452 [PMID: 21406627 DOI: 10.1148/radiol.11101133]
15 **Best LM**, Rawji V, Pereira SP, Davidson BR, Gurusamy KS. Imaging modalities for characterising focal pancreatic lesions. *Cochrane Database Syst Rev* 2017; **4**: CD010213 [PMID: 28415140 DOI: 10.1002/14651858.CD010213.pub2]
16 **Francis IR**. Pancreatic adenocarcinoma: diagnosis and staging using multidetector-row computed tomography (MDCT) and magnetic resonance imaging (MRI). *Cancer Imaging* 2007; **7** Spec No A: S160-S165 [PMID: 17921087 DOI: 10.1102/1470-7330.2007.9010]
17 **Burk KS**, Lo GC, Gee MS, Sahani DV. Imaging and Screening of Pancreatic Cancer. *Radiol Clin North Am* 2017; **55**:

1223-1234 [PMID: 28991562 DOI: 10.1016/j.rcl.2017.06.006]
18 **Raman SP**, Horton KM, Fishman EK. Multimodality imaging of pancreatic cancer-computed tomography, magnetic resonance imaging, and positron emission tomography. *Cancer J* 2012; **18**: 511-522 [PMID: 23187837 DOI: 10.1097/PPO.0b013e318274a461]
19 **Loperfido S**, Angelini G, Benedetti G, Chilovi F, Costan F, De Berardinis F, De Bernardin M, Ederle A, Fina P, Fratton A. Major early complications from diagnostic and therapeutic ERCP: a prospective multicenter study. *Gastrointest Endosc* 1998; **48**: 1-10 [PMID: 9684657 DOI: 10.1016/S0016-5107(98)70121-X]
20 **Maccioni F**, Martinelli M, Al Ansari N, Kagarmanova A, De Marco V, Zippi M, Marini M. Magnetic resonance cholangiography: past, present and future: a review. *Eur Rev Med Pharmacol Sci* 2010; **14**: 721-725 [PMID: 20707292]
21 **Adamek HE**, Albert J, Breer H, Weitz M, Schilling D, Riemann JF. Pancreatic cancer detection with magnetic resonance cholangiopancreatography and endoscopic retrograde cholangiopancreatography: a prospective controlled study. *Lancet* 2000; **356**: 190-193 [PMID: 10963196 DOI: 10.1016/S0140-6736(00)02479-X]
22 **Tamm EP**, Bhosale PR, Vikram R, de Almeida Marcal LP, Balachandran A. Imaging of pancreatic ductal adenocarcinoma: State of the art. *World J Radiol* 2013; **5**: 98-105 [PMID: 23671746 DOI: 10.4329/wjr.v5.i3.98]
23 **Fukukura Y**, Takumi K, Kamimura K, Shindo T, Kumagae Y, Tateyama A, Nakajo M. Pancreatic adenocarcinoma: variability of diffusion-weighted MR imaging findings. *Radiology* 2012; **263**: 732-740 [PMID: 22623694 DOI: 10.1148/radiol.12111222]
24 **Wang Y**, Miller FH, Chen ZE, Merrick L, Mortele KJ, Hoff FL, Hammond NA, Yaghmai V, Nikolaidis P. Diffusion-weighted MR imaging of solid and cystic lesions of the pancreas. *Radiographics* 2011; **31**: E47-E64 [PMID: 21721197 DOI: 10.1148/rg.313105174]
25 **Jia H**, Li J, Huang W, Lin G. Multimodel magnetic resonance imaging of mass-forming autoimmune pancreatitis: differential diagnosis with pancreatic ductal adenocarcinoma. *BMC Med Imaging* 2021; **21**: 149 [PMID: 34654379 DOI: 10.1186/s12880-021-00679-0]
26 **Lopes Vendrami C**, Shin JS, Hammond NA, Kothari K, Mittal PK, Miller FH. Differentiation of focal autoimmune pancreatitis from pancreatic ductal adenocarcinoma. *Abdom Radiol (NY)* 2020; **45**: 1371-1386 [PMID: 31493022 DOI: 10.1007/s00261-019-02210-0]
27 **Wakabayashi T**, Kawaura Y, Satomura Y, Watanabe H, Motoo Y, Okai T, Sawabu N. Clinical and imaging features of autoimmune pancreatitis with focal pancreatic swelling or mass formation: comparison with so-called tumor-forming pancreatitis and pancreatic carcinoma. *Am J Gastroenterol* 2003; **98**: 2679-2687 [PMID: 14687817 DOI: 10.1111/j.1572-0241.2003.08727.x]
28 **Triantopoulou C**, Dervenis C, Giannakou N, Papailiou J, Prassopoulos P. Groove pancreatitis: a diagnostic challenge. *Eur Radiol* 2009; **19**: 1736-1743 [PMID: 19238393 DOI: 10.1007/s00330-009-1332-7]
29 **Blasbalg R**, Baroni RH, Costa DN, Machado MC. MRI features of groove pancreatitis. *AJR Am J Roentgenol* 2007; **189**: 73-80 [PMID: 17579155 DOI: 10.2214/AJR.06.1244]
30 **Zhang TT**, Wang L, Liu HH, Zhang CY, Li XM, Lu JP, Wang DB. Differentiation of pancreatic carcinoma and mass-forming focal pancreatitis: qualitative and quantitative assessment by dynamic contrast-enhanced MRI combined with diffusion-weighted imaging. *Oncotarget* 2017; **8**: 1744-1759 [PMID: 27661003 DOI: 10.18632/oncotarget.12120]
31 **Levy MJ**, Wiersema MJ, Chari ST. Chronic pancreatitis: focal pancreatitis or cancer? *Endoscopy* 2006; **38** Suppl 1: S30-S35 [PMID: 16802220 DOI: 10.1055/s-2006-946648]
32 **Gonzalo-Marin J**, Vila JJ, Perez-Miranda M. Role of endoscopic ultrasound in the diagnosis of pancreatic cancer. *World J Gastrointest Oncol* 2014; **6**: 360-368 [PMID: 25232461 DOI: 10.4251/wjgo.v6.i9.360]
33 **Cho MK**, Moon SH, Song TJ, Kim RE, Oh DW, Park DH, Lee SS, Seo DW, Lee SK, Kim MH. Contrast-Enhanced Endoscopic Ultrasound for Differentially Diagnosing Autoimmune Pancreatitis and Pancreatic Cancer. *Gut Liver* 2018; **12**: 591-596 [PMID: 29699060 DOI: 10.5009/gnl17391]
34 **D'Onofrio M**, De Robertis R, Barbi E, Martone E, Manfrin E, Gobbo S, Puntel G, Bonetti F, Pozzi Mucelli R. Ultrasound-guided percutaneous fine-needle aspiration of solid pancreatic neoplasms: 10-year experience with more than 2,000 cases and a review of the literature. *Eur Radiol* 2016; **26**: 1801-1807 [PMID: 26373764 DOI: 10.1007/s00330-015-4003-x]
35 **Varadarajulu S**, Tamhane A, Eloubeidi MA. Yield of EUS-guided FNA of pancreatic masses in the presence or the absence of chronic pancreatitis. *Gastrointest Endosc* 2005; **62**: 728-36; quiz 751, 753 [PMID: 16246688 DOI: 10.1016/j.gie.2005.06.051]
36 **Eloubeidi MA**, Jhala D, Chhieng DC, Chen VK, Eltoum I, Vickers S, Mel Wilcox C, Jhala N. Yield of endoscopic ultrasound-guided fine-needle aspiration biopsy in patients with suspected pancreatic carcinoma. *Cancer* 2003; **99**: 285-292 [PMID: 14579295 DOI: 10.1002/cncr.11643]
37 **DeWitt J**, McGreevy K, Sherman S, LeBlanc J. Utility of a repeated EUS at a tertiary-referral center. *Gastrointest Endosc* 2008; **67**: 610-619 [PMID: 18279866 DOI: 10.1016/j.gie.2007.09.037]
38 **Suzuki R**, Lee JH, Krishna SG, Ramireddy S, Qiao W, Weston B, Ross WA, Bhutani MS. Repeat endoscopic ultrasound-guided fine needle aspiration for solid pancreatic lesions at a tertiary referral center will alter the initial inconclusive result. *J Gastrointestin Liver Dis* 2013; **22**: 183-187 [PMID: 23799217]
39 **Mitchell RA**, Stanger D, Shuster C, Telford J, Lam E, Enns R. Repeat Endoscopic Ultrasound-Guided Fine-Needle Aspiration in Patients with Suspected Pancreatic Cancer: Diagnostic Yield and Associated Change in Access to Appropriate Care. *Can J Gastroenterol Hepatol* 2016; **2016**: 7678403 [PMID: 27648440 DOI: 10.1155/2016/7678403]
40 **Kleeff J**, Korc M, Apte M, La Vecchia C, Johnson CD, Biankin AV, Neale RE, Tempero M, Tuveson DA, Hruban RH, Neoptolemos JP. Pancreatic cancer. *Nat Rev Dis Primers* 2016; **2**: 16022 [PMID: 27158978 DOI: 10.1038/nrdp.2016.22]
41 **Apte MV**, Wilson JS. The desmoplastic reaction in pancreatic cancer: an increasingly recognized foe. *Pancreatology* 2007; **7**: 378-379 [DOI: 10.1159/000107399]
42 **Whitcomb DC**, Frulloni L, Garg P, Greer JB, Schneider A, Yadav D, Shimosegawa T. Chronic pancreatitis: An international draft consensus proposal for a new mechanistic definition. *Pancreatology* 2016; **16**: 218-224 [PMID: 26924663 DOI: 10.1016/j.pan.2016.02.001]
43 **Al-Hawary MM**, Kaza RK, Azar SF, Ruma JA, Francis IR. Mimics of pancreatic ductal adenocarcinoma. *Cancer Imaging*

2013; **13**: 342-349 [PMID: 24060833 DOI: 10.1102/1470-7330.2013.9012]

44 **Ren S**, Chen X, Cui W, Chen R, Guo K, Zhang H, Chen S, Wang Z. Differentiation of chronic mass-forming pancreatitis from pancreatic ductal adenocarcinoma using contrast-enhanced computed tomography. *Cancer Manag Res* 2019; **11**: 7857-7866 [PMID: 31686905 DOI: 10.2147/CMAR.S217033]

45 **Tong GX**, Geng QQ, Chai J, Cheng J, Chen PL, Liang H, Shen XR, Wang DB. Association between pancreatitis and subsequent risk of pancreatic cancer: a systematic review of epidemiological studies. *Asian Pac J Cancer Prev* 2014; **15**: 5029-5034 [PMID: 24998582 DOI: 10.7314/APJCP.2014.15.12.5029]

46 **Al Zahrani H**, Kyoung Kim T, Khalili K, Vlachou P, Yu H, Jang HJ. IgG4-related disease in the abdomen: a great mimicker. *Semin Ultrasound CT MR* 2014; **35**: 240-254 [PMID: 24929264 DOI: 10.1053/j.sult.2013.12.002]

47 **Javadi S**, Menias CO, Korivi BR, Shaaban AM, Patnana M, Alhalabi K, Elsayes KM. Pancreatic Calcifications and Calcified Pancreatic Masses: Pattern Recognition Approach on CT. *AJR Am J Roentgenol* 2017; **209**: 77-87 [PMID: 28418702 DOI: 10.2214/AJR.17.17862]

48 **Oshikawa O**, Tanaka S, Ioka T, Nakaizumi A, Hamada Y, Mitani T. Dynamic sonography of pancreatic tumors: comparison with dynamic CT. *AJR Am J Roentgenol* 2002; **178**: 1133-1137 [PMID: 11959716 DOI: 10.2214/ajr.178.5.1781133]

49 **D'Onofrio M**, Barbi E, Dietrich CF, Kitano M, Numata K, Sofuni A, Principe F, Gallotti A, Zamboni GA, Mucelli RP. Pancreatic multicenter ultrasound study (PAMUS). *Eur J Radiol* 2012; **81**: 630-638 [PMID: 21466935 DOI: 10.1016/j.ejrad.2011.01.053]

50 **Catalano MF**, Sahai A, Levy M, Romagnuolo J, Wiersema M, Brugge W, Freeman M, Yamao K, Canto M, Hernandez LV. EUS-based criteria for the diagnosis of chronic pancreatitis: the Rosemont classification. *Gastrointest Endosc* 2009; **69**: 1251-1261 [PMID: 19243769 DOI: 10.1016/j.gie.2008.07.043]

51 **Braganza JM**, Lee SH, McCloy RF, McMahon MJ. Chronic pancreatitis. *Lancet* 2011; **377**: 1184-1197 [PMID: 21397320 DOI: 10.1016/S0140-6736(10)61852-1]

52 **Nicaud M**, Hou W, Collins D, Wagh MS, Chauhan S, Draganov PV. The utility of repeat endoscopic ultrasound-guided fine needle aspiration for suspected pancreatic cancer. *Gastroenterol Res Pract* 2010; **2010**: 268290 [PMID: 21234311 DOI: 10.1155/2010/268290]

53 **Löhr JM**, Vujasinovic M, Rosendahl J, Stone JH, Beuers U. IgG4-related diseases of the digestive tract. *Nat Rev Gastroenterol Hepatol* 2022; **19**: 185-197 [PMID: 34750548 DOI: 10.1038/s41575-021-00529-y]

54 **Martín-Nares E**, Hernández-Molina G, Baenas DF, Paira S. IgG4-Related Disease: Mimickers and Diagnostic Pitfalls. *J Clin Rheumatol* 2022; **28**: e596-e604 [PMID: 34538846 DOI: 10.1097/RHU.0000000000001787]

55 **Cao Z**, Tian R, Zhang T, Zhao Y. Localized Autoimmune Pancreatitis: Report of a Case Clinically Mimicking Pancreatic Cancer and a Literature Review. *Medicine (Baltimore)* 2015; **94**: e1656 [PMID: 26496272 DOI: 10.1097/MD.0000000000001656]

56 **Gardner TB**, Adler DG, Forsmark CE, Sauer BG, Taylor JR, Whitcomb DC. ACG Clinical Guideline: Chronic Pancreatitis. *Am J Gastroenterol* 2020; **115**: 322-339 [PMID: 32022720 DOI: 10.14309/ajg.0000000000000535]

57 **Storz P**, Crawford HC. Carcinogenesis of Pancreatic Ductal Adenocarcinoma. *Gastroenterology* 2020; **158**: 2072-2081 [PMID: 32199881 DOI: 10.1053/j.gastro.2020.02.059]

58 **Masamune A**, Kikuta K, Hamada S, Tsuji I, Takeyama Y, Shimosegawa T, Okazaki K; Collaborators. Nationwide epidemiological survey of autoimmune pancreatitis in Japan in 2016. *J Gastroenterol* 2020; **55**: 462-470 [PMID: 31872350 DOI: 10.1007/s00535-019-01658-7]

59 **Kennedy T**, Preczewski L, Stocker SJ, Rao SM, Parsons WG, Wayne JD, Bell RH, Talamonti MS. Incidence of benign inflammatory disease in patients undergoing Whipple procedure for clinically suspected carcinoma: a single-institution experience. *Am J Surg* 2006; **191**: 437-441 [PMID: 16490563 DOI: 10.1016/j.amjsurg.2005.10.051]

60 **Pelaez-Luna M**, Soriano-Rios A, Lira-Treviño AC, Uscanga-Domínguez L. Steroid-responsive pancreatitides. *World J Clin Cases* 2020; **8**: 3411-3430 [PMID: 32913848 DOI: 10.12998/wjcc.v8.i16.3411]

61 **Soriano Rios A**, Paredes H, Hernández-Calleros J, Uscanga-Domínguez L, Peláez-Luna M. Retroperitoneal fibrosis. Steroid treatment response seems to depend on its association to IgG4 related disease. *Med Hypotheses* 2019; **122**: 120-123 [PMID: 30593393 DOI: 10.1016/j.mehy.2018.11.005]

62 **Umehara H**, Okazaki K, Masaki Y, Kawano M, Yamamoto M, Saeki T, Matsui S, Sumida T, Mimori T, Tanaka Y, Tsubota K, Yoshino T, Kawa S, Suzuki R, Takegami T, Tomosugi N, Kurose N, Ishigaki Y, Azumi A, Kojima M, Nakamura S, Inoue D; Research Program for Intractable Disease by Ministry of Health, Labor and Welfare (MHLW) Japan G4 team. A novel clinical entity, IgG4-related disease (IgG4RD): general concept and details. *Mod Rheumatol* 2012; **22**: 1-14 [PMID: 21881964 DOI: 10.1007/s10165-011-0508-6]

63 **Dite P**, Novotny I, Dvorackova J, Kianicka B, Blaho M, Svoboda P, Uvirova M, Rohan T, Maskova H, Kunovsky L. Pancreatic Solid Focal Lesions: Differential Diagnosis between Autoimmune Pancreatitis and Pancreatic Cancer. *Dig Dis* 2019; **37**: 416-421 [PMID: 31079114 DOI: 10.1159/000499762]

64 **Culver EL**, Sadler R, Simpson D, Cargill T, Makuch M, Bateman AC, Ellis AJ, Collier J, Chapman RW, Klenerman P, Barnes E, Ferry B. Elevated Serum IgG4 Levels in Diagnosis, Treatment Response, Organ Involvement, and Relapse in a Prospective IgG4-Related Disease UK Cohort. *Am J Gastroenterol* 2016; **111**: 733-743 [PMID: 27091321 DOI: 10.1038/ajg.2016.40]

65 **Kiyama K**, Yoshifuji H, Kandou T, Hosono Y, Kitagori K, Nakashima R, Imura Y, Yukawa N, Ohmura K, Fujii T, Kawabata D, Mimori T. Screening for IgG4-type anti-nuclear antibodies in IgG4-related disease. *BMC Musculoskelet Disord* 2015; **16**: 129 [PMID: 26018403 DOI: 10.1186/s12891-015-0584-4]

66 **Aparisi L**, Farre A, Gomez-Cambronero L, Martinez J, De Las Heras G, Corts J, Navarro S, Mora J, Lopez-Hoyos M, Sabater L, Ferrandez A, Bautista D, Perez-Mateo M, Mery S, Sastre J. Antibodies to carbonic anhydrase and IgG4 levels in idiopathic chronic pancreatitis: relevance for diagnosis of autoimmune pancreatitis. *Gut* 2005; **54**: 703-709 [PMID: 15831920 DOI: 10.1136/gut.2004.047142]

67 **Peláez-Luna M**, Medina-Campos C, Uscanga-Domínuez L, Hernandez-Calleros J, Chan-Nuñez C, Negrete E, Angeles A. A Nondilated Main Pancreatic Duct Predicts Type 2 Autoimmune Pancreatitis: Comparative Study of Resected Pancreatic

Head Masses. *Digestion* 2020; **101**: 137-143 [PMID: 30759428 DOI: 10.1159/000497140]

68 **Ráty S**, Sand J, Nordback I, Rinta-Kiikka I, Vasama K, Hagström J, Nordling S, Sirén J, Kiviluoto T, Haglund C. Tumor-like Chronic Pancreatitis Is Often Autoimmune Pancreatitis. *Anticancer Res* 2015; **35**: 6163-6166 [PMID: 26504044]

69 **Dickerson LD**, Farooq A, Bano F, Kleeff J, Baron R, Raraty M, Ghaneh P, Sutton R, Whelan P, Campbell F, Healey P, Neoptolemos JP, Yip VS. Differentiation of Autoimmune Pancreatitis from Pancreatic Cancer Remains Challenging. *World J Surg* 2019; **43**: 1604-1611 [PMID: 30815742 DOI: 10.1007/s00268-019-04928-w]

70 **Kamisawa T**, Zen Y, Pillai S, Stone JH. IgG4-related disease. *Lancet* 2015; **385**: 1460-1471 [PMID: 25481618 DOI: 10.1016/S0140-6736(14)60720-0]

71 **Takuma K**, Kamisawa T, Gopalakrishna R, Hara S, Tabata T, Inaba Y, Egawa N, Igarashi Y. Strategy to differentiate autoimmune pancreatitis from pancreas cancer. *World J Gastroenterol* 2012; **18**: 1015-1020 [PMID: 22416175 DOI: 10.3748/wjg.v18.i10.1015]

72 **Chang WI**, Kim BJ, Lee JK, Kang P, Lee KH, Lee KT, Rhee JC, Jang KT, Choi SH, Choi DW, Choi DI, Lim JH. The clinical and radiological characteristics of focal mass-forming autoimmune pancreatitis: comparison with chronic pancreatitis and pancreatic cancer. *Pancreas* 2009; **38**: 401-408 [PMID: 18981953 DOI: 10.1097/MPA.0b013e31818d92c0]

73 **Kwon JH**, Kim JH, Kim SY, Byun JH, Kim HJ, Lee MG, Lee SS. Differentiating focal autoimmune pancreatitis and pancreatic ductal adenocarcinoma: contrast-enhanced MRI with special emphasis on the arterial phase. *Eur Radiol* 2019; **29**: 5763-5771 [PMID: 31028441 DOI: 10.1007/s00330-019-06200-0]

74 **Schima W**, Böhm G, Rösch CS, Klaus A, Függer R, Kopf H. Mass-forming pancreatitis versus pancreatic ductal adenocarcinoma: CT and MR imaging for differentiation. *Cancer Imaging* 2020; **20**: 52 [PMID: 32703312 DOI: 10.1186/s40644-020-00324-z]

75 **Treadwell JR**, Zafar HM, Mitchell MD, Tipton K, Teitelbaum U, Jue J. Imaging Tests for the Diagnosis and Staging of Pancreatic Adenocarcinoma: A Meta-Analysis. *Pancreas* 2016; **45**: 789-795 [PMID: 26745859 DOI: 10.1097/MPA.0000000000000524]

76 **Naitoh I**, Nakazawa T, Hayashi K, Okumura F, Miyabe K, Shimizu S, Kondo H, Yoshida M, Yamashita H, Ohara H, Joh T. Clinical differences between mass-forming autoimmune pancreatitis and pancreatic cancer. *Scand J Gastroenterol* 2012; **47**: 607-613 [PMID: 22416894 DOI: 10.3109/00365521.2012.667147]

77 **Vlachou PA**, Khalili K, Jang HJ, Fischer S, Hirschfield GM, Kim TK. IgG4-related sclerosing disease: autoimmune pancreatitis and extrapancreatic manifestations. *Radiographics* 2011; **31**: 1379-1402 [PMID: 21918050 DOI: 10.1148/rg.315105735]

78 **Carbognin G**, Girardi V, Biasiutti C, Camera L, Manfredi R, Frulloni L, Hermans JJ, Mucelli RP. Autoimmune pancreatitis: imaging findings on contrast-enhanced MR, MRCP and dynamic secretin-enhanced MRCP. *Radiol Med* 2009; **114**: 1214-1231 [PMID: 19789959 DOI: 10.1007/s11547-009-0452-0]

79 **Löhr JM**, Beuers U, Vujasinovic M, Alvaro D, Frøkjær JB, Buttgereit F, Capurso G, Culver EL, de-Madaria E, Della-Torre E, Detlefsen S, Dominguez-Muñoz E, Czubkowski P, Ewald N, Frulloni L, Gubergrits N, Duman DG, Hackert T, Iglesias-Garcia J, Kartalis N, Laghi A, Lammert F, Lindgren F, Okhlobystin A, Oracz G, Parniczky A, Mucelli RMP, Rebours V, Rosendahl J, Schleinitz N, Schneider A, van Bommel EF, Verbeke CS, Vullierme MP, Witt H; UEG guideline working group. European Guideline on IgG4-related digestive disease - UEG and SGF evidence-based recommendations. *United European Gastroenterol J* 2020; **8**: 637-666 [PMID: 32552502 DOI: 10.1177/2050640620934911]

80 **Ichikawa T**, Sou H, Araki T, Arbab AS, Yoshikawa T, Ishigame K, Haradome H, Hachiya J. Duct-penetrating sign at MRCP: usefulness for differentiating inflammatory pancreatic mass from pancreatic carcinomas. *Radiology* 2001; **221**: 107-116 [PMID: 11568327 DOI: 10.1148/radiol.2211001157]

81 **Chamokova B**, Bastati N, Poetter-Lang S, Bican Y, Hodge JC, Schindl M, Matos C, Ba-Ssalamah A. The clinical value of secretin-enhanced MRCP in the functional and morphological assessment of pancreatic diseases. *Br J Radiol* 2018; **91**: 20170677 [PMID: 29206061 DOI: 10.1259/bjr.20170677]

82 **Hsu WL**, Chang SM, Wu PY, Chang CC. Localized autoimmune pancreatitis mimicking pancreatic cancer: Case report and literature review. *J Int Med Res* 2018; **46**: 1657-1665 [PMID: 29332510 DOI: 10.1177/0300060517742303]

83 **Backhus J**, Seufferlein T, Perkhofer L, Hermann PC, Kleger A. IgG4-Related Diseases in the Gastrointestinal Tract: Clinical Presentation, Diagnosis and Treatment Challenges. *Digestion* 2019; **100**: 1-14 [PMID: 30384361 DOI: 10.1159/000492814]

84 **Kawakami H**, Zen Y, Kuwatani M, Eto K, Haba S, Yamato H, Shinada K, Kubota K, Asaka M. IgG4-related sclerosing cholangitis and autoimmune pancreatitis: histological assessment of biopsies from Vater's ampulla and the bile duct. *J Gastroenterol Hepatol* 2010; **25**: 1648-1655 [PMID: 20880174 DOI: 10.1111/j.1440-1746.2010.06346.x]

85 **Yadav AK**, Sharma R, Kandasamy D, Pradhan RK, Garg PK, Bhalla AS, Gamanagatti S, Srivastava DN, Sahni P, Upadhyay AD. Perfusion CT - Can it resolve the pancreatic carcinoma versus mass forming chronic pancreatitis conundrum? *Pancreatology* 2016; **16**: 979-987 [PMID: 27568845 DOI: 10.1016/j.pan.2016.08.011]

86 **Aslan S**, Nural MS, Camlidag I, Danaci M. Efficacy of perfusion CT in differentiating of pancreatic ductal adenocarcinoma from mass-forming chronic pancreatitis and characterization of isoattenuating pancreatic lesions. *Abdom Radiol (NY)* 2019; **44**: 593-603 [PMID: 30225610 DOI: 10.1007/s00261-018-1776-9]

87 **Macari M**, Spieler B, Kim D, Graser A, Megibow AJ, Babb J, Chandarana H. Dual-source dual-energy MDCT of pancreatic adenocarcinoma: initial observations with data generated at 80 kVp and at simulated weighted-average 120 kVp. *AJR Am J Roentgenol* 2010; **194**: W27-W32 [PMID: 20028887 DOI: 10.2214/AJR.09.2737]

88 **Shi Y**, Cang L, Zhang X, Cai X, Wang X, Ji R, Wang M, Hong Y. The use of magnetic resonance elastography in differentiating autoimmune pancreatitis from pancreatic ductal adenocarcinoma: A preliminary study. *Eur J Radiol* 2018; **108**: 13-20 [PMID: 30396645 DOI: 10.1016/j.ejrad.2018.09.001]

89 **Zhu L**, Guo J, Jin Z, Xue H, Dai M, Zhang W, Sun Z, Xu J, Marticorena Garcia SR, Asbach P, Hamm B, Sack I. Distinguishing pancreatic cancer and autoimmune pancreatitis with in vivo tomoelastography. *Eur Radiol* 2021; **31**: 3366-3374 [PMID: 33125553 DOI: 10.1007/s00330-020-07420-5]

90 **Iglesias-Garcia J**, Lindkvist B, Lariño-Noia J, Abdulkader-Nallib I, Dominguez-Muñoz JE. Differential diagnosis of solid

pancreatic masses: contrast-enhanced harmonic (CEH-EUS), quantitative-elastography (QE-EUS), or both? *United European Gastroenterol J* 2017; **5**: 236-246 [PMID: 28344791 DOI: 10.1177/2050640616640635]

91 **Iglesias-García J**, Lariño-Noia J, Domínguez-Muñoz JE. New Imaging Techniques: Endoscopic Ultrasound-Guided Elastography. *Gastrointest Endosc Clin N Am* 2017; **27**: 551-567 [PMID: 28918798 DOI: 10.1016/j.giec.2017.06.001]

92 **Giovannini M**, Thomas B, Erwan B, Christian P, Fabrice C, Benjamin E, Geneviève M, Paolo A, Pierre D, Robert Y, Walter S, Hanz S, Carl S, Christoph D, Pierre E, Jean-Luc VL, Jacques D, Peter V, Andrian S. Endoscopic ultrasound elastography for evaluation of lymph nodes and pancreatic masses: a multicenter study. *World J Gastroenterol* 2009; **15**: 1587-1593 [PMID: 19340900 DOI: 10.3748/wjg.15.1587]

93 **Hou J**, Li X, Xie KP. Coupled liquid biopsy and bioinformatics for pancreatic cancer early detection and precision prognostication. *Mol Cancer* 2021; **20**: 34 [PMID: 33593396 DOI: 10.1186/s12943-021-01309-7]

94 **Cohen JD**, Javed AA, Thoburn C, Wong F, Tie J, Gibbs P, Schmidt CM, Yip-Schneider MT, Allen PJ, Schattner M, Brand RE, Singhi AD, Petersen GM, Hong SM, Kim SC, Falconi M, Doglioni C, Weiss MJ, Ahuja N, He J, Makary MA, Maitra A, Hanash SM, Dal Molin M, Wang Y, Li L, Ptak J, Dobbyn L, Schaefer J, Silliman N, Popoli M, Goggins MG, Hruban RH, Wolfgang CL, Klein AP, Tomasetti C, Papadopoulos N, Kinzler KW, Vogelstein B, Lennon AM. Combined circulating tumor DNA and protein biomarker-based liquid biopsy for the earlier detection of pancreatic cancers. *Proc Natl Acad Sci U S A* 2017; **114**: 10202-10207 [PMID: 28874546 DOI: 10.1073/pnas.1704961114]

95 **Yan TB**, Huang JQ, Huang SY, Ahir BK, Li LM, Mo ZN, Zhong JH. Advances in the Detection of Pancreatic Cancer Through Liquid Biopsy. *Front Oncol* 2021; **11**: 801173 [PMID: 34993149 DOI: 10.3389/fonc.2021.801173]

96 **Javadrashid D**, Baghbanzadeh A, Derakhshani A, Leone P, Silvestris N, Racanelli V, Solimando AG, Baradaran B. Pancreatic Cancer Signaling Pathways, Genetic Alterations, and Tumor Microenvironment: The Barriers Affecting the Method of Treatment. *Biomedicines* 2021; **9** [PMID: 33918146 DOI: 10.3390/biomedicines9040373]

97 **Sherman MH**, Beatty GL. Tumor Microenvironment in Pancreatic Cancer Pathogenesis and Therapeutic Resistance. *Annu Rev Pathol* 2023; **18**: 123-148 [PMID: 36130070 DOI: 10.1146/annurev-pathmechdis-031621-024600]

98 **Luchini C**, Capelli P, Scarpa A. Pancreatic Ductal Adenocarcinoma and Its Variants. *Surg Pathol Clin* 2016; **9**: 547-560 [PMID: 27926359 DOI: 10.1016/j.path.2016.05.003]

99 **Valdez-Hernández P**, Pérez-Díaz I, Soriano-Rios A, Gómez-Islas V, García-Fong K, Hernández-Calleros J, Uscanga-Dominguez L, Pelaez-Luna M. Pancreatogenic Diabetes, 2 Onset Forms and Lack of Metabolic Syndrome Components Differentiate It From Type 2 Diabetes. *Pancreas* 2021; **50**: 1376-1381 [PMID: 35041336 DOI: 10.1097/MPA.0000000000001930]

100 **Hadidi A**. Pancreatic duct diameter: sonographic measurement in normal subjects. *J Clin Ultrasound* 1983; **11**: 17-22 [PMID: 6403583 DOI: 10.1002/jcu.1870110105]

101 **Kamat R**, Gupta P, Rana S. Imaging in chronic pancreatitis: State of the art review. *Indian J Radiol Imaging* 2019; **29**: 201-210 [PMID: 31367093 DOI: 10.4103/ijri.IJRI_484_18]

102 **Shankar A**, Srinivas S, Kalyanasundaram S. Icicle sign: autoimmune pancreatitis. *Abdom Radiol (NY)* 2020; **45**: 245-246 [PMID: 31712867 DOI: 10.1007/s00261-019-02323-6]

103 **Hur BY**, Lee JM, Lee JE, Park JY, Kim SJ, Joo I, Shin CI, Baek JH, Kim JH, Han JK, Choi BI. Magnetic resonance imaging findings of the mass-forming type of autoimmune pancreatitis: comparison with pancreatic adenocarcinoma. *J Magn Reson Imaging* 2012; **36**: 188-197 [PMID: 22371378 DOI: 10.1002/jmri.23609]

104 **Campisi A**, Brancatelli G, Vullierme MP, Levy P, Ruszniewski P, Vilgrain V. Are pancreatic calcifications specific for the diagnosis of chronic pancreatitis? *Clin Radiol* 2009; **64**: 903-911 [PMID: 19664481 DOI: 10.1016/j.crad.2009.05.005]

105 **Negrelli R**, Manfredi R, Pedrinolla B, Boninsegna E, Ventriglia A, Mehrabi S, Frulloni L, Pozzi Mucelli R. Pancreatic duct abnormalities in focal autoimmune pancreatitis: MR/MRCP imaging findings. *Eur Radiol* 2015; **25**: 359-367 [PMID: 25106489 DOI: 10.1007/s00330-014-3371-y]

106 **Zaheer A**, Singh VK, Akshintala VS, Kawamoto S, Tsai SD, Gage KL, Fishman EK. Differentiating autoimmune pancreatitis from pancreatic adenocarcinoma using dual-phase computed tomography. *J Comput Assist Tomogr* 2014; **38**: 146-152 [PMID: 24424563 DOI: 10.1097/RCT.0b013e3182a9a431]

107 **Palazzo M**, Palazzo L, Aubert A, Fabre M, Couvelard A, Vullierme MP, Maire F, Lévy P, Ruszniewski P. Irregular narrowing of the main pancreatic duct in association with a wall thickening is a key sign at endoscopic ultrasonography for the diagnosis of autoimmune pancreatitis. *Pancreas* 2015; **44**: 211-215 [PMID: 25394223]

108 **Bang SJ**, Kim MH, Kim DH, Lee TY, Kwon S, Oh HC, Kim JY, Hwang CY, Lee SS, Seo DW, Lee SK, Song DE, Jang SJ. Is pancreatic core biopsy sufficient to diagnose autoimmune chronic pancreatitis? *Pancreas* 2008; **36**: 84-89 [PMID: 18192887 DOI: 10.1097/mpa.0b013e318135483d]

109 **Berger Z**. [Focal autoimmune pancreatitis versus pancreatic cancer: value of steroid treatment in the diagnosis]. *Rev Med Chil* 2014; **142**: 413-417 [PMID: 25117030 DOI: 10.4067/S0034-98872014000400001]

World Journal of Gastrointestinal Oncology

Submit a Manuscript: https://www.f6publishing.com

World J Gastrointest Oncol 2023 June 15; 15(6): 943-958

DOI: 10.4251/wjgo.v15.i6.943

ISSN 1948-5204 (online)

MINIREVIEWS

Vitamin E in the management of pancreatic cancer: A scoping review

Sophia Ogechi Ekeuku, Effiong Paul Etim, Kok-Lun Pang, Kok-Yong Chin, Chun-Wai Mai

Specialty type: Oncology

Provenance and peer review: Invited article; Externally peer reviewed.

Peer-review model: Single blind

Peer-review report's scientific quality classification

Grade A (Excellent): 0
Grade B (Very good): 0
Grade C (Good): C, C
Grade D (Fair): D
Grade E (Poor): 0

P-Reviewer: Laranjeira C, Portugal; Qi L, China

Received: November 8, 2022
Peer-review started: November 8, 2022
First decision: January 3, 2023
Revised: February 3, 2023
Accepted: April 7, 2023
Article in press: April 7, 2023
Published online: June 15, 2023

Sophia Ogechi Ekeuku, Kok-Yong Chin, Department of Pharmacology, Faculty of Medicine, Universiti Kebangsaan Malaysia, Kuala Lumpur 56000, Malaysia

Effiong Paul Etim, Faculty of Applied Sciences, UCSI University, Kuala Lumpur 56000, Malaysia

Kok-Lun Pang, Newcastle University Medicine Malaysia, Iskandar Puteri 79200, Johor, Malaysia

Kok-Yong Chin, Chun-Wai Mai, State Key Laboratory of Oncogenes and Related Genes, Renji-Med X Clinical Stem Cell Research Center, Ren Ji Hospital, School of Medicine, Shanghai Jiao Tong University, Shanghai 200127, China

Chun-Wai Mai, Department of Pharmaceutical Chemistry, Faculty of Pharmaceutical Sciences, UCSI University, Kuala Lumpur 56000, Malaysia

Corresponding author: Chun-Wai Mai, BPharm, PhD, Associate Professor, Department of Pharmaceutical Chemistry, Faculty of Pharmaceutical Sciences, UCSI University, No. 1, Jalan Menara Gading, UCSI Heights (Taman Connaught), Cheras, Kuala Lumpur 56000, Malaysia. mai.chunwai@gmail.com

Abstract

Pancreatic cancer is the leading cause of cancer mortality worldwide. Research investigating effective management strategies for pancreatic cancer is ongoing. Vitamin E, consisting of both tocopherol and tocotrienol, has demonstrated debatable effects on pancreatic cancer cells. Therefore, this scoping review aims to summarize the effects of vitamin E on pancreatic cancer. In October 2022, a literature search was conducted using PubMed and Scopus since their inception. Original studies on the effects of vitamin E on pancreatic cancer, including cell cultures, animal models and human clinical trials, were considered for this review. The literature search found 75 articles on this topic, but only 24 articles met the inclusion criteria. The available evidence showed that vitamin E modulated proliferation, cell death, angiogenesis, metastasis and inflammation in pancreatic cancer cells. However, the safety and bioavailability concerns remain to be answered with more extensive preclinical and clinical studies. More in-depth analysis is necessary to investigate further the role of vitamin E in the management of pancreatic cancers.

Key Words: Anti-cancer treatment; Pancreatic cancer; Scoping review; Tocopherol; Tocotrienol; Vitamin E

Core Tip: Vitamin E is a natural bioactive agent found in a variety of foods. Our scoping review found that it inhibits pancreatic tumor progression, and modulates key pathways in carcinogenesis. Vitamin E might support the current pharmacological approach for treating pancreatic cancer. However, more studies are needed to investigate its safety and efficacy.

Citation: Ekeuku SO, Etim EP, Pang KL, Chin KY, Mai CW. Vitamin E in the management of pancreatic cancer: A scoping review. *World J Gastrointest Oncol* 2023; 15(6): 943-958
URL: https://www.wjgnet.com/1948-5204/full/v15/i6/943.htm
DOI: https://dx.doi.org/10.4251/wjgo.v15.i6.943

INTRODUCTION

Pancreatic cancer is a disease with a poor prognosis and high mortality rate[1,2]. Pancreatic ductal adenocarcinoma (PDAC) is categorized as an exocrine tumor that accounts for 80%-90% of pancreatic cancer cases. Less common types of exocrine tumors, such as squamous cell carcinoma and small cell carcinomas, constitute the remaining cases[2]. PDAC can evade from the host's cell death[3-5] and immune defense[5-8]. The lack of effective PDAC therapy emphasizes the need for the development of new treatment modalities.

Background

Just like other cancers, pancreatic cancer is characterized by uncontrolled proliferation and the ability to resist eradication[1]. Over the past few decades, there has been a dramatic surge in pancreatic cancer cases. The number of cases worldwide has increased from 196000 in 1991 to 495773 in 2010. The global number of new cases is expected to increase by 1.1% annually. By 2050, the incidence could rise to 18.6 cases for every 100000 individuals[9]. Mortality-wise, cases have increased by 53% in the last 25 years and as of 2020, there were 466003 deaths recorded and PDAC-linked deaths account for 4.6% of all cancer deaths[10]. The high fatality rate of pancreatic cancer is linked to the inability of detecting early malignancy. Hence, late diagnosis at an advanced stage is often the case with a 5-year survival rate of less than 5%.

The ability of pancreatic cancer cells to evade the host's apoptotic and immune pathways make intervention difficult[3-8]. The activation of the extrinsic death receptor-mediated apoptosis pathway is dependent on the ligand-receptor binding of tumor necrosis factor-related apoptosis-inducing ligand (TRAIL)[11]. Pancreatic cancer cells have also shown resistance to the apoptotic effects of TRAIL[11]. There are several pathways and mechanisms that drive the oncogenic progression of pancreatic cancer cells. Kirsten rat sarcoma viral oncogene homolog (KRAS) is the most frequently onset driver of pancreatic cancer. It captures the cell machinery *via* the phosphoinositide-3-kinases/protein kinase B (PI3K/AKT) and the rat sarcoma virus/rapidly accelerated fibrosarcoma/mitogen-activated protein kinase (MAPK) kinase/extracellular signal-regulated kinase (Ras/Raf/MEK/ERK) signaling pathways [12]. The signal transducer and activator of transcription 3 (STAT3) pathway is constitutively activated in pancreatic cancer cells[13]. Pancreatic cancer disrupts the cancer-immunity cycle, supporting cancer cells to evade host immunity and immunotherapy[4-7]. Pancreatic cancer stem cells (CSCs) that break off from the primary tumor and metastases have made treatment and recovery options even more challenging as most patients go into relapse. This is because CSCs renew themselves, become tumorigenic, metastatic and develop differentiated progenies that further increases the resistance to treatment[14,15].

Unfortunately, treatment options available for patients with pancreatic cancer are limited. The only effective treatment method with the possibility of full recovery remains surgery either by pancreatic-duodenectomy (Whipple's procedure), distal or total pancreatectomy[16]. The risk associated with the procedure is daunting and less safe once metastasis ensues. Most patients are then given gemcitabine, the first-line chemotherapy used to eliminate pancreatic cancer, which only merely extends the survival rate marginally[17]. Other chemotherapeutic regimes, such as 5-fluorouracil, Partenariat de Recherche en Oncologie Digestive 24/Canadian Cancer Trial Group, and modified FOLFIRONOX (a combination of 5-fluorouracil, leucovorin, irinotecan, and oxaliplatin), and immunotherapy have shown some benefits among patients with pancreatic cancer[2]. However, pancreatic cancer eventually develops chemoresistance towards these clinically used agents. Many combination agents[7,18,19] and novel drug delivery methods[20-22] are currently under investigation in hope that a safe and effective treatment for pancreatic cancer patients can be found.

Dietary modulation is a good strategy with the potential for prevention and treatment of many disorders including cancers[23,24]. The naturally occurring vitamin E with all its isoforms have shown potential as a stand-alone treatment in disrupting the cancer mechanism pathways and in several combination treatments[25]. Vitamin E comprises a chromanol ring with an isoprenoid side chain (Figure 1)[26]. There are two common homologues of vitamin E, *i.e.* tocopherol (TP) and tocotrienols (TT). Natural occurring TPs exhibit three *R*-configuration asymmetric carbons, namely C2 (chromanol ring), C4′ and C8′ (side chain)[26]. For TT, the three double bonds are *all-trans* configuration. Both groups exist in α-, β-, γ- and δ-isomer, with different methyl groups. Stereoisomerism of TP and TT may have an impact on their biological activity. Both TP and TT can be prepared in ester forms, namely acetate, nicotinate, succinate or phosphate, at the hydroxyl group at the chromanol head to reduce the oxidation of TP or TT. Vitamin E isoforms can be prepared *via* total or semi-synthesis for industrial application[26]. Unfortunately, the investigation of α-TP as an agent of cancer prevention has only yielded disappointing results since it required a high anti-cancer dose *in vitro* but failed to suppress the growth in pancreatic carcinoma *in vivo*[27]. As a consequence, the study of α-TPs has not reached clinical trial and are not being investigated as treatment for pancreatic cancer[27]. Molecularly, TTs differ from TPs since the former have an unsaturated isoprenoid side chain (Figure 1). Compared to most TP isoforms, δ- and γ-TT possess stronger anti-cancer properties. This unsaturated side chain may confer an extra anticancer/anti-proliferative property that the TPs are lacking[28]. However, due to the strong binding of α-TP with α-TP transfer protein, TTs have a low bioavailability which might hinder their anti-cancer activities *in vivo* when present together with α-TP [27]. A study also showed that δ- and γ-TT exhibited a much stronger inhibitory effect on eicosanoid formation than α-TPs[27]. Moreover, compared to α-TP, TT has much stronger inhibitory effects on canonical inflammatory markers[27]. Thus, δ-TT and γ-TT are widely studied for their anti-cancer properties, but not β-TT probably because it is not commonly found in nature compared to other isoforms[25,27].

Purpose

Given the unique properties of TPs and TTs, this review aims to summarize the effects of vitamin E against PDAC cells lines, *in vivo* tumor models and pancreatic cancer patients. In addition to identifying research gaps in the existing literature, this study will look at the quantity, variety, and type of research activity that is currently available on this subject.

MATERIALS AND METHODOLOGY

This scoping review was performed according to the Preferred Reporting Items for Systematic Reviews and Meta-Analyses extension for Scoping Reviews (PRISMA-ScR) guidelines[29]. The methodology was according to the Arksey and O'Malley framework[30]. Steps of the literature search selection process, from identification, screening and eligibility for the inclusion of articles are shown in Figure 2. The protocol of this scoping review has not been registered before the study.

Research question

The research question for this scoping review was: *What are the effects of vitamin E on pancreatic cancer?* α-TP, α-, β-, γ- and δ-TT are different types of vitamin E included in the study. Pre-clinical models such as *in vitro* cell lines, *in vivo* mouse models and clinical trial findings from pancreatic cancer patients were included in the study. This scoping review has included findings from all stages of pancreatic cancer.

Study identification

A literature search was conducted by two authors (SOE and EPE) in October 2022 using PubMed and Scopus to identify studies on the association between vitamin E and pancreatic cancer. The search string used was ("vitamin E" OR TPs [MeSH] OR OR tocopheryl OR TTs [MeSH] OR TT) AND "pancreatic cancer".

Study selection

Studies with the following characteristics were included: (1) Studies that aimed at determining the effects of vitamin E (mixture or single isomer) on pancreatic cancer; (2) Studies published in English; and (3) Studies conducted on pancreatic cancer cells (primary culture or cell lines), animal models or patients with pancreatic cancers. We excluded: (1) Articles that did not contain original data, such as reviews, letters, commentaries, or opinions; (2) Conference abstracts, considering the results might have been published as full articles; and (3) Studies that use a combination of vitamin E and other compounds, whereby the effects of vitamin E could not be clearly delineated. The search results were organized using Mendeley software (Elsevier, Amsterdam). Duplicates were identified using Mendeley and confirmed by manual checking.

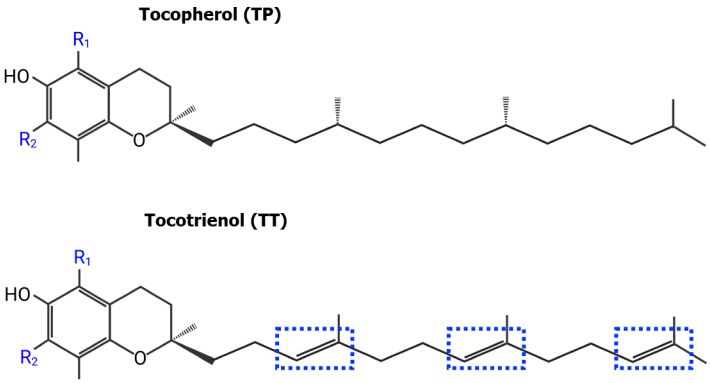

	α	β	γ	δ
R_1	CH_3	CH_3	H	H
R_2	CH_3	H	CH_3	H

DOI: 10.4251/wjgo.v15.i6.943 **Copyright** ©The Author(s) 2023.

Figure 1 Chemical structure of vitamin E homologues, namely tocopherol, and tocotrienol. TP has a saturated phytyl side chain, while tocopherol has three double bonds (indicated in blue line dotted box) on the side chain. The α-, β-, γ-, δ-isomers differ in the position of the methyl group on the chromanol ring (R_1 and R_2).

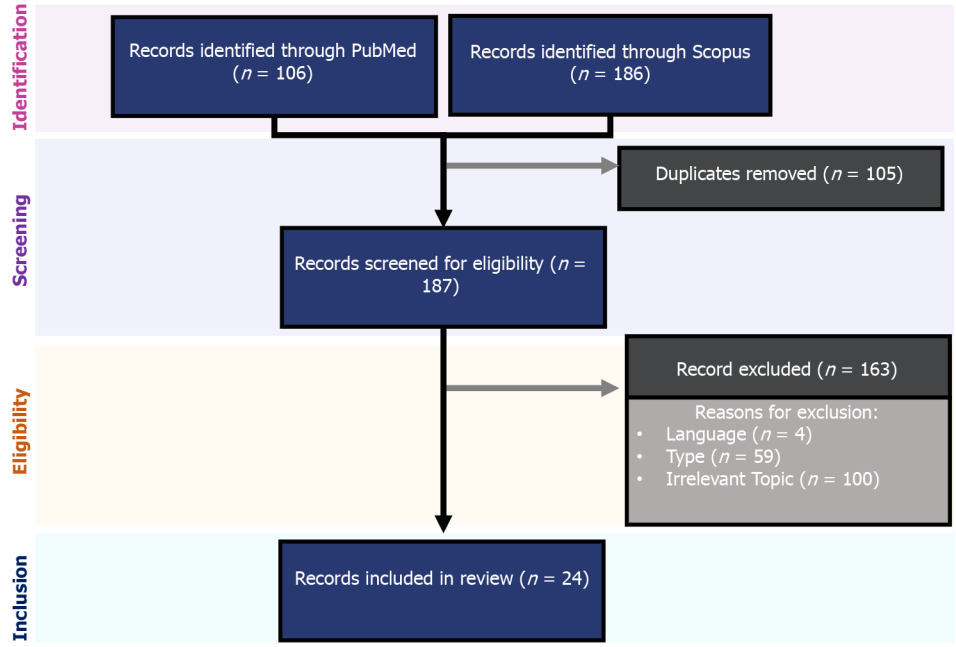

DOI: 10.4251/wjgo.v15.i6.943 **Copyright** ©The Author(s) 2023.

Figure 2 Process of article selection in this scoping review.

Data charting

Two authors (SOE and EPE) screened the search results based on titles, abstracts and full texts. Any disagreement on the inclusion or exclusion of articles was resolved through discussion among the two authors. The corresponding author (CWM) had the final decision on articles included if a consensus could not be reached between authors. Data charting was performed by two authors (SOE and EPE) using a standardized table and validated by two other authors (KYC and KLP). The data extracted included researchers, years of inclusion, study design and major findings.

RESULTS

Selection of articles

The literature search yielded 292 results (106 from PubMed and 186 from Scopus). After removing the duplicated items (n = 105), 187 articles were screened for eligibility. During the screening, 163 articles were removed due to various reasons (100 articles were not relevant, 4 non-English articles, 41 review articles, 4 conference proceedings, 3 book chapters, 3 meta-analyses, 2 notes, 2 "Patients-Oriented

Evidence that Matters" articles, 1 editorial, 1 guideline, 1 letter and 1 short communication). Finally, 24 papers that met all the criteria were included in the current review.

Study characteristics

Articles that passed the inclusion criteria were published from 2000 to 2019. Three studies used vitamin E succinate (VES)[31-33], two studies used alpha-tocopheryl succinate (α-TPS)[34,35], four studies used α-TP[36-39], one study used α-TT[39], one study used β-TT[39], four studies used γ-TT[12,39-41], and 11 studies used δ-TT[39-51]. Nineteen studies were *in vitro* experiments using human pancreatic cancer cell lines, namely AsPC-1, BxPC-3, Capan-1, Capan-2, COLO-357, MIA PaCa-2, PANC-1, Pan02, Panc 28, PSN-1, SW1990, and L3.6pI[12,31,33-36,39-48,51,52]; human pancreatic cancer stem-like cells (PCSCs) [48] and primary culture of human pancreatic cancer cells[32]. The concentrations of vitamin E ranged from 0 to 500 μM *in vitro* up to 72 h[12,31,33-36,39-43,45-48,51,52]. In terms of animal studies, 11 studies used either athymic nude mice[41-43,48,51], severe-combined immunodeficient (SCID) nude mice[39] , $LSL^{KrasG12D/+}$; *Pdx-1-Cre* transgenic mice[47,50], $LSL^{KrasG12D/+}$; $LSL^{Trp53R172H/+}$; *Pdx-1-Cre* (KPC) transgenic mice [49] or Syrian hamsters[37,38]. The dose of vitamin E used in animal studies was between 4 to 400 mg/kg/day and the study duration ranged from 3 wk to 12 mo[37-39,41-43,47-51]. Only one Phase I clinical trial of vitamin E (NCT00985777) on patients diagnosed with pancreatic ductal neoplasia was reported [53]. It was a single-center, open-label, phase I dose escalation trial. Patients with presumptive premalignant (intraductal papillary mucinous neoplasm or mucinous cystic neoplasm of the pancreas) or malignant (pancreatic carcinoma) exocrine pancreas neoplasms were given 200-1600 mg vitamin E twice daily for 2 wk before surgery and once on the day of surgery[53].

Evidence from cell culture studies

As illustrated in Table 1, several *in vitro* studies applied various types of vitamin E in pancreatic cancer cell lines[12,31,33-36,39-43,45-48,51,52], PCSCs[48] and primary culture of human pancreatic cancer cells [32]. VES (0.000023-500 μM) reduced the growth[32-34] or proliferation[31] of pancreatic cancer cells after 24-72 h of treatment. Protein expression studies revealed that VES induced pancreatic cancer cell death with the increase of cleaved poly adenosine diphosphate ribose polymerase (cPARP), caspase-3, and p21 expression but decreased the cell division cycle protein 2 (Cdc2), survivin, and X-linked inhibitor of apoptosis protein (XIAP) expression[31]. Debele *et al*[35] reported that α-TPS and α-TPS-loaded poly(allylamine)-citraconic anhydride-poly(lactic-co-glycolic acid)-cystamine (PAH-SS-PLGA) micelle (PAH-SS-PLGA-TOS) exhibited cytotoxicity, apoptosis induction and G0/G1 and G2/M arrest in Pan02 cells. However, the effect of α-TPS was only significant at a higher concentration (100 μM). Husain *et al*[39] reported that α-TP at doses between 0-100 μM did not affect growth, survival, colony formation and nuclear factor kappa-light-chain-enhancer of activated B cells (NF-κB) activity in the pancreatic cancer cell lines. Independently, Greco *et al*[34] reported that pancreatic cancer cell lines were only responsive to the anti-proliferative effects of α-TPS at a concentration greater than 200 μM. Similarly, Blanchard *et al*[36] also reported decreased expression of interleukin 6 (IL-6) in both CAPAN 1 and CAPAN 2; IL-8 and NF-κB in CAPAN 2 pancreatic cancer cell lines at a high dose (500 μM). These results suggest that α-TP may only be effective against pancreatic cancer cell lines at high doses greater than 100 μM.

Independently, TTs also reduced proliferation, and modulated apoptosis of pancreatic cancer cells[12, 39,41,42,44-48]. TT suppressed pancreatic cancer cell proliferation as indicated by the downregulation of proliferation markers (cyclin D1, cellular myelocytomatosis or c-Myc) in a concentration-dependent manner[41]. After treatment with δ- or γ-TT (0-100 μM for 2-6 d), pancreatic cancer cells underwent apoptosis as downregulated anti-apoptotic proteins such as B-cell lymphoma 2 (Bcl2), Bcl-extra-large (Bcl-xL), XIAP, and cellular inhibitors of apoptosis protein (cIAP), as well as increasing the expression of apoptotic proteins namely, caspase 3, caspase 8, Bcl-2 associated X protein (Bax), early growth response factor (EGR) 1 , and poly(adenosine diphosphate-ribose) polymerase 1 (PARP-1)[39,41,42,48]. However, δ-TT (50 μM for 12 h) did not significantly affect Bcl-2, survivin, XIAP and cIAP1 protein expression, suggesting that TT has conflicting effects on anti-apoptotic markers of pancreatic cancer cells[47]. Additionally, γ-TT (40 μM for 2-6 d) induced apoptosis by upregulating ceramide synthesis in pancreatic cancer through stimulating the synthesis of serine palmitoyl transferase, ceramide synthase 6 and delta 4-desaturase, sphingolipid 1. As a result, γ-TT prevented the conversion of ceramides to sphingomyelin and glucosylceramide, which contributes to the apoptotic effect of γ-TT on pancreatic cancer cells[12].

NF-κB transcription factor in pancreatic cancer cells was significantly decreased after the treatment with 500 μM of α-TP for 18 h[36] or 50 μM of d- or γ-TT for 72 h[39] suggesting that vitamin E modulates inflammation in pancreatic cells. Both γ- and δ-TT (10-100 μM for 72 h) reduced MAPK/ERK activation and that of its downstream mediator ribosomal protein S6 kinase, as well as suppressed AKT activation. TT-mediated inactivation of MAPK, AKT and ERK through the induced expression of $p27^{Kip1}$, suggests that oncogenic signaling was inhibited through cell cycle inhibition[40,43,48]. Suppression of AKT phosphorylation by γ- and δ-TT led to downregulation of phosphorylated glycogen synthase kinase-3 beta and upregulation accompanied by nuclear translocation of forkhead box transcription factor-3a (Foxo3a). These effects were mediated by messenger-level receptor tyrosine-protein kinase erythroblastic oncogene B-2 downregulation[40]. Additionally, δ-TT (10-100 μM for 72 h) decreased the

Table 1 *In vitro* studies investigating effect of vitamin E on pancreatic cancer

Type	Pancreatic cells	Dosing regimen	Statistically significant effect (compared to negative control)	Ref.
VES	AsPC-1, COLO 357, PANC-1	10-80 μM; 24, 48, 72 h	↓ Proliferation; ↑ Apoptosis; ↑ Cell cycle arrest; ↓Antiapoptotic markers	[31]
VES	LPC 1-7 (Primary Culture)	0.001-1 μM; 48 h	↓ Proliferation	[32]
VES	MIA PaCa-2	0.000023 μM; 24, 48, 72 h	↓ Proliferation	[33]
α-TPS	BxPC-3, Capan-1,MIA PaCa-2, PANC1, PSN-1	5-500 μM; 72h	↓ Proliferation	[34]
α-TPS, PAH-SS-PLGA-TOS	Pan02	1.45-232.2 μM; 48 h	↓ Proliferation; ↑ Apoptosis; ↑ Cell cycle arrest	[35]
α-TP	Capan-1, Capan-2	500 μM; 18 h	↓ NF-κB activity; ↓ IL-6; ↓ IL-8	[36]
α-TP, α-TT, β-TT, γ-TT, δ-TT	AsPC1, MIA PaCa-2	0-100 μM; 72 h	↓ Proliferation; ↑ Apoptosis;↓ NF-κB activity; ↓ NF-κB DNA binding activity; ↓ Antiapoptotic markers	[39]
γ-TT, δ-TT	BxPC-3, MIA PaCa-2, PANC-1, Panc 28	10, 20, 40, 60, 80, 100 μM; 24 h	↑ Apoptosis; ↓ MAPK related markers	[40]
γ-TT	BxPC-3, MIA PaCa-2, PANC-1	10, 50 μM; 48, 96, 144 h	↓ Proliferation; ↓ NF-κB activity; ↓Antiapoptotic markers; ↓Angiogenesis markers; ↓ Invasion markers	[41]
γ-TT	BxPC-3, MIA PaCa-2, PANC-1	40 μM; 2, 4, 6 h	↑ Apoptosis	[12]
-TT	BxPC-3, MIA PaCa-2, SW1990	0-50μM; 24, 48, 72h	↓ Proliferation; ↑ Cell cycle arrest; ↓ MAPK related markers	[43]
δ-TT	BxPC-3, MIA PaCa-2, PANC-1	0-64 μM; 24-72 h	↓ Proliferation; ↑ Apoptosis	[44]
δ-TT	Human pancreatic cancer cells from ATCC	2.5-80 μM; 48 h	↓ Proliferation	[45]
δ-TT	PANC-1	12.5 μM; 48 h	↓ Proliferation	[46]
δ-TT	MIA PaCa-2	50 μM; 0-12 h	↓ Proliferation; ↑ Apoptosis; = Antiapoptotic markers	[47]
δ-TT	MIA PaCa-2, PCSCs	10-100 μM; 72 h	↓ MAPK related markers; ↓ Invasion markers; ↓ Angiogenesis markers	[48]
δ-TT	AsPc-1, BxPC-3, MIA PaCa-2, PANC-1, SW1990	20-100 μM; 72 h	↓ Proliferation; ↑ Apoptosis	[42]

"=" represents no difference; "↑" represents increase; "↓" represents reduction; PAH-SS-PLGA-TOS: Poly (allylamine)-citraconic anhydride-poly(lactic-co-glycolic acid)-cystamine micelle-α-tocopheryl succinate conjugate; α-TP: Alpha tocopherol; β-TT: Beta tocotrienol; γ-TT: Gamma tocotrienol; δ-TT: Delta tocotrienol; LPC: Low passage primary pancreatic cancer cells; ATCC: American Type Culture Collection; PCSC: Pancreatic cancer stem cells; NF-kappa B: Nuclear factor kappa-light-chain-enhancer of activated B cells; IL: Interleukin; MAPK: Mitogen-activated protein kinase.

pluripotency of pancreatic CSCs as shown by a reduction in the expression of Nanog, octamer-binding transcription factor 4 and sex-determining region Y-box 2 as well as blocking the Notch 1 receptor[48].

δ- or γ-TT (0-100 μM for 2-6 d) prevented the invasion, adhesion, and angiogenesis of pancreatic cancer cells by reducing the protein expression of matrix metalloproteinase 9 (MMP-9), intercellular adhesion molecule 1 (ICAM-1), vascular endothelial growth factor (VEGF) and C-X-C chemokine receptor type 4[41,48]. Additionally, TT increased the protein expression of the E-cadherin and reduced the expression of vimentin and N-cadherin in pancreatic cancer cells, indicating the role of TT in suppressing epithelial-to-mesenchymal tumor transition (EMT) of pancreatic cancer cells[48].

Evidence from animal studies

Several studies suggest that TT treatment can reduce the growth of pancreatic tumors *in vivo* (Table 2). A significantly smaller pancreatic tumor was observed after 100 mg/kg of δ-TT daily (3 wk)[43], 200mg/kg of δ-TT once/twice daily (4 wk)[42], 200 mg/kg of δ-TT twice daily (4 wk)[48], or 400 mg/kg of γ--TT (28 d)[41], was given to the athymic nude mice with pancreatic cancer cell line-derived xenografts. The xenografts were established using subcutaneous xenograft implantation in the flank of mice[42,43] or orthotopic xenograft implantation in the subcapsular region of the pancreas[41,48], or spleen[51] of the mice. In another subcutaneous xenograft of AsPC-1-induced pancreatic tumors[39], the team reported a 50% reduction, 42% reduction and 32% reduction of tumor volume after δ-TT, γ--TT

Table 2 *In vivo* studies investigating effect of vitamin E on pancreatic cancer

Type	Model	Dosing regimen	Statistically significant effect (compared to negative control)	Ref.
δ-TT	Subcutaneous xenograft of MIA PaCa-2 induced pancreatic tumor in athymic nude mice	PO 100 mg/kg, 1 x/day for 3 wk	↓ Tumor volume; ↓ Proliferation markers; ↓ MAPK related markers	[43]
δ-TT	Subcutaneous xenograft of MIA PaCa-2 induced pancreatic tumor in athymic nude mice	PO 200 mg/kg, 2 x/day during weekday & 1 x/day during weekend for 4 wk	↓ Tumor volume; ↑ Apoptotic markers	[42]
δ-TT	Subcutaneous xenograft of L3.6pl cells and PCSC- induced pancreatic tumor in athymic nude mice	PO 200 mg/kg, 2x/day for 4 wk	↓ Tumor volume; ↓ Proliferation markers; ↑ Apoptotic markers; ↓ Invasion markers; ↓ Angiogenesis markers	[48]
δ-TT	Orthotopic xenograft of MIA PaCa-2 induced pancreatic tumor in athymic nude mice	PO 400 mg/kg, 1 x/day for 28 d	↓ Tumor volume; ↓ Proliferation markers; ↓ NF-κB activity; ↓ Invasion markers; ↓ Angiogenesis markers	[41]
δ-TT	*LSL*$^{KrasG12D/+}$; *LSL*$^{Trp53R172H/+}$; *Pdx-1-Cre* (KPC) transgenic mice	PO 200 mg/kg, 2 x/day for 12 wk	↑ Survival; ↓ Tumor volume; = Body weight; ↓ Proliferation markers; ↑ Apoptotic markers; ↓ MAPK related markers	[49]
δ-TT	*LSL*$^{KrasG12D/+}$; *Pdx-1-Cre* transgenic mice	PO 200 mg/kg, 2 x/day for 12 mo	↑ Apoptotic markers	[47]
δ-TT	*LSL*$^{KrasG12D/+}$; *Pdx-1-Cre* transgenic mice	PO 200 mg/kg, 2 x/day for 12 mo	↑ Survival; ↓ Tumor progression; = Body weight; ↑ Apoptotic markers; ↓ NF-κB markers; ↓ MAPK related markers	[50]
δ-TT	Orthotopic xenograft of MIA PaCa-2 induced pancreatic tumours in athymic nude mice	PO 50-100 mg/kg, 2 x/day during weekday & 1 x/day during weekend for 6 wk	↑ δ-TT concentration in pancreas; = Body weight; = Histopathology	[51]
α-TT, β-TT, γ-TT, δ-TT	Subcutaneous xenograft of AsPC-1 induced pancreatic tumor in SCID mice	PO 200 mg/kg, 2 x/day for 4 wk	↓ Tumor volume; ↑ Apoptotic markers; ↓ Antiapoptotic markers; ↓ NF-κB activity and markers	[39]
α-TP	*N*-nitrosobis (2-oxopropyl) amine-induced pancreatic cancer in Syrian hamster	PO 4 mg/kg, 3 x/wk for 12 wk	= Tumor incidence; = Body weight; ↓ Liver metastasis incidence; = Liver metastasis number; = Liver metastasis size	[37]
α-TP	*N*-nitrosobis (2-oxopropyl) amine-induced pancreatic cancer in Syrian hamster	PO 4 mg/kg, 3 x/wk for 12 wk	= Tumor incidence; = Body weight;	[38]

"=" represents no difference; "↑" represents increase; "↓" represents reduction; α-TP: Alpha tocopherol; α-TT: Alpha tocotrienol; γ-TT: Gamma tocotrienol; δ-TT: Delta tocotrienol; SCID: Severe-combined immunodeficient; PO: Oral administration; PCSC: Pancreatic cancer stem cells; MAPK: Mitogen-activated protein kinase; NF-κB: Nuclear factor kappa-light-chain-enhancer of activated B cells.

and β-TT treatment, respectively. However, there was no tumor volume reduction after α-TT treatment. The treated tumor also showed a lower expression of Ki-67 protein expression among the treatment group compared to the negative controls[41,43,48]. Similarly, δ-TT of 200 mg/kg (12 wk) reduced the Ki-67 staining in pancreatic tumor formed among the KPC transgenic mice[49], indicating the role of TT in reducing pancreatic tumor proliferation and growth *in vivo*.

δ-TT treatment (200 mg/kg) for 12 wk[49], or 12 mo[47,50] induced apoptosis on the pancreatic tumors of KPC transgenic mice with a lower level of antiapoptotic protein Bcl-xL but increased expression of apoptotic proteins Bax, PARP-1, EGR1, and cleaved caspase-3. Similarly, increased apoptosis was found among the pancreatic cancer cell line-derived xenograft in the SCID nude mice[39] or athymic nude mice[42,48] upon δ-TT or -TT (200-400mg/kg) treatment for 4 wk. This was evidenced by an increase in Bax and PARP-1 protein expression; increased cPARP-1, caspase-3 and -8 protein activity and reduction of antiapoptotic proteins such as Bcl-xL, survivin, cFLIP and XIAP in the TT-treated tumors[39,42,48].

Tumor formation in the KPC transgenic mice treated with δ-TT (200mg/kg) for 12 wk[49] or *LSL*$^{KrasG12D/+}$; *Pdx-1-Cre* transgenic mice treated with δ-TT (200mg/kg) for 12 mo[50] expressed lower levels of KRAS related oncogenic events including AKT, MEK and ERK activation. Researchers also observed cell cycle arrest, as evidenced by an increase of $p27^{kip-1}$ (a cell cycle repressor protein)[49,50] and $p21^{Cip1}$ (a cycle-dependent kinase inhibitor)[49] in pancreatic cancer tumors. Similarly, Hodul *et al*[43] also reported an increase in $p21^{Cip1}$ protein expression in athymic nude mice carrying MIA PaCa-2 cell-induced pancreatic tumors treated with 100 mg/kg of δ-TT daily for 3 wk.

Husain *et al*[49] also reported a decrease in the invasion, adhesion, and angiogenesis in tumors from KPC transgenic mice treated with δ-TT (200mg/kg) for 12 wk. It was evidenced by a decrease in angiogenic factors such as VEGF and clusters of differentiation (CD) 31 immunoreactivity[49]. Similarly, athymic nude mice with pancreatic cancer cell line derived xenografts when being treated with 400 mg/kg of g-TT for 28 d[41] and 200 mg/kg of δ-TT (twice daily) for 4 wk[48] showed a reduction in VEGF, MMP-9, CD31 and CD44. The same group also reported an inhibition in EMT, shown by reduced expression of the mesenchymal markers (N-cadherin and vimentin), and increased expression of the epithelial marker (E-cadherin)[48,49]. Interestingly, 12 wk of oral administration of 4 mg/kg α-TP (thrice weekly) in the *N*-nitrosobis (2-oxopropyl) amine-induced pancreatic cancer in the Syrian hamster did not affect the incidence of pancreatic tumor formation[37,38]. However, α-TP treatment decreased the incidence of liver metastasis compared to the negative control but not the number and size of liver metastasis *per* animal compared to the negative control[37].

Evidence from human clinical trial

Based on the selection criteria for this review, only one human study (NCT0098577) passed our selection criteria, in which vitamin E was used as a single drug intervention with complete peer-reviewed response in pancreatic cancer[53]. In this single-center, open-label, dose-escalation phase I trial conducted by Springett *et al*[53], 25 patients with resectable pancreatic ductal neoplasia were treated with δ-TT (200, 300, 400, 800 and 1600 mg twice daily) for 2 wk before and one dose on the day of pancreatectomy (day 14)[53]. Dysplastic and malignant tissues excised from these patients showed increased caspase-3 staining suggesting that oral δ-TT has beneficial effects on patients with pancreatic cancer[53].

A total of 5 trials (including NCT0098577) were found on ClinicalTrials.gov registry (https://clinicaltrials.gov/; Accessed 1 September 2022) using the search term "Vitamin E" and "Pancreatic Cancer". Two of the trials (NCT01446952 and NCT01450046) investigated the safety profile of vitamin E by the same team and reported the finding in NCT0098577. No data were made available from these two trials, so they were excluded from this review. The other study (NCT02681601) was filed by the University of California Los Angeles Hirshberg Pancreatic Cancer Centre to investigate the clinical outcomes of a dietary supplement enriched with natural vitamin E for pancreatic cancer patients. This study was also excluded from our review because it was terminated due to a low number of participants with no data published by the research team. Moreover, the supplement is a combination of natural vitamin E and other ingredients, so the efficacy of vitamin E cannot be accurately determined from this study. Another study (NCT04315311) which was also excluded from our review because this study investigated the role of pancrelipase rather than vitamin E in a patient with exocrine pancreatic insufficiency other than pancreatic cancer. As a result, there is no other good quality vitamin E intervention studies on human pancreatic cancer except the cited study (NCT0098577)[53]. Therefore, further larger and multi-center clinical studies are warranted to understand the effects of oral vitamin E on pancreatic cancer.

Mechanistic studies of vitamin E in the treatment of pancreatic cancer

The development and progression of pancreatic cancer relies heavily on its capability to proliferate and resist cell death[1,7,54]. Early stages of pancreatic tumors development are associated with a fibrogenic response that favors cancer cell proliferation and survival[1,4,5]. Vitamin E could exhibit its promising anticancer effect by disrupting cancer proliferation. -TT suppresses cell proliferation in pancreatic cancer cells by downregulating cell proliferative markers, namely cyclin D1[41], c-Myc[41], and Ki-67[43,48,49]. Overriding the cell cycle checkpoint is a common phenomenon in carcinogenesis, allowing tumor cells to replicate indefinitely[1]. Cell cycle entry is modulated by cyclin-dependent kinases (CDK) activity and its inhibitors ($p21^{Cip1}$and $p27^{kip-1}$). Activating the checkpoint inhibitor is thus a logical approach to limit cancer cell proliferation[1]. α-TP succinate induced G0/G1 cell cycle arrest in pancreatic cancer[35], while -TT induced G1 cell cycle arrest through increased expression of $p21^{Cip1}$[49] and $p27^{kip}$[43,49,50]. VES[31] and α-TP succinate[35] induced G2/M cell cycle arrest by suppressing Cdc2 (CDK1)[31], resulting in reduced proliferation among the pancreatic cancer cells.

Apoptosis is essential for cell survival, and its dysregulation drives the development of several diseases, including pancreatic cancer[8]. One of the hallmarks of pancreatic cancer is the ability to avoid cell death (such as apoptosis) and thus creating a conducive tumor microenvironment for tumor progression[8]. The sensitivity of cancer cells to treatment is modulated by the pro- and anti-apoptotic genes[18,55-58]. Treatment with VES, - or -TT induced apoptosis in pancreatic cancers by upregulating the apoptotic markers (Bax, and caspase-3) and downregulating the anti-apoptotic markers[31,39,41,42,47-50]. - and -TT suppressed expression of anti-apoptotic proteins Bcl-2, Bcl-xL, cIAP-1, XIAP and c-Flip [39,41,42]. However, Wang *et al*[47] reported that -TT did not affect protein expression of Bcl-xL, cIAP-1 and XIAP, suggesting there might be a varied response by vitamin E in regulating anti-apoptotic proteins of pancreatic cancers.

Inflammation-induced cancer progression is one of the inevitable oncogenic events in pancreatic cancer[3]. Activation of NF-κB is known to interfere with apoptosis processes and enhance cell survival [59]. NF-κB will be activated when IkappaB kinase phosphorylates the NF-κB-bound IκBα, leading to the ubiquitin-degradation of IκBα, and the nuclear translocation of the NF-κB p65-p50 dimer. This process activates inflammation-induced proliferation and cell survival[3,60], α-TP succinate[36] and -TT

[41] suppressed NF-κB activity in pancreatic cancer cells. Husain *et al*[39] demonstrated that - and -TT prevented the degradation of IκBα, thus suppressing the nuclear translocation of p65/p50 dimer. As a nuclear factor, NF-κB controls the transcription of proteins related to proliferation, apoptosis and cell cycle[61]. Both intrinsic (Bcl-2 and Bcl-xL) and extrinsic (cIAPs, caspase-8, and c-Flip) pathways are regulated by NF-κB, and NF-κB activation frequently tips the scales in favor of anti-apoptotic markers such as cFlip or the IAP (cIAP1/2 and XIAP)[61].

Additionally, KRAS-induced inflammation is another key oncogenic event in PDAC[62]. However, KRAS remains "undruggable" because of a lack of efficient inhibitors[63]. KRAS mutation accounts for 90–95% of fatal and metastatic PDAC[64]. Even though oncogenic KRAS remains "undruggable", KRAS relies on the two major downstream pathways, namely: (1) PI3K/AKT; and (2) Ras/Raf/MEK/ERK pathways to promote proliferation, and survival. Therefore, a prospective method of treating these KRAS-driven pancreatic cancers could be achieved by inhibiting its KRAS downstream signals[63,65].

The PI3K/AKT survival pathway is primarily involved in cancer cell proliferation[66]. The dysregulation of PI3K/AKT accounts for nearly 60% of PDAC patients[66]. Through phosphorylation, AKT activates the Bcl-2-associated death promoter, glycogen synthase kinase 3 (GSK-3), and FoxO-related transcription factors, all of which mediate cancer cell proliferation[66]. AKT activation was suppressed by -TT[40] or -TT[40,43,48,50], as evidenced by a reduction in phosphorylated AKT (pAKT). By inhibiting pAKT, -TT or -TT also modulated GSK-3β and Foxo3a as well as nuclear translocation in pancreatic cancer cells[40]. Foxo3a suppresses tumor growth by promoting cell cycle arrest and apoptosis. Phosphorylated AKT inhibits Foxo3a, resulting in its cytoplasmic sequestration. Dephosphorylation of FoxO3a leads to nuclear translocation and transcriptional activity conducive to apoptosis or cell cycle arrest[40].

The RAS/RAF/MEK/ERK pathway is one of the critical pathways in MAPK, that regulates proliferation, apoptosis, and cell cycle. The G0–G1–S phase cell cycle progression is also regulated by the RAF–MEK–ERK pathway in response to growth factor stimulation or oncogene activation. As a result, the pathway regulates the expression/activity of CDK and CDK inhibitors ($p21^{Cip1}$ and $p27^{kip-1}$)[67]. -TT or -TT inhibited the RAS/RAF/MEK/ERK pathway by suppressing MEK and ERK activation, which subsequently increased the expression of $p27^{kip-1}$, leading to cell cycle arrest at G1[40,43,48-50].

Tumor angiogenesis is a tightly controlled process, in which new blood vessels form in the tumor environment to provide oxygen and support tumor growth[1]. Apart from its role in the maintenance of the primary tumor ecosystem, tumor angiogenesis promotes tumor cell invasion and dissemination and the formation of new secondary tumor ecosystems at metastasized sites[68]. This process necessitates extensive interactions between endothelial cells, angiogenic growth factors, and extracellular matrix *via* pro-angiogenic signals[1,68]. -TT reduced angiogenesis in pancreatic tumor cells and thus reduced the oxygen supply to the tumor cells and slowed their growth[41,43,48]. -TT also inhibited the angiogenic factor as confirmed by a reduction in the CD31 immunostaining in tumor blood vessels[48,50]. To direct the tip cell migration and stalk cell proliferation during sprouting angiogenesis, VEGF and Notch signaling are activated[69]. In a bid to promote Notch-dependent angiogenesis, VEGF can cause the production of jagged ligands, which in turn boosts Notch expression in cancer endothelial cells[69]. The Notch signaling pathway is important in cancer stem cell renewal, differentiation, and survival[70]. Husain *et al*[48] supported the application of -TT in targeting the PCSCs' self-renewal capacity by suppressing Notch 1 receptors and other pluripotent transcription factors.

Tumor cells will eventually gain the ability to metastasize, leaving the primary site and spreading throughout the body, causing severe organ failure and eventually death[71]. Invasion, the first step in tumor cell metastasis, begins when cancer cells detach from the tumor mass, acquire the ability to actively move, and invade surrounding tissues through the adjacent basement membrane[71]. - and -TT downregulated the tumor invasion biomarker MMP9 and prevented tumor invasion[41,48]. Adhesion is another critical step in metastasis, and it can occur directly between tumor cells and endothelial cells with the help of adhesion-associated proteins[72]. -TT also prevented the adhesion in cancer cells by suppressing the adhesion marker ICAM[41]. One of the key events in driving tumor metastasis is EMT, a complex biological process in which epithelial cells lose their phenotype and gain mesenchymal characteristics[73]. EMT is a potential target for cancer metastases due to the tight coupling of these growth factors that sustain the growth of cancer cells. Preventing the activation signal of EMT markers, such as E-cadherin, N-cadherin and vimentin, is one of the ways to target the EMT process in cancer [73]. On that note, -T3 treatment reversed EMT by increasing the expression of the epithelial marker (E-cadherin) and decreasing the expression of the mesenchymal markers (N-cadherin and vimentin)[48,49], indicating its potential in preventing metastasis in pancreatic cancer. Based on our scoping review, vitamin E modulates proliferation, cell death, inflammation angiogenesis, and metastasis in pancreatic cancer cells (Figure 3).

DISCUSSION

Safety and bioavailability concerns of vitamin E

There is a global initiative to promote the consumption of vitamin E *via* supplementation or vitamin E-

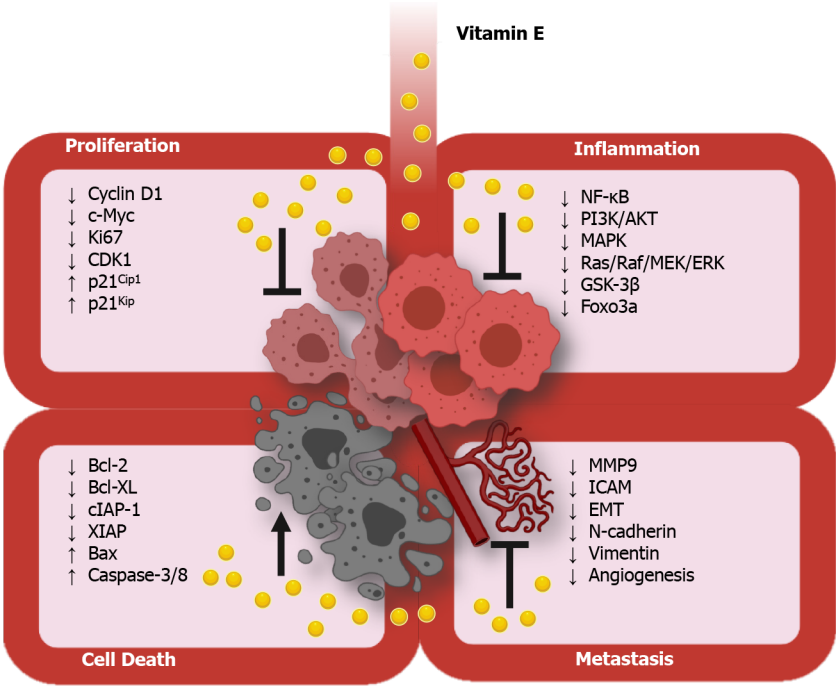

DOI: 10.4251/wjgo.v15.i6.943 **Copyright** ©The Author(s) 2023.

Figure 3 Role of vitamin E in modulating proliferation, cell death, inflammation and metastasis in pancreatic cancer. c-Myc: Cellular myelocytomatosis; CDK1: Cyclin-dependent kinase 1; Bcl-2: B-cell lymphoma 2; Bcl-xL: B-cell lymphoma-extra-large; cIAP-1: Cellular inhibitor of apoptosis protein-1; XIAP: X-linked inhibitor of apoptosis protein; Bax: Bcl-2 associated X protein; NF-κB: Nuclear factor kappa-light-chain-enhancer of activated B cells; PI3K: Phosphoinositide 3-kinase; AKT, Protein kinase B; MAPKL Microtubule-associated protein kinase; Ras/Raf/MEK/ERK: Rat sarcoma virus/rapidly accelerated fibrosarcoma/mitogen-activated protein kinase (MAPK) kinase/extracellular signal-regulated kinase; GSK-3β: Glycogen synthase kinase-3 beta; Foxo3a: Forkhead box transcription factor-3a; MMP9: Matrix metalloproteinase 9; ICAM-1, Intercellular adhesion molecule 1; EMT: Epithelial-to-mesenchymal tumor transition. The figure is created by author and generated using Biorender.com.

fortified food since the majority of the intake values are far below average[74]. As a result, the clinical safety and toxicity of vitamin E supplementation must be evaluated. Regrettably, there has been only a small number of conflicting reports on vitamin E safety evaluation in recent years[53,75-78]. For the present review, animal doses were translatable to human equivalent doses by multiplying the animal doses with a factor of 0.081 or 0.135 for mouse or hamster models, respectively, assuming a human adult's average weight is 60 kg[79]. In a meta-analysis by Miller *et al*[75], it was discovered that the elevated risk of death was only noticeable at a vitamin E dose of 2000 IU/d (1340 mg/d or 22.3 mg/kg), which is higher than the adult upper limit. According to El-Hak *et al*[76], subacute administration of 2000 mg/kg (324 mg/kg in humans) α-TP acetate for 30 d in male albino rats caused liver toxicity by altering the levels of alanine transaminase, aspartate transaminase, and the histological structure of the liver. However, no mortality or adverse reproductive effects was reported[76]. In contrast, female mice treated with 500 and 1000 mg/kg (40.5 and 81.08 mg/kg in humans) of palm vitamin E for 14 and 42 d had a higher bleeding and clotting time[77]. Serum creatinine and kidney weight were increased in these mice but no renal impairment was observed[77]. However, Kappus *et al*[78] noted that numerous scientifically credible studies consistently did not identify any significant negative effects related to α-TP supplementation at intakes up to 3200 IU/d (2144 mg/d or 35.7 mg/kg). A clinical trial recorded no adverse effects in pancreatic cancer patients treated with 3200 mg/d (53.33 mg/kg) of δ-TT[53]. More conclusive safety studies are warranted to investigate whether high-dose vitamin E is safe for humans.

One of the possible underlying reasons for variable efficacy and safety of vitamin E could be attributed to its poor oral bioavailability, particularly TTs[20,80]. In the mice given δ-TT (100 mg/kg for 6 wk), Husain *et al*[51] found that δ-TT was 10-fold more concentrated in the pancreas than in tumor, indicating that δ-TT may not be available for pancreatic tumor through oral administration. The pharmacokinetic limitation of TT is caused by its solubility, absorption, distribution, and rate of elimination[80]. In healthy human volunteers, the 24-hour area under the curve (0-∞) of TT rich fraction increased by roughly 2-fold in the fed state compared to the fasting state, showing that food consumption increased the absorption of vitamin E, thereby enhancing its bioavailability[81]. TTs reach their peak plasma concentration (Tmax) at 3-4 h after a meal but α-TP took 6 h to reach its Tmax[82]. However, α-TP achieved a higher peak plasma concentration compared to TTs (1.82-2.92 μM *vs* 0.89-1.92 μM, respectively)[82]. The elimination half-life (t1/2) of α-TP in humans ranged from 2.3 to 4.4 h for various TT isomers[83]. Therefore, TT supplementation is typically advised to be taken twice daily to maintain its bioactive levels[80]. This was used in most of the reviewed studies where TT was

administered twice daily to mice[39,42,43,47,48,50,51] and humans[53].

To address the issue of low bioavailability, researchers are altering or modifying the composition of TT isomers in a fraction, developing new emulsification with cyclodextrin, or constructing new nano-formulations such as nano-vesicles, solid-lipid nano-particles, nano-structured lipid carriers, nano-emulsions, and polymeric nano-particles[20,80]. However, very few studies have reported the bioavailability and toxicity profiles of nano-formulations[20,80]. Debele *et al*[35] illustrated that a nanoparticle-based drug delivery system using glutathione-sensitive micelle loaded with α-TP succinate (PAH-SS-PLGA-TOS), was more effective at increasing the cytotoxicity, apoptosis and G2/M cell cycle arrest in Pan02 pancreatic cancer cell compared to free α-TP succinate. The synergistic effects of the nano-formulated TOS in the study suggest that PAH-SS-PLGA micelles may be a good carrier for TOS, increasing the therapeutic potency of the compound[35]. Independently, Maniam *et al*[21] also showed the niosomes entrapped TT and gemcitabine can enhance activity of gemcitabine. More studies are therefore required to provide important insights into the various applications, toxicity, and pharmacokinetics of vitamin E formulations.

Limitations of the current preclinical and clinical models in evaluating the role of vitamin E in cancer

It is critical to select an appropriate cancer model to investigate the respective research hypothesis[84]. PDAC induced by nitroso-bis(2-oxopropyl) amine in the Syrian hamster shared common human genetic alteration including KRAS mutation. However, the development of concomitant malignancies in the liver and lung jeopardized this pancreatic cancer model[85]. Moreover, a rat-based PDAC model had a limited subset of tumor types and grades. Similar to other cancers, these limitations prompt the development of mouse xenograft and transgenic mouse models. These mouse models demonstrate a greater advantage given the animals' small size, lower cost, ease of breeding, short life span of 1-2 years, and ability to recapitulate genomic and pathological alteration in humans[84]. Only two studies used the *N*-nitrosobis(2-oxopropyl) amine-induced pancreatic cancer in Syrian hamsters[37,38]. Almost all animal studies reviewed used the subcutaneous[39,42,43] or orthotopic[41,48,51] tumor xenograft or transgenic[47,49,50] mouse model. Out of 291 registered trials under the search term 'vitamin E' (https://clinicaltrials.gov/; accessed on 22nd August 2022), only three trials were on pancreatic cancer. Two studies were conducted using multiple dosing δ-TT (NCT01450046) or single dosing (NCT01446952) in healthy humans. Only one study was conducted using δ-TT on patients with resectable pancreatic exocrine neoplasia (NCT00985777)[53]. Therefore, to better determine the effects of vitamin E for pancreatic cancer patients, we advocate for more studies using cutting edge genetical engineered mouse models[86-88], organoids[89,90] or organ-on-chip[91] to further evaluate the role of vitamin E in pancreatic cancer. A novel drug delivery system using a novel nanoformulation[20,80] or complex ion delivery system[54,92] may strengthen vitamin E's efficacy in cancer.

Considerations for clinical use of vitamin E as an anticancer treatment

Assuming a healthy adult is 60 kg in weight, the American Food and Nutrition Board recommends a daily upper limit of 1000 mg/day (or 16.67 mg/kg) of vitamin E[93]. The human equivalence dose (HED) of vitamin E used in hamsters (4-100 mg/kg) was only 0.54-8.1mg/kg, which is far from the adults' daily upper limit of 16.67 mg/kg. However, the HED doses in mice (200-400 mg/kg) were 16.216-32.43 mg/kg, which is approximate the adult's daily upper limit. Although 32.43 mg/kg exceeds the recommended intake for adults, Kappus and Diplock[78] noted that there was no significant negative effects associated with α-TP supplementation even up to 3200 IU/d (2144 mg/d or 35.7 mg/kg). Independently, Springett *et al*[53] also recorded no adverse effects in pancreatic cancer patients treated with 3200 mg/d (53.33 mg/kg) of δ-TT. All findings suggest that vitamin E could be a safe therapeutic agent even above the recommended daily intake.

Our review concluded α-TP supplementation failed to inhibit the growth of pancreatic carcinoma *in vivo*[37,38] and only suppressed the proliferation of pancreatic cancer cells growth at high doses[34-36]. None-the-less, mounting mechanistic and preclinical animal studies demonstrated that - and -TT have a significantly better pancreatic cancer-preventive activity than other forms of vitamin E. However, α-TP could reduce TT's antioxidant potential, impairs its anticancer effects and accelerates the breakdown of TT in the body[94,95]. As a result, it appears that TP-TT mixtures may not be efficient in preventing or treating pancreatic cancer. Furthermore, compared to -TT, -TT or gemcitabine alone, both - and -TT in combination with gemcitabine are more effective in the treatment of pancreatic cancer. - and -TT improve the antitumor efficacy of gemcitabine by inhibiting NF-κB, cell proliferation, and inducing apoptosis, implying that TT may be more effective as an adjuvant rather than a replacement for standard therapy in pancreatic cancer treatment.

LIMITATIONS OF THIS SCOPING REVIEW

We only considered articles that were indexed by PubMed and Scopus; therefore, studies published in non-indexed journals and grey literature may have been overlooked. Furthermore, no critical appraisal of evidence sources was performed since only a small number of papers were eligible for the review.

Future scoping review on the similar topic may include a critical appraisal when more peer-reviewed studies have been published.

To comprehend the molecular actions of vitamin E, only studies that focused on vitamin E or its isomers were included in this scoping review. In reality, vitamin E is present in many foods and it may interact with other nutrients to produce more complex pharmacokinetic and pharmacodynamic interactions. This aspect was not considered in the current study. Most studies did not compare the effect of vitamin E on cancer cells or tumors with standard therapy. We are not able to draw any conclusive remarks on this aspect as well. Thus, more thorough research is required to validate vitamin E as a clinical therapeutic option for PDAC.

CONCLUSION

Based on the available studies, vitamin E modulates proliferation, cell death, angiogenesis, metastasis and inflammation in pancreatic cancer cells (Figure 3). However, there are limited studies to address its safety concern and low bioavailability. Currently, available preclinical and clinical studies should be re-visited with a more in-depth analysis to further investigate the efficacy and safety of vitamin E in pancreatic cancer.

FOOTNOTES

Author contributions: Ekeuku SO, Etim EP, Pang KL, Chin KY, Mai CW were involved in the data collection and validation; Ekeuku SO, Etim EP provided the first draft of the manuscript; Ekeuku SO, Etim BP, Mai CW prepared the figures and tables; Ekeuku SO, Etim EP, Pang KL, Chin KY, Mai CW wrote and finalized the manuscript; Chin KY and Mai CW designed the outline and coordinated the writing of the paper.

Supported by Universiti Kebangsaan Malaysia Through Research University Grant, No. GUP-2020-021; and Shanghai Municipal Science and Technology Commission, No. 20WZ2504600.

Conflict-of-interest statement: All the authors report having no relevant conflicts of interest for this article.

Country/Territory of origin: Malaysia

ORCID number: Sophia Ogechi Ekeuku 0000-0002-5485-4592; Effiong Paul Etim 0000 0001 6437 8772; Kok-Lun Pang 0000-0003-2219-6297; Kok-Yong Chin 0000-0001-6628-1552; Chun-Wai Mai 0000-0001-6532-184X.

Corresponding Author's Membership in Professional Societies: Chinese Society for Cell Biology, S233103897M; European Association for Cancer Research, EACR27345; International Pharmaceutical Federation, 36982; Royal Society of Chemistry, 538435; Malaysian Pharmaceutical Society, 8141.

S-Editor: Liu GL
L-Editor: Filipodia
P-Editor: Liu GL

REFERENCES

1 **Hanahan D**. Hallmarks of Cancer: New Dimensions. *Cancer Discov* 2022; **12**: 31-46 [PMID: 35022204 DOI: 10.1158/2159-8290.CD-21-1059]
2 **Wood LD**, Canto MI, Jaffee EM, Simeone DM. Pancreatic Cancer: Pathogenesis, Screening, Diagnosis, and Treatment. *Gastroenterology* 2022; **163**: 386-402.e1 [PMID: 35398344 DOI: 10.1053/j.gastro.2022.03.056]
3 **Mai CW**, Kang YB, Pichika MR. Should a Toll-like receptor 4 (TLR-4) agonist or antagonist be designed to treat cancer? *Onco Targets Ther* 2013; **6**: 1573-1587 [PMID: 24235843 DOI: 10.2147/OTT.S50838]
4 **Looi CK**, Chung FF, Leong CO, Wong SF, Rosli R, Mai CW. Therapeutic challenges and current immunomodulatory strategies in targeting the immunosuppressive pancreatic tumor microenvironment. *J Exp Clin Cancer Res* 2019; **38**: 162 [PMID: 30987642 DOI: 10.1186/s13046-019-1153-8]
5 **Gan LL**, Hii LW, Wong SF, Leong CO, Mai CW. Molecular Mechanisms and Potential Therapeutic Reversal of Pancreatic Cancer-Induced Immune Evasion. *Cancers (Basel)* 2020; **12** [PMID: 32664564 DOI: 10.3390/cancers12071872]

6 **Looi CK**, Hii LW, Ngai SC, Leong CO, Mai CW. The Role of Ras-Associated Protein 1 (Rap1) in Cancer: Bad Actor or Good Player? *Biomedicines* 2020; **8** [PMID: 32906721 DOI: 10.3390/biomedicines8090334]

7 **Sim W**, Lim WM, Hii LW, Leong CO, Mai CW. Targeting pancreatic cancer immune evasion by inhibiting histone deacetylases. *World J Gastroenterol* 2022; **28**: 1934-1945 [PMID: 35664961 DOI: 10.3748/wjg.v28.i18.1934]

8 **Chen X**, Zeh HJ, Kang R, Kroemer G, Tang D. Cell death in pancreatic cancer: from pathogenesis to therapy. *Nat Rev Gastroenterol Hepatol* 2021; **18**: 804-823 [PMID: 34331036 DOI: 10.1038/s41575-021-00486-6]

9 **Hu JX**, Zhao CF, Chen WB, Liu QC, Li QW, Lin YY, Gao F. Pancreatic cancer: A review of epidemiology, trend, and risk factors. *World J Gastroenterol* 2021; **27**: 4298-4321 [PMID: 34366606 DOI: 10.3748/wjg.v27.i27.4298]

10 **Rawla P**, Sunkara T, Gaduputi V. Epidemiology of Pancreatic Cancer: Global Trends, Etiology and Risk Factors. *World J Oncol* 2019; **10**: 10-27 [PMID: 30834048 DOI: 10.14740/wjon1166]

11 **Kretz AL**, von Karstedt S, Hillenbrand A, Henne-Bruns D, Knippschild U, Trauzold A, Lemke J. Should We Keep Walking along the Trail for Pancreatic Cancer Treatment? *Cancers (Basel)* 2018; **10** [PMID: 29562636 DOI: 10.3390/cancers10030077]

12 **Palau VE**, Chakraborty K, Wann D, Lightner J, Hilton K, Brannon M, Stone W, Krishnan K. γ-Tocotrienol induces apoptosis in pancreatic cancer cells by upregulation of ceramide synthesis and modulation of sphingolipid transport. *BMC Cancer* 2018; **18**: 564 [PMID: 29769046 DOI: 10.1186/s12885-018-4462-y]

13 **Chen H**, Bian A, Yang LF, Yin X, Wang J, Ti C, Miao Y, Peng S, Xu S, Liu M, Qiu WW, Yi Z. Targeting STAT3 by a small molecule suppresses pancreatic cancer progression. *Oncogene* 2021; **40**: 1440-1457 [PMID: 33420372 DOI: 10.1038/s41388-020-01626-z]

14 **Patil K**, Khan FB, Akhtar S, Ahmad A, Uddin S. The plasticity of pancreatic cancer stem cells: implications in therapeutic resistance. *Cancer Metastasis Rev* 2021; **40**: 691-720 [PMID: 34453639 DOI: 10.1007/s10555-021-09979-x]

15 **Subramaniam D**, Kaushik G, Dandawate P, Anant S. Targeting Cancer Stem Cells for Chemoprevention of Pancreatic Cancer. *Curr Med Chem* 2018; **25**: 2585-2594 [PMID: 28137215 DOI: 10.2174/0929867324666170127095832]

16 **Jiang YL**, Zhang RC, Zhou YC. Comparison of overall survival and perioperative outcomes of laparoscopic pancreaticoduodenectomy and open pancreaticoduodenectomy for pancreatic ductal adenocarcinoma: a systematic review and meta-analysis. *BMC Cancer* 2019; **19**: 781 [PMID: 31391085 DOI: 10.1186/s12885-019-6001-x]

17 **Schultheis B**, Reuter D, Ebert MP, Siveke J, Kerkhoff A, Berdel WE, Hofheinz R, Behringer DM, Schmidt WE, Goker E, De Dosso S, Kneba M, Yalcin S, Overkamp F, Schlegel F, Dommach M, Rohrberg R, Steinmetz T, Bulitta M, Strumberg D. Gemcitabine combined with the monoclonal antibody nimotuzumab is an active first-line regimen in KRAS wildtype patients with locally advanced or metastatic pancreatic cancer: a multicenter, randomized phase IIb study. *Ann Oncol* 2017; **28**: 2429-2435 [PMID: 28961832 DOI: 10.1093/annonc/mdx343]

18 **Hii LW**, Lim SE, Leong CO, Chin SY, Tan NP, Lai KS, Mai CW. The synergism of Clinacanthus nutans Lindau extracts with gemcitabine: downregulation of anti-apoptotic markers in squamous pancreatic ductal adenocarcinoma. *BMC Complement Altern Med* 2019; **19**: 257 [PMID: 31521140 DOI: 10.1186/s12906-019-2663-9]

19 **Looi CK**, Gan LL, Sim W, Hii LW, Chung FF, Leong CO, Lim WM, Mai CW. Histone Deacetylase Inhibitors Restore Cancer Cell Sensitivity towards T Lymphocytes Mediated Cytotoxicity in Pancreatic Cancer. *Cancers (Basel)* 2022; **14** [PMID: 35954379 DOI: 10.3390/cancers14153709]

20 **Maniam G**, Mai CW, Zulkefeli M, Dufès C, Tan DM, Fu JY. Challenges and Opportunities of Nanotechnology as Delivery Platform for Tocotrienols in Cancer Therapy. *Front Pharmacol* 2018; **9**: 1358 [PMID: 30534071 DOI: 10.3389/fphar.2018.01358]

21 **Maniam G**, Mai CW, Zulkefeli M, Fu JY. Co-encapsulation of gemcitabine and tocotrienols in nanovesicles enhanced efficacy in pancreatic cancer. *Nanomedicine (Lond)* 2021; **16**: 373-389 [PMID: 33543651 DOI: 10.2217/nnm-2020-0374]

22 **Liew HS**, Mai CW, Zulkefeli M, Madheswaran T, Kiew LV, Pua LJW, Hii LW, Lim WM, Low ML. Novel Gemcitabine-Re(I) Bisquinolinyl Complex Combinations and Formulations With Liquid Crystalline Nanoparticles for Pancreatic Cancer Photodynamic Therapy. *Front Pharmacol* 2022; **13**: 903210 [PMID: 35873548 DOI: 10.3389/fphar.2022.903210]

23 **Meganathan P**, Mai CW, Selvaduray KR, Zainal Z, Fu JY. Effect of Carotenes against Oxidative Stress Induced Age-Related Macular Degeneration in Human Retinal Pigment Cells. *ACS Food Sci Tech* 2022; **2**: 1719-27 [DOI: 10.1021/acsfoodscitech.2c00205]

24 **Shyam S**, Greenwood D, Mai CW, Tan SS, Mohd Yusof BN, Moy FM, Cade J. Traditional and Novel Adiposity Indicators and Pancreatic Cancer Risk: Findings from the UK Women's Cohort Study. *Cancers (Basel)* 2021; **13** [PMID: 33801191 DOI: 10.3390/cancers13051036]

25 **Tham SY**, Loh HS, Mai CW, Fu JY. Tocotrienols Modulate a Life or Death Decision in Cancers. *Int J Mol Sci* 2019; **20** [PMID: 30654580 DOI: 10.3390/ijms20020372]

26 **Theodosis-Nobelos P**, Papagiouvannis G, Rekka EA. A Review on Vitamin E Natural Analogues and on the Design of Synthetic Vitamin E Derivatives as Cytoprotective Agents. *Mini Rev Med Chem* 2021; **21**: 10-22 [PMID: 32767937 DOI: 10.2174/1389557520666200807132617]

27 **Jiang Q**. Natural Forms of Vitamin E as Effective Agents for Cancer Prevention and Therapy. *Adv Nutr* 2017; **8**: 850-867 [PMID: 29141970 DOI: 10.3945/an.117.016329]

28 **Wong SK**, Kamisah Y, Mohamed N, Muhammad N, Masbah N, Fahami NAM, Mohamed IN, Shuid AN, Saad QM, Abdullah A, Mohamad NV, Ibrahim NI, Pang KL, Chow YY, Thong BKS, Subramaniam S, Chan CY, Ima-Nirwana S, Chin AK. Potential Role of Tocotrienols on Non-Communicable Diseases: A Review of Current Evidence. *Nutrients* 2020; **12** [PMID: 31963885 DOI: 10.3390/nu12010259]

29 **Moher D**, Liberati A, Tetzlaff J, Altman DG; PRISMA Group. Preferred reporting items for systematic reviews and meta-analyses: the PRISMA statement. *BMJ* 2009; **339**: b2535 [PMID: 19622551 DOI: 10.1136/bmj.b2535]

30 **Arksey H**, O'Malley L. Scoping studies: towards a methodological framework. *Int J Soc Res Methodol* 2005; **8**: 19-32 [DOI: 10.1080/1364557032000119616]

31 **Patacsil D**, Osayi S, Tran AT, Saenz F, Yimer L, Shajahan AN, Gokhale PC, Verma M, Clarke R, Chauhan SC, Kumar D. Vitamin E succinate inhibits survivin and induces apoptosis in pancreatic cancer cells. *Genes Nutr* 2012; **7**: 83-89 [PMID: 21842182 DOI: 10.1007/s12263-011-0242-x]

32 **Ohlsson B**, Albrechtsson E, Axelson J. Vitamins A and D but not E and K decreased the cell number in human pancreatic cancer cell lines. *Scand J Gastroenterol* 2004; **39**: 882-885 [PMID: 15513387 DOI: 10.1080/00365520410006701]

33 **Heisler T**, Towfigh S, Simon N, Liu C, McFadden DW. Peptide YY augments gross inhibition by vitamin E succinate of human pancreatic cancer cell growth. *J Surg Res* 2000; **88**: 23-25 [PMID: 10644462 DOI: 10.1006/jsre.1999.5775]

34 **Greco E**, Basso D, Fadi E, Padoan A, Fogar P, Zambon CF, Navaglia F, Bozzato D, Moz S, Pedrazzoli S, Plebani M. Analogs of vitamin E epitomized by alpha-tocopheryl succinate for pancreatic cancer treatment: *in vitro* results induce caution for *in vivo* applications. *Pancreas* 2010; **39**: 662-668 [PMID: 20562578 DOI: 10.1097/MPA.0b013e3181c8b48c]

35 **Debele TA**, Wu HC, Wu SR, Shan YS, Su WP. Combination Delivery of Alpha-Tocopheryl Succinate and Curcumin Using a GSH-Sensitive Micelle (PAH-SS-PLGA) to Treat Pancreatic Cancer. *Pharmaceutics* 2020; **12** [PMID: 32824299 DOI: 10.3390/pharmaceutics12080778]

36 **Blanchard JA 2nd**, Barve S, Joshi-Barve S, Talwalker R, Gates LK Jr. Antioxidants inhibit cytokine production and suppress NF-kappaB activation in CAPAN-1 and CAPAN-2 cell lines. *Dig Dis Sci* 2001; **46**: 2768-2772 [PMID: 11768272 DOI: 10.1023/a:1012795900871]

37 **Heukamp I**, Kilian M, Gregor JI, Neumann A, Jacobi CA, Guski H, Schimke I, Walz MK, Wenger FA. Effects of the antioxidative vitamins A, C and E on liver metastasis and intrametastatic lipid peroxidation in BOP-induced pancreatic cancer in Syrian hamsters. *Pancreatology* 2005; **5**: 403-409 [PMID: 15985764 DOI: 10.1159/000086541]

38 **Wenger FA**, Kilian M, Ridders J, Stahlknecht P, Schimke I, Guski H, Jacobi CA, Müller JM. Influence of antioxidative vitamins A, C and E on lipid peroxidation in BOP-induced pancreatic cancer in Syrian hamsters. *Prostaglandins Leukot Essent Fatty Acids* 2001; **65**: 165-171 [PMID: 11728167 DOI: 10.1054/plef.2001.0305]

39 **Husain K**, Francois RA, Yamauchi T, Perez M, Sebti SM, Malafa MP. Vitamin E δ-tocotrienol augments the antitumor activity of gemcitabine and suppresses constitutive NF-κB activation in pancreatic cancer. *Mol Cancer Ther* 2011; **10**: 2363-2372 [PMID: 21971120 DOI: 10.1158/1535-7163.MCT-11-0424]

40 **Shin-Kang S**, Ramsauer VP, Lightner J, Chakraborty K, Stone W, Campbell S, Reddy SA, Krishnan K. Tocotrienols inhibit AKT and ERK activation and suppress pancreatic cancer cell proliferation by suppressing the ErbB2 pathway. *Free Radic Biol Med* 2011; **51**: 1164-1174 [PMID: 21723941 DOI: 10.1016/j.freeradbiomed.2011.06.008]

41 **Kunnumakkara AB**, Sung B, Ravindran J, Diagaradjane P, Deorukhkar A, Dey S, Koca C, Yadav VR, Tong Z, Gelovani JG, Guha S, Krishnan S, Aggarwal BB. {Gamma}-tocotrienol inhibits pancreatic tumors and sensitizes them to gemcitabine treatment by modulating the inflammatory microenvironment. *Cancer Res* 2010; **70**: 8695-8705 [PMID: 20864511 DOI: 10.1158/0008-5472.CAN-10-2318]

42 **Francois RA**, Zhang A, Husain K, Wang C, Hutchinson S, Kongnyuy M, Batra SK, Coppola D, Sebti SM, Malafa MP. Vitamin E δ-tocotrienol sensitizes human pancreatic cancer cells to TRAIL-induced apoptosis through proteasome-mediated down-regulation of c-FLIP(s). *Cancer Cell Int* 2019; **19**: 189 [PMID: 31367187 DOI: 10.1186/s12935-019-0876-0]

43 **Hodul PJ**, Dong Y, Husain K, Pimiento JM, Chen J, Zhang A, Francois R, Pledger WJ, Coppola D, Sebti SM, Chen DT, Malafa MP. Vitamin E δ-tocotrienol induces p27(Kip1)-dependent cell-cycle arrest in pancreatic cancer cells *via* an E2F-1-dependent mechanism. *PLoS One* 2013; **8**: e52526 [PMID: 23393547 DOI: 10.1371/journal.pone.0052526]

44 **Hussein D**, Mo H. d-δ-Tocotrienol-mediated suppression of the proliferation of human PANC-1, MIA PaCa-2, and BxPC-3 pancreatic carcinoma cells. *Pancreas* 2009; **38**: e124-e136 [PMID: 19346993 DOI: 10.1097/MPA.0b013e3181a20f9c]

45 **Qureshi AA**, Zuvanich EG, Khan DA, Mushtaq S, Silswal N, Qureshi N. Proteasome inhibitors modulate anticancer and anti-proliferative properties *via* NF-kB signaling, and ubiquitin-proteasome pathways in cancer cell lines of different organs. *Lipids Health Dis* 2018; **17**: 62 [PMID: 29606130 DOI: 10.1186/s12944-018-0697-5]

46 **Eitsuka T**, Tatewaki N, Nishida H, Kurata T, Nakagawa K, Miyazawa T. Synergistic inhibition of cancer cell proliferation with a combination of δ-tocotrienol and ferulic acid. *Biochem Biophys Res Commun* 2014; **453**: 606-611 [PMID: 25285637 DOI: 10.1016/j.bbrc.2014.09.126]

47 **Wang C**, Husain K, Zhang A, Centeno BA, Chen DT, Tong Z, Sebti SM, Malafa MP. EGR-1/Bax pathway plays a role in vitamin E δ-tocotrienol-induced apoptosis in pancreatic cancer cells. *J Nutr Biochem* 2015; **26**: 797-807 [PMID: 25997867 DOI: 10.1016/j.jnutbio.2015.02.008]

48 **Husain K**, Centeno BA, Coppola D, Trevino J, Sebti SM, Malafa MP. δ-Tocotrienol, a natural form of vitamin E, inhibits pancreatic cancer stem-like cells and prevents pancreatic cancer metastasis. *Oncotarget* 2017; **8**: 31554-31567 [PMID: 28404939 DOI: 10.18632/oncotarget.15767]

49 **Husain K**, Centeno BA, Chen DT, Hingorani SR, Sebti SM, Malafa MP. Vitamin E δ-tocotrienol prolongs survival in the LSL-KrasG12D/+;LSL-Trp53R172H/+;Pdx-1-Cre (KPC) transgenic mouse model of pancreatic cancer. *Cancer Prev Res (Phila)* 2013; **6**: 1074-1083 [PMID: 23963802 DOI: 10.1158/1940-6207.CAPR-13-0157]

50 **Husain K**, Centeno BA, Chen DT, Fulp WJ, Perez M, Zhang Lee G, Luetteke N, Hingorani SR, Sebti SM, Malafa MP. Prolonged survival and delayed progression of pancreatic intraepithelial neoplasia in LSL-KrasG12D/+;Pdx-1-Cre mice by vitamin E δ-tocotrienol. *Carcinogenesis* 2013; **34**: 858-863 [PMID: 23302291 DOI: 10.1093/carcin/bgt002]

51 **Husain K**, Francois RA, Hutchinson SZ, Neuger AM, Lush R, Coppola D, Sebti S, Malafa MP. Vitamin E delta-tocotrienol levels in tumor and pancreatic tissue of mice after oral administration. *Pharmacology* 2009; **83**: 157-163 [PMID: 19142032 DOI: 10.1159/000190792]

52 **Abu-Fayyad A**, Nazzal S. Extraction of Vitamin E Isomers from Palm Oil: Methodology, Characterization, and in Vitro Anti-Tumor Activity. *J Am Oil Chem Soc* 2017; **94**: 1209-1217 [PMID: 33518766 DOI: 10.1007/s11746-017-3025-8]

53 **Springett GM**, Husain K, Neuger A, Centeno B, Chen DT, Hutchinson TZ, Lush RM, Sebti S, Malafa MP. A Phase I Safety, Pharmacokinetic, and Pharmacodynamic Presurgical Trial of Vitamin E δ-tocotrienol in Patients with Pancreatic Ductal Neoplasia. *EBioMedicine* 2015; **2**: 1987-1995 [PMID: 26844278 DOI: 10.1016/j.ebiom.2015.11.025]

54 **Liew HS**, Mai CW, Zulkefeli M, Madheswaran T, Kiew LV, Delsuc N, Low ML. Recent Emergence of Rhenium(I) Tricarbonyl Complexes as Photosensitisers for Cancer Therapy. *Molecules* 2020; **25** [PMID: 32932573 DOI: 10.3390/molecules25184176]

55 **Soo HC**, Chung FF, Lim KH, Yap VA, Bradshaw TD, Hii LW, Tan SH, See SJ, Tan YF, Leong CO, Mai CW.

Cudraflavone C Induces Tumor-Specific Apoptosis in Colorectal Cancer Cells through Inhibition of the Phosphoinositide 3-Kinase (PI3K)-AKT Pathway. *PLoS One* 2017; **12**: e0170551 [PMID: 28107519 DOI: 10.1371/journal.pone.0170551]

56 **Mai CW**, Yaeghoobi M, Abd-Rahman N, Kang YB, Pichika MR. Chalcones with electron-withdrawing and electron-donating substituents: anticancer activity against TRAIL resistant cancer cells, structure-activity relationship analysis and regulation of apoptotic proteins. *Eur J Med Chem* 2014; **77**: 378-387 [PMID: 24675137 DOI: 10.1016/j.ejmech.2014.03.002]

57 **Er JL**, Goh PN, Lee CY, Tan YJ, Hii LW, Mai CW, Chung FF, Leong CO. Identification of inhibitors synergizing gemcitabine sensitivity in the squamous subtype of pancreatic ductal adenocarcinoma (PDAC). *Apoptosis* 2018; **23**: 343-355 [PMID: 29740790 DOI: 10.1007/s10495-018-1459-6]

58 **Mai CW**, Kang YB, Nadarajah VD, Hamzah AS, Pichika MR. Drug-like dietary vanilloids induce anticancer activity through proliferation inhibition and regulation of bcl-related apoptotic proteins. *Phytother Res* 2018; **32**: 1108-1118 [PMID: 29464796 DOI: 10.1002/ptr.6051]

59 **Gilmore TD**. NF-κB and Human Cancer: What Have We Learned over the Past 35 Years? *Biomedicines* 2021; **9** [PMID: 34440093 DOI: 10.3390/biomedicines9080889]

60 **Hou J**, Karin M, Sun B. Targeting cancer-promoting inflammation - have anti-inflammatory therapies come of age? *Nat Rev Clin Oncol* 2021; **18**: 261-279 [PMID: 33469195 DOI: 10.1038/s41571-020-00459-9]

61 **Silke J**, O'Reilly LA. NF-κB and Pancreatic Cancer; Chapter and Verse. *Cancers (Basel)* 2021; **13** [PMID: 34572737 DOI: 10.3390/cancers13184510]

62 **Leinwand J**, Miller G. Regulation and modulation of antitumor immunity in pancreatic cancer. *Nat Immunol* 2020; **21**: 1152-1159 [PMID: 32807942 DOI: 10.1038/s41590-020-0761-y]

63 **Kinsey CG**, Camolotto SA, Boespflug AM, Guillen KP, Foth M, Truong A, Schuman SS, Shea JE, Seipp MT, Yap JT, Burrell LD, Lum DH, Whisenant JR, Gilcrease GW 3rd, Cavalieri CC, Rehbein KM, Cutler SL, Affolter KE, Welm AL, Welm BE, Scaife CL, Snyder EL, McMahon M. Protective autophagy elicited by RAF→MEK→ERK inhibition suggests a treatment strategy for RAS-driven cancers. *Nat Med* 2019; **25**: 620-627 [PMID: 30833748 DOI: 10.1038/s41591-019-0367-9]

64 **Luo J**. KRAS mutation in pancreatic cancer. *Semin Oncol* 2021; **48**: 10-18 [PMID: 33676749 DOI: 10.1053/j.seminoncol.2021.02.003]

65 **Muzumdar MD**, Chen PY, Dorans KJ, Chung KM, Bhutkar A, Hong E, Noll EM, Sprick MR, Trumpp A, Jacks T. Survival of pancreatic cancer cells lacking KRAS function. *Nat Commun* 2017; **8**: 1090 [PMID: 29061961 DOI: 10.1038/s41467-017-00942-5]

66 **Murthy D**, Attri KS, Singh PK. Phosphoinositide 3-Kinase Signaling Pathway in Pancreatic Ductal Adenocarcinoma Progression, Pathogenesis, and Therapeutics. *Front Physiol* 2018; **9**: 335 [PMID: 29670543 DOI: 10.3389/fphys.2018.00335]

67 **Mollinedo F**, Gajate C. Novel therapeutic approaches for pancreatic cancer by combined targeting of RAF→MEK→ERK signaling and autophagy survival response. *Ann Transl Med* 2019; **7**: S153 [PMID: 31576360 DOI: 10.21037/atm.2019.06.40]

68 **Zuazo-Gaztelu I**, Casanovas O. Unraveling the Role of Angiogenesis in Cancer Ecosystems. *Front Oncol* 2018; **8**: 248 [PMID: 30013950 DOI: 10.3389/fonc.2018.00248]

69 **Hasan SS**, Fischer A. Notch Signaling in the Vasculature: Angiogenesis and Angiocrine Functions. *Cold Spring Harb Perspect Med* 2023; **13** [PMID: 35667708 DOI: 10.1101/cshperspect.a041166]

70 **Venkatesh V**, Nataraj R, Thangaraj GS, Karthikeyan M, Gnanasekaran A, Kaginelli SB, Kuppanna G, Kallappa CG, Basalingappa KM. Targeting Notch signalling pathway of cancer stem cells. *Stem Cell Investig* 2018; **5**: 5 [PMID: 29682512 DOI: 10.21037/sci.2018.02.02]

71 **Gerashchenko TS**, Novikov NM, Krakhmal NV, Zolotaryova SY, Zavyalova MV, Cherdyntseva NV, Denisov EV, Perelmuter VM. Markers of Cancer Cell Invasion: Are They Good Enough? *J Clin Med* 2019; **8** [PMID: 31344926 DOI: 10.3390/jcm8081092]

72 **Smart JA**, Oleksak JE, Hartsough EJ. Cell Adhesion Molecules in Plasticity and Metastasis. *Mol Cancer Res* 2021; **19**: 25-37 [PMID: 33004622 DOI: 10.1158/1541-7786.MCR-20-0595]

73 **Pastushenko I**, Blanpain C. EMT Transition States during Tumor Progression and Metastasis. *Trends Cell Biol* 2019; **29**: 212-226 [PMID: 30594349 DOI: 10.1016/j.tcb.2018.12.001]

74 **Péter S**, Eggersdorfer M, Weber P. Vitamin E Intake and Serum Levels in the General Population: A Global Perspective. In: Weber P, Birringer M, Blumberg JB, Eggersdorfer M, Frank J, editors. Vitamin E in Human Health. Springer International Publishing; 2019. 175-88 [DOI: 10.1007/978-3-030-05315-4_13]

75 **Miller ER 3rd**, Pastor-Barriuso R, Dalal D, Riemersma RA, Appel LJ, Guallar E. Meta-analysis: high-dosage vitamin E supplementation may increase all-cause mortality. *Ann Intern Med* 2005; **142**: 37-46 [PMID: 15537682 DOI: 10.7326/0003-4819-142-1-200501040-00110]

76 **El-Hak HNG**, ELaraby EE, Hassan AK, Abbas OA. Study of the toxic effect and safety of vitamin E supplement in male albino rats after 30 days of repeated treatment. *Heliyon* 2019; **5**: e02645 [PMID: 31667433 DOI: 10.1016/j.heliyon.2019.e02645]

77 **Ima-Nirwana S**, Nurshazwani Y, Nazrun A, Norliza M, Norazlina M. Subacute and Subchronic Toxicity Studies of Palm Vitamin E in Mice. *J Pharmacol Toxicol* 2011; **6**: 166-73 [DOI: 10.3923/jpt.2011.166.173]

78 **Kappus H**, Diplock AT. Tolerance and safety of vitamin E: a toxicological position report. *Free Radic Biol Med* 1992; **13**: 55-74 [PMID: 1628854 DOI: 10.1016/0891-5849(92)90166-e]

79 **Nair AB**, Jacob S. A simple practice guide for dose conversion between animals and human. *J Basic Clin Pharm* 2016; **7**: 27-31 [PMID: 27057123 DOI: 10.4103/0976-0105.177703]

80 **Mohd Zaffarin AS**, Ng SF, Ng MH, Hassan H, Alias E. Pharmacology and Pharmacokinetics of Vitamin E: Nanoformulations to Enhance Bioavailability. *Int J Nanomedicine* 2020; **15**: 9961-9974 [PMID: 33324057 DOI: 10.2147/IJN.S276355]

81 **Yap SP**, Yuen KH, Wong JW. Pharmacokinetics and bioavailability of alpha-, gamma- and delta-tocotrienols under

different food status. *J Pharm Pharmacol* 2001; **53**: 67-71 [PMID: 11206194 DOI: 10.1211/0022357011775208]

82 **Qureshi AA**, Khan DA, Silswal N, Saleem S, Qureshi N. Evaluation of Pharmacokinetics, and Bioavailability of Higher Doses of Tocotrienols in Healthy Fed Humans. *J Clin Exp Cardiolog* 2016; **7** [PMID: 27493840 DOI: 10.4172/2155-9880.1000434]

83 **Mahipal A**, Klapman J, Vignesh S, Yang CS, Neuger A, Chen DT, Malafa MP. Pharmacokinetics and safety of vitamin E δ-tocotrienol after single and multiple doses in healthy subjects with measurement of vitamin E metabolites. *Cancer Chemother Pharmacol* 2016; **78**: 157-165 [PMID: 27278668 DOI: 10.1007/s00280-016-3048-0]

84 **Mai CW**, Chin KY, Foong LC, Pang KL, Yu B, Shu Y, Chen S, Cheong SK, Chua CW. Modeling prostate cancer: What does it take to build an ideal tumor model? *Cancer Lett* 2022; **543**: 215794 [PMID: 35718268 DOI: 10.1016/j.canlet.2022.215794]

85 **Bisht S**, Feldmann G. Animal models for modeling pancreatic cancer and novel drug discovery. *Expert Opin Drug Discov* 2019; **14**: 127-142 [PMID: 30657339 DOI: 10.1080/17460441.2019.1566319]

86 **da Silva L**, Jiang J, Perkins C, Atanasova KR, Bray JK, Bulut G, Azevedo-Pouly A, Campbell-Thompson M, Yang X, Hakimjavadi H, Chamala S, Ratnayake R, Gharaibeh RZ, Li C, Luesch H, Schmittgen TD. Pharmacological inhibition and reversal of pancreatic acinar ductal metaplasia. *Cell Death Discov* 2022; **8**: 378 [PMID: 36055991 DOI: 10.1038/s41420-022-01165-4]

87 **Baslan T**, Morris JP 4th, Zhao Z, Reyes J, Ho YJ, Tsanov KM, Bermeo J, Tian S, Zhang S, Askan G, Yavas A, Lecomte N, Erakky A, Varghese AM, Zhang A, Kendall J, Ghiban E, Chorbadjiev L, Wu J, Dimitrova N, Chadalavada K, Nanjangud GJ, Bandlamudi C, Gong Y, Donoghue MTA, Socci ND, Krasnitz A, Notta F, Leach SD, Iacobuzio-Donahue CA, Lowe SW. Ordered and deterministic cancer genome evolution after p53 loss. *Nature* 2022; **608**: 795-802 [PMID: 35978189 DOI: 10.1038/s41586-022-05082-5]

88 **Shankar S**, Tien JC, Siebenaler RF, Chugh S, Dommeti VL, Zelenka-Wang S, Wang XM, Apel IJ, Waninger J, Eyunni S, Xu A, Mody M, Goodrum A, Zhang Y, Tesmer JJ, Mannan R, Cao X, Vats P, Pitchiaya S, Ellison SJ, Shi J, Kumar-Sinha C, Crawford HC, Chinnaiyan AM. An essential role for Argonaute 2 in EGFR-KRAS signaling in pancreatic cancer development. *Nat Commun* 2020; **11**: 2817 [PMID: 32499547 DOI: 10.1038/s41467-020-16309-2]

89 **Shi X**, Li Y, Yuan Q, Tang S, Guo S, Zhang Y, He J, Zhang X, Han M, Liu Z, Zhu Y, Gao S, Wang H, Xu X, Zheng K, Jing W, Chen L, Wang Y, Jin G, Gao D. Integrated profiling of human pancreatic cancer organoids reveals chromatin accessibility features associated with drug sensitivity. *Nat Commun* 2022; **13**: 2169 [PMID: 35449156 DOI: 10.1038/s41467-022-29857-6]

90 **Beato F**, Reverón D, Dezsi KB, Ortiz A, Johnson JO, Chen DT, Ali K, Yoder SJ, Jeong D, Malafa M, Hodul P, Jiang K, Centeno BA, Abdalah MA, Balasi JA, Tassielli AF, Sarcar B, Teer JK, DeNicola GM, Permuth JB, Fleming JB. Establishing a living biobank of patient-derived organoids of intraductal papillary mucinous neoplasms of the pancreas. *Lab Invest* 2021; **101**: 204-217 [PMID: 33037322 DOI: 10.1038/s41374-020-00494-1]

91 **Haque MR**, Wessel CR, Leary DD, Wang C, Bhushan A, Bishehsari F. Patient-derived pancreatic cancer-on-a-chip recapitulates the tumor microenvironment. *Microsyst Nanoeng* 2022; **8**: 36 [PMID: 35450328 DOI: 10.1038/s41378-022-00370-6]

92 **Sharma H**, Chaudhary S, Nirwan S, Kakkar R, Liew HS, Low ML, Mai CW, Hii LW, Leong CO, Daisy Milton M. N, N'-Disubstituted Benzimidazolium Salts: Synthesis, Characterization, Micromolar Detection of Fe(III) ions in Aqueous system, Biological Evaluation and Molecular Docking Studies. *ChemistrySelect* 2022; **7**: e202203239 [DOI: 10.1002/slct.202203239]

93 **Monsen ER**. Dietary reference intakes for the antioxidant nutrients: vitamin C, vitamin E, selenium, and carotenoids. *J Am Diet Assoc* 2000; **100**: 637-640 [PMID: 10863565 DOI: 10.1016/S0002-8223(00)00189-9]

94 **Shibata A**, Nakagawa K, Sookwong P, Tsuduki T, Asai A, Miyazawa T. alpha-Tocopherol attenuates the cytotoxic effect of delta-tocotrienol in human colorectal adenocarcinoma cells. *Biochem Biophys Res Commun* 2010; **397**: 214-219 [PMID: 20493172 DOI: 10.1016/j.bbrc.2010.05.087]

95 **Sontag TJ**, Parker RS. Influence of major structural features of tocopherols and tocotrienols on their omega-oxidation by tocopherol-omega-hydroxylase. *J Lipid Res* 2007; **48**: 1090-1098 [PMID: 17284776 DOI: 10.1194/jlr.M600514-JLR200]

World Journal of Gastrointestinal Oncology

Submit a Manuscript: https://www.f6publishing.com

World J Gastrointest Oncol 2023 June 15; 15(6): 959-972

DOI: 10.4251/wjgo.v15.i6.959

ISSN 1948-5204 (online)

MINIREVIEWS

Paradigm shift of chemotherapy and systemic treatment for biliary tract cancer

Wattana Leowattana, Tawithep Leowattana, Pathomthep Leowattana

Specialty type: Oncology

Provenance and peer review: Invited article; Externally peer reviewed.

Peer-review model: Single blind

Peer-review report's scientific quality classification

Grade A (Excellent): 0
Grade B (Very good): B, B, B
Grade C (Good): 0
Grade D (Fair): 0
Grade E (Poor): 0

P-Reviewer: Govindarajan KK, India; Hori T, Japan; Roy S, United States

Received: January 26, 2023
Peer-review started: January 26, 2023
First decision: April 11, 2023
Revised: April 14, 2023
Accepted: May 5, 2023
Article in press: May 5, 2023
Published online: June 15, 2023

Wattana Leowattana, Pathomthep Leowattana, Department of Clinical Tropical Medicine, Faculty of Tropical Medicine, Mahidol University, Rachatawee 10400, Bangkok, Thailand

Tawithep Leowattana, Department of Medicine, Faculty of Medicine, Srinakharinwirot University, Wattana 10110, Bangkok, Thailand

Corresponding author: Wattana Leowattana, BMed, MD, MSc, PhD, Full Professor, Department of Clinical Tropical Medicine, Faculty of Tropical Medicine, Mahidol University, 420/6 Rajavithi Road, Rachatawee 10400, Bangkok, Thailand. wattana.leo@mahidol.ac.th

Abstract

Biliary tract cancers (BTC) are frequently identified at late stages and have a poor prognosis due to limited systemic treatment regimens. For more than a decade, the combination of gemcitabine and cis-platin has served as the first-line standard treatment. There are few choices for second-line chemo-therapy. Targeted treatment with fibroblast growth factor receptor 2 inhibitors, neurotrophic tyrosine receptor kinase inhibitors, and isocitrate dehydrogenase 1 inhibitors has had important results. Immune checkpoint inhibitors (ICI) such as pembrolizumab are only used in first-line treatment for microsatellite instability high patients. The TOPAZ-1 trial's outcome is encouraging, and there are several trials underway that might soon put targeted treatment and ICI combos into first-line options. Newer targets and agents for existing goals are being studied, which may represent a paradigm shift in BTC management. Due to a scarcity of targetable mutations and the higher toxicity profile of the current medications, the new category of drugs may occupy a significant role in BTC therapies.

Key Words: Biliary tract cancers; Gemcitabine and cisplatin combination; Fibroblast growth factor receptor 2 inhibitors; Isocitrate dehydrogenase 1 inhibitors; Neurotrophic tyrosine receptor kinase gene fusion inhibitors; Immune checkpoint inhibitors; Microsatellite instability high; Infrigatinib; Pemigatinib

Core Tip: There have been several developments in the field of advanced biliary tract cancer (BTC) therapy in recent years. First, the care of these hepatobiliary malignancies has improved as a result of better knowledge of the molecular basis of BTC. The Food and Drug Administration's approval of pemigatinib, infigratinib, and ivosidenib for fibroblast growth factor receptor 2-rearranged and isocitrate dehydrogenase 1-mutant cholangiocarcinoma illustrates the paradigm shift that the arrival of targeted agents has really brought about. Second, patients receiving modified fluorouracil, oxaliplatin, and liposomal irinotecan with fluorouracil-leucovorin, respectively, as second-line treatments after progressing to first-line cisplatin-gemcitabine, showed an overall survival advantage in the newly released Advanced Biliary Tract Cancer-06 and NIFTY studies.

Citation: Leowattana W, Leowattana T, Leowattana P. Paradigm shift of chemotherapy and systemic treatment for biliary tract cancer. *World J Gastrointest Oncol* 2023; 15(6): 959-972
URL: https://www.wjgnet.com/1948-5204/full/v15/i6/959.htm
DOI: https://dx.doi.org/10.4251/wjgo.v15.i6.959

INTRODUCTION

The term "biliary tract cancers" (BTCs) refers to a group of aggressive and invasive hepatobiliary tumors that include ampulla of Vater cancer (AVC), gallbladder carcinoma (GBC), perihilar cholangiocarcinoma (pCCA), distal cholangiocarcinoma (dCCA), and intrahepatic cholangiocarcinoma (iCCA). The anatomical location of iCCA is within the biliary tree, whereas dCCA and pCCA, which are sometimes combined under the term extrahepatic cholangiocarcinoma (eCCA), originate outside the liver[1-3]. Between BTC subgroups and geographical areas, incidence and causes differ. In high-income nations, the incidence of CCA is modest (between 0.35 and 2 cases per 100000 people), but it can be up to 40 times higher in areas of Thailand and China where the disease is endemic. The incidence of iCCA is increasing in high-income countries. Statistics from the United Kingdom, the United States, and other countries show a consistent and steady growth in incidence from 0.1 to 0.6 instances per 100000 people during the last 30 years[4-6]. Hepatitis B and C infection, primary sclerosing cholangitis, liver fluke infections, liver cirrhosis, hepatolithiasis, Caroli's disease, obesity-associated liver disease, and diabetes are risk factors that have historically been associated to the development of BTC. It should be highlighted that the epidemiological disparities in the occurrence of different BTC types worldwide are also reflected in these risk variables[7-9]. The median overall survival (OS) for BTCs is 12 mo. Depending on stage, the 5-year relative survival rate for iCCA is from 9% to 25%, for eCCA it is between 10% and 15%, and for GBC it is between 15% and 35%[10,11]. The basic principle of curative therapy is radical surgery with negative margins; patients with early-stage illness, however, usually show no symptoms. Regrettably, the majority of BTC patients present with advanced BTC, with just a tiny fraction of BTCs being identified with a resectable condition[12,13]. The current gold standard for first-line treatment is still combined chemotherapy (CT) with gemcitabine and cisplatin (Gem/Cis) and second-line leucovorin (LV) calcium (folinic acid), fluorouracil, and oxaliplatin (FOLFOX)[14,15]. However, there is no solid data concerning what to do next following the poor prognosis of chemotherapeutic treatment. The BTC landscape has recently witnessed the introduction of innovative medicines, including targeted medications like pemigatinib, infigratinib, and ivosidenib. Additionally, a number of cutting-edge therapies are being evaluated and have the potential to alter the therapeutic picture for these cancers, including immune checkpoint inhibitors (ICIs), either alone or in combination with other anticancer medicines[16-19]. In this review, we summarized recent clinical data on CT, targeted treatments, ICIs, and immunotherapy in the context of systemic treatment for BTCs.

CHEMOTHERAPY

First-line CT

Based on the outcomes of the Japanese BT22 Phase 2 and the Advanced Biliary Tract Cancer (ABC-02) Phase 3 studies, which showed that this combination was superior to gemcitabine alone, Gem/Cis is presently the recommended first-line treatment for patients with advanced BTC (aBTC)[14,20]. The results of this ground-breaking trial reported by Valle *et al*[21] showed that the combination of cisplatin and gemcitabine was associated with a longer median OS [11.7 mo *vs* 8.1 mo, HR: 0.64, 95% confidence interval (CI): 0.52-0.80; $P < 0.001$] and median progression-free survival (PFS) (8.0 mo *vs* 5.0 mo) compared with gemcitabine alone. Similar advantages of cisplatin-gemcitabine vs. gemcitabine monotherapy were also shown in the phase 2 BT22 study for Asian patients[22]. The efficacy of many combination CT treatments has been studied over the past ten years, including the triplet-agent

regimen, which combines Gem, Cis, and nab-paclitaxel (nab-P), and which has shown positive clinical results. Particularly, OS and PFS had medians of 19.2 and 11.8 mo, respectively[23,24]. In the real-world situation, Cheon *et al*[25] conducted a retrospective analysis in 178 Asian patients with advanced BTC to evaluate the treatment outcomes of Gem/Cis/nab-P. Gem/Cis/nab-P was administered as the initial course of treatment to 117 (65.7%) patients, whereas gemcitabine-based CT with nab-P was administered to 61 (34.3%) patients. The total objective response rate (ORR) for all patients was 42.1%, with a disease control rate (DCR) of 84.8%. In Korean patients with advanced BTC, they discovered that Gem/Cis/nab-P had positive real-life effectiveness and safety results that were consistent with the findings of the phase II study. However, Jung *et al*[26] evaluated the efficacy of triplet and normal doublet CT in a real-world scenario of 68 BTC patients and discovered that Gem/Cis/nab-P treatment did not increase PFS or OS compared to regular CT in patients with advanced BTC. They recommended that sizable randomized controlled studies are necessary to examine the advantages of triplet CT in advanced BTC.

A French team recently compared 5-fluorouracil (5-FU), oxaliplatin, irinotecan, and leucovorin (FOLFIRINOX) with the standard of care (SOC). One hundred and ninety-one patients with locally advanced or metastatic BTCs were randomized to receive either Gem/Cis for a maximum of 6 mo or infusional 5-FU without bolus, oxaliplatin, and irinotecan [modified FOLFIRINOX (mFOLFIRINOX)]. The study's primary OS endpoint was not met; the SOC in the first-line scenario was maintained with a median OS of 11.7 mo for mFOLFIRINOX and 13.8 mo for the Gem/Cis arm[27]. The development of S-1 in conjunction with platinum is ongoing in this line for BTC. In a phase 3 randomized controlled trial, the FUGA-BT study comprised 354 CT-unexperienced patients with recurrent or unresectable BTC with an ECOG of 0 or 1. OS is the primary endpoint of the non-inferiority study FUGA-BT, which compares Gem/S-1 to Gem/Cis. In Japanese patients, CT based on Gem/S-1 was not inferior to Gem/Cis. Patients allocated to the Gem/Cis group had a median OS of 13.4 mo, whereas those assigned to the S1-gemcitabine group had a median OS of 15.1 mo. Overall, there was good tolerability of the side effects, which did not substantially differ across treatment arms[28]. Recently, Ioka *et al*[29] conducted a multicenter, randomized phase 3 trial in 246 patients from 39 medical centers in Japan. Patients who had been enrolled were randomly assigned (1:1) to the Gem/Cis/S-1 (GCS) or Gem/Cis arm. The GCS regimen included 80 mg/m^2 of S-1 on days 1 through 7 every 2 wk, as well as infusions of cisplatin (25 mg/m^2) and gemcitabine (1000 mg/m^2) on day 1. OS was the main outcome, whereas PFS, ORR, and adverse events (AEs) were the secondary endpoints. They discovered that the median OS and 1-year OS rates in the GCS arm were 13.5 mo and 59.4%, respectively, whereas in the GC arm they were 12.6 mo and 53.7%. In the GCS arm, the median PFS was 7.4 mo, whereas in the GC arm, it was 5.5 mo. RR in the GCS arm was 41.5%, compared to 15.0% in the GC arm. AEs with a grade of 3 or below did not reveal any appreciable variations between the two arms. They stated that GCS may become the new first-line SOC for advanced BTC because it was the first regimen to show survival advantages as well as a higher RR than GC in a randomized phase 3 study (Figure 1).

Second-line CT

Combination regimens utilizing fluoropyrimidines, platinum salts, and other chemotherapies have been evaluated for the second-line situation. Results from a second-line randomized phase 3 trial were recently published. A United Kingdom population with locally advanced or metastatic BTC after progressing to first-line Gem/Cis CT with an ECOG 0-1 was involved in the open-label, phase 3 ABC-06 clinical research. The treatment of active symptom management plus FOLFOX or active symptom control alone was randomly allocated to 162 patients. Oxaliplatin (85 mg/m^2) was administered as a 2-h infusion on day 1 of the FOLFOX CT regimen, followed by a 2-h infusion of LV (175 mg/m^2/day), a 5-FU bolus (400 mg/m^2/day), and a 46-h infusion of 5-FU (2400 mg/m^2) every two weeks. OS among the population who were being treated intentionally was the main result. With 6.2 mo as opposed to 5.3 mo in the control group, FOLFOX slightly increased the median OS. Compared to 39% of patients in the control arm, 59% of patients in the experimental arm had grade 3/4 toxicities, such as fatigue and neutropenia. All subtypes of BTC tumors improved equally after FOLFOX in the subgroup study[30]. Patients who received FOLFOX as second-line treatment had a clinically significant increase in OS rates at 6 and 12 mo, despite the small absolute median OS difference between the two groups, and the study has produced clinical data for the first time in this context (Figure 1). For advanced BTCs, more cutting-edge CT regimens are being investigated in the second-line setting. A phase 2 study assigned 120 patients to either modified fluorouracil, and oxaliplatin (mFOLFOX) (5-FU 2400 mg/m^2 over 46 h, LV 100 mg/m^2 over 2 h, and oxaliplatin 100 mg/m^2 over 2 h, every 2 wk) or mFOLFIRI (5-FU 2400 mg/m^2 over 46 h, LV 100 mg/m^2 over 2 h, and irinotecan 150 mg/m^2 over 2 h, every 2 wk). The mFOLFOX group had a higher median OS (6.6 mo), ORR (5.9%), and median PFS (2.8 mo)[31].

A novel regimen, platinum-free liposomal irinotecan in combination with 5-FU/LV, has recently been studied in second-line BTC. In a randomized, open-label, phase IIb study, 174 Korean patients were randomly allocated to receive 5-FU/LV every two weeks or nal-IRI 70 mg/m^2 combined with 2400 mg/m^2 intravenous fluorouracil and intravenous LV 400 mg/m^2 for 46 h) (NIFTY study). When compared to 5 FU/LV, the nal-IRI with 5-FU/LV improved PFS and OS significantly. In comparison to the 5-FU/LV group, which had a median PFS of 5.5 mo *vs* 1.4 mo, the nal-IRI plus 5-FU/LV group had a median PFS of 3.9 mo and a median OS of 8.6 mo. Even though this clinical trial is in phase 2b, there are

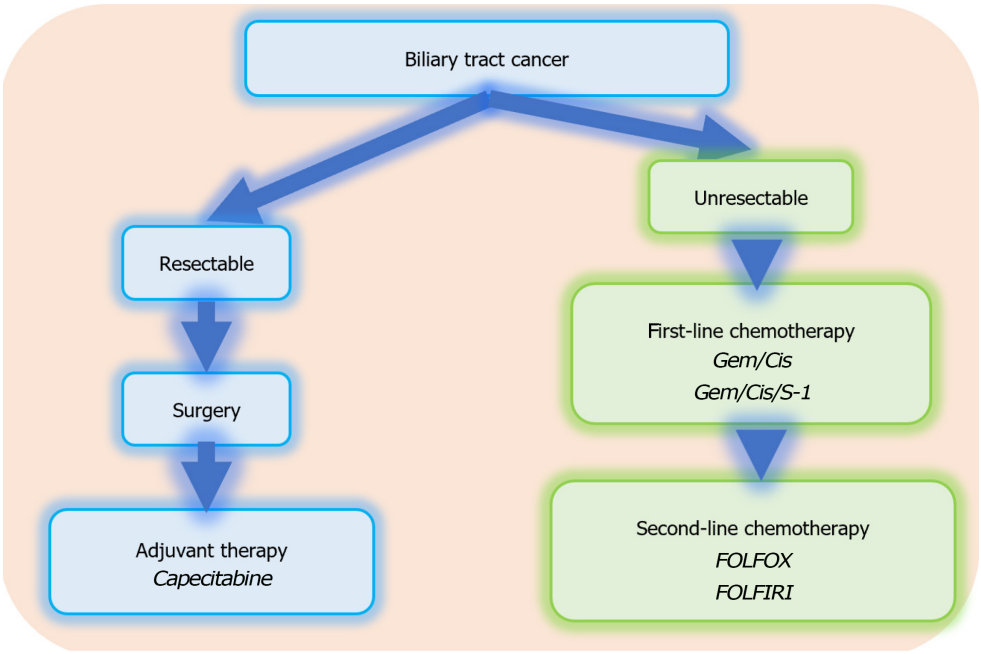

DOI: 10.4251/wjgo.v15.i6.959

Figure 1 Treatment strategy in biliary tract cancers. FOLFIRI: 5-fluorouracil plus irinotecan; FOLFOX: 5-fluorouracil plus oxaliplatin; Gem/Cis: Gemcitabine plus cisplatin; Gem/Cis/S-1: Gemcitabine plus cisplatin plus S-1.

exactly the same number of participants as in the single-phase 3 study that has been conducted to date (ABC-06). In the nal-IRI plus 5-FU/LV group, 70% of patients and 31% of patients in the 5-FU/LV group experienced grade 3 side effects, such as neutropenia and asthenia. Despite the fact that these outcomes are encouraging, they must be validated in global phase 3 clinical studies[32]. In a phase 2 trial in 2018, irinotecan 180 mg/m^2 on day 1 combined with capecitabine 1000 mg/m^2 twice daily on days 1 through 10 (XELIRI-arm) or irinotecan 180 mg/m^2 on day 1 alone (IRI-arm) were the two therapy options given to 60 Gem/Cis refractory aBTC patients by Zheng *et al*[33] over the course of a cycle of 14 d. Treatments were continued until the condition became worse or the side effects became too severe. They discovered that the median PFS was 3.7 *vs* 2.4 mo, the 9-mo survival rate was 60.9% *vs* 32.0%, the median OS was 10.1 *vs* 7.3 mo, and the DCR was 63.3% *vs* 50.0% for the XELIRI-arm and IRI-arm, respectively. Leucopenia and neutropenia were the two grade 3 or 4 toxicities that were most prevalent.

Because of a number of factors, including the proportion of patients deemed suitable for third- or later-line treatment and the absence of agreement for second-line therapy prior to ABC-06 and NIFTY, few studies have looked at the usefulness of systemic CT in the third-line situation. There are few data on third-line CT for highly pretreated patients. As a result, the clinical choice of third-line CT in metastatic BTC remains complex and is based on a number of factors, including the patient's motivation, performance status, response to prior therapies, and quality of life[34,35].

TARGETED THERAPIES

More driving genes are being discovered because of the advancement of next-generation sequencing, which is assisting in the creation of new treatments as well as the explanation of the pathophysiology of BTC. In the BTC landscape, iCCA, eCCA, GBC, and AVC appear to differ significantly from one another based on this technology. Kirsten rat sarcoma virus (RAS), AT-rich interactive domain B mutations, and erb-b2 receptor tyrosine kinase 2 (ERBB2) are more common in eCCA and GBC, whereas isocitrate dehydrogenase (IDH)-1, IDH-2 mutations, and FGFR2 fusions or rearrangements are almost exclusively detected in intrahepatic variants[36,37].

FGFR2 inhibitors

According to several genetic studies, FGFR2 abnormalities are seen in about 15%–25% of iCCAs. Tyrosine kinase receptors known as FGFRs are implicated in regulating RAS, Janus kinase 2, and phosphoi-nositide 3-kinases (PI3K)/mammalian target of rapamycin pathways, and FGFR2 abnormalities affect cellular migration, angiogenesis, proliferation, and survival processes[38,39]. Numerous medications that target FGFR isoforms, including infigratinib, pemigatinib, derazantinib, erdafitinib (ATP-competitive, reversible inhibitors), and futibatinib (non-ATP-competitive, covalent

inhibitor), have been studied in iCCA patients during the past ten years[40,41]. In a phase 1 clinical trial with 3 CCA patients carrying FGFR2 abnormalities, the pan-FGFR tyrosine kinase inhibitor infigratinib was originally evaluated, and all patients had stable condition[42]. In a further phase 2 study, infigratinib was investigated in 61 gemcitabine-resistant CCA patients with *FGFR2* gene mutations, fusions, or amplifications. In the subset of CCAs with *FGFR2* gene fusions, the ORR and DCR, respectively, were 19% and 83%; the most frequently reported side effects were tiredness, hyperphosphatemia, baldness, and stomatitis[43]. Javle *et al*[44] recently published the complete data of this single-arm, phase 2 study, in which infigratinib showed a median PFS and OS of 7.3 mo and 12.2 mo, respectively (Table 1).

In a multicenter, open-label, single-arm phase 2 trial (FIGHT-202) with three cohorts: 107 patients with FGFR2 fusions or rearrangements, 20 patients with other FGFR alterations, or 18 patients without such changes, pemigatinib, another reversible inhibitor, was investigated. The main outcome measure was ORR in patients with FGFR2 fusions or rearrangements who took pemigatinib at least once. With three cases of full response and a median treatment time of 7.2 mo, ORR was observed in 35.5% (38/107) of patients with *FGFR2* gene fusions and/or rearrangements during the course of their median follow-up of 17.8 mo. The median PFS and OS for this cohort were 6.9 and 21.1 mo, respectively. The other two cohorts of CCA patients, however, did not have any responses; in patients with additional FGF/FGFR mutations, the median PFS was 2.1 mo and the median OS was 4.0 mo, whereas the median PFS in patients with FGFR wild type was 1.7 mo. Patients with *FGFR2* gene fusions and/or rearrangements had a median OS of 17.5 mo (95%CI: 14.4-22.9)[45]. Pemigatinib was given fast approval by the United States Food and Drug Administration for pretreated patients with metastatic CCA that included FGFR2 fusions or rearrangements as a consequence of the findings of FIGHT-202. Following these encouraging findings, in patients with FGFR2 rearrangements as the first-line scenario, the phase 3 FIGHT-302 and PROOF-301 investigations, in which both therapies are contrasted with Gem/Cis, are evaluating FGFR2 inhibitors[46,47].

In a phase 1/2 study (AR087-101) involving 29 CCA patients with *FGFR2* gene fusion, the pan-FGFR inhibitor derazantinib (ARQ087) was first analyzed. Two cases of therapy-naive CCA were included, although the bulk of the patients (n = 27) had had disease progression after at least one systemic treatment. According to the study's findings, with a median PFS of 5.7 mo, the ORR and DCR were 20.7% and 82.8%, respectively[48]. Erdafitinib (JNJ-42756493), a different pan-FGFR inhibitor, was studied in a phase 1 study and shown to be effective in CCA patients with FGFR mutations or gene fusions, with an ORR of 27.3% and an average response time of 11.4 mo[49]. Futibatinib (TAS-120), an irreversible, highly selective pan-FGFR inhibitor that can overcome resistance to ATP-competitive inhibitors, is the final potential drug. All iCCA patients (n = 3) exhibited a partial response in the first dose-escalation phase 1 study that included metastatic solid tumors with FGFR abnormalities[50]. Following the findings of this trial, 67 pretreatment iCCA patients with FGFR2 gene fusions or rearrangements were included in the FOENIX-CCA2 single-arm, multicenter, phase 2 trial. The findings of this trial showed that an ORR was noted in 42.0% of patients receiving futibatinib, with a median PFS of 9.0 mo and a median OS of 21.7 mo[51]. Futibatinib was associated with a number of the same treatment-related side effects as other FGFR inhibitors, such as diarrhea, hyperphosphatemia, alopecia, and dry mouth. The phase 3 FOENIX-CCA3 clinical research is evaluating futibatinib *vs* Gem/Cis as a first-line treatment for locally progressed, unresectable, or metastatic iCCA patients with FGFR2 gene fusions or rearrangements in light of the encouraging signs of efficacy reported in FOENIX-CCA2 (Figure 2).

IDH inhibitors

IDH mutations are very uncommon findings in the other BTC subtypes, such as eCCA and GBC; however, they have been documented in about 15% of all cases with iCCA. From a biological perspective, IDH mutations inhibit enhanced IDH1/2 activity, resulting in modifications to cellular metabolism and a buildup of the tumor metabolite 2-hydroxyglutaric acid (2-HG). IDH1/2 mutations in the isocitrate binding region reduce enzyme activity for oxidative decarboxylation of isocitrate to α-ketoglutarate. In turn, 2-HG alters DNA methylation and chromatin structure in a number of ways that hinder normal cell differentiation and promote cancer. This genetic change allows tumors to catalyze the conversion of α-ketoglutarate to 2-HG. This has recently been studied in patients with CCA, and several of these drugs have already demonstrated encouraging benefits in other malignancies with IDH mutations[52,53]. A number of IDH1/2 inhibitors, including ivosidenib, enasidenib, and others, have lately been investigated in CCA patients; some of these drugs have already shown notable benefit in other malignancies with IDH mutations.

An oral IDH1 targeted inhibitor called ivosidenib (AG-120) has demonstrated efficacy in preliminary clinical studies. The pivotal experiment that led to the approval of ivosidenib was the multicenter, randomized, double-blind, placebo-controlled ClarIDHy phase 3 study, patients with advanced, IDH1-mutant CCA who had progressed on up to two prior therapy regimens were enrolled. IDH1 mutations were prescreened in a total of 780 individuals, and 187 were randomly assigned to receive either 500 mg of ivosidenib once daily or a placebo. The majority of them were advanced iCCA at the time of randomization. In the ivosidenib group, the median PFS was 2.7 mo as opposed to 1.4 mo in the placebo group; this improvement was statistically significant. Ivosidenib's median OS was 10.3 mo while the placebo

Table 1 Summary of main clinical trials evaluating the targeted therapies in advanced biliary tract cancer patients

Ref.	Country	Drug(s)	Number of patients	Study phase	ORR (%)	Mean OS (months)	Mean PFS (months)	Adverse events
FGFR2 inhibitors								
Javle *et al* [44]	United States, Belgium, Spain, Germany, Singapore, Taiwan, and Thailand	Infigratinib (BGJ398)	108	2	23.1	12.2	7.3	Tiredness, baldness, hyperphosphatemia, and stomatitis
Abou-Alfa *et al*[45]	United States, France, Italy, Germany, Belgium, and South Korea	Pemigatinib (FIGHT-202)	146	2	35.5	21.1 (FGFR2 fusion)	6.9 (FGFR2 fusion)	Hypophosphatemia, arthralgia, stomatitis, hyponatremia, and abdominal pain
Mazzaferro *et al*[48]	United States and Italy	Derazantinib (AR087-101)	29	1/2	20.7	12.7	5.7	Fatigue, eye toxicity, hyperphosphatemia, and increase in ALT/AST
Bahleda *et al* [49]	United States, France, and Spain	Erdafitinib (JNJ-42756493)	11	1	27.0	12.0	7.5	Fatigue, eye toxicity, hyperphosphatemia, and increase in ALT/AST
Goyal *et al* [51]	United States, France, Spain, United Kingdom, Netherland, Japan, Germany, and South Korea	Futibatinib (TAS-120)	103	2	42.0	21.7	9.0	Hyperphosphatemia, diarrhea, fatigue, alopecia, and stomatitis
IDH inhibitors								
Zhu *et al*[54]	United States, China, Spain, United Kingdom, Ireland, and South Korea	Ivosidenib (AG-120)	187	3	51.0	10.3	2.7	Ascites, anemia, increase bilirubin level, and hyponatremia
BRAF inhibitors								
Subbiah *et al* [59]	United States, Denmark, United Kingdom, Austria, France, Italy, Spain, Germany, Netherland, Switzerland, Japan, and South Korea	Trametinib and Dabrafenib	43	2	47.0	14.0	9.0	Hypertension, reduced white blood cell count, and elevated gamma-glutamyl transferase
NTRK inhibitors								
Doebele *et al* [67]	United States, France, Italy, Spain, Germany, Australia, Hong Kong, Switzerland, Japan, and South Korea	Entrectinib	54	1/2	57.0	21.0	11.0	Anemia, increased weight, dyspnea, and fatigue

BRAF: B-Raf gene; FGFR2: Fibroblast growth factor receptor 2; IDH: Isocitrate dehydrogenase; NTRK: Neurotrophic tyrosine receptor kinase; ORR: Objective response rate; OS: Overall survival; PFS: Progression-free survival; ALT: Alanine aminotransferase; AST: Aspartate aminotransferase.

group's median OS was 7.5 mo. The 57% crossover from placebo to ivosidenib, which was authorized on the basis of radiological advancement, may be the cause of the OS difference that was not statistically significant. Nausea, diarrhea, and exhaustion were common side effects that affected 41%, 35%, and 31% of individuals, respectively[54]. Rimini *et al*[55] presented the first real-world experience in 2022, with eight patients with previously treated locally advanced or metastatic IDH1-mutated CCA treated with ivosidenib after a median follow-up of 9.4 mo. They discovered that the median OS was not attained, while the median PFS from the commencement of therapy with ivosidenib was 4.4 mo. The DCR was 62.5%, with two patients attaining a partial response (at a rate of 25%). 12.5% of patients had side effects due to the therapy, however, none of grade 3 or higher were noted. Hypomagnesemia and a longer QT interval were the grade 2 AEs that were detected. They concluded that the effectiveness results were in line with those mentioned in the ClarIDHy study. Larger samples of real-world data are required to corroborate the findings[56]. Other IDH inhibitors, like as enasidenib (AG-221), and combination therapy combining these targeted drugs with additional anticancer drugs, such PARP inhibitors, are now being evaluated in IDH-mutated CCAs.

BRAF inhibitors

BRAF is a growth signal transduction protein kinase that belongs to the Raf kinase family. The mitogen-activated protein (MAP) kinase/extracellular signal-regulated kinases signaling system, which controls

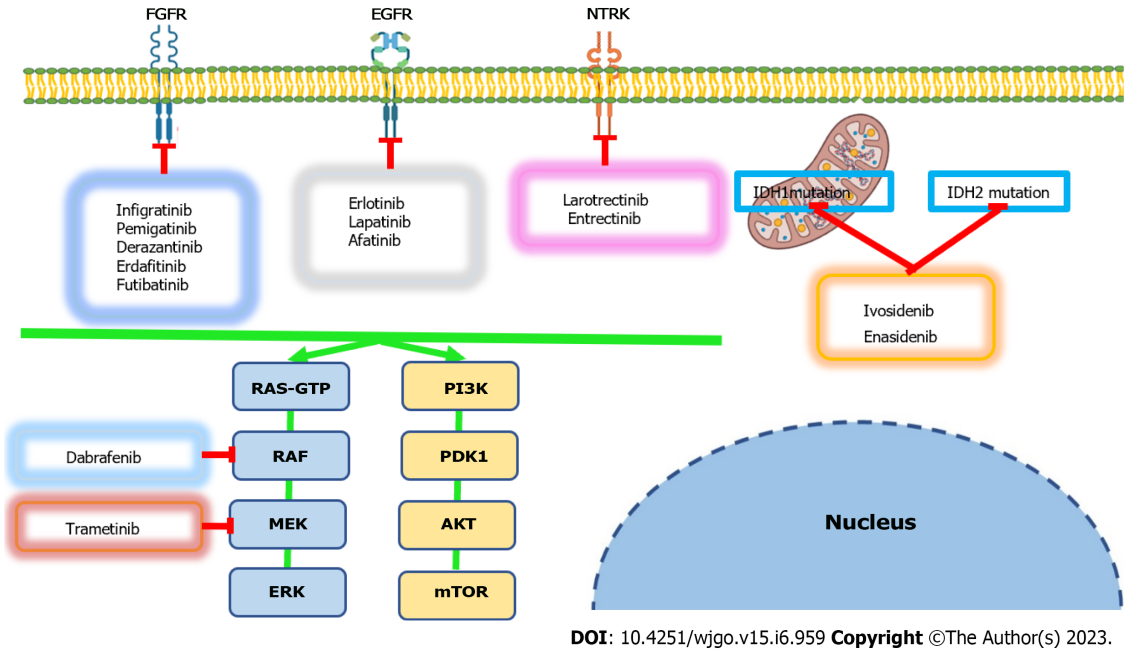

DOI: 10.4251/wjgo.v15.i6.959

Figure 2 Targeted therapies used in systemic treatment for biliary tract cancers. AKT: Protein kinase B; EGFR: Epidermal growth factor receptor; ERK: Extracellular signal-related kinase; FGFR: Fibroblast growth factor receptor; GTP: Guanosine triphosphate; IDH1: Isocitrate dehydrogenase 1; IDH2: Isocitrate dehydrogenase 2; MEK: Mitogen-activated protein kinase; mTOR: Mammalian target of rapamycin; NTRK: Neurotrophic tyrosine receptor kinase; PI3K: Phosphoinositide-3-kinase; PKD1: Polycystic kidney disease 1; RAF: Raf proto-oncogene; RAS: RAS proto-oncogene.

cell division, differentiation, and secretion, is regulated by this protein. Approximately 5% of BTCs have been shown to contain BRAF gene alterations, particularly in iCCA. Fascinatingly, individuals with BRAFV600E mutations experience more aggressive clinical behavior, have more advanced tumors upon diagnosis, and are more likely to have lymph node involvement. Similar to other BRAF-mutated cancers, this situation has exhibited the early emergence of treatment resistance and transient responses to BRAF inhibitor monotherapy[57,58]. Consequently, combination therapies combining BRAF inhibitors and MEK inhibitors have been investigated. Subbiah *et al*[59] conducted a phase 2, open-label, single-arm study, the Rare Oncology Agnostic Research, to assess the effectiveness and safety of trametinib and dabrafenib in 43 patients, including 91% with iCCA, 2% with pCCA, 2% with GBC, and 2% with unclear origins. Independent analysis revealed a 47% ORR, a 9-mo median PFS, and a 14-mo median OS. These results demonstrated that, in contrast to metastatic colorectal cancer, where EGFR inhibition is crucial, BRAF inhibition is critical in BTC. Among patients taking dabrafenib with trametinib, hypertension (7%), a decrease in white blood cell count (7%), and an increase in gamma-glutamyl transferase (12%) were the most common grade 3 or 4 AEs. The dual-targeting treatment appears to produce better results than BRAF inhibition alone. Future research should concentrate on the use of combination drugs for early therapy.

EGFR inhibitors

Human EGFR2 (HER2) is a tumor-promoting growth factor receptor. EGFR, HER1 (ERBB1), HER2 (ERBB2), HER3 (ERBB3), and HER4 (ERBB4) are all members of the same family. These transmembrane growth factor receptors activate downstream secondary messengers when their intracellular domains are phosphorylated, resulting in a variety of physiologic consequences. HER2 activation causes cancer by activating the MAP kinase and PI3K pathways, as well as a loss of cell polarity and adhesion and a disrupted cell cycle by activating cyclin D and inhibiting p27. The most active catalytic kinase is seen in HER2, especially when HER3 is involved. The HER2 protein has been shown to be overexpressed in 13% of GBCs and up to 18% of eCCA[60,61]. Although HER2 overexpression has been correlated with a poorer prognosis and a higher tendency to metastasize, it has also been associated with increased cytotoxic and targeted agent sensitivity. Javle *et al*[62] retrospectively analyzed patients with advanced GBC and CCA who had HER2/neu-directed therapy between 2007 and 2014 and who had HER2/neu genetic abnormalities or protein overexpression. HER2/neu-directed treatment (trastuzumab, lapatinib, or pertuzumab) had been administered to five patients with CCA and nine patients with GBC at some point throughout the research. Eight incidences of HER2/neu gene amplification or overexpression in GBC patients were found. With HER2/neu-directed treatment, these patients either had a full response (n = 1), a partial response (n = 4), or disease stability (n = 3). A HER2/neu mutation caused a patient who received lapatinib therapy to have a mixed response. Response times ranged from 8 to 168 wk (median 40 wk). The CCA cases in this series that were treated had a greater proportion of HER2/neu mutations,

and despite HER2/neu-directed treatment, these patients showed no radiological responses. They recommended that HER2/neu blocking is a promising therapeutic approach for patients with gene amplification for GBC and merits more investigation in multicenter research.

Neurotrophic tyrosine receptor kinase inhibitors

Three membrane-bound receptors known as tropomyosin receptor kinases (Trk A, B, and C) are encoded by the neurotrophic tyrosine receptor kinase genes (NTRK1-3), which are exceedingly uncommon in BTC (0.67%) and present in between 0.3% and 1% of all solid tumors. The cytoplasmic kinase is activated by neurotrophin binding, which also activates the MAPK, PI3K, and phospholipase C-γ1 pathways and downstream signaling cascades. One of the three *NTRK* genes can combine with a number of partners to form oncogenic fusions, which constitutively activate the Trk pathway and promote cancer[63-65]. Larotrectinib and entrectinib, two extremely specific small compounds that inhibit all three TRK proteins, were discovered and demonstrated efficacy in preliminary clinical studies. Larotrectinib (LOXO-101) phase 1 clinical trial, which recruited 55 patients, was analyzed, and it was revealed that the ORR was 75% and the median PFS was not attained until 9.9 mo. There were only 2 CCA patients included, and both had an ORR of 80%. One patient had a progressing condition[66]. Three entrectinib phase 1 or 2 clinical studies (STARTRK-1, STARTRK-2, and ALKA-372-001) were analyzed together. Fifty-four patients from 10 distinct NTRK fusion-positive tumor types were enrolled in all of the studies, which showed a median PFS of 12.9 mo and an ORR of 57%[67].

ICIS

The incorrect insertions or deletions that happen during DNA replication are recognized and corrected by the mismatch repair (MMR) mechanism. ICIs are particularly effective against cancers with a deficient MMR (dMMR) system because these cancers frequently have somatic mutations. Adenocarcinomas of the liver, cervix, endometrium, and gastrointestinal tract all have dMMR in more than 5% of cases. They are observed in localized phases more frequently (8%) than in metastatic stages (4%). Depending on the region and published series, dMMR accounts for 2%–18% of tumors in BTC. In contrast to eCCA or GBC (5%–8%), it is more common in iCCA (10%) and AVC (6%–20%)[68,69]. ICIs can boost anticancer activity by inhibiting immune system regulators like cytotoxic T lymphocyte antigen 4 (CTLA-4), programmed cell death protein 1 (PD-1), programmed cell death-ligand 1 (PD-L1), and lymphocyte activating gene 3. This results in increased cytotoxicity in T lymphocytes (Figure 3). ICIs have recently been tested in BTC, either by alone or in combination with other anticancer drugs[70-73].

Both the phase 1b and phase 2 KEYNOTE-158 studies used the PD-1 inhibitor pembrolizumab. In these two studies, a limited group of BTC patients who had already had treatment and whose conditions had gotten worse on traditional therapy were involved. The median PFS and OS for KEYNOTE-158 were 2.0 and 7.4 mo, respectively, whereas the ORR, median PFS, and median OS for KEYNOTE-028 were 13.0%, 1.8 mo, and 5.7 mo, respectively, in the intention-to-treat group. Microsatellite instability (MSI) status was used by the investigators to stratify their data, and patients with MSI-H/dMMR had an ORR of 40.9% with median PFS and OS of 4.2 and 24.3 mo, respectively [74]. Metastatic BTC was treated with nivolumab, a human immunoglobulin G4 monoclonal antibody that prevents PD-1 interaction with PD-L1 and PD-L2. Early results from a single-group, multicenter phase 2 study of nivolumab monotherapy showed partial responses in 10 of 45 patients with CCA who had previously received treatment, with 27 of them reaching a stable status. It is also worth noting that the median PFS and OS were 3.68 and 14.24 mo, respectively. Nivolumab was further assessed as a first-line treatment for patients with metastatic condition when combined with the traditional doublet Gem/Cis, with results indicating a median OS of 15.4 mo and a median PFS of 4.2 mo. Moreover, 11 out of 30 patients showed an objective response[75].

Ueno *et al*[76] performed a multicenter, open-label, phase 1 trial in 60 patients with BTCs to investigate the safety and tolerability of the ICI nivolumab as monotherapy or in combination with Gem/Cis CT. Nivolumab monotherapy (240 mg every 2 wk) was given to 30 patients with unresectable or recurrent BTC that was resistant or intolerant to Gem/Cis. Thirty CT-naive patients with unresectable or recurrent BTC were given nivolumab (240 mg every two weeks) in addition to Gem/Cis CT. In the monotherapy cohort, they found that the median OS was 5.2 mo, the median PFS was 1.4 mo, and just one patient out of thirty exhibited an objective response. Eleven out of 30 patients in the combination treatment cohort showed an objective response, and the median OS and PFS were 15.4 and 4.2 mo, respectively. They concluded that nivolumab showed evidence of therapeutic effectiveness in individuals with unresectable or recurrent BTC and had a tolerable safety profile. This preliminary evaluation of nivolumab for the treatment of advanced BTC offers encouraging data for upcoming larger randomized studies of nivolumab in this challenging malignancy.

Nivolumab was also investigated in a phase 2 trial on 54 patients with refractory BTC at doses of 240 mg intravenously every two weeks for 16 wk, followed by 480 mg intravenously every four weeks, until disease progression or unacceptable toxicity. According to the research, the ORR by central review was

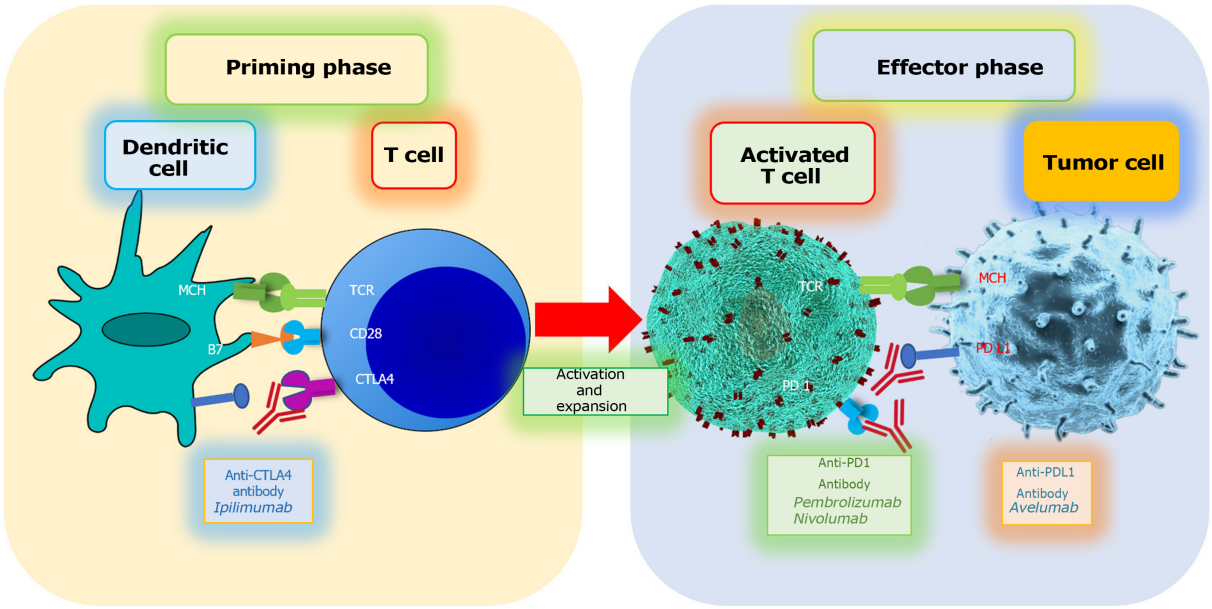

DOI: 10.4251/wjgo.v15.i6.959 **Copyright** ©The Author(s) 2023.

Figure 3 The mechanisms of action of immune checkpoint inhibitors in cancer immunotherapy. CTLA-4: Cytotoxic T lymphocyte antigen 4; MHC: Major histocompatibility complex; PD-1: Programmed cell death protein 1; PD-L1: Programmed death-ligand 1; TCR: T cell receptor.

11%, the DCR was 50%, the median PFS was 3.7 mo, and the median OS was 14 mo. The median PFS and OS were higher for patients who were stratified by positive PD-L1 expression status than for patients who had PD-L1-negative expression[77]. Nivolumab and the anti-CTLA-4 drug ipilimumab were studied in combination in patients with advanced BTCs by Klein *et al*[78]. The median PFS was 2.9 mo, the ORR was 23%, 17 out of 39 patients had disease control, and the median OS was 5.7 mo. The ORR for patients with iCCA and GBC was 31%, while there was no response seen in individuals with eCCA, suggesting that the effectiveness of ICIs varied depending on the anatomic locations. In an advanced BTC patient without prior systemic treatment and an ECOG score of 0-1, Sahai *et al*[79] conducted a phase 2 randomized study to assess the impact of adding an anti-PD-1/PD-L1 antibody to either systemic CT or an anti-CTLA4 antibody. Nivolumab (360 mg) was given to patients in Arm A (35) on day one, along with Gem/Cis on days one and eight, every three weeks for six months, followed by Nivolumab (240 mg) every two weeks. Patients in Arm B (33) received nivolumab (240 mg) every two weeks, and Ipilimumab (1 mg/kg) every six weeks. They discovered that the 6-mo PFS rates in Arm A were 59.4% and Arm B was 21.2% for the observed main endpoint. The median PFS and OS in Arm A were 6.6 and 10.6 mo, respectively, while they were 3.9 and 8.2 mo in Arm B. The most common grade 3 or higher hematologic AE related to therapy was neutropenia (34.3%, Arm A), while tiredness (8.6%, Arm A) and elevated transaminases (9.1%, Arm B) were the most common nonhematologic AEs. They determined that when combined with CT or Ipilimumab, Nivolumab did not improve 6-mo PFS. Although both arms' median OS was less than 12 mo, Arm A's high OS rate at 2 years suggested benefit in a small patient cohort.

A phase 2 trial with advanced BTC examined gemcitabine and oxaliplatin (GEMOX) and the PD-1 antibody, camrelizumab. Fever and exhaustion were the side effects of therapy that occurred most frequently (both 73%). In 54% of patients, the combination produced an objective response. When compared to those for GEMOX alone, the median PFS was 6.1 mo and the median OS 11.8 mo[80]. Patients with advanced BTC were evaluated in a phase 2 research study in China using camrelizumab plus an oxaliplatin-based CT regimen. Similar to the ABC-02 study, the reported ORR was 16.3%, the median PFS was 5.3 mo, and the median OS was 12.4 mo. These encouraging findings imply that a novel first-line treatment for advanced BTC, camrelizumab plus oxaliplatin-based CT, may be possible [81]. In a phase 2 study, individuals with advanced BTC who had never had CT were given a combination of Gem/Cis plus durvalumab, with or without tremelimumab. Three regimens of CT and immunotherapy were administered to all patients, and the medication dosages across the regimens were all the same. They enrolled 128 patients; 32 in the Gem/Cis, followed by the Gem/Cis plus durvalumab and tremelimumab, 49 in the Gem/Cis plus durvalumab, and 47 in the Gem/Cis plus durvalumab and tremelimumab. The total median PFS was 12.1 mo and the median OS was 18.4 mo, which was encouraging compared with traditional CT. The research, however, lacked a control group. There were no appreciable changes in OS or PFS across the three regimens. After one cycle of therapy, the researchers discovered that lower PD-L1 expression in immune and tumor cells was linked to a shorter PFS. Immune cell PD-L1 expression was connected to the median OS. The findings suggested that PD-L1 expression variations following therapy may help predict clinical outcomes. Considering the

promising potential of CT combined with durvalumab in advanced BTC[82].

Peng *et al*[83] conducted a meta-analysis to assess the predictive and clinicopathological significance of the systemic immune-inflammation index (SII) in BTC. A combined study revealed that those with high SII levels had worse OS than people with low SII levels. Moreover, a higher SII was linked to lymph node metastases, TNM stage, and vascular invasion. In contrast, no significant relationship was discovered between a high SII and sex or tumor differentiation. These data indicated that high SII levels were associated with poor survival outcomes in individuals with BTC, as well as certain more malignant aspects of BTC.

CONCLUSION

Since BTC is frequently discovered at advanced stages, the disease is usually incurable. The best currently available, possibly curative treatment for a primary tumor found in the early stages in a subset of people is surgery; however, the treatment of advanced cancer is still in its early phases. As a result of biology's present understanding, new tactics are becoming possible because BTCs have several chemical changes that may be altered. Since several genetic abnormalities may be discovered and will affect our patients' outcomes, it is strongly recommended that all BTC patients receive a thorough molecular test before beginning systemic medication. There are several clinical trials taking place right now that use various methods to examine the safety and effectiveness of many medications in first- and second-line settings. Following the encouraging findings of phase 3 ABC-02, which showed an improvement in median OS compared with gemcitabine alone, the first-line recommended therapy is still Gem/Cis. However, the TOPAZ-1 clinical study, which revealed an improvement in OS, PFS, and ORR with immunotherapy combined with CT, has set a new course for patients who do not carry driver mutations. When compared to active symptom management, FOLFOX has demonstrated a little but statistically significant improvement in median OS. For BTC patients with certain genetic problems, targeted drugs such FGFR2, IDH1, and BRAF inhibitors have already demonstrated good outcomes in clinical trials. Targeted medicines, CT combinations, and ICIs are other approaches under investigation that will have an influence on the treatment of BTC in the future.

FOOTNOTES

Author contributions: Leowattana W wrote the paper; Leowattana T and Leowattana P collected the data.

Conflict-of-interest statement: All the authors report no relevant conflicts of interest for this article.

Country/Territory of origin: Thailand

ORCID number: Wattana Leowattana 0000-0003-4257-2480; Tawithep Leowattana 0000-0003-2316-3585.

S-Editor: Fan JR
L-Editor: A
P-Editor: Ji MX

REFERENCES

1 **Valle JW**, Kelley RK, Nervi B, Oh DY, Zhu AX. Biliary tract cancer. *Lancet* 2021; **397**: 428-444 [PMID: 33516341 DOI: 10.1016/S0140-6736(21)00153-7]

2 **Bridgewater JA**, Goodman KA, Kalyan A, Mulcahy MF. Biliary Tract Cancer: Epidemiology, Radiotherapy, and Molecular Profiling. *Am Soc Clin Oncol Educ Book* 2016; **35**: e194-e203 [PMID: 27249723 DOI: 10.1200/EDBK_160831]

3 **Lendvai G**, Szekerczés T, Illyés I, Dóra R, Kontsek E, Gógl A, Kiss A, Werling K, Kovalszky I, Schaff Z, Borka K. Cholangiocarcinoma: Classification, Histopathology and Molecular Carcinogenesis. *Pathol Oncol Res* 2020; **26**: 3-15 [PMID: 30448973 DOI: 10.1007/s12253-018-0491-8]

4 **Saha SK**, Zhu AX, Fuchs CS, Brooks GA. Forty-Year Trends in Cholangiocarcinoma Incidence in the U.S.: Intrahepatic Disease on the Rise. *Oncologist* 2016; **21**: 594-599 [PMID: 27000463 DOI: 10.1634/theoncologist.2015-0446]

5 **West J**, Wood H, Logan RF, Quinn M, Aithal GP. Trends in the incidence of primary liver and biliary tract cancers in

England and Wales 1971-2001. *Br J Cancer* 2006; **94**: 1751-1758 [PMID: 16736026 DOI: 10.1038/sj.bjc.6603127]

6 **Florio AA**, Ferlay J, Znaor A, Ruggieri D, Alvarez CS, Laversanne M, Bray F, McGlynn KA, Petrick JL. Global trends in intrahepatic and extrahepatic cholangiocarcinoma incidence from 1993 to 2012. *Cancer* 2020; **126**: 2666-2678 [PMID: 32129902 DOI: 10.1002/cncr.32803]

7 **Massarweh NN**, El-Serag HB. Epidemiology of Hepatocellular Carcinoma and Intrahepatic Cholangiocarcinoma. *Cancer Control* 2017; **24**: 1073274817729245 [PMID: 28975830 DOI: 10.1177/1073274817729245]

8 **Clements O**, Eliahoo J, Kim JU, Taylor-Robinson SD, Khan SA. Risk factors for intrahepatic and extrahepatic cholangiocarcinoma: A systematic review and meta-analysis. *J Hepatol* 2020; **72**: 95-103 [PMID: 31536748 DOI: 10.1016/j.jhep.2019.09.007]

9 **Sithithaworn P**, Yongvanit P, Duenngai K, Kiatsopit N, Pairojkul C. Roles of liver fluke infection as risk factor for cholangiocarcinoma. *J Hepatobiliary Pancreat Sci* 2014; **21**: 301-308 [PMID: 24408775 DOI: 10.1002/jhbp.62]

10 **Spolverato G**, Kim Y, Alexandrescu S, Marques HP, Lamelas J, Aldrighetti L, Clark Gamblin T, Maithel SK, Pulitano C, Bauer TW, Shen F, Poultsides GA, Tran TB, Wallis Marsh J, Pawlik TM. Management and Outcomes of Patients with Recurrent Intrahepatic Cholangiocarcinoma Following Previous Curative-Intent Surgical Resection. *Ann Surg Oncol* 2016; **23**: 235-243 [PMID: 26059651 DOI: 10.1245/s10434-015-4642-9]

11 **Alabraba E**, Joshi H, Bird N, Griffin R, Sturgess R, Stern N, Sieberhagen C, Cross T, Camenzuli A, Davis R, Evans J, O'Grady E, Palmer D, Diaz-Nieto R, Fenwick S, Poston G, Malik H. Increased multimodality treatment options has improved survival for Hepatocellular carcinoma but poor survival for biliary tract cancers remains unchanged. *Eur J Surg Oncol* 2019; **45**: 1660-1667 [PMID: 31014988 DOI: 10.1016/j.ejso.2019.04.002]

12 **Tariq NU**, McNamara MG, Valle JW. Biliary tract cancers: current knowledge, clinical candidates and future challenges. *Cancer Manag Res* 2019; **11**: 2623-2642 [PMID: 31015767 DOI: 10.2147/CMAR.S157092]

13 **Rizzo A**, Brandi G. Pitfalls, challenges, and updates in adjuvant systemic treatment for resected biliary tract cancer. *Expert Rev Gastroenterol Hepatol* 2021; **15**: 547-554 [PMID: 33571059 DOI: 10.1080/17474124.2021.1890031]

14 **Valle J**, Wasan H, Palmer DH, Cunningham D, Anthoney A, Maraveyas A, Madhusudan S, Iveson T, Hughes S, Pereira SP, Roughton M, Bridgewater J; ABC-02 Trial Investigators. Cisplatin plus gemcitabine versus gemcitabine for biliary tract cancer. *N Engl J Med* 2010; **362**: 1273-1281 [PMID: 20375404 DOI: 10.1056/NEJMoa0908721]

15 **Abdel-Rahman O**, Elsayed Z, Elhalawani H. Gemcitabine-based chemotherapy for advanced biliary tract carcinomas. *Cochrane Database Syst Rev* 2018; **4**: CD011746 [PMID: 29624208 DOI: 10.1002/14651858.CD011746.pub2]

16 **Chakrabarti S**, Kamgar M, Mahipal A. Targeted Therapies in Advanced Biliary Tract Cancer: An Evolving Paradigm. *Cancers (Basel)* 2020; **12** [PMID: 32722188 DOI: 10.3390/cancers12082039]

17 **Lamarca A**, Barriuso J, McNamara MG, Valle JW. Molecular targeted therapies: Ready for "prime time" in biliary tract cancer. *J Hepatol* 2020; **73**: 170-185 [PMID: 32171892 DOI: 10.1016/j.jhep.2020.03.007]

18 **Rizzo A**, Ricci AD, Brandi G. Pemigatinib: Hot topics behind the first approval of a targeted therapy in cholangiocarcinoma. *Cancer Treat Res Commun* 2021; **27**: 100337 [PMID: 33611090 DOI: 10.1016/j.ctarc.2021.100337]

19 **Zhang W**, Shi J, Wang Y, Zhou H, Zhang Z, Han Z, Li G, Yang B, Cao G, Ke Y, Zhang T, Song T, QiangLi. Next-generation sequencing-guided molecular-targeted therapy and immunotherapy for biliary tract cancers. *Cancer Immunol Immunother* 2021; **70**: 1001-1014 [PMID: 33095329 DOI: 10.1007/s00262-020-02745-y]

20 **Okusaka T**, Nakachi K, Fukutomi A, Mizuno N, Ohkawa S, Funakoshi A, Nagino M, Kondo S, Nagaoka S, Funai J, Koshiji M, Nambu Y, Furuse J, Miyazaki M, Nimura Y. Gemcitabine alone or in combination with cisplatin in patients with biliary tract cancer: a comparative multicentre study in Japan. *Br J Cancer* 2010; **103**: 469-474 [PMID: 20628385 DOI: 10.1038/sj.bjc.6605779]

21 **Valle JW**, Furuse J, Jitlal M, Beare S, Mizuno N, Wasan H, Bridgewater J, Okusaka T. Cisplatin and gemcitabine for advanced biliary tract cancer: a meta-analysis of two randomised trials. *Ann Oncol* 2014; **25**: 391-398 [PMID: 24351397 DOI: 10.1093/annonc/mdt540]

22 **Furuse J**, Okusaka T, Bridgewater J, Taketsuna M, Wasan H, Koshiji M, Valle J. Lessons from the comparison of two randomized clinical trials using gemcitabine and cisplatin for advanced biliary tract cancer. *Crit Rev Oncol Hematol* 2011; **80**: 31-39 [PMID: 21094052 DOI: 10.1016/j.critrevonc.2010.10.009]

23 **Shroff RT**, Javle MM, Xiao L, Kaseb AO, Varadhachary GR, Wolff RA, Raghav KPS, Iwasaki M, Masci P, Ramanathan RK, Ahn DH, Bekaii-Saab TS, Borad MJ. Gemcitabine, Cisplatin, and nab-Paclitaxel for the Treatment of Advanced Biliary Tract Cancers: A Phase 2 Clinical Trial. *JAMA Oncol* 2019; **5**: 824-830 [PMID: 30998813 DOI: 10.1001/jamaoncol.2019.0270]

24 **Roth MT**, Goff LW. Gemcitabine, Cisplatin, and nab-Paclitaxel for Patients With Advanced Biliary Tract Cancer: Closing the GAP. *JAMA Oncol* 2019; **5**: 831-832 [PMID: 30998823 DOI: 10.1001/jamaoncol.2019.0269]

25 **Cheon J**, Lee CK, Sang YB, Choi HJ, Kim MH, Ji JH, Ko KH, Kwon CI, Kim DJ, Choi SH, Kim C, Kang B, Chon HJ. Real-world efficacy and safety of nab-paclitaxel plus gemcitabine-cisplatin in patients with advanced biliary tract cancers: a multicenter retrospective analysis. *Ther Adv Med Oncol* 2021; **13**: 17588359211035983 [PMID: 34394748 DOI: 10.1177/17588359211035983]

26 **Jung K**, Park J, Jung JH, Lee JC, Kim J, Hwang JH. Real-World Outcomes of Gemcitabine, Cisplatin, and Nab-Paclitaxel Chemotherapy Regimen for Advanced Biliary Tract Cancer: A Propensity Score-Matched Analysis. *Gut Liver* 2022; **16**: 798-805 [PMID: 35000934 DOI: 10.5009/gnl210346]

27 **Phelip JM**, Desrame J, Edeline J, Barbier E, Terrebonne E, Michel P, Perrier H, Dahan L, Bourgeois V, Akouz FK, Soularue E, Ly VL, Molin Y, Lecomte T, Ghiringhelli F, Coriat R, Louafi S, Neuzillet C, Manfredi S, Malka D; PRODIGE 38 AMEBICA Investigators/Collaborators. Modified FOLFIRINOX Versus CISGEM Chemotherapy for Patients With Advanced Biliary Tract Cancer (PRODIGE 38 AMEBICA): A Randomized Phase II Study. *J Clin Oncol* 2022; **40**: 262-271 [PMID: 34662180 DOI: 10.1200/JCO.21.00679]

28 **Morizane C**, Okusaka T, Mizusawa J, Katayama H, Ueno M, Ikeda M, Ozaka M, Okano N, Sugimori K, Fukutomi A, Hara H, Mizuno N, Yanagimoto H, Wada K, Tobimatsu K, Yane K, Nakamori S, Yamaguchi H, Asagi A, Yukisawa S, Kojima Y, Kawabe K, Kawamoto Y, Sugimoto R, Iwai T, Nakamura K, Miyakawa H, Yamashita T, Hosokawa A, Ioka T, Kato N, Shioji K, Shimizu K, Nakagohri T, Kamata K, Ishii H, Furuse J; members of the Hepatobiliary and Pancreatic

Oncology Group of the Japan Clinical Oncology Group (JCOG-HBPOG). Combination gemcitabine plus S-1 versus gemcitabine plus cisplatin for advanced/recurrent biliary tract cancer: the FUGA-BT (JCOG1113) randomized phase III clinical trial. *Ann Oncol* 2019; **30**: 1950-1958 [PMID: 31566666 DOI: 10.1093/annonc/mdz402]

29 **Ioka T**, Kanai M, Kobayashi S, Sakai D, Eguchi H, Baba H, Seo S, Taketomi A, Takayama T, Yamaue H, Takahashi M, Sho M, Kamei K, Fujimoto J, Toyoda M, Shimizu J, Goto T, Shindo Y, Yoshimura K, Hatano E, Nagano H; Kansai Hepatobiliary Oncology Group (KHBO). Randomized phase III study of gemcitabine, cisplatin plus S-1 versus gemcitabine, cisplatin for advanced biliary tract cancer (KHBO1401- MITSUBA). *J Hepatobiliary Pancreat Sci* 2023; **30**: 102-110 [PMID: 35900311 DOI: 10.1002/jhbp.1219]

30 **Lamarca A**, Palmer DH, Wasan HS, Ross PJ, Ma YT, Arora A, Falk S, Gillmore R, Wadsley J, Patel K, Anthoney A, Maraveyas A, Iveson T, Waters JS, Hobbs C, Barber S, Ryder WD, Ramage J, Davies LM, Bridgewater JA, Valle JW; Advanced Biliary Cancer Working Group. Second-line FOLFOX chemotherapy versus active symptom control for advanced biliary tract cancer (ABC-06): a phase 3, open-label, randomised, controlled trial. *Lancet Oncol* 2021; **22**: 690-701 [PMID: 33798493 DOI: 10.1016/S1470-2045(21)00027-9]

31 **Choi IS**, Kim KH, Lee JH, Suh KJ, Kim JW, Park JH, Kim YJ, Kim JS, Kim JH. A randomised phase II study of oxaliplatin/5-FU (mFOLFOX) versus irinotecan/5-FU (mFOLFIRI) chemotherapy in locally advanced or metastatic biliary tract cancer refractory to first-line gemcitabine/cisplatin chemotherapy. *Eur J Cancer* 2021; **154**: 288-295 [PMID: 34303267 DOI: 10.1016/j.ejca.2021.06.019]

32 **Yoo C**, Kim KP, Jeong JH, Kim I, Kang MJ, Cheon J, Kang BW, Ryu H, Lee JS, Kim KW, Abou-Alfa GK, Ryoo BY. Liposomal irinotecan plus fluorouracil and leucovorin versus fluorouracil and leucovorin for metastatic biliary tract cancer after progression on gemcitabine plus cisplatin (NIFTY): a multicentre, open-label, randomised, phase 2b study. *Lancet Oncol* 2021; **22**: 1560-1572 [PMID: 34656226 DOI: 10.1016/S1470-2045(21)00486-1]

33 **Zheng Y**, Tu X, Zhao P, Jiang W, Liu L, Tong Z, Zhang H, Yan C, Fang W, Wang W. A randomised phase II study of second-line XELIRI regimen versus irinotecan monotherapy in advanced biliary tract cancer patients progressed on gemcitabine and cisplatin. *Br J Cancer* 2018; **119**: 291-295 [PMID: 29955136 DOI: 10.1038/s41416-018-0138-2]

34 **Zhang W**, Zhou H, Wang Y, Zhang Z, Cao G, Song T, Zhang T, Li Q. Systemic treatment of advanced or recurrent biliary tract cancer. *Biosci Trends* 2020; **14**: 328-341 [PMID: 32830166 DOI: 10.5582/bst.2020.03240]

35 **Rizzo A**, Ricci AD, Cusmai A, Acquafredda S, De Palma G, Brandi G, Palmiotti G. Systemic Treatment for Metastatic Biliary Tract Cancer: State of the Art and a Glimpse to the Future. *Curr Oncol* 2022; **29**: 551-564 [PMID: 35200550 DOI: 10.3390/curroncol29020050]

36 **Wakai T**, Nagahashi M, Shimada Y, Prasoon P, Sakata J. Genetic analysis in the clinical management of biliary tract cancer. *Ann Gastroenterol Surg* 2020; **4**: 316-323 [PMID: 32724874 DOI: 10.1002/ags3.12334]

37 **Berchuck JE**, Facchinetti F, DiToro DF, Baiev I, Majeed U, Reyes S, Chen C, Zhang K, Sharman R, Uson Junior PLS, Maurer J, Shroff RT, Pritchard CC, Wu MJ, Catenacci DVT, Javle M, Friboulet L, Hollebecque A, Bardeesy N, Zhu AX, Lennerz JK, Tan B, Borad M, Parikh AR, Kiedrowski LA, Kelley RK, Mody K, Juric D, Goyal L. The clinical landscape of cell-free DNA alterations in 1671 patients with advanced biliary tract cancer. *Ann Oncol* 2022; **33**: 1269-1283 [PMID: 36089135 DOI: 10.1016/j.annonc.2022.09.150]

38 **Arai Y**, Totoki Y, Hosoda F, Shirota T, Hama N, Nakamura H, Ojima H, Furuta K, Shimada K, Okusaka T, Kosuge T, Shibata T. Fibroblast growth factor receptor 2 tyrosine kinase fusions define a unique molecular subtype of cholangiocarcinoma. *Hepatology* 2014; **59**: 1427-1434 [PMID: 24122810 DOI: 10.1002/hep.26890]

39 **Pu X**, Ye Q, Cai J, Yang X, Fu Y, Fan X, Wu H, Chen J, Qiu Y, Yue S. Typing FGFR2 translocation determines the response to targeted therapy of intrahepatic cholangiocarcinomas. *Cell Death Dis* 2021; **12**: 256 [PMID: 33692336 DOI: 10.1038/s41419-021-03548-4]

40 **Mirallas O**, López-Valbuena D, García-Illescas D, Fabregat-Franco C, Verdaguer H, Tabernero J, Macarulla T. Advances in the systemic treatment of therapeutic approaches in biliary tract cancer. *ESMO Open* 2022; **7**: 100503 [PMID: 35696747 DOI: 10.1016/j.esmoop.2022.100503]

41 **Aitcheson G**, Mahipal A, John BV. Targeting FGFR in intrahepatic cholangiocarcinoma [iCCA]: leading the way for precision medicine in biliary tract cancer [BTC]? *Expert Opin Investig Drugs* 2021; **30**: 463-477 [PMID: 33678096 DOI: 10.1080/13543784.2021.1900821]

42 **Nogova L**, Sequist LV, Perez Garcia JM, Andre F, Delord JP, Hidalgo M, Schellens JH, Cassier PA, Camidge DR, Schuler M, Vaishampayan U, Burris H, Tian GG, Campone M, Wainberg ZA, Lim WT, LoRusso P, Shapiro GI, Parker K, Chen X, Choudhury S, Ringeisen F, Graus-Porta D, Porter D, Isaacs R, Buettner R, Wolf J. Evaluation of BGJ398, a Fibroblast Growth Factor Receptor 1-3 Kinase Inhibitor, in Patients With Advanced Solid Tumors Harboring Genetic Alterations in Fibroblast Growth Factor Receptors: Results of a Global Phase I, Dose-Escalation and Dose-Expansion Study. *J Clin Oncol* 2017; **35**: 157-165 [PMID: 27870574 DOI: 10.1200/JCO.2016.67.2048]

43 **Javle M**, Lowery M, Shroff RT, Weiss KH, Springfeld C, Borad MJ, Ramanathan RK, Goyal L, Sadeghi S, Macarulla T, El-Khoueiry A, Kelley RK, Borbath I, Choo SP, Oh DY, Philip PA, Chen LT, Reungwetwattana T, Van Cutsem E, Yeh KH, Ciombor K, Finn RS, Patel A, Sen S, Porter D, Isaacs R, Zhu AX, Abou-Alfa GK, Bekaii-Saab T. Phase II Study of BGJ398 in Patients With FGFR-Altered Advanced Cholangiocarcinoma. *J Clin Oncol* 2018; **36**: 276-282 [PMID: 29182496 DOI: 10.1200/JCO.2017.75.5009]

44 **Javle M**, Roychowdhury S, Kelley RK, Sadeghi S, Macarulla T, Weiss KH, Waldschmidt DT, Goyal L, Borbath I, El-Khoueiry A, Borad MJ, Yong WP, Philip PA, Bitzer M, Tanasanvimon S, Li A, Pande A, Soifer HS, Shepherd SP, Moran S, Zhu AX, Bekaii-Saab TS, Abou-Alfa GK. Infigratinib (BGJ398) in previously treated patients with advanced or metastatic cholangiocarcinoma with FGFR2 fusions or rearrangements: mature results from a multicentre, open-label, single-arm, phase 2 study. *Lancet Gastroenterol Hepatol* 2021; **6**: 803-815 [PMID: 34358484 DOI: 10.1016/S2468-1253(21)00196-5]

45 **Abou-Alfa GK**, Sahai V, Hollebecque A, Vaccaro G, Melisi D, Al-Rajabi R, Paulson AS, Borad MJ, Gallinson D, Murphy AG, Oh DY, Dotan E, Catenacci DV, Van Cutsem E, Ji T, Lihou CF, Zhen H, Féliz L, Vogel A. Pemigatinib for previously treated, locally advanced or metastatic cholangiocarcinoma: a multicentre, open-label, phase 2 study. *Lancet Oncol* 2020; **21**: 671-684 [PMID: 32203698 DOI: 10.1016/S1470-2045(20)30109-1]

46 **Makawita S**, K Abou-Alfa G, Roychowdhury S, Sadeghi S, Borbath I, Goyal L, Cohn A, Lamarca A, Oh DY, Macarulla T, T Shroff R, Howland M, Li A, Cho T, Pande A, Javle M. Infigratinib in patients with advanced cholangiocarcinoma with FGFR2 gene fusions/translocations: the PROOF 301 trial. *Future Oncol* 2020; **16**: 2375-2384 [PMID: 32580579 DOI: 10.2217/fon-2020-0299]

47 **Bekaii-Saab TS**, Valle JW, Van Cutsem E, Rimassa L, Furuse J, Ioka T, Melisi D, Macarulla T, Bridgewater J, Wasan H, Borad MJ, Abou-Alfa GK, Jiang P, Lihou CF, Zhen H, Asatiani E, Féliz L, Vogel A. FIGHT-302: first-line pemigatinib vs gemcitabine plus cisplatin for advanced cholangiocarcinoma with FGFR2 rearrangements. *Future Oncol* 2020; **16**: 2385-2399 [PMID: 32677452 DOI: 10.2217/fon-2020-0429]

48 **Mazzaferro V**, El-Rayes BF, Droz Dit Busset M, Cotsoglou C, Harris WP, Damjanov N, Masi G, Rimassa L, Personeni N, Braiteh F, Zagonel V, Papadopoulos KP, Hall T, Wang Y, Schwartz B, Kazakin J, Bhoori S, de Braud F, Shaib WL. Derazantinib (ARQ 087) in advanced or inoperable FGFR2 gene fusion-positive intrahepatic cholangiocarcinoma. *Br J Cancer* 2019; **120**: 165-171 [PMID: 30420614 DOI: 10.1038/s41416-018-0334-0]

49 **Bahleda R**, Italiano A, Hierro C, Mita A, Cervantes A, Chan N, Awad M, Calvo E, Moreno V, Govindan R, Spira A, Gonzalez M, Zhong B, Santiago-Walker A, Poggesi I, Parekh T, Xie H, Infante J, Tabernero J. Multicenter Phase I Study of Erdafitinib (JNJ-42756493), Oral Pan-Fibroblast Growth Factor Receptor Inhibitor, in Patients with Advanced or Refractory Solid Tumors. *Clin Cancer Res* 2019; **25**: 4888-4897 [PMID: 31088831 DOI: 10.1158/1078-0432.CCR-18-3334]

50 **Bahleda R**, Meric-Bernstam F, Goyal L, Tran B, He Y, Yamamiya I, Benhadji KA, Matos I, Arkenau HT. Phase I, first-in-human study of futibatinib, a highly selective, irreversible FGFR1-4 inhibitor in patients with advanced solid tumors. *Ann Oncol* 2020; **31**: 1405-1412 [PMID: 32622884 DOI: 10.1016/j.annonc.2020.06.018]

51 **Goyal L**, Meric-Bernstam F, Hollebecque A, Valle JW, Morizane C, Karasic TB, Abrams TA, Furuse J, Kelley RK, Cassier PA, Klümpen HJ, Chang HM, Chen LT, Tabernero J, Oh DY, Mahipal A, Moehler M, Mitchell EP, Komatsu Y, Masuda K, Ahn D, Epstein RS, Halim AB, Fu Y, Salimi T, Wacheck V, He Y, Liu M, Benhadji KA, Bridgewater JA; FOENIX-CCA2 Study Investigators. Futibatinib for FGFR2-Rearranged Intrahepatic Cholangiocarcinoma. *N Engl J Med* 2023; **388**: 228-239 [PMID: 36652354 DOI: 10.1056/NEJMoa2206834]

52 **Boscoe AN**, Rolland C, Kelley RK. Frequency and prognostic significance of isocitrate dehydrogenase 1 mutations in cholangiocarcinoma: a systematic literature review. *J Gastrointest Oncol* 2019; **10**: 751-765 [PMID: 31392056 DOI: 10.21037/jgo.2019.03.10]

53 **Lee K**, Song YS, Shin Y, Wen X, Kim Y, Cho NY, Bae JM, Kang GH. Intrahepatic cholangiocarcinomas with IDH1/2 mutation-associated hypermethylation at selective genes and their clinicopathological features. *Sci Rep* 2020; **10**: 15820 [PMID: 32978444 DOI: 10.1038/s41598-020-72810-0]

54 **Zhu AX**, Macarulla T, Javle MM, Kelley RK, Lubner SJ, Adeva J, Cleary JM, Catenacci DVT, Borad MJ, Bridgewater JA, Harris WP, Murphy AG, Oh DY, Whisenant JR, Lowery MA, Goyal L, Shroff RT, El-Khoueiry AB, Chamberlain CX, Aguado-Fraile E, Choe S, Wu B, Liu H, Gliser C, Pandya SS, Valle JW, Abou-Alfa GK. Final Overall Survival Efficacy Results of Ivosidenib for Patients With Advanced Cholangiocarcinoma With IDH1 Mutation: The Phase 3 Randomized Clinical ClarIDHy Trial. *JAMA Oncol* 2021; **7**: 1669-1677 [PMID: 34554208 DOI: 10.1001/jamaoncol.2021.3836]

55 **Rimini M**, Burgio V, Antonuzzo L, Rimassa L, Oneda E, Lavacchi D, Personeni N, Ratti F, Pedica F, Della Corte A, Persano M, De Cobelli F, Aldrighetti L, Scartozzi M, Cascinu S, Casadei-Gardini A. Real-World Data on Ivosidenib in Patients with Previously Treated Isocitrate Dehydrogenase 1-Mutated Intrahepatic Cholangiocarcinomas: An Early Exploratory Analysis. *Target Oncol* 2022; **17**: 591-596 [PMID: 36114954 DOI: 10.1007/s11523-022-00917-7]

56 **Casak SJ**, Pradhan S, Fashoyin-Aje LA, Ren Y, Shen YL, Xu Y, Chow ECY, Xiong Y, Zirklelbach JF, Liu J, Charlab R, Pierce WF, Fesenko N, Beaver JA, Pazdur R, Kluetz PG, Lemery SJ. FDA Approval Summary: Ivosidenib for the Treatment of Patients with Advanced Unresectable or Metastatic, Chemotherapy Refractory Cholangiocarcinoma with an IDH1 Mutation. *Clin Cancer Res* 2022; **28**: 2733-2737 [PMID: 35259259 DOI: 10.1158/1078-0432.CCR-21-4462]

57 **Weinberg BA**, Xiu J, Lindberg MR, Shields AF, Hwang JJ, Poorman K, Salem ME, Pishvaian MJ, Holcombe RF, Marshall JL, Morse MA. Molecular profiling of biliary cancers reveals distinct molecular alterations and potential therapeutic targets. *J Gastrointest Oncol* 2019; **10**: 652-662 [PMID: 31392046 DOI: 10.21037/jgo.2018.08.18]

58 **Tsimafeyeu I**, Temper M. Cholangiocarcinoma: An Emerging Target for Molecular Therapy. *Gastrointest Tumors* 2021; **8**: 153-158 [PMID: 34722468 DOI: 10.1159/000517258]

59 **Subbiah V**, Lassen U, Élez E, Italiano A, Curigliano G, Javle M, de Braud F, Prager GW, Greil R, Stein A, Fasolo A, Schellens JHM, Wen PY, Viele K, Boran AD, Gasal E, Burgess P, Ilankumaran P, Wainberg ZA. Dabrafenib plus trametinib in patients with BRAF(V600E)-mutated biliary tract cancer (ROAR): a phase 2, open-label, single-arm, multicentre basket trial. *Lancet Oncol* 2020; **21**: 1234-1243 [PMID: 32818466 DOI: 10.1016/S1470-2045(20)30321-1]

60 **Kim HJ**, Yoo TW, Park DI, Park JH, Cho YK, Sohn CI, Jeon WK, Kim BI, Kim MK, Chae SW, Sohn JH. Gene amplification and protein overexpression of HER-2/neu in human extrahepatic cholangiocarcinoma as detected by chromogenic in situ hybridization and immunohistochemistry: its prognostic implication in node-positive patients. *Ann Oncol* 2007; **18**: 892-897 [PMID: 17322545 DOI: 10.1093/annonc/mdm006]

61 **Detarya M**, Lert-Itthiporn W, Mahalapbutr P, Klaewkla M, Sorin S, Sawanyawisuth K, Silsirivanit A, Seubwai W, Wongkham C, Araki N, Wongkham S. Emerging roles of GALNT5 on promoting EGFR activation in cholangiocarcinoma: a mechanistic insight. *Am J Cancer Res* 2022; **12**: 4140-4159 [PMID: 36225633]

62 **Javle M**, Churi C, Kang HC, Shroff R, Janku F, Surapaneni R, Zuo M, Barrera C, Alshamsi H, Krishnan S, Mishra L, Wolff RA, Kaseb AO, Thomas MB, Siegel AB. HER2/neu-directed therapy for biliary tract cancer. *J Hematol Oncol* 2015; **8**: 58 [PMID: 26022204 DOI: 10.1186/s13045-015-0155-z]

63 **Javle M**, Borad MJ, Azad NS, Kurzrock R, Abou-Alfa GK, George B, Hainsworth J, Meric-Bernstam F, Swanton C, Sweeney CJ, Friedman CF, Bose R, Spigel DR, Wang Y, Levy J, Schulze K, Cuchelkar V, Patel A, Burris H. Pertuzumab and trastuzumab for HER2-positive, metastatic biliary tract cancer (MyPathway): a multicentre, open-label, phase 2a, multiple basket study. *Lancet Oncol* 2021; **22**: 1290-1300 [PMID: 34339623 DOI: 10.1016/S1470-2045(21)00336-3]

64 **Okamura R**, Boichard A, Kato S, Sicklick JK, Bazhenova L, Kurzrock R. Analysis of NTRK Alterations in Pan-Cancer Adult and Pediatric Malignancies: Implications for NTRK-Targeted Therapeutics. *JCO Precis Oncol* 2018; **2018** [PMID:

30637364 DOI: 10.1200/PO.18.00183]

65 **Grant CS**, Van Heerden JA. Anastomotic ulceration following subtotal and total pancreatectomy. *Ann Surg* 1979; **190**: 1-5 [PMID: 313757 DOI: 10.1038/s41379-019-0324-7]

66 **Drilon A**, Laetsch TW, Kummar S, DuBois SG, Lassen UN, Demetri GD, Nathenson M, Doebele RC, Farago AF, Pappo AS, Turpin B, Dowlati A, Brose MS, Mascarenhas L, Federman N, Berlin J, El-Deiry WS, Baik C, Deeken J, Boni V, Nagasubramanian R, Taylor M, Rudzinski ER, Meric-Bernstam F, Sohal DPS, Ma PC, Raez LE, Hechtman JF, Benayed R, Ladanyi M, Tuch BB, Ebata K, Cruickshank S, Ku NC, Cox MC, Hawkins DS, Hong DS, Hyman DM. Efficacy of Larotrectinib in TRK Fusion-Positive Cancers in Adults and Children. *N Engl J Med* 2018; **378**: 731-739 [PMID: 29466156 DOI: 10.1056/NEJMoa1714448]

67 **Doebele RC**, Drilon A, Paz-Ares L, Siena S, Shaw AT, Farago AF, Blakely CM, Seto T, Cho BC, Tosi D, Besse B, Chawla SP, Bazhenova L, Krauss JC, Chae YK, Barve M, Garrido-Laguna I, Liu SV, Conkling P, John T, Fakih M, Sigal D, Loong HH, Buchschacher GL Jr, Garrido P, Nieva J, Steuer C, Overbeck TR, Bowles DW, Fox E, Riehl T, Chow-Maneval E, Simmons B, Cui N, Johnson A, Eng S, Wilson TR, Demetri GD; trial investigators. Entrectinib in patients with advanced or metastatic NTRK fusion-positive solid tumours: integrated analysis of three phase 1-2 trials. *Lancet Oncol* 2020; **21**: 271-282 [PMID: 31838007 DOI: 10.1016/S1470-2045(19)30691-6]

68 **Le DT**, Durham JN, Smith KN, Wang H, Bartlett BR, Aulakh LK, Lu S, Kemberling H, Wilt C, Luber BS, Wong F, Azad NS, Rucki AA, Laheru D, Donehower R, Zaheer A, Fisher GA, Crocenzi TS, Lee JJ, Greten TF, Duffy AG, Ciombor KK, Eyring AD, Lam BH, Joe A, Kang SP, Holdhoff M, Danilova L, Cope L, Meyer C, Zhou S, Goldberg RM, Armstrong DK, Bever KM, Fader AN, Taube J, Housseau F, Spetzler D, Xiao N, Pardoll DM, Papadopoulos N, Kinzler KW, Eshleman JR, Vogelstein B, Anders RA, Diaz LA Jr. Mismatch repair deficiency predicts response of solid tumors to PD-1 blockade. *Science* 2017; **357**: 409-413 [PMID: 28596308 DOI: 10.1126/science.aan6733]

69 **Zhao P**, Li L, Jiang X, Li Q. Mismatch repair deficiency/microsatellite instability-high as a predictor for anti-PD-1/PD-L1 immunotherapy efficacy. *J Hematol Oncol* 2019; **12**: 54 [PMID: 31151482 DOI: 10.1186/s13045-019-0738-1]

70 **de Miguel M**, Calvo E. Clinical Challenges of Immune Checkpoint Inhibitors. *Cancer Cell* 2020; **38**: 326-333 [PMID: 32750319 DOI: 10.1016/j.ccell.2020.07.004]

71 **Goleva E**, Lyubchenko T, Kraehenbuehl L, Lacouture ME, Leung DYM, Kern JA. Our current understanding of checkpoint inhibitor therapy in cancer immunotherapy. *Ann Allergy Asthma Immunol* 2021; **126**: 630-638 [PMID: 33716146 DOI: 10.1016/j.anai.2021.03.003]

72 **Gani F**, Nagarajan N, Kim Y, Zhu Q, Luan L, Bhaijjee F, Anders RA, Pawlik TM. Program Death 1 Immune Checkpoint and Tumor Microenvironment: Implications for Patients With Intrahepatic Cholangiocarcinoma. *Ann Surg Oncol* 2016; **23**: 2610-2617 [PMID: 27012989 DOI: 10.1245/s10434-016-5101-y]

73 **Rizzo A**, Ricci AD, Brandi G. Recent advances of immunotherapy for biliary tract cancer. *Expert Rev Gastroenterol Hepatol* 2021; **15**: 527-536 [PMID: 33215952 DOI: 10.1080/17474124.2021.1853527]

74 **Piha-Paul SA**, Oh DY, Ueno M, Malka D, Chung HC, Nagrial A, Kelley RK, Ros W, Italiano A, Nakagawa K, Rugo HS, de Braud F, Varga AI, Hansen A, Wang H, Krishnan S, Norwood KG, Doi T. Efficacy and safety of pembrolizumab for the treatment of advanced biliary cancer: Results from the KEYNOTE-158 and KEYNOTE-028 studies. *Int J Cancer* 2020; **147**: 2190-2198 [PMID: 32359091 DOI: 10.1002/ijc.33013]

75 **Feng K**, Liu Y, Zhao Y, Yang Q, Dong L, Liu J, Li X, Zhao Z, Mei Q, Han W. Efficacy and biomarker analysis of nivolumab plus gemcitabine and cisplatin in patients with unresectable or metastatic biliary tract cancers: results from a phase II study. *J Immunother Cancer* 2020; **8** [PMID: 32487569 DOI: 10.1136/jitc-2019-000367]

76 **Ueno M**, Ikeda M, Morizane C, Kobayashi S, Ohno I, Kondo S, Okano N, Kimura K, Asada S, Namba Y, Okusaka T, Furuse J. Nivolumab alone or in combination with cisplatin plus gemcitabine in Japanese patients with unresectable or recurrent biliary tract cancer: a non-randomised, multicentre, open-label, phase 1 study. *Lancet Gastroenterol Hepatol* 2019; **4**: 611-621 [PMID: 31109808 DOI: 10.1016/S2468-1253(19)30086-X]

77 **Kim RD**, Chung V, Alese OB, El-Rayes BF, Li D, Al-Toubah TE, Schell MJ, Zhou JM, Mahipal A, Kim BH, Kim DW. A Phase 2 Multi-institutional Study of Nivolumab for Patients With Advanced Refractory Biliary Tract Cancer. *JAMA Oncol* 2020; **6**: 888-894 [PMID: 32352498 DOI: 10.1001/jamaoncol.2020.0930]

78 **Klein O**, Kee D, Nagrial A, Markman B, Underhill C, Michael M, Jackett L, Lum C, Behren A, Palmer J, Tebbutt NC, Carlino MS, Cebon J. Evaluation of Combination Nivolumab and Ipilimumab Immunotherapy in Patients With Advanced Biliary Tract Cancers: Subgroup Analysis of a Phase 2 Nonrandomized Clinical Trial. *JAMA Oncol* 2020; **6**: 1405-1409 [PMID: 32729929 DOI: 10.1001/jamaoncol.2020.2814]

79 **Sahai V**, Griffith KA, Beg MS, Shaib WL, Mahalingam D, Zhen DB, Deming DA, Zalupski MM. A randomized phase 2 trial of nivolumab, gemcitabine, and cisplatin or nivolumab and ipilimumab in previously untreated advanced biliary cancer: BilT-01. *Cancer* 2022; **128**: 3523-3530 [PMID: 35895381 DOI: 10.1002/cncr.34394]

80 **Chen X**, Wu X, Wu H, Gu Y, Shao Y, Shao Q, Zhu F, Li X, Qian X, Hu J, Zhao F, Mao W, Sun J, Wang J, Han G, Li C, Xia Y, Seesaha PK, Zhu D, Li H, Zhang J, Wang G, Wang X, Shu Y. Camrelizumab plus gemcitabine and oxaliplatin (GEMOX) in patients with advanced biliary tract cancer: a single-arm, open-label, phase II trial. *J Immunother Cancer* 2020; **8** [PMID: 33172881 DOI: 10.1136/jitc-2020-001240]

81 **Chen X**, Qin S, Gu S, Ren Z, Chen Z, Xiong J, Liu Y, Meng Z, Zhang X, Wang L, Zou J. Camrelizumab plus oxaliplatin-based chemotherapy as first-line therapy for advanced biliary tract cancer: A multicenter, phase 2 trial. *Int J Cancer* 2021; **149**: 1944-1954 [PMID: 34309846 DOI: 10.1002/ijc.33751]

82 **Oh DY**, Lee KH, Lee DW, Yoon J, Kim TY, Bang JH, Nam AR, Oh KS, Kim JM, Lee Y, Guthrie V, McCoon P, Li W, Wu S, Zhang Q, Rebelatto MC, Kim JW. Gemcitabine and cisplatin plus durvalumab with or without tremelimumab in chemotherapy-naive patients with advanced biliary tract cancer: an open-label, single-centre, phase 2 study. *Lancet Gastroenterol Hepatol* 2022; **7**: 522-532 [PMID: 35278356 DOI: 10.1016/S2468-1253(22)00043-7]

83 **Peng X**, Wang X, Hua L, Yang R. Prognostic and Clinical Value of the Systemic Immune-Inflammation Index in Biliary Tract Cancer: A Meta-Analysis. *J Immunol Res* 2022; **2022**: 6988489 [PMID: 36438200 DOI: 10.1155/2022/6988489]

World Journal of Gastrointestinal Oncology

Submit a Manuscript: https://www.f6publishing.com

World J Gastrointest Oncol 2023 June 15; 15(6): 973-978

DOI: 10.4251/wjgo.v15.i6.973

ISSN 1948-5204 (online)

MINIREVIEWS

Analysis of load status and management strategies of main caregivers of patients with malignant tumors of digestive tract

Xiao-Yan Wang, Jing Wang, Shu Zhang

Specialty type: Gastroenterology and hepatology

Provenance and peer review: Unsolicited article; Externally peer reviewed.

Peer-review model: Single blind

Peer-review report's scientific quality classification

Grade A (Excellent): 0
Grade B (Very good): B
Grade C (Good): C
Grade D (Fair): 0
Grade E (Poor): 0

P-Reviewer: Andersen JB, Denmark; Elkord E, Qatar

Received: March 17, 2023
Peer-review started: March 17, 2023
First decision: April 7, 2023
Revised: April 12, 2023
Accepted: April 23, 2023
Article in press: April 23, 2023
Published online: June 15, 2023

Xiao-Yan Wang, Shu Zhang, Emergency Department, West China Hospital of Sichuan University, Chengdu 610000, Sichuan Province, China

Jing Wang, ENT (Ear-Nose-Throat) Department, Chengdu Hospital of Combination of Chinese Traditional and Western Medicine, Chengdu 610000, Sichuan Province, China

Corresponding author: Shu Zhang, MD, Associate Professor, Emergency Department, West China Hospital of Sichuan University, No. 37 Guoxue Lane, Wuhou District, Chengdu 610000, Sichuan Province, China. dr.zhangshu@qq.com

Abstract

Caregiver load refers to the subjective and objective negative impact of caregivers in the care of patients, and excessive load will have a serious impact on patients and caregivers themselves and can reduce their quality of life. For the main caregivers, it not only needs to care for the patients in life and daily life, but also needs to pay the cost of treatment for the patients, coupled with the need to carry out their own original work, life, *etc.* excessive life pressure, economic pressure, work pressure, emotional pressure, *etc.* lead to heavy load of the main caregivers, which can easily cause caregivers to have different degrees of psychological problems, which will cause serious adverse effects on the caregivers themselves and cancer patients, not conducive to the construction of a harmonious family and society. This article analyzes the current situation of primary caregiver burden in patients with gastrointestinal malignant tumors, analyzes its influencing factors, and specifies specific treatment strategies. It is hoped to provide scientific guidance for later related research and application.

Key Words: Malignant tumors; Digestive tract; Primary caregivers; Current load situation; Handling measures

Core Tip: This article analyzes the current situation of primary caregiver burden in patients with gastrointestinal malignant tumors, analyzes its influencing factors, and specifies specific treatment strategies. It is hoped to provide scientific guidance for later related research and application.

Citation: Wang XY, Wang J, Zhang S. Analysis of load status and management strategies of main caregivers of patients with malignant tumors of digestive tract. *World J Gastrointest Oncol* 2023; 15(6): 973-978
URL: https://www.wjgnet.com/1948-5204/full/v15/i6/973.htm
DOI: https://dx.doi.org/10.4251/wjgo.v15.i6.973

INTRODUCTION

With the change of life structure and dietary habits, the incidence of malignant tumors of the digestive tract has increased in recent years, which poses a threat to public health safety and also increases the social burden[1]. Because patients with malignant tumors have certain particularities, the demand for care is high. And caregivers are mostly family members of patients, and there are many death concerns among caring patients, and a variety of stresses can have a serious impact on the physical and mental health of caregivers[2]. Therefore, it is a hot issue in clinical practice to analyze the load status of the main caregivers of patients with malignant tumors of the digestive tract and make targeted treatment strategies.

STATUS OF LOAD OF MAIN CAREGIVERS OF PATIENTS WITH MALIGNANT TUMORS OF DIGESTIVE TRACT

The load of the main caregivers of patients with malignant tumors of the digestive tract includes five dimensions: Time-dependent load, development-limited load, physical load, sociability load, and affective load, which are described separately as follows.

Time-dependent loads

In studies of the load status of primary caregivers of patients with gastrointestinal malignancies[3,4], it was concluded that the time-dependent load score was 9.17 points, which was the dimension with the highest load score (Table 1 for specific data), which was consistent with the conclusions of many researchers in China[5].

Developmental limited burden

Development limitation load is influenced by time-dependent load, and the main caregivers of patients with gastrointestinal malignancies spend all their time and energy on patients, resulting in no time belonging to themselves to enjoy life. In related research, it is found that caring for and accompanying patients has become the main care of the only life content, their original lifestyle is completely changed, social activities such as parties, games, shopping are forced to cancel, and even hobbies are forced to give up, and their career planning, life planning and other forced changes make the main caregivers have serious adverse emotions[6,7]. A domestic study on the load bearing by the main caregivers of patients with malignant tumors of the digestive tract found that time-dependent load and development-limited load were the main loads, 25.4% of the main caregivers expected to rest briefly, and 16.4% wanted to be shared. In many foreign studies, it is emphasized that the main caregivers of patients with chronic diseases need more support, encouragement and proper rest, otherwise long-term accumulation will lead to their emotional breakdown and produce heavier emotional burden[8].

Physical load

The nursing tasks of patients with malignant tumors of digestive tract are relatively heavy. Prolonged care and companionship of patients make the main caregivers have obvious physical load, causing headache, physical decline, fatigue, drowsiness, palpitation and other physical symptoms due to affected sleep and mood, accompanied by anxiety, upset, depression, restlessness and other psychological symptoms[9]. In a foreign study, 35% of cancer patients were found to be mainly cared for the presence of physical stress symptoms, accompanied by significant physical load. However, relevant domestic surveys have found that most of the main caregivers of cancer patients believe that their health status is fair, and only a small number believe that their health status has problems due to caring for patients, which may be related to different study groups, or may have a greater impact on the psychological function and social function of caregivers than physical aspects, so that they automatically ignore the changes in health status[10,11]. In conclusion, physical load is also one of the main caregivers of patients with gastrointestinal malignancies.

Social load

The main caregivers of patients with malignant tumors of the digestive tract spent almost all their time caring for and accompanying the patients, and the lack of social support made them feel socially

Table 1 Total score and dimension scores of primary caregivers of patients with malignant tumors of digestive tract (*n* = 189)

Items	mean (Standard mean)	SD
Time dependent load (5 entries)	9.17 (1.83)	5.51
Developmental limiting load (5 items)	6.08 (1.22)	5.65
Physical load (4 items)	2.86 (0.97)	4.29
Social load (4 items)	2.02 (0.51)	2.47
Affective load (6 items)	0.92 (0.15)	1.45
Total load (24 items)	22.05 (0.92)	15.35

isolated[12]. Once problems of not being understood and not being able to get along with each other emerged in caring patients, the primary caregiver could easily experience sociability load. Relevant domestic studies have found that most primary caregivers can be understood and supported in caring patients, and only a small proportion have significant sociability load[13].

Affective load

Induced by traditional Chinese culture, most families can help each other. When a family member has a problem or disease, other members will actively and actively help and take care of it. In the hearts of most people, family members are superior to their own interests and hobbies. Therefore, it can be found in a number of studies that the emotional load is the lowest in the load of the main caregivers of cancer patients[14]. However, it has also been stated that a small number of people experience feelings such as complaints and anxiety after their lives have changed due to caring for patients, triggering emotional load[15].

INFLUENCING FACTORS OF MAIN CAREGIVER LOAD IN PATIENTS WITH MALIGNANT TUMORS OF DIGESTIVE TRACT

Economic situation

Economic situation is one of the important factors affecting the load of the main caregivers of patients with malignant tumors of the digestive tract, and in families with better economic conditions, they can choose more treatment options, and carers can be invited to take care of patients together, which greatly reduces the pressure on the caring load of the main caregivers[16]. In families with poor economic conditions, they should not only bear the responsibility of caring for patients independently, but also consider daily expenses, patients' treatment costs, *etc.*, in addition to the fact that caring for patients may not be able to participate in work, the decline in economic income makes the load of the main caregivers more emotional. Some studies have found that economic pressure is the main factor affecting the care load of the main caregivers of cancer patients, caregivers with relatively poor economic situation need to bear the comprehensive pressure of economic, mental, social, and life, and there is bound to be a high economic load in the face of cancer, a disease that costs "no bottom hole". Second, poor economic conditions limit the choice of patient treatment and examination options, and these pressures also increase the load on the main caregiver[17].

Caregiving impacts income

Malignant tumors of the digestive tract are cancers with high morbidity and mortality among all malignant tumors. In most cases, patients need to be cared for and accompanied by others every day, and even need members of the entire family to care for them when they are severely ill, which makes the main caregivers unable to have time and energy to work, which will have a serious impact on their economic income. However, the daily treatment or rehabilitation of patients requires a certain cost, and this economic pressure makes the load of the main caregiver heavy. Some studies have found that in families with heavy income due to caring for patients with advanced cancer, the degree of caring load appears to be heavy, which is consistent with the conclusions of a number of domestic and foreign studies[18].

Patient self-care ability

The self-care ability of patients is the main factor affecting the load of the main caregivers of patients with malignant tumors of the digestive tract. The worse the self-care ability of patients, the heavier the load of care of the main caregivers. The analysis of the reasons may be related to the following points: (1) With the progression of the disease, patients may experience a variety of complications, the decline of body function makes their own care ability also decline, followed by an increase in dependence on

the main caregiver, which directly leads to caregivers need to pay more time and energy, and the load naturally borne is also relatively heavy; (2) With the progression of the disease, the number of chemoradiotherapy increases, which aggravates the medical burden, coupled with the lack of professional nursing skills and knowledge of the main caregiver, resulting in a higher load of their own care. Some related studies have pointed out that among the main caregivers of patients with advanced cancer, most people crave professional disease knowledge training; and (3) With the progression of the disease, patients may experience cancer pain symptoms, especially aggravated in the evening, and it is often necessary for the main caregivers to take relevant measures to relieve cancer pain, which undoubtedly has a serious impact on the sleep of the main caregivers, and then can make the main caregivers experience a significant load[19].

Time to care for patients

The time of caring for patients is one of the important factors affecting the load of the main caregivers of patients with malignant tumors of the digestive tract, and the longer the total time of caring for patients, the heavier the load of the main caregivers. The reason may be due to the care of patients, the main caregivers can freely control the time significantly shortened, the reduction of social activities makes it easy to collapse mentally, and the mental load it bears is also relatively heavy. At the same time, the longer the patient is cared for, the greater the impact on work, and the natural income will be greatly reduced. However, the cost of patient treatment makes the main caregiver bear heavy economic pressure, and the spirit is in a state of high tension and fatigue for a long time. Finally, because caring for patients, their own lifestyle, routines are changed, lack of sleep, irregular life and other adverse effects on the physical health of the main caregivers have also caused adverse effects, in the double adverse effects of physical and mental, the main caregivers are prone to higher physical and mental, spiritual load.

COUNTERMEASURES TO REDUCE THE LOAD OF MAIN CAREGIVERS OF PATIENTS WITH MALIGNANT TUMORS OF THE DIGESTIVE TRACT

Develop a diagnosis and care plan according to the actual situation to reduce the medical costs of patients

In the actual diagnosis and treatment, the economic situation of the patient 's family and main caregivers shall be evaluated to understand whether the patient pays medical insurance or commercial insurance, the actual situation of the patient' s disease shall be analyzed for the patient with poor economic conditions, and the drugs and consumables with higher selectivity and higher reimbursement rate of medical insurance shall be tried in the treatment and examination. During hospitalization, appropriate care plans are developed to reduce unnecessary treatment and nursing procedures, so as to appropriately reduce their medical costs.

Strengthening the care of patients with poor self-care ability in clinical nursing

In clinical nursing, the actual situation and self-care ability of patients are assessed to determine the level of care of patients. Special care patients were given 24-h care, primary care patients were given circuit observation every 1 h, secondary care patients were given circuit observation every 2 h, and patients with poor self-care ability were given more care and attention, mainly including the following points: (1) Strengthen the nursing patrol of patients, include patients with critical condition and poor self-care ability in the focus of nursing observation, especially during the shift, do a good job of work handover and information check; (2) help patients turn over and pat their back when they are awake, assist patients to complete daily face washing, tooth brushing, dressing and other operations, especially to strengthen the care of the patient's mouth and skin; (3) Regularly evaluate the patient 's condition, predict the possible risk events or complications, and formulate response plans. Once abnormal phenomena are found, they should be immediately reported to the doctor and emergency treatment should be made according to the doctor's advice; (4) strengthen the health education for patients and main caregivers, tell the behaviors conducive to disease or physical rehabilitation, guide them to develop good health habits, and improve their own rehabilitation; and (5) develop an out-of-hospital follow-up plan after discharge, among which telephone follow-up: 2 wk after discharge, 1 return visit every 3 days; 2-4 wk after discharge, once a week; 4-8 wk after discharge, once every 2 wk, 8-12 wk after discharge, once every 4 wk; door-to-door follow-up: 1 time a month, face-to-face communication with patients, telephone and door-to-door follow-up contents include the patient's recent pain, health behaviors, medication, physical condition, psychological emotions, *etc.*, and make adjustments to the nursing plan according to the actual situation of patients; Inform patients of any questions they may have at any time in the group and provide remote guidance on relevant care. By strengthening the care of patients with poor self-care ability, nursing staff can reduce the care burden of the main caregiver to a large extent, which can effectively alleviate or prevent the emergence of care load[20].

Improving the time to get along with and accompany patients in clinical nursing

During the patient's hospitalization, improve the time for communication and companionship. In the nursing operation, it is necessary to pay attention to establishing communication with the patient, give them more spiritual encouragement and comfort, and then accompany the patient to walk outside the ward every day when their physical condition permits, so as to replace the main caregiver to accompany the patient. For special patients, the accompany model without family members can be carried out. The accompany nursing without family members is not to ask the family members of patients to hire professional accompany personnel for daily nursing, nor to limit the family members to visit the patients, but to let the family members of patients accompany but not protect. On the basis of completing their own work, the nursing staff replaces the family members of patients to complete the relevant nursing services, so as to improve the time to get along with the patients.

Actively communicate with the main caregivers of patients and provide psychological counseling and support for them.

Communicate regularly with the main caregivers of patients, evaluate their psychological status, understand their existing difficulties and inner real ideas, physical and mental status, targeted psychological counseling. Pay attention to protecting the privacy of patients' families when communicating, have polite, sincere and friendly tone, have natural and appropriate language, and conduct non-verbal communication when necessary[21,22]. Professional psychotherapy is carried out for primary caregivers who have significant psychological problems or severe load[23,24].

CONCLUSION

Due to economic situation, care will affect income, patients' self-care ability and care time of patients and other factors, the main caregivers of patients with digestive tract malignant tumors generally have different degrees of load, which will not only affect the care of patients, but also cause serious adverse effects on the physical and mental health of caregivers themselves. Therefore, in the later work, it is necessary to strengthen the load on the main caregivers of patients with malignant tumors of the digestive tract, alleviate or prevent the occurrence of load by formulating a targeted diagnosis and care plan, reducing the medical costs of patients, strengthening the time to care for patients with poor self-care ability, get along, and accompany them and carrying out psychological counseling and support for the main caregivers.

FOOTNOTES

Author contributions: Wang XY designed the research study and performed the research; Wang J contributed analytic tools; Zhang S analyzed the data and wrote the manuscript; and all authors have read and approve the final manuscript.

Conflict-of-interest statement: No conflict of interest.

Country/Territory of origin: China

ORCID number: Xiao-Yan Wang 0000-0002-0480-3869; Shu Zhang 0000-0002-2568-9153.

S-Editor: Wang JL
L-Editor: A
P-Editor: Yu HG

REFERENCES

1 **Owoo B**, Ninnoni JP, Ampofo EA, Seidu AA. Challenges encountered by family caregivers of prostate cancer patients in Cape Coast, Ghana: a descriptive phenomenological study. *BMC Palliat Care* 2022; **21**: 108 [PMID: 35701817 DOI: 10.1186/s12904-022-00993-6]

2 **Carter J**, Huang HQ, Armer J, Carlson JW, Lockwood S, Nolte S, Kauderer J, Hutson A, Walker JL, Fleury AC,

Bonebrake A, Soper JT, Mathews C, Zivanovic O, Richards WE, Tan A, Alberts DS, Barakat RR, Wenzel LB. GOG 244 - The Lymphedema and Gynecologic cancer (LeG) study: The impact of lower-extremity lymphedema on quality of life, psychological adjustment, physical disability, and function. *Gynecol Oncol* 2021; **160**: 244-251 [PMID: 33109392 DOI: 10.1016/j.ygyno.2020.10.023]

3 **Sutherland AE**, Bennett NC, Herst PM. Psychological stress affects the severity of radiation-induced acute skin reactions in breast cancer patients. *Eur J Cancer Care (Engl)* 2017; **26** [PMID: 28707369 DOI: 10.1111/ecc.12737]

4 **Kim SH**, Kim JH, Shim EJ, Hahm BJ, Yu ES. Patients' communication preferences for receiving a cancer diagnosis: Differences depending on cancer stage. *Psychooncology* 2020; **29**: 1540-1548 [PMID: 32567081 DOI: 10.1002/pon.5447]

5 **Liu W**, Zhang H. Do sleep quality and psychological factors link precancerous conditions of colorectal cancer? A retrospective case-control study. *Expert Rev Gastroenterol Hepatol* 2022; **16**: 173-179 [PMID: 35043737 DOI: 10.1080/17474124.2022.2029701]

6 **Jeong A**, An JY. The moderating role of social support on depression and anxiety for gastric cancer patients and their family caregivers. *PLoS One* 2017; **12**: e0189808 [PMID: 29284033 DOI: 10.1371/journal.pone.0189808]

7 **Miyashita M**, Wada M, Morita T, Ishida M, Onishi H, Tsuneto S, Shima Y. Development and validation of the Comprehensive Quality of Life Outcome (CoQoLo) inventory for patients with advanced cancer. *BMJ Support Palliat Care* 2019; **9**: 75-83 [PMID: 26497747 DOI: 10.1136/bmjspcare-2014-000725]

8 **Otto AK**, Soriano EC, Birmingham WC, Vadaparampil ST, Heyman RE, Ellington L, Reblin M. Impact of Relationship and Communication Variables on Ambulatory Blood Pressure in Advanced Cancer Caregivers. *Ann Behav Med* 2022; **56**: 405-413 [PMID: 34244701 DOI: 10.1093/abm/kaab057]

9 **Mosher CE**, Winger JG, Hanna N, Jalal SI, Einhorn LH, Birdas TJ, Ceppa DP, Kesler KA, Schmitt J, Kashy DA, Champion VL. Randomized Pilot Trial of a Telephone Symptom Management Intervention for Symptomatic Lung Cancer Patients and Their Family Caregivers. *J Pain Symptom Manage* 2016; **52**: 469-482 [PMID: 27401514 DOI: 10.1016/j.jpainsymman.2016.04.006]

10 **Maeda K**, Hasegawa D, Urayama KY, Tsujimoto S, Azami Y, Ozawa M, Manabe A. Risk factors for psychological and psychosomatic symptoms among children with malignancies. *J Paediatr Child Health* 2018; **54**: 411-415 [PMID: 29105206 DOI: 10.1111/jpc.13771]

11 **Tay CT**, Loxton D, Khomami MB, Teede H, Joham AE. Negative associations of ideal family size achievement with hypertension, obesity and maternal age in women with and without polycystic ovary syndrome. *Clin Endocrinol (Oxf)* 2022; **97**: 217-226 [PMID: 35394665 DOI: 10.1111/cen.14736]

12 **Mosher CE**, Secinti E, Hirsh AT, Hanna N, Einhorn LH, Jalal SI, Durm G, Champion VL, Johns SA. Acceptance and Commitment Therapy for Symptom Interference in Advanced Lung Cancer and Caregiver Distress: A Pilot Randomized Trial. *J Pain Symptom Manage* 2019; **58**: 632-644 [PMID: 31255586 DOI: 10.1016/j.jpainsymman.2019.06.021]

13 **Byrne A**, Torrens-Burton A, Sivell S, Moraes FY, Bulbeck H, Bernstein M, Nelson A, Fielding H. Early palliative interventions for improving outcomes in people with a primary malignant brain tumour and their carers. *Cochrane Database Syst Rev* 2022; **1**: CD013440 [PMID: 34988973 DOI: 10.1002/14651858.CD013440.pub2]

14 **Gangane N**, Khairkar P, Hurtig AK, San Sebastián M. Quality of Life Determinants in Breast Cancer Patients in Central Rural India. *Asian Pac J Cancer Prev* 2017; **18**: 3325-3332 [PMID: 29286227 DOI: 10.22034/APJCP.2017.18.12.3325]

15 **Shamloo MBB**, Nasiri M, Maneiy M, Kiarsi M, Madmoli Y. Correlation between ways of coping and quality of life in Iranian husbands of women with breast cancer. *Int J Palliat Nurs* 2020; **26**: 84-90 [PMID: 32125917 DOI: 10.12968/ijpn.2020.26.2.84]

16 **Costas-Muñiz R**, Garduño-Ortega O, Hunter-Hernández M, Morales J, Castro-Figueroa EM, Gany F. Barriers to Psychosocial Services Use For Latina Versus Non-Latina White Breast Cancer Survivors. *Am J Psychother* 2021; **74**: 13-21 [PMID: 33028079 DOI: 10.1176/appi.psychotherapy.20190036]

17 **Jack BA**, Mitchell TK, Cope LC, O'Brien MR. Supporting older people with cancer and life-limiting conditions dying at home: a qualitative study of patient and family caregiver experiences of Hospice at Home care. *J Adv Nurs* 2016; **72**: 2162-2172 [PMID: 27113470 DOI: 10.1111/jan.12983]

18 **Hartman SJ**, Weiner LS, Nelson SH, Natarajan L, Patterson RE, Palmer BW, Parker BA, Sears DD. Mediators of a Physical Activity Intervention on Cognition in Breast Cancer Survivors: Evidence From a Randomized Controlled Trial. *JMIR Cancer* 2019; **5**: e13150 [PMID: 31605514 DOI: 10.2196/13150]

19 **Taub CJ**, Lippman ME, Hudson BI, Blomberg BB, Diaz A, Fisher HM, Nahin ER, Lechner SC, Kwak T, Hwang GH, Antoni MH. The effects of a randomized trial of brief forms of stress management on RAGE-associated S100A8/A9 in patients with breast cancer undergoing primary treatment. *Cancer* 2019; **125**: 1717-1725 [PMID: 30633331 DOI: 10.1002/cncr.31965]

20 **Ferguson RJ**, Sigmon ST, Pritchard AJ, LaBrie SL, Goetze RE, Fink CM, Garrett AM. A randomized trial of videoconference-delivered cognitive behavioral therapy for survivors of breast cancer with self-reported cognitive dysfunction. *Cancer* 2016; **122**: 1782-1791 [PMID: 27135464 DOI: 10.1002/cncr.29891]

21 **Reese JB**, Zimmaro LA, Lepore SJ, Sorice KA, Handorf E, Daly MB, Schover LR, Kashy D, Westbrook K, Porter LS. Evaluating a couple-based intervention addressing sexual concerns for breast cancer survivors: study protocol for a randomized controlled trial. *Trials* 2020; **21**: 173 [PMID: 32051002 DOI: 10.1186/s13063-019-3975-2]

22 **Leclair T**, Carret AS, Samson Y, Sultan S. Stability and Repeatability of the Distress Thermometer (DT) and the Edmonton Symptom Assessment System-Revised (ESAS-r) with Parents of Childhood Cancer Survivors. *PLoS One* 2016; **11**: e0159773 [PMID: 27454432 DOI: 10.1371/journal.pone.0159773]

23 **Victorson D**, Morgan T, Kutikov A, Novakovic K, Kundu S, Horowitz B, Jackson K, Addington E, Murphy K, Sauer C, Brendler C. Mindfulness-based stress reduction for men on active surveillance for prostate cancer and their spouses: Design and methodology of a randomized controlled trial. *Contemp Clin Trials* 2023; **125**: 107059 [PMID: 36563902 DOI: 10.1016/j.cct.2022.107059]

24 **Marzorati C**, Renzi C, Russell-Edu SW, Pravettoni G. Telemedicine Use Among Caregivers of Cancer Patients: Systematic Review. *J Med Internet Res* 2018; **20**: e223 [PMID: 29914858 DOI: 10.2196/jmir.9812]

World Journal of Gastrointestinal Oncology

Submit a Manuscript: https://www.f6publishing.com

World J Gastrointest Oncol 2023 June 15; 15(6): 979-987

DOI: 10.4251/wjgo.v15.i6.979

ISSN 1948-5204 (online)

MINIREVIEWS

Emerging role of autophagy in colorectal cancer: Progress and prospects for clinical intervention

Tian-Fei Ma, Yue-Ren Fan, Yi-Hang Zhao, Bin Liu

Specialty type: Oncology

Provenance and peer review: Unsolicited article; Externally peer reviewed.

Peer-review model: Single blind

Peer-review report's scientific quality classification

Grade A (Excellent): 0
Grade B (Very good): B
Grade C (Good): C
Grade D (Fair): 0
Grade E (Poor): 0

P-Reviewer: Alonso C, Spain; Bottalico L, Italy

Received: March 28, 2023
Peer-review started: March 28, 2023
First decision: April 11, 2023
Revised: April 17, 2023
Accepted: May 12, 2023
Article in press: May 12, 2023
Published online: June 15, 2023

Tian-Fei Ma, Yue-Ren Fan, Yi-Hang Zhao, Bin Liu, Department of Breast Internal Medicine II, Cancer Hospital of China Medical University, Liaoning Cancer Hospital & Institute, Shenyang 110042, Liaoning Province, China

Corresponding author: Tian-Fei Ma, MBBS, Doctor, Department of Breast Internal Medicine II, Cancer Hospital of China Medical University, Liaoning Cancer Hospital and Institute, No. 44 Xiaoheyan Road, Dadong District, Shenyang 110042, Liaoning Province, China.
lnskaxh6@163.com

Abstract

Autophagy is a physiological mechanism in which cells degrade themselves and quickly recover the degraded cell components. Recent studies have shown that autophagy plays an important role in the occurrence, development, treatment, and prognosis of colorectal cancer. In the early stages of colorectal cancer, autophagy can inhibit the production and development of tumors through multiple mechanisms such as maintaining DNA stability, inducing tumor death, and enhancing immune surveillance. However, as colorectal cancer progresses, autophagy may mediate tumor resistance, enhance tumor metabolism, and other pathways to promote tumor development. Therefore, intervening in autophagy at the appropriate time has broad clinical application prospects. This article summarizes the recent research progress of autophagy and colorectal cancer and is expected to provide new theoretical basis and reference for clinical treatment of colorectal cancer.

Key Words: Autophagy; Self-degradation; Colorectal cancer; Phosphatidylinositol-3-phosphate; Immune cells

Core Tip: In the early stages of colon cancer, autophagy can inhibit the production and development of tumors through multiple mechanisms such as maintaining DNA stability, inducing tumor death, and enhancing immune surveillance. However, as colorectal cancer progresses, autophagy may mediate tumor resistance, enhance tumor metabolism, and other pathways to promote tumor development. Therefore, intervening in autophagy at the appropriate time has broad clinical application prospects.

Citation: Ma TF, Fan YR, Zhao YH, Liu B. Emerging role of autophagy in colorectal cancer: Progress and prospects for clinical intervention. *World J Gastrointest Oncol* 2023; 15(6): 979-987
URL: https://www.wjgnet.com/1948-5204/full/v15/i6/979.htm
DOI: https://dx.doi.org/10.4251/wjgo.v15.i6.979

INTRODUCTION

Colorectal cancer (CRC) refers to malignant epithelial tumors of the colon, rectum, and anal canal. In 2020, CRC was the third most common malignancy and the second most deadly cancer worldwide, with an estimated 1.88 million new cases (9.8%) and 910000 deaths (9.2%)[1]. Great progress has been made in CRC diagnosis and treatment with the availability of routine health check-ups and new techniques. At present, surgery remains the mainstay of treatment for CRC, while chemotherapy, targeted therapy, and immunotherapy have also been applied in clinical settings. However, due to its insidious onset, CRC is mostly diagnosed in advanced stages and becomes resistant to chemotherapy and targeted therapy[2]. Therefore, the prognosis of CRC is poor. Autophagy plays a critical role in regulating cancer development, and autophagy-based clinical interventions may address this clinical dilemma. This article reviews the recent progress in the research on the association between autophagy and CRC.

AUTOPHAGY

Autophagy is a highly conserved eukaryotic macromolecular degradation process that degrades and recycles macromolecular substances such as damaged organelles and sirtuins inside the cells to quickly replenish the substances required for normal physiological activities of cells[3]. Autophagy is strictly regulated by a variety of autophagy-related genes (ATGs). Under stressful conditions such as organelle damage, production of abnormal proteins, and nutrient deficiency, autophagosomes are formed, which fuse with intracellular lysosomes to form autophagolysosomes by wrapping or binding to the components to be degraded, thus initiating the degradation and recycling process[4]. In both normal and malignant cells, autophagy may be a response to cellular stresses including nutrient deficiencies, hypoxia, and toxin accumulation[5]. Nevertheless, the impact of autophagy on cells can be multi-faceted: It may be a protective factor that promotes cell survival, but can also lead to growth arrest and/or apoptosis.

Autophagy, as a metabolic regulatory mechanism widely present within cells, can lead to various diseases such as neurodegenerative diseases and tumors once dysregulated. As shown in Figure 1, the molecular mechanism *via* which autophagy is regulated mainly includes the following three aspects: (1) The adenosine monophosphate-activated protein kinase (AMPK)/mammalian target of rapamycin (mTOR) pathway: The mTOR kinase, as a receptor for amino acids, energy, and hormones in cells, can regulate autophagy in a negative feedback manner[6]; (2) The phosphatidylinositol 3-kinase (PI3K)/AKT signaling pathway: Different types of PI3K play different roles in autophagy regulation, among which type I PI3K can inhibit autophagy after binding to AKT, whereas type III PI3K can induce the enhancement of autophagy by binding to the ultraviolet resistance-associated gene (UURAG) product; and (3) The negative feedback signaling pathway of G protein subunit Gai3 and amino acids: GTP can bind to Gai3 intracellularly and is an inhibitory signal of autophagy; GDP binds to Gai3 protein to activate autophagy; and, as the end products of protein degradation, amino acids negatively regulate the autophagy[7-8].

Autophagy can be divided into three types depending on the mechanism by which intracellular materials are delivered into the lysosome for degradation: Macroautophagy, microautophagy, and chaperone-mediated autophagy (CMA)[9]. Macroautophagy is a selective autophagy process that occurs mainly in macrophages. They can form phagosomes that ingest cytoplasmic proteins and damaged organelles and then further mature into double-membrane binding vesicles (known as autophagosomes). These autophagosomes are transported to lysosomes, where they degrade the damaged mitochondria, the invading microorganisms, and other components, thus maintaining the homeostasis of cells during the stress response. During macroautophagy, autophagy is mainly regulated *via* the AMPK/mTOR signaling pathway[10]. Microautophagy occurs through the invagination of lysosomes or endosomal membranes, which directly phagocytosize the substances to be degraded, during which the proteases in lysosomes play a degrading role. Microautophagy occurs in almost all normal cells and therefore is a widely existing intracellular energy and material circulation mechanism[11-12]. Notably, no direct link between microautophagy and tumorigenesis has been found.

Unlike macroautophagy and microautophagy, CMA is a selective lysosome-dependent protein-degrading mechanism[13]. CMA exists in most cells but exerts only basal activities under physiological conditions. Once cell stress occurs, the activity of CMA is rapidly enhanced, which facilitates the rapid circulation of intracellular proteins under stress conditions and minimizes the need for new protein

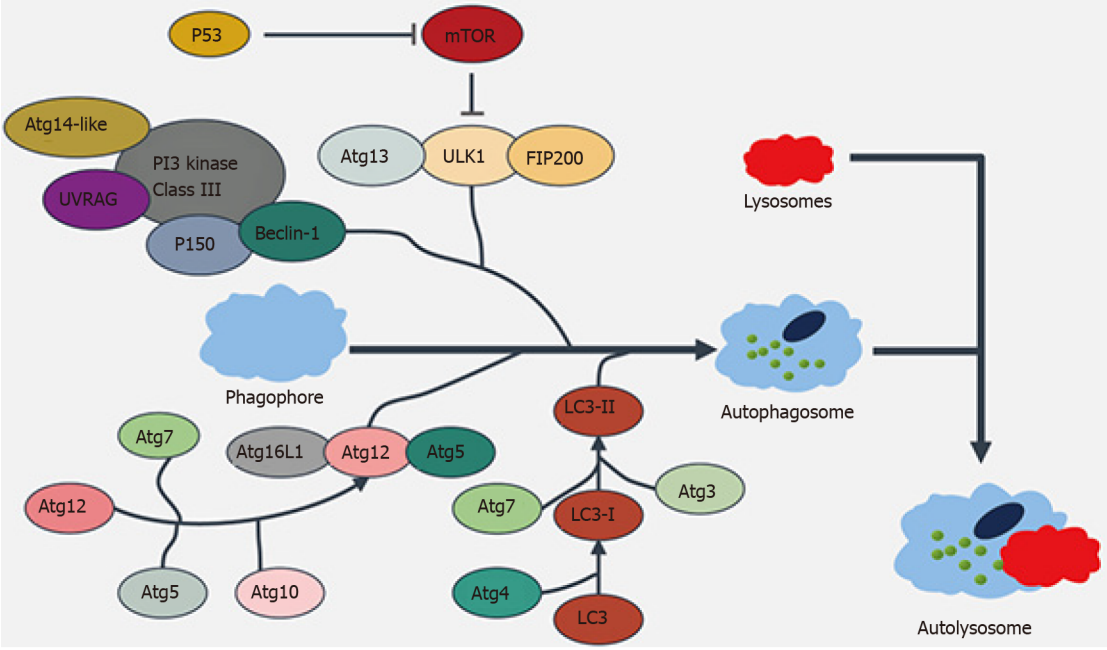

DOI: 10.4251/wjgo.v15.i6.979 **Copyright** ©The Author(s) 2023.

Figure 1 Autophagy-related gene signaling pathway schematic. Autophagy can be mainly divided into five stages according to its development process: induction, autophagosome nucleation, autophagosome formation, lysosome fusion, and degradation. As shown in the diagram, the entire process is strictly regulated by over 36 autophagy-related genes and their corresponding proteins. The mammalian target of rapamycin is a key factor in autophagy. Mature autophagosomes can merge with lysosomes to form autolysosomes, which selectively remove proteins and damaged organelles through autophagy and participate in autophagic body formation. mTOR: Mammalian target of rapamycin.

degradation and production, thereby maximizing energy savings and improving cell survival. Compared to normal cells, tumor cells have increased CMA activity. Blocking CMA significantly inhibited tumor growth and induced regression of lung cancer or melanoma xenografts in mouse models[14]. Therefore, intervening in the CMA pathways may have broad antitumor activity. In the form of autophagy, all the proteins targeted by CMA contain KFERQ-like pentapeptide motifs, which can be recognized by heat shock protein family A (Hsp70) member 8 (HSPA8/HSC70) and form a complex with lysosome-associated membrane protein type 2a (LAMP-2A)[15]. No vesicle structure will be formed during this process; rather, the proteins to be degraded pass directly through the lysosomal membrane to enter the lysosomal cavity for degradation.

In addition to autophagy's important regulatory role in energy and material metabolism, the endosomal protein sorting nexin 5 (SNX5) interacts with beclin 1 and ATG14-containing class III phosphatidylinositol-3-kinase (PI3KC3) complex 1 (PI3KC3-C1), increases the lipid kinase activity of purified PI3KC3-C1, and is required for the endosomal generation of phosphatidylinositol-3-phosphate (PI3P) and recruitment of the PI3P-binding protein WIPI2 to virion-containing endosomes, thus mediating virus-induced autophagy[16]. Therefore, autophagy can also play an immune- and host-protecting role when cells are invaded by viruses.

REGULATORY ROLES OF AUTOPHAGY IN CRC

As a regulatory mechanism of intracellular substance and energy metabolism, autophagy is deeply involved in a variety of biological behaviors such as cell repair, transformation, proliferation, senescence, and apoptosis[17]. With increasing in-depth research, the roles of autophagy in the pathogenesis, drug resistance, and therapeutic options of CRC have been revealed. For CRC, autophagy is a "double-edged sword": On the one hand, autophagy can significantly suppress proliferation and induce apoptosis in CRC cells; on the other hand, it can also provide CRC cells with additional energy to promote their abnormal proliferation and can reduce the response of CRC to various treatment measures[18].

Autophagy acts as a CRC suppressor

As a housekeeping mechanism in normal cells, autophagy can scavenge and repair DNA damage, abnormal folding of proteins or abnormal accumulation of normal proteins, accumulation of oxygen free radicals, and damage to organelles (*e.g.* mitochondria) during normal physiological processes and under stress, which is extremely important for maintaining cell stability and avoiding carcinogenesis[3,

19-21]. Therefore, as an early cancer-suppressing mechanism, autophagy can protect the human body through multiple pathways.

SRC kinases are non-receptor tyrosine kinases that mediate carcinogenesis. An abnormal elevation of SRC can be detected in about 80% of CRC patients, and sorting nexin 10 (SNX10), an endosomal protein, is negatively correlated with SRC expression. The downregulated expression of SNX10 is significantly associated with SRC activation, tumor differentiation, tumor metastasis, and patient survival. SNX10 regulates the fusion between autophagy and lysosomes. SNX10 deficiency can lead to impaired autophagic degradation of SRC, which ultimately promotes the occurrence and development of CRC. Interfering with the SRC autophagy pathway can achieve the regulation of tumor growth[22].

The level of the imprinted gene pleckstrin homology like domain family A member 2 (PHLDA2) can also be up-regulated in CRC tissues. Knockdown of PHLDA2 inhibited cellular proliferation, invasion, migration, and epithelial-mesenchymal transition (EMT) *in vitro* by activating the autophagy of CRC cells through the PI3K/AKT/mTOR and PI3K/AKT/GSK-3β signaling pathways[23]. Decreased or absent expressions of ATGs BeclinI and ATG5 can also lead to CRC progression and are significantly associated with poor prognosis[24,25]. Therefore, ATGs can exert a cancer-suppressing effect by inducing autophagy. In addition to ATGs that directly regulate the biological behaviors of tumor cells, epigenetic regulation of autophagy can also be a molecular basis for the body to inhibit tumorigenesis by regulating autophagy. BRG1, the ATPase subunit of the SWI/SNF chromatin remodeling complex, is required for maintaining the homeostasis of intestinal epithelial cells (IECs) to prevent inflammation and tumorigenesis. BRG1 is a key regulator that directly regulates Atg16 L1, Ambra1, Atg7, and Wipi2 transcription, which is important for autophagosome biogenesis. Defective autophagy in BRG1-deficient IECs results in excess reactive oxygen species (ROS), which leads to defects in barrier integrity and thus causes the occurrence of CRC[26].

Autophagy acts as a CRC promoter

Compared with normal tissue cells, tumor cells have unlimited self-replication ability and ultra-high metabolic level. The bulky growth of CRC creates a unique environment featured by hypoxia, low pH, and high metabolites within the tumor tissue[27]. On the one hand, it makes the energy acquisition of tumor cells more dependent on glycolytic pathways and autophagy[28-30]; on the other hand, the enhanced autophagy can further promote tumor progression by affecting the expressions of tumor suppressor genes (*e.g.*, p53), the degradation of major histocompatibility complex I (MHC-I), and the infiltration of various immune cells[31,32]. In solid tumors, the autophagosome content receptor NBR1 mainly regulates the localization of MHC-I on the tumor cell surface, autophagosomes, and lysosomes, whereas MHC-I is closely related to the antigen presentation and anti-tumor activity of immune cells. Intervening with NBR1 can regulate autophagy, thereby affecting the expression of MHC-I and the immune status of the body[33], suggesting that autophagy may promote tumor progression *via* immune mechanisms.

The increased activity of autophagy in solid tumors is also closely related to the activation of intracellular oncogenes such as RAS[34]. The activation of RAS helps CRC cells maintain their energy and material supply under stress conditions[35]. Hu *et al*[36] have found that IL-6 accumulates in the tumor microenvironment, which can activate autophagy through the IL-6/JAK2/BECN1 pathway and promote the chemotherapy resistance of CRC cells. BECN1 Y333 phosphorylation is a predictive marker of poor prognosis and chemotherapy resistance in CRC. Under hypoxic conditions, tumor-initiating cells (TICs) can maintain their tumor initiation capacity and stemness through the autophagy-related PRKC/PKC-EZR pathway[37], thereby regulating the progression of CRC. CRC stem cells can also maintain the expressions of stemness markers Oct4, SOX2, and Nanog through autophagy-related proteins ATG5 and ATG7, and intervention in ATG5 and ATG7 can reduce stem cell proliferation and promote cell senescence and apoptosis[38,39]. E3 ubiquitin ligase TRAF6 interacts with MAP1LC3B/LC3B in colonic epithelial cells through its LC3 interaction region "YxxL" and catalyzes K63-linked LC3B polyubiquitination to trigger selective CTNNB1 degradation by autophagy, thereby playing an inhibitory role on epithelial mesenchymal transition (EMT) and CRC metastasis[40] (Table 1).

Autophagy in CRC therapies

Since autophagy plays an important role in the physiological activities of CRC cells, regulating key elements of the autophagy pathway may be a promising strategy for CRC treatment. For different tumors, autophagy can either suppress or promote tumorigenesis; therefore, the treatment strategies should be tailored (*i.e.*, up-regulation or inhibition of autophagy according to different tumor types).

Mycobacterium tuberculosis and Bacillus Calmette–Guérin (BCG) vaccine can induce the death of autophagic cells through the TLR2 and TLR4 signaling pathways, thereby enhancing radiosensitization in CRC cell lines. *In vivo* evidence further supports that BCG-mediated radiosensitization is an autophagy-dependent pathway[41]. The combination of BCG and ionizing radiation can induce autophagy, providing a potential strategy to enhance the radiotherapeutic effect in CRC cells. As an antimalarial drug, chloroquine has recently been found to prevent autophagosome-lysosome fusion in tumor cells; thus, it may act as an autophagy inhibitor on the autophagy pathway of tumor cells[42].

Table 1 Research advances in the role of autophagy in colorectal cancer

Effects	Action cells	Targets	Pathways and mechanisms
As a tumor suppressor	CRC	SNX10	SRC-STAT3 and SRC-TNNB1
	CRC	PHLDA2	PI3K/AKT/GSK-3β
	CRC	BRG1	Defective autophagy results in excess reactive oxygen species
	CRC	BeclinI	PI3K/AKT/mTOR
As a tumor promoter	CRC and macrophages	NBR1	After being regulated, MHC-I can affect the immune system and lead to immune evasion
	CRC	RAS	MEK/ERK
	Regulatory T cells (Treg)	Atg7	Down-regulation of the immune-suppressive protein FOXP3 promotes immune evasion
	CSC	ATG5, ATG7	Affects the expressions of stemness markers Oct4, SOX2 and Nanog
	Tumor-initiating cells	PRKC	PRKC/PKC-EZR
	CRC	IL-6	IL-6/JAK2/BECN1
	Normal Colonic epithelial cells	TRAF6	MAP1LC3B/LC3B ubiquitination

CSC: Cancer stem cell; CRC: Colorectal cancer; SNX10: Sorting nexin 10; PHLDA2: Pleckstrin homology-like domain family A member 2; PI3K: Phosphatidylinositol 3-kinase; mTOR: Mammalian target of rapamycin; MHC-I: Major histocompatibility complex I.

CRC cells can develop autophagy-dependent chemotherapy resistance by activating autophagy to combat 5-fluorouracil (5-FU). Clinically, chloroquine is used in combination with chemotherapy drugs such as 5-FU[43] or trifluorothymidine (TFT)[44] to enhance the cytotoxicity of chemotherapy drugs against tumor cells. Preoperative use of chloroquine in CRC patients significantly increases the sensitivity of CRC to 5-FU and radiotherapy; in addition, it enhances intracellular ROS production in tumor cells, further promoting tumor cell death[45-46]. As a widely used antitumor drug, temsirolimus (TEM) can inhibit CRC cells by inducing G1 cell cycle arrest and reducing HIF1A and VEGF levels[47]. Meanwhile, as an mTOR inhibitor, TEM also has the function of autophagy inhibitors[48]. When used in combination with chloroquine, TEM can significantly increase the apoptosis level of CRC cells and increase the BAX: BCL2 ratio. Thus, TEM and chloroquine have synergistic anti-tumor effects, which sheds new light on the treatment of CRC. Fu *et al*[49] discovered an autophagy-targeting small molecule S130 by integrating into silico screening and *in vitro* assays. S130 binds to ATG4B with strong affinity and specifically suppresses the activity of ATG4B, thereby limiting the autophagic activity of CRC cells. *In vitro* and *in vivo* experiments confirmed that S130 could significantly inhibit the growth of CRC cells, suggesting the potential clinical value of small-molecule autophagy inhibitors.

Housekeeping and regulatory immune factors [*e.g.*, macrophages and regulatory T lymphocytes (Tregs) in the tumor microenvironment] are also involved in the occurrence and development of CRC [50-52]. Akbari-Birgani *et al*[53] found that autophagy targeting Tregs and tumor cells can improve the therapeutic effect against CRC, possibly due to the fact that specific deletion of the Atg7 gene in Treg cells is associated with the increase of apoptosis and the downregulation of the transcription factor FOXP3. The loss of autophagy leads to the upregulation of metabolic mediators (such as MTORC1 and MYC), thereby removing the negative regulatory effect of Tregs on autoimmunity and improving the body's anti-tumor ability[54-56]. In addition, downregulating the autophagy activity of tumor cells and macrophages by chloroquine or other autophagy inhibitors[57,58] can avoid the downregulation of MHC-I expression on their surfaces; meanwhile, it can also enhance the presentation of tumor-associated antigens by antigen-presenting cells (APCs) and induce immune cells to exert their antitumor effects[33].

In addition to the direct use of autophagy inhibitors and the use of autophagy's regulatory role in immune cells for treating CRC, photodynamic therapy (PDT) combined with proteasome inhibitors (*e.g.*, bortezomib) may also enhance tumor sensitivity to PDT through the autophagy pathway[59]. Protoporphyrin IX mediates PDT to induce autophagy in CRC stem cells. The inhibition of PDT-induced autophagy by gene knockout or pharmacological means can trigger apoptosis of tumor stem cells and decrease the ability of colonosphere formation *in vitro* and tumorigenicity *in vivo*[60].

In general, artificial intervention in tumor biological behavior can be achieved by directly targeting the autophagy mechanism using autophagy modulators in CRC experimental models. Autophagy modulators, chemotherapy drugs, radiotherapy, and immunotherapy have synergistic anti-tumor effects, and their combined use can enhance the efficacy of existing therapies. In fact, autophagy-based treatments have broad applications in CRC treatments.

CONCLUSION

Autophagy is an extremely potential therapeutic target for the treatment of rectal cancer, but appropriate interventions should be selected according to the different stages of colorectal cancer. Autophagy can inhibit tumorigenesis in the early stages of CRC by preventing DNA damage, maintaining genomic stability, and inducing apoptosis. However, with the progression of tumors, autophagy can promote CRC growth by enhancing energy metabolism in tumor cells, by mediating drug resistance, and by avoiding tumor cell death. Therefore, autophagy-based CRC treatment strategies should be tailored according to the specific CRC type, tumor stage, and tumor metabolic characteristics. The combination of multiple therapeutic methods can enhance the inhibitory effect of autophagy on tumors and weaken its role as a tumor promoter, therefore playing a key role in CRC treatment.

FOOTNOTES

Author contributions: Ma TF and Liu B contributed equally to the conception and design; Ma TF and Fan YR searched the literature, drafted the manuscript and prepared the tables; Liu B and Zhao YH modified and revised the manuscript.

Conflict-of-interest statement: All authors report no relevant conflicts of interest for this article.

Country/Territory of origin: China

ORCID number: Tian-Fei Ma 0000-0003-2226-3648.

S-Editor: Li L
L-Editor: A
P-Editor: Li L

REFERENCES

1 **Sung H**, Ferlay J, Siegel RL, Laversanne M, Soerjomataram I, Jemal A, Bray F. Global Cancer Statistics 2020: GLOBOCAN Estimates of Incidence and Mortality Worldwide for 36 Cancers in 185 Countries. *CA Cancer J Clin* 2021; **71**: 209-249 [PMID: 33538338 DOI: 10.3322/caac.21660]

2 **Aparicio C**, Belver M, Enríquez L, Espeso F, Núñez L, Sánchez A, de la Fuente MÁ, González-Vallinas M. Cell Therapy for Colorectal Cancer: The Promise of Chimeric Antigen Receptor (CAR)-T Cells. *Int J Mol Sci* 2021; **22** [PMID: 34769211 DOI: 10.3390/ijms222111781]

3 **Galluzzi L**, Pietrocola F, Bravo-San Pedro JM, Amaravadi RK, Baehrecke EH, Cecconi F, Codogno P, Debnath J, Gewirtz DA, Karantza V, Kimmelman A, Kumar S, Levine B, Maiuri MC, Martin SJ, Penninger J, Piacentini M, Rubinsztein DC, Simon HU, Simonsen A, Thorburn AM, Velasco G, Ryan KM, Kroemer G. Autophagy in malignant transformation and cancer progression. *EMBO J* 2015; **34**: 856-880 [PMID: 25712477 DOI: 10.15252/embj.201490784]

4 **Cao W**, Li J, Yang K, Cao D. An overview of autophagy: Mechanism, regulation and research progress. *Bull Cancer* 2021; **108**: 304-322 [PMID: 33423775 DOI: 10.1016/j.bulcan.2020.11.004]

5 **Ferro F**, Servais S, Besson P, Roger S, Dumas JF, Brisson L. Autophagy and mitophagy in cancer metabolic remodelling. *Semin Cell Dev Biol* 2020; **98**: 129-138 [PMID: 31154012 DOI: 10.1016/j.semcdb.2019.05.029]

6 **Yamazaki T**, Bravo-San Pedro JM, Galluzzi L, Kroemer G, Pietrocola F. Autophagy in the cancer-immunity dialogue. *Adv Drug Deliv Rev* 2021; **169**: 40-50 [PMID: 33301821 DOI: 10.1016/j.addr.2020.12.003]

7 **Wang Y**, Zhang H. Regulation of Autophagy by mTOR Signaling Pathway. *Adv Exp Med Biol* 2019; **1206**: 67-83 [PMID: 31776980 DOI: 10.1007/978-981-15-0602-4_3]

8 **Klionsky DJ**, Petroni G, Amaravadi RK, Baehrecke EH, Ballabio A, Boya P, Bravo-San Pedro JM, Cadwell K, Cecconi F, Choi AMK, Choi ME, Chu CT, Codogno P, Colombo MI, Cuervo AM, Deretic V, Dikic I, Elazar Z, Eskelinen EL, Fimia GM, Gewirtz DA, Green DR, Hansen M, Jäättelä M, Johansen T, Juhász G, Karantza V, Kraft C, Kroemer G, Ktistakis NT, Kumar S, Lopez-Otin C, Macleod KF, Madeo F, Martinez J, Meléndez A, Mizushima N, Münz C, Penninger JM, Perera RM, Piacentini M, Reggiori F, Rubinsztein DC, Ryan KM, Sadoshima J, Santambrogio L, Scorrano L, Simon HU, Simon AK, Simonsen A, Stolz A, Tavernarakis N, Tooze SA, Yoshimori T, Yuan J, Yue Z, Zhong Q, Galluzzi L, Pietrocola F. Autophagy in major human diseases. *EMBO J* 2021; **40**: e108863 [PMID: 34459017 DOI: 10.15252/embj.2021108863]

9 **Li X**, He S, Ma B. Autophagy and autophagy-related proteins in cancer. *Mol Cancer* 2020; **19**: 12 [PMID: 31969156 DOI:

10.1186/s12943-020-1138-4]
10 **Hardie DG**. AMPK: positive and negative regulation, and its role in whole-body energy homeostasis. *Curr Opin Cell Biol* 2015; **33**: 1-7 [PMID: 25259783 DOI: 10.1016/j.ceb.2014.09.004]
11 **Deretic V**. Autophagy in inflammation, infection, and immunometabolism. *Immunity* 2021; **54**: 437-453 [PMID: 33691134 DOI: 10.1016/j.immuni.2021.01.018]
12 **Takamura A**, Komatsu M, Hara T, Sakamoto A, Kishi C, Waguri S, Eishi Y, Hino O, Tanaka K, Mizushima N. Autophagy-deficient mice develop multiple liver tumors. *Genes Dev* 2011; **25**: 795-800 [PMID: 21498569 DOI: 10.1101/gad.2016211]
13 **Dong S**, Wang Q, Kao YR, Diaz A, Tasset I, Kaushik S, Thiruthuvanathan V, Zintiridou A, Nieves E, Dzieciatkowska M, Reisz JA, Gavathiotis E, D'Alessandro A, Will B, Cuervo AM. Chaperone-mediated autophagy sustains haematopoietic stem-cell function. *Nature* 2021; **591**: 117-123 [PMID: 33442062 DOI: 10.1038/s41586-020-03129-z]
14 **Qiao L**, Ma J, Zhang Z, Sui W, Zhai C, Xu D, Wang Z, Lu H, Zhang M, Zhang C, Chen W, Zhang Y. Deficient Chaperone-Mediated Autophagy Promotes Inflammation and Atherosclerosis. *Circ Res* 2021; **129**: 1141-1157 [PMID: 34704457 DOI: 10.1161/CIRCRESAHA.121.318908]
15 **Anding AL**, Baehrecke EH. Cleaning House: Selective Autophagy of Organelles. *Dev Cell* 2017; **41**: 10-22 [PMID: 28399394 DOI: 10.1016/j.devcel.2017.02.016]
16 **Dong X**, Yang Y, Zou Z, Zhao Y, Ci B, Zhong L, Bhave M, Wang L, Kuo YC, Zang X, Zhong R, Aguilera ER, Richardson RB, Simonetti B, Schoggins JW, Pfeiffer JK, Yu L, Zhang X, Xie Y, Schmid SL, Xiao G, Gleeson PA, Ktistakis NT, Cullen PJ, Xavier RJ, Levine B. Sorting nexin 5 mediates virus-induced autophagy and immunity. *Nature* 2021; **589**: 456-461 [PMID: 33328639 DOI: 10.1038/s41586-020-03056-z]
17 **Glick D**, Barth S, Macleod KF. Autophagy: cellular and molecular mechanisms. *J Pathol* 2010; **221**: 3-12 [PMID: 20225336 DOI: 10.1002/path.2697]
18 **Long J**, He Q, Yin Y, Lei X, Li Z, Zhu W. The effect of miRNA and autophagy on colorectal cancer. *Cell Prolif* 2020; **53**: e12900 [PMID: 32914514 DOI: 10.1111/cpr.12900]
19 **Li W**, He P, Huang Y, Li YF, Lu J, Li M, Kurihara H, Luo Z, Meng T, Onishi M, Ma C, Jiang L, Hu Y, Gong Q, Zhu D, Xu Y, Liu R, Liu L, Yi C, Zhu Y, Ma N, Okamoto K, Xie Z, Liu J, He RR, Feng D. Selective autophagy of intracellular organelles: recent research advances. *Theranostics* 2021; **11**: 222-256 [PMID: 33391472 DOI: 10.7150/thno.49860]
20 **Liu K**, Wang L, Zhao T. Autophagy in Normal Stem Cells and Specialized Cells. *Adv Exp Med Biol* 2019; **1206**: 489-508 [PMID: 31777000 DOI: 10.1007/978-981-15-0602-4_23]
21 **White E**, Mehnert JM, Chan CS. Autophagy, Metabolism, and Cancer. *Clin Cancer Res* 2015; **21**: 5037-5046 [PMID: 26567363 DOI: 10.1158/1078-0432.CCR-15-0490]
22 **Zhang S**, Yang Z, Bao W, Liu L, You Y, Wang X, Shao L, Fu W, Kou X, Shen W, Yuan C, Hu B, Dang W, Nandakumar KS, Jiang H, Zheng M, Shen X. SNX10 (sorting nexin 10) inhibits colorectal cancer initiation and progression by controlling autophagic degradation of SRC. *Autophagy* 2020; **16**: 735-749 [PMID: 31208298 DOI: 10.1080/15548627.2019.1632122]
23 **Ma Z**, Lou S, Jiang Z. PHLDA2 regulates EMT and autophagy in colorectal cancer *via* the PI3K/AKT signaling pathway. *Aging (Albany NY)* 2020; **12**: 7985-8000 [PMID: 32385195 DOI: 10.18632/aging.103117]
24 **Zhao Y**, Yang J, Liao W, Liu X, Zhang H, Wang S, Wang D, Feng J, Yu L, Zhu WG. Cytosolic FoxO1 is essential for the induction of autophagy and tumour suppressor activity. *Nat Cell Biol* 2010; **12**: 665-675 [PMID: 20543840 DOI: 10.1038/ncb2069]
25 **Peng X**, Wang Y, Li H, Fan J, Shen J, Yu X, Zhou Y, Mao H. ATG5-mediated autophagy suppresses NF-κB signaling to limit epithelial inflammatory response to kidney injury. *Cell Death Dis* 2019; **10**: 253 [PMID: 30874544 DOI: 10.1038/s41419-019-1483-7]
26 **Liu M**, Sun T, Li N, Peng J, Fu D, Li W, Li L, Gao WQ. BRG1 attenuates colonic inflammation and tumorigenesis through autophagy-dependent oxidative stress sequestration. *Nat Commun* 2019; **10**: 4614 [PMID: 31601814 DOI: 10.1038/s41467-019-12573-z]
27 **Hinshaw DC**, Shevde LA. The Tumor Microenvironment Innately Modulates Cancer Progression. *Cancer Res* 2019; **79**: 4557-4566 [PMID: 31350295 DOI: 10.1158/0008-5472.CAN-18-3962]
28 **Ganapathy-Kanniappan S**, Geschwind JF. Tumor glycolysis as a target for cancer therapy: progress and prospects. *Mol Cancer* 2013; **12**: 152 [PMID: 24298908 DOI: 10.1186/1476-4598-12-152]
29 **Paul S**, Ghosh S, Kumar S. Tumor glycolysis, an essential sweet tooth of tumor cells. *Semin Cancer Biol* 2022; **86**: 1216-1230 [PMID: 36330953 DOI: 10.1016/j.semcancer.2022.09.007]
30 **Li CH**, Liao CC. The Metabolism Reprogramming of microRNA Let-7-Mediated Glycolysis Contributes to Autophagy and Tumor Progression. *Int J Mol Sci* 2021; **23** [PMID: 35008539 DOI: 10.3390/ijms23010113]
31 **Mizushima N**, Levine B. Autophagy in Human Diseases. *N Engl J Med* 2020; **383**: 1564-1576 [PMID: 33053285 DOI: 10.1056/NEJMra2022774]
32 **White E**. Autophagy and p53. *Cold Spring Harb Perspect Med* 2016; **6**: a026120 [PMID: 27037419 DOI: 10.1101/cshperspect.a026120]
33 **Yamamoto K**, Venida A, Yano J, Biancur DE, Kakiuchi M, Gupta S, Sohn ASW, Mukhopadhyay S, Lin EY, Parker SJ, Banh RS, Paulo JA, Wen KW, Debnath J, Kim GE, Mancias JD, Fearon DT, Perera RM, Kimmelman AC. Autophagy promotes immune evasion of pancreatic cancer by degrading MHC-I. *Nature* 2020; **581**: 100-105 [PMID: 32376951 DOI: 10.1038/s41586-020-2229-5]
34 **Guo JY**, Chen HY, Mathew R, Fan J, Strohecker AM, Karsli-Uzunbas G, Kamphorst JJ, Chen G, Lemons JM, Karantza V, Coller HA, Dipaola RS, Gelinas C, Rabinowitz JD, White E. Activated Ras requires autophagy to maintain oxidative metabolism and tumorigenesis. *Genes Dev* 2011; **25**: 460-470 [PMID: 21317241 DOI: 10.1101/gad.2016311]
35 **Wang Y**, Xiong H, Liu D, Hill C, Ertay A, Li J, Zou Y, Miller P, White E, Downward J, Goldin RD, Yuan X, Lu X. Autophagy inhibition specifically promotes epithelial-mesenchymal transition and invasion in RAS-mutated cancer cells. *Autophagy* 2019; **15**: 886-899 [PMID: 30782064 DOI: 10.1080/15548627.2019.1569912]
36 **Hu F**, Song D, Yan Y, Huang C, Shen C, Lan J, Chen Y, Liu A, Wu Q, Sun L, Xu F, Hu F, Chen L, Luo X, Feng Y,

Huang S, Hu J, Wang G. IL-6 regulates autophagy and chemotherapy resistance by promoting BECN1 phosphorylation. *Nat Commun* 2021; **12**: 3651 [PMID: 34131122 DOI: 10.1038/s41467-021-23923-1]

37 **Qureshi-Baig K**, Kuhn D, Viry E, Pozdeev VI, Schmitz M, Rodriguez F, Ullmann P, Koncina E, Nurmik M, Frasquilho S, Nazarov PV, Zuegel N, Boulmont M, Karapetyan Y, Antunes L, Val D, Mittelbronn M, Janji B, Haan S, Letellier E. Hypoxia-induced autophagy drives colorectal cancer initiation and progression by activating the PRKC/PKC-EZR (ezrin) pathway. *Autophagy* 2020; **16**: 1436-1452 [PMID: 31775562 DOI: 10.1080/15548627.2019.1687213]

38 **Sharif T**, Martell E, Dai C, Kennedy BE, Murphy P, Clements DR, Kim Y, Lee PW, Gujar SA. Autophagic homeostasis is required for the pluripotency of cancer stem cells. *Autophagy* 2017; **13**: 264-284 [PMID: 27929731 DOI: 10.1080/15548627.2016.1260808]

39 **Ma Y**, Qi M, An Y, Zhang L, Yang R, Doro DH, Liu W, Jin Y. Autophagy controls mesenchymal stem cell properties and senescence during bone aging. *Aging Cell* 2018; **17** [PMID: 29210174 DOI: 10.1111/acel.12709]

40 **Wu H**, Lu XX, Wang JR, Yang TY, Li XM, He XS, Li Y, Ye WL, Wu Y, Gan WJ, Guo PD, Li JM. TRAF6 inhibits colorectal cancer metastasis through regulating selective autophagic CTNNB1/β-catenin degradation and is targeted for GSK3B/GSK3β-mediated phosphorylation and degradation. *Autophagy* 2019; **15**: 1506-1522 [PMID: 30806153 DOI: 10.1080/15548627.2019.1586250]

41 **Yuk JM**, Shin DM, Song KS, Lim K, Kim KH, Lee SH, Kim JM, Lee JS, Paik TH, Kim JS, Jo EK. Bacillus calmette-guerin cell wall cytoskeleton enhances colon cancer radiosensitivity through autophagy. *Autophagy* 2010; **6**: 46-60 [PMID: 19901560 DOI: 10.4161/auto.6.1.10325]

42 **Ferreira PMP**, Sousa RWR, Ferreira JRO, Militão GCG, Bezerra DP. Chloroquine and hydroxychloroquine in antitumor therapies based on autophagy-related mechanisms. *Pharmacol Res* 2021; **168**: 105582 [PMID: 33775862 DOI: 10.1016/j.phrs.2021.105582]

43 **Bijnsdorp IV**, Peters GJ, Temmink OH, Fukushima M, Kruyt FA. Differential activation of cell death and autophagy results in an increased cytotoxic potential for trifluorothymidine compared to 5-fluorouracil in colon cancer cells. *Int J Cancer* 2010; **126**: 2457-2468 [PMID: 19816940 DOI: 10.1002/ijc.24943]

44 **Jia HJ**, Zhou M, Vashisth MK, Xia J, Hua H, Dai QL, Bai SR, Zhao Q, Wang XB, Shi YL. Trifluridine induces HUVECs senescence by inhibiting mTOR-dependent autophagy. *Biochem Biophys Res Commun* 2022; **610**: 119-126 [PMID: 35462092 DOI: 10.1016/j.bbrc.2022.04.063]

45 **Kimura T**, Takabatake Y, Takahashi A, Isaka Y. Chloroquine in cancer therapy: a double-edged sword of autophagy. *Cancer Res* 2013; **73**: 3-7 [PMID: 23288916 DOI: 10.1158/0008-5472.CAN-12-2464]

46 **Xu R**, Ji Z, Xu C, Zhu J. The clinical value of using chloroquine or hydroxychloroquine as autophagy inhibitors in the treatment of cancers: A systematic review and meta-analysis. *Medicine (Baltimore)* 2018; **97**: e12912 [PMID: 30431566 DOI: 10.1097/MD.0000000000012912]

47 **Kaneko M**, Nozawa H, Hiyoshi M, Tada N, Murono K, Nirei T, Emoto S, Kishikawa J, Iida Y, Sunami E, Tsuno NH, Kitayama J, Takahashi K, Watanabe T. Temsirolimus and chloroquine cooperatively exhibit a potent antitumor effect against colorectal cancer cells. *J Cancer Res Clin Oncol* 2014; **140**: 769-781 [PMID: 24619662 DOI: 10.1007/s00432-014-1628-0]

48 **Yurube T**, Ito M, Kakiuchi Y, Kuroda R, Kakutani K. Autophagy and mTOR signaling during intervertebral disc aging and degeneration. *JOR Spine* 2020; **3**: e1082 [PMID: 32211593 DOI: 10.1002/jsp2.1082]

49 **Fu Y**, Hong L, Xu J, Zhong G, Gu Q, Guan Y, Zheng X, Dai Q, Luo X, Liu C, Huang Z, Yin XM, Liu P, Li M. Discovery of a small molecule targeting autophagy *via* ATG4B inhibition and cell death of colorectal cancer cells *in vitro* and in vivo. *Autophagy* 2019; **15**: 295-311 [PMID: 30176161 DOI: 10.1080/15548627.2018.1517073]

50 **Toor SM**, Murshed K, Al-Dhaheri M, Khawar M, Abu Nada M, Elkord E. Immune Checkpoints in Circulating and Tumor-Infiltrating CD4(+) T Cell Subsets in Colorectal Cancer Patients. *Front Immunol* 2019; **10**: 2936 [PMID: 31921188 DOI: 10.3389/fimmu.2019.02936]

51 **Liu P**, Zhu H, Zhang X, Feng A, Zhu X, Sun Y. Predicting Survival for Hepatic Arterial Infusion Chemotherapy of Unresectable Colorectal Liver Metastases: Radiomics Analysis of Pretreatment Computed Tomography. *J Transl Int Med* 2022; **10**: 56-64 [PMID: 35702189 DOI: 10.2478/jtim-2022-0004]

52 **Gao Z**, Jiang J, Hou L, Zhang B. Dysregulation of MiR-144-5p/RNF187 Axis Contributes To the Progression of Colorectal Cancer. *J Transl Int Med* 2022; **10**: 65-75 [PMID: 35702180 DOI: 10.2478/jtim-2021-0043]

53 **Akbari-Birgani S**, Paranjothy T, Zuse A, Janikowski T, Cieślar-Pobuda A, Likus W, Urasińska E, Schweizer F, Ghavami S, Klonisch T, Łos MJ. Cancer stem cells, cancer-initiating cells and methods for their detection. *Drug Discov Today* 2016; **21**: 836-842 [PMID: 26976692 DOI: 10.1016/j.drudis.2016.03.004]

54 **Kato H**, Perl A. Blockade of Treg Cell Differentiation and Function by the Interleukin-21-Mechanistic Target of Rapamycin Axis Via Suppression of Autophagy in Patients With Systemic Lupus Erythematosus. *Arthritis Rheumatol* 2018; **70**: 427-438 [PMID: 29161463 DOI: 10.1002/art.40380]

55 **Rabanal-Ruiz Y**, Otten EG, Korolchuk VI. mTORC1 as the main gateway to autophagy. *Essays Biochem* 2017; **61**: 565-584 [PMID: 29233869 DOI: 10.1042/EBC20170027]

56 **Jahangiri L**, Pucci P, Ishola T, Trigg RM, Williams JA, Pereira J, Cavanagh ML, Turner SD, Gkoutos GV, Tsaprouni L. The Contribution of Autophagy and LncRNAs to MYC-Driven Gene Regulatory Networks in Cancers. *Int J Mol Sci* 2021; **22** [PMID: 34445233 DOI: 10.3390/ijms22168527]

57 **Oh DS**, Lee HK. Autophagy protein ATG5 regulates CD36 expression and anti-tumor MHC class II antigen presentation in dendritic cells. *Autophagy* 2019; **15**: 2091-2106 [PMID: 30900506 DOI: 10.1080/15548627.2019.1596493]

58 **Shao BZ**, Han BZ, Zeng YX, Su DF, Liu C. The roles of macrophage autophagy in atherosclerosis. *Acta Pharmacol Sin* 2016; **37**: 150-156 [PMID: 26750103 DOI: 10.1038/aps.2015.87]

59 **Szokalska A**, Makowski M, Nowis D, Wilczynski GM, Kujawa M, Wójcik C, Mlynarczuk-Bialy I, Salwa P, Bil J, Janowska S, Agostinis P, Verfaillie T, Bugajski M, Gietka J, Issat T, Glodkowska E, Mrówka P, Stoklosa T, Hamblin MR, Mróz P, Jakóbisiak M, Golab J. Proteasome inhibition potentiates antitumor effects of photodynamic therapy in mice through induction of endoplasmic reticulum stress and unfolded protein response. *Cancer Res* 2009; **69**: 4235-4243 [PMID: 19435917 DOI: 10.1158/0008-5472.CAN-08-3439]

60 **Wei MF**, Chen MW, Chen KC, Lou PJ, Lin SY, Hung SC, Hsiao M, Yao CJ, Shieh MJ. Autophagy promotes resistance to photodynamic therapy-induced apoptosis selectively in colorectal cancer stem-like cells. *Autophagy* 2014; **10**: 1179-1192 [PMID: 24905352 DOI: 10.4161/auto.28679]

World Journal of Gastrointestinal Oncology

Submit a Manuscript: https://www.f6publishing.com

World J Gastrointest Oncol 2023 June 15; 15(6): 988-1004

DOI: 10.4251/wjgo.v15.i6.988

ISSN 1948-5204 (online)

ORIGINAL ARTICLE

Basic Study

Transcription factor glucocorticoid modulatory element-binding protein 1 promotes hepatocellular carcinoma progression by activating Yes-associate protein 1

Cheng Chen, Hai-Guan Lin, Zheng Yao, Yi-Ling Jiang, Hong-Jin Yu, Jing Fang, Wei-Na Li

Specialty type: Gastroenterology and hepatology

Provenance and peer review: Unsolicited article; Externally peer reviewed.

Peer-review model: Single blind

Peer-review report's scientific quality classification

Grade A (Excellent): 0
Grade B (Very good): 0
Grade C (Good): C, C
Grade D (Fair): 0
Grade E (Poor): 0

P-Reviewer: Elshimi E, Egypt; He D, China

Received: January 17, 2023
Peer-review started: January 17, 2023
First decision: February 28, 2023
Revised: March 18, 2023
Accepted: April 12, 2023
Article in press: April 12, 2023
Published online: June 15, 2023

Cheng Chen, Yi-Ling Jiang, Hong-Jin Yu, Jing Fang, Wei-Na Li, Department of Medical Oncology, Zhejiang Xiaoshan Hospital, Hangzhou 311202, Zhejiang Province, China

Hai-Guan Lin, Department of General Surgery, People's Liberation Army Strategic Support Force Characteristic Medical Center, Beijing 100101, China

Zheng Yao, Department of Radiation Oncology, Cancer Hospital of The University of Chinese Academy of Sciences, Hangzhou 310022, Zhejiang Province, China

Corresponding author: Cheng Chen, MM, Attending Doctor, Department of Medical Oncology, Zhejiang Xiaoshan Hospital, No. 728 Yucai North Road, Xiaoshan District, Hangzhou 311202, Zhejiang Province, China. chencheng858@126.com

Abstract

BACKGROUND

Glucocorticoid modulatory element-binding protein 1 (GMEB1), which has been identified as a transcription factor, is a protein widely expressed in various tissues. Reportedly, the dysregulation of GMEB1 is linked to the genesis and development of multiple cancers.

AIM

To explore GMEB1's biological functions in hepatocellular carcinoma (HCC) and figuring out the molecular mechanism.

METHODS

GMEB1 expression in HCC tissues was analyzed employing the StarBase database. Immunohistochemical staining, Western blotting and quantitative real-time PCR were conducted to examine GMEB1 and Yes-associate protein 1 (YAP1) expression in HCC cells and tissues. Cell counting kit-8 assay, Transwell assay and flow cytometry were utilized to examine HCC cell proliferation, migration, invasion and apoptosis, respectively. The JASPAR database was employed for predicting the binding site of GMEB1 with YAP1 promoter. Dual-luciferase reporter gene assay and chromatin immunoprecipitation-qPCR were conducted to verify the binding relationship of GMEB1 with YAP1 promoter region.

RESULTS

GMEB1 was up-regulated in HCC cells and tissues, and GMEB1 expression was correlated to the tumor size and TNM stage of HCC patients. GMEB1 overexpression facilitated HCC cell multiplication, migration, and invasion, and suppressed the apoptosis, whereas GMEB1 knockdown had the opposite effects. GMEB1 bound to YAP1 promoter region and positively regulated YAP1 expression in HCC cells.

CONCLUSION

GMEB1 facilitates HCC malignant proliferation and metastasis by promoting the transcription of the YAP1 promoter region.

Key Words: Hepatocellular carcinoma; Glucocorticoid modulatory element-binding protein 1; Yes-associate protein 1; Apoptosis; Proliferation

Core Tip: Glucocorticoid modulatory element-binding protein 1 (GMEB1) was highly expressed in hepatocellular carcinoma (HCC) tissues. Functionally, GMEB1 modulates the malignant biological behaviors of HCC cells. Mechanistically, GMEB1 promotes the expression of Yes-associate protein 1 at transcriptional level. In short, the present study suggested that for HCC, GMEB1 might be a diagnostic biomarker and treatment target.

Citation: Chen C, Lin HG, Yao Z, Jiang YL, Yu HJ, Fang J, Li WN. Transcription factor glucocorticoid modulatory element-binding protein 1 promotes hepatocellular carcinoma progression by activating Yes-associate protein 1. *World J Gastrointest Oncol* 2023; 15(6): 988-1004
URL: https://www.wjgnet.com/1948-5204/full/v15/i6/988.htm
DOI: https://dx.doi.org/10.4251/wjgo.v15.i6.988

INTRODUCTION

Liver cancer is the third leading cause of cancer-related deaths worldwide, with more than 780000 deaths due to liver cancer in 2018. Approximately 90% of liver cancer cases originate in hepatocytes and are referred to as hepatocellular carcinoma (HCC)[1]. HCC is the fifth most common cancer in males and the ninth most common cancer in females, with an estimated 500000 and 200000 new cases annually in the world, respectively. The pathogenesis of hepatocellular carcinoma is complicated by structural mutations in the proto-oncogene and the addition of exogenous pathogenic factors such as viruses, excessive alcohol consumption, obesity and aflatoxins, which have contributed to the development of HCC[2,3]. Therefore, HCC is one of the most common types of clinical malignancies in the digestive system, and it also ranks fourth among the causes of cancer death globally[4]. Currently, the predominant treatment options for HCC include surgical resection, liver transplantation, radiotherapy and chemotherapy[5]. Nevertheless, most HCC cases have already been in an intermediate to advanced stage at diagnosis, missing the optimal time for surgical treatment[6]. Besides, the high cost and huge shortage of donors greatly limit the clinical application of liver transplantation[7,8]. In this context, it is necessary to identify more reliable early diagnostic markers for HCC diagnosis and to discover more effective new therapeutic targets for clinical intervention, thus providing new insights to improve the prognosis and overall survival rate of HCC patients.

Glucocorticoid modulatory element-binding protein 1 (GMEB1) is a nucleoprotein with a molecular weight of 88 kDa, and can interact with GMEB2 and bind with the glucocorticoid regulatory element (GME) of the tyrosine aminotransferase (TAT) gene promoter sequence, thereby regulating the glucocorticoid receptor transactivation[9]. It has been demonstrated that IL-2 can inhibit glucocorticoid-induced T-cell apoptosis by boosting GMEB1 expression and activating the PI3K/AKT pathway[10], which is a preliminary indication of the anti-apoptotic function of GMEB1. Meanwhile, FOXL2 is an important transcription factor involved in the transcriptional regulation of several target genes, and GMEB1 was found to bind to FOXL2, whose interaction with FOXL2 could regulate the apoptotic process of cells[11]. Additionally, GMEB1 can also bind to pro-caspases and repress its activation and apoptosis[12,13]. Given that tumor development cannot occur without uncontrolled cell proliferation and apoptotic escape, the anti-apoptotic effect of GMEB1 has prompted researchers to explore the relevance of GMEB1 dysregulation to tumorigenesis and development. For example, GMEB1 suppresses CASP8 activation *via* regulating $CFLAR_L$ ubiquitination and degradation to repress the cellular apoptosis and thereby promoting malignant progression of non-small cell lung cancer[9]. Additional bioinformatics studies have further shown that high expression of several transcription factors,

including GMEB1, is a promising biomarker and/or therapeutic target for prostate cancer[14]. Thus, it becomes clear that GMEB1 can contribute to malignant progression in various tumor types through different mechanisms. Nonetheless, the expression of GMEB1 in HCC and the molecular mechanism to promote the malignant evolution of HCC have not been elucidated.

Yes-associate protein 1 (YAP1) is one of the prime effector proteins downstream of the Hippo pathway, which controls organ size, normal tissue homeostasis and stem cell function through modulating cell proliferation and apoptosis[15]. YAP1 has been proved to play an important role as an oncoprotein in a variety of tumors. For example, in clinical specimens, YAP has been reported to be overexpressed and overactivated after nucleation in prostate, colon, breast and non-small cell lung cancers, as well as ovarian and hepatocellular carcinomas[16-20], significantly contributing to the development and progression of these tumors. More importantly, in studies surrounding the pathogenesis of HCC, there is a growing consensus that abnormalities in the Hippo signaling pathway are closely associated with the development of HCC. The abnormal expression and dysfunction of YAP1, a key protein in the Hippo signaling pathway, is directly related to the malignant progression of HCC[21]. A clinical study including 177 HCC patients further indicated that YAP1 was an independent prognostic marker significantly associated with shorter disease-free and overall survival in hepatocellular carcinoma[22]. Currently, the mechanisms underlying the promotion of tumor progression by YAP1 revolve around the binding of YAP1 to the transcription factor TEAD[23], which in turn initiates the transcription of many genes involved in cell proliferation and survival, including downstream target genes such as *BIRC5*, *CTGF* and *Cyclin D1*[24]. However, as research has continued, the upstream proteins that regulate YAP1 have been further identified. In addition to the classical upstream LATS1/2 that regulates YAP1 expression[25], it has been reported that, for example, the transcription factor FOXM1 promotes the proliferation, migration and invasion of breast cancer cells through promoting YAP1 transcription activation[26]. Furthermore, in HCC, SIX4 can promote cell metastasis by upregulating YAP1 and c-MET[27].

Could GMEB1, a transcription factor closely associated with tumor development, also promote the malignant progression of HCC by regulating the transcription of YAP1 and thus affecting the normal function of the Hippo signaling pathway? With this question in mind, we would like to confirm the potential regulatory relationship between GMEB1 and YAP1 in this study, thus providing a new intervention target for the Hippo signaling pathway, a key signaling pathway in HCC pathogenesis. To this end, we will firstly focus on examining the expression of GMEB1 in human HCC tissues and HCC cell lines, and clarifying the regulatory mechanism of the interaction between GMEB1 and YAP1 in promoting HCC progression in this study. We hope that our study will reveal the crucial role of GMEB1 in the development of HCC, explore the additional biological functions of GMEB1, and provide new therapeutic strategies for the clinical treatment of patients with HCC accompanied with YAP1 overexpression.

MATERIALS AND METHODS

Case collection

With the approval of Zhejiang Xiaoshan Hopital's Ethics Committee, cancerous tissues and their corresponding para-cancerous tissues from 55 patients with HCC previously admitted to our hospital were selected for this study. Immediately after surgical removal, the tissues were frozen at -196 °C and kept at -80 °C until use. The clinical data and clinicopathological data of all subjects were complete, and none of them underwent preoperative chemotherapy or radiotherapy.

Immunohistochemistry

We fixed the cancerous and normal para-cancerous tissues in 10% formaldehyde and embedded them in paraffin. Afterwards, the tissues were cut into 4-μm-thick slices, deparaffinized with xylene, and washed with PBS. The antigen retrieval was induced by heat in PBS (microwave heating, 96 °C, 15 min), and then the tissues were treated with 3% H_2O_2 for removing endogenous peroxidases. The slices were incubated with citrate buffer to repair the antigen, and blocked with 5% bovine serum albumin (Sangon Biotech Co., Ltd., Shanghai, China) at 4 °C for 30 min. The slices were incubated at 4 °C overnight with the primary antibody GMEB1 (ab240646, 1:100, Abcam, Cambridge, United Kingdom) and then with horseradish peroxidase-conjugated secondary antibody (1:5000, ab6721, Abcam) for 30 min at room temperature. The sections were stained with diaminobenzidine (Sigma-Aldrich, St. Louis, MO, United States) at room temperature for 10 min. Ultimately, the slices were counter-stained with hematoxylin and sealed and fixed with PerMount (BIOS, Beijing, China). Eventually, the slices were observed and photographed under an optical microscope (Olympus Optical Company, Tokyo, Japan).

As previously mentioned, the staining signals were scored by the percentage of positive tumor cells and staining intensity[28]. The grading of the positive tumor cell ratio is as follows: 0% (0 point), 0.01%-25% (1 point), 25.01%-50% (2 points), 50.01%-75% (3 points) and ≥ 75% (4 points). The degree of staining intensity: no staining (0 point), weak staining (1 point), medium staining (2 points) and strong staining (3 points). The following formula was adopted to calculate the immunohistochemistry (IHC) score of

each section: IHC score = staining intensity × percentage of positively stained tumor cells. The total score is 0-12 points. The score > 4 was defined as high expression, while the score ≤ 4 was defined as low expression.

Cell culture and transfection

From the Chinese Center for Type Culture Collection (Wuhan, China), we bought human HCC cell lines (HepG2, HCCLM3, Huh7 and MHCC97H) and human-derived liver cell line (HL-7702). All cells were cultured in RPMI-1640 medium (Thermo Fisher Scientific, Carlsbad, MA, United States) with 10% fetal bovine serum (Thermo Fisher Scientific, Waltham, MA, United States) and 100 μg/mL streptomycin and 100 U/mL penicillin (Invitrogen, Carlsbad, CA, United States) at 37 °C in 5% CO_2. From GenePharma Co., Ltd. (Shanghai, China), we purchased pcDNA-GMEB1, pcDNA empty vector (NC), small interfering RNA (siRNA) negative control (si-NC), siRNAs against GMEB1 (si-GMEB1#1 and si-GMEB1#2), pcDNA-YAP1 and siRNA against YAP1 (si-YAP1). HepG2 and Huh7 cells were transfected employing Lipofectamine® 3000 (Invitrogen, Carlsbad, CA, United States) under the supplier's instructions. At 48 h after transfection, Western blot was conducted to verify the transfection efficiency.

Lentiviral infection

The lentiviral overexpression vector pCDH-CMV-MCS-EF1-Puro and the shRNA vector pLKO.1-puro were purchased from GenScript Biotech. The HCC cell line HepG2 was inoculated in 6-well cell culture plates with 2 mL of medium containing 10% fetal bovine serum 1 d prior to the infection and incubated in a constant temperature incubator at 37 °C with 5% CO_2. The lentivirus was transfected when the cell density reached 80%. An appropriate amount of lentivirus was added to the cell culture plate according to the MOI (multiplicity of infection) = 5 and incubated overnight at 37 °C with 5% CO_2. Change to fresh medium 24 h after infection. The puromycin was added 36 h after infection to allow the cells infected with the puromycin resistance gene to proliferate sufficiently. 72 h later the puromycin medium was withdrawn and the remaining cells continued to be cultured to obtain stable overexpression or silenced cell lines.

Quantitative real-time PCR

TRIzol reagent (Invitrogen, Carlsbad, CA, United States) was utilized to extract total RNA from tissues and cells, and the RNA purity and concentration were determined by UV absorption method. Subsequently, a PrimeScript-RT Kit (Takara, Shiga, Japan) was employed for synthesizing complementary DNA (cDNA) from 1 μg of total RNA under the manufacturer's protocol, and then ABI7300 Real-Time PCR System (Applied Biosystems, Foster City, CA, United States) and SYBR® Premix Ex Taq™ (TaKaRa, Dalian, China) were used for quantitative real-time PCR (qRT-PCR). All fluorescence data were converted to relative quantification, and the $2^{-\Delta\Delta Ct}$ method was utilized to calculate the relative expression, with GAPDH as the internal control. GMEB1 primer sequence: forward, 5'-GCACCAAAUUUGAUCUUCU-3', reverse, 5'-GCACACACAUUUGGCCUAA-3'; YAP1 primer sequence: forward, 5'-CCCTCGTTTTGCCATGAACC-3', reverse, 5'-GTTGCTGCTGGTTGGAGTTG-3'; GAPDH primer sequence: forward, 5'-CGACACTTTATCATGGCTA-3', reverse, 5'-TTGTTGCCGATCACTGAAT-3'.

Western blot analysis

The cells were harvested and incubated with pre-cooled radioimmunoprecipitation assay (RIPA) lysis buffer (Beyotime, Shanghai, China) for 20 min on ice. We collected the supernatant following centrifuging the cell lysis solution for 20 min at 13000 r/min at 4 °C. Then, a BCA protein quantification kit was utilized to measure the concentration of protein. The protein was isolated by 12% SDS-PAGE, and transferred onto a polyvinylidene difluoride membrane. After being blocked with Tris-buffered saline Tween (TBST) solution containing 3% bovine serum albumin at room temperature for 1 h, the membrane was incubated overnight with diluted primary antibodies at 4 °C: anti-GMEB1 antibody (Abcam, 1:1000, ab240646), anti-GAPDH antibody (1:1000, Abcam, ab8245), and anti-YAP1 antibody (1:1000, Abcam, ab52771). The membrane was washed 5 times with TBST, 3 min for each time. Then, the membrane and the added diluted secondary antibody (1:5000, Abcam, ab6721) were incubated at room temperature for 40 min. The protein bands were observed employing the ECL Western blot kit (Beyotime, Shanghai, China). ImageJ software (NIH, Bethesda, MD, United States) was adopted for analyzing each band's gray value, and the ratio of the target protein's gray value to that of GAPDH functioned as the relative protein expression for analysis.

Cell proliferation assay

Cell Counting Kit-8 (CCK-8) (Beyotime, Shanghai, China) was employed for detecting cell proliferation. HepG2 and Huh7 cells during logarithmic growth were taken and inoculated into 96-well plates (5×10^3 cells/well), which were incubated in a 37 °C, 5% CO_2 incubator for 1, 2 and 3 days, respectively. After that, 10 μL of CCK-8 reagent was added to each well and incubated for 2 h at 37 °C. We discarded the supernatant, and used an automatic microplate reader (Bio-Rad, Hercules, CA, United States) to determine the absorbance (OD) value at 450 nm of each well.

Transwell assays

Matrigel (BD Biosciences, Franklin Lakes, NJ, United States) preserved at -20 °C was melted at 4 °C overnight and mixed with serum-free medium. 100 μL of the medium was pipetted into the upper Transwell chamber, which was then let stand for 5 h at 37 °C. HepG2 and Huh7 cells were collected to prepare single-cell suspension with a density of 5 × 10^5 cells/mL. 500 μL of 10% fetal bovine serum-containing medium was added to the lower compartment, and 200 μL of cell suspension was added to the top compartment. The Transwell chamber was incubated at 37 °C for 48 h. We wiped off the remaining cells and Matrigel carefully. The migrated cells in the lower compartment were fixed with 4% formaldehyde at room temperature for 30 min and stained with crystal violet for 20 min at room temperature. The cells in 5 random views were photographed and counted under the inverted microscope (Nikon, Tokyo, Japan). In the migration assay, Matrigel was not added to the top compartment of Transwell, and the rest was as same as that in the invasion assay.

Flow cytometry

Cell apoptosis was detected *via* the Annexin V-fluorescein isothiocyanate (FITC)/propidium iodide (PI) apoptosis detection kit (Southern Biotechnology, Birmingham, Al, United States). Huh7 and HepG2 cells 48 h after transfection were trypsinized and collected and inoculated into 6-well plates. The cell density was adjusted to 2 × 10^4 cells/well, and the culturing was continued for 24 h. After washing with precooled PBS twice, the cells were re-suspended in 1×Binding buffer. We added 5 μL of PI and 5 μL of Annexin V-FITC to the cell suspension, which was subsequently mixed fully and incubated for 15 min at room temperature away from light. Afterwards, under the requirements of the instructions, the apoptosis was detected by the flow cytometer (BD Biosciences, San Jose, CA, United States) within 1 h.

Dual-luciferase reporter gene assay

We employed the JASPR database (http://jaspar.genereg.net/) for predicting the binding sites of GMEB1 to YAP1 promoter region. The target fragments of mutant YAP1 and wild-type YAP1 were established and inserted into the pGL3 vector (Promega, Madison, WI, United States) to construct pGL3-YAP1-mutant (YAP1-MUT) and pGL3-YAP1-wild type (YAP1-WT) reporter vectors. YAP1-MUT or YAP1-WT and pcDNA-GMEB1 overexpression plasmids or si-GMEB1#1 were cotransfected into HepG2 and Huh7 cells. The luciferase activity was measured 48 h after transfection with the Dual-Luciferase Reporter Assay system (Promega, Madison, WI, United States) under the instructions.

Chromatin immunoprecipitation assay

A EZ-ChIP™ kit (Millipore, Billerica, MA, United States) was adopted for performing chromatin immunoprecipitation (ChIP) assay. About 1 × 10^7 HepG2 and Huh7 cells were cross-linked at 37 °C for 10 min in 1% formaldehyde, and reacted with 125 mmol/L glycine solution at room temperature for 5 min. The mixture was sonicated on ice, 15 s each time, and 15 times at 15-second intervals. Following that, the sonicated product was centrifuged for 10 min at 4 °C at 12000 *g*. The supernatant was harvested, divided into two tubes, and was incubated with negative control IgG antibody (Abcam, ab6721) or GMEB1 antibody (Abcam, ab240646) at 4 °C overnight. Next, protein agarose/agarose gel was utilized to precipitate DNA-protein complexes which were then centrifuged for 5 min at 12000 *g* at 4 °C. Subsequently, the cross-linking was reversed at 65 °C overnight, and DNA fragments were recovered after extraction and purification by phenol/chloroform. Eventually, the binding of GMEB1 with YAP1 promoter region and YAP1 specific primers was detected *via* qRT-PCR.

Balb/c nude mouse subcutaneous transplantation tumour model

5-6 wk C57BL/6 mice (purchased from Beijing Viton Lever Laboratory Animal Technology Co., Ltd.) were housed under pathogenic conditions at 26-28 °C and 50-65% humidity. All animal experiments conformed to ethical norms and were approved by the animal ethics committee of our institution. To construct subcutaneous tumors, sh-NC (shRNA negative control), sh-GMEB1, oe-NC (overexpression negative control), oe-YAP1, sh-GMEB1+oe-YAP1 cells were suspended in 100 μL PBS diluted in Matrigel matrix gel (356234, Corning) in quantities of 1 × 10^6 (PBS:Matrigel = 2:1), cells were injected subcutaneously into the right axilla of mice (n = 5/group) and tumor size was measured every 3 days. Tumor volume was calculated using the formula: $V = (L \times W^2)/2$, where V is the volume (mm^3), L is the long diameter and W is the short diameter. Transplanted tumors were taken from Balb/c nude mice after 30 d for subsequent experiments.

To examine the effect on metastatic capacity, sh-NC (shRNA negative control), sh-GMEB1, oe-NC, oe-YAP1, sh-GMEB1+ oe-YAP1 cells were injected into nude mice (n = 5/group) *via* tail vein at an amount of 1 × 10^6, respectively. Mice were executed 60 days after injection, and number of metastatic foci on the lungs of each group were counted.

Statistical analysis

SPSS22.0 statistical software was employed to carry out statistical analysis of the data. All experiments were independently repeated three times. The results of *in vitro* experiments were presented as mean ± SD, and the results of all *in vivo* experiments were expressed as mean ± SEM. Comparisons between

groups were conducted using Student's t test or one-way ANOVA. Pearson correlation analysis was utilized for evaluate the correlation between GMEB1 and YAP1 expression in HCC tissues. The relationship between GMEB1 expression and the clinicopathological characteristics of HCC patients was assessed by the χ^2 test. $P < 0.05$ was considered a statistically significant difference between groups.

RESULTS

GMEB1 is up-regulated in HCC tissues and cells

To investigate GMEB1 expression in HCC, we analyzed GMEB1 expression in HCC through the StarBase database (http://starbase.sysu.edu.cn/), and it was unveiled that GMEB1 is aberrantly upregulated in HCC tissue samples (Figure 1A). Furthermore, we performed another database analysis of GMEB1 expression level in different subtypes of hepatocellular carcinoma (https://ualcan.path.uab.edu/), and the results revealed that GMEB1 expression was still significantly higher in HCC than in normal liver tissues (Supplementary Figure 1A). Interestingly, GMEB1 expression was further upregulated with the increasing tumor stage (Supplementary Figure 1B), tentatively suggesting a correlation between high GMEB1 expression and poorer liver cancer stage. Subsequently, we validated results from the database on clinical samples. IHC was adopted to detect GMEB1 expression in 55 selected HCC patients' cancer tissues and corresponding para-cancer tissues. Statistical analysis manifested that GMEB1 expression in the cancerous tissues of HCC patients was significantly higher as opposed to the para-cancer tissues (Figure 1B). Additionally, qRT-PCR analysis found that GMEB1 mRNA was markedly upregulated in HCC tissues and cells (HepG2, HCCLM3, MHCC97H and Huh7) as against para-cancerous tissues or the HL-7702 cell line (Figure 1C and D). Western blot analysis manifested that relative to HL-7702 cells, the GMEB1 protein level in HCC cells was remarkably elevated (Figure 1E).

Due to the high expression of GMEB1 in HCC tissues, we further explored the association between GMEB1 expression level and patient prognosis through the database analysis. The results from StarBase database suggested that high GMEB1 expression was linked to HCC patients' short overall survival (Figure 1F). At the same time, the overall survival of patients with the same stage of hepatocellular carcinoma was significantly longer in patients with low GMEB1 expression compared to those with high GMEB1 expression (Supplementary Figure 1C). Chi-square test revealed that high GMEB1 expression was related to advanced TNM stage and large tumor size in HCC patients (Table 1). These results indicated that GMEB1 is highly expressed in HCC tissues and that upregulation of GMEB1 expression is strongly associated with an exacerbation of the malignant phenotype and poor prognosis. Also, this section provisionally suggested that the upregulation of GMEB1 may play a role in the malignant progression of hepatocellular carcinoma.

GMEB1 facilitates HCC cell multiplication, migration and invasion, and suppresses cell apoptosis

To delve into the biological function of GMEB1 in HCC cells, we transfected HepG2 cells with pcDNA-GMEB1 to construct the GMEB1 overexpression cell model, and transfected Huh7 cells with si-GMEB1#1 or si-GMEB1#2 to construct the GMEB1 knockdown cell model. Western blot analysis showed that the plasmids were successfully transfected into cells, which was reflected in the results that GMEB1 was successfully overexpressed in HepG2 cells while GMEB1 was effectively silenced and down-regulated in Huh7 cells (Figure 2A). Next, to investigate the effect of GMEB1 on the proliferation of hepatocellular carcinoma cells, CCK8 assay was performed to assess the alteration in cell viability and proliferation rate following changes in GMEB1 expression levels. Results from CCK-8 assay demonstrated that overexpression of GMEB1 significantly promoted the proliferation of HepG2 cells while GMEB1 knockdown dramatically inhibited the proliferation of Huh7 cells compared to the si-NC group (Figure 2B). Furthermore, we continued to examine the effect of altered GMEB1 expression levels on cellular apoptosis in different groups by flow cytometry, and analysis of the PI/Annexin V double staining results showed that the percentage of apoptotic cells increased substantially after GMEB1 silencing, while the percentage of apoptotic cells in the overexpression group decreased markedly compared to the control group, suggesting that GMEB1 could enhance the anti-apoptotic ability of cells and promote cell survival (Figure 2C and D). The above results indicated that GMEB1 had a remarkable promotion effect on the growth of hepatocellular carcinoma cells, which was mainly achieved through the dual effect on inhibiting apoptosis and promoting proliferation.

In addition to promoting proliferation, we'd also like to know whether GMEB1 could alter the migration and invasion ability of hepatocellular carcinoma cells as well. The UALCAN database was firstly employed to analyze the correlation between GMEB1 and nodal metastasis status. As we can see in Supplementary Figure 1D, with the increase of nodal metastasis status, the expression level of GMEB1 was boosted as well. In order to further verify this conjecture, we conducted Transwell assay. The results indicated that overexpression of GMEB1 significantly promoted the migration and invasion of HepG2 cells, while knockdown of GMEB1 strongly inhibited the motor ability of Huh7 cells, suggesting that GMEB1 also plays an important role in promoting the migration and invasion ability of hepatocellular carcinoma cells and increasing the metastatic potential of tumors (Figure 2E-H).

Table 1 Correlation between glucocorticoid modulatory element-binding protein 1 expression and multiple clinicopathological characteristics in hepatocellular carcinoma patients (*n* = 55)

Characteristic	Number	GMEB1 expression		χ^2	*P* value
		High (*n* = 29)	Low (*n* = 26)		
Age (yr)					
< 60	25	14	11		
≥ 60	30	15	15	0.197	0.657
Gender					
Male	23	17	13		
Female	32	12	13	0.419	0.517
Alcoholism					
Negative	24	15	9		
Positive	31	14	17	1.632	0.201
HBV					
Negative	28	16	12		
Positive	27	13	14	0.446	0.504
Tumor size (cm)					
≤ 3	18	12	6		
> 3	37	10	27	7.928	0.005[b]
TNM stage					
I-II	20	11	9		
III-IV	35	7	28	7.081	0.007[b]
Differentiation					
Well/moderate	28	13	15		
Poor	27	16	11	0.980	0.322

[b]*P* < 0.01. GMEB1: Glucocorticoid modulatory element-binding protein 1; HBV: Hepatitis B virus; TNM: Tumor node metastasis.

Taken together, we can easily infer that GMEB1 can enhance the proliferation and anti-apoptotic ability of tumor cells, thus promoting unlimited proliferation of tumor. In addition, the enhancement of the migration and invasion ability of tumor cells further increases the possibility of tumor metastasis.

GMEB1 binds to the YAP1 promoter to promote transcription of YAP1

The next question is how GMEB1 promotes malignant proliferation and invasion of hepatocellular carcinoma cells and what are the downstream target genes, which we will then explore in more depth. Firstly, we analyzed the JASPAR databases (http://jaspar.genereg.net/) and found that GMEB1 may bind to three sites in the promoter region of YAP1 (Figure 3A). The StarBase database (http://starbase.sysu.edu.cn/) showed that GMEB1 and YAP1 expression are positively correlated in hepatic cancer tissue samples (Figure 3B). To verify the relationship between GMEB1 and YAP1, we then constructed wild-type plasmids with YAP1 promoter binding region and plasmids with mutations in the predicted binding sites, and then transfected cells with plasmids separately and collected them for dual luciferase reporter gene assays. The results revealed that overexpression of GMEB1 enhanced the luciferase activity of YAP1-WT in HepG2 cells, whereas GMEB1 knockdown reduced the luciferase activity of YAP1-WT in Huh7 cells (Figure 3C); neither GMEB1 overexpression nor knockdown had any significant effect on the luciferase activity of YAP1-MUT (Figure 3C), suggesting that GMEB1 can specifically bind to the YAP1 promoter region, and the binding site predicted by the database is the region where GMEB1 binds to the YAP1 promoter, and GMEB1 can positively regulate YAP1 expression at the transcriptional level. Moreover, ChIP-qPCR analysis demonstrated that GMEB1 was markedly enriched in the promoter region of YAP1 compared to the IgG control (Figure 3D), further confirming that GMEB1 directly regulates the transcriptional activation of YAP1. To this end, we examined the effects of altered GMEB1 expression on YAP1 at the mRNA and protein levels, respectively, and found that overexpression of GMEB1 promoted YAP1 expression in HepG2 cells, whereas knockdown of

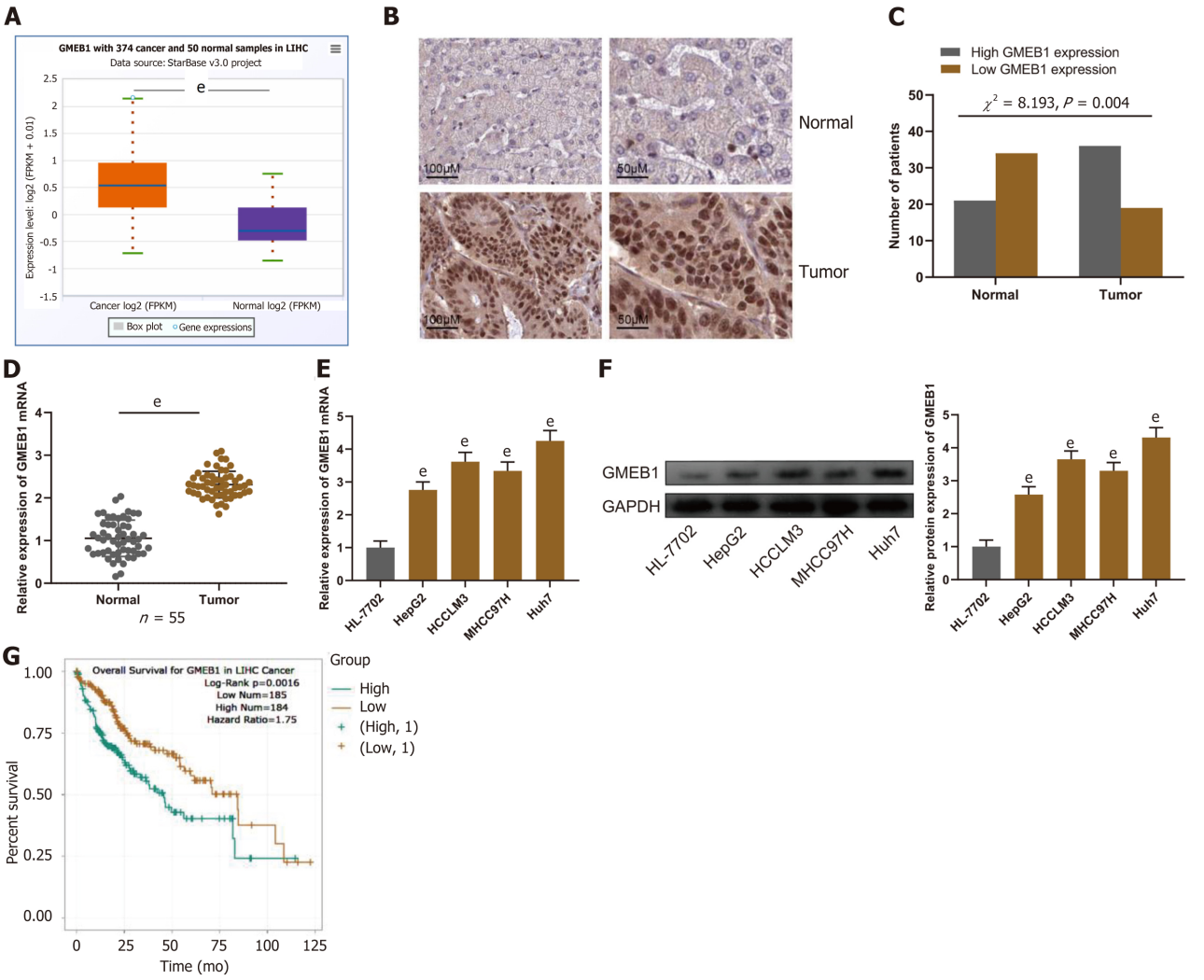

DOI: 10.4251/wjgo.v15.i6.988 **Copyright** ©The Author(s) 2023.

Figure 1 Glucocorticoid modulatory element-binding protein 1 is highly expressed in hepatocellular carcinoma. A: StarBase database (http://starbase.sysu.edu.cn/) analysis of glucocorticoid modulatory element-binding protein 1 (GMEB1) expression in hepatocellular carcinoma (HCC) tissues. B: Immunohistochemical assay was conducted to detect GMEB1 expression in HCC and para-cancerous tissues. C: IHC scores of GMEB1 expression in HCC and para-cancerous tissues. D and E: Detection by qRT-PCR of GMEB1 mRNA expression in HCC and para-cancer tissues, as well as in HCC cells (HepG2, HCCML3, MHCC97H and Huh7) and normal human hepatocytes (HL-7702). F: Detection by Western blot of GMEB1 protein expression in HCC cells and HL-7702 hepatocytes. G: The StarBase database analysis of the relationship between GMEB1 expression and HCC patients' overall survival. $^{e}P < 0.001$. GMEB1: Glucocorticoid modulatory element-binding protein 1; YAP1: Yes-associate protein 1.

GMEB1 inhibited YAP1 expression in Huh7 cells (Figure 3E and F). In addition, we also examined the expression of YAP1 in HCC tissues. qRT-PCR results illustrated that the expression of YAP1 mRNA was much higher in HCC tissues than in para-cancerous tissues (Figure 3G); Pearson analysis indicated that GMEB1 mRNA was positively correlated with YAP1 mRNA expression in HCC tissues (Figure 3H).

GMEB1 boosts HCC cell multiplication, migration and invasion and suppresses cell apoptosis through targeting YAP1

To verify the effect of GMEB1/YAP1 regulatory circuit on proliferation, migration, invasion and apoptosis of HCC cells, we co-transfected HepG2 cells with pcDNA-GMEB1 and si-YAP1; co-transfected Huh7 cells with si-GMEB1#1 and pcDNA-YAP1, respectively. qRT-PCR and Western blot assays illustrated that GMEB1 overexpression and YAP1 protein silencing were successful (Figure 4A and B). The results of CCK-8 assay, Transwell and flow cytometry demonstrated that the promotion of proliferation, migration and invasion as well as the anti-apoptotic effect of GMEB1 overexpression on HepG2 cells was reversed by the knockdown of YAP1; on the other hand, the upregulation of YAP1 also reversed the effect of knockdown of GMEB1 on the proliferation, migration, invasion and anti-apoptotic effect of YAP1 on Huh7 cells (Figure 4C-F).

To further validate this effect, we then constructed sh-GMEB1, oe-YAP1 and sh-GMEB1+oeYAP1 stable expression cell lines by lentiviral infection and investigated the effect of the GMEB1/YAP1 regulatory loop on tumor proliferation by Cell-derived xenografts (CDX) model in nude mice. The

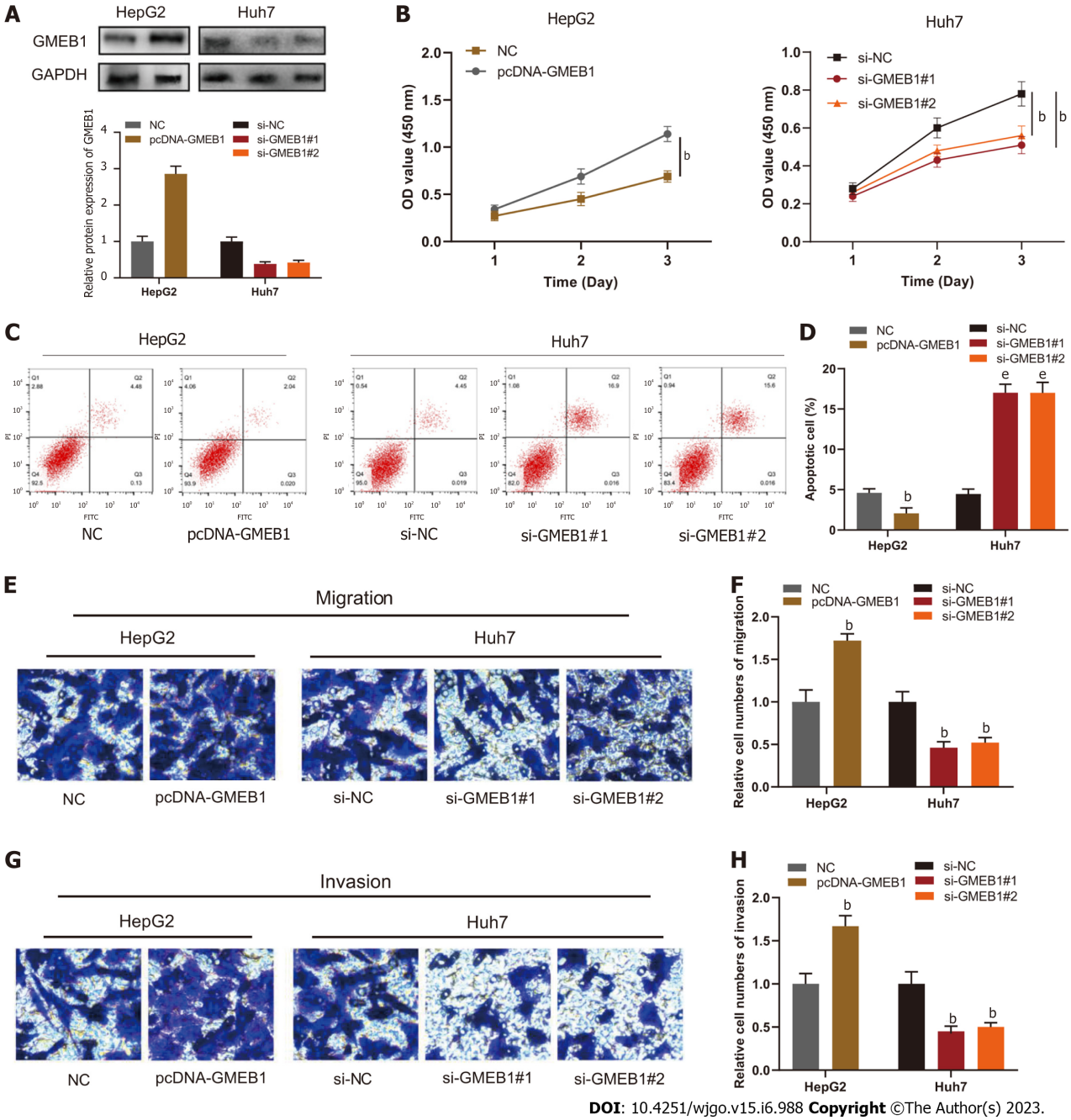

DOI: 10.4251/wjgo.v15.i6.988

Figure 2 Biological functions of glucocorticoid modulatory element-binding protein 1 in hepatocellular carcinoma. A: Western blotting was utilized to detect glucocorticoid modulatory element-binding protein 1 (GMEB1) expression in HepG2 cells transfected with GMEB1 overexpression plasmids and Huh7 cells transfected with si-GMEB1#1 and si-GMEB1#2; B: Evaluation of cell proliferation by the CCK-8 method; C and D: Detection of cell apoptosis *via* flow cytometry. E and F: Transwell assays were carried out to detect cell migration; G and H: Transwell assays were carried out to detect cell invasion. $^{b}P < 0.01$; and $^{e}P < 0.001$. GMEB1: Glucocorticoid modulatory element-binding protein 1; YAP1: Yes-associate protein 1.

results revealed that sh-GMEB1 remarkably slowed down the proliferation rate of HepG2-derived xenografts, whereas overexpression of YAP1 significantly enhanced the proliferation ability of tumors compared with the oe-NC group. More interestingly, silencing GMEB1 followed by overexpression of YAP1 markedly reversed the proliferation inhibitory effect of silencing GMEB1 (Figure 5A and B). The above data suggested that the GMEB1/YAP1-regulated signaling axis can effectively increase the level of malignant proliferation of tumor. Subsequently, we examined whether the number of HCC metastasis foci forming in the lung would be altered by tail vein injection of the above cells. As we can see, silencing of GMEB1 significantly reduced the number of metastatic foci, whereas overexpression of YAP1 did the opposite. Furthermore, silencing of GMEB1 followed by overexpression of YAP1 also reversed the inhibitory effect of GMEB1 silencing on the metastatic ability, with no significant difference from the control group (Figure 5C and D). Taken together, these data further confirmed our findings at the cellular level from the perspective of CDX mice model and emphasized the positive regulation of the GMEB1/YAP1 signaling axis on the malignant proliferation and metastasis of hepatocellular carcinoma.

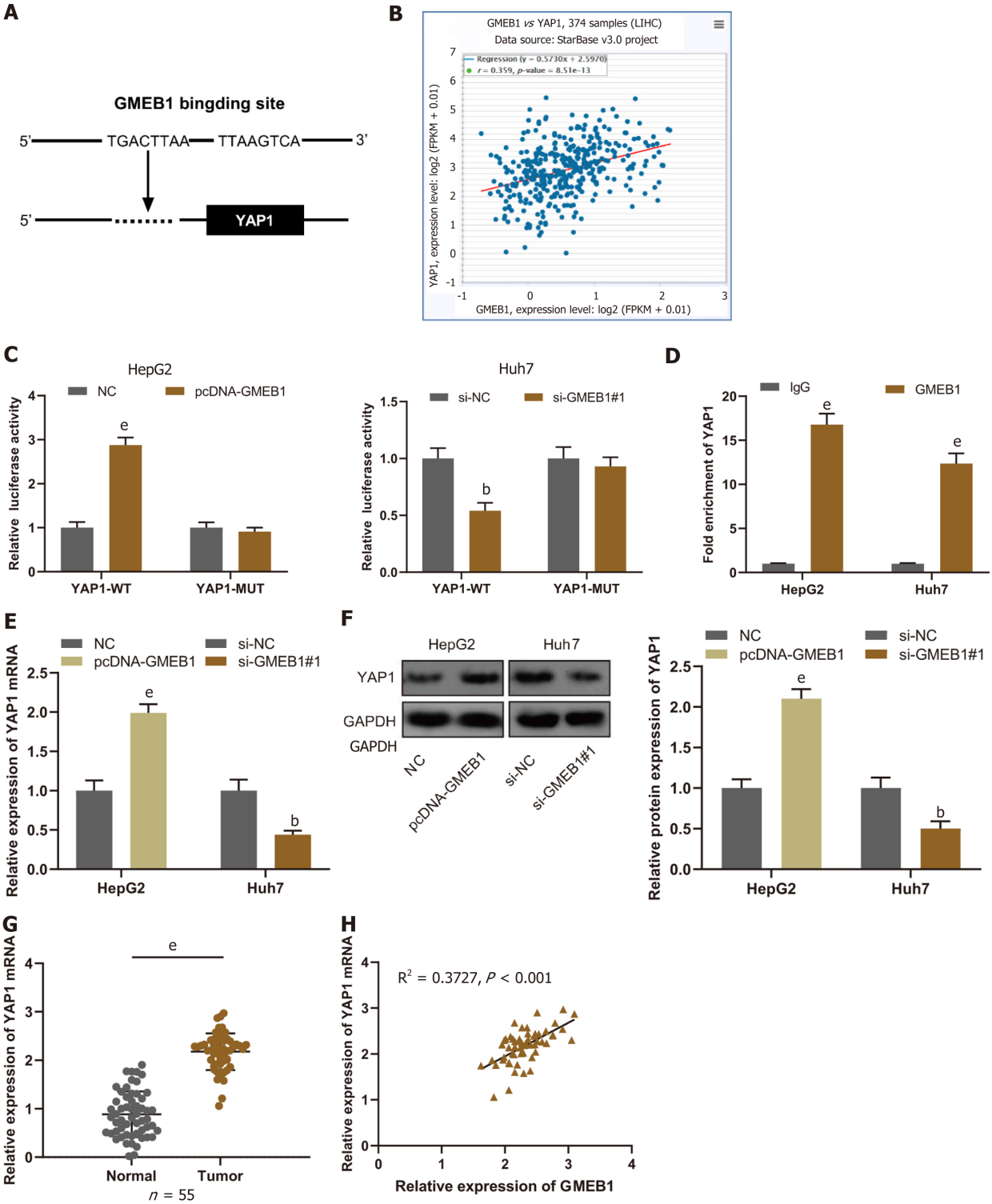

DOI: 10.4251/wjgo.v15.i6.988 **Copyright** ©The Author(s) 2023.

Figure 3 Glucocorticoid modulatory element-binding protein 1 targets and binds to Yes-associate protein 1. A: The JASPR database (http://jaspar.genereg.net/) was employed to predict the binding site of glucocorticoid modulatory element-binding protein 1 (GMEB1) and Yes-associate protein 1 (YAP1) promoter region. B: The StarBase database was employed to analyze the correlation between GMEB1 and YAP1 expression in hepatocellular carcinoma (HCC) tissues. C: Verification by dual-luciferase reporter gene assay of the binding relationship between GMEB1 and YAP1 promoter sequence. D: Detection *via* ChIP-qPCR assay of the binding of GMEB1 to the YAP1 promoter region. E and F: qRT-PCR and Western blotting were conducted to detect the effects of GMEB1 overexpression or knockdown on YAP1 mRNA and protein expression in HepG2 and Huh7 cells. G: Detection of YAP1 mRNA expression in HCC and para-tumorous tissues by qRT-PCR. H: Pearson correlation analysis of the correlation between GMEB1 mRNA and YAP1 mRNA expression in 55 cases of HCC tissues. $^{b}P < 0.01$; and $^{e}P < 0.001$. GMEB1: Glucocorticoid modulatory element-binding protein 1; YAP1: Yes-associate protein 1.

DISCUSSION

Transcription factors are a major type of DNA-binding protein that regulates gene expression *via*

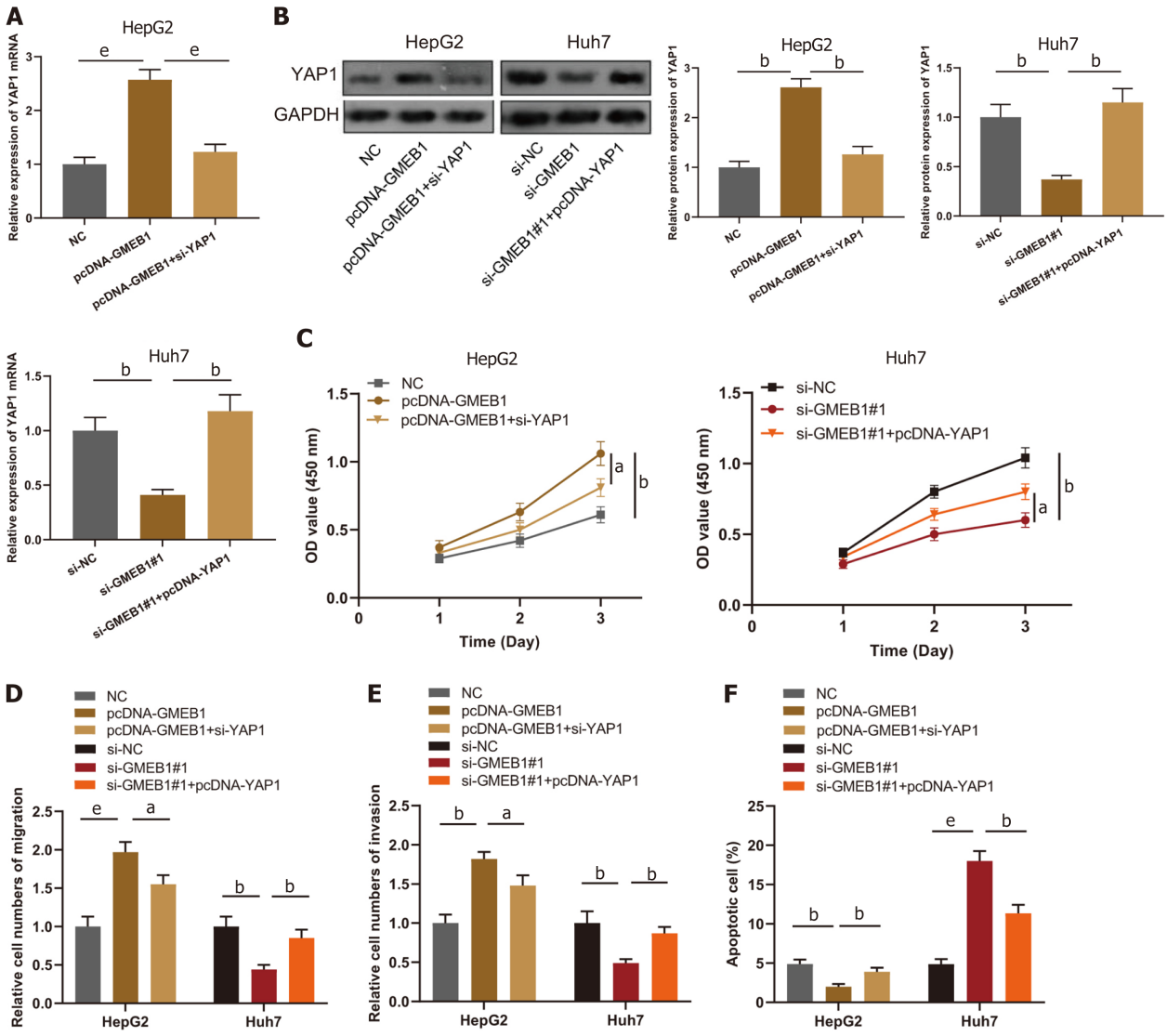

DOI: 10.4251/wjgo.v15.i6.988 **Copyright** ©The Author(s) 2023.

Figure 4 Effects of the interaction between glucocorticoid modulatory element-binding protein 1 and Yes-associate protein 1 on the biological functions of hepatocellular carcinoma cells. A and B: qRT-PCR and Western blot were utilized to detect YAP1 mRNA and protein expression in HepG2 cells transfected with NC, pcDNA-GMEB1, pcDNA-GMEB1+si-YAP1 and Huh7 cells transfected with si-NC, si-GMEB1#1, si-GMEB1#1+pcDNA-YAP1. C: Evaluation of HepG2 and Huh7 cell proliferation after transfection through the CCK-8 method. D and E: Transwell assays were conducted to detect HepG2 and Huh7 cell migration and invasion after transfection. F: Detection of HepG2 and Huh7 cell apoptosis after transfection *via* flow cytometry. $^{a}P < 0.05$; $^{b}P < 0.01$; and $^{e}P < 0.001$. GMEB1: Glucocorticoid modulatory element-binding protein 1; YAP1: Yes-associate protein 1.

binding with specific DNA sequences in gene promoter regions, thereby affecting cell growth, differentiation and apoptosis[29,30]. Many studies have shown that transcription factors can partake in regulating HCC occurrence and development. For instance, the transcription factor FOXN3 is downregulated in HCC and can inhibit cancer cell proliferation *via* negatively regulating E2F5 expression[31]; the transcription factor ATF3 suppresses HCC cell metastasis and proliferation by upregulating CYR61 expression[32]; the transcription factor KLF5 boosts HCC cell multiplication and metastasis by activating the PI3K/AKT/Snail signal pathway[33]. GMEB1 is a glucocorticoid regulatory element-binding protein, a ubiquitous multifunctional DNA-binding protein, and a transcription factor, which features prominently in the modulation of transcription after steroid hormone activation[34,35]. For the first time, this study discovered that GMEB1 was up-regulated in HCC tissues and cells. High GMEB1 expression was correlated to the advanced TNM stage, relatively large tumor size, and relatively short overall survival time of HCC patients. *In-vitro* functional research indicated that GMEB1 overexpression facilitated HCC cell multiplication, migration and invasion, and repressed the apoptosis, yet knocking down GMEB1 resulted in the opposite effects. This demonstrates that GMEB1 plays a vital role in the malignant progression of HCC.

In the further mechanism study, we mainly focused on the exploration for the downstream target gene of GMEB1, and finally determined that YAP1 was a new downstream target gene of GMEB1 through database prediction and experimental verification.YAP1, located on human chromosome 11q22,

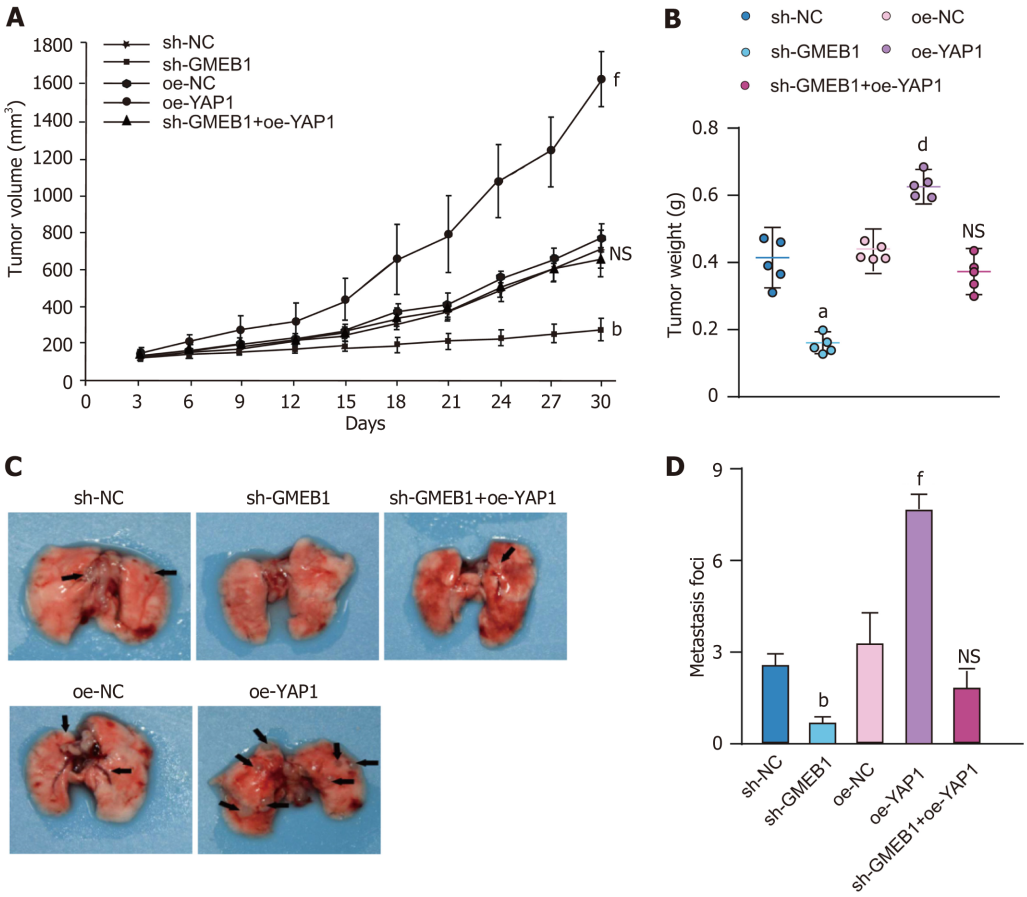

DOI: 10.4251/wjgo.v15.i6.988

Figure 5 Effects of the interaction between glucocorticoid modulatory element-binding protein 1 and Yes-associate protein 1 on the biological functions of hepatocellular carcinoma CDX mice models. A and B: HepG2 CDX mice model. Sh-NC, sh-GMEB1, oe-NC, oe-YAP1, sh-GMEB1+oe-YAP1 cells were injected subcutaneously into the right axilla of mice (n = 5/group) and tumor size was measured every 3 d. Tumor volume was calculated using the formula: V = (L x W^2)/2. 30 days post injection, mice were sacrificed and tumors were peeled and weighted. C and D: HepG2 metastasis mice model. Sh-NC, sh-GMEB1, oe-NC, oe-YAP1, sh-GMEB1+oe-YAP1 cells were injected into nude mice (n = 5/group) *via* tail vein, respectively. Mice were sacrificed 60 d after injection, and number of metastatic foci on the lungs of each group were photographed and counted. $^{a}P < 0.05$, $^{b}P < 0.01$, and $^{e}P < 0.001$ *vs* sh-NC group; $^{d}P < 0.01$ and $^{f}P < 0.001$ *vs* oe-NC group. NS: Not significant. GMEB1: Glucocorticoid modulatory element-binding protein 1; YAP1: Yes-associate protein 1.

is a transcriptional coactivator of the Hippo pathway, and it modulates the transcription of downstream target genes and intracellular signal transduction through phosphorylation, thus maintaining the balance of cell multiplication and apoptosis[36]. Some studies have found that YAP1 is targeted and regulated by multiple microRNAs (miRs), such as miR-506[37], miR-200a[38], miR-139-5p[39] and miR-27b-3p[40]. Reportedly, YAP1 is abnormally high-expressed in various tumor tissues, and participates in facilitating tumor cell multiplication, invasion and migration and the activation of multiple signaling pathways[36-38,41,42]. For example, YAP1 is up-regulated in bladder carcinoma tissues and can interact with mTOR protein to promote bladder carcinoma cell proliferation[43]. The increase in YAP1 expression is connected with the poor prognosis of BC patients, and inhibits PTEN expression to boost BC cell multiplication and repress the apoptosis[44]. In HCC, YAP1 can facilitate cell proliferation, invasion and EMT process *in vitro*[45]. In our study, we first found that GMEB1 could bind with the YAP1 promoter region and could positively modulate YAP1 expression in HCC cells. Also, there was a positive correlation between YAP1 and GMEB1 expression in HCC tissues. Moreover, alteration of YAP1 expression could mediate GMEB1-induced HCC cell multiplication, migration, invasion and apoptosis.

The crucial role of the Hippo signaling pathway, with YAP/TAZ as the main effector proteins, in the development of hepatocellular carcinoma has been confirmed and highlighted by numerous studies [46], however, no inhibitors directly targeting core proteins of the Hippo signaling pathway have been successfully marketed, making direct intervention of the Hippo signaling pathway difficult and preventing patients with excessive Hippo activation from benefiting more from conventional therapies. For this reason, a number of studies have begun to attempt to interfere with the Hippo signaling pathway through the inhibition of indirectly regulated proteins. These include PFI-2, a highly selective inhibitor of SETD7 methyltransferase, which inhibits YAP nuclear translocation and Hippo pathway activation through direct interaction with SETD7[47], and Ki-16425, a competitive inhibitor of LPA1/2/

3, which inhibits Hippo signaling by blocking LPA receptor-induced YAP/TAZ dephosphorylation[48]. The discovery of our study further enriches the range of target options for indirect intervention in the Hippo signaling pathway, thus providing new candidate proteins for inhibitor development.

CONCLUSION

In conclusion, our study revealed for the first time that GMEB1 is highly expressed in both HCC tissues and cells. Furthermore, we confirmed that YAP1 is a novel transcriptional target gene of GMEB1 and demonstrated that GMEB1/YAP1 regulatory axis has a key role in promoting HCC cell proliferation, migration and invasion and anti-apoptosis. As this suggests that, on the one hand, GMEB1 can be a candidate molecular marker for accurate diagnosis of early-stage liver cancer; on the other hand, targeting GMEB1 may be a potential therapeutic approach to improve the efficiency of HCC treatment. However, our study also has some limitations. Firstly, we only used the CDX animal model to verify the regulation of GMEB1 on the malignant progression of HCC; we lacked samples from clinical sources for further corroboration. In addition, we lacked follow-up studies on patients so as to further corroborate the effect of GMEB1 on the prognosis of hepatocellular carcinoma. In subsequent studies, we will continue to refine our findings in the follow-up study and continue to obtain more reliable experimental conclusions.

ARTICLE HIGHLIGHTS

Research background

Most hepatocellular carcinoma (HCC) cases have already been in an intermediate to advanced stage at diagnosis, missing the optimal time for surgical treatment. Besides, the high cost and huge shortage of donors greatly limit the clinical application of liver transplantation. Therefore, the lack of reliable diagnostic markers and interventions makes the overall survival rate of HCC patients hardly improved, and the prognosis of patients is generally poor.

Research motivation

Mechanistic understanding of proliferation promotion, increased metastatic potential and cellular defense against apoptosis can inform novel therapeutic strategies in HCC treatment. We would like to clarify the biological functions and clinical significance of glucocorticoid modulatory element-binding protein 1 (GMEB1) in HCC to provide more reliable biomarkers and target candidates for HCC diagnosis and treatment.

Research objectives

Due to the lack of reliable early diagnosis biomarkers and clinical intervention targets, patients with HCC are often diagnosed in the middle and late stages with poor prognosis. This study aims to find new molecular biomarkers with high reference value and effective candidate targets for the treatment of HCC.

Research methods

GMEB1 expression level was detected through bioinformatics analysis first and further validation was conducted in HCC clinical tissue samples by using immunohistochemistry and qPCR; immunoblotting and qPCR were used to detect the expression of GMEB1 in HCC cell lines. Cell counting kit-8 assay, Transwell and flow cytometry were performed to assess the alteration on proliferation and metastasis potential of HCC cells after changes on GMEB1 expression level in HCC cell lines. The binding site of GMEB1 to Yes-associate protein 1 (YAP1) promoter was predicted by bioinformatics analysis and verified by dual luciferase reporter gene assay and ChIP-qPCR.

Research results

GMEB1 was abnormally highly expressed in HCC, whose expression correlates with some clinicopathological features of HCC patients, such as tumor size and TNM stage. According to i*n vitro* results, overexpression of GEMB1 promotes the malignant proliferation and metastasis of HCC cell lines, while knockdown of GMEB1 suppresses the degree of malignancy. In mechanism, GEMB1 positively regulates the expression of YAP1 in transcription level, which finally promote the progression of HCC.

Research conclusions

GMEB1 is a new oncogenic factor of HCC, which promotes the malignant proliferation and metastasis of HCC by promoting YAP1 transcriptional activation.

Research perspectives

This study reveals that GMEB1, a member of KDWK gene family to modulate the transactivation of the glucocorticoid receptor, has a previously unrecognized role in HCC progression, suggesting that it may be a promising biomarker for early-stage HCC diagnosis and it is possible to intervene in anti-tumor therapy against HCC by inhibiting GMEB1-mediated tumor proliferation, metastasis and anti-apoptosis effect.

FOOTNOTES

Author contributions: Chen C and Lin HG contributed equally to this work; Chen C, Lin HG and Yao Z designed the research; Lin HG, Yao Z, Jiang YL and Yu HJ contributed to methodological establishment and completion of experiments; Lin HG, Yao Z, Jiang YL, Yu HJ, Fang J and Li WN analyzed and interpreted the data; Chen C and Lin HG drafted the manuscript; Chen C and Fang J and Li WN critically revised the manuscript for important intellectual content.

Institutional review board statement: The study was reviewed and approved by Ethics Committee of Zhejiang Xiaoshan Hopital.

Institutional animal care and use committee statement: The experimental protocol was approved by the Animal Care and Use Committee of Zhejiang Xiaoshan Hopital.

Conflict-of-interest statement: All the authors report no relevant conflicts of interest for this article.

Data sharing statement: No additional data are available.

ARRIVE guidelines statement: The authors have read the ARRIVE guidelines, and the manuscript was prepared and revised according to the ARRIVE guidelines.

Country/Territory of origin: China

ORCID number: Cheng Chen 0000-0003-4867-0727.

S-Editor: Gong ZM
L-Editor: A
P-Editor: Zhang YL

REFERENCES

1 **de Castria TB**, Khalil DN, Harding JJ, O'Reilly EM, Abou-Alfa GK. Tremelimumab and durvalumab in the treatment of unresectable, advanced hepatocellular carcinoma. *Future Oncol* 2022; **18**: 3769-3782 [PMID: 36399155 DOI: 10.2217/fon-2022-0652]

2 **Hernández-Aquino E**, Muriel P. Beneficial effects of naringenin in liver diseases: Molecular mechanisms. *World J Gastroenterol* 2018; **24**: 1679-1707 [PMID: 29713125 DOI: 10.3748/wjg.v24.i16.1679]

3 **Bray F**, Ren JS, Masuyer E, Ferlay J. Global estimates of cancer prevalence for 27 sites in the adult population in 2008. *Int J Cancer* 2013; **132**: 1133-1145 [PMID: 22752881 DOI: 10.1002/ijc.27711]

4 **Global Burden of Disease Cancer Collaboration**, Fitzmaurice C, Abate D, Abbasi N, Abbastabar H, Abd-Allah F, Abdel-Rahman O, Abdelalim A, Abdoli A, Abdollahpour I, Abdulle ASM, Abebe ND, Abraha HN, Abu-Raddad LJ, Abualhasan A, Adedeji IA, Advani SM, Afarideh M, Afshari M, Aghaali M, Agius D, Agrawal S, Ahmadi A, Ahmadian E, Ahmadpour E, Ahmed MB, Akbari ME, Akinyemiju T, Al-Aly Z, AlAbdulKader AM, Alahdab F, Alam T, Alamene GM, Alemnew BTT, Alene KA, Alinia C, Alipour V, Aljunid SM, Bakeshei FA, Almadi MAH, Almasi-Hashiani A, Alsharif U, Alsowaidi S, Alvis-Guzman N, Amini E, Amini S, Amoako YA, Anbari Z, Anber NH, Andrei CL, Anjomshoa M, Ansari F, Ansariadi A, Appiah SCY, Arab-Zozani M, Arabloo J, Arefi Z, Aremu O, Areri HA, Artaman A, Asayesh H, Asfaw ET, Ashagre AF, Assadi R, Ataeinia B, Atalay HT, Ataro Z, Atique S, Ausloos M, Avila-Burgos L, Avokpaho EFGA, Awasthi A, Awoke N, Ayala Quintanilla BP, Ayanore MA, Ayele HT, Babaee E, Bacha U, Badawi A, Bagherzadeh M, Bagli E, Balakrishnan S, Balouchi A, Bärnighausen TW, Battista RJ, Behzadifar M, Bekele BB, Belay YB, Belayneh YM, Berfield KKS, Berhane A, Bernabe E, Beuran M, Bhakta N, Bhattacharyya K, Biadgo B, Bijani A, Bin Sayeed MS, Birungi C, Bisignano C, Bitew H, Bjørge T, Bleyer A, Bogale KA, Bojia HA, Borzì AM, Bosetti C, Bou-Orm IR, Brenner H, Brewer JD, Briko AN, Briko NI, Bustamante-Teixeira MT, Butt ZA, Carreras G, Carrero JJ, Carvalho F,

Castro C, Castro F, Catalá-López F, Cerin E, Chaiah Y, Chanie WF, Chattu VK, Chaturvedi P, Chauhan NS, Chehrazi M, Chiang PP, Chichiabellu TY, Chido-Amajuoyi OG, Chimed-Ochir O, Choi JJ, Christopher DJ, Chu DT, Constantin MM, Costa VM, Crocetti E, Crowe CS, Curado MP, Dahlawi SMA, Damiani G, Darwish AH, Daryani A, das Neves J, Demeke FM, Demis AB, Demissie BW, Demoz GT, Denova-Gutiérrez E, Derakhshani A, Deribe KS, Desai R, Desalegn BB, Desta M, Dey S, Dharmaratne SD, Dhimal M, Diaz D, Dinberu MTT, Djalalinia S, Doku DT, Drake TM, Dubey M, Dubljanin E, Duken EE, Ebrahimi H, Effiong A, Eftekhari A, El Sayed I, Zaki MES, El-Jaafary SI, El-Khatib Z, Elemineh DA, Elkout H, Ellenbogen RG, Elsharkawy A, Emamian MH, Endalew DA, Endries AY, Eshrati B, Fadhil I, Fallah Omrani V, Faramarzi M, Farhangi MA, Farioli A, Farzadfar F, Fentahun N, Fernandes E, Feyissa GT, Filip I, Fischer F, Fisher JL, Force LM, Foroutan M, Freitas M, Fukumoto T, Futran ND, Gallus S, Gankpe FG, Gayesa RT, Gebrehiwot TT, Gebremeskel GG, Gedefaw GA, Gelaw BK, Geta B, Getachew S, Gezae KE, Ghafourifard M, Ghajar A, Ghashghaee A, Gholamian A, Gill PS, Ginindza TTG, Girmay A, Gizaw M, Gomez RS, Gopalani SV, Gorini G, Goulart BNG, Grada A, Ribeiro Guerra M, Guimaraes ALS, Gupta PC, Gupta R, Hadkhale K, Haj-Mirzaian A, Hamadeh RR, Hamidi S, Hanfore LK, Haro JM, Hasankhani M, Hasanzadeh A, Hassen HY, Hay RJ, Hay SI, Henok A, Henry NJ, Herteliu C, Hidru HD, Hoang CL, Hole MK, Hoogar P, Horita N, Hosgood HD, Hosseini M, Hosseinzadeh M, Hostiuc M, Hostiuc S, Househ M, Hussen MM, Ileanu B, Ilic MD, Innos K, Irvani SSN, Iseh KR, Islam SMS, Islami F, Jafari Balalami N, Jafarinia M, Jahangiry L, Jahani MA, Jahanmehr N, Jakovljevic M, James SL, Javanbakht M, Jayaraman S, Jee SH, Jenabi E, Jha RP, Jonas JB, Jonnagaddala J, Joo T, Jungari SB, Jürisson M, Kabir A, Kamangar F, Karch A, Karimi N, Karimian A, Kasaeian A, Kasahun GG, Kassa B, Kassa TD, Kassaw MW, Kaul A, Keiyoro PN, Kelbore AG, Kerbo AA, Khader YS, Khalilarjmandi M, Khan EA, Khan G, Khang YH, Khatab K, Khater A, Khayamzadeh M, Khazaee-Pool M, Khazaei S, Khoja AT, Khosravi MH, Khubchandani J, Kianipour N, Kim D, Kim YJ, Kisa A, Kisa S, Kissimova-Skarbek K, Komaki H, Koyanagi A, Krohn KJ, Bicer BK, Kugbey N, Kumar V, Kuupiel D, La Vecchia C, Lad DP, Lake EA, Lakew AM, Lal DK, Lami FH, Lan Q, Lasrado S, Lauriola P, Lazarus JV, Leigh J, Leshargie CT, Liao Y, Limenih MA, Listl S, Lopez AD, Lopukhov PD, Lunevicius R, Madadin M, Magdeldin S, El Razek HMA, Majeed A, Maleki A, Malekzadeh R, Manafi A, Manafi N, Manamo WA, Mansourian M, Mansournia MA, Mantovani LG, Maroufizadeh S, Martini SMS, Mashamba-Thompson TP, Massenburg BB, Maswabi MT, Mathur MR, McAlinden C, McKee M, Meheretu HAA, Mehrotra R, Mehta V, Meier T, Melaku YA, Meles GG, Meles HG, Melese A, Melku M, Memiah PTN, Mendoza W, Menezes RG, Merat S, Meretoja TJ, Mestrovic T, Miazgowski B, Miazgowski T, Mihretie KMM, Miller TR, Mills EJ, Mir SM, Mirzaei H, Mirzaei HR, Mishra R, Moazen B, Mohammad DK, Mohammad KA, Mohammad Y, Darwesh AM, Mohammadbeigi A, Mohammadi H, Mohammadi M, Mohammadian M, Mohammadian-Hafshejani A, Mohammadoo-Khorasani M, Mohammadpourhodki R, Mohammed AS, Mohammed JA, Mohammed S, Mohebi F, Mokdad AH, Monasta L, Moodley Y, Moosazadeh M, Moossavi M, Moradi G, Moradi-Joo M, Moradi-Lakeh M, Moradpour F, Morawska L, Morgado-da-Costa J, Morisaki N, Morrison SD, Mosapour A, Mousavi SM, Muche AA, Muhammed OSS, Musa J, Nabhan AF, Naderi M, Nagarajan AJ, Nagel G, Nahvijou A, Naik G, Najafi F, Naldi L, Nam HS, Nasiri N, Nazari J, Negoi I, Neupane S, Newcomb PA, Nggada HA, Ngunjiri JW, Nguyen CT, Nikniaz L, Ningrum DNA, Nirayo YL, Nixon MR, Nnaji CA, Nojomi M, Nosratnejad S, Shiadeh MN, Obsa MS, Ofori-Asenso R, Ogbo FA, Oh IH, Olagunju AT, Olagunju TO, Oluwasanu MM, Omonisi AE, Onwujekwe OE, Oommen AM, Oren E, Ortega-Altamirano DDV, Ota E, Otstavnov SS, Owolabi MO, P A M, Padubidri JR, Pakhale S, Pakpour AH, Pana A, Park EK, Parsian H, Pashaei T, Patel S, Patil ST, Pennini A, Pereira DM, Piccinelli C, Pillay JD, Pirestani M, Pishgar F, Postma MJ, Pourjafar H, Pourmalek F, Pourshams A, Prakash S, Prasad N, Qorbani M, Rabiee M, Rabiee N, Radfar A, Rafiei A, Rahim F, Rahimi M, Rahman MA, Rajati F, Rana SM, Raoofi S, Rath GK, Rawaf DL, Rawaf S, Reiner RC, Renzaho AMN, Rezaei N, Rezapour A, Ribeiro AI, Ribeiro D, Ronfani L, Roro EM, Roshandel G, Rostami A, Saad RS, Sabbagh P, Sabour S, Saddik B, Safiri S, Sahebkar A, Salahshoor MR, Salehi F, Salem H, Salem MR, Salimzadeh H, Salomon JA, Samy AM, Sanabria J, Santric Milicevic MM, Sartorius B, Sarveazad A, Sathian B, Satpathy M, Savic M, Sawhney M, Sayyah M, Schneider IJC, Schöttker B, Sekerija M, Sepanlou SG, Sepehrimanesh M, Seyedmousavi S, Shaahmadi F, Shabaninejad H, Shahbaz M, Shaikh MA, Shamshirian A, Shamsizadeh M, Sharafi H, Sharafi Z, Sharif M, Sharifi A, Sharifi H, Sharma R, Sheikh A, Shirkoohi R, Shukla SR, Si S, Siabani S, Silva DAS, Silveira DGA, Singh A, Singh JA, Sisay S, Sitas F, Sobngwi E, Soofi M, Soriano JB, Stathopoulou V, Sufiyan MB, Tabarés-Seisdedos R, Tabuchi T, Takahashi K, Tamtaji OR, Tarawneh MR, Tassew SG, Taymoori P, Tehrani-Banihashemi A, Temsah MH, Temsah O, Tesfay BE, Tesfay FH, Teshale MY, Tessema GA, Thapa S, Tlaye KG, Topor-Madry R, Tovani-Palone MR, Traini E, Tran BX, Tran KB, Tsadik AG, Ullah I, Uthman OA, Vacante M, Vaezi M, Varona Pérez P, Veisani Y, Vidale S, Violante FS, Vlassov V, Vollset SE, Vos T, Vosoughi K, Vu GT, Vujcic IS, Wabinga H, Wachamo TM, Wagnew FS, Waheed Y, Weldegebreal F, Weldesamuel GT, Wijeratne T, Wondafrash DZ, Wonde TE, Wondmieneh AB, Workie HM, Yadav R, Yadegar A, Yadollahpour A, Yaseri M, Yazdi-Feyzabadi V, Yeshaneh A, Yimam MA, Yimer EM, Yisma E, Yonemoto N, Younis MZ, Yousefi B, Yousefifard M, Yu C, Zabeh E, Zadnik V, Moghadam TZ, Zaidi Z, Zamani M, Zandian H, Zangeneh A, Zaki L, Zendehdel K, Zenebe ZM, Zewale TA, Ziapour A, Zodpey S, Murray CJL. Global, Regional, and National Cancer Incidence, Mortality, Years of Life Lost, Years Lived With Disability, and Disability-Adjusted Life-Years for 29 Cancer Groups, 1990 to 2017: A Systematic Analysis for the Global Burden of Disease Study. *JAMA Oncol* 2019; **5**: 1749-1768 [PMID: 31560378 DOI: 10.1001/jamaoncol.2019.2996]

5 **Kirstein MM**, Wirth TC. [Multimodal treatment of hepatocellular carcinoma]. *Internist (Berl)* 2020; **61**: 164-169 [PMID: 31919533 DOI: 10.1007/s00108-019-00722-x]

6 **Zhou ZF**, Peng F, Li JY, Ye YB. Intratumoral IL-12 Gene Therapy Inhibits Tumor Growth In A HCC-Hu-PBL-NOD/SCID Murine Model. *Onco Targets Ther* 2019; **12**: 7773-7784 [PMID: 31571927 DOI: 10.2147/OTT.S222097]

7 **Dageforde LA**, Fowler KJ, Chapman WC. Liver transplantation for hepatocellular carcinoma: current update on treatment and allocation. *Curr Opin Organ Transplant* 2017; **22**: 128-134 [PMID: 27926548 DOI: 10.1097/MOT.0000000000000385]

8 **O'Rourke JM**, Shetty S, Shah T, Perera MTPR. Liver transplantation for hepatocellular carcinoma: pushing the boundaries. *Transl Gastroenterol Hepatol* 2019; **4**: 1 [PMID: 30854488 DOI: 10.21037/tgh.2018.12.07]

9 **An W**, Yao S, Sun X, Hou Z, Lin Y, Su L, Liu X. Glucocorticoid modulatory element-binding protein 1 (GMEB1) interacts with the de-ubiquitinase USP40 to stabilize CFLAR(L) and inhibit apoptosis in human non-small cell lung cancer

cells. *J Exp Clin Cancer Res* 2019; **38**: 181 [PMID: 31046799 DOI: 10.1186/s13046-019-1182-3]

10 **Kawabe K**, Lindsay D, Braitch M, Fahey AJ, Showe L, Constantinescu CS. IL-12 inhibits glucocorticoid-induced T cell apoptosis by inducing GMEB1 and activating PI3K/Akt pathway. *Immunobiology* 2012; **217**: 118-123 [PMID: 21840619 DOI: 10.1016/j.imbio.2011.07.018]

11 **L'Hôte D**, Georges A, Todeschini AL, Kim JH, Benayoun BA, Bae J, Veitia RA. Discovery of novel protein partners of the transcription factor FOXL2 provides insights into its physiopathological roles. *Hum Mol Genet* 2012; **21**: 3264-3274 [PMID: 22544055 DOI: 10.1093/hmg/dds170]

12 **Tsuruma K**, Nakagawa T, Morimoto N, Minami M, Hara H, Uehara T, Nomura Y. Glucocorticoid modulatory element-binding protein 1 binds to initiator procaspases and inhibits ischemia-induced apoptosis and neuronal injury. *J Biol Chem* 2006; **281**: 11397-11404 [PMID: 16497673 DOI: 10.1074/jbc.M510597200]

13 **Nakagawa T**, Tsuruma K, Uehara T, Nomura Y. GMEB1, a novel endogenous caspase inhibitor, prevents hypoxia- and oxidative stress-induced neuronal apoptosis. *Neurosci Lett* 2008; **438**: 34-37 [PMID: 18455874 DOI: 10.1016/j.neulet.2008.04.023]

14 **Jiang M**, Cheng Y, Wang D, Lu Y, Gu S, Wang C, Huang Y, Li Y. Transcriptional network modulated by the prognostic signature transcription factors and their long noncoding RNA partners in primary prostate cancer. *EBioMedicine* 2021; **63**: 103150 [PMID: 33279858 DOI: 10.1016/j.ebiom.2020.103150]

15 **Shibata M**, Ham K, Hoque MO. A time for YAP1: Tumorigenesis, immunosuppression and targeted therapy. *Int J Cancer* 2018; **143**: 2133-2144 [PMID: 29696628 DOI: 10.1002/ijc.31561]

16 **Zagiel B**, Melnyk P, Cotelle P. Progress with YAP/TAZ-TEAD inhibitors: a patent review (2018-present). *Expert Opin Ther Pat* 2022; **32**: 899-912 [PMID: 35768160 DOI: 10.1080/13543776.2022.2096436]

17 **Hao B**, Chen X, Cao Y. Yes-associated protein 1 promotes the metastasis of U251 glioma cells by upregulating Jagged-1 expression and activating the Notch signal pathway. *Exp Ther Med* 2018; **16**: 1411-1416 [PMID: 30112068 DOI: 10.3892/etm.2018.6322]

18 **Shao DD**, Xue W, Krall EB, Bhutkar A, Piccioni F, Wang X, Schinzel AC, Sood S, Rosenbluh J, Kim JW, Zwang Y, Roberts TM, Root DE, Jacks T, Hahn WC. KRAS and YAP1 converge to regulate EMT and tumor survival. *Cell* 2014; **158**: 171-184 [PMID: 24954536 DOI: 10.1016/j.cell.2014.06.004]

19 **Zhao B**, Wei X, Li W, Udan RS, Yang Q, Kim J, Xie J, Ikenoue T, Yu J, Li L, Zheng P, Ye K, Chinnaiyan A, Halder G, Lai ZC, Guan KL. Inactivation of YAP oncoprotein by the Hippo pathway is involved in cell contact inhibition and tissue growth control. *Genes Dev* 2007; **21**: 2747-2761 [PMID: 17974916 DOI: 10.1101/gad.1602907]

20 **Sheen-Chen SM**, Huang CY, Tsai CH, Liu YW, Wu SC, Huang CC, Eng HL, Chan YC, Ko SF, Tang RP. Yes-associated protein is not an independent prognostic marker in breast cancer. *Anticancer Res* 2012; **32**: 3321-3325 [PMID: 22843909]

21 **Zender L**, Spector MS, Xue W, Flemming P, Cordon-Cardo C, Silke J, Fan ST, Luk JM, Wigler M, Hannon GJ, Mu D, Lucito R, Powers S, Lowe SW. Identification and validation of oncogenes in liver cancer using an integrative oncogenomic approach. *Cell* 2006; **125**: 1253-1267 [PMID: 16814713 DOI: 10.1016/j.cell.2006.05.030]

22 **Xu MZ**, Yao TJ, Lee NP, Ng IO, Chan YT, Zender L, Lowe SW, Poon RT, Luk JM. Yes-associated protein is an independent prognostic marker in hepatocellular carcinoma. *Cancer* 2009; **115**: 4576-4585 [PMID: 19551889 DOI: 10.1002/cncr.24495]

23 **Xie Q**, Chen J, Feng H, Peng S, Adams U, Bai Y, Huang L, Li J, Huang J, Meng S, Yuan Z. YAP/TEAD-mediated transcription controls cellular senescence. *Cancer Res* 2013; **73**: 3615-3624 [PMID: 23576552 DOI: 10.1158/0008-5472.CAN-12-3793]

24 **Piccolo FM**, Kastan NR, Haremaki T, Tian Q, Laundos TL, De Santis R, Beaudoin AJ, Carroll TS, Luo JD, Gnedeva K, Etoc F, Hudspeth AJ, Brivanlou AH. Role of YAP in early ectodermal specification and a Huntington's Disease model of human neurulation. *Elife* 2022; **11** [PMID: 35451959 DOI: 10.7554/eLife.73075]

25 **Kastan N**, Gnedeva K, Alisch T, Petelski AA, Huggins DJ, Chiaravalli J, Aharanov A, Shakked A, Tzahor E, Nagiel A, Segil N, Hudspeth AJ. Small-molecule inhibition of Lats kinases may promote Yap-dependent proliferation in postmitotic mammalian tissues. *Nat Commun* 2021; **12**: 3100 [PMID: 34035288 DOI: 10.1038/s41467-021-23395-3]

26 **Sun HL**, Men JR, Liu HY, Liu MY, Zhang HS. FOXM1 facilitates breast cancer cell stemness and migration in YAP1-dependent manner. *Arch Biochem Biophys* 2020; **685**: 108349 [PMID: 32209309 DOI: 10.1016/j.abb.2020.108349]

27 **He Q**, Lin Z, Wang Z, Huang W, Tian D, Liu M, Xia L. SIX4 promotes hepatocellular carcinoma metastasis through upregulating YAP1 and c-MET. *Oncogene* 2020; **39**: 7279-7295 [PMID: 33046796 DOI: 10.1038/s41388-020-01500-y]

28 **Chen Z**, Wang HW, Wang S, Fan L, Feng S, Cai X, Peng C, Wu X, Lu J, Chen D, Chen Y, Wu W, Lu D, Liu N, You Y, Wang H. USP9X deubiquitinates ALDH1A3 and maintains mesenchymal identity in glioblastoma stem cells. *J Clin Invest* 2019; **129**: 2043-2055 [PMID: 30958800 DOI: 10.1172/JCI126414]

29 **Inoue K**. Feedback enrichment analysis for transcription factor-target genes in signaling pathways. *Biosystems* 2020; **198**: 104262 [PMID: 33002527 DOI: 10.1016/j.biosystems.2020.104262]

30 **Turner D**, Kim R, Guo JT. TFinDit: transcription factor-DNA interaction data depository. *BMC Bioinformatics* 2012; **13**: 220 [PMID: 22943312 DOI: 10.1186/1471-2105-13-220]

31 **Sun J**, Li H, Huo Q, Cui M, Ge C, Zhao F, Tian H, Chen T, Yao M, Li J. The transcription factor FOXN3 inhibits cell proliferation by downregulating E2F5 expression in hepatocellular carcinoma cells. *Oncotarget* 2016; **7**: 43534-43545 [PMID: 27259277 DOI: 10.18632/oncotarget.9780]

32 **Chen C**, Ge C, Liu Z, Li L, Zhao F, Tian H, Chen T, Li H, Yao M, Li J. ATF3 inhibits the tumorigenesis and progression of hepatocellular carcinoma cells *via* upregulation of CYR61 expression. *J Exp Clin Cancer Res* 2018; **37**: 263 [PMID: 30376856 DOI: 10.1186/s13046-018-0919-8]

33 **An T**, Dong T, Zhou H, Chen Y, Zhang J, Zhang Y, Li Z, Yang X. The transcription factor Krüppel-like factor 5 promotes cell growth and metastasis *via* activating PI3K/AKT/Snail signaling in hepatocellular carcinoma. *Biochem Biophys Res Commun* 2019; **508**: 159-168 [PMID: 30473218 DOI: 10.1016/j.bbrc.2018.11.084]

34 **Kaul S**, Blackford JA Jr, Chen J, Ogryzko VV, Simons SS Jr. Properties of the glucocorticoid modulatory element binding proteins GMEB-1 and -2: potential new modifiers of glucocorticoid receptor transactivation and members of the family of KDWK proteins. *Mol Endocrinol* 2000; **14**: 1010-1027 [PMID: 10894151 DOI: 10.1210/mend.14.7.0494]

35 **Oshima H**, Szapary D, Simons SS Jr. The factor binding to the glucocorticoid modulatory element of the tyrosine aminotransferase gene is a novel and ubiquitous heteromeric complex. *J Biol Chem* 1995; **270**: 21893-21901 [PMID: 7665613 DOI: 10.1074/jbc.270.37.21893]

36 **Pan Y**, Tong JHM, Lung RWM, Kang W, Kwan JSH, Chak WP, Tin KY, Chung LY, Wu F, Ng SSM, Mak TWC, Yu J, Lo KW, Chan AWH, To KF. RASAL2 promotes tumor progression through LATS2/YAP1 axis of hippo signaling pathway in colorectal cancer. *Mol Cancer* 2018; **17**: 102 [PMID: 30037330 DOI: 10.1186/s12943-018-0853-6]

37 **Deng J**, Lei W, Xiang X, Zhang L, Yu F, Chen J, Feng M, Xiong J. MicroRNA-506 inhibits gastric cancer proliferation and invasion by directly targeting Yap1. *Tumour Biol* 2015; **36**: 6823-6831 [PMID: 25846731 DOI: 10.1007/s13277-015-3364-8]

38 **Yu SJ**, Hu JY, Kuang XY, Luo JM, Hou YF, Di GH, Wu J, Shen ZZ, Song HY, Shao ZM. MicroRNA-200a promotes anoikis resistance and metastasis by targeting YAP1 in human breast cancer. *Clin Cancer Res* 2013; **19**: 1389-1399 [PMID: 23340296 DOI: 10.1158/1078-0432.CCR-12-1959]

39 **Zhu X**, Bu F, Tan T, Luo Q, Zhu J, Lin K, Huang J, Luo C, Zhu Z. Long noncoding RNA RP11-757G1.5 sponges miR-139-5p and upregulates YAP1 thereby promoting the proliferation and liver, spleen metastasis of colorectal cancer. *J Exp Clin Cancer Res* 2020; **39**: 207 [PMID: 33023613 DOI: 10.1186/s13046-020-01717-5]

40 **Miao W**, Li N, Gu B, Yi G, Su Z, Cheng H. MiR-27b-3p suppresses glioma development *via* targeting YAP1. *Biochem Cell Biol* 2020; **98**: 466-473 [PMID: 32567955 DOI: 10.1139/bcb-2019-0300]

41 **Zhang P**, Liu L, Zhang L, He X, Xu X, Lu Y, Li F. Runx2 is required for activity of CD44(+)/CD24(-/Low) breast cancer stem cell in breast cancer development. *Am J Transl Res* 2020; **12**: 2305-2318 [PMID: 32509221]

42 **Wu S**, Wang H, Li Y, Xie Y, Huang C, Zhao H, Miyagishi M, Kasim V. Transcription Factor YY1 Promotes Cell Proliferation by Directly Activating the Pentose Phosphate Pathway. *Cancer Res* 2018; **78**: 4549-4562 [PMID: 29921695 DOI: 10.1158/0008-5472.CAN-17-4047]

43 **Xu M**, Gu M, Zhou J, Da J, Wang Z. Interaction of YAP1 and mTOR promotes bladder cancer progression. *Int J Oncol* 2020; **56**: 232-242 [PMID: 31789387 DOI: 10.3892/ijo.2019.4922]

44 **Guo L**, Chen Y, Luo J, Zheng J, Shao G. YAP1 overexpression is associated with poor prognosis of breast cancer patients and induces breast cancer cell growth by inhibiting PTEN. *FEBS Open Bio* 2019; **9**: 437-445 [PMID: 30868052 DOI: 10.1002/2211-5463.12597]

45 **Guo L**, Zheng J, Luo J, Zhang Z, Shao G. Targeting Yes1 Associated Transcriptional Regulator Inhibits Hepatocellular Carcinoma Progression and Improves Sensitivity to Sorafenib: An *in vitro* and *in vivo* Study. *Onco Targets Ther* 2020; **13**: 11071-11087 [PMID: 33149619 DOI: 10.2147/OTT.S249412]

46 **Roßner F**, Sinn BV, Horst D. Pathology of Combined Hepatocellular Carcinoma-Cholangiocarcinoma: An Update. *Cancers (Basel)* 2023; **15** [PMID: 36672443 DOI: 10.3390/cancers15020494]

47 **Liu B**, Nie J, Liang H, Liang Z, Huang J, Yu W, Wen S. Pharmacological inhibition of SETD7 by PFI-2 attenuates renal fibrosis following folic acid and obstruction injury. *Eur J Pharmacol* 2021; **901**: 174097 [PMID: 33848540 DOI: 10.1016/j.ejphar.2021.174097]

48 **Ueda H**, Neyama H, Sasaki K, Miyama C, Iwamoto R. Lysophosphatidic acid LPA(1) and LPA(3) receptors play roles in the maintenance of late tissue plasminogen activator-induced central poststroke pain in mice. *Neurobiol Pain* 2019; **5**: 100020 [PMID: 31194070 DOI: 10.1016/j.ynpai.2018.07.001]

World Journal of Gastrointestinal Oncology

Submit a Manuscript: https://www.f6publishing.com

World J Gastrointest Oncol 2023 June 15; 15(6): 1005-1018

DOI: 10.4251/wjgo.v15.i6.1005

ISSN 1948-5204 (online)

ORIGINAL ARTICLE

Basic Study

5'tiRNA-Pro-TGG, a novel tRNA halve, promotes oncogenesis in sessile serrated lesions and serrated pathway of colorectal cancer

Xin-Yuan Wang, Yu-Jie Zhou, Hai-Ying Chen, Jin-Nan Chen, Shan-Shan Chen, Hui-Min Chen, Xiao-Bo Li

Specialty type: Oncology

Provenance and peer review: Unsolicited article; Externally peer reviewed.

Peer-review model: Single blind

Peer-review report's scientific quality classification
Grade A (Excellent): A
Grade B (Very good): B
Grade C (Good): 0
Grade D (Fair): 0
Grade E (Poor): 0

P-Reviewer: Elpek GO, Turkey; Zhang Z, China

Received: February 1, 2023
Peer-review started: February 1, 2023
First decision: February 16, 2023
Revised: February 27, 2023
Accepted: April 17, 2023
Article in press: April 17, 2023
Published online: June 15, 2023

Xin-Yuan Wang, Yu-Jie Zhou, Hai-Ying Chen, Jin-Nan Chen, Hui-Min Chen, Xiao-Bo Li, Division of Gastroenterology and Hepatology, Renji Hospital, Shanghai Jiaotong University School of Medicine, Shanghai 200000, China

Shan-Shan Chen, Department of Spleen and Stomach and Rheumatology, Affiliated Traditional Chinese Medicine Hospital of Southwest Medical University, Luzhou 646000, Sichuan Province, China

Corresponding author: Xiao-Bo Li, PhD, Chief Doctor, Chief Physician, Professor, Division of Gastroenterology and Hepatology, Renji Hospital, Shanghai Jiaotong University School of Medicine, No. 145 Middle Shandong Road, Shanghai 200000, China. lxb_1969@163.com

Abstract

BACKGROUND

Transfer RNA (tRNA)-derived small RNAs (tsRNAs) are small fragments that form when tRNAs severe. tRNA halves (tiRNAs), a subcategory of tsRNA, are involved in the oncogenic processes of many tumors. However, their specific role in sessile serrated lesions (SSLs), a precancerous lesion often observed in the colon, has not yet been elucidated.

AIM

To identify SSL-related tiRNAs and their potential role in the development of SSLs and serrated pathway of colorectal cancer (CRC).

METHODS

Small-RNA sequencing was conducted in paired SSLs and their adjacent normal control (NC) tissues. The expression levels of five SSL-related tiRNAs were validated by q-polymerase chain reaction. Cell counting kit-8 and wound healing assays were performed to detect cell proliferation and migration. The target genes and sites of tiRNA-1:33-Pro-TGG-1 (5'tiRNA-Pro-TGG) were predicted by TargetScan and miRanda algorithms. Metabolism-associated and immune-related pathways were analyzed by single-sample gene set enrichment analysis. Functional analyses were performed to establish the roles of 5'tiRNA-Pro-TGG based on the target genes.

RESULTS

In total, we found 52 upregulated tsRNAs and 28 downregulated tsRNAs in SSLs compared to NC. The expression levels of tiRNA-1:33-Gly-CCC-2, tiRNA-1:33-

Pro-TGG-1, and tiRNA-1:34-Thr-TGT-4-M2 5'tiRNAs were higher in SSLs than those in NC, while that of 5'tiRNA-Pro-TGG was associated with the size of SSLs. It was demonstrated that 5'tiRNA-Pro-TGG promoted cell proliferation and migration of RKO cell *in vitro*. Then, heparanase 2 (*HPSE2*) was identified as a potential target gene of 5'tiRNA-Pro-TGG. Its lower expression was associated with a worse prognosis in CRC. Further, lower expression of *HPSE2* was observed in SSLs compared to normal controls or conventional adenomas and in *BRAF*-mutant CRC compared to *BRAF*-wild CRC. Bioinformatics analyses revealed that its low expression was associated with a low interferon γ response and also with many metabolic pathways such as riboflavin, retinol, and cytochrome p450 drug metabolism pathways.

CONCLUSION

tiRNAs may profoundly impact the development of SSLs. 5'tiRNA-Pro-TGG potentially promotes the progression of serrated pathway CRC through metabolic and immune pathways by interacting with *HPSE2* and regulating its expression in SSLs and *BRAF*-mutant CRC. In the future, it may be possible to use tiRNAs as novel biomarkers for early diagnosis of SSLs and as potential therapeutic targets in serrated pathway of CRC.

Key Words: Noncoding RNA; tRNA halves; Sessile serrated lesions; Colon cancer; Serrated pathway

Core Tip: Our study identified the transfer RNA-derived small RNAs expression profile of sessile serrated lesions (SSLs) for the first time and found that tRNA halves (tiRNAs)-1:33-Pro-TGG-1, which was associated with polyp size, were highly expressed in SSLs and promoted oncogenesis in colorectal cancer cell. Furthermore, tiRNA-1:33-Pro-TGG-1 potentially promotes the progression of serrated pathway colorectal cancer (CRC) through metabolic and immune pathways by interacting with HPSE2 in SSLs and *BRAF* mutant CRC. In the future, tiRNA-1:33-Pro-TGG-1 may serve as a potential target for the early diagnosis of SSLs and treatment of CRC that arises from the serrated pathway.

Citation: Wang XY, Zhou YJ, Chen HY, Chen JN, Chen SS, Chen HM, Li XB. 5'tiRNA-Pro-TGG, a novel tRNA halve, promotes oncogenesis in sessile serrated lesions and serrated pathway of colorectal cancer. *World J Gastrointest Oncol* 2023; 15(6): 1005-1018
URL: https://www.wjgnet.com/1948-5204/full/v15/i6/1005.htm
DOI: https://dx.doi.org/10.4251/wjgo.v15.i6.1005

INTRODUCTION

Colorectal cancer (CRC) typically develops from colorectal polyps. there are two main categories: Conventional adenomas (ADs) and serrated lesions (SLs)[1]. SLs, precancerous lesions often observed in the colorectum, are again of four subtypes: (1) Sessile SLs with or without dysplasia (SSLs-D and SSLs, respectively); (2) Traditional serrated adenomas; (3) Hyperplastic polyps; and (4) Unclassified serrated adenomas[2].

The association between common colorectal polyps and the development of CRC has been well-studied. In recent years, a large number of studies have also confirmed the malignant potential of SLs, in particular, that of SSLs[3]. Unlike ADs, which tend to develop into microsatellite-stability or microsatellite-instability–low CRC and carry a mutation in the Kirsten Rat Sarcoma Viral Oncogene Homolog (*KRAS*) gene, SSLs tend to develop into microsatellite-instability–high (MSI-H) CRC and carry a mutation in the v-raf murine sarcoma viral oncogene homolog B (*BRAF*) gene[4,5]. At present, we do not know much about the exact mechanisms through which SSLs develop and how they progress to CRC. In addition, endoscopic detection of SSLs is very difficult because of the flattened morphology, surface coverage with an overlying mucus cap, and greyish hue of the lesion[6]. Several studies have shown that patients with SSLs are at an increased risk of developing both concurrent and heterochronic advanced adenomas[7-9]. As the effective intervention in CRC depends on early detection and diagnosis, there is an urgent need to find effective early diagnostic markers for SSLs, which will help in the prevention and accurate treatment of CRC.

Recent research has revealed the essential role of non-coding RNAs, including long non-coding RNAs, transfer (t) RNAs, and micro (mi) RNAs, in the development and progression of various diseases [10-12]. tRNAs play an important role in the translation of proteins by transporting amino acids to the ribosome[13]. However, under conditions of nutritional, physicochemical, and oxidative stress, cells

selectively reduce protein synthesis to conserve energy. Under these situations, tRNAs may be enzymatically cleaved to form tRNA-derived small RNAs (tsRNAs)[14,15]. tsRNAs can be classified into two categories based on their length and enzymatic cleavage sites: tRNA halves (tiRNAs) and tRNA-related fragments (tRFs). tiRNAs comprise 31–40 nucleotides (nt). They form when mature tRNAs are cleaved in the anticodon loop region comprising 5′tiRNAs and 3′tiRNAs. tRFs are 14–30 nt in length and form from mature or precursor tRNA. tRFs have four isoforms: tRF-1, tRF-2, tRF-3, and tRF-5.

It was reported in the last decade that tsRNAs are involved in the regulation of several physiological processes. For example, 5′tiRNA-GLY can promote the proliferative and invasive capabilities of papillary thyroid cancer cells by binding to RBM17[16]. Other studies have shown that tRF-Val can attach directly to binding protein EEF1A1 to promote proliferation and inhibit apoptosis of gastric cancer cells[17]. It was also reported that tRF-Gly promotes migration of hepatocellular carcinoma cells by binding to NDFIP2 in liver cancer[18]. Thus, although the role of tsRNAs in diseases remains an interesting research topic, dysregulation of their expression may present possible biomarkers for many diseases, such as CRC and breast cancer[19-21]. However, the expression and function of tsRNAs and small tRNA-derived fragments in colorectal polyps, particularly those of SSLs, have not yet been explored.

This study aims to identify the expression profiles of tsRNAs in SSLs and paired normal control (NC) tissues using small-RNA sequencing and their potential role in the development of SSLs and serrated pathway of CRC.

MATERIALS AND METHODS

Clinical samples

Twenty paired SSL tissues and adjacent normal tissues belonging to the same patient were collected from Renji Hospital, School of Medicine, Shanghai JiaoTong University (China). The inclusion criteria were as follows: Age, ≥ 18 years; adequate bowel preparation and cecum reach; and received a colonoscopy with an assured diagnosis of SSL by experienced endoscopists. Two pathologists confirmed the diagnosis using biopsy specimens according to the 2019 World Health Organization 5th classification. Our study was approved by the Ethics Committee of Renji Hospital No. KY2021-004.

Data collection

RNA sequencing (RNA-Seq) data of SSLs, ADs, and the corresponding control tissue were obtained from GSE76987 from the Gene Expression Omnibus database (https://www.ncbi.nlm.nih.gov/gds/). The gene expression data of colorectal adenocarcinoma were downloaded from The Cancer Genome Atlas Program (TCGA, https://portal.gdc.cancer.gov/) and cBioPortal for Cancer Genomics (https://www.cbioportal.org/).

RNA extraction

Total RNA was extracted from fresh tissues stored in RNA using TRIzol (Invitrogen, CA, United States). The purity and concentration of the total RNA samples were determined with NanoDrop ND-1000 (Thermo Fisher Scientific, DE, United States).

Sequence processing of tRFs and tiRNAs

RNA samples were extracted from four paired SSL tissues and adjacent normal tissues. The purity and concentration of the total RNA samples were determined before conducting small-RNA sequencing, as mentioned before. Next, a commercial RNA pretreatment kit (rtStar™ tRF and tiRNA Pretreatment Kit, AS-FS-005, Arraystar Inc., MD, United States) for tRF and tiRNA-seq library preparation was used, which was then used to remove some RNA modifications that interfered with small RNA-seq library construction, including 3′-aminoacyl (charged) deacylation to 3′-OH for 3′adaptor ligation, 3′-cP (2′,3′-cyclic phosphate) removal to 3′-OH for 3′adaptor ligation, 5′-OH (hydroxyl group) phosphorylation to 5′-P for 5′-adaptor ligation, m1A and m^{3}C demethylation for reverse transcription, cDNA synthesis, and library polymerase chain reaction (PCR) amplification. The prepared RNA of each sample was ligated to 3′ and 5′ small-RNA adapters. Then, cDNA was synthesized and amplified using proprietary reverse transcription primers and amplification primers (Illumina). Subsequently, approximately 134–160 bp PCR-amplified fragments were extracted and purified using the PAGE gel. The concentration and quality of the libraries were assessed *via* absorbance spectrometry on Agilent BioAnalyzer 2100 (Agilent Technologies Inc., CA, United States). The libraries were denatured and diluted to a loading volume of 1.3 mL and a loading concentration of 1.8 pM. Then, they were loaded onto a reagent cartridge and forwarded to sequencing run on the Illumina NextSeq 500 system using NextSeq 500/550 V2 kit (FC-404- 2005, Illumina), according to the manufacturer's instructions. Raw sequencing read data that passed the Illumina chastity filter were used for subsequent analysis. Trimmed reads (with 5′,3′-adaptor bases removed) were aligned to mature-tRNA and pre-tRNA reference sequences. Statistical analysis of the alignment results was applied to retain the valid sequences for subsequent tRF and tiRNA expression

profiling analysis.

Sequencing data analysis

Sequencing quality was examined using the FastQC software (v0.11.7) and trimmed reads were aligned allowing for only one mismatch to mature-tRNA sequences. The reads that do not map are aligned allowing for only one mismatch to precursor tRNA sequences using the Bowtie software (v1.2.2, http://bowtie-bio.sourceforge.net/index.shtml). The abundance of tRF and tiRNA was evaluated using their sequencing counts and is normalized as counts per million of the total aligned reads. The differentially expressed tRFs and tiRNAs were screened based on the count value with R package edgeR. The R packages (R 4.1.2), including FactoMineR, factoextra, ggvenn, pheatmap, and ggplot2, were used for principal component analysis (PCA), Venn plots, Hierarchical clustering heatmap analysis, and Volcano plots.

Quantitative real-time reverse-transcription PCR

Total RNA collected from 16 paired SSLs and adjacent normal tissues was extracted using TRIzol (Invitrogen, CA, United States), as stated previously. tiRNAs were reverse-transcribed into cDNA using a Bulge-Loop miRNA qRT-PCR Starter Kit (Ribobio, Guangzhou, China). Subsequently, qPCR was performed with SYBR Premix Ex Taq (Takara), as instructed by the manufacturer. The expression levels of tiRNAs were normalized to that of U6. The primers of qPCR were as follows: *HPSE2*-F: 5′-ATGGCCGGGCAGTAAATGG-3′; *HPSE2*-R: 5′-GCTGGCTCTGGAATAAATCCG -3′; *ACTB*-F: 5′-CACCATTGGCAATGAGCGGTTC-3′, and *ACTB*-R: 5′-AGGTCTTTGCGGATGTCCACGT-3′. Other primers involved in reverse transcription and qPCR were purchased from RiboBio (China).

Cell culture

The RKO cell line was purchased from the Typical Culture Preservation Commission Cell Bank, Chinese Academy of Sciences (Shanghai, China). The cell was cultured in the RPMI 1640 medium with 10% fetal bovine serum (Gibco, United States) at 37 °C with 5% CO_2.

Cell transfection

The RKO cell was seeded in plates (Corning Life Sciences, United States) the day before transfection. The 5′tiRNA-Pro-TGG mimic and inhibitor (50 nM), both modified with 2′-O-methyl, were purchased from GenePharma Technology (Shanghai, China) and transfected using DharmaFECT 1 siRNA transfection reagent (Thermo Fisher Scientific Dharmacon Inc., United States). The corresponding scramble sequences were used as negative controls. The RNA oligonucleotide sequences were as follows: 5′tiRNA-Pro-TGG mimic: 5′-GGCUCGUUGGUCUAGUGGUAUGAUUCUCGCUUU-3′; 5′tiRNA-Pro-TGG inhibitor: 5′-AAAGCGAGAAUCAUACCACUAGACCAACGAGCC-3′; mimic scramble control: 5′-ACGUUUGACCUGUGUCGAGUUUUCUGUUUGGCG-3′; and inhibitor scramble control: 5′-GGGAAAGCGAAUAAAUCCAAACACCCAAUCCGC-3′.

Cell counting kit-8 (CCK-8) assay

Cell proliferation was measured by CCK-8 (Dojindo, Japan). The RKO cell was seeded in 96-well plates at a density of 2 × 10^3 cells per well. After transfection for 48 h, 10 μL of CCK-8 solution and 100 μL of the RPMI 1640 medium per well were added to the wells after discarding the previous medium; the OD values (450 nm) were measured after 2 h. All assays were conducted three times.

Wound-healing assay

The cells were inoculated in a 6-well plate. When 90% confluence was reached, a sterile 200-μL pipette tip was used to create vertical wounds. Finally, the wells were photographed under a microscope (Olympus, Japan) at × 200 magnification. The pictures were analyzed by ImageJ. All assays were conducted three times.

Single-sample gene set enrichment analysis (ssGSEA)

The ssGSEA analysis was used to investigate the expression levels of immune- and metabolism-related pathways by GSVA R package. Next, 41 metabolism pathway gene sets and 29 immune pathway gene sets were obtained from Molecular Signatures Database (MSigDB; https://www.gsea-msigdb.org/).

Gene ontology (GO) and Kyoto encyclopedia of genes and genome (KEGG) enrichment analyses of target genes

To investigate the potential biological function of dysregulated tiRNAs in SSLs, the target gene predictions were conducted by TargetScan (http://www.targetscan.org/vert72/) and Miranda (http://www.microrna.org/microrna/) with a context score < -0.1. KEGG pathway and GO analyses to the target gene sets were performed by using the clusterProfiler R package.

Statistical analysis

Mean and standard deviations (mean ± SD) were used to analyze all quantitative variables. Two-tailed Student's *t*-tests and Wilcoxon rank test were performed. A P value < 0.05 was considered statistically significant. Spearman correlation analysis was used to determine the relationship between 5′tiRNAs and polyp size. Pearson correlation analysis was used to determine the relationship between tiRNA-1:33-Pro-TGG-1 and *HPSE2*. Kaplan–Meier survival analysis was performed to evaluate the association between the *HPSE2*-expression level and the overall survival of CRC patients. All analyses were performed by GraphPad Prism 9.3.1 (GraphPad Software, United States).

RESULTS

Expression profiles of tRFs and tiRNAs in paired SSL and NC groups

To identify the expression profiles of tRFs and tiRNAs in patients with SSLs, four pairs of SSLs and the corresponding NC tissues from different patients were collected for small-RNA sequencing analysis. Variations in all tRFs and tiRNAs expressed in SSL and NC groups are shown using a heatmap (Figure 1A). The expression levels of tRFs and tiRNAs in SSLs were different from those in NC groups, as determined by PCA (Figure 1B). We used a Venn diagram to show the tRFs and tiRNAs that were both generally and specifically expressed between the SSL and NC groups (Figure 1C). As seen in Figure 1C, 54 types of tRFs and tiRNAs were exclusively found in SSLs, while 123 types were found only in NCs. Differences in tRFs and tiRNAs found in SSLs and NCs were determined under the following conditions: absolute log2 (fold change) ≥ 1.5 and P < 0.05. Under these conditions, we identified 52 upregulated and 28 downregulated tRFs and tiRNAs and have shown them in a hierarchical cluster heatmap (Figure 1D).

Distribution of tRF and tiRNA subtypes in SSL and NC groups

The expression of tRF-1 and 5′tiRNA increased, while that of tRF-5c and tRF-3b decreased in SSLs compared with that of NCs (Figure 2A and B). tRNAs with the same anticodon translate the same amino acid. Hence, we herein separately determined the number of different tRFs and tiRNAs with the same anticodon (Figure 2C and D).

Validation for discrepant expression levels of 5′tiRNAs

5′tiRNAs play an important role in the development of many diseases, including CRC. Because our analysis showed a significant increase in tiRNA-5 in SSLs compared to that in NCs, we further verified the expression of 5′tiRNA in SSLs. Our previous screening criteria showed that six 5′tiRNAs (five upregulated and one downregulated) with different expression levels emerged between SSLs and NCs. tiRNA-1:33-Gly-CCC-2, tiRNA-1:33-Pro-TGG-1, tiRNA-1:34-Thr-TGT-4-M2, tiRNA-1:34-Lys-CTT-1-M2, and tiRNA-1:32-chrM.Val-TAC were upregulated in SSLs with 43.99-, 25.50-, 24.00-, 12.61-, and 8.73-fold change, respectively (P < 0.05), while tiRNA-1:33-Gly-CCC-3 was downregulated with a 36.95-fold change in SSLs compared to that in NCs (P < 0.05, Figure 3A and B).

Since we previously reported increased levels of 5′tiRNA expression in SSLs (Figure 2A and B), we herein focus on the abovementioned five upregulated 5′tiRNAs in SSLs. To further validate our sequencing data, we collected 16 pairs of SSLs and the corresponding NCs to confirm the expressions of the five upregulated 5′tiRNAs using RT-PCR (Figure 3C-G). The size of all collected lesions ranged from 4 to 15 mm, with an average of 6.31 ± 3.07 mm. tiRNA-1:33-Gly-CCC-2, tiRNA-1:33-Pro-TGG-1, and tiRNA-1:34-Thr-TGT-4-M2 were significantly upregulated in SSLs compared to those in the paired NC (P = 0.0059, 0.0309, and 0.0008, respectively). The expression of tiRNA-1:34-Lys-CTT-1-M2 and tiRNA-1:32-chrM.Val-TAC did not show any statistically significant differences between SSLs and NCs (P = 0.0641 and 0.9838, respectively).

Association of tiRNA-1:33-Pro-TGG-1 with lesion size and promotion of oncogenesis in CRC cells

We further analyzed the correlation between the lesion size and the expression levels of the three 5′tiRNAs that had been validated as significantly highly expressed in SSLs. It was tiRNA-1:33-Pro-TGG-1 (Figure 4A and B), not tiRNA-1:33-Gly-CCC-2 or tiRNA-1:34-Thr-TGT-4-M2 (Figure 4C and D), that positively correlated with lesion size. Therefore, we focused on tiRNA-1:33-Pro-TGG-1, also known as 5′tiRNA-Pro-TGG. It comprises 33 nucleotides and is a type of 5′tiRNA that originated in tRNA-Pro-TGG-1 (Figure 4E). The inhibition of 5′tiRNA-Pro-TGG reduces the proliferation (Figure 4F) and migratory capacity of cancer cells in RKO, a colon cancer cell line carrying the *BRAF* V600E mutation, while its overexpression enhanced the migratory capacity of the cancer cells (Figure 4G and H).

Involvement of potential target gene HPSE2 in the serrated pathway

To further investigate the potential functions of upregulated 5′tiRNAs in the progression of SSLs, we identified potential target genes that might bind to 5′tiRNA-Pro-TGG using TargetScan and miRanda algorithms and could predict 502 target genes. When context plus score < -0.5 and structure score > 300,

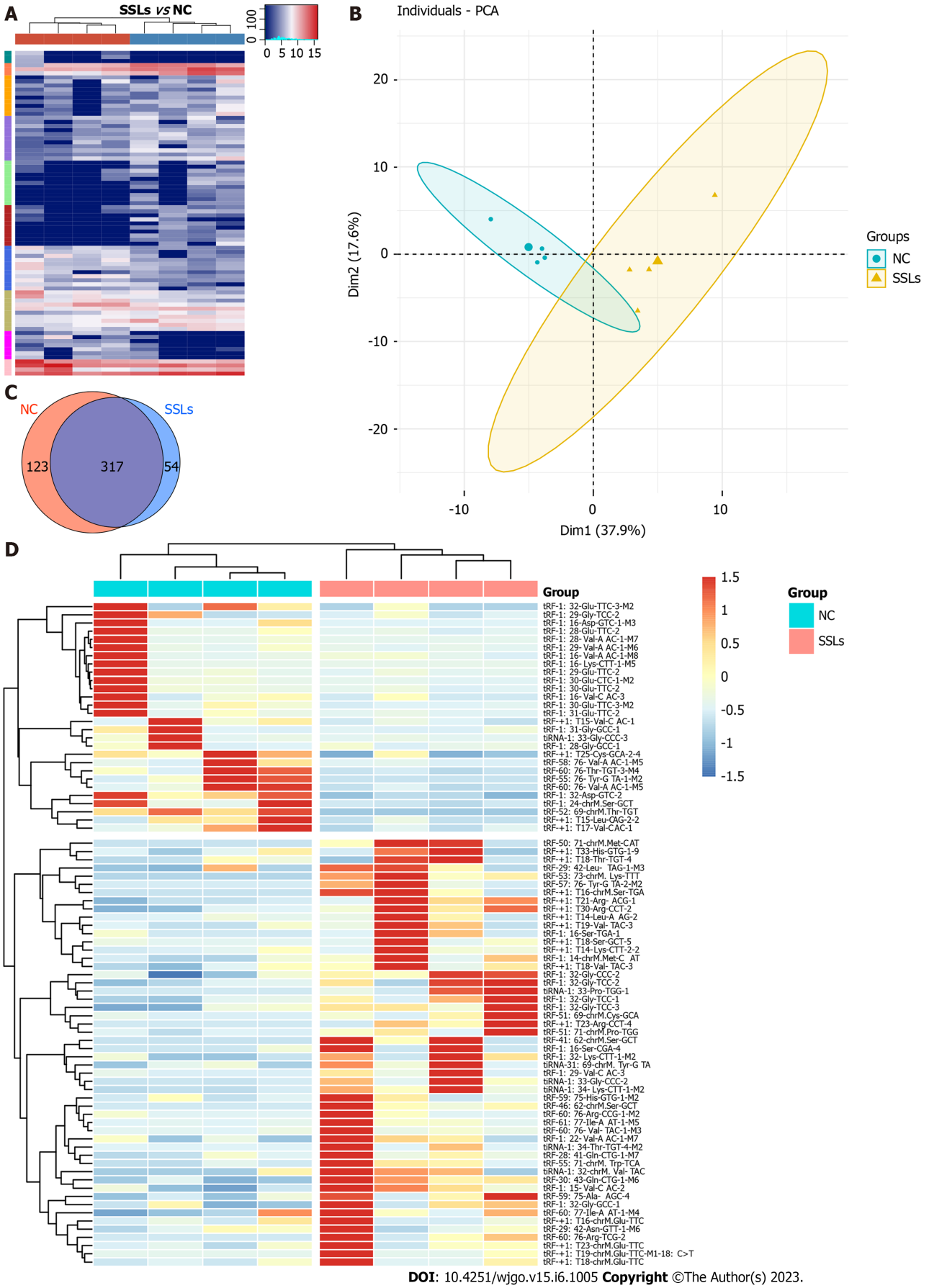

DOI: 10.4251/wjgo.v15.i6.1005

Figure 1 Expression profiles of transfer RNA-related fragments and transfer RNA halves in paired sessile serrated lesions and normal control groups. A: Hierarchical clustering analysis of transfer RNA (tRNA)-related fragment (tRF)- and tRNA halves (tiRNAs)-expression data obtained from paired

sessile serrated lesions (SSLs) and normal control (NC) groups. Cluster analysis arranged samples into groups based on the counts per million. All samples were categorized in 10 clusters using K-means clustering. B: Principal component analysis showed a distinguishable tRF- and tiRNA-expression profile among SSLs and NC. C: Venn diagram based on the number of basically expressed and specifically expressed tRFs and tiRNAs. D: Heatmap revealed results of dysregulated tRFs and tiRNAs obtained using hierarchical clustering analysis. SSLs: Sessile serrated lesions; NC: Normal control; PCA: Principal component analysis.

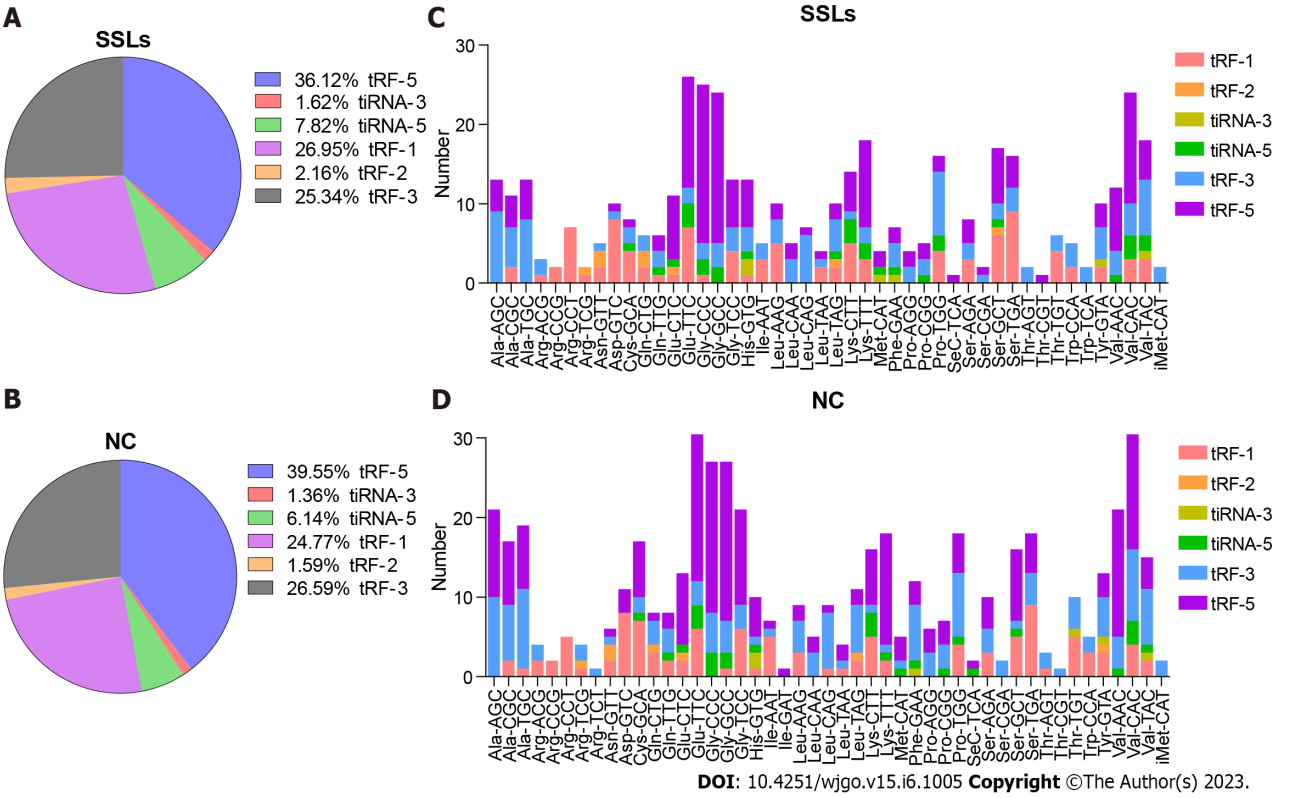

DOI: 10.4251/wjgo.v15.i6.1005 **Copyright** ©The Author(s) 2023.

Figure 2 Distribution of transfer RNA-related fragment and transfer RNA halves subtypes in sessile serrated lesions and normal control groups. A and B: Pie charts for all kinds of subtype of transfer RNA-related fragment (tRFs) and transfer RNA halves (tiRNAs) in the two separated groups. The values in the pie chart are ratios of each subtype of tRFs and tiRNAs in sessile serrated lesions (SSLs) and normal control (NC), respectively. C and D: Stacked plot for all subtypes of tRFs and tiRNAs of each group clustered based on the anticodons of tRNAs. The X-axis represents tRNAs with the same anticodon and the Y-axis shows the number of all subtype tRFs and tiRNAs derived from the same anticodon tRNA. The color bar represents the number of each subtype tRFs and tiRNAs. SSLs: Sessile serrated lesions; NC: Normal control; tRF: Transfer RNA-related fragment; tiRNA: Transfer RNA halves.

the filtering parameters of the TargetScan and miRanda algorithms were predicted to be 33 and 10 target genes, respectively, with the intersection at *HPSE2* (Figure 5A). Two possible binding sites were predicted within the 3′UTR of *HPSE2* for the seed regions of 5′tiRNA-Pro-TGG (Figure 5B). *HPSE2* encodes heparinase II. A mutation in *HPSE2* is responsible for the urofacial syndrome and has been progressively identified as a tumor suppressor. We examined the expression levels of 5′tiRNA-Pro-TGG and *HPSE2* and found a significant negative correlation between their expression levels (Figure 5C). We also found that the expression level of *HPSE2* in SSLs was significantly lower than that in the uninvolved right colon, control right colon tissue, and common adenoma ($P < 0.05$; Figure 5D). The qPCR results also confirmed that the expression level of *HPSE2* in SSLs was lower than that in NC ($P < 0.05$; Figure 5E). Not coincidentally, the *HPSE2* expression level was lower in CRC lesions carrying *BRAF* mutations than those with *BRAF* wild-type CRC (Figure 5F). An analysis of survival outcomes in CRC patients demonstrated that the lower level of *HPSE2* was associated with poorer prognosis (Figure 5G).

HPSE2-associated immune and metabolic profiles in CRC

To explore the function of *HPSE2* in the development of serrated pathway of CRC, we grouped CRC patients into *HPSE2* high (*HPSE2*-high) and low (*HPSE2*-low) expression groups. We then scored both groups for the immune cell type (Figure 6A), immune cell function (Figure 6B), and metabolic pathways (Figure 6C) using the ssGSEA algorithm. In the *HPSE2*-low group, a part of the immune cell scores were lower, including that for tumor infiltration lymphocyte (TIL), dendritic cells, T helper cells, B cells, and mast cells. The scores for response to interferon γ (IFNγ) and T-cell co-stimulation were lower in the *HPSE2*-low group than they were in the *HPSE2*-high group. Notably, many metabolic pathways scored lower in the *HPSE2*-low-expression group, implying the downregulation of these pathways, including

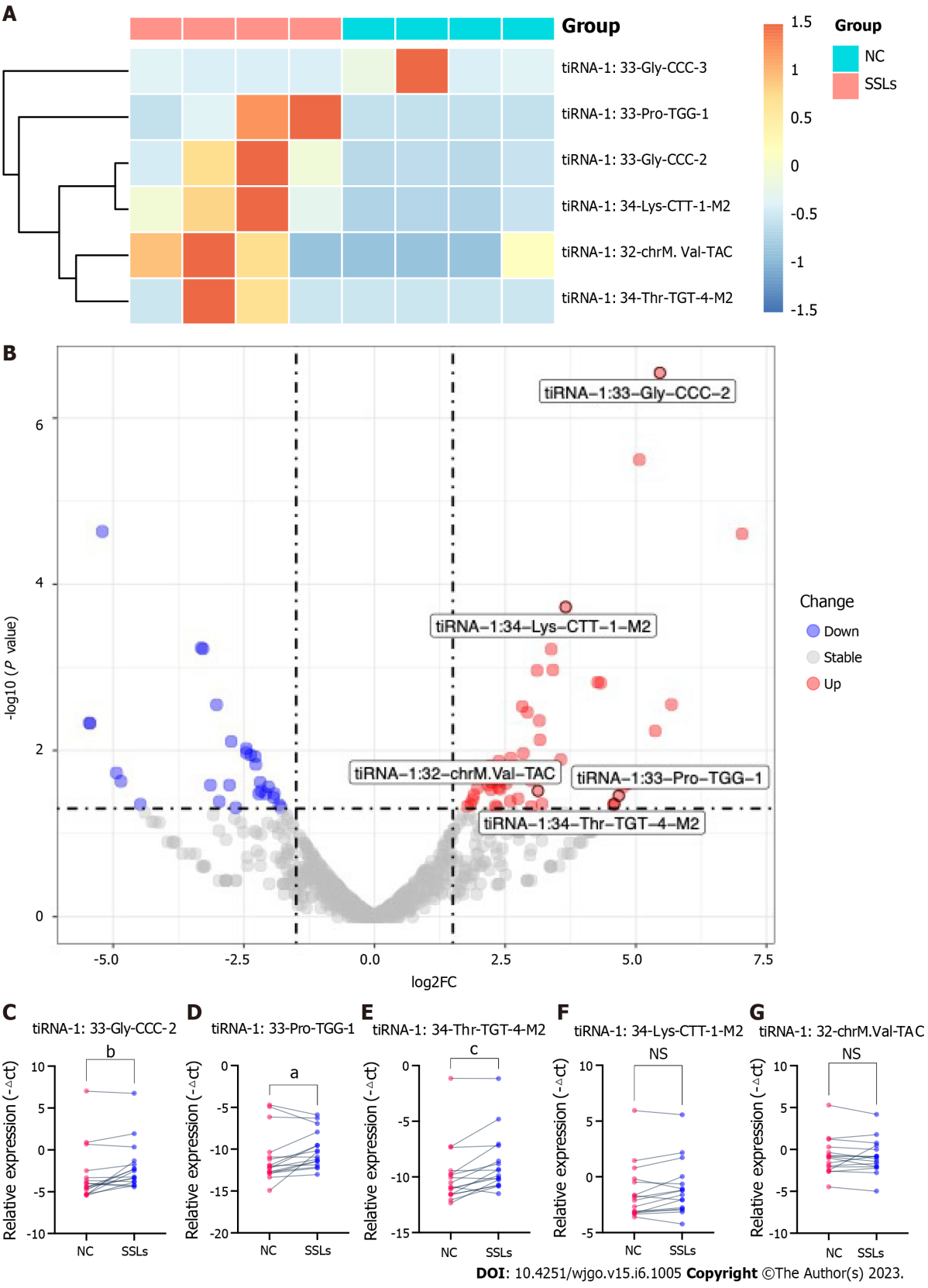

DOI: 10.4251/wjgo.v15.i6.1005

Figure 3 Validation for the discrepant expression levels of 5'transfer RNA halves. A: Heatmap of the expression levels of six differently expressed 5'transfer RNA halves (tiRNAs) in sessile serrated lesions (SSLs) *vs* normal control (NC). B: Volcano chart of transfer RNA-related fragments (tRFs) and tiRNAs. Red/blue circles indicate statistically significant differentially expressed tRFs and tiRNAs with the absolute log2 (fold change) of no < 1.5 and a *P* value ≤ 0.05 (red: Upregulated; blue: Downregulated). Gray circles indicate nondifferentially expressed tRFs and tiRNAs, with fold changes and/or *P* values not meeting the cutoff thresholds. C-G: qRT-polymerase chain reaction for the validation of five upregulated 5'tiRNAs in 16 paired SSLs and NC tissues. All data were analyzed using paired Student's *t*-test. The asterisk indicates a significant difference between the two groups ($^{a}P < 0.05$, $^{b}P < 0.01$, $^{c}P < 0.001$). NS: Not significant; SSLs: Sessile serrated lesions; NC: Normal control; tRF: Transfer RNA-related fragment; tiRNA: Transfer RNA halves.

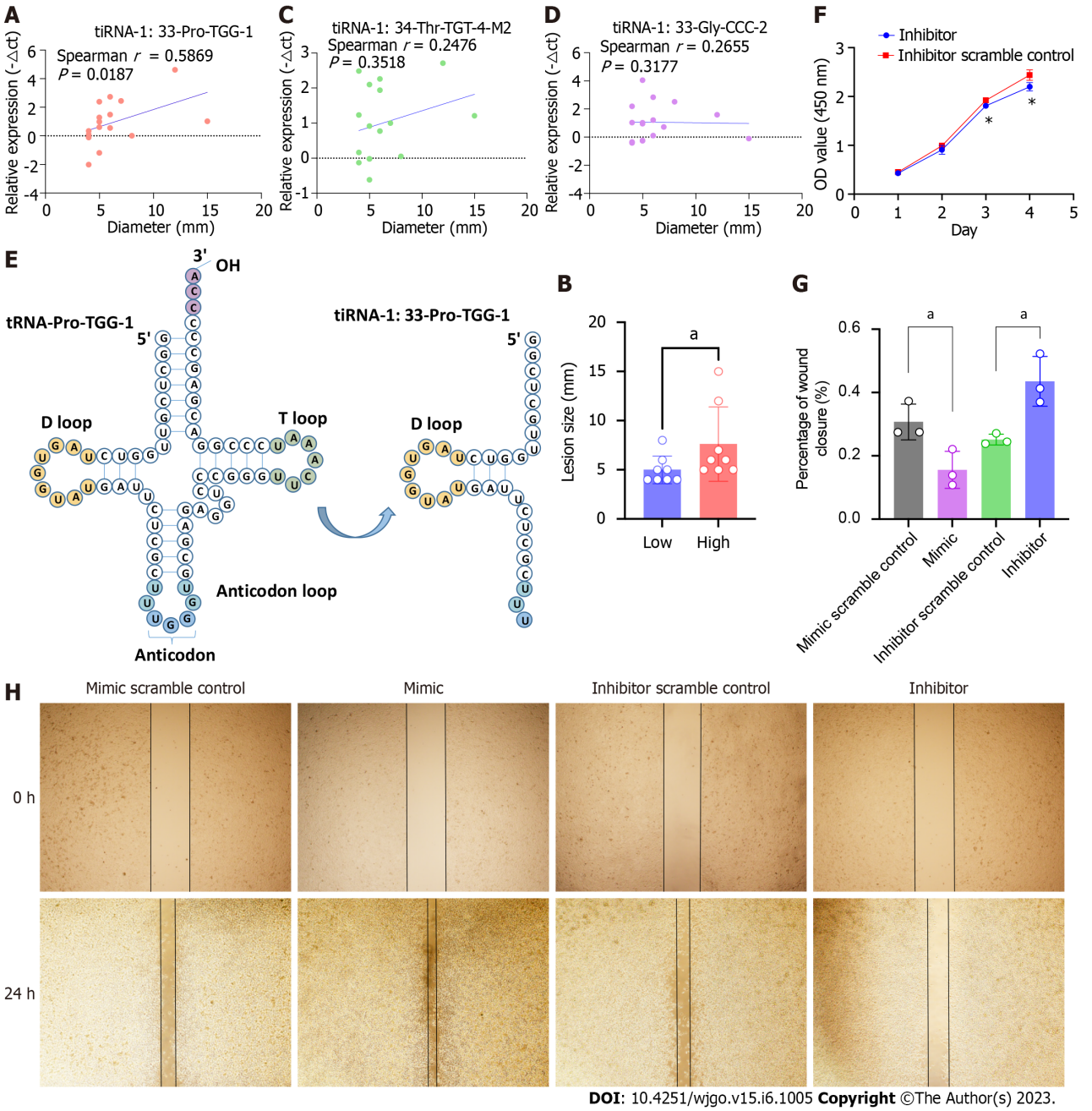

DOI: 10.4251/wjgo.v15.i6.1005 **Copyright** ©The Author(s) 2023.

Figure 4 Transfer RNA halves-1:33-Pro-TGG-1 is associated with lesion size and promotes oncogenesis in colorectal cancer cells. A: Correlation analysis of the lesion sizes and expressions of transfer RNA halves (tiRNA)-1:33-Pro-TGG-1 of SSLs. The X-axis represents the diameter of the lesion and the Y-axis represents the expression level of tiRNA-1:33-Pro-TGG-1. B: Lesions in the tiRNA-1:33-Pro-TGG-1 high-expression group are larger than that of the low-expression group. Lesions are divided into high- and low-expression groups based on the median tiRNA-1:33-Pro-TGG-1 expression levels. The lesion sizes are compared between the two groups. C and D: Correlation analysis of lesion sizes and the expressions of tiRNA-1:34-Thr-TGT-4-M2 and tiRNA-1:33-Gly-CCC-2 of SSLs. E: 5'tiRNA-Pro-TGG is a type of 5'tiRNA that originated in tRNA-Pro-TGG-1. F: 5'tiRNA-Pro-TGG knockdown suppressed the proliferation of RKO cells compared to that of the scramble control as determined by CCK-8 assays. G and H: Wound-healing assays demonstrated that the overexpression of 5'tiRNA-Pro-TGG promotes cell migration and knockdown of 5'tiRNA-Pro-TGG inhibits cell migration when compared to those of the corresponding scramble control, respectively. The asterisk indicates a significant difference between the two groups ($^aP < 0.05$). SSLs: Sessile serrated lesions; tiRNA: Transfer RNA halves.

that of riboflavin, retinol, and cytochrome P450 drug metabolism pathways. However, the metabolism of glyoxylate, dicarboxylate, and pyrimidine upregulated in the *HPSE2*-low group.

We next performed KEGG and GO enrichment analyses using the potential target genes of 5'tiRNA-Pro-TGG. KEGG enrichment analysis revealed that these target genes could be involved in pathways such as the biosynthesis of cofactors, antifolate resistance, and choline metabolism in cancer (Figure 6D). GO enrichment analysis demonstrated the possible target genes involved in cell-to-cell adhesion and regulation of the secretory pathway and exocytosis (Figure 6E).

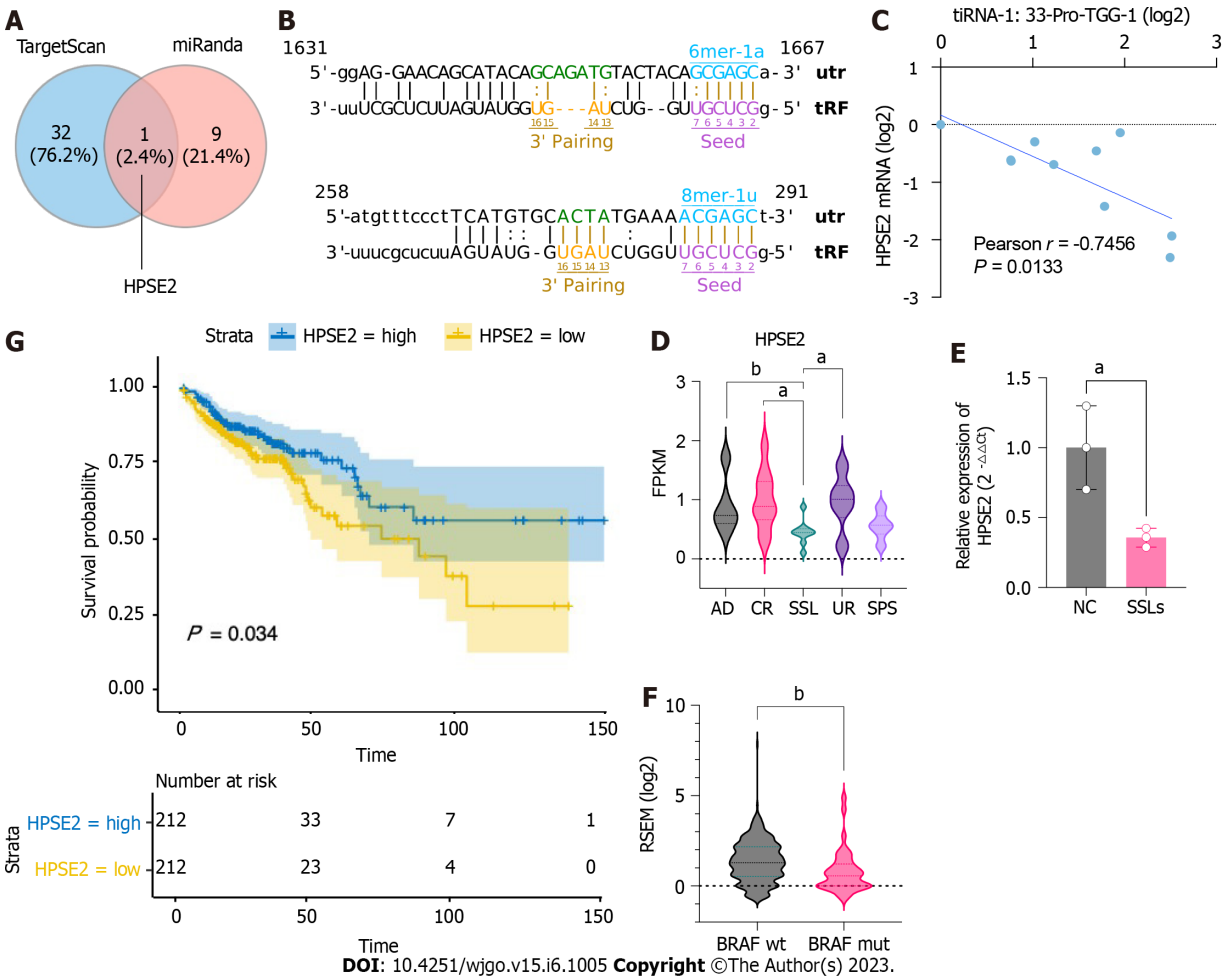

DOI: 10.4251/wjgo.v15.i6.1005

Figure 5 Potential target gene *HPSE2* is involved in the serrated pathway. A: Schematic Venn diagram of transfer RNA halves (5'tiRNA)-Pro-TGG target gene prediction. B: Predicted interaction position between 5'tiRNA-Pro-TGG and 3'UTR of *HPSE2*. C: Correlation analysis of the expression of 5'tiRNA-Pro-TGG and *HPSE2* (n = 10). D: Expression level of *HPSE2* in common adenoma, right control colon tissue, sessile serrated lesion (SSL), right uninvolved colon, and serrated polyp syndrome in GSE76987. E: Expression level of *HPSE2* in SSLs and normal control (n = 3). F: *HPSE2* expression in *BRAF*-mut colorectal cancer (CRC) was lower in *BRAF*-wild CRC. G: Kaplan–Meier survival curves for the overall survival (OS) of CRC patients in HPSE2-high and HPSE2-low groups. The OS of patients with HPSE2-low was worse compared to that of patients with HPSE2-high. [a]P < 0.05, [b]P < 0.01. AD: Common adenoma; CR: Right control colon tissue; SSL: Sessile serrated lesion; UR: Right uninvolved colon; SPS: Serrated polyp syndrome; OS: Overall survival; CRC: Colorectal cancer; NC: Normal control; tRF: Transfer RNA-related fragment; tiRNA: Transfer RNA halves.

DISCUSSION

Formation of SSLs and the process by which they progress to CRC is known as the serrated neoplastic pathway. However, the mechanisms and processes involved in this pathway are still not fully understood. SSLs that progress to CRC have a prevalence of 10%–15% in the general population. The main pathology of this type of cancer involves a structurally distorted serrated crypt, with a *BRAF* mutation (*BRAF*mut), MSI-H, and CpG island methylator phenotype-high[22]. SSLs presenting with *BRAF*mut often develop into CRC with a worse prognosis[23]. Therefore, early diagnosis of SSLs can help in reducing the incidence of *BRAF*mut CRC. In addition, understanding the pathogenesis of SSLs can help identify new targets for intervention in the early and precise treatment of *BRAF*mut CRC.

Studies conducted in the last decade reported that tsRNAs can play an important role as a biomarker in colon cancer[24], and that 5′-tiRNA-Pro-TGG levels can be used as an independent prognostic marker in CRC for predicting its recurrence[20]. Another study showed that in CRC, higher levels of tRF-phe-GAA-031 and tRF-VAL-TCA-002 expression were associated with reduced survival. Hence, they could also be used as prognostic predictors of CRC[19]. Therefore, the present study investigated the expression levels of tsRNAs, specifically that of 5′tiRNAs, in SSLs and their potential biological roles. We sequenced small RNAs from SSLs and their corresponding NCs, and found that among the 80 dysregulated tsRNAs, 5′tiRNAs, 3′tiRNAs, and tRFs-1 were more highly expressed in the SSLs, which suggests that tiRNAs may play an important role in these lesions.

Further analysis confirmed tiRNA-1:33-Gly-CCC-2, tiRNA-1:33-Pro-TGG-1, and tiRNA-1:34-Thr-TGT-4-M2 to be significantly upregulated in SSLs with a 2.92-, 3.69-, and 2.37-fold change, respectively. The expression level of 5′tiRNA-Pro-TGG was positively correlated with the size of SSLs. In addition,

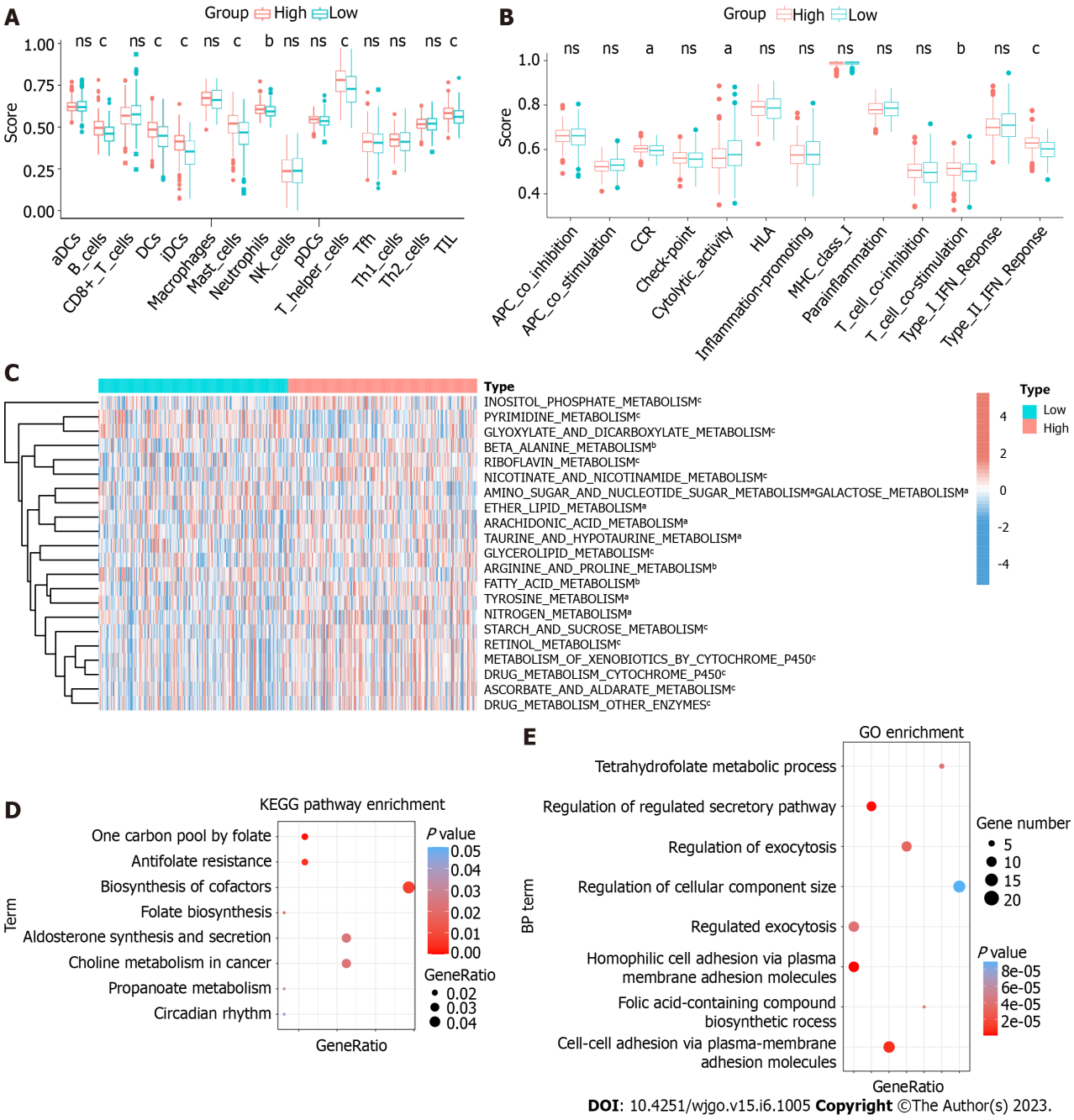

DOI: 10.4251/wjgo.v15.i6.1005

Figure 6 *HPSE2*-associated immune and metabolic profiles in colorectal cancer. A and B: Scores of immune cells and immune functions by ssGSEA in the colorectal cancer (CRC) patients of *HPSE2*-low and *HPSE2*-high groups. C: Unsupervised clustering of metabolic pathways in CRC patients of *HPSE2*-low and *HPSE2*-high groups by ssGSEA. D: Kyoto Encyclopedia of Genes and Genome pathway analysis and gene ontology enrichment analysis; E: For 5'transfer RNA halves-Pro-TGG predicted genes. The vertical axis shows the annotated functions of the predicted genes. The horizontal axis shows the ratio of different genes in the specific pathway/progress and *P* value (showed by colors) of each cluster, respectively. $^{a}P < 0.05$, $^{b}P < 0.01$, $^{c}P < 0.001$. ns: Not significant; CRC: Colorectal cancer; KEGG: Kyoto Encyclopedia of Genes and Genome; BP: Biological process; GO: Gene ontology; HLA: Human leukocyte antigen; IFN: Interferon.

5′tiRNA-Pro-TGG promoted carcinogenic processes in the colon cancer cell. We further screened *HPSE2* as the potential target gene. Interestingly, we found that *HPSE2* appeared to be specifically hypo-expressed in SSLs, as well as in *BRAF*-mutant CRC, and its low expression predicted lower survival. 5′tiRNA-Pro-TGG is associated with poor prognosis in CRC[20]. *HPSE2*, a novel tumor-suppressor gene, has been reported to have reduced expression levels and poor prognosis in colon and breast cancers[25, 26]. Our study identifies for the first time the specific low expression of *HPSE2* in SSLs and *BRAF*mut CRC and reveals that it may play an essential role in the serrated pathway but not in other colorectal carcinogenesis pathways. To the best of our knowledge, this study is the first to report the high expression of 5′tiRNA-Pro-TGG in SSLs and its potential regulatory relationship with *HPSE2*.

Analysis of immune cells and their functions suggested that *HPSE2* is involved in regulating the functions of various immune cells in CRC, including TIL, particularly in response to IFNγ. IFNγ promotes antigen presentation and tumor killing[27]. Our finding that patients with low *HPSE2* had

lower IFNγ-response scores suggested that it might be involved in regulating the tumor immune escape. Metabolic analysis revealed that *HPSE2* could downregulate various metabolic pathways, such as riboflavin and retinol metabolism. Riboflavin may reduce the risk of CRC in women[28]. In addition, a negative association between the plasma retinol concentration and the risk of proximal colon cancer has also been reported[29]. Recently, a lack of retinoic acid synthesis was found to promote the accumulation of myeloid-derived suppressor cells (MDSC) in CRC, thereby mediating the immune escape, while exogenous retinoic acid supplementation in an *in vitro* model attenuated the polymorphonuclear MDSC production[30].

Our study has some limitations. Firstly, more *in vitro* and *in vivo* experiments are needed to validate the function of the tiRNAs discussed. Secondly, because of the low prevalence of SSLs and their frequent neglect by endoscopists, it became difficult to collect a large number of samples. In addition, the expression level of 5′tiRNA-Pro-TGG and its association with recurrence and prognosis in SSL patients require further studies in large samples.

CONCLUSION

Our study is the first to identify the tsRNA expression profile of SSLs. It also reported that tiRNA-1:33-Gly-CCC-2, tiRNA-1:33-Pro-TGG-1, and tiRNA-1:34-Thr-TGT-4-M2 were highly expressed in SSLs. tiRNA-1:33-Pro-TGG-1 potentially promotes the serrated pathway for CRC progression through metabolic and immune pathways by interacting with *HPSE2* in SSLs and *BRAF*mut CRC. Our results showed that tiRNA-1:33-Pro-TGG-1 may serve as a potential target for early diagnosis of SSLs and treatment of CRC arising from the serrated pathway.

ARTICLE HIGHLIGHTS

Research background

tRNA halves (tiRNAs), a subcategory of tRNA-derived small RNAs (tsRNA), are involved in the oncogenic processes of many tumors, yet their specific role in sessile serrated lesions (SSLs) has not yet been elucidated.

Research motivation

The motivation for this study is to identify SSL-related tiRNAs and their potential role in the development of SSLs and serrated pathways in colorectal cancer (CRC).

Research objectives

Endoscopic detection of SSLs is very difficult and we do not know much about the exact mechanisms through which SSLs develop and how they progress to CRC in present.

Research methods

Small-RNA sequencing was conducted in paired SSLs and their adjacent normal control (NC) tissues. The expression levels of five SSL-related tiRNAs were validated by q-polymerase chain reaction. Cell counting kit and wound healing assays were performed to detect cell proliferation and migration. The target genes and sites of tiRNA-1:33-Pro-TGG-1 (5′tiRNA-Pro-TGG) were predicted by TargetScan and miRanda algorithms. Metabolism-associated and immune-related pathways were analyzed by single-sample gene set enrichment analysis. Functional analyses were performed to establish the roles of 5′tiRNA-Pro-TGG based on the target genes.

Research results

The expression levels of tiRNA-1:33-Gly-CCC-2, tiRNA-1:33-Pro-TGG-1, and tiRNA-1:34-Thr-TGT-4-M2 5′tiRNAs were higher in SSLs than those in NC, while that of 5′tiRNA-Pro-TGG was associated with the size of SSLs. It was demonstrated that 5′tiRNA-Pro-TGG promoted cell proliferation and migration of RKO cell *in vitro*. Then, heparanase 2 (*HPSE2*) was identified as a potential target gene of 5′tiRNA-Pro-TGG. Its lower expression was associated with a worse prognosis in CRC. Further, lower expression of *HPSE2* was observed in SSLs compared to NC or adenomas and in *BRAF*-mutant CRC compared to *BRAF*-wild CRC. Bioinformatics analyses revealed that its low expression was associated with a low interferon γ response and also with many metabolic pathways such as riboflavin, retinol, and cytochrome p450 drug metabolism pathways.

Research conclusions

5′tiRNA-Pro-TGG potentially promotes the progression of serrated pathway CRC through metabolic and immune pathways by interacting with *HPSE2* and regulating its expression in SSLs and *BRAF*-

mutant CRC.

Research perspectives

In the future, it may be possible to use 5′tiRNA-Pro-TGG as a novel biomarker for early diagnosis of SSLs and as a potential therapeutic target in serrated pathway of CRC.

ACKNOWLEDGEMENTS

The authors are grateful to all the individuals who participated in the study.

FOOTNOTES

Author contributions: Li XB was the guarantor of the paper; Wang XY and Chen SS collected clinical samples and performed the experiments; Chen HY analyzed data; Wang XY and Zhou YJ wrote the original draft; Chen JN revised the manuscript; Li XB and Chen HM conceived and supervised the study; All the authors revised and approved the final manuscript.

Supported by the Program of Health and Family Planning Research Project Plan of Pudong New Area Health Committee, No. PW2020D-12.

Institutional review board statement: This study was approved by Shanghai Jiaotong University School of Medicine, Renji Hospital Ethics Committee, No. KY2021-004.

Informed consent statement: All study participants, or their legal guardian, provided informed written consent prior to study enrollment.

Conflict-of-interest statement: All the authors report no relevant conflicts of interest for this article.

Data sharing statement: No additional data are available.

Country/Territory of origin: China

ORCID number: Hui-Min Chen 0000-0002-2940-2295; Xiao-Bo Li 0000-0003-1755-1135.

S-Editor: Li L
L-Editor: A
P-Editor: Zhao S

REFERENCES

1 **Crockett SD**, Nagtegaal ID. Terminology, Molecular Features, Epidemiology, and Management of Serrated Colorectal Neoplasia. *Gastroenterology* 2019; **157**: 949-966.e4 [PMID: 31323292 DOI: 10.1053/j.gastro.2019.06.041]
2 **Ahadi M**, Sokolova A, Brown I, Chou A, Gill AJ. The 2019 World Health Organization Classification of appendiceal, colorectal and anal canal tumours: an update and critical assessment. *Pathology* 2021; **53**: 454-461 [PMID: 33461799 DOI: 10.1016/j.pathol.2020.10.010]
3 **Meester RGS**, Ladabaum U. Sessile serrated polyps and colorectal cancer mortality. *Lancet Gastroenterol Hepatol* 2020; **5**: 516-517 [PMID: 32192629 DOI: 10.1016/S2468-1253(20)30074-1]
4 **Bell PD**, Anderson JC, Srivastava A. The Frontiers of Serrated Polyps. *Am J Surg Pathol* 2022; **46**: e64-e70 [PMID: 34545859 DOI: 10.1097/PAS.0000000000001806]
5 **Yang HM**, Mitchell JM, Sepulveda JL, Sepulveda AR. Molecular and histologic considerations in the assessment of serrated polyps. *Arch Pathol Lab Med* 2015; **139**: 730-741 [PMID: 26030242 DOI: 10.5858/arpa.2014-0424-RA]
6 **Hazewinkel Y**, López-Cerón M, East JE, Rastogi A, Pellisé M, Nakajima T, van Eeden S, Tytgat KM, Fockens P, Dekker E. Endoscopic features of sessile serrated adenomas: validation by international experts using high-resolution white-light endoscopy and narrow-band imaging. *Gastrointest Endosc* 2013; **77**: 916-924 [PMID: 23433877 DOI: 10.1016/j.gie.2012.12.018]
7 **Erichsen R**, Baron JA, Hamilton-Dutoit SJ, Snover DC, Torlakovic EE, Pedersen L, Frøslev T, Vyberg M, Hamilton SR, Sørensen HT. Increased Risk of Colorectal Cancer Development Among Patients With Serrated Polyps. *Gastroenterology*

2016; **150**: 895-902.e5 [PMID: 26677986 DOI: 10.1053/j.gastro.2015.11.046]

8 **He X**, Hang D, Wu K, Nayor J, Drew DA, Giovannucci EL, Ogino S, Chan AT, Song M. Long-term Risk of Colorectal Cancer After Removal of Conventional Adenomas and Serrated Polyps. *Gastroenterology* 2020; **158**: 852-861.e4 [PMID: 31302144 DOI: 10.1053/j.gastro.2019.06.039]

9 **Lu FI**, van Niekerk de W, Owen D, Tha SP, Turbin DA, Webber DL. Longitudinal outcome study of sessile serrated adenomas of the colorectum: an increased risk for subsequent right-sided colorectal carcinoma. *Am J Surg Pathol* 2010; **34**: 927-934 [PMID: 20551824 DOI: 10.1097/PAS.0b013e3181e4f256]

10 **Fabbri M**, Girnita L, Varani G, Calin GA. Decrypting noncoding RNA interactions, structures, and functional networks. *Genome Res* 2019; **29**: 1377-1388 [PMID: 31434680 DOI: 10.1101/gr.247239.118]

11 **Hulshoff MS**, Del Monte-Nieto G, Kovacic J, Krenning G. Non-coding RNA in endothelial-to-mesenchymal transition. *Cardiovasc Res* 2019; **115**: 1716-1731 [PMID: 31504268 DOI: 10.1093/cvr/cvz211]

12 **Zang J**, Lu D, Xu A. The interaction of circRNAs and RNA binding proteins: An important part of circRNA maintenance and function. *J Neurosci Res* 2020; **98**: 87-97 [PMID: 30575990 DOI: 10.1002/jnr.24356]

13 **Phizicky EM**, Hopper AK. tRNA biology charges to the front. *Genes Dev* 2010; **24**: 1832-1860 [PMID: 20810645 DOI: 10.1101/gad.1956510]

14 **Tao EW**, Cheng WY, Li WL, Yu J, Gao QY. tiRNAs: A novel class of small noncoding RNAs that helps cells respond to stressors and plays roles in cancer progression. *J Cell Physiol* 2020; **235**: 683-690 [PMID: 31286522 DOI: 10.1002/jcp.29057]

15 **Park J**, Ahn SH, Shin MG, Kim HK, Chang S. tRNA-Derived Small RNAs: Novel Epigenetic Regulators. *Cancers (Basel)* 2020; **12** [PMID: 32992597 DOI: 10.3390/cancers12102773]

16 **Han L**, Lai H, Yang Y, Hu J, Li Z, Ma B, Xu W, Liu W, Wei W, Li D, Wang Y, Zhai Q, Ji Q, Liao T. A 5'-tRNA halve, tiRNA-Gly promotes cell proliferation and migration *via* binding to RBM17 and inducing alternative splicing in papillary thyroid cancer. *J Exp Clin Cancer Res* 2021; **40**: 222 [PMID: 34225773 DOI: 10.1186/s13046-021-02024-3]

17 **Cui H**, Li H, Wu H, Du F, Xie X, Zeng S, Zhang Z, Dong K, Shang L, Jing C, Li L. A novel 3'tRNA-derived fragment tRF-Val promotes proliferation and inhibits apoptosis by targeting EEF1A1 in gastric cancer. *Cell Death Dis* 2022; **13**: 471 [PMID: 35585048 DOI: 10.1038/s41419-022-04930-6]

18 **Zhou Y**, Hu J, Liu L, Yan M, Zhang Q, Song X, Lin Y, Zhu D, Wei Y, Fu Z, Hu L, Chen Y, Li X. Gly-tRF enhances LCSC-like properties and promotes HCC cells migration by targeting NDFIP2. *Cancer Cell Int* 2021; **21**: 502 [PMID: 34537070 DOI: 10.1186/s12935-021-02102-8]

19 **Chen H**, Xu Z, Cai H, Peng Y, Yang L, Wang Z. Identifying Differentially Expressed tRNA-Derived Small Fragments as a Biomarker for the Progression and Metastasis of Colorectal Cancer. *Dis Markers* 2022; **2022**: 2646173 [PMID: 35035608 DOI: 10.1155/2022/2646173]

20 **Tsiakanikas P**, Adamopoulos PG, Tsirba D, Artemaki PI, Papadopoulos IN, Kontos CK, Scorilas A. High Expression of a tRNA(Pro) Derivative Associates with Poor Survival and Independently Predicts Colorectal Cancer Recurrence. *Biomedicines* 2022; **10** [PMID: 35625858 DOI: 10.3390/biomedicines10051120]

21 **Wang J**, Ma G, Li M, Han X, Xu J, Liang M, Mao X, Chen X, Xia T, Liu X, Wang S. Plasma tRNA Fragments Derived from 5' Ends as Novel Diagnostic Biomarkers for Early-Stage Breast Cancer. *Mol Ther Nucleic Acids* 2020; **21**: 954-964 [PMID: 32814252 DOI: 10.1016/j.omtn.2020.07.026]

22 **De Palma FDE**, D'Argenio V, Pol J, Kroemer G, Maiuri MC, Salvatore F. The Molecular Hallmarks of the Serrated Pathway in Colorectal Cancer. *Cancers (Basel)* 2019; **11** [PMID: 31330830 DOI: 10.3390/cancers11071017]

23 **Angerilli V**, Sabella G, Centonze G, Lonardi S, Bergamo F, Mangogna A, Pietrantonio F, Fassan M, Milione M. BRAF-mutated colorectal adenocarcinomas: Pathological heterogeneity and clinical implications. *Crit Rev Oncol Hematol* 2022; **172**: 103647 [PMID: 35248712 DOI: 10.1016/j.critrevonc.2022.103647]

24 **Li S**, Shi X, Chen M, Xu N, Sun D, Bai R, Chen H, Ding K, Sheng J, Xu Z. Angiogenin promotes colorectal cancer metastasis *via* tiRNA production. *Int J Cancer* 2019; **145**: 1395-1407 [PMID: 30828790 DOI: 10.1002/ijc.32245]

25 **Zhang H**, Xu C, Shi C, Zhang J, Qian T, Wang Z, Ma R, Wu J, Jiang F, Feng J. Hypermethylation of heparanase 2 promotes colorectal cancer proliferation and is associated with poor prognosis. *J Transl Med* 2021; **19**: 98 [PMID: 33663522 DOI: 10.1186/s12967-021-02770-0]

26 **Wu B**, Liu G, Jin Y, Yang T, Zhang D, Ding L, Zhou F, Pan Y, Wei Y. miR-15b-5p Promotes Growth and Metastasis in Breast Cancer by Targeting HPSE2. *Front Oncol* 2020; **10**: 108 [PMID: 32175269 DOI: 10.3389/fonc.2020.00108]

27 **Alspach E**, Lussier DM, Schreiber RD. Interferon γ and Its Important Roles in Promoting and Inhibiting Spontaneous and Therapeutic Cancer Immunity. *Cold Spring Harb Perspect Biol* 2019; **11** [PMID: 29661791 DOI: 10.1101/cshperspect.a028480]

28 **de Vogel S**, Dindore V, van Engeland M, Goldbohm RA, van den Brandt PA, Weijenberg MP. Dietary folate, methionine, riboflavin, and vitamin B-6 and risk of sporadic colorectal cancer. *J Nutr* 2008; **138**: 2372-2378 [PMID: 19022960 DOI: 10.3945/jn.108.091157]

29 **Leenders M**, Leufkens AM, Siersema PD, van Duijnhoven FJ, Vrieling A, Hulshof PJ, van Gils CH, Overvad K, Roswall N, Kyrø C, Boutron-Ruault MC, Fagerhazzi G, Cadeau C, Kühn T, Johnson T, Boeing H, Aleksandrova K, Trichopoulou A, Klinaki E, Androulidaki A, Palli D, Grioni S, Sacerdote C, Tumino R, Panico S, Bakker MF, Skeie G, Weiderpass E, Jakszyn P, Barricarte A, María Huerta J, Molina-Montes E, Argüelles M, Johansson I, Ljuslinder I, Key TJ, Bradbury KE, Khaw KT, Wareham NJ, Ferrari P, Duarte-Salles T, Jenab M, Gunter MJ, Vergnaud AC, Wark PA, Bueno-de-Mesquita HB. Plasma and dietary carotenoids and vitamins A, C and E and risk of colon and rectal cancer in the European Prospective Investigation into Cancer and Nutrition. *Int J Cancer* 2014; **135**: 2930-2939 [PMID: 24771392 DOI: 10.1002/ijc.28938]

30 **Sun HW**, Chen J, Wu WC, Yang YY, Xu YT, Yu XJ, Chen HT, Wang Z, Wu XJ, Zheng L. Retinoic Acid Synthesis Deficiency Fosters the Generation of Polymorphonuclear Myeloid-Derived Suppressor Cells in Colorectal Cancer. *Cancer Immunol Res* 2021; **9**: 20-33 [PMID: 33177108 DOI: 10.1158/2326-6066.CIR-20-0389]

World Journal of Gastrointestinal Oncology

Submit a Manuscript: https://www.f6publishing.com

World J Gastrointest Oncol 2023 June 15; 15(6): 1019-1035

DOI: 10.4251/wjgo.v15.i6.1019

ISSN 1948-5204 (online)

ORIGINAL ARTICLE

Clinical and Translational Research

Comprehensive analysis of distal-less homeobox family gene expression in colon cancer

Yong-Cheng Chen, Dong-Bing Li, Dong-Liang Wang, Hui Peng

Specialty type: Oncology

Provenance and peer review: Unsolicited article; Externally peer reviewed.

Peer-review model: Single blind

Peer-review report's scientific quality classification

Grade A (Excellent): 0
Grade B (Very good): B
Grade C (Good): C
Grade D (Fair): 0
Grade E (Poor): 0

P-Reviewer: Abdalla AN, Saudi Arabia; Zhang W, China

Received: January 6, 2023
Peer-review started: January 6, 2023
First decision: January 23, 2023
Revised: February 6, 2023
Accepted: April 27, 2023
Article in press: April 27, 2023
Published online: June 15, 2023

Yong-Cheng Chen, Department of General Surgery (Endoscopic Surgery), The Sixth Affiliated Hospital, Sun Yat-sen University, Guangzhou 510655, Guangdong Province, China

Yong-Cheng Chen, Hui Peng, Guangdong Provincial Key Laboratory of Colorectal and Pelvic Floor Diseases, The Sixth Affiliated Hospital, Sun Yat-sen University, Guangzhou 510655, Guangdong Province, China

Yong-Cheng Chen, Hui Peng, Biomedical Innovation Center, The Sixth Affiliated Hospital, Sun Yat-sen University, Guangzhou 510655, Guangdong Province, China

Dong-Bing Li, Dong-Liang Wang, Department of Medicine, ChosenMed Technology (Beijing) Co., Ltd., Beijing 100176, China

Hui Peng, Department of General Surgery (Anorectal Surgery), The Sixth Affiliated Hospital, Sun Yat-sen University, Guangzhou 510655, Guangdong Province, China

Corresponding author: Hui Peng, MD, Chief Doctor, Department of General Surgery (Anorectal Surgery), The Sixth Affiliated Hospital, Sun Yat-sen University, No. 26 Yuancun Erheng Road, Tianhe District, Guangzhou 510655, Guangdong Province, China. phui@mail.sysu.edu.cn

Abstract

BACKGROUND

The distal-less homeobox (*DLX*) gene family plays an important role in the development of several tumors. However, the expression pattern, prognostic and diagnostic value, possible regulatory mechanisms, and the relationship between *DLX* family genes and immune infiltration in colon cancer have not been systematically reported.

AIM

We aimed to comprehensively analyze the biological role of the *DLX* gene family in the pathogenesis of colon cancer.

METHODS

Colon cancer tissue and normal colon tissue samples were collected from the Cancer Genome Atlas and Gene Expression Omnibus databases. Wilcoxon rank sum test and *t*-test were used to assess *DLX* gene family expression between colon cancer tissue and unpaired normal colon tissue. cBioPortal was used to analyze *DLX* gene family variants. R software was used to analyze *DLX* gene expression

in colon cancer and the relationship between *DLX* gene family expression and clinical features and correlation heat map. The survival package and Cox regression module were used to assess the prognostic value of the *DLX* gene family. The pROC package was used to analyze the diagnostic value of the *DLX* gene family. R software was used to analyze the possible regulatory mechanisms of *DLX* gene family members and related genes. The GSVA package was used to analyze the relationship between the *DLX* gene family and immune infiltration. The ggplot2, the survminer package, and the clusterProfiler package were used for visualization.

RESULTS

DLX1/2/3/4/5 were significantly aberrantly expressed in colon cancer patients. The expression of *DLX* genes were associated with M stage, pathologic stage, primary therapy outcome, residual tumor, lymphatic invasion, T stage, N stage, age, perineural invasion, and history of colon polyps. *DLX5* was independently correlated with the prognosis of colon cancer in multivariate analysis. *DLX1/2/3/4/5/6* were involved in the development and progression of colon cancer by participating in immune infiltration and associated pathways, including the Hippo signaling pathway, the Wnt signaling pathway, several signaling pathways regulating the pluripotency of stem cells, and *Staphylococcus aureus* infection.

CONCLUSION

The results of this study suggest a possible role for the *DLX* gene family as potential diagnostic or prognostic biomarkers and therapeutic targets in colon cancer.

Key Words: Colon cancer; The Cancer Genome Atlas; Distal-less homeobox genes; Prognosis; Immune infiltration

Core Tip: The distal-less homeobox (*DLX*) gene family plays an important role in the pathogenesis of several tumors. However, the expression pattern, prognostic and diagnostic value, possible regulatory mechanisms, and the relationship between *DLX* family genes and immune infiltration in colon cancer have not been systematically reported. In this study, we aimed to investigate the expression level, clinical significance, and relationship between *DLX* genes and immune infiltration in colon cancer to establish an adequate scientific basis for clinical decision making and risk management. The *DLX* gene family holds promise as a potential diagnostic or prognostic biomarker and therapeutic target for colon cancer.

Citation: Chen YC, Li DB, Wang DL, Peng H. Comprehensive analysis of distal-less homeobox family gene expression in colon cancer. *World J Gastrointest Oncol* 2023; 15(6): 1019-1035
URL: https://www.wjgnet.com/1948-5204/full/v15/i6/1019.htm
DOI: https://dx.doi.org/10.4251/wjgo.v15.i6.1019

INTRODUCTION

Colon cancer comprises a widely study group of tumors whose incidence is on the rise. Approximately 10% of all cancer deaths are caused by colon cancer and related complications[1]. Colon adenocarcinoma (COAD) is the most common, accounting for 98% of colon cancer cases[2]. Colon cancer has a high recurrence rate after treatment, with 42% of patients recurring within 5 y and a median time from recurrence to death of 12 mo[3]. Unfortunately, about 20% of colon cancer patients are diagnosed with stage IV each year[4]. Therefore, exploring novel molecular markers is of great clinical significance to improve the diagnosis and treatment of colon cancer.

The distal-less homeobox (*DLX*) gene is a homolog of *Drosophila* distal-less and consists of 6 members, including *DLX1, DLX2, DLX3, DLX4, DLX5*, and *DLX6*[5]. *DLX1* can be used to identify prostate cancer for early diagnosis[6]. Overexpression of *DLX2* has been associated with poor prognosis in hepatocellular carcinoma (HCC)[7]. High expression of *DLX2* has been shown to be a poor prognostic marker for patients with glioblastoma multiforme[8]. *DLX3* has been demonstrated as a key regulator of the STAT3 signaling network that maintains skin homeostasis[9]. *DLX4* can also be used as a prognostic marker for HCC[10]. *DLX5* has been shown to be a potential diagnostic biomarker and therapeutic target for oral squamous cell carcinoma (OSCC)[11]. *DLX6* has been shown to promote cell proliferation and survival in OSCC[12]. To our knowledge, no studies have systematically assessed the role of the *DLX* gene family in colon cancer using bioinformatics methods. In this study, we aimed to investigate

the expression level, clinical significance, and relationship between *DLX* family genes and immune infiltration in colon cancer to establish an adequate scientific basis for clinical decision making and risk management.

MATERIALS AND METHODS

CBioPortal analysis

The cBio Cancer Genomics Portal (cBioPortal) (http://cbioportal.org) was used to study mutations in *DLX* genes in colon cancer[13]. Queries for visualization and analysis were performed using the following entries: (1) Cancer type: COAD; (2) 2 selected studies: COAD (CaseCCC, PNAS 2015), colon cancer (CPTAC-2 Prospective, Cell 2019); (3) Molecular profile: Mutations and copy number alterations (CNAs); (4) Selection of patients/case sets: All samples (139); and (5) Input genes: *DLX1*(ENSG-00000144355), *DLX2*(ENSG00000115844), *DLX3*(ENSG00000064195), *DLX4*(ENSG00000108813), *DLX5* (ENSG00000105880), and *DLX6*(ENSG00000006377). After submission of queries, accessions were made including origin studies, mutation profiles, mutation number, overall survival (OS) status, OS (months), disease-free status, and disease-free period (months) tracks.

Dysregulation of DLX genes in colon cancer

R software (version 3.6.3) was used for statistical analysis and visualization[14,15]. The R packages used included ggplot2 (version 3.3.3) for visualization. UCSC XENA (https://xenabrowser.net/datapages/) RNAseq data were uniformly processed by the Toil process into TPM (transcripts per million reads) format for the Cancer Genome Atlas (TCGA) and GTEx[16]. Data for colon cancer were extracted from the TCGA and corresponding normal tissue data were extracted from GTEx. RNAseq data were in TPM format and log2 transformed for expression comparisons between samples. The data filtering condition was set to retain paired samples.

Correlation heat map

Correlation between every 2 genes of the *DLX* family was assessed using a Pearson's correlation coefficient. The R package used was mainly ggplot2 (version 3.3.3). The filter condition was set to remove data from the normal/control groups (of note, not every item had a normal/control group).

Association of DLX gene expression with clinical features of TCGA-colon cancer

The R package used was the basic R package[17]. Grouping was based on the median.

Survival analysis

The survminer package (version 0.4.9) was used for visualizing survival data, and the survival package (version 3.2-10) allowed statistical analysis of survival data. Subgroups included 0-50 and 50-100. The prognosis types were OS, progression-free interval (PFS), and disease specific survival (DSS). Supplementary data were prognostic data from the reference literature[18]. The filter condition was set to remove data from the normal/control groups (of note, not every item had a normal/control group) and keep the data for clinical information.

Univariate and multivariate Cox regression analysis

The R package used was the survivor package (version 3.2-10). Statistical analysis was performed using the Cox regression module. Prognosis types were OS, PFS, and DSS, and included variables were *DLX1, DLX2, DLX3, DLX4, DLX5*, and *DLX6*. Supplementary data were prognostic data from the reference literature[18]. The filter condition was set to remove data from the normal/control groups (of note, not every item had a normal/control group) and keep the data for clinical information.

ROC curve analysis

Two R packages were used: the pROC package (for analysis) and ggplot2 package (version 3.3.3). Clinical variables were "tumor" and "normal". UCSC XENA (https://xenabrowser.net/datapages/) RNAseq data were uniformly processed by the Toil process into TPM format for TCGA and GTEx[16]. Data for colon cancer were extracted from TCGA and corresponding normal tissue data were extracted from GTEx. The RNAseq data were in TPM format and log2 transformed for expression comparison between samples. Data were not filtered. The horizontal coordinate was the false positive rate and the vertical coordinate was the true positive rate.

Correlation analysis for genes associated with DLX genes

The R package used was the stat package (version 3.6.3) (base package). The TCGA colon cancer project provided the RNAseq data in level 3 HTSeq-FPKM format. The TPM format was converted to FPKM, and log2 transformation was applied to the transformed data. The control/normal groups were removed from the results (of note, not all projects had control/normal groups).

Functional enrichment analysis of genes associated with DLX genes

The R packages used were mainly ggplot2 package (version 3.3.3) and clusterProfiler package (version 3.14.3).

Correlation between the expression of DLX genes in colon cancer and immune cells

The R package used was the GSVA package (version 1.34.0)[19]. For immune infiltration, the GSVA package had a built-in algorithm, ssGSEA. Immune cells included were activated dendritic cells (aDCs), B-cells, CD8 T-cells, cytotoxic cells, dendritic cells (DCs), eosinophils, immature DCs (iDCs), macrophages, mast cells, neutrophils, natural killer (NK) CD56bright cells, NK CD56dim cells, NK cells, plasmacytoid DCs (pDCs), T-cells, T helper (Th) cells, T central memory cells, T effector memory (Tem) cells, T follicular helper (TFH) cells, T gamma delta (Tgd) cells, Th1 cells, Th17 cells, Th2 cells, and regulatory T (Treg) cells[20]. The data filtering condition was set to remove the control/normal group (of note, not all projects had control/normal groups). Markers for 24 immune cells were obtained from the reference literature[21].

Validation of DLX gene expression

To further verify the accuracy of the TCGA database, we downloaded colon cancer samples from the Gene Expression Omnibus database for analysis. The 30 colon cancer tissue samples and 30 normal colon tissue samples contained in GSE74062 were used for *DLX* gene expression analysis.

Statistical analysis

All statistical analyses were performed using R software (v.3.6.3). The Wilcoxon rank sum test, chi-square test, and Fisher exact test were used to analyze the relationship between clinical characteristics and *DLX* genes. *P* values less than 0.05 were considered statistically significant.

RESULTS

DLX gene alterations and mRNA expression in colon cancer

The cBioPortal online tool was used to analyze the expression of *DLX* family genes in colon cancer patients. Alterations in the expression of *DLX* genes in colon cancer ranged from 0.7% to 3% (Figure 1). The mutation data, CNA data, and deep deletion from the 2 studies are depicted in Figure 2. The analysis of *DLX* gene expression was performed based on 41 colon cancer tissue samples and 41 paired samples of normal colon tissue (Figure 3). The results showed that the expression level of *DLX1* in colon cancer was significantly lower than that in normal colon tissue (0.199 ± 0.026 *vs* 0.867 ± 0.031; $P < 0.001$). The expression level of *DLX2* in colon cancer was significantly lower than that in normal colon tissue (0.129 ± 0.020 *vs* 0.211 ± 0.011; $P = 0.0074$). The expression level of *DLX3* in colon cancer was significantly higher than that in normal colon tissue (0.593 ± 0.052 *vs* 0.171 ± 0.008; $P < 0.001$). The expression level of *DLX4* in colon cancer was significantly higher than in normal colon tissue (0.635 ± 0.027 *vs* 0.229 ± 0.009; $P < 0.001$). The expression level of *DLX5* in colon cancer was significantly lower than that in normal colon tissue (0.416 ± 0.036 *vs* 0.463 ± 0.022; $P < 0.001$). There was no significant difference in *DLX6* expression in colon cancer compared to normal colon tissue (0.229 ± 0.014 *vs* 0.449 ± 0.037; $P = 0.554$). We examined the correlation between *DLX* genes using Pearson correlation analysis. There was no significant correlation between *DLX1* and *DLX3*, *DLX1* and *DLX6*; there was a significant positive correlation between other *DLX* genes (Figure 4).

Relationship between DLX gene expression and clinical characteristics and prognosis of colon cancer patients

Clinical characteristics data and gene expression data for 478 colon cancer samples were downloaded from the TCGA database (Supplementary Table 1). *DLX2* expression was associated with M stage ($P = 0.005$), pathologic stage ($P = 0.014$), primary therapy outcome ($P = 0.036$), residual tumor ($P = 0.002$), and lymphatic invasion ($P = 0.013$). *DLX3* expression was associated with N stage ($P < 0.001$), M stage ($P < 0.001$), pathologic stage ($P < 0.001$), height ($P = 0.045$), and residual tumor ($P < 0.001$). *DLX5* expression was associated with T stage ($P < 0.001$), N stage ($P < 0.001$), M stage ($P = 0.005$), pathologic stage ($P < 0.001$), primary therapy outcome ($P = 0.005$), age ($P < 0.001$), perineural invasion ($P = 0.023$), lymphatic invasion ($P < 0.001$), and history of colon polyps ($P = 0.009$). However, the expression of *DLX1, DLX4*, and *DLX6* did not significantly correlate with any clinical characteristic of colon cancer patients.

A low expression of *DLX1* was associated with PFS ($P = 0.013$); a low expression of *DLX2* was associated with OS ($P = 0.006$), PFS ($P = 0.003$), and DSS ($P = 0.007$); a high expression of *DLX3* was associated with OS ($P = 0.010$), PFS ($P = 0.004$), and DSS ($P = 0.007$); a high expression of *DLX4* was associated with OS ($P = 0.030$) and PFS ($P = 0.023$); a low expression of *DLX5* was associated with poor OS ($P = 0.048$), PFS ($P = 0.002$), and DSS ($P = 0.007$). However, a high expression of *DLX6* was not significantly associated with prognosis in colon cancer (Figure 5).

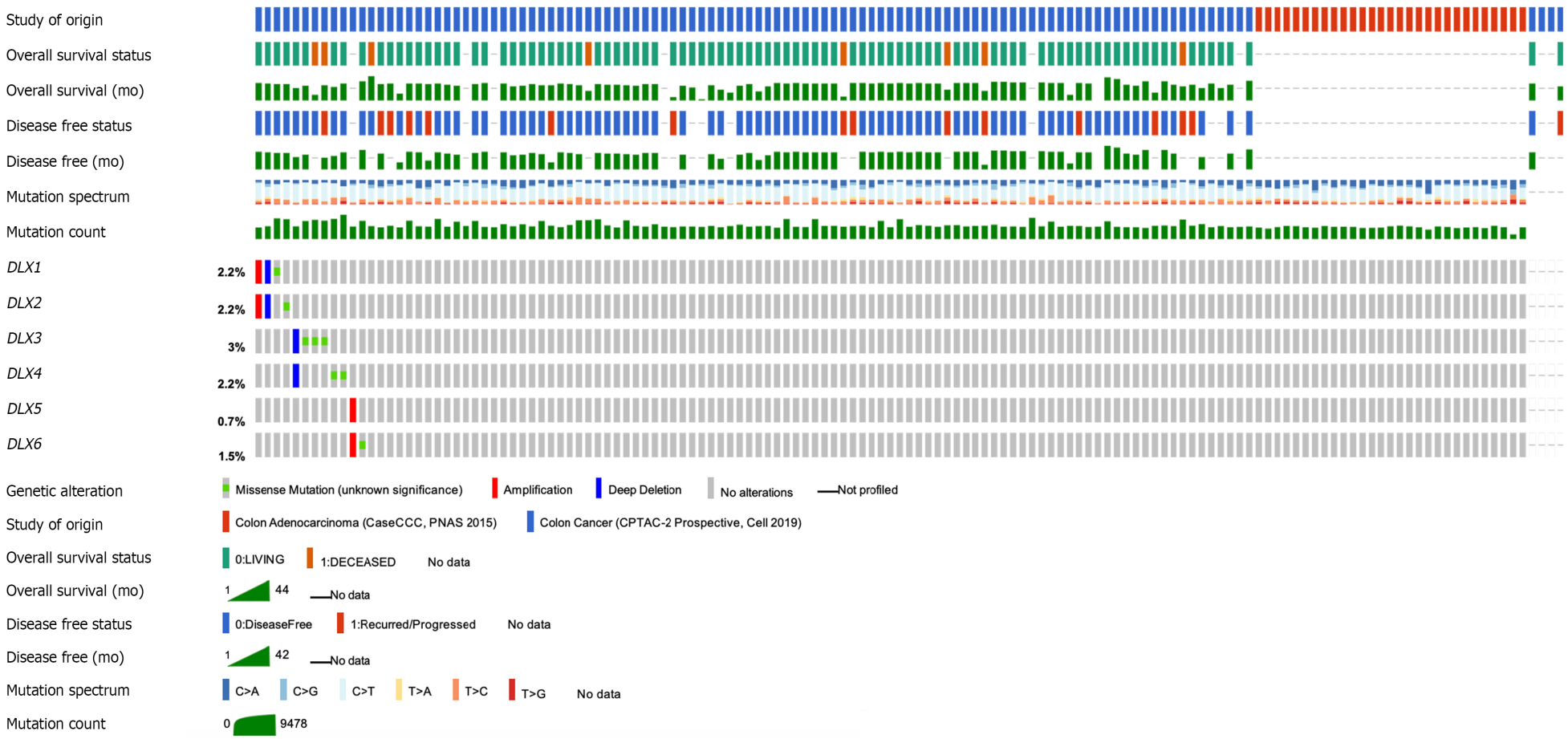

DOI: 10.4251/wjgo.v15.i6.1019

Figure 1 mRNA expression of distal-less homeobox genes in colon adenocarcinoma in cBioPortal (RNA Seq V2 RSEM). DLX: Distal-less homeobox.

Univariate Cox regression analysis for OS showed that *DLX2* ($P = 0.007$), *DLX3* ($P = 0.011$), *DLX4* ($P = 0.031$), and *DLX5* ($P = 0.049$) were associated with OS, and *DLX1* ($P = 0.014$), *DLX2* ($P = 0.003$), *DLX3* ($P = 0.004$), *DLX4* ($P = 0.024$), and *DLX5* ($P = 0.002$) were associated with PFS. *DLX2* ($P = 0.008$), *DLX3* ($P = 0.008$), and *DLX5* ($P = 0.009$) were associated with DSS. *DLX5* was independently correlated with PFS ($P = 0.012$) and DSS ($P = 0.035$) in multivariate analysis (Table 1).

DLX1 had some accuracy in diagnosing normal and tumor outcomes [area under curve (AUC) = 0.893; 95%CI: 0.867-0.920]. *DLX2* also had some accuracy in diagnosing normal and tumor outcomes

Table 1 Univariate and multivariate Cox regression analyses with distal-less homeobox genes and prognosis of colon adenocarcinoma patients

Survival	Characteristics	Total, *n*	Univariate analysis		Multivariate analysis	
			HR (95%CI)	*P* value	HR (95%CI)	*P* value
Overall	*DLX1* (low *vs* high)	477	1.299 (0.880-1.917)	0.186		
	DLX2 (low *vs* high)	477	1.736 (1.167-2.584)	0.007	1.502 (0.988-2.285)	0.057
	DLX3 (low *vs* high)	477	1.668 (1.123-2.476)	0.011	1.374 (0.900-2.099)	0.142
	DLX4 (low *vs* high)	477	1.538 (1.039-2.276)	0.031	1.197 (0.783-1.830)	0.405
	DLX5 (low *vs* high)	477	1.485 (1.001-2.202)	0.049	1.334 (0.893-1.993)	0.159
	DLX6 (low *vs* high)	477	0.935 (0.634-1.379)	0.734		
Progression-free	*DLX1* (low *vs* high)	477	1.557 (1.094-2.214)	0.014	1.316 (0.901-1.921)	0.155
	DLX2 (low *vs* high)	477	1.715 (1.201-2.449)	0.003	1.317 (0.883-1.964)	0.178
	DLX3 (low *vs* high)	477	1.670 (1.174-2.376)	0.004	1.365 (0.937-1.990)	0.105
	DLX4 (low *vs* high)	477	1.497 (1.054-2.125)	0.024	1.181 (0.813-1.715)	0.382
	DLX5 (low *vs* high)	477	1.742 (1.217-2.492)	0.002	1.588 (1.105-2.283)	0.012
	DLX6 (low *vs* high)	477	0.914 (0.646-1.294)	0.613		
Disease specific	*DLX1* (low *vs* high)	461	1.426 (0.865-2.349)	0.164		
	DLX2 (low *vs* high)	461	2.014 (1.202-3.376)	0.008	1.666 (0.971-2.857)	0.064
	DLX3 (low *vs* high)	461	2.007 (1.202-3.349)	0.008	1.570 (0.909-2.713)	0.106
	DLX4 (low *vs* high)	461	1.617 (0.981-2.664)	0.059	1.179 (0.692-2.011)	0.545
	DLX5 (low *vs* high)	461	2.011 (1.193-3.390)	0.009	1.765 (1.039-2.998)	0.035
	DLX6 (low *vs* high)	461	0.852 (0.520-1.395)	0.524		

CI: Confidence interval; *DLX*: Distal-less homeobox; HR: Hazard ratio.

(AUC = 0.731; 95%CI: 0.691-0.771), while *DLX3* had a lower accuracy in diagnosing these outcomes (AUC = 0.561; 95%CI: 0.512-0.611). *DLX4* also had some accuracy in diagnosing normal and tumor outcomes (AUC = 0.834; 95%CI: 0.802-0.867), while *DLX5* had low accuracy in diagnosing these outcomes (AUC = 0.590; 95%CI: 0.546-0.635). Lastly, *DLX6* had poor accuracy in diagnosing normal and tumor outcomes (AUC = 0.486; 95%CI: 0.439-0.534) (Figure 6).

The function of genes associated with DLX genes

The top 10 significantly associated genes for each *DLX* gene are shown in the single gene co-expression heat map (Figure 7). Genes significantly associated with *DLX1* included *DLX2, KLF14, CHRND, KCNN1, IGDCC3, ARHGAP36, NCAN, TFAP2B, CNPY1*, and *CACNG7*. Genes significantly associated with *DLX2* included *DLX1, CNPY1, CHRND, NEUROD1, IGDCC3, TNFRSF19, KLF14, NELL2, HS3ST4*, and *SLC38A8*. Genes significantly associated with *DLX3* included *NOTUM, NKD1, APCDD1, ADAMTSL2, MYH7B, PRR9, LRRC43, CAB39L, ABCC2*, and *DLX4*. Genes significantly associated with *DLX4* included *DLX3, TTLL4, DNMT3B, CDK5R1, IGF2BP1, STK36, UNK, AMER3, PHF12*, and *WNT3*. Genes significantly associated with *DLX5* included *DYNC1I1, DLX6, RASL11B, ID4, SP7, AMBN, KRT31, MYL3, VENTX*, and *ISM1*. Genes significantly associated with *DLX6* included *DLX5, TRIM71, SH3GL2, SLC46A1, DYNC1I1, PGBD5, GAL, COCH, AXIN2*, and *CKB*. The top 30 genes significantly associated with each *DLX* gene (147 in total) were analyzed for Gene Ontology and Kyoto Encyclopedia of Genes and Genomes enrichment (Supplementary Table 2). The top biological processes included pattern specification, regionalization, ossification, connective tissue development, cell fate commitment, hippocampus development, biomineral tissue development, biomineralization, skeletal system morphogenesis, and odontogenesis. The significantly related molecular functions included DNA-binding transcription activator activity, RNA polymerase II-specificity, fibroblast growth factor receptor binding, DNA-binding transcription activator activity (Figure 8 and Supplementary Table 3). The significantly related pathways included the Hippo signaling pathway, the Wnt signaling pathway, and signaling pathways regulating the pluripotency of stem cells and *Staphylococcus aureus* infection (Figure 9 and Supplementary Table 3).

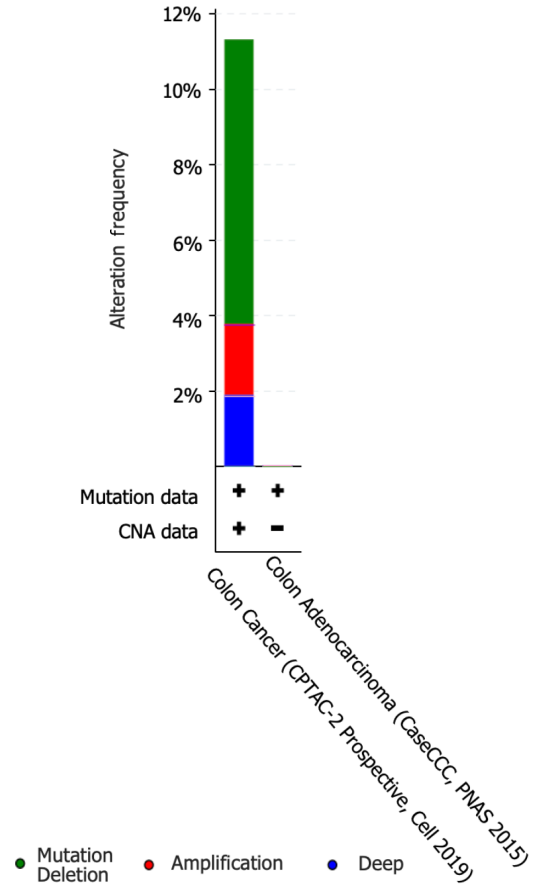

DOI: 10.4251/wjgo.v15.i6.1019 **Copyright** ©The Author(s) 2023.

Figure 2 Percentage of distal-less homeobox genes in colon adenocarcinoma cases calculated using the cancer type summary in cBioPortal.

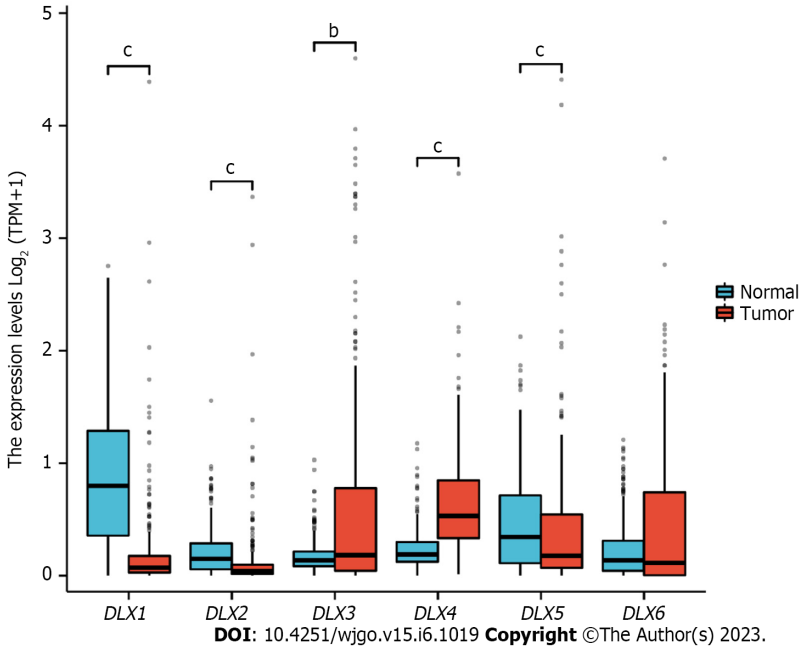

DOI: 10.4251/wjgo.v15.i6.1019 **Copyright** ©The Author(s) 2023.

Figure 3 mRNA levels of distal-less homeobox genes between colon adenocarcinoma tissue and unpaired normal stomach tissue in the Cancer Genome Atlas. $^{b}P < 0.01$; $^{c}P < 0.001$. *DLX*: Distal-less homeobox.

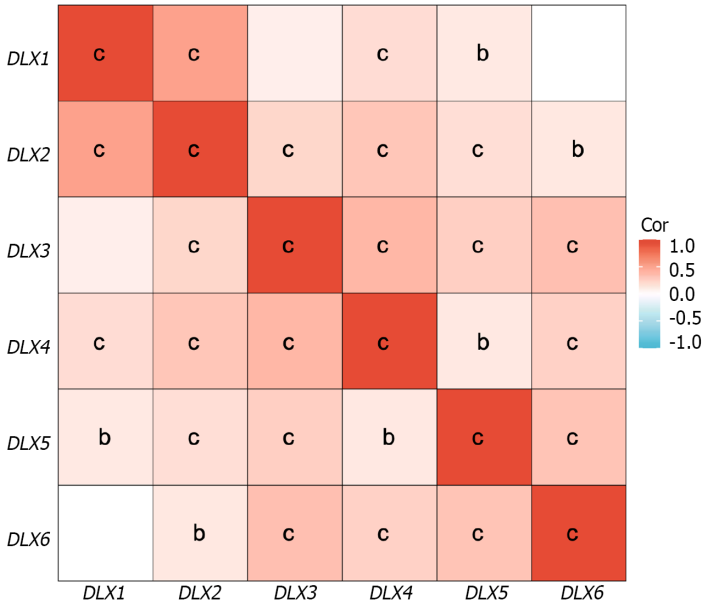

DOI: 10.4251/wjgo.v15.i6.1019 **Copyright** ©The Author(s) 2023.

Figure 4 Correlation between every two genes of distal-less homeobox genes in colon adenocarcinoma. $^{b}P < 0.01$; $^{c}P < 0.001$. *DLX*: Distal-less homeobox.

Correlation of DLX gene expression and immune cells in colon cancer

There was a correlation between *DLX* gene expression and immune cells in colon cancer (Figure 10). *DLX1* gene expression positively correlated with some tumor-infiltrating immune cells (TIICs), including aDCs, cytotoxic cells, DCs, eosinophils, iDCs, macrophages, mast cells, neutrophils, NK CD56dim cells, NK cells, Tem cells, TFH cells, Tgd cells, Th1 cells, and Treg cells; *DLX1* expression negatively correlated with Th17 cells. *DLX2* gene expression positively correlated with mast cells and TFH cells and negatively correlated with pDCs and Th17 cells. *DLX3* gene expression negatively correlated with some TIICs, including aDCs, CD8 T-cells, cytotoxic cells, DCs, macrophages, neutrophils, T-cells, Th cells, Th1 cells, Th2 cells, and Treg cells. *DLX4* gene expression positively correlated with NK cells and negatively correlated with some TIICs, including cytotoxic cells, DCs, macrophages, pDCs, Th1 cells, and Th2 cells. *DLX5* gene expression positively correlated with some TIICs, including B-cells, CD8 T-cells, DCs, iDCs, macrophages, mast cells, neutrophils, NK cells, pDCs, Tem cells, TFH cells, Tgd cells, and Treg cells; *DLX5* expression negatively correlated with Th17 cells and Th2 cells. *DLX6* gene expression negatively correlated with some TIICs, including aDCs, cytotoxic cells, DCs, macrophages, neutrophils, NK CD56dim cells, T-cells, Tem cells, and Th1 cells.

DLX genes were aberrantly expressed in colon cancer tissue

Compared to normal colon, *DLX1* (P = 7.6e-08), *DLX2* (P = 5.7e-08), *DLX4* (P = 0.00013), and *DLX5* (P = 0.0084) were aberrantly expressed in colon cancer tissue. However, *DLX3* and *DLX6* were not aberrantly expressed in colon cancer (Figure 11).

DISCUSSION

DLX1 has been shown to be significantly upregulated in prostate cancer tissues and cells[22]. *DLX2* is known to be significantly upregulated in HCC tissues and cell lines[7,23], and its expression in gastric cancer has been shown to significantly correlated with tumor size, depth of infiltration, lymph node metastasis, and tumor-lymph node metastasis stage[24]. *DLX4* has been demonstrated to be upregulated in nasopharyngeal carcinoma (NPC) cell lines[25], and its expression was shown to be elevated in HCC and correlated significantly with tumor size, histopathological classification, and serum alpha-fetoprotein[10]. *DLX5* has been shown to be upregulated in OSCC tissues and cell lines, and has been associated with advanced TNM staging, lymph node metastasis, poor cell differentiation, and tumor location[11]. *DLX6* has been shown to be upregulated in oral cancer and has been associated with advanced tumor stage and poor prognosis[12]. In this study, *DLX1/2/3/4/5* were aberrantly expressed in colon cancer tissue samples. The expression of *DLX* family genes was associated with M stage, pathologic stage, primary therapy outcome, residual tumor, lymphatic invasion, T stage, N stage, age, perineural invasion, and history of colon polyps. In the multivariate analysis, *DLX5* was independently related to PFS and OS. In diagnosing the outcome of normal and tumor tissues, *DXL1/2/4* had some

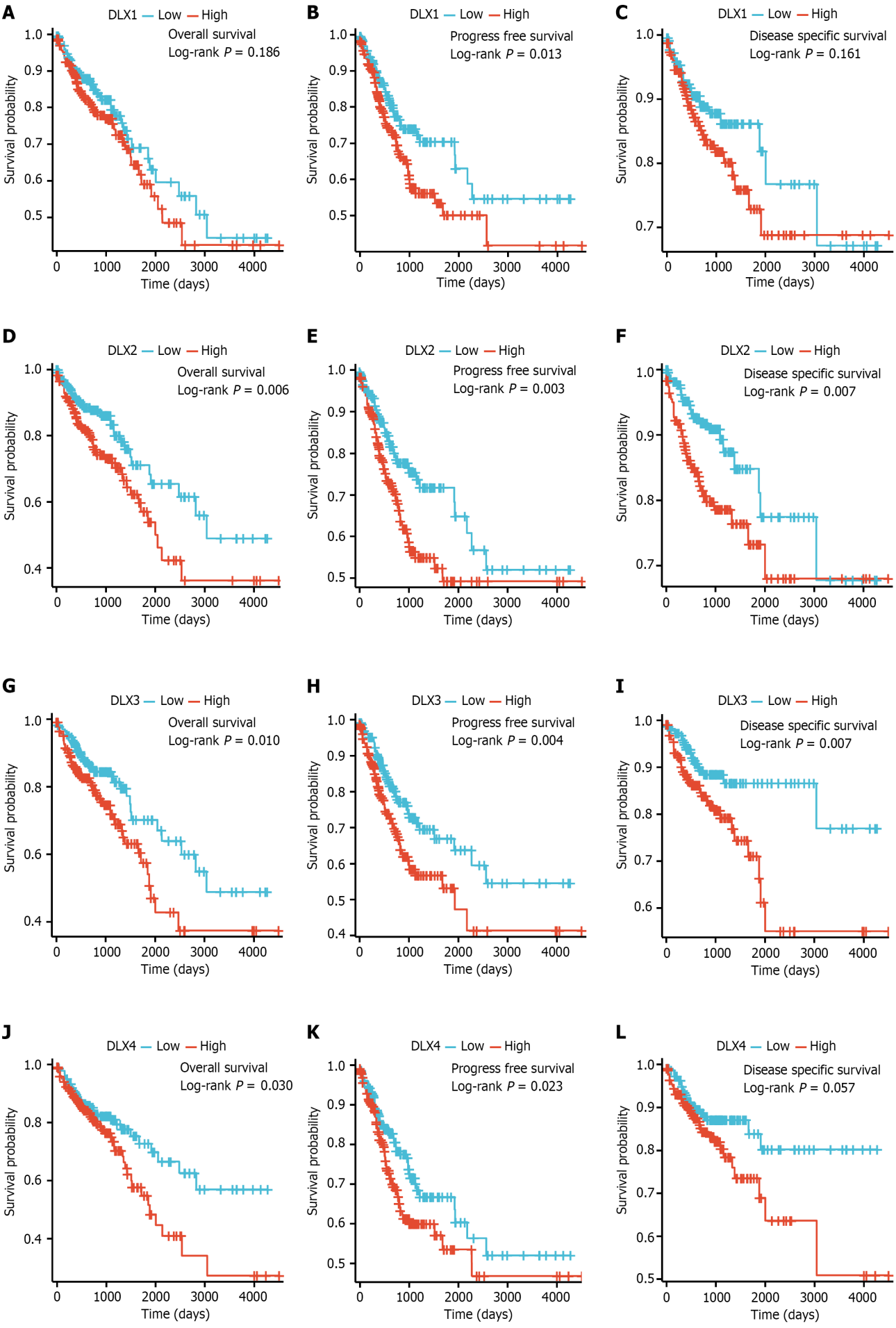
A
DLX1 Low High
Overall survival
Log-rank P = 0.186
B
DLX1 Low High
Progress free survival
Log-rank P = 0.013
C
DLX1 Low High
Disease specific survival
Log-rank P = 0.161
D
DLX2 Low High
Overall survival
Log-rank P = 0.006
E
DLX2 Low High
Progress free survival
Log-rank P = 0.003
F
DLX2 Low High
Disease specific survival
Log-rank P = 0.007
G
DLX3 Low High
Overall survival
Log-rank P = 0.010
H
DLX3 Low High
Progress free survival
Log-rank P = 0.004
I
DLX3 Low High
Disease specific survival
Log-rank P = 0.007
J
DLX4 Low High
Overall survival
Log-rank P = 0.030
K
DLX4 Low High
Progress free survival
Log-rank P = 0.023
L
DLX4 Low High
Disease specific survival
Log-rank P = 0.057
Survival probability
Time (days)

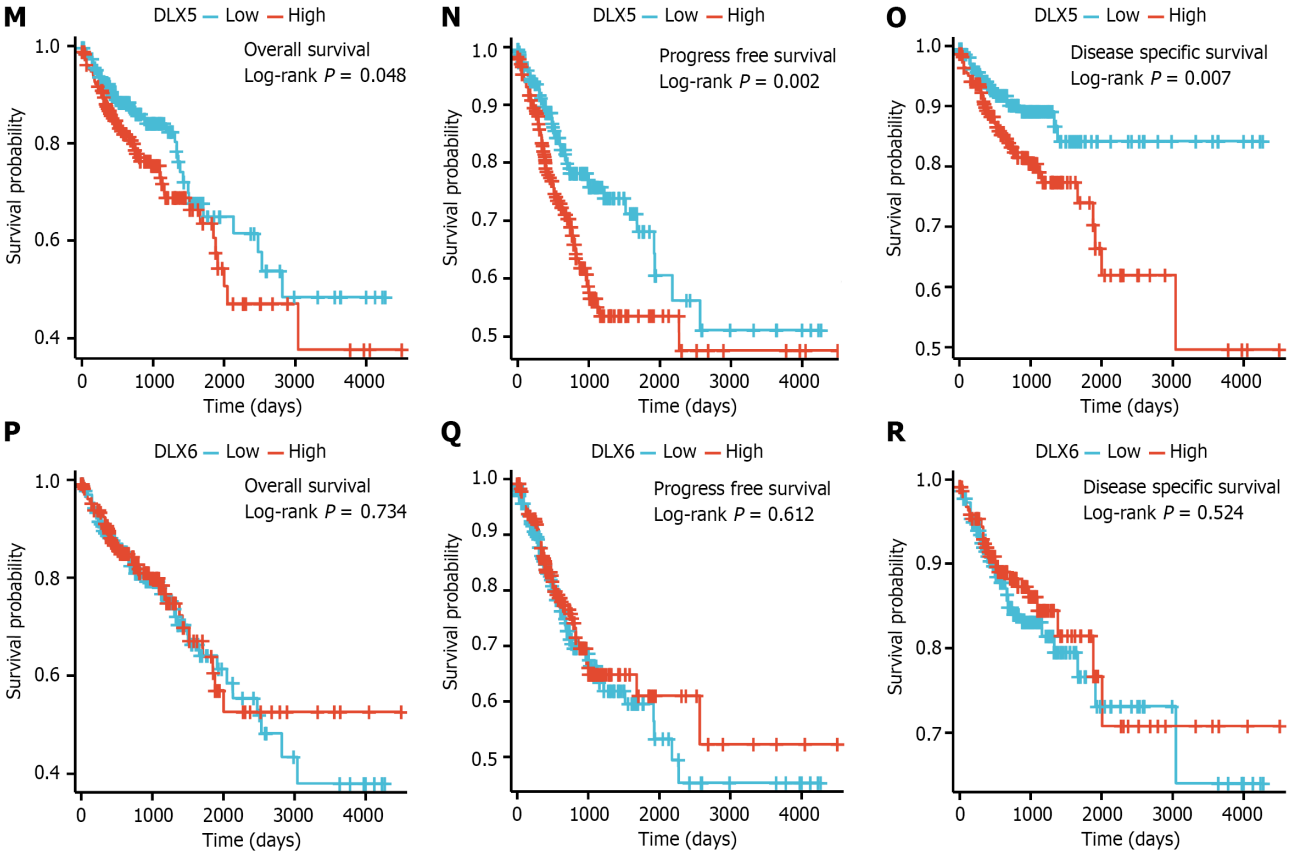

DOI: 10.4251/wjgo.v15.i6.1019 **Copyright** ©The Author(s) 2023.

Figure 5 Survival analysis results for distal-less homeobox genes. A: Overall survival (OS) of distal-less homeobox (*DLX*)1; B: Progression-free survival (PFS) of *DLX1*; C: Disease specific survival (DSS) of *DLX1*; D: OS of *DLX2*; E: PFS of *DLX2*; F: DSS of *DLX2*; G: OS of *DLX3*; H: PFS of *DLX3*; I: DSS of *DLX3*; J: OS of *DLX4*; K: PFS of *DLX4*; L: DSS of *DLX4*; M: OS of *DLX5*; N: PFS of *DLX5*; O: DSS of *DLX5*; P: OS of *DLX6*; Q: PFS of *DLX6*; R: DSS of *DLX6*. *DLX*: Distal-less homeobox.

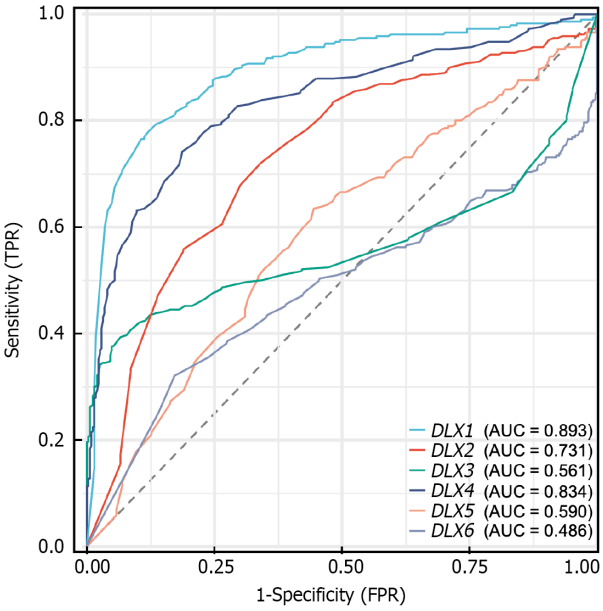

DOI: 10.4251/wjgo.v15.i6.1019 **Copyright** ©The Author(s) 2023.

Figure 6 Receiver operating characteristic curves of distal-less homeobox genes in colon adenocarcinoma and normal colon tissues. The area under the receiver operating characteristic curve is between 0.5 and 1. The closer the area under the curve (AUC) is to 1, the better the diagnosis. the AUC is between 0.5 and 0.7 with low accuracy, the AUC is between 0.7 and 0.9 with some accuracy, and the AUC is above 0.9 with high accuracy. AUC: Area under the curve; *DLX*: Distal-less homeobox; FPR: False positive rate; TPR: True positive rate.

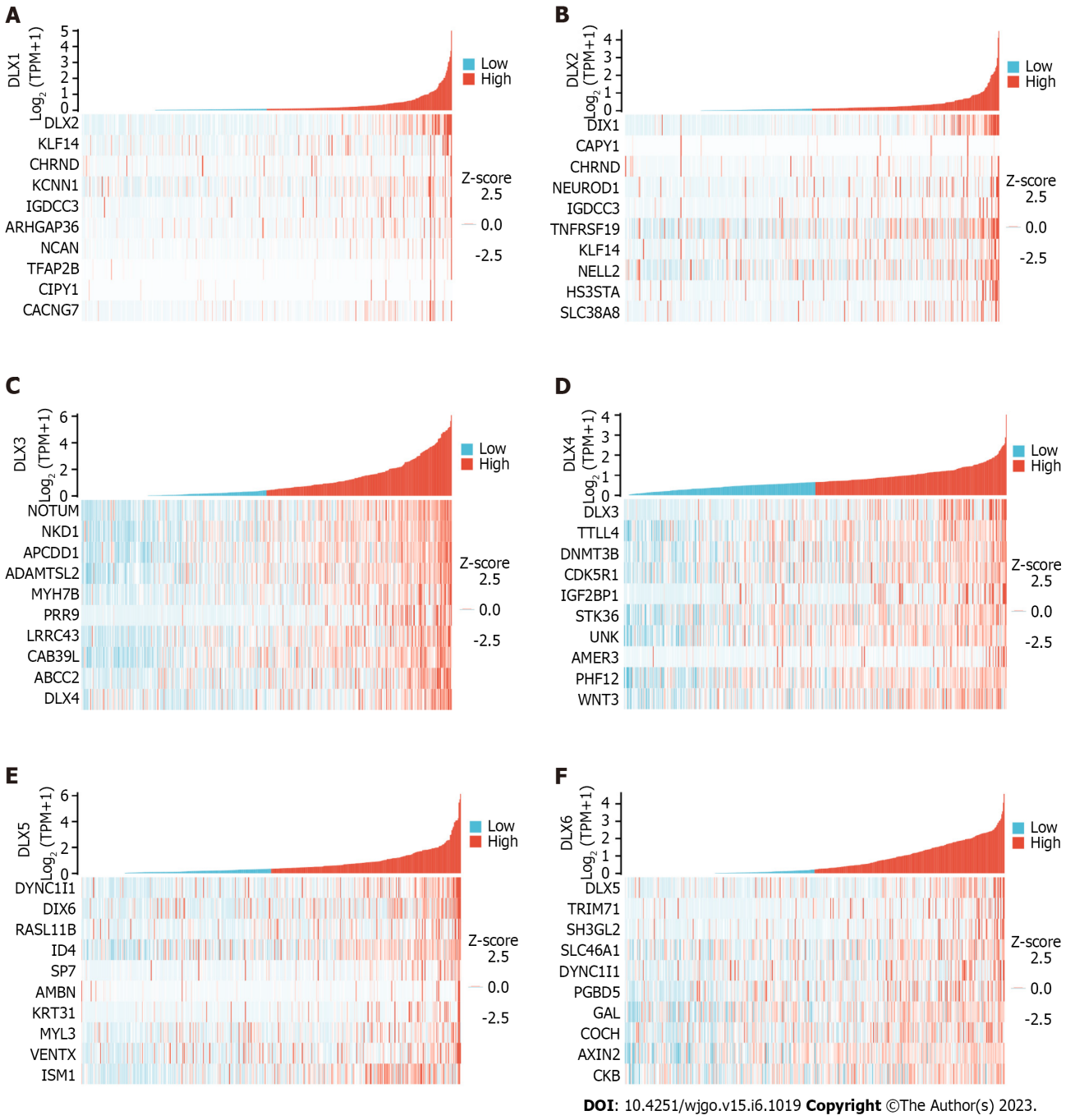

DOI: 10.4251/wjgo.v15.i6.1019

Figure 7 Heatmap plot of top 10 correlated genes to distal-less homeobox genes. A: Distal-less homeobox (*DLX*)1; B: *DLX2*; C: *DLX3*; D: *DLX4*; E: *DLX5*; F: *DLX6*. *DLX*: Distal-less homeobox.

accuracy.

MiR-129-5p has been shown to impede the biological function of cancer cells by inhibiting *DLX1* expression[26]. *DLX1*, a key target of *FOXM1*, has been shown to promote ovarian cancer aggressiveness by enhancing transforming growth factor (TGF)-β/SMAD4 signaling[27]. Circ_*HIPK3* has been demonstrated to promote HCC progression by mediating the miR-582-3p/*DLX2* pathway[23]. In tumor cells, *DLX2/3/4* can be involved in the control of fenretinide (4HPR)-mediated apoptosis[28]. *DLX3* has been shown to be downregulated by miR-133[29]. The homology domain protein *DLX4* has been shown to promote NPC progression through the upregulation of YB-1[25]. *DLX5* regulation of *CCND1* affected the progression of OSCC[11]. *DLX5* has been shown to promote osteosarcoma progression through activation of the NOTCH signaling pathway[30]. *DLX6* has been demonstrated to regulate OSCC cell proliferation through the *EGFR-CCND1* axis[12]. In this study, the *DLX* gene family is suggested to be involved in the development and progression of colon cancer by participating in several pathways, including breast cancer, gastric cancer, the Hippo signaling pathway, the Wnt signaling pathway, and signaling pathways regulating the pluripotency of stem cells, basal cell carcinoma, melanoma, and *Staphylococcus aureus* infection. Dlx-2 is involved in TGF-β- and Wnt-induced inhibition of mitochondria

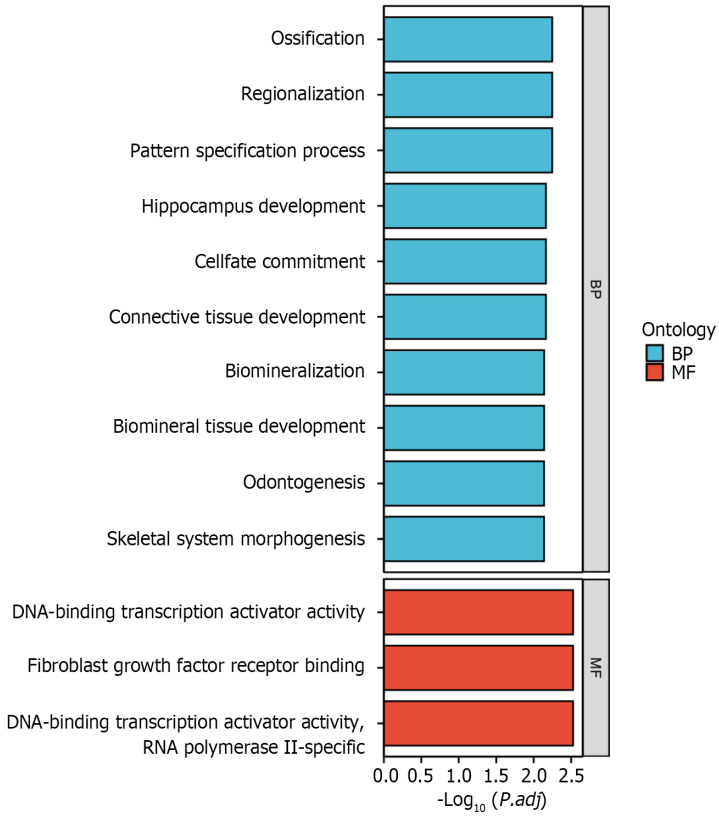

DOI: 10.4251/wjgo.v15.i6.1019 **Copyright** ©The Author(s) 2023.

Figure 8 Gene Ontology analysis of genes associated with distal-less homeobox genes. BP: Biological process; MF: Molecular function.

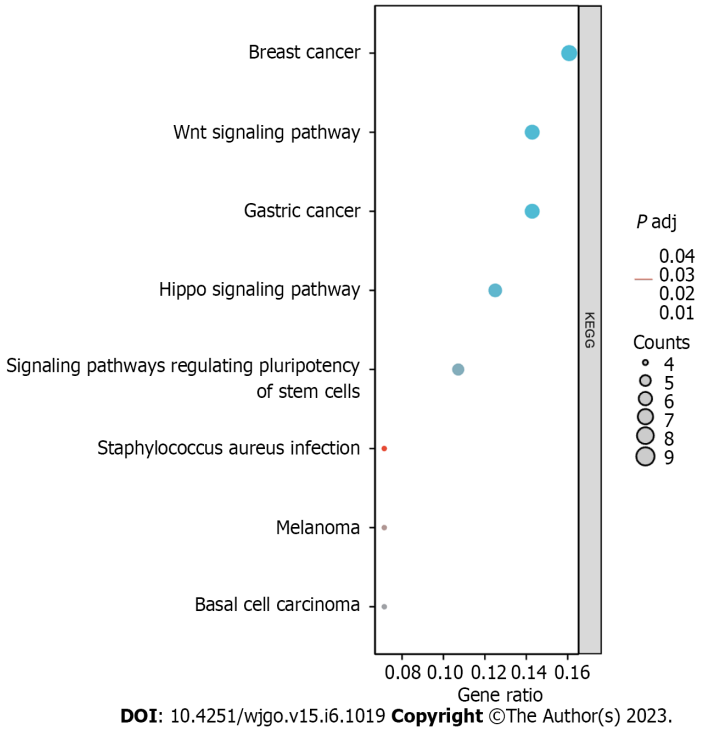

DOI: 10.4251/wjgo.v15.i6.1019 **Copyright** ©The Author(s) 2023.

Figure 9 Kyoto Encyclopedia of Genes and Genomes analysis of genes associated with distal-less homeobox genes. KEGG: Kyoto Encyclopedia of Genes and Genomes.

by epithelial-mesenchymal transition, glycolytic conversion, and Snail activation[31]. However, the specific mechanisms by which the *DLX* gene family mediates the pathways involved in the development of colon cancer need to be further investigated.

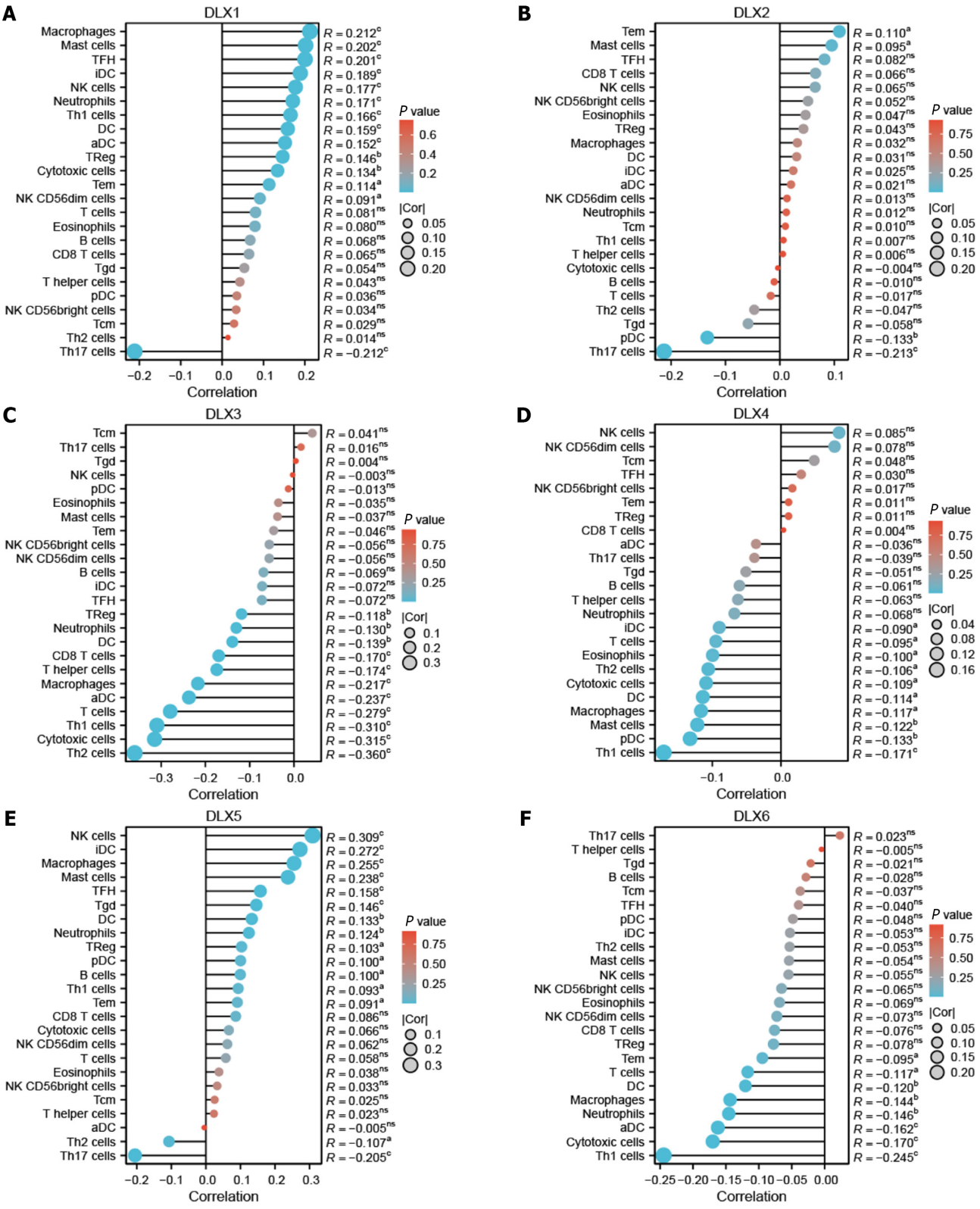

DOI: 10.4251/wjgo.v15.i6.1019

Figure 10 Correlation between the expression of each distal-less homeobox gene and the 24 tumor-infiltrating immune cells of colon adenocarcinoma (lollipop plot). In the color bar, the darker the color, the smaller the *P*-value, indicating a higher statistical significance. The bubble size represents the correlation value, the larger the bubble, the larger the correlation value. A: Correlation between distal-less homeobox (*DLX1*) expression and immune infiltration; B: Correlation between *DLX2* expression and immune infiltration; C: Correlation between *DLX3* expression and immune infiltration; D: Correlation between *DLX4* expression and immune infiltration; E: Correlation between *DLX5* expression and immune infiltration; F: Correlation between *DLX6* expression and immune infiltration. $^{a}P < 0.05$; $^{b}P < 0.01$; $^{c}P < 0.001$. aDC: Activated dendritic cell; DC: Dendritic cell; *DLX*: Distal-less homeobox; iDC: Immature dendritic cell; NK: Natural killer; Tcm: T central memory; Tem: T effector memory; TFH: T follicular helper; Tgd: T gamma delta; Th: T helper.

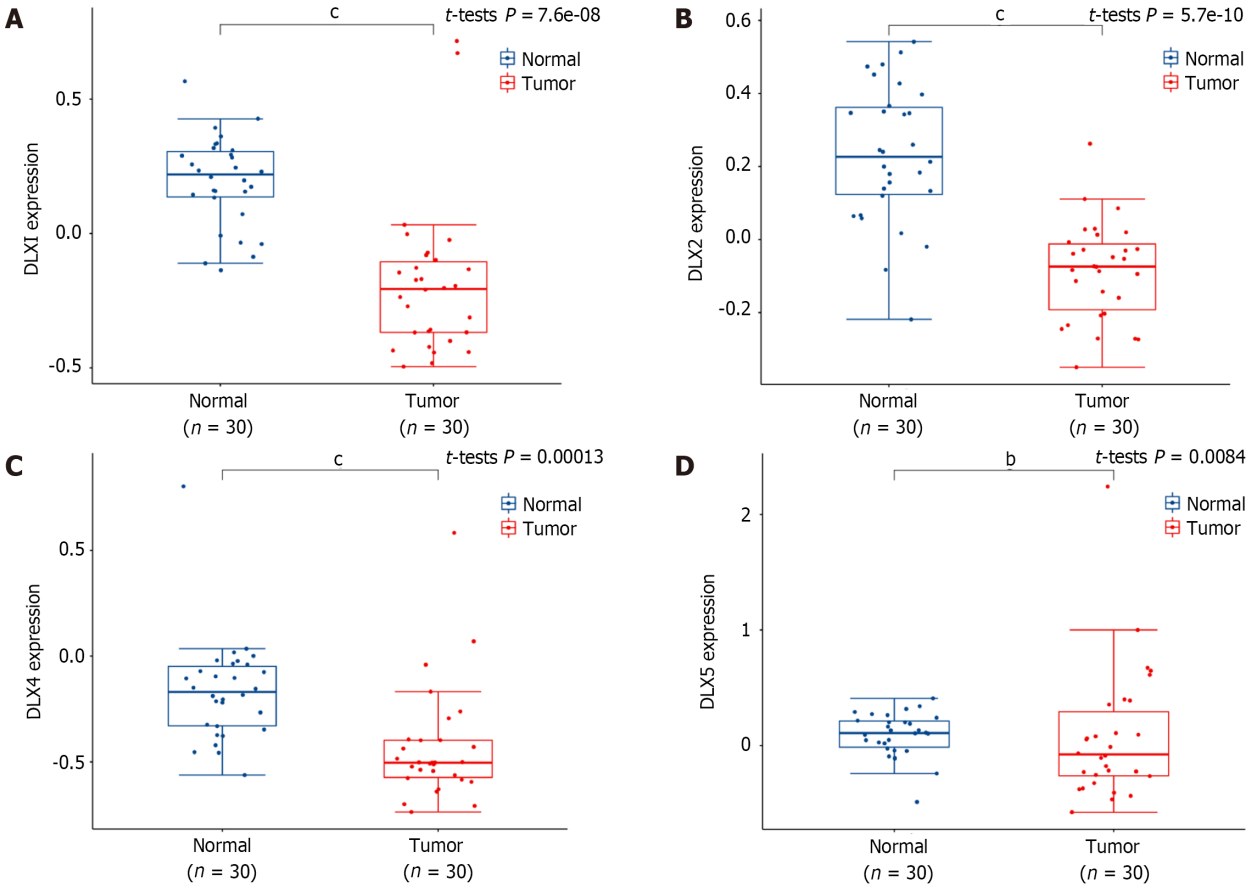

DOI: 10.4251/wjgo.v15.i6.1019

Figure 11 Differential expression of distal-less homeobox genes in colon adenocarcinoma and normal colon tissues (GSE74062). A: Distal-less homeobox (*DLX*)1; B: *DLX2*; C: *DLX4*; D: *DLX5*. $^{b}P < 0.01$; $^{c}P < 0.001$. *DLX*: Distal-less homeobox.

Immune-related mechanisms play an important role in the development of colon cancer, and immunotherapeutic strategies are considered a promising direction for the treatment of this disease[32]. Another important aspect of the current study was that the expression of the *DLX* gene family correlated with different levels of immune infiltration. Here, the expression levels of *DLX* family genes were negatively correlated with some TIICs, and positively correlated with other TIICs. The *DLX* gene family plays an important role in the recruitment and regulation of immune infiltrating cells in colon cancer.

The present study has several limitations. Firstly, colon cancer shows strong heterogeneity, and the mRNA expression levels in the TCGA database are the average mRNA expression levels for all cell types within various colon tumors. Single-cell sequencing is needed to further elucidate the role of *DLX* genes in colon cancer and its subtypes. Secondly, our study findings are not confirmed by biological or molecular experiments.

CONCLUSION

DLX1/2/3/4/5 were significantly aberrantly expressed in colon cancer tissue samples. *DLX 2/3/5* were associated with M stage, pathologic stage, primary therapy outcome, residual tumor, lymphatic invasion, T stage, N stage, age, perineural invasion, and history of colon polyps. *DLX5* was independently correlated with the prognosis of colon cancer in multivariate analysis. *DLX1/2/4* had some accuracy in diagnosing normal and tumor conditions. The *DLX* gene family may be involved in the development and progression of colon cancer by participating in immune infiltration and pathways, including the Hippo signaling pathway, the Wnt signaling pathway, and signaling pathways regulating the pluripotency of stem cells and *Staphylococcus aureus* infection. The results of this study suggest a role for *DLX* family genes as a potential diagnostic or prognostic biomarkers and therapeutic targets in colon cancer.

ARTICLE HIGHLIGHTS

Research background

The distal-less homeobox (*DLX*) gene family plays an important role in several tumors. However, the role of *DLX* gene family in colon cancer is not yet clear.

Research motivation

The aim of this study was to investigate the role of the *DLX* gene family in colon cancer and to establish a sound scientific basis for clinical decision making and risk management.

Research objectives

In this study, we aimed to comprehensively analyze the biological role of the *DLX* gene family in colon cancer.

Research methods

Colon cancer and normal colon tissue samples were collected from the Cancer Genome Atlas (TCGA) and Gene Expression Omnibus databases. We used Wilcoxon rank sum test and t-test to assess *DLX* gene family expression between colon cancer tissue samples and unpaired normal colon tissue samples, cBioPortal to analyze *DLX* gene family variants, R software (version 3.6.3) to analyze *DLX* gene expression in colon cancer and the relationship between *DLX* gene family expression and clinical features and correlation heat map, the survival package [version 3.2-10] and Cox regression module to assess the prognostic value of the *DLX* gene family, the pROC package [version 1.17.0.1] to analyze the diagnostic value of the *DLX* gene family, R software (version 3.6.3) to analyze the possible regulatory mechanisms of *DLX* gene family members and related genes, the GSVA package [version 1.34.0] to analyze the relationship between the *DLX* gene family and immune infiltration, and the ggplot2 [version 3.3.3], the survminer package [version 0.4.9], and the clusterProfiler package [version 3.14.3] for visualization.

Research results

Expression levels of *DLX1/2/3/4/5* were significantly abnormal in tissue from patients with colon cancer. *DLX* gene family expression in colon cancer was significantly associated with clinical characteristics, including M stage, pathological stage, primary treatment outcome, residual tumor, lymphatic invasion, T stage, N stage, age, peripheral invasion, and history of colonic polyps. Results of the multivariate Cox analysis showed *DLX5* to be an independent prognostic factor in patients with colon cancer. *DLX1/2/3/4/5/6* may be involved in the development and progression of colon cancer through mediation of multiple pathways, including the Hippo signaling pathway, the Wnt signaling pathway, and signaling pathways regulating the pluripotency of stem cells. *DLX1/2/3/4/5/6* are associated with immune infiltration.

Research conclusions

DLX family genes may function as potential diagnostic or prognostic biomarkers and therapeutic targets for colon cancer.

Research perspectives

It may be possible to use *DLX* family genes as a diagnostic or prognostic biomarkers or therapeutic targets for colon cancer.

FOOTNOTES

Author contributions: Chen YC and Peng H participated in study design, and data collection and analysis; Chen YC, Li DB, and Wang DL performed the data analysis; Chen YC and Peng H drafted the manuscript; Chen YC and Peng H revised the manuscript; All authors read and approved the final manuscript.

Institutional review board statement: The current study does not require approval from an ethics committee.

Clinical trial registration statement: This study did not involve a clinical trial registration statement.

Informed consent statement: The data that support the findings of this study are publicly available. The current study does not require signed informed consent documents.

Conflict-of-interest statement: All the authors report having no relevant conflicts of interest for this article.

Data sharing statement: All data and material are public.

Country/Territory of origin: China

ORCID number: Yong-Cheng Chen 0000-0002-9594-9512; Dong-Bing Li 0000-0002-5227-9643; Dong-Liang Wang 0000-0003-4073-3332; Hui Peng 0000-0001-9970-1947.

S-Editor: Wang JJ
L-Editor: Filipodia
P-Editor: Zhang XD

REFERENCES

1 **Bray F**, Ferlay J, Soerjomataram I, Siegel RL, Torre LA, Jemal A. Global cancer statistics 2018: GLOBOCAN estimates of incidence and mortality worldwide for 36 cancers in 185 countries. *CA Cancer J Clin* 2018; **68**: 394-424 [PMID: 30207593 DOI: 10.3322/caac.21492]

2 **Alibolandi M**, Rezvani R, Farzad SA, Taghdisi SM, Abnous K, Ramezani M. Tetrac-conjugated polymersomes for integrin-targeted delivery of camptothecin to colon adenocarcinoma *in vitro* and in vivo. *Int J Pharm* 2017; **532**: 581-594 [PMID: 28935257 DOI: 10.1016/j.ijpharm.2017.09.039]

3 **Sargent DJ**, Wieand HS, Haller DG, Gray R, Benedetti JK, Buyse M, Labianca R, Seitz JF, O'Callaghan CJ, Francini G, Grothey A, O'Connell M, Catalano PJ, Blanke CD, Kerr D, Green E, Wolmark N, Andre T, Goldberg RM, De Gramont A. Disease-free survival versus overall survival as a primary end point for adjuvant colon cancer studies: individual patient data from 20,898 patients on 18 randomized trials. *J Clin Oncol* 2005; **23**: 8664-8670 [PMID: 16260700 DOI: 10.1200/jco.2005.01.6071]

4 **Zhou Y**, Zang Y, Yang Y, Xiang J, Chen Z. Candidate genes involved in metastasis of colon cancer identified by integrated analysis. *Cancer Med* 2019; **8**: 2338-2347 [PMID: 30884206 DOI: 10.1002/cam4.2071]

5 **Cohen SM**, Brönner G, Küttner F, Jürgens G, Jäckle H. Distal-less encodes a homoeodomain protein required for limb development in Drosophila. *Nature* 1989; **338**: 432-434 [PMID: 2564639 DOI: 10.1038/338432a0]

6 **Leyten GH**, Hessels D, Smit FP, Jannink SA, de Jong H, Melchers WJ, Cornel EB, de Reijke TM, Vergunst H, Kil P, Knipscheer BC, Hulsbergen-van de Kaa CA, Mulders PF, van Oort IM, Schalken JA. Identification of a Candidate Gene Panel for the Early Diagnosis of Prostate Cancer. *Clin Cancer Res* 2015; **21**: 3061-3070 [PMID: 25788493 DOI: 10.1158/1078-0432.CCR-14-3334]

7 **Liu J**, Cui X, Qu L, Hua L, Wu M, Shen Z, Lu C, Ni R. Overexpression of DLX2 is associated with poor prognosis and sorafenib resistance in hepatocellular carcinoma. *Exp Mol Pathol* 2016; **101**: 58-65 [PMID: 27302463 DOI: 10.1016/j.yexmp.2016.06.003]

8 **Yan ZH**, Bao ZS, Yan W, Liu YW, Zhang CB, Wang HJ, Feng Y, Wang YZ, Zhang W, You G, Zhang QG, Jiang T. Upregulation of DLX2 confers a poor prognosis in glioblastoma patients by inducing a proliferative phenotype. *Curr Mol Med* 2013; **13**: 438-445 [PMID: 23331016]

9 **Bhattacharya S**, Kim JC, Ogawa Y, Nakato G, Nagle V, Brooks SR, Udey MC, Morasso MI. DLX3-Dependent STAT3 Signaling in Keratinocytes Regulates Skin Immune Homeostasis. *J Invest Dermatol* 2018; **138**: 1052-1061 [PMID: 29246798 DOI: 10.1016/j.jid.2017.11.033]

10 **Gao Y**, Li Z, Guo X, Liu Y, Zhang K. DLX4 as a prognostic marker for hepatocellular carcinoma. *Neoplasma* 2014; **61**: 318-323 [PMID: 24824934 DOI: 10.4149/neo_2014_041]

11 **Zhang J**, Wu J, Chen Y, Zhang W. Dlx5 promotes cancer progression through regulation of CCND1 in oral squamous cell carcinoma (OSCC). *Biochem Cell Biol* 2021; **99**: 424-434 [PMID: 34283652 DOI: 10.1139/bcb-2020-0523]

12 **Liang J**, Liu J, Deng Z, Liu Z, Liang L. DLX6 promotes cell proliferation and survival in oral squamous cell carcinoma. *Oral Dis* 2022; **28**: 87-96 [PMID: 33215805 DOI: 10.1111/odi.13728]

13 **Chen J**, Tang H, Li T, Jiang K, Zhong H, Wu Y, He J, Li D, Li M, Cai X. Comprehensive Analysis of the Expression, Prognosis, and Biological Significance of OVOLs in Breast Cancer. *Int J Gen Med* 2021; **14**: 3951-3960 [PMID: 34345183 DOI: 10.2147/IJGM.S326402]

14 **Lin Z**, Huang W, Yi Y, Li D, Xie Z, Li Z, Ye M. LncRNA ADAMTS9-AS2 is a Prognostic Biomarker and Correlated with Immune Infiltrates in Lung Adenocarcinoma. *Int J Gen Med* 2021; **14**: 8541-8555 [PMID: 34849000 DOI: 10.2147/IJGM.S340683]

15 **Liang W**, Lu Y, Pan X, Zeng Y, Zheng W, Li Y, Nie Y, Li D, Wang D. Decreased Expression of a Novel lncRNA FAM181A-AS1 is Associated with Poor Prognosis and Immune Infiltration in Lung Adenocarcinoma. *Pharmgenomics Pers Med* 2022; **15**: 985-998 [PMID: 36482943 DOI: 10.2147/PGPM.S384901]

16 **Vivian J**, Rao AA, Nothaft FA, Ketchum C, Armstrong J, Novak A, Pfeil J, Narkizian J, Deran AD, Musselman-Brown A, Schmidt H, Amstutz P, Craft B, Goldman M, Rosenbloom K, Cline M, O'Connor B, Hanna M, Birger C, Kent WJ, Patterson DA, Joseph AD, Zhu J, Zaranek S, Getz G, Haussler D, Paten B. Toil enables reproducible, open source, big biomedical data analyses. *Nat Biotechnol* 2017; **35**: 314-316 [PMID: 28398314 DOI: 10.1038/nbt.3772]

17 **Yang D**, Liu M, Jiang J, Luo Y, Wang Y, Chen H, Li D, Wang D, Yang Z. Comprehensive Analysis of DMRT3 as a Potential Biomarker Associated with the Immune Infiltration in a Pan-Cancer Analysis and Validation in Lung Adenocarcinoma. *Cancers (Basel)* 2022; **14** [PMID: 36551704 DOI: 10.3390/cancers14246220]

18 **Liu J**, Lichtenberg T, Hoadley KA, Poisson LM, Lazar AJ, Cherniack AD, Kovatich AJ, Benz CC, Levine DA, Lee AV, Omberg L, Wolf DM, Shriver CD, Thorsson V; Cancer Genome Atlas Research Network, Hu H. An Integrated TCGA Pan-Cancer Clinical Data Resource to Drive High-Quality Survival Outcome Analytics. *Cell* 2018; **173**: 400-416.e11 [PMID: 29625055 DOI: 10.1016/j.cell.2018.02.052]

19 **Hänzelmann S**, Castelo R, Guinney J. GSVA: gene set variation analysis for microarray and RNA-seq data. *BMC Bioinformatics* 2013; **14**: 7 [PMID: 23323831 DOI: 10.1186/1471-2105-14-7]

20 **Lu X**, Jing L, Liu S, Wang H, Chen B. miR-149-3p Is a Potential Prognosis Biomarker and Correlated with Immune Infiltrates in Uterine Corpus Endometrial Carcinoma. *Int J Endocrinol* 2022; **2022**: 5006123 [PMID: 35719192 DOI: 10.1155/2022/5006123]

21 **Bindea G**, Mlecnik B, Tosolini M, Kirilovsky A, Waldner M, Obenauf AC, Angell H, Fredriksen T, Lafontaine L, Berger A, Bruneval P, Fridman WH, Becker C, Pagès F, Speicher MR, Trajanoski Z, Galon J. Spatiotemporal dynamics of intratumoral immune cells reveal the immune landscape in human cancer. *Immunity* 2013; **39**: 782-795 [PMID: 24138885 DOI: 10.1016/j.immuni.2013.10.003]

22 **Sun B**, Fan Y, Yang A, Liang L, Cao J. MicroRNA-539 functions as a tumour suppressor in prostate cancer *via* the TGF-β /Smad4 signalling pathway by down-regulating DLX1. *J Cell Mol Med* 2019; **23**: 5934-5948 [PMID: 31298493 DOI: 10.1111/jcmm.14402]

23 **Zhang H**, Dai Q, Zheng L, Yuan X, Pan S, Deng J. Knockdown of circ_HIPK3 inhibits tumorigenesis of hepatocellular carcinoma *via* the miR-582-3p/DLX2 axis. *Biochem Biophys Res Commun* 2020; **533**: 501-509 [PMID: 32977948 DOI: 10.1016/j.bbrc.2020.09.050]

24 **Tang P**, Huang H, Chang J, Zhao GF, Lu ML, Wang Y. Increased expression of DLX2 correlates with advanced stage of gastric adenocarcinoma. *World J Gastroenterol* 2013; **19**: 2697-2703 [PMID: 23674878 DOI: 10.3748/wjg.v19.i17.2697]

25 **Ling Z**, Long X, Li J, Feng M. Homeodomain protein DLX4 facilitates nasopharyngeal carcinoma progression *via* up-regulation of YB-1. *Genes Cells* 2020; **25**: 466-474 [PMID: 32281175 DOI: 10.1111/gtc.12772]

26 **Li Q**, Xu K, Tian J, Lu Z, Pu J. MiR-129-5p/DLX1 signalling axis mediates functions of prostate cancer during malignant progression. *Andrologia* 2021; **53**: e14230 [PMID: 34472106 DOI: 10.1111/and.14230]

27 **Chan DW**, Hui WW, Wang JJ, Yung MM, Hui LM, Qin Y, Liang RR, Leung TH, Xu D, Chan KK, Yao KM, Tsang BK, Ngan HY. DLX1 acts as a crucial target of FOXM1 to promote ovarian cancer aggressiveness by enhancing TGF-β/ SMAD4 signaling. *Oncogene* 2017; **36**: 1404-1416 [PMID: 27593933 DOI: 10.1038/onc.2016.307]

28 **Ferrari N**, Paleari L, Palmisano GL, Tammaro P, Levi G, Albini A, Brigati C. Induction of apoptosis by fenretinide in tumor cell lines correlates with DLX2, DLX3 and DLX4 gene expression. *Oncol Rep* 2003; **10**: 973-977 [PMID: 12792755]

29 **Qadir AS**, Lee J, Lee YS, Woo KM, Ryoo HM, Baek JH. Distal-less homeobox 3, a negative regulator of myogenesis, is downregulated by microRNA-133. *J Cell Biochem* 2019; **120**: 2226-2235 [PMID: 30277585 DOI: 10.1002/jcb.27533]

30 **Zhang X**, Bian H, Wei W, Wang Q, Chen J, Hei R, Chen C, Wu X, Yuan H, Gu J, Lu Y, Cai C, Zheng Q. DLX5 promotes osteosarcoma progression *via* activation of the NOTCH signaling pathway. *Am J Cancer Res* 2021; **11**: 3354-3374 [PMID: 34249467]

31 **Lee SY**, Jeon HM, Ju MK, Jeong EK, Kim CH, Yoo MA, Park HG, Han SI, Kang HS. Dlx-2 is implicated in TGF-β- and Wnt-induced epithelial-mesenchymal, glycolytic switch, and mitochondrial repression by Snail activation. *Int J Oncol* 2015; **46**: 1768-1780 [PMID: 25651912 DOI: 10.3892/ijo.2015.2874]

32 **Procaccio L**, Schirripa M, Fassan M, Vecchione L, Bergamo F, Prete AA, Intini R, Manai C, Dadduzio V, Boscolo A, Zagonel V, Lonardi S. Immunotherapy in Gastrointestinal Cancers. *Biomed Res Int* 2017; **2017**: 4346576 [PMID: 28758114 DOI: 10.1155/2017/4346576]

World Journal of Gastrointestinal Oncology

Submit a Manuscript: https://www.f6publishing.com

World J Gastrointest Oncol 2023 June 15; 15(6): 1036-1050

DOI: 10.4251/wjgo.v15.i6.1036

ISSN 1948-5204 (online)

ORIGINAL ARTICLE

Retrospective Cohort Study

Development of a model based on the age-adjusted Charlson comorbidity index to predict survival for resected perihilar cholangiocarcinoma

Yu Pan, Zhi-Peng Liu, Hai-Su Dai, Wei-Yue Chen, Ying Luo, Yu-Zhu Wang, Shu-Yang Gao, Zi-Ran Wang, Jin-Ling Dong, Yun-Hua Liu, Xian-Yu Yin, Xing-Chao Liu, Hai-Ning Fan, Jie Bai, Yan Jiang, Jun-Jie Cheng, Yan-Qi Zhang, Zhi-Yu Chen

Specialty type: Oncology

Provenance and peer review: Unsolicited article; Externally peer reviewed.

Peer-review model: Single blind

Peer-review report's scientific quality classification

Grade A (Excellent): A, A
Grade B (Very good): 0
Grade C (Good): 0
Grade D (Fair): 0
Grade E (Poor): 0

P-Reviewer: Broering DC, Saudi Arabia; Yildiz K, Turkey

Received: February 11, 2023
Peer-review started: February 11, 2023
First decision: April 10, 2023
Revised: April 18, 2023
Accepted: May 4, 2023
Article in press: May 4, 2023
Published online: June 15, 2023

Yu Pan, Zhi-Peng Liu, Hai-Su Dai, Wei-Yue Chen, Yu-Zhu Wang, Shu-Yang Gao, Yun-Hua Liu, Xian-Yu Yin, Jie Bai, Yan Jiang, Jun-Jie Cheng, Zhi-Yu Chen, Department of Hepatobiliary Surgery, Southwest Hospital, Third Military Medical University (Army Medical University), Chongqing 400038, China

Wei-Yue Chen, Clinical Research Center of Oncology, Lishui Hospital of Zhejiang University, Lishui 323000, Zhejiang Province, China

Ying Luo, Faculty of Education, Southwest University, Chongqing 400715, China

Zi-Ran Wang, Department of General Surgery, 903rd Hospital of People's Liberation Army, Hangzhou 310000, Zhejiang Province, China

Jin-Ling Dong, Department of Clinical Pharmacy, The General Hospital of Western Theater Command, Chengdu 610000, Sichuan Province, China

Xing-Chao Liu, Department of Hepatobiliary Surgery, Sichuan Provincial People's Hospital, Chengdu 610000, Sichuan Province, China

Hai-Ning Fan, Department of Hepatobiliary Surgery, Affiliated Hospital of Qinghai University, Xining 810000, Qinghai Province, China

Yan-Qi Zhang, Department of Health Statistics, College of Military Preventive Medicine, Third Military Medical University (Army Medical University), Chongqing 400038, China

Corresponding author: Zhi-Yu Chen, MD, PhD, Academic Editor, Academic Research, Deputy Director, Doctor, Professor, Surgeon, Department of Hepatobiliary Surgery, Southwest Hospital, Third Military Medical University (Army Medical University), No. 30 Gaotanyan Road, Chongqing 400038, China. chenzhiyu_umn@163.com

Abstract

BACKGROUND

Perihilar cholangiocarcinoma (pCCA) has a poor prognosis and urgently needs a better predictive method. The predictive value of the age-adjusted Charlson

comorbidity index (ACCI) for the long-term prognosis of patients with multiple malignancies was recently reported. However, pCCA is one of the most surgically difficult gastrointestinal tumors with the poorest prognosis, and the value of the ACCI for the prognosis of pCCA patients after curative resection is unclear.

AIM

To evaluate the prognostic value of the ACCI and to design an online clinical model for pCCA patients.

METHODS

Consecutive pCCA patients after curative resection between 2010 and 2019 were enrolled from a multicenter database. The patients were randomly assigned 3:1 to training and validation cohorts. In the training and validation cohorts, all patients were divided into low-, moderate-, and high-ACCI groups. Kaplan-Meier curves were used to determine the impact of the ACCI on overall survival (OS) for pCCA patients, and multivariate Cox regression analysis was used to determine the independent risk factors affecting OS. An online clinical model based on the ACCI was developed and validated. The concordance index (C-index), calibration curve, and receiver operating characteristic (ROC) curve were used to evaluate the predictive performance and fit of this model.

RESULTS

A total of 325 patients were included. There were 244 patients in the training cohort and 81 patients in the validation cohort. In the training cohort, 116, 91 and 37 patients were classified into the low-, moderate- and high-ACCI groups. The Kaplan-Meier curves showed that patients in the moderate- and high-ACCI groups had worse survival rates than those in the low-ACCI group. Multivariable analysis revealed that moderate and high ACCI scores were independently associated with OS in pCCA patients after curative resection. In addition, an online clinical model was developed that had ideal C-indexes of 0.725 and 0.675 for predicting OS in the training and validation cohorts. The calibration curve and ROC curve indicated that the model had a good fit and prediction performance.

CONCLUSION

A high ACCI score may predict poor long-term survival in pCCA patients after curative resection. High-risk patients screened by the ACCI-based model should be given more clinical attention in terms of the management of comorbidities and postoperative follow-up.

Key Words: Perihilar cholangiocarcinoma; Age-adjusted Charlson comorbidity index; Resection; Survival; Model; Prognosis

Core Tip: Our study assessed the prognostic value of the age-adjusted Charlson comorbidity index (ACCI) and designed an online clinical model for perihilar cholangiocarcinoma (pCCA). We retrospectively evaluated 496 pCCA patients from multiple centers who underwent radical resection. This study proposed that the ACCI is an independent predictor of pCCA prognosis, and a nomogram based on the ACCI is a promising predictive model for overall survival in pCCA patients.

Citation: Pan Y, Liu ZP, Dai HS, Chen WY, Luo Y, Wang YZ, Gao SY, Wang ZR, Dong JL, Liu YH, Yin XY, Liu XC, Fan HN, Bai J, Jiang Y, Cheng JJ, Zhang YQ, Chen ZY. Development of a model based on the age-adjusted Charlson comorbidity index to predict survival for resected perihilar cholangiocarcinoma. *World J Gastrointest Oncol* 2023; 15(6): 1036-1050

URL: https://www.wjgnet.com/1948-5204/full/v15/i6/1036.htm

DOI: https://dx.doi.org/10.4251/wjgo.v15.i6.1036

INTRODUCTION

Cholangiocarcinoma (CCA) is the most common biliary malignancy and the second most common hepatic malignancy after hepatocellular carcinoma (HCC)[1]. Perihilar CCA (pCCA), arising at the site of biliary fusion or in the right or left hepatic duct, represents 60% of CCA cases[2,3]. The overall

incidence of pCCA has increased progressively worldwide over the past four decades[4-6]. Curative resection provides a possible cure for eligible patients with pCCA[7]. However, even after successful curative resection, the prognosis of most pCCA patients remains unsatisfactory, with a five-year survival rate of approximately 20%[8]. Therefore, the accurate identification of important factors affecting long-term prognosis and screening of patients with a high survival risk is essential to improve long-term survival. However, the specificity and complexity of the anatomical location of pCCA greatly increases the difficulty of surgery. The relationship between whether a patient is "strong" enough to withstand the shock of surgery and long-term prognosis may be overlooked in existing forecasting models.

Comorbidity is defined as the "coexistence of disorders in addition to a primary disease of interest"[9]. The coexistence of cancer and other chronic diseases has significant implications for cancer treatment decisions and outcomes[10-12]. Recent studies indicated the substantial influence of comorbidities on postoperative survival in different kinds of solid neoplasms, including breast, vulvar and colorectal cancers[13,14]. Regrettably, most cancer treatment guidelines do not consider the complex interrelationships between cancer and comorbidities and instead adopt a "single-disease" approach to management. Currently, most clinicians also judge prognosis based on tumor-related information alone, ignoring the patient's own disease status. Although some previous studies have taken comorbidities into account, the simple classification into the presence/absence of comorbidities is not comprehensive[13].

At present, the most frequently used system for evaluating the grade of patients' comorbidity burden is the Charlson comorbidity index (CCI). The CCI has excellent clinical efficacy in predicting patient prognosis by assessing the number of certain comorbidities and their severity[15]. Since age had been determined to affect prognosis, Charlson *et al* developed an additional age-adjusted CCI (ACCI) to correct the final score of the CCI[16]. Recently, the predictive value of the ACCI for long-term prognosis in patients with multiple malignancies, such as prostate cancer, pancreatic cancer, colorectal cancer and HCC, has been determined[17-20]. Nevertheless, pCCA is one of the most surgically difficult gastrointestinal tumors with the poorest prognosis, and the relationship between the ACCI and the prognosis of pCCA has not been studied.

Therefore, a multicenter database was utilized to assess the impact of the ACCI on the long-term prognosis of patients with pCCA after curative resection. Furthermore, to help surgeons make better clinical decisions, a prognostic model to predict the overall survival (OS) of pCCA patients after curative resection was developed in this study based on the ACCI and tumor-related indicators.

MATERIALS AND METHODS

Patient selection

This study retrospectively enrolled newly diagnosed pCCA patients who underwent curative resection between January 2010 and December 2019 at three institutions (Southwest Hospital, Sichuan Provincial People's Hospital and the Affiliated Hospital of Qinghai University) in China. Computer-generated random numbers were used to assign three-quarters of the patients to the training cohort and the remaining one-quarter to the validation cohort. Drawing on the previous methods, the patients in the training and validation cohorts were categorized into three groups by the ACCI score: Low-ACCI (ACCI = 0-1), moderate-ACCI (ACCI = 2-3) and high-ACCI (ACCI ≥ 4) groups[20,21]. The patients were classified by the CCI into low- and high-risk groups according to zero and nonzero scores. All tumors originated from the left or right hepatic ducts, biliary confluence, or common hepatic duct, which were confirmed by postoperative histological examination. All patients underwent hepatectomy, bile duct resection, locoregional lymphadenectomy and choledochojejunostomy. Hepatectomy-pancreaticoduodenectomy and revascularization were performed when necessary. Curative resection was defined as a clear-cut edge without tumor cells under macroscopy and microscopy. The exclusion criteria included the following: (1) Recurrent pCCA; (2) death within 30 d after resection; (3) incomplete medical records; and (4) loss to follow-up.

The study followed the ethical guidelines of the World Medical Association and Declaration of Helsinki. Approval for the present study was obtained from the Ethics Committee of Southwest Hospital (approval number: KY2021129). An informed consent form was signed by all patients prior to surgery.

Data collection

The multicenter database was prospectively created and dynamically maintained, and data were retrospectively collected. Demographic information included sex, age, American Society of Anesthesiologists score, various comorbidities and preoperative percutaneous transhepatic cholangial drainage. Preoperative laboratory variables included alanine aminotransferase, aspartate transaminase, platelet count, albumin, total bilirubin, international normalized ratio, and carbohydrate antigen 19-9 (CA19-9). Surgical variables included extent of hepatectomy, intraoperative blood loss and perioperative blood transfusion. Pathological variables included cirrhosis, maximum tumor size, macrovascular invasion,

microvascular invasion, peripheral nerve invasion, tumor differentiation, lymphoid metastasis, 8th American Joint Committee on Cancer (AJCC) stage[22] and Bismuth classification[23].

Major hepatectomy was defined as three or more resected Couinaud liver segments, while minor hepatectomy was defined as two or fewer resected Couinaud liver segments. All pathological variables were confirmed by postoperative pathological examination.

Assessment of comorbidities

The patients' preoperative comorbidities were rigorously assessed based on the disease definition[15]. The comorbidity severity was assessed by the CCI and ACCI[16]. The CCI incorporates nineteen common preoperative comorbidities, with each weighing from 1 to 6 points. On the basis of the CCI, the ACCI considers the influence of age on prognosis. As shown in Table 1, the risk increases by 1 point for each decade of age over 40 years (50-59 years, 1 point; 60-69 years, 2 points; 70-79 years, 3 points; and > 80 years, 4 points), and the points for age are added to the total ACCI score.

Follow-up

All patients were followed up in the participating hospitals after discharge. A standardized follow-up protocol was strictly followed, which included a physical examination, laboratory tests (tumor biomarkers and liver function) and imaging examinations. Imaging examinations included abdominal contrast-enhanced ultrasound (CEUS), contrast-enhanced computed tomography (CT) and magnetic resonance imaging (MRI). Imaging examinations were performed at least once every 2 mo in the first year after resection and then every 3 mo from the second year on. Recurrence was defined as the appearance of a new lesion or multiple new lesions on CEUS, contrast-enhanced CT or MRI. In the case of recurrence, conservative treatment, systemic chemotherapy, and repeat surgical resection were available options, and the treatment strategy was determined considering the doctor's advice and the patient's own wishes. The endpoint was OS after pCCA resection, which was defined as the interval between the date of surgery and the date of patient death or the last follow-up. The last follow-up date for all patients was September 2022.

Statistical analysis

Continuous variables with a normal distribution are expressed as the mean ± SD or median (range), and Student's *t* test or the Mann-Whitney *U* test was used as appropriate. Categorical variables are expressed as numbers and percentages, and the χ^2 test or Fisher's exact test was used as appropriate. According to our previous studies, the included continuous variables were transformed into categorical variables[24,25]. The Kaplan-Meier method was used to calculate the OS of patients. The log-rank test was used to compare OS between the low- and moderate-ACCI groups and between the low- and high-ACCI groups. Multivariate Cox regression analysis was then performed to determine independent risk factors associated with reduced OS after curative resection of pCCA. The hazard ratio (HR) and its 95% confidence interval (CI) were estimated in univariate and multivariate Cox regression analyses. In particular, variables with a significant P value < 0.10 in the univariate analysis were included in the multivariate Cox regression analysis.

The nomogram factors were selected based on the independent variables associated with OS in multivariate Cox regression analysis to construct the nomogram model. Calibration curves and Harrell's concordance index (C-index) were applied to evaluate the fit and accuracy of the nomogram. Furthermore, the discriminative power of the model was assessed by a receiver operating characteristic (ROC) curve through the "survivalROC" package in R. The comparison between the nomogram and the 8th AJCC staging system was achieved using decision curve analysis (DCA) through the "rmda" package in R. For the validation cohort, the performance evaluation of the model was performed using the same approach as that in the training cohort. According to the ROC curve for the prediction of 1-year OS, the optimal cutoff value of the nomogram score was calculated, and all patients were divided into high- and low-risk groups. Using the Kaplan-Meier method and the log-rank test, OS rates were compared between the low- and high-risk groups.

Statistical analysis was performed using SPSS 26.0 (SPSS, Chicago, IL, United States) and R software (version 4.1.3. https://www.r-project.org/wDyn). An internet browser calculator based on the model was constructed by using the "DynNom" package in R. Statistical significance was set at $P < 0.05$ for all analyses.

RESULTS

Baseline characteristics and clinical variables

Of 496 pCCA patients who underwent radical resection during the study period, 171 patients were excluded according to the exclusion criteria, and 325 pCCA patients were finally included in this study. Of these, 244 patients were assigned to the training cohort, and the remaining 81 patients were assigned to the validation cohort, as shown in Supplementary Figure 1. In the training cohort, the low-, mode-

Table 1 Weighted index of comorbidities in the age-adjusted Charlson comorbidity index and patient distribution

Conditions	Training cohort (*n* = 244)	Validation cohort (*n* = 81)	Total patients (*n* = 325)
1 point per decade for age > 40 (0 to 4 points)			
< 50	88 (36.1)	27 (33.3)	115 (35.4)
50-59	64 (26.2)	25 (30.9)	89 (27.4)
60-69	55 (22.5)	19 (23.5)	74 (22.8)
70-79	27 (11.1)	7 (8.6)	34 (10.5)
≥ 80	10 (4.1)	3 (3.7)	13 (4.0)
1 point			
Mild liver disease	42 (17.2)	12 (14.8)	54 (16.6)
Peptic ulcer disease	11 (4.5)	4 (4.9)	15 (4.6)
Congestive heart failure	9 (3.6)	2 (2.4)	11 (3.4)
Peripheral vascular disease	9 (3.6)	5 (6.1)	14 (4.3)
Cerebrovascular disease	6 (2.4)	1 (1.2)	7 (2.2)
Chronic pulmonary disease	6 (2.4)	1 (1.2)	7 (2.2)
Connective tissue disease	4 (1.6)	3 (3.7)	7 (2.2)
Myocardial infarction	0 (0.0)	0 (0.0)	0 (0.0)
Dementia	0 (0.0)	0 (0.0)	0 (0.0)
Diabetes without end-organ damage	42 (17.2)	12 (14.8)	54 (16.6)
2 points			
Diabetes with end-organ damage	10 (4.1)	4 (4.9)	14 (4.3)
Moderate/severe renal disease	8 (3.2)	1 (1.2)	9 (2.8)
Other tumor	0 (0.0)	0 (0.0)	0 (0.0)
Leukemia	0 (0.0)	0 (0.0)	0 (0.0)
Hemiplegia/paraplegia	0 (0.0)	0 (0.0)	0 (0.0)
Malignant lymphoma	0 (0.0)	0 (0.0)	0 (0.0)
3 points			
Moderate/severe liver disease	3 (1.2)	0 (0.0)	3 (0.9)
6 points			
Metastatic solid tumor	0 (0.0)	0 (0.0)	0 (0.0)
AIDS	0 (0.0)	0 (0.0)	0 (0.0)

AIDS: Acquired immune deficiency syndrome.

rate-, and high-ACCI groups had 116, 91 and 37 patients, respectively. The distribution of the different comorbidities is summarized in Table 1. Among 325 patients, the most common comorbidities were mild liver disease and diabetes mellitus without end-organ damage, with 54 cases each (16.6%). Of the 1-point comorbidities, mild liver disease, peptic ulcer disease and peripheral vascular disease were the most frequent, with proportions of 16.6%, 4.6% and 4.3%, followed by congestive heart failure. Among the 2-point comorbidities, 14 patients (4.3%) were diagnosed with moderate/severe renal disease, and 9 patients (2.8%) were diagnosed with diabetes with end-organ damage. Of all comorbidities greater than 2 points, 3 patients (0.9%) were diagnosed with moderate/severe liver disease. A comparison of patient characteristics across the ACCI groups in the training cohort is shown in Table 2. Compared to patients in the low-ACCI and moderate-ACCI groups, those in the high-ACCI group were more often older than 70 years and had higher CCI scores. There were no significant differences in other characteristics across the groups. Similar results for the comparison of patient characteristics by the ACCI groups in the validation cohort are shown in Supplementary Table 1.

Table 2 Comparison of patient characteristics between the age-adjusted Charlson comorbidity index groups in the training cohort

Patient demographics	Total (*n* = 244)	ACCI = 0-1 (*n* = 116)	ACCI = 2-3 (*n* = 91)	ACCI ≥ 4 (*n* = 37)	*P* value
Sex, Female/Male	102/142 (41.8/58.2)	48/68 (41.4/58.6)	38/53 (41.8/58.2)	16/21 (43.2/56.8)	0.980
Age (years), ≤ 70/> 70	207/37 (84.8/15.2)	116/0 (100.0/0)	91/0 (100.0/0)	0/37 (0/100.0)	< 0.001
CCI, Low/High	96/148 (39.3/60.7)	57/59 (49.1/50.9)	34/57 (37.4/62.6)	5/22 (13.5/86.5)	0.001
Diabetes, No/Yes	224/20 (91.8/8.2)	106/10 (91.4/8.6)	85/6 (93.4/6.6)	33/4 (89.2/10.8)	0.714
Cirrhosis, No/Yes	222/22 (91.0/9.0)	109/7 (94.0/6.0)	82/9 (90.1/9.9)	31/6 (83.8/16.2)	0.159
ALT (U/L), ≤ 40/> 40	64/180 (26.2/73.8)	28/88 (24.1/75.9)	29/62 (31.9/68.1)	7/30 (18.9/81.1)	0.249
AST (U/L), ≤ 40/> 40	63/181 (25.8/74.2)	35/81 (30.2/69.8)	21/70 (23.1/76.9)	7/30 (18.9/81.1)	0.297
PLT (× 10^9/L), ≥ 100/< 100	11/233 (4.5/95.5)	6/110 (5.2/94.8)	4/87 (4.4/95.6)	1/36 (2.7/97.3)	0.818
ALB (g/L), ≥ 35/< 35	161/83 (66.0/34.0)	80/38 (69.0/31.0)	60/31 (65.9/34.1)	21/16 (56.8/43.2)	0.394
TB (mg/dL), ≤ 1/> 1	51/193 (20.9/79.1)	26/90 (22.4/77.6)	20/71 (22.0/78.0)	5/32 (13.5/86.5)	0.485
INR, ≤ 1.25/> 1.25	211/33 (86.5/13.5)	102/14 (87.9/12.1)	78/13 (85.7/14.3)	31/6 (83.8/16.2)	0.785
CA19-9 (U/L), ≤ 150/> 150	111/133 (45.5/54.5)	57/59 (49.1/50.9)	37/54 (40.7/59.3)	17/20 (45.9/54.1)	0.477
Preoperative PTCD, No/Yes	168/76 (68.9/31.1)	82/34 (70.7/29.3)	60/31 (65.9/34.1)	26/11 (70.3/29.7)	0.749
Maximum tumor size (cm), < 3/3-5/> 5	101/117/26 (41.4/48.0/10.7)	55/49/12 (47.4/42.2/10.3)	35/46/10 (38.5/50.5/11.0)	11/22/4 (29.7/59.5/10.8)	0.357
Macrovascular invasion, No/Yes	183/61 (75.0/25.0)	89/27 (76.7./23.3)	66/25 (72.5/27.5)	28/9 (75.7/24.3)	0.783
Microvascular invasion, No/Yes	199/45 (81.6/18.4)	99/17 (85.3/14.7)	69/22 (75.8/24.2)	31/6 (83.8/16.2)	0.200
Perineural infiltration, No/Yes	196/48 (80.3/19.7)	96/20 (82.8/17.2)	70/21 (76.9/23.1)	30/7 (81.1/18.9)	0.573
Tumor differentiation, well/(moderate/poor)	202/42 (82.8/17.2)	98/18 (84.5/15.5)	72/19 (79.1/20.9)	32/5 (86.5/13.5)	0.485
Extent of resection, Minor/Major	62/182 (25.4/74.6)	34/82 (29.3/70.7)	21/70 (23.1/76.9)	7/30 (18.9/81.1)	0.365
8th AJCC staging system, I-II/III/IV	134/99/11 (54.9/40.6/4.5)	67/45/4 (57.8/38.8/3.4)	52/35/4 (57.1/38.5/4.4)	15/19/3 (40.5/51.4/8.1)	0.373
Bismuth classification, I-II/III/IV	55/51/138 (22.5/20.9/56.6)	25/23/68 (21.6/19.8/58.6)	21/22/48 (23.1/24.2/52.7)	9/6/22 (24.3/16.2/59.5)	0.843
Lymphoid metastasis, No (ELN > 4)/No (ELN ≤ 4)/Yes	85/91/68 (34.8/37.3/27.9)	44/40/32 (37.9/34.5/27.6)	31/37/23 (34.1/40.7/25.3)	10/14/13 (27.0/37.8/35.1)	0.657
Intraoperative blood loss (mL), ≤ 500/> 500	91/153 (37.3/62.7)	42/74 (36.2/63.8)	37/54 (40.7/59.3)	12/25 (32.4/67.6)	0.646
Perioperative blood transfusion, No/Yes	85/159 (34.8/65.2)	42/74 (36.2/63.8)	30/61 (33.0/67.0)	13/24 (35.1/64.9)	0.888
Period of follow-up, months[1]	25.7 ± 22.7	32.7 ± 25.4	20.9 ± 18.9	15.7 ± 14.5	0.222
Recurrence during follow-up	183 (75.0)	81 (69.8)	69 (75.8)	33 (89.2)	0.059
Death during follow-up	166 (68.0)	69 (59.5)	66 (72.5)	31 (83.8)	0.011
OS, months[2]	23.0 (19.1-26.9)	34.0 (27.1-40.9)	18.0 (12.9-23.1)	11.0 (9.1-12.9)	< 0.001
1-yr OS rate, %	72.7	91.4	74.6	39.3	
3-yr OS rate, %	32.4	45.6	19.8	14.6	
5-yr OS rate, %	22.3	31.1	11.9	6.0	

[1]Values are the mean ± SD.
[2]Values are the median and 95% confidence interval.
ACCI: Age-adjusted Charlson comorbidity index; AJCC: American Joint Committee on Cancer; ALT: Alanine aminotransferase; ASA: American Society of Anesthesiologists; AST: Aspartate transaminase; CA19-9: Carbohydrate antigen 19-9; CCI: Charlson comorbidity index; INR: International normalized ratio; PLT: Platelet count; PTCD: Percutaneous transhepatic cholangial drainage; OS: Overall survival; ALB: Albumin; TB: Total bilirubin.

Long-term outcomes after resection

The median follow-up time was 24.0 (21.2-26.8) mo in the whole dataset. In the training cohort, 75.0% of the patients (183/244) developed recurrence, and 68.0% of the patients (166/244) died during follow-up. The 1-, 3- and 5-year OS rates were 72.7%, 32.4% and 22.9%, respectively. The 1-, 3-, and 5-year OS rates were 81.7%, 45.6%, and 31.1% in the low-ACCI group; 74.7%, 19.8%, and 15.8% in the moderate-ACCI group; and 39.9%, 14.6%, and 6.0% in the high-ACCI group, as shown in Table 2. The survival rate was lowest in the high-ACCI group and the highest in the low-ACCI group, with a significant difference in survival rates among the three groups ($P < 0.001$), as shown in Figure 1A. In the validation cohort, 73.8% of the patients (59/81) developed recurrence, and 63.0% of the patients (51/81) died during follow-up. The 1-, 3- and 5-year OS rates were 80.1%, 34.7% and 25.2%, respectively, as shown in Supplementary Table 1. Compared with the low-ACCI group, the survival rates were lower in the moderate-ACCI and high-ACCI groups ($P = 0.018$), as shown in Figure 1B.

Multivariable Cox regression analysis of OS

The results of univariate and multivariate analyses of OS for pCCA patients after curative resection are shown in Table 3. Considering the effect of covariance between covariates on the results, age was excluded from the Cox regression model. Finally, seven variables were found to be independently associated with the OS of pCCA, as shown in Table 3: ACCI (2-3 *vs* 0-1) (HR: 1.605, 95%CI: 1.133-2.273, $P = 0.008$); ACCI (≥ 4 *vs* 0-1) (HR: 2.498, 95%CI: 1.614-3.866, $P < 0.001$); CA19-9 (> 150 *vs* ≤ 150 U/L) (HR: 1.471, 95%CI: 1.059-2.043, $P = 0.021$); maximum tumor size (> 5 *vs* < 3 cm) (HR: 1.990, 95%CI: 1.166-3.396, $P = 0.011$); macrovascular invasion (yes *vs* no) (HR: 1.700, 95%CI: 1.198-2.412, $P = 0.003$); microvascular invasion (yes *vs* no) (HR: 1.752, 95%CI: 1.166-2.634, $P = 0.007$); tumor differentiation (poor *vs* well/moderate) (HR: 1.550, 95%CI: 1.042-2.305, $P = 0.030$); and lymphoid metastasis [yes *vs* no (ELN > 4)] (HR: 2.549, 95%CI: 1.684-3.859, $P < 0.001$).

Development and validation of a nomogram for OS

Using the variables from multivariate analysis, a nomogram to assess the OS of patients after curative resection was constructed based on the clinically relevant factors, as shown in Figure 2. To optimize its practicality, the nomogram was also transformed into an internet browser calculator (https://acci.shinyapps.io/newDynNomapp/). The relevant information of patients can be input, and information on the postoperative survival of patients could be obtained. The C-indexes of the prognostic nomogram for predicting OS were 0.725 (95%CI: 0.706-0.744) and 0.675 (95%CI: 0.635-0.715) in the training and validation cohorts, respectively. The calibration curves for the probability of 1-year OS in the training and validation cohorts were plotted, and the results revealed optimal accordance between the nomogram predictions and actual observations in both cohorts, as shown in Figure 3A and B.

Comparing the predictive power of the nomogram and 8th AJCC staging system

The ROC curves for the training and validation cohorts suggested that the nomogram performed better than the 8th AJCC staging system in predicting OS within 1 year after curative resection, as shown in Figure 3C and D. Furthermore, the nomogram was compared with the 8th AJCC staging system by utilizing DCA. As shown in Figure 3E and F, the nomogram demonstrated superior net benefits with a wider range of threshold probabilities compared to the 8th AJCC staging system in predicting the OS of patients in both the training and validation cohorts. All these results indicated that this nomogram was an excellent predictive model for predicting the long-term outcomes of pCCA patients following curative resection.

Risk classification based on the nomogram

According to the ROC curve for the prediction of 1-year OS, the optimal cutoff value of the nomogram score was 156. Therefore, all patients were effectively separated into low- and high-risk groups. In the training cohort, patients in the high-risk group had 1-, 3-, and 5-year OS rates of 51.1%, 11.1%, and 0%, and patients in the low-risk group had 1-, 3-, and 5-year OS rates of 91.5%, 50.1%, and 36.5%, as shown in Figure 4A. The high-risk group had a significantly lower survival rate than the low-risk group ($P < 0.001$). In the validation cohort, patients in the high-risk group had 1-, 3-, and 5-year OS rates of 64.5%, 23.0%, and 0%, and patients in the low-risk group had 1-, 3-, and 5-year OS rates of 91.5%, 61.2%, and 35.7%, as shown in Figure 4B. Similarly, the survival rate was found to be significantly lower in the high-risk group than in the low-risk group ($P = 0.012$).

DISCUSSION

Comorbidities are common in cancer patients and are becoming more prevalent as the population ages [26]. An increasing number of studies have demonstrated that comorbidities potentially affect the development, diagnosis, treatment and prognosis of patients with cancer[11,12,27]. The ACCI is an excellent indicator that combines age and comorbidities. A higher ACCI implies a more complex

Table 3 Univariable and multivariable Cox regression analyses of overall survival in the training cohort

Variable	R comparison	Univariable Cox regression		Multivariable Cox regression	
		HR (95%CI)	*P* value	HR (95%CI)	*P* value[1]
Age	> 70 *vs* ≤ 70 yr	1.793 (1.314-2.447)	< 0.001		
Sex	Male *vs* Female	1.141 (0.838-1.555)	0.402		
Diabetes	Yes *vs* No	1.203 (0.718-2.017)	0.482		
Cirrhosis	Yes *vs* No	1.220 (0.738-2.016)	0.438		
PLT	> 100 *vs* ≤ 100 × 10^9/L	1.538 (0.719-3.290)	0.267		
Albumin	< 35 *vs* ≥ 35	1.131 (0.823-1.555)	0.447		
ALT	> 40 *vs* ≤ 40 U/L	1.202 (0.848-1.704)	0.302		
AST	> 40 *vs* ≤ 40 U/L	1.155 (0.815-1.638)	0.418		
TB	> 1 *vs* ≤ 1 mg/dL	1.204 (0.813-1.785)	0.354		
INR	> 1.25 *vs* ≤ 1.25	1.217 (0.795-1.863)	0.365		
CA19-9	> 150 *vs* ≤ 150 U/L	1.768 (1.289-2.426)	< 0.001	1.471 (1.059-2.043)	0.021
Preoperative PTCD	Yes *vs* No	1.172 (0.848-1.620)	0.336		
Maximum tumor size	3-5 *vs* < 3 cm	1.777 (1.269-2.488)	0.001	1.236 (0.858-1.779)	0.255
	> 5 *vs* < 3 cm	2.289 (1.377-3.803)	0.001	1.990 (1.166-3.396)	0.011
Macrovascular invasion	Yes *vs* No	2.165 (1.539-3.045)	< 0.001	1.700 (1.198-2.412)	0.003
Microvascular invasion	Yes *vs* No	2.212 (1.526-3.205)	< 0.001	1.752 (1.166-2.634)	0.007
Perineural infiltration	Yes *vs* No	1.267 (0.878-1.827)	0.205		
Tumor differentiation	Poor *vs* Well/moderate	1.616 (1.102-2.369)	0.014	1.550 (1.042-2.305)	0.030
Extent of resection	Major *vs* Minor	1.348 (0.941-1.931)	0.104		
Intraoperative blood loss	> 500 *vs* ≤ 500 mL	1.128 (0.821-1.550)	0.457		
Perioperative blood transfusion	Yes *vs* No	1.069 (0.773-1.477)	0.688		
Lymphoid metastasis	No (ELN ≤ 4) *vs* No (ELN > 4)	1.673 (1.146-2.441)	0.008	1.454 (0.987-2.141)	0.058
	Yes *vs* No (ELN > 4)	2.403 (1.618-3.567)	< 0.001	2.549 (1.684-3.859)	< 0.001
CCI	High *vs* Low	1.239 (0.901-1.703)	0.187		
ACCI	Moderate *vs* Low	1.818 (1.292-2.558)	0.001	1.605 (1.133-2.273)	0.008
	High *vs* Low	2.791 (1.818-4.287)	< 0.001	2.498 (1.614-3.866)	< 0.001

[1]Variables found significant at $P < 0.10$ in univariable analysis.

ACCI: Age-adjusted Charlson comorbidity index; ALT: Alanine aminotransferase; ASA: American Society of Anesthesiologists; AST: Aspartate transaminase; CA19-9: Carbohydrate antigen 19-9; CCI: Charlson comorbidity index; CI: Confidence interval; HR: Hazard ratio; INR: International normalized ratio; PLT: Platelet count; PTCD: Percutaneous transhepatic cholangial drainage; ALB: Albumin; TB: Total bilirubin.

preoperative situation, lower tolerance for complicated surgery, more difficult postoperative care and longer postoperative recovery. These conditions will directly impact the patient's perioperative safety and long-term prognosis. There is evidence that patient comorbidities can directly affect the choice of patient treatment modality[28]. Recently, the impact of the ACCI on the long-term prognosis of patients with various gastrointestinal carcinomas, such as gastric, colorectal, and pancreatic cancers, has been demonstrated[18,29,30]. Nevertheless, pCCA is one of the most surgically difficult gastrointestinal tumors with a poor prognosis, but the relationship between the ACCI and the prognosis of pCCA has not been studied. Therefore, our team conducted the first multicenter study to explore the impact of the ACCI on the long-term prognosis of patients after curative resection for pCCA.

In this study, we investigated for the first time the comorbidity distribution of 325 pCCA patients from multiple centers who underwent curative resection. The ACCI was used to assess comorbidity status, and drawing on previous methods, the patients were categorized into three groups by the ACCI score: Low-ACCI (ACCI = 0-1), moderate-ACCI (ACCI = 2-3) and high-ACCI (ACCI ≥ 4) groups. Multivariable analysis revealed that moderate and high ACCI scores were independently associated

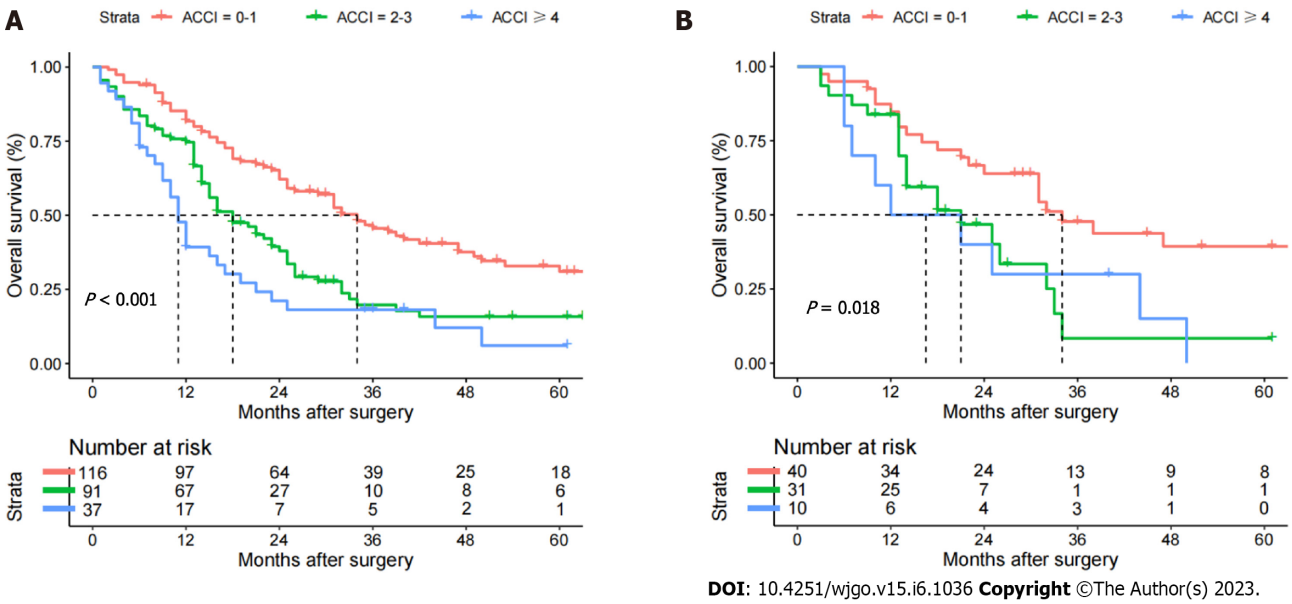

DOI: 10.4251/wjgo.v15.i6.1036 **Copyright** ©The Author(s) 2023.

Figure 1 Overall survival of perihilar cholangiocarcinoma patients in the training and validation cohorts according to the three age-adjusted Charlson comorbidity index groups. Low age-adjusted Charlson comorbidity index (ACCI): 0-1; moderate ACCI: 2-3; high ACCI: ≥ 4. A: Training; B: Validation cohorts. ACCI: Age-adjusted Charlson comorbidity index.

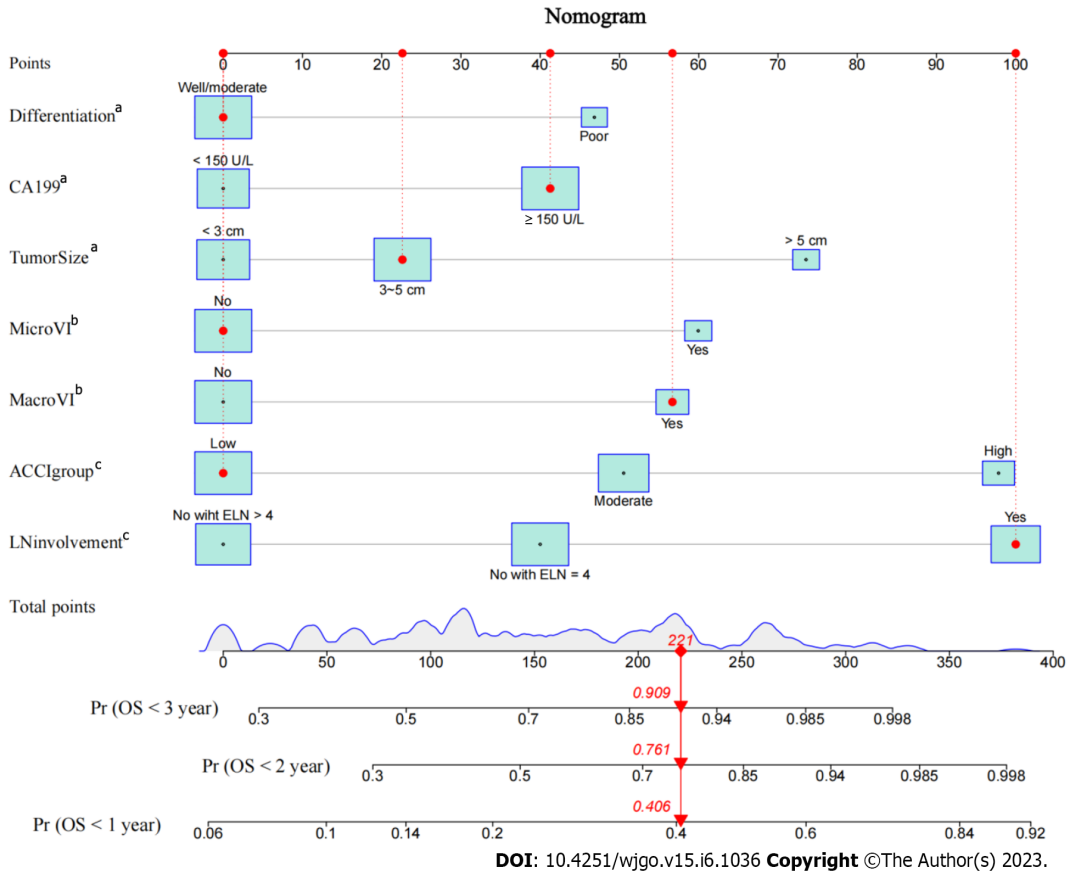

DOI: 10.4251/wjgo.v15.i6.1036 **Copyright** ©The Author(s) 2023.

Figure 2 Age-adjusted Charlson comorbidity index-based enhanced regression nomogram to predict the overall survival of perihilar cholangiocarcinoma patients. ACCI: Age-adjusted Charlson comorbidity index; OS: Overall survival. [a]*P* < 0.05, [b]*P* < 0.01, [c]*P* < 0.001.

with reduced OS after curative resection for pCCA. To enhance guidance on treatment strategies, a clinical prediction model for the OS of pCCA patients after curative resection was constructed based on the ACCI and other independent risk factors associated with worse OS and validated. The satisfactory predictive performance of the model and its ability to identify patients with a high-risk prognosis allows

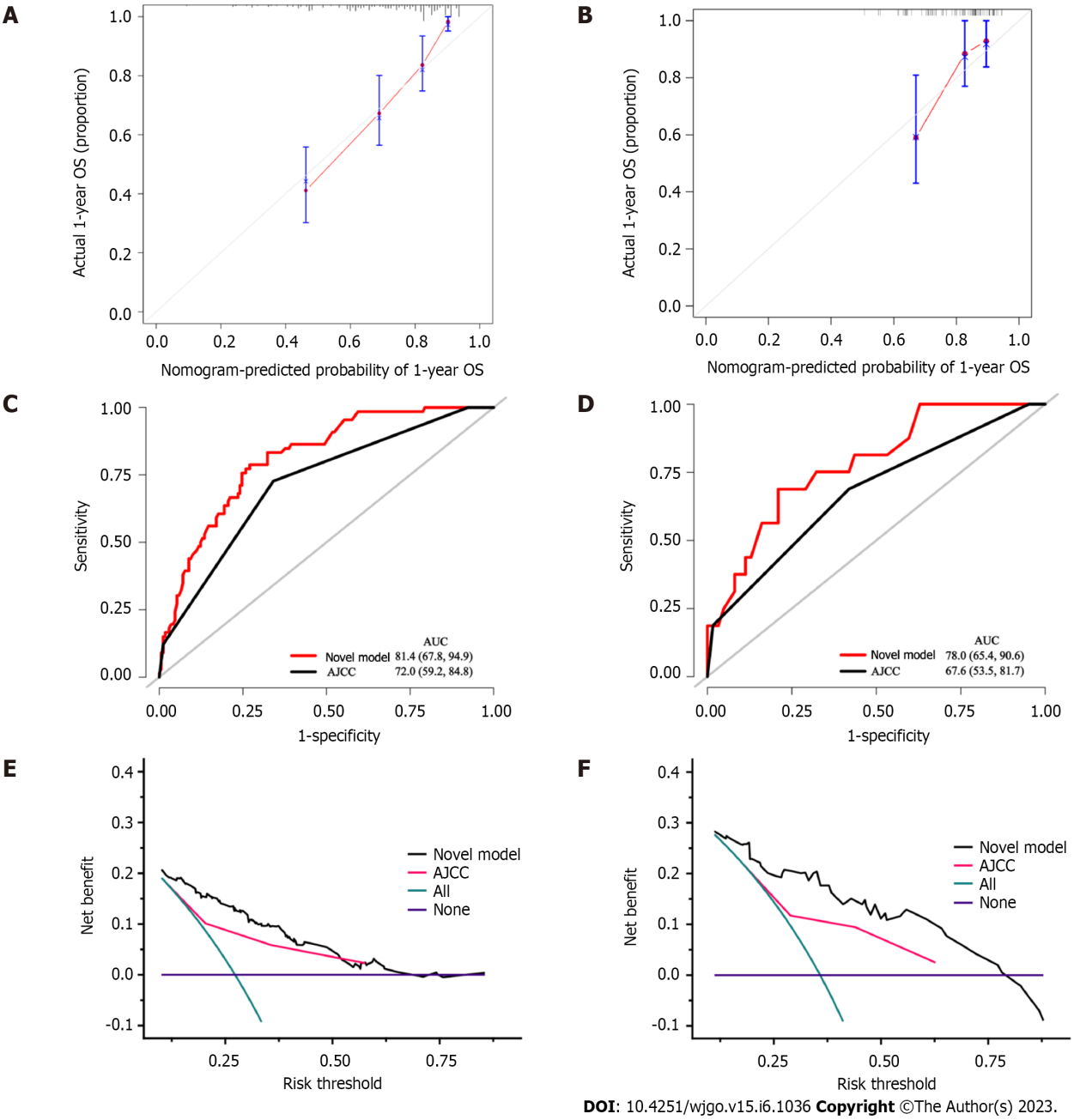

DOI: 10.4251/wjgo.v15.i6.1036 **Copyright** ©The Author(s) 2023.

Figure 3 Calibration curves, receiver operating characteristic curves and decision curve. A and B: Calibration curves for predicting 1-yr overall survival in the training (A) and validation cohorts (B); C-F: Receiver operating characteristic curves (C and D) and decision curve analysis (E and F) for the prognostic model and 8th American Joint Committee on Cancer staging system in the training (C and E) and validation cohorts (D and F). AJCC: American Joint Committee on Cancer; AUC: Area under the curve; OS: Overall survival.

it to guide clinical decision making.

In the long-term survival analysis, the univariate analysis results indicated that CCI did not significantly affect the long-term prognosis of pCCA, whereas ACCI was ultimately proven to be an independent prognostic factor for pCCA. This result suggests that the ACCI, a composite of age and comorbidity, provides a better prognostic assessment for patients. Multivariate Cox regression analysis revealed that moderate and high ACCI scores were independently associated with reduced OS in patients with pCCA after curative resection. This exciting and interesting result might be explained by the following findings.

Advanced age is not a contraindication to hepatobiliary surgery[31], nor is it a comorbidity[32]. However, elderly patients with comorbidities have a slow metabolism and poor recovery. The ACCI is a composite of age and comorbidities, and a high ACCI score indicates that the patient is elderly and/or has one or more comorbidities. Preoperative comorbidities, including diabetes, respiratory disease, and cardiovascular disease, are more common in older patients. Organ reserve function is reduced, and the long-term use of multiple medications can lead to further liver damage. Some pCCA patients may have prolonged obstructive jaundice prior to admission, which leads to a further decline in liver function.

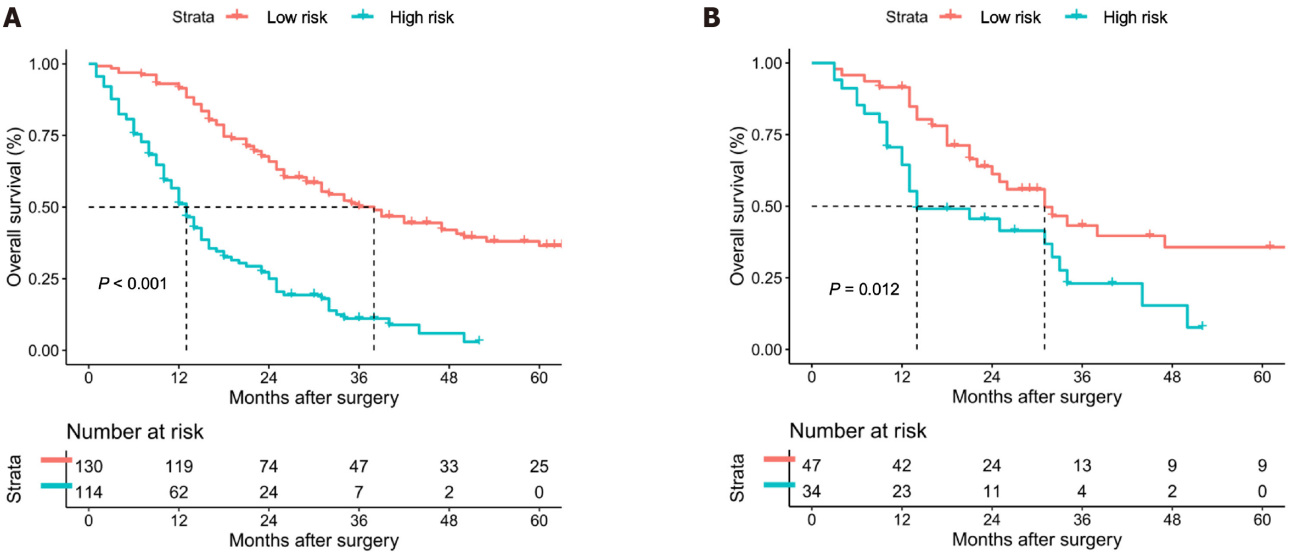

DOI: 10.4251/wjgo.v15.i6.1036

Figure 4 Risk classifications satisfactorily determined the risk of postoperative survival in perihilar cholangiocarcinoma patients after curative resection in the training and validation cohorts. A: Training; B: Validation cohorts.

Moreover, pCCA patients may require hemihepatectomy or more extensive liver resection to achieve radical resection, further increasing the risk of perioperative liver failure. In addition, patients with high ACCI scores have worse nutritional status[33], and gastrointestinal diseases such as pCCA often lead to a reduction in the nutritional intake of patients, resulting in a substantially increased incidence of perioperative malnutrition. The combination of these factors leads to a significant increase in the perioperative risk of patients with high ACCI scores.

The National Comprehensive Cancer Network guidelines recommend that adjuvant therapy be considered after pCCA resection, especially for patients at high risk of recurrence with lymphatic metastases or R1 resection[34]. Cisplatin and S1 are two key drugs used in the postoperative adjuvant treatment of CCA, and their combination with gemcitabine significantly prolongs survival in patients with bile duct cancer[35]. However, some elderly patients with comorbidities cannot tolerate this treatment, resulting in the need for dose adjustment or contraindication[35,36]. Indeed, age and comorbidity burden led to lower rates of introduction of first-line combination chemotherapy and second-line chemotherapy[37]. In addition, various reasons, such as damage to liver and kidney function after adjuvant therapy, have forced patients to discontinue adjuvant therapy midway, resulting in a worse prognosis for the patient. Hence, reduced intensity or discontinuation of postoperative adjuvant therapy in elderly patients with comorbidities may be associated with poor prognosis.

In our opinion, patients with high ACCI scores should undergo a more careful multidisciplinary evaluation in terms of both the choice of the surgical procedure and the choice of postoperative adjuvant treatment.

In addition to the ACCI, a number of other independent risk factors for reduced OS were identified in the present study. These risk factors included CA19-9 (> 150 U/L), maximum tumor size (> 5 cm), lymphoid metastasis (yes), macrovascular invasion, microvascular invasion, and tumor differentiation. All these risk factors have been reported previously[38-40]. We constructed a nomogram using the above independent risk factors.

Nomograms are a visual tool for predicting the prognosis of patients with various cancers and are widely recognized in clinical practice for their applicability and accuracy[41]. Thus, based on the ACCI and these independent risk factors, a clinical prediction model to assess the OS of pCCA patients after curative resection was constructed and validated. To optimize its practicality, the nomogram was also further transformed into an internet browser calculator. According to the nomogram, we were able to identify high-risk patients (nomogram score > 156), who had a worse OS.

The ROC curves and DCA results for both the training and validation cohorts showed that the nomogram performed better than the 8th AJCC staging system in terms of its ability to predict OS after curative resection and its superior net clinical benefits. The TNM staging system has been promoted in abdominal surgery for a long time. With the continuous optimization of the staging system, the prediction of prognosis for many gastrointestinal tumors, such as gastric and colon cancers, has become increasingly accurate[42]. However, for parenchymal organs, whether pancreatic or liver tumors, the predictive accuracy of TNM staging is greatly reduced. For HCC, the clinical significance of N stage may be overestimated by the TNM staging system due to the exceptionally small probability of lymphatic metastasis. For pCCA, in addition to N stage, MVI and degree of differentiation are also critical in predicting prognosis. Thus, our model not only incorporates more comprehensive oncological

information, including a highly specific serum tumor marker of pCCA, CA19-9, but also takes into account the patient's comorbidity status. This allows our model to obtain a better predictive performance than TNM staging and to better guide clinical decisions.

Nevertheless, this study has several limitations. First, this was a retrospective study, and bias in data collection was inevitable. However, we included consecutive patients, so this study was closer to the real world than a randomized controlled trial. Second, although this was a multicenter study, there was a dearth of patient data from Western countries. We tried external validation using data from public databases such as surveillance, epidemiology, and end results but ultimately failed because only CCA but not pCCA could be identified in the database. Third, this study lacks data on postoperative adjuvant therapy. The patients in this study were recruited between 2010 and 2019. Due to the uncertainty of the efficacy, we did not record the adjuvant treatment in detail and will add these data in the future[43].

CONCLUSION

In conclusion, this multicenter study showed that a high ACCI score was independently associated with worse OS following curative resection for pCCA. The nomogram based on the ACCI provides a good prediction of OS, which can help surgeons make better clinical decisions.

ARTICLE HIGHLIGHTS

Research background

Curative resection provides a possible cure for eligible patients with perihilar cholangiocarcinoma (pCCA). The predictive value of the age-adjusted Charlson comorbidity index (ACCI) for the long-term prognosis of patients with multiple malignancies was recently reported. However, pCCA is one of the most surgically difficult gastrointestinal tumors with the poorest prognosis, and the value of the ACCI for the prognosis of pCCA patients after curative resection is unclear.

Research motivation

The present study attempted to evaluate the prognostic value of the ACCI and to design an online clinical model to predict the overall survival (OS) of pCCA patients after curative resection.

Research objectives

This study aimed to identify the prognostic value of the ACCI in pCCA patients and to construct an online clinical model to predict the OS of pCCA patients after curative resection.

Research methods

Consecutive pCCA patients after curative resection between 2010 and 2019 were enrolled from a multicenter database. The patients were randomly assigned 3:1 to training and validation cohorts. In the training and validation cohorts, all patients were divided into low-, moderate-, and high-ACCI groups. Kaplan-Meier curves were used to determine the impact of the ACCI on OS for pCCA patients, and multivariate Cox regression analysis was used to determine the independent risk factors affecting OS. An online clinical model based on the ACCI was developed and validated. The concordance index (C-index), calibration curve, and receiver operating characteristic (ROC) curve were used to evaluate the predictive performance and fit of this model.

Research results

Mild liver disease and diabetes were the most common comorbidities in pCCA patients undergoing radical surgery. The Kaplan-Meier curves showed that patients in the moderate- and high-ACCI groups had worse survival rates than those in the low-ACCI group. Multivariable analysis revealed that moderate and high ACCI scores were independently associated with OS in pCCA patients after curative resection. In addition, an online clinical model was developed that had ideal C-indexes of 0.725 and 0.675 for predicting OS in the training and validation cohorts, respectively. The calibration curve and ROC curve indicated that the model had a good fit and prediction performance.

Research conclusions

A high ACCI score may predict poor long-term survival in pCCA patients after curative resection. High-risk patients screened by the ACCI-based model should be given more clinical attention in terms of the management of comorbidities and postoperative follow-up.

Research perspectives

Although our multicenter study identified the prognostic value of the ACCI in pCCA patients after

curative resection, future prospective studies with larger samples should be conducted to further explore the association between the ACCI and the prognosis of pCCA patients and the guidance of the ACCI on treatment allocation.

FOOTNOTES

Author contributions: Pan Y, Liu ZP, Dai HS, and Chen ZY contributed to the conception; Pan Y, Liu ZP, Wang YZ, Chen WY, Luo Y, Gao SY, Chen ZY, and Dai HS designed the study; Chen ZY and Dai HS performed the administrative support; Pan Y, Dong JL, Liu YH, Yin XY, Liu XC, Fan HN, Bai J, Jiang Y, and Cheng JJ contributed to the data collection and acquisition; Pan Y, Liu ZP, Chen WY, Luo Y, Gao SY, Wang ZR, and Zhang YQ performed the data analysis; Pan Y, Liu ZP, and Dai HS contributed to the manuscript preparation; Chen ZY and Dai HS performed the critical revision; All authors agree to the final approval of the manuscript.

Supported by National Natural Science Foundation of China, No. 81874211; and Chongqing Technology Innovation and Application Development Special Key Project, No. CSTC2021jscx-gksb-N0009.

Institutional review board statement: The study was approved by the Institutional Review Board of the Southwest Hospital, China, No. KY2021129.

Informed consent statement: Patients were not required to give informed consent to the study because the analysis used anonymized clinical data, which were obtained after each patient gave written consent to treatment. For full disclosure, the details of the study are published on the home page of Southwest Hospital.

Conflict-of-interest statement: All the authors report no relevant conflicts of interest for this article.

Data sharing statement: Technical appendix, statistical code, and dataset available from the corresponding author at chenzhiyu_umn@163.com. Participants gave informed consent for data sharing.

STROBE statement: The authors have read the STROBE Statement—checklist of items, and the manuscript was prepared and revised according to the STROBE Statement—checklist of items.

Country/Territory of origin: China

ORCID number: Yu Pan 0000-0003-3827-2418; Zhi-Peng Liu 0000-0001-7652-1783; Hai-Su Dai 0000-0001-9896-6249; Wei-Yue Chen 0000-0001-6922-8888; Ying Luo 0000-0003-2692-0676; Yu-Zhu Wang 0000-0003-2101-0673; Shu-Yang Gao 0000-0002-1490-8533; Zi-Ran Wang 0000-0002-5499-7737; Jin-Ling Dong 0000-0001-6970-6341; Yun-Hua Liu 0000-0001-9967-7676; Xian-Yu Yin 0000-0003-1881-0215; Xing-Chao Liu 0000-0001-9086-6139; Hai-Ning Fan 0000-0002-3869-9406; Jie Bai 0000-0003-3031-8434; Yan Jiang 0000-0003-4628-7150; Jun-Jie Cheng 0000-0002-8536-2347; Yan-Qi Zhang 0000-0001-9438-0953; Zhi-Yu Chen 0000-0002-1321-1793.

S-Editor: Fan JR
L-Editor: A
P-Editor: Zhang XD

REFERENCES

1 **Welzel TM**, McGlynn KA, Hsing AW, O'Brien TR, Pfeiffer RM. Impact of classification of hilar cholangiocarcinomas (Klatskin tumors) on the incidence of intra- and extrahepatic cholangiocarcinoma in the United States. *J Natl Cancer Inst* 2006; **98**: 873-875 [PMID: 16788161 DOI: 10.1093/jnci/djj234]

2 **Cardinale V**. Classifications and misclassification in cholangiocarcinoma. *Liver Int* 2019; **39**: 260-262 [PMID: 30694026 DOI: 10.1111/liv.13998]

3 **Klatskin G**. Adenocarcinoma of the hepatic duct at its bifurcation within the PORTA hepatis. An unusual tumor with distinctive clinical and pathological features. *Am J Med* 1965; **38**: 241-256 [PMID: 14256720 DOI: 10.1016/0002-9343(65)90178-6]

4 **Saha SK**, Zhu AX, Fuchs CS, Brooks GA. Forty-Year Trends in Cholangiocarcinoma Incidence in the U.S.: Intrahepatic Disease on the Rise. *Oncologist* 2016; **21**: 594-599 [PMID: 27000463 DOI: 10.1634/theoncologist.2015-0446]

5 **Khan SA**, Taylor-Robinson SD, Toledano MB, Beck A, Elliott P, Thomas HC. Changing international trends in mortality rates for liver, biliary and pancreatic tumours. *J Hepatol* 2002; **37**: 806-813 [PMID: 12445422 DOI: 10.1016/s0168-8278(02)00297-0]

6 **Taylor-Robinson SD**, Toledano MB, Arora S, Keegan TJ, Hargreaves S, Beck A, Khan SA, Elliott P, Thomas HC. Increase in mortality rates from intrahepatic cholangiocarcinoma in England and Wales 1968-1998. *Gut* 2001; **48**: 816-820 [PMID: 11358902 DOI: 10.1136/gut.48.6.816]

7 **van Keulen AM**, Franssen S, van der Geest LG, de Boer MT, Coenraad M, van Driel LMJW, Erdmann JI, Haj Mohammad N, Heij L, Klümpen HJ, Tjwa E, Valkenburg-van Iersel L, Verheij J, Groot Koerkamp B, Olthof PB; Dutch Hepatocellular & Cholangiocarcinoma Group (DHCG). Nationwide treatment and outcomes of perihilar cholangiocarcinoma. *Liver Int* 2021; **41**: 1945-1953 [PMID: 33641214 DOI: 10.1111/liv.14856]

8 **DeOliveira ML**, Cunningham SC, Cameron JL, Kamangar F, Winter JM, Lillemoe KD, Choti MA, Yeo CJ, Schulick RD. Cholangiocarcinoma: thirty-one-year experience with 564 patients at a single institution. *Ann Surg* 2007; **245**: 755-762 [PMID: 17457168 DOI: 10.1097/01.sla.0000251366.62632.d3]

9 **Feinstein AR**. The pre-therapeutic classification of co-morbidity in chronic disease. *J Chronic Dis* 1970; **23**: 455-468 [PMID: 26309916 DOI: 10.1016/0021-9681(70)90054-8]

10 **Extermann M**. Measurement and impact of comorbidity in older cancer patients. *Crit Rev Oncol Hematol* 2000; **35**: 181-200 [PMID: 10960800 DOI: 10.1016/s1040-8428(00)00090-1]

11 **Satariano WA**, Silliman RA. Comorbidity: implications for research and practice in geriatric oncology. *Crit Rev Oncol Hematol* 2003; **48**: 239-248 [PMID: 14607386 DOI: 10.1016/j.critrevonc.2003.08.002]

12 **Liu ZP**, Chen WY, Zhang YQ, Jiang Y, Bai J, Pan Y, Zhong SY, Zhong YP, Chen ZY, Dai HS. Postoperative morbidity adversely impacts oncological prognosis after curative resection for hilar cholangiocarcinoma. *World J Gastroenterol* 2022; **28**: 948-960 [PMID: 35317056 DOI: 10.3748/wjg.v28.i9.948]

13 **Boakye D**, Rillmann B, Walter V, Jansen L, Hoffmeister M, Brenner H. Impact of comorbidity and frailty on prognosis in colorectal cancer patients: A systematic review and meta-analysis. *Cancer Treat Rev* 2018; **64**: 30-39 [PMID: 29459248 DOI: 10.1016/j.ctrv.2018.02.003]

14 **Di Donato V**, Page Z, Bracchi C, Tomao F, Musella A, Perniola G, Panici PB. The age-adjusted Charlson comorbidity index as a predictor of survival in surgically treated vulvar cancer patients. *J Gynecol Oncol* 2019; **30**: e6 [PMID: 30479090 DOI: 10.3802/jgo.2019.30.e6]

15 **Charlson ME**, Pompei P, Ales KL, MacKenzie CR. A new method of classifying prognostic comorbidity in longitudinal studies: development and validation. *J Chronic Dis* 1987; **40**: 373-383 [PMID: 3558716 DOI: 10.1016/0021-9681(87)90171-8]

16 **Charlson M**, Szatrowski TP, Peterson J, Gold J. Validation of a combined comorbidity index. *J Clin Epidemiol* 1994; **47**: 1245-1251 [PMID: 7722560 DOI: 10.1016/0895-4356(94)90129-5]

17 **Lee JY**, Kang HW, Rha KH, Cho NH, Choi YD, Hong SJ, Cho KS. Age-adjusted Charlson comorbidity index is a significant prognostic factor for long-term survival of patients with high-risk prostate cancer after radical prostatectomy: a Bayesian model averaging approach. *J Cancer Res Clin Oncol* 2016; **142**: 849-858 [PMID: 26660495 DOI: 10.1007/s00432-015-2093-0]

18 **Dias-Santos D**, Ferrone CR, Zheng H, Lillemoe KD, Fernández-Del Castillo C. The Charlson age comorbidity index predicts early mortality after surgery for pancreatic cancer. *Surgery* 2015; **157**: 881-887 [PMID: 25704415 DOI: 10.1016/j.surg.2014.12.006]

19 **Wu CC**, Hsu TW, Chang CM, Yu CH, Lee CC. Age-adjusted Charlson comorbidity index scores as predictor of survival in colorectal cancer patients who underwent surgical resection and chemoradiation. *Medicine (Baltimore)* 2015; **94**: e431 [PMID: 25590852 DOI: 10.1097/MD.0000000000000431]

20 **Shinkawa H**, Tanaka S, Takemura S, Amano R, Kimura K, Nishioka T, Miyazaki T, Kubo S. Predictive Value of the Age-Adjusted Charlson Comorbidity Index for Outcomes After Hepatic Resection of Hepatocellular Carcinoma. *World J Surg* 2020; **44**: 3901-3914 [PMID: 32651603 DOI: 10.1007/s00268-020-05686-w]

21 **Kahl A**, du Bois A, Harter P, Prader S, Schneider S, Heitz F, Traut A, Alesina PF, Meier B, Walz M, Brueckner A, Groeben HT, Brunkhorst V, Heikaus S, Ataseven B. Prognostic Value of the Age-Adjusted Charlson Comorbidity Index (ACCI) on Short- and Long-Term Outcome in Patients with Advanced Primary Epithelial Ovarian Cancer. *Ann Surg Oncol* 2017; **24**: 3692-3699 [PMID: 28871563 DOI: 10.1245/s10434-017-6079-9]

22 **Chun YS**, Pawlik TM, Vauthey JN. 8th Edition of the AJCC Cancer Staging Manual: Pancreas and Hepatobiliary Cancers. *Ann Surg Oncol* 2018; **25**: 845-847 [PMID: 28752469 DOI: 10.1245/s10434-017-6025-x]

23 **Bismuth H**, Corlette MB. Intrahepatic cholangioenteric anastomosis in carcinoma of the hilus of the liver. *Surg Gynecol Obstet* 1975; **140**: 170-178 [PMID: 1079096]

24 **Liu ZP**, Cheng ZJ, Dai HS, Zhong SY, Zhao DC, Gong Y, Zuo JH, Che XY, Chen WY, Wang ZR, Yu T, Cheng JJ, Liu XC, Bai J, Jiang Y, Zhang YQ, Lau WY, Deng SQ, Chen ZY. Impact of perioperative blood transfusion on long-term survival in patients with different stages of perihilar cholangiocarcinoma treated with curative resection: A multicentre propensity score matching study. *Front Oncol* 2022; **12**: 1059581 [PMID: 36387093 DOI: 10.3389/fonc.2022.1059581]

25 **Chen C**, Liu ZP, Chen WY, Wang X, Liu YH, Wang Y, Liu XC, Fan HN, Bai J, Jiang Y. Anatomical hepatectomy for achieving textbook outcome for perihilar cholangiocarcinoma treated with curative-intent resection A multicenter study. *iLIVER* 2022; **1**: 7

26 **Williams GR**, Deal AM, Lund JL, Chang Y, Muss HB, Pergolotti M, Guerard EJ, Shachar SS, Wang Y, Kenzik K, Sanoff HK. Patient-Reported Comorbidity and Survival in Older Adults with Cancer. *Oncologist* 2018; **23**: 433-439 [PMID: 29242282 DOI: 10.1634/theoncologist.2017-0404]

27 **Lee L**, Cheung WY, Atkinson E, Krzyzanowska MK. Impact of comorbidity on chemotherapy use and outcomes in solid tumors: a systematic review. *J Clin Oncol* 2011; **29**: 106-117 [PMID: 21098314 DOI: 10.1200/JCO.2010.31.3049]

28 **Gross CP**, McAvay GJ, Guo Z, Tinetti ME. The impact of chronic illnesses on the use and effectiveness of adjuvant chemotherapy for colon cancer. *Cancer* 2007; **109**: 2410-2419 [PMID: 17510973 DOI: 10.1002/cncr.22726]

29 **Kellokumpu I**, Kairaluoma M, Mecklin JP, Kellokumpu H, Väyrynen V, Wirta EV, Sihvo E, Kuopio T, Seppälä TT. Impact of Age and Comorbidity on Multimodal Management and Survival from Colorectal Cancer: A Population-Based Study. *J Clin Med* 2021; **10** [PMID: 33920665 DOI: 10.3390/jcm10081751]

30 **Lin JX**, Huang YQ, Xie JW, Wang JB, Lu J, Chen QY, Cao LL, Lin M, Tu R, Huang ZN, Lin JL, Zheng CH, Huang CM,

Li P. Association of the age-adjusted Charlson Comorbidity Index and systemic inflammation with survival in gastric cancer patients after radical gastrectomy. *Eur J Surg Oncol* 2019; **45**: 2465-2472 [PMID: 31350072 DOI: 10.1016/j.ejso.2019.07.010]

31 **Fong Y**, Blumgart LH, Fortner JG, Brennan MF. Pancreatic or liver resection for malignancy is safe and effective for the elderly. *Ann Surg* 1995; **222**: 426-34; discussion 434 [PMID: 7574924 DOI: 10.1097/00000658-199522240-00002]

32 **Cucchetti A**, Ercolani G, Vivarelli M, Cescon M, Ravaioli M, Ramacciato G, Grazi GL, Pinna AD. Is portal hypertension a contraindication to hepatic resection? *Ann Surg* 2009; **250**: 922-928 [PMID: 19855258 DOI: 10.1097/SLA.0b013e3181b977a5]

33 **Takada Y**, Kawashima H, Ohno E, Ishikawa T, Mizutani Y, Iida T, Yamamura T, Kakushima N, Furukawa K, Nakamura M, Honda T, Ishigami M, Ito A, Hirooka Y. The impact of the age-adjusted Charlson comorbidity index as a prognostic factor for endoscopic papillectomy in ampullary tumors. *J Gastroenterol* 2022; **57**: 199-207 [PMID: 35098349 DOI: 10.1007/s00535-022-01853-z]

34 **Benson AB**, D'Angelica MI, Abbott DE, Anaya DA, Anders R, Are C, Bachini M, Borad M, Brown D, Burgoyne A, Chahal P, Chang DT, Cloyd J, Covey AM, Glazer ES, Goyal L, Hawkins WG, Iyer R, Jacob R, Kelley RK, Kim R, Levine M, Palta M, Park JO, Raman S, Reddy S, Sahai V, Schefter T, Singh G, Stein S, Vauthey JN, Venook AP, Yopp A, McMillian NR, Hochstetler C, Darlow SD. Hepatobiliary Cancers, Version 2.2021, NCCN Clinical Practice Guidelines in Oncology. *J Natl Compr Canc Netw* 2021; **19**: 541-565 [PMID: 34030131 DOI: 10.6004/jnccn.2021.0022]

35 **Morizane C**, Okusaka T, Mizusawa J, Katayama H, Ueno M, Ikeda M, Ozaka M, Okano N, Sugimori K, Fukutomi A, Hara H, Mizuno N, Yanagimoto H, Wada K, Tobimatsu K, Yane K, Nakamori S, Yamaguchi H, Asagi A, Yukisawa S, Kojima Y, Kawabe K, Kawamoto Y, Sugimoto R, Iwai T, Nakamura K, Miyakawa H, Yamashita T, Hosokawa A, Ioka T, Kato N, Shioji K, Shimizu K, Nakagohri T, Kamata K, Ishii H, Furuse J; members of the Hepatobiliary and Pancreatic Oncology Group of the Japan Clinical Oncology Group (JCOG-HBPOG). Combination gemcitabine plus S-1 versus gemcitabine plus cisplatin for advanced/recurrent biliary tract cancer: the FUGA-BT (JCOG1113) randomized phase III clinical trial. *Ann Oncol* 2019; **30**: 1950-1958 [PMID: 31566666 DOI: 10.1093/annonc/mdz402]

36 **Takahara N**, Isayama H, Nakai Y, Sasaki T, Ishigaki K, Saito K, Akiyama D, Uchino R, Mizuno S, Yagioka H, Kogure H, Togawa O, Matsubara S, Ito Y, Toda N, Tada M, Koike K. Gemcitabine and S-1 versus gemcitabine and cisplatin treatment in patients with advanced biliary tract cancer: a multicenter retrospective study. *Invest New Drugs* 2017; **35**: 269-276 [PMID: 28124197 DOI: 10.1007/s10637-017-0430-7]

37 **Takahara N**, Nakai Y, Saito K, Sasaki T, Suzuki Y, Inokuma A, Oyama H, Kanai S, Suzuki T, Sato T, Hakuta R, Ishigaki K, Saito T, Hamada T, Mizuno S, Kogure H, Tada M, Isayama H, Koike K. The impact of age and comorbidity in advanced or recurrent biliary tract cancer receiving palliative chemotherapy. *J Gastroenterol Hepatol* 2020; **35**: 1828-1835 [PMID: 32267557 DOI: 10.1111/jgh.15066]

38 **Liu ZP**, Zhang QY, Chen WY, Huang YY, Zhang YQ, Gong Y, Jiang Y, Bai J, Chen ZY, Dai HS. Evaluation of Four Lymph Node Classifications for the Prediction of Survival in Hilar Cholangiocarcinoma. *J Gastrointest Surg* 2022; **26**: 1030-1040 [PMID: 34973138 DOI: 10.1007/s11605-021-05211-x]

39 **Ercolani G**, Dazzi A, Giovinazzo F, Ruzzenente A, Bassi C, Guglielmi A, Scarpa A, D'Errico A, Pinna AD. Intrahepatic, peri-hilar and distal cholangiocarcinoma: Three different locations of the same tumor or three different tumors? *Eur J Surg Oncol* 2015; **41**: 1162-1169 [PMID: 26095704 DOI: 10.1016/j.ejso.2015.05.013]

40 **Fabris L**, Alvaro D. The prognosis of perihilar cholangiocarcinoma after radical treatments. *Hepatology* 2012; **56**: 800-802 [PMID: 22532318 DOI: 10.1002/hep.25808]

41 **Balachandran VP**, Gonen M, Smith JJ, DeMatteo RP. Nomograms in oncology: more than meets the eye. *Lancet Oncol* 2015; **16**: e173-e180 [PMID: 25846097 DOI: 10.1016/S1470-2045(14)71116-7]

42 **Oh SE**, An JY, Choi MG, Lee JH, Sohn TS, Bae JM. Comparisons of remnant primary, residual, and recurrent gastric cancer and applicability of the 8th AJCC TNM classification for remnant gastric cancer staging. *Eur J Surg Oncol* 2020; **46**: 2236-2242 [PMID: 32788098 DOI: 10.1016/j.ejso.2020.06.032]

43 **Mallick S**, Benson R, Haresh KP, Julka PK, Rath GK. Adjuvant radiotherapy in the treatment of gall bladder carcinoma: What is the current evidence. *J Egypt Natl Canc Inst* 2016; **28**: 1-6 [PMID: 26265290 DOI: 10.1016/j.jnci.2015.07.004]

World Journal of Gastrointestinal Oncology

Submit a Manuscript: https://www.f6publishing.com

World J Gastrointest Oncol 2023 June 15; 15(6): 1051-1061

DOI: 10.4251/wjgo.v15.i6.1051

ISSN 1948-5204 (online)

ORIGINAL ARTICLE

Retrospective Study

Diagnostic accuracy of apparent diffusion coefficient to differentiate intrapancreatic accessory spleen from pancreatic neuroendocrine tumors

Shuai Ren, Kai Guo, Yuan Li, Ying-Ying Cao, Zhong-Qiu Wang, Ying Tian

Specialty type: Oncology

Provenance and peer review: Unsolicited article; Externally peer reviewed.

Peer-review model: Single blind

Peer-review report's scientific quality classification

Grade A (Excellent): 0
Grade B (Very good): B
Grade C (Good): C
Grade D (Fair): 0
Grade E (Poor): 0

P-Reviewer: Gokce E, Turkey; Uhlmann D, Germany

Received: December 30, 2022
Peer-review started: December 30, 2022
First decision: January 22, 2023
Revised: February 1, 2023
Accepted: April 19, 2023
Article in press: April 19, 2023
Published online: June 15, 2023

Shuai Ren, Kai Guo, Yuan Li, Ying-Ying Cao, Zhong-Qiu Wang, Ying Tian, Department of Radiology, Jiangsu Province Hospital of Chinese Medicine, Affiliated Hospital of Nanjing University of Chinese Medicine, Nanjing 210029, Jiangsu Province, China

Corresponding author: Zhong-Qiu Wang, MD, PhD, Chief Doctor, Department of Radiology, Jiangsu Province Hospital of Chinese Medicine, Affiliated Hospital of Nanjing University of Chinese Medicine, No. 155 Hanzhong Road, Nanjing 210029, Jiangsu Province, China. zhongqiuwang0815@163.com

Abstract

BACKGROUND

Intrapancreatic accessory spleen (IPAS) shares similar imaging findings with hypervascular pancreatic neuroendocrine tumors (PNETs), which may lead to unnecessary surgery.

AIM

To investigate and compare the diagnostic performance of absolute apparent diffusion coefficient (ADC) and normalized ADC (lesion-to-spleen ADC ratios) in the differential diagnosis of IPAS from PNETs.

METHODS

A retrospective study consisting of 29 patients (16 PNET patients *vs* 13 IPAS patients) who underwent preoperative contrast-enhanced magnetic resonance imaging together with diffusion-weighted imaging/ADC maps between January 2017 and July 2020 was performed. Two independent reviewers measured ADC on all lesions and spleens, and normalized ADC was calculated for further analysis. The receiver operating characteristics analysis was carried out for evaluating the diagnostic performance of both absolute ADC and normalized ADC values in the differential diagnosis between IPAS and PNETs by clarifying sensitivity, specificity, and accuracy. Inter-reader reliability for the two methods was evaluated.

RESULTS

IPAS had a significantly lower absolute ADC ($0.931 \pm 0.773 \times 10^{-3}$ mm^2/s *vs* $1.254 \pm 0.219 \times 10^{-3}$ mm^2/s) and normalized ADC value (1.154 ± 0.167 *vs* 1.591 ± 0.364) compared to PNET. A cutoff value of 1.046×10^{-3} mm^2/s for absolute ADC was

associated with 81.25% sensitivity, 100% specificity, and 89.66% accuracy with an area under the curve of 0.94 (95% confidence interval: 0.8536-1.000) for the differential diagnosis of IPAS from PNET. Similarly, a cutoff value of 1.342 for normalized ADC was associated with 81.25% sensitivity, 92.31% specificity, and 86.21% accuracy with an area under the curve of 0.91 (95% confidence interval: 0.8080-1.000) for the differential diagnosis of IPAS from PNET. Both methods showed excellent inter-reader reliability with intraclass correlation coefficients for absolute ADC and ADC ratio being 0.968 and 0.976, respectively.

CONCLUSION
Both absolute ADC and normalized ADC values can facilitate the differentiation between IPAS and PNET.

Key Words: Pancreas; Neuroendocrine tumors; Accessory spleen; Diffusion-weighted imaging; Diagnostic performance

Core Tip: Intrapancreatic accessory spleen (IPAS) presents as a solitary, well-defined, hypervascular mass on contrast-enhanced computed tomography or contrast-enhanced magnetic resonance imaging. They are often misdiagnosed as small (< 3 cm) hypervascular pancreatic neuroendocrine tumors (PNETs). IPAS is innocuous in nature and does not require treatment. However, surgery and/or chemotherapy are recommended for PNETs. The overlap of imaging characteristics between IPAS and PNETs often requires surgical management. Therefore, preoperative characterization is of utmost importance. Our study demonstrated that both absolute apparent diffusion coefficient (ADC) and normalized ADC values (lesion-to-spleen ADC ratios) allow clinically relevant differentiation of IPAS from PNET.

Citation: Ren S, Guo K, Li Y, Cao YY, Wang ZQ, Tian Y. Diagnostic accuracy of apparent diffusion coefficient to differentiate intrapancreatic accessory spleen from pancreatic neuroendocrine tumors. *World J Gastrointest Oncol* 2023; 15(6): 1051-1061
URL: https://www.wjgnet.com/1948-5204/full/v15/i6/1051.htm
DOI: https://dx.doi.org/10.4251/wjgo.v15.i6.1051

INTRODUCTION

Ectopic splenic tissue, also known as an accessory spleen, is found in up to 30% of the population[1]. While accessory spleens are often observed at the splenic hilum, they can also be present in the pancreatic parenchyma[2]. Accessory spleens are usually of little clinical consequence and found incidentally during surgery for other indications. They can cause symptoms, most often hematologic, after a splenectomy has been carried out[3,4]. Intrapancreatic accessory spleen (IPAS) typically presents as a solitary, well-defined, hypervascular, ovoid or round mass with a maximum diameter < 3 cm on contrast-enhanced computed tomography (CE-CT) or magnetic resonance imaging (CE-MRI). They are often misdiagnosed as small (< 3 cm) hypervascular pancreatic neuroendocrine tumors (PNETs) since they share similar imaging findings[1,4-9]. IPAS is innocuous in nature and generally does not require any treatment. However, surgery and/or chemotherapy are recommended for PNETs[10]. Unfortunately, the overlap of imaging features between IPAS and small (< 3 cm) hypervascular PNETs often requires surgical management[11]. Therefore, preoperative characterization of IPAS *vs* small (< 3 cm) hypervascular PNETs is of utmost importance.

The investigation of diffusion-weighted imaging (DWI) in evaluating and characterizing pancreatic masses is increasing, with several studies clarifying its application in pancreatic tumor detection or the differentiation between benign and malignant pancreatic masses[12-14]. DWI is a method of signal contrast generation based on tissue cellularity, architecture, and cell membrane integrity, which can be quantified by apparent diffusion coefficient (ADC) maps. DWI can reflect the random microscopic motion of water molecules and provide information for tumor characterizing, staging, and differential diagnosis[12,14,15]. Recently, technical advancements have been achieved in decreasing imaging time and improving image quality. As a result, DWI is preferred and recommended since it allows non-invasive functional evaluation without the use of contrast media or ionizing radiation.

It has been shown that the splenic parenchyma possesses a markedly lower ADC value than the pancreatic parenchyma due to its unique organ composition. Obviously, significant differences with regard to ADC values have been observed between IPAS and PNETs since IPAS has similar tissue

structures and properties as the spleen[6]. However, concerns have been raised about inter- and intra-scanner ADC variability with contradicting results[16]. A recent study showed that though ADC measurements of the pancreas may be affected by the field strength of an MRI scanner, they demonstrate good reproducibility between different MR systems with the same field strength[17]. Notably, it has also been reported that ADC variability may be minimized by calculation of the normalized ADC value (lesion-to-spleen ADC ratios) with the assistance of technical factors in different organs and pathologies[18,19]. Therefore, the objective of our study was to investigate and compare the diagnostic accuracy of absolute ADC and normalized ADC values in differentiating IPAS from small (< 3 cm) hypervascular PNETs.

MATERIALS AND METHODS

Patients

This study was approved by our ethics committee with a waiver of informed consent due to its retrospective nature. We carried out a search of our radiology database of focal pancreatic masses to identify patients with IPAS and PNETs between January 2017 and July 2020. A total of 132 patients were identified from the database search (51 IPAS and 81 PNETs). Inclusion criteria for IPAS were as follows: (1) CE-MRI images together with DWI/ADC maps were available; (2) IPAS showed a purely solid lesion without cystic changes on MRI images; (3) Diagnosis of IPAS was made pathologically following surgical resection or endoscopic ultrasound-guided fine needle aspiration; and (4) IPAS cases without pathology or cytopathology were also included under the following criteria: the lesion was located at the tail of the pancreas and showed similar signal intensity/enhancement pattern compared with spleen; and the lesion remained stable in size (< 3 cm) and shape over at least 18 mo[1,6]. According to these criteria, 38 patients were excluded from the study, *i.e.* 34 patients did not have available CE-MRI or DWI/ADC, 1 patient had surgically-proven cystic changes within the lesion, and 3 patients were diagnosed based on imaging findings although the follow-up period was less than 18 mo. Finally, 13 patients with IPAS whose diagnosis was made by surgery (n = 4), biopsy (n = 3), and typical imaging findings (n = 6, follow-up period ≥ 18 mo) were included in this study (Figure 1).

Inclusion criteria for PNETs were as follows: (1) CE-MRI images together with DWI/ADC maps were available; (2) PNET showed a hypervascular purely solid mass without cystic changes on MRI images; (3) Diagnosis of PNET was made pathologically following surgical resection or endoscopic ultrasound-guided fine needle aspiration; and (4) PNET had a size < 3 cm without apparent distant metastasis on MRI images. According to these criteria, 65 patients were excluded from the study, *i.e.* 49 patients without available CE-MRI or DWI/ADC, 5 patients with hypovascular enhancement pattern or surgically-proven cystic changes within the lesion, 8 patients with a mass size > 3 cm, and 3 patients with metastasis. Finally, 16 patients with PNET whose diagnoses were made by surgery (n = 11) and biopsy (n = 5) were included into this study (Figure 1).

MRI protocol

A preoperative MRI scan was performed for all enrolled patients using a standard imaging protocol as described in our previous study[20]. A 3.0-T MRI system (Sigma HDx; GE Medical Systems, Milwaukee, WI, United States) with an eight-channel phased-array torso coil was adopted. DWI was obtained prior to contrast administration in all patients. DWI images with b values of 0, 50, and 1000 s/mm^2 were performed using a respiration-triggered single-shot echo-planar sequence. The imaging parameters were: a spectral pre-saturation with inversion recovery for fat suppression; repetition time, 8000 ms; echo time, 60 ms; slice thickness, 5 mm; interslice gap, 2 mm; flip angle 90°; matrix, 196 × 133; and field of view, 36 cm × 30 cm. In addition to DWI sequence, this study also adopted T1-weighted fat-suppressed liver acquisition with volume acceleration sequence (repetition time, 3100 ms; echo time, 15 ms; imaging duration, 60-120 s; slice thickness, 5 mm; interslice gap, 2 mm; flip angle, 12°; matrix, 384 × 256; and field of view, 22 cm × 22 cm) and fast spin-echo T2-weighted fat-suppressed sequence (repetition time, 6000 ms; echo time, 80 ms; imaging duration, 120-180 s; slice thickness, 5 mm; interslice gap, 2 mm; flip angle, 90°; matrix, 384 × 256; and field of view, 22 cm × 22 cm). T1-weighted contrast-enhanced images with triple phases including pancreatic parenchyma, portal venous, and delayed phases were obtained at 35 s, 70 s, and 240 s after bolus intravenous administration of gadopentetate dimeglumine (Bayer HealthCare Pharmaceuticals, Berlin, Germany) at a dose of 0.2 mmol/kg body weight followed by a 20-mL saline flush. The ADC values were calculated using a monoexponential function with b values of 0 and 1000 s/mm^2 due to the fact that high b-value DWI images contribute to better contrast, greater tissue diffusivity, and a lower T2 shine through effect[7].

Image analysis

One abdominal radiologist with 10 years of experience who was blinded to the final diagnosis performed all the ADC measurements of the lesions and spleens on ADC maps using circular or oval regions of interest (ROIs). ROIs of pancreatic lesions were placed to include maximum lesion areas, while the most peripheral portions were avoided to exclude volume averaging. The ROIs of the spleen

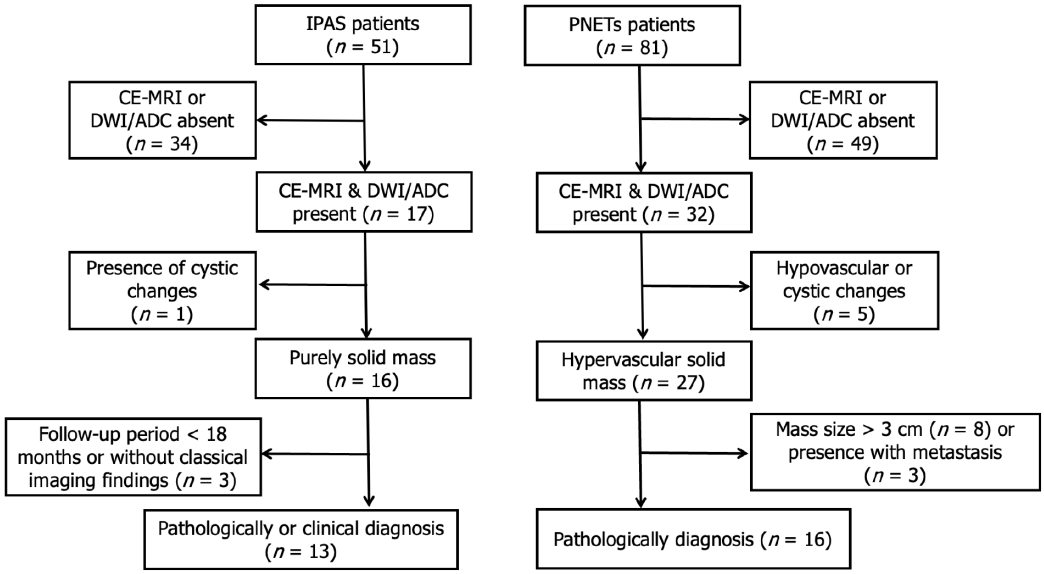

DOI: 10.4251/wjgo.v15.i6.1051

Figure 1 Flowchart of patients throughout the study. ADC: Apparent diffusion coefficient; CE-MRI: Contrast-enhanced magnetic resonance imaging; DWI: Diffusion-weighted imaging; IPAS: Intrapancreatic accessory spleen; PNETs: Pancreatic neuroendocrine tumors.

were placed on each of the anterior pole, mid pole, and posterior pole of the spleen with the purpose of avoiding volume averaging by excluding vessels and artifacts as much as possible. Finally, the average of the three splenic ADC measurements was adopted for the calculation of normalized ADC value (ADC of the pancreatic lesion/the average ADC of spleen).

Similar image analysis was carried out by a second abdominal radiologist (with 8 years of experience) with no prior knowledge of detailed histopathological information of any patients for inter-reader variability analysis. Quantitative data including absolute ADC and normalized ADC values from the reader with greater experience in abdominal MRI diagnosis was adopted for further analysis.

Statistical analysis

Statistical analysis was carried out using SPSS 20.0 and GraphPad Prism 8.0 software. The normal distribution and variance homogeneity of variables were analyzed by using the Kolmogorov-Smirnov test and Levene test, respectively. Normal distributed variables were described by mean ± standard deviation (SD). The non-normal distributed variables were expressed as medians (first quartile, third quartile). The quantitative variables were compared by the two-tailed independent *t*-test or the Mann-Whitney *U* test. The receiver operating characteristics (ROC) analysis was carried out for evaluating the diagnostic performance of both absolute ADC and normalized ADC values in the differential diagnosis between IPAS and PNETs by clarifying sensitivity, specificity, and accuracy. The areas under the curves (AUCs) were determined for both absolute ADC and normalized ADC values, and the AUCs between these two methods were compared using the DeLong's test. Inter-reader reliability for both absolute ADC and normalized ADC values were assessed by using Bland-Altman analyses and intraclass correlation coefficient (ICC)[21]. ICC coefficients were defined as poor (< 0.40), fair (0.40 ≤ ICC < 0.60), good (0.60 ≤ ICC < 0.75), and excellent (ICC ≥ 0.75). The statistical significance level was set at a *P* value < 0.05.

RESULTS

Patient characteristics and imaging analysis

Twenty-nine patients including 16 PNET patients [10 males and 6 females; age range: 22-72 years; mean age: 52.38 years ± 13.72 (SD)] and 13 IPAS patients [6 males and 7 females; age range: 27-78 years; mean age: 56.15 years ± 15.78 (SD)] were finally included into the study. Among them, 16 PNET patients and 7 IPAS patients were diagnosed by pathology/cytopathology, while the remaining cases with IPAS were selected out based on typical imaging findings. No significant differences were found in sex or age between the two groups. All IPAS lesions were located at the tail of the pancreas. PNETs were located as follows: six tumors at the head and neck of the pancreas; and 7 at the body and tail of the pancreas.

MRI findings in patients with IPAS and PNET were shown in Table 1. No significant differences were found in lesion diameter, lesion ROI, or spleen ROI. Mean absolute ADC values for the spleen were not significantly different between the IPAS and PNET groups (0.817 ± 0.943 × 10^{-3} mm^2/s *vs* 0.806 ± 0.145 ×

Table 1 Magnetic resonance imaging findings in patients with intrapancreatic accessory spleen and small hypervascular pancreatic neuroendocrine tumors

Parameters	IPAS	PNETs	*P* value
Lesion diameter in mm	17.71 ± 5.09	18.21 ± 5.47	0.803
Lesion ROI in cm^2	0.685 ± 0.601	0.866 ± 0.567	0.413
Spleen ROI in cm^2	2.134 ± 0.805	2.753 ± 0.910	0.066
Spleen ADC as × 10^{-3} mm^2/s	0.817 ± 0.943	0.806 ± 0.145	0.825
aADC as × 10^{-3} mm^2/s	0.931 ± 0.773	1.254 ± 0.219	< 0.001
rADC	1.154 ± 0.167	1.591 ± 0.364	< 0.001

aADC: Absolute apparent diffusion coefficient; ADC: Apparent diffusion coefficient; IPAS: Intrapancreatic accessory spleen; PNETs: Pancreatic neuroendocrine tumors; rADC: Normalized apparent diffusion coefficient (lesion-to-spleen apparent diffusion coefficient ratios); ROI: Regions of interest.

10^{-3} mm^2/s, P = 0.825). The absolute ADC and normalized ADC values were significantly different between IPAS and PNET (both P < 0.001), with IPAS showing lower absolute ADC values (0.931 ± 0.773 × 10^{-3} mm^2/s *vs* 1.254 ± 0.219 × 10^{-3} mm^2/s) and lower normalized ADC values (1.154 ± 0.167 *vs* 1.591 ± 0.364) compared to PNET. Figure 2 shows two representative cases of IPAS and PNET. The absolute ADC and normalized ADC values of IPAS were significantly lower than those of PNET.

Diagnostic performance of ADC values

We subsequently evaluated the diagnostic performance of absolute ADC and normalized ADC values in differentiating IPAS from PNET. Table 2 summarized the sensitivity, specificity, accuracy, positive predictive value, negative predictive value, and cutoff value of absolute ADC and normalized ADC values by ROC analysis. ROC analysis demonstrated the optimum cutoff value by maximizing the sum of sensitivity and specificity for differentiating IPAS from PNET. A cutoff value of 1.046 × 10^{-3} mm^2/s for absolute ADC was associated with 81.25% sensitivity, 100% specificity, and 89.66% accuracy with an AUC of 0.94 (95%CI: 0.8536-1.000) for the differential diagnosis of IPAS from PNET. Similarly, a cutoff value of 1.342 for normalized ADC was associated with 81.25% sensitivity, 92.31% specificity, and 86.21% accuracy with an AUC of 0.91 (95%CI: 0.8080-1.000) for the differential diagnosis of IPAS from PNET. Figure 3 shows the ROC curves for absolute ADC and normalized ADC values. DeLong's test was used to compare the AUCs of two models established with absolute ADC and normalized ADC values in the differential diagnosis of IPAS from PNET. No statistically significant difference was found (P = 0.6668).

Inter-reader reliability analysis

The ICCs to evaluate inter-reader reliability for absolute ADC and normalized ADC values were 0.968 (95%CI: 0.933-0.985) and 0.976 (95%CI: 0.950-0.989), respectively. Bland-Altman analysis (Figure 4) revealed that the bias between two readers (solid blue line) was not significant for both absolute ADC and normalized ADC values, with the line of quality (dotted orange line) falling within the 95%CI of the mean difference (dotted blue lines).

DISCUSSION

An IPAS is typically asymptomatic and has an innocuous nature, which does not require needle biopsy or surgery[11]. However, overlapping imaging features of IPAS and PNET may lead to unnecessary surgery. In many cases, despite imaging and other diagnostic studies, malignancy cannot be excluded, and patients are subjected to pancreatic resection. Therefore, there is a dire need to preoperatively characterize IPAS and differentiate them from PNET. Conventional MRI paved the way for differentiating IPAS from PNET in a non-invasive way since IPAS has similar tissue structure and properties as the spleen, which can be reflected by DWI, demonstrating that IPAS possesses a markedly lower ADC value than PNET[1,7]. In our current study, we found that absolute ADC and normalized ADC values can be used for the differential diagnosis between IPAS and PNET and showed a high pooled sensitivity and specificity.

Multiple modalities including contrast-enhanced ultrasound (CE-US), CT, superparamagnetic iron oxide-enhanced MRI, and nuclear medicine have been proven to be effective in discriminating IPAS from pancreatic solid tumors[5,8,22,23]. Among these, CE-US, ^{99m}Tc scintigraphy, and superparamagnetic iron oxide-enhanced MRI are performed with the intravenous administration of contrast media or the phagocytosis of nuclear pharmaceuticals by macrophages of the reticuloendothelial system

Table 2 Diagnostic performances of absolute apparent diffusion coefficient and normalized apparent diffusion coefficient values

Variables	AUC	Sensitivity, %	Specificity, %	PPV, %	NPV, %	Accuracy, %
aADC as × 10^{-3} mm^2/s	0.94	81.25	100	100	81.25	89.66
rADC	0.91	81.25	92.31	92.86	80.00	86.21

aADC: Absolute apparent diffusion coefficient; AUC: Area under curve; NPV: Negative predictive value; PPV: Positive predictive value; rADC: Normalized apparent diffusion coefficient (lesion-to-spleen apparent diffusion coefficient ratios).

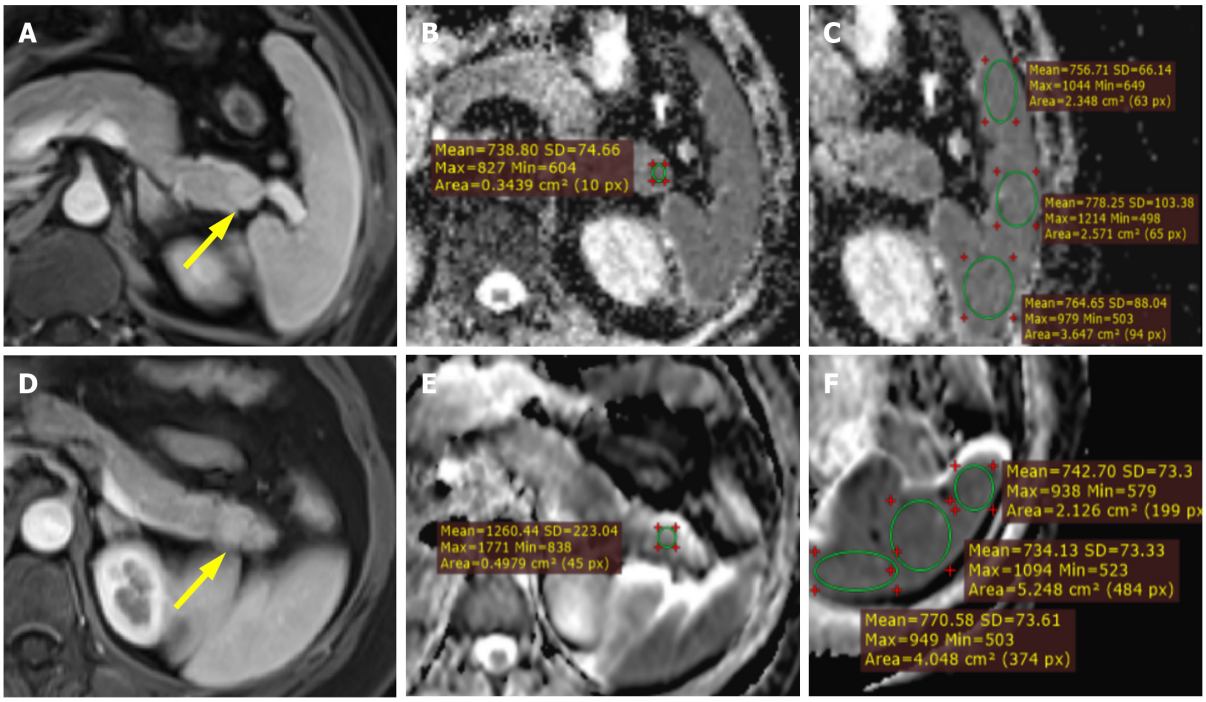

DOI: 10.4251/wjgo.v15.i6.1051

Figure 2 Magnetic resonance images. A-C: Magnetic resonance images in a 51-year-old male with pathologically proven intrapancreatic accessory spleen. The lesion was located at the tail of the pancreas with a hypervascular enhancement pattern on contrast-enhanced arterial phase T1 weighted imaging (T1WI) (yellow arrow, A). After confirming the lesion on arterial phase T1WI and diffusion-weighted imaging (B), circular regions of interest (ROI) were placed within the lesion on the apparent diffusion coefficient (ADC) map (B) and showed an ADC value of 0.738 × 10^{-3} mm^2/s. Similarly, ADC measurement was carried out on the adjacent spleen using circular ROIs (C) and demonstrated an average splenic ADC of 0.767 × 10^{-3} mm^2/s. The normalized ADC (lesion-to-spleen ADC ratio) was 0.962; D-F: Magnetic resonance images in a 45-year-old female with pathologically proven G2 pancreatic neuroendocrine tumor. The lesion was located at the tail of the pancreas with a hypervascular enhancement pattern on contrast-enhanced arterial phase T1WI (yellow arrow, D). After confirming the lesion on arterial phase T1WI and diffusion-weighted imaging (B), circular ROI was placed within the lesion on the ADC map (B) and showed an ADC value of 1.260 × 10^{-3} mm^2/s. Similarly, ADC measurement was carried out on the adjacent spleen using circular ROIs (C) and demonstrated an average splenic ADC of 0.749 × 10^{-3} mm^2/s. The normalized ADC (lesion-to-spleen ADC ratio) was 1.682.

in the spleen[7]. Although these modalities showed high pooled sensitivity and specificity, they have the following shortcomings: They rely on phagocytosis of macrophages, the application of which in splenic visualization is quite limited as it requires minimal functioning of splenic tissues; and contrast agents or exogenous nuclear pharmaceuticals[7]. In addition, scintigraphy has limited value when the pancreatic lesion has a relatively small size since it has lower spatial resolution compared with CT or MRI. In addition, CE-US has limited diagnostic utility in fully examining the pancreatic tail due to the limited sonic window and operator-independent nature[24]. In contrast, DWI does not require any exogenous contrast media or ionizing radiation and can be performed comparatively rapidly.

It has been reported that ADC variability may be minimized by calculation of the normalized ADC value (lesion-to-spleen ADC ratios) with the help of technical factors in different organs and pathologies [18,19]. In our study, we used absolute ADC and normalized ADC values to differentiate IPAS from PNET. The key findings of our study fall into two main categories: (1) Both absolute and normalized ADC values performed equally well in the discrimination of IPAS from PNET. A cutoff value of 1.046 × 10^{-3} mm^2/s for absolute ADC was associated with 81.25% sensitivity, 100% specificity, and 89.66% accuracy with an AUC of 0.94 (95%CI: 0.8536-1.000) for the differential diagnosis of IPAS from PNET. Similarly, a cutoff value of 1.342 for normalized ADC was associated with 81.25% sensitivity, 92.31%

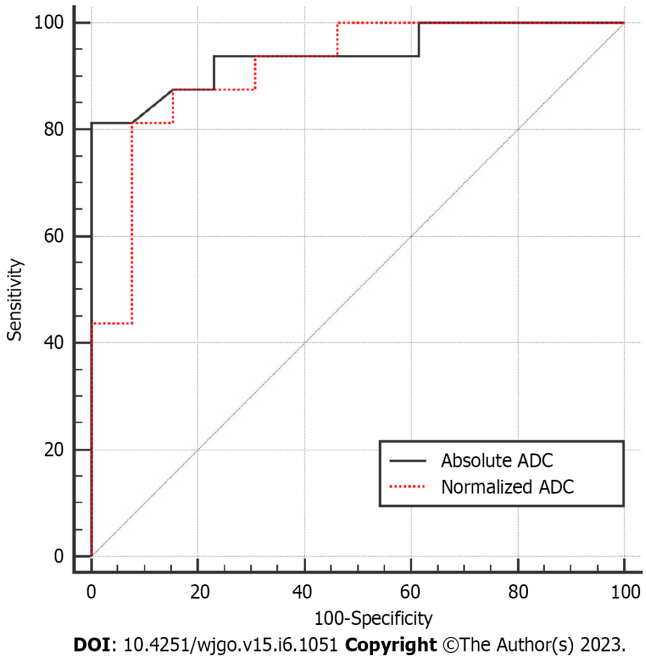

DOI: 10.4251/wjgo.v15.i6.1051 **Copyright** ©The Author(s) 2023.

Figure 3 Receiver operating characteristic curve for diagnostic performance of absolute apparent diffusion coefficient and normalized apparent diffusion coefficient values regarding the differentiation between intrapancreatic accessory spleen and pancreatic neuroendocrine tumor. ADC: Apparent diffusion coefficient.

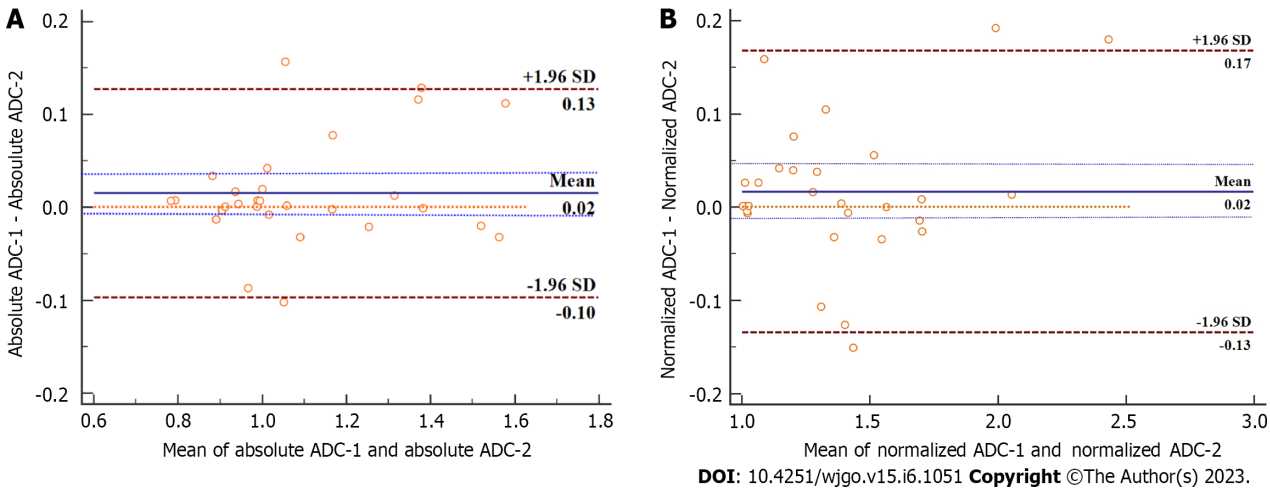

DOI: 10.4251/wjgo.v15.i6.1051 **Copyright** ©The Author(s) 2023.

Figure 4 Bland-Altman plots of absolute apparent diffusion coefficient and normalized apparent diffusion coefficient for the two readers' measurements with the representation of the 95% limits of agreement (dotted and dashed brown lines). A: Absolute apparent diffusion coefficient (ADC); B: Normalized ADC. For both absolute ADC and normalized ADC values, the bias between two readers (solid blue line) was not significant, with the line of equality (dotted orange line) falling within the 95% confidence interval of the mean difference (dashed blue lines). SD: Standard deviation.

specificity, and 86.21% accuracy with an AUC of 0.91 (95%CI: 0.8080-1.000) for the differential diagnosis of IPAS from PNET; and (2) A high degree of inter-reader reliability for absolute ADC [0.968 (95%CI: 0.933-0.985)] and normalized ADC values [0.976 (95%CI: 0.950-0.989)] were obtained in our study. There was no significant difference in diagnostic performance between absolute ADC and normalized ADC values with high inter-reader reliability. In clinical practice, absolute ADC provides the ease of a single measurement. However, further studies with a larger cohort size may be necessary to evaluate the definite superiority of one method over the other.

The spleen has a much lower ADC compared to the pancreas since it has a unique organ composition. A previous study revealed that the mean ADC value of IPAS was significantly lower than that of PNET (0.90×10^{-3} mm^2/s *vs* 1.44×10^{-3} mm^2/s, $P < 0.001$); A cutoff value of 1.07×10^{-3} mm^2/s demonstrated high pooled sensitivity (96.0%) and specificity (93.5%) in the differential diagnosis between IPAS and PNET[6]. In our study, the absolute ADC and normalized ADC values of the IPAS were $0.931 \pm 0.773 \times 10^{-3}$ mm^2/s and 1.154 ± 0.167, respectively, which were significantly lower than those of PNETs ($1.254 \pm$

0.219 × 10^{-3} mm^2/s and 1.591 ± 0.364). Our study was consistent with the previous study[6]. However, they did not investigate the potential value of the normalized ADC and their diagnostic performance in the differential diagnosis between the two entities. Our study showed an equal performance of both absolute ADC and normalized ADC values in the discrimination of IPAS from PNET and revealed a high degree of inter-reader reliability, which corroborated the findings a previous study demonstrated [1]. However, this study had unbalanced data with 51 PNETs and 11 IPAS lesions, and no algorithm was used to balance the data for further analysis.

Additionally, all patients underwent MRI scans using a 1.5-T MRI system, and a single scanner from one vendor was used to scan the patients. It is unclear whether the results can be generalized to all vendors. A recent study showed that ADC measurements of the pancreas may be affected by the field strength of the MRI scanner[17]. Our studies further validated that both absolute ADC and normalized ADC values are useful in the discrimination of IPAS from PNET with the 3.0-T MRI system and may be attributed to the fact that the IPAS has similar tissue structure and properties as the spleen, which possesses the lowest ADC values among the upper abdominal viscera.

Our study had several limitations. First, selection bias may be present due to its retrospective nature. Second, the number of enrolled patients is small. As we know, an IPAS is an uncommon condition, with a prevalence ranging from 1.1%-3.4% in individuals[25]. We could not include more IPAS patients in a short period of time. We will recruit more patients for further validation and reliability testing of our results. Third, although no difference regarding diagnostic performance of absolute ADC and normalized ADC values in discrimination of IPAS from PNET was observed, further studies with a larger cohort size may be needed to evaluate the definite superiority of one method over another. Fourth, there was no histopathological confirmation of IPAS in 6 cases since surgical resection is not recommended for IPAS. However, reasonable confidence was acquired with the criteria for the imaging diagnosis of IPAS combing typical imaging features and stability on imaging follow-up.

CONCLUSION

In conclusion, our study demonstrated that both absolute ADC and normalized ADC values allow clinically relevant differentiation of IPAS from PNET. Large-scale multicenter prospective cohort studies are needed to validate the potential value of absolute and normalized ADC values in differentiating IPAS from PNET.

ARTICLE HIGHLIGHTS

Research background

Intrapancreatic accessory spleen (IPAS) typically presents as a solitary, well-defined, hypervascular, ovoid or round mass with a maximum diameter < 3 cm on contrast-enhanced (CE) computed tomography or CE magnetic resonance imaging. They are often misdiagnosed as small (< 3 cm) hypervascular pancreatic neuroendocrine tumors (PNETs) since they share similar imaging findings. IPAS is innocuous in nature and generally does not require any treatment. However, surgery and/or chemotherapy are recommended for PNETs.

Research motivation

The overlap of imaging features between IPAS and small (< 3 cm) hypervascular PNET often requires surgical management. Therefore, preoperative characterization of IPAS *vs* small (< 3 cm) hypervascular PNET is of utmost importance. This study provided a non-invasive method for preoperatively differentiating these two entities.

Research objectives

This study aimed to investigate and compare the diagnostic performance of absolute apparent diffusion coefficient (ADC) and normalized ADC (lesion-to-spleen ADC ratios) in the differential diagnosis of IPAS from PNET.

Research methods

A retrospective study consisting of 16 PNET patients and 13 IPAS patients who underwent preoperative CE-magnetic resonance imaging together with diffusion-weighted imaging/ADC maps was performed. Two independent reviewers measured ADC on all lesions and spleens, and normalized ADC was calculated for further analysis. The receiver operating characteristics analysis was carried out for evaluating the diagnostic performance of both absolute ADC and normalized ADC values. Inter-reader reliability for the two methods was evaluated.

Research results

IPAS had significantly lower absolute ADC (0.931 ± 0.773 × 10^{-3} mm^2/s *vs* 1.254 ± 0.219 × 10^{-3} mm^2/s) and normalized ADC values (1.154 ± 0.167 *vs* 1.591 ± 0.364) as compared to PNET. A cutoff value of 1.046 × 10^{-3} mm^2/s for absolute ADC was associated with 81.25% sensitivity, 100% specificity, and 89.66% accuracy with an area under curve of 0.94 for the differential diagnosis of IPAS from PNET. Similarly, a cutoff value of 1.342 for normalized ADC was associated with 81.25% sensitivity, 92.31% specificity, and 86.21% accuracy with an area under the curve of 0.91 for the differential diagnosis of IPAS from PNET. Both methods showed excellent inter-reader reliability with intraclass correlation coefficients for absolute ADC and ADC ratio of 0.968 and 0.976, respectively.

Research conclusions

This study demonstrated that both absolute ADC and normalized ADC values allow clinically relevant differentiation of IPAS from PNET.

Research perspectives

This study provided a non-invasive method to preoperatively differentiate IPAS from PNET, which has a profound clinical significance in guiding treatment strategy and predicting prognosis for patients with IPAS and PNET. Large-scale multicenter prospective cohort studies are needed to validate the potential value of absolute and normalized ADC values in differentiating IPAS from PNET.

ACKNOWLEDGEMENTS

We thank all authors for their continuous and excellent support with patient data collection, imaging analysis, statistical analysis, and valuable suggestions for the article.

FOOTNOTES

Author contributions: Ren S, Guo K, and Li Y contributed equally to this work; Ren S, Wang ZQ, and Tian Y designed the research study; Ren S, Guo K, Li Y, and Cao YY performed the research; Ren S, Guo K, and Li Y analyzed the data; Ren S wrote the manuscript; Wang ZQ and Tian Y revised the manuscript; All authors read and approved the final manuscript.

Supported by the National Natural Science foundation of China, No. 82202135, and No. 82171925; Foundation of Excellent Young Doctor of Jiangsu Province Hospital of Chinese Medicine, No. 2023QB0112; Innovative Development Foundation of Department in Jiangsu Hospital of Chinese Medicine, No. Y2021CX19; and Developing Program for High-level Academic Talent in Jiangsu Hospital of TCM, No. y2021rc03.

Institutional review board statement: The study was reviewed and approved by the ethics committee of Affiliated Hospital of Nanjing University of Chinese Medicine (Approval No. 2017NL-137-05).

Informed consent statement: Informed consent statement was waived due to the retrospective nature of the study.

Conflict-of-interest statement: The authors declare that they have no conflicts of interest.

Data sharing statement: Patient imaging data and histopathology reports contain sensitive patient information and cannot be released publicly due to the legal and ethical restrictions imposed by the institutional ethics committee (Affiliated Hospital of Nanjing University of Chinese Medicine). Data is available upon reasonable request from the following e-mail address: zhongqiuwang@njucm.edu.cn.

Country/Territory of origin: China

ORCID number: Shuai Ren 0000-0003-4902-6298; Kai Guo 0000-0002-7593-2510; Yuan Li 0000-0002-1454-3976; Ying-Ying Cao 0000-0001-9067-6319; Zhong-Qiu Wang 0000-0001-6681-7345; Ying Tian 0000-0002-1525-0614.

S-Editor: Yan JP
L-Editor: Filipodia
P-Editor: Zhang XD

REFERENCES

1 **Pandey A**, Pandey P, Ghasabeh MA, Varzaneh FN, Khoshpouri P, Shao N, Pour MZ, Fouladi DF, Hruban RH, O'Broin-Lennon AM, Kamel IR. Accuracy of apparent diffusion coefficient in differentiating pancreatic neuroendocrine tumour from intrapancreatic accessory spleen. *Eur Radiol* 2018; **28**: 1560-1567 [PMID: 29134352 DOI: 10.1007/s00330-017-5122-3]

2 **Smith HC**, Kakar N, Shadid AM. Accessory Spleen Masquerading as an Intrapancreatic Tumor: A Case Report. *Cureus* 2022; **14**: e24677 [PMID: 35663712 DOI: 10.7759/cureus.24677]

3 **Wong A**, Fung KFK, Wong WC, Ng KK, Kung BT, Kan YLE. Multimodality imaging of developmental splenic anomalies: tips and pitfalls. *Clin Radiol* 2022; **77**: 319-325 [PMID: 35000764 DOI: 10.1016/j.crad.2021.12.014]

4 **Bhutiani N**, Egger ME, Doughtie CA, Burkardt ES, Scoggins CR, Martin RC 2nd, McMasters KM. Intrapancreatic accessory spleen (IPAS): A single-institution experience and review of the literature. *Am J Surg* 2017; **213**: 816-820 [PMID: 27894508 DOI: 10.1016/j.amjsurg.2016.11.030]

5 **Ishigami K**, Nishie A, Nakayama T, Asayama Y, Kakihara D, Fujita N, Ushijima Y, Okamoto D, Ohtsuka T, Mori Y, Ito T, Mochidome N, Honda H. Superparamagnetic iron-oxide-enhanced diffusion-weighted magnetic resonance imaging for the diagnosis of intrapancreatic accessory spleen. *Abdom Radiol (NY)* 2019; **44**: 3325-3335 [PMID: 31420705 DOI: 10.1007/s00261-019-02189-8]

6 **Kang BK**, Kim JH, Byun JH, Lee SS, Kim HJ, Kim SY, Lee MG. Diffusion-weighted MRI: usefulness for differentiating intrapancreatic accessory spleen and small hypervascular neuroendocrine tumor of the pancreas. *Acta Radiol* 2014; **55**: 1157-1165 [PMID: 24259300 DOI: 10.1177/0284185113513760]

7 **Jang KM**, Kim SH, Lee SJ, Park MJ, Lee MH, Choi D. Differentiation of an intrapancreatic accessory spleen from a small (<3-cm) solid pancreatic tumor: value of diffusion-weighted MR imaging. *Radiology* 2013; **266**: 159-167 [PMID: 23093681 DOI: 10.1148/radiol.12112765]

8 **Lin X**, Xu L, Wu A, Guo C, Chen X, Wang Z. Differentiation of intrapancreatic accessory spleen from small hypervascular neuroendocrine tumor of the pancreas: textural analysis on contrast-enhanced computed tomography. *Acta Radiol* 2019; **60**: 553-560 [PMID: 30086651 DOI: 10.1177/0284185118788895]

9 **Yin Q**, Wang M, Wang C, Wu Z, Yuan F, Chen K, Tang Y, Zhao X, Miao F. Differentiation between benign and malignant solid pseudopapillary tumor of the pancreas by MDCT. *Eur J Radiol* 2012; **81**: 3010-3018 [PMID: 22520082 DOI: 10.1016/j.ejrad.2012.03.013]

10 **Huang M**, Li J, Yin Q, Xiong L. Surgical Strategy and Prognosis of Pancreatic Neuroendocrine Tumors Based on Smart Medical Imaging. *Contrast Media Mol Imaging* 2022; **2022**: 8752375 [PMID: 35821889 DOI: 10.1155/2022/8752375]

11 **Kato T**, Matsuo Y, Ueda G, Aoyama Y, Omi K, Hayashi Y, Imafuji H, Saito K, Tsuboi K, Morimoto M, Ogawa R, Takahashi H, Kato H, Yoshida M, Naitoh I, Hayashi K, Takahashi S, Takiguchi S. Epithelial cyst arising in an intrapancreatic accessory spleen: a case report of robotic surgery and review of minimally invasive treatment. *BMC Surg* 2020; **20**: 263 [PMID: 33129283 DOI: 10.1186/s12893-020-00927-0]

12 **Kurita A**, Mori Y, Someya Y, Kubo S, Azuma S, Iwano K, Ikeda S, Okumura R, Yazumi S. High signal intensity on diffusion-weighted magnetic resonance images is a useful finding for detecting early-stage pancreatic cancer. *Abdom Radiol (NY)* 2021; **46**: 4817-4827 [PMID: 34223962 DOI: 10.1007/s00261-021-03199-1]

13 **Gong XH**, Xu JR, Qian LJ. Atypical and uncommon CT and MR imaging presentations of pancreatic ductal adenocarcinoma. *Abdom Radiol (NY)* 2021; **46**: 4226-4237 [PMID: 33914139 DOI: 10.1007/s00261-021-03089-6]

14 **Jia H**, Li J, Huang W, Lin G. Multimodel magnetic resonance imaging of mass-forming autoimmune pancreatitis: differential diagnosis with pancreatic ductal adenocarcinoma. *BMC Med Imaging* 2021; **21**: 149 [PMID: 34654379 DOI: 10.1186/s12880-021-00679-0]

15 **Zeng P**, Ma L, Liu J, Song Z, Yuan H. The diagnostic value of intravoxel incoherent motion diffusion-weighted imaging for distinguishing nonhypervascular pancreatic neuroendocrine tumors from pancreatic ductal adenocarcinomas. *Eur J Radiol* 2022; **150**: 110261 [PMID: 35316674 DOI: 10.1016/j.ejrad.2022.110261]

16 **Grech-Sollars M**, Hales PW, Miyazaki K, Raschke F, Rodriguez D, Wilson M, Gill SK, Banks T, Saunders DE, Clayden JD, Gwilliam MN, Barrick TR, Morgan PS, Davies NP, Rossiter J, Auer DP, Grundy R, Leach MO, Howe FA, Peet AC, Clark CA. Multi-centre reproducibility of diffusion MRI parameters for clinical sequences in the brain. *NMR Biomed* 2015; **28**: 468-485 [PMID: 25802212 DOI: 10.1002/nbm.3269]

17 **Ye XH**, Gao JY, Yang ZH, Liu Y. Apparent diffusion coefficient reproducibility of the pancreas measured at different MR scanners using diffusion-weighted imaging. *J Magn Reson Imaging* 2014; **40**: 1375-1381 [PMID: 24222019 DOI: 10.1002/jmri.24492]

18 **Jang W**, Song JS, Kwak HS, Hwang SB, Paek MY. Intra-individual comparison of conventional and simultaneous multislice-accelerated diffusion-weighted imaging in upper abdominal solid organs: value of ADC normalization using the spleen as a reference organ. *Abdom Radiol (NY)* 2019; **44**: 1808-1815 [PMID: 30737546 DOI: 10.1007/s00261-019-01924-5]

19 **Ding X**, Xu H, Zhou J, Xu J, Mei H, Long Q, Wang Y. Reproducibility of normalized apparent diffusion coefficient measurements on 3.0-T diffusion-weighted imaging of normal pancreas in a healthy population. *Medicine (Baltimore)* 2019; **98**: e15104 [PMID: 30946375 DOI: 10.1097/MD.0000000000015104]

20 **Guo CG**, Ren S, Chen X, Wang QD, Xiao WB, Zhang JF, Duan SF, Wang ZQ. Pancreatic neuroendocrine tumor: prediction of the tumor grade using magnetic resonance imaging findings and texture analysis with 3-T magnetic resonance. *Cancer Manag Res* 2019; **11**: 1933-1944 [PMID: 30881119 DOI: 10.2147/CMAR.S195376]

21 **Ma C**, Yang P, Li J, Bian Y, Wang L, Lu J. Pancreatic adenocarcinoma: variability in measurements of tumor size among computed tomography, magnetic resonance imaging, and pathologic specimens. *Abdom Radiol (NY)* 2020; **45**: 782-788 [PMID: 31292672 DOI: 10.1007/s00261-019-02125-w]

22 **Vandekerckhove E**, Ameloot E, Hoorens A, De Man K, Berrevoet F, Geboes K. Intrapancreatic accessory spleen mimicking pancreatic NET: can unnecessary surgery be avoided? *Acta Clin Belg* 2021; **76**: 492-495 [PMID: 32394810 DOI: 10.1080/17843286.2020.1762351]

23 **Kim SH**, Lee JM, Han JK, Lee JY, Kang WJ, Jang JY, Shin KS, Cho KC, Choi BI. MDCT and superparamagnetic iron oxide (SPIO)-enhanced MR findings of intrapancreatic accessory spleen in seven patients. *Eur Radiol* 2006; **16**: 1887-1897 [PMID: 16547707 DOI: 10.1007/s00330-006-0193-6]

24 **Kim SH**, Lee JM, Han JK, Lee JY, Kim KW, Cho KC, Choi BI. Intrapancreatic accessory spleen: findings on MR Imaging, CT, US and scintigraphy, and the pathologic analysis. *Korean J Radiol* 2008; **9**: 162-174 [PMID: 18385564 DOI: 10.3348/kjr.2008.9.2.162]

25 **Li BQ**, Xu XQ, Guo JC. Intrapancreatic accessory spleen: a diagnostic dilemma. *HPB (Oxford)* 2018; **20**: 1004-1011 [PMID: 29843985 DOI: 10.1016/j.hpb.2018.04.004]

World Journal of Gastrointestinal Oncology

Submit a Manuscript: https://www.f6publishing.com

World J Gastrointest Oncol 2023 June 15; 15(6): 1062-1072

DOI: 10.4251/wjgo.v15.i6.1062

ISSN 1948-5204 (online)

ORIGINAL ARTICLE

Retrospective Study

Chicken skin mucosa surrounding small colorectal cancer could be an endoscopic predictive marker of submucosal invasion

Ying-Jie Zhang, Wu Wen, Fan Li, Yi Jian, Chuan-Ming Zhang, Meng-Xia Yuan, Ye Yang, Feng-Lin Chen

Specialty type: Gastroenterology and hepatology

Provenance and peer review: Unsolicited article; Externally peer-reviewed.

Peer-review model: Single-blind

Peer-review report's scientific quality classification

Grade A (Excellent): 0
Grade B (Very good): B, B, B
Grade C (Good): C, C
Grade D (Fair): 0
Grade E (Poor): 0

P-Reviewer: Ichita C, Japan; Musa Y, Nigeria; Osera S, Japan

Received: January 13, 2023
Peer-review started: January 13, 2023
First decision: February 9, 2023
Revised: February 23, 2023
Accepted: April 23, 2023
Article in press: April 23, 2023
Published online: June 15, 2023

Ying-Jie Zhang, Wu Wen, Fan Li, Yi Jian, Chuan-Ming Zhang, Meng-Xia Yuan, Department of Digestive Diseases, Chengdu Second People's Hospital, Chengdu 610000, Sichuan Province, China

Ye Yang, Feng-Lin Chen, Graduate School, Chengdu Medical College, Chengdu 610000, Sichuan Province, China

Corresponding author: Meng-Xia Yuan, MD, Doctor, Department of Digestive Diseases, Chengdu Second People's Hospital, No. 10 Qingyun South Street, Chengdu 610000, Sichuan Province, China. 1062274198@qq.com

Abstract

BACKGROUND

Chicken skin mucosa (CSM) surrounding colon polyps is a common endoscopic finding with pale yellow-speckled mucosa during a colonoscopy screening. Although reports about CSM surrounding small colorectal cancer are scarce, and its clinical significance in intramucosal and submucosal cancers is unclear, previous studies have suggested it could be an endoscopic predictive marker for colonic neoplastic and advanced polyps. Currently, because of the inaccurate preoperative evaluation by endoscopists, many small colorectal cancers, particularly lesions with a diameter < 2 cm, are improperly treated. Therefore, more effective methods are required to better assess the depth of the lesion before treatment.

AIM

To explore potential markers of small colorectal cancer early invasion under white light endoscopy, providing patients with better treatment alternatives.

METHODS

This retrospective cross-sectional study included 198 consecutive patients [233 early colorectal cancers (ECCs)] who underwent endoscopy or surgical procedures at the Digestive Endoscopy Center of Chengdu Second People's Hospital between January 2021 and August 2022. The participants had pathologically confirmed colorectal cancer with a lesion diameter < 2 cm and received endoscopic or surgical treatment, including endoscopic mucosal resection and submucosal dissection. Clinical pathology and endoscopy parameters, including tumor size, invasion depth, anatomical position, and morphology, were reviewed. Fisher's exact test, the χ^2 test, and Student's *t*-test were used to analyze the

patient's basic characteristics. Logistic regression analysis was used to examine the relationship between morphological characteristics, size, CSM prevalence, and ECC invasion depth under white light endoscopy. Statistical significance was set at $P < 0.05$.

RESULTS

The submucosal carcinoma (SM stage) was larger than the mucosal carcinoma (M stage) with a significant difference (17.2 ± 4.1 *vs* 13.4 ± 4.6 mm, $P < 0.01$). M- and SM-stage cancers were common in the left colon; however, no significant differences were found between them (151/196, 77% and 32/37, 86.5%, respectively, $P = 0.199$). The endoscopic features of colorectal cancer revealed that CSM, depressed areas with clear boundaries, and erosion or ulcer bleeding were more common in the SM-stage cancer group than in the M-stage cancer group (59.5% *vs* 26.2%, 46% *vs* 8.7%, and 27.3% *vs* 4.1%, respectively, $P < 0.05$). CSM prevalence in this study was 31.3% (73/233). The positive rates of CSM in flat, protruded, and sessile lesions were 18% (11/61), 30.6% (30/98), and 43.2% (32/74), respectively, with significant differences ($P = 0.007$).

CONCLUSION

CSM-related small colorectal cancer was primarily located in the left colon and could be a predictive marker of submucosal invasion in the left colon.

Key Words: Chicken skin mucosa; Colonoscopy; Colorectal cancer; Submucosal invasion; White light endoscopy; Endoscopic features

Core Tip: Chicken skin mucosa (CSM) surrounding colorectal polyps is a relatively common clinical feature. Previous studies have found that it could be an endoscopic predictor of neoplastic and advanced colorectal polyps. However, it is unclear whether it is associated with early colorectal cancer or invasion. In our study, CSM-related small colorectal cancer was mainly found in the distal colon; this could be a potential predictive marker of submucosal invasion cancers located in the left colon. Since these cancers cannot be treated as a normal polyp, biopsy snare, cold-snare polypectomy, and cold-snare endoscopic mucosal resection may not be the appropriate options.

Citation: Zhang YJ, Wen W, Li F, Jian Y, Zhang CM, Yuan MX, Yang Y, Chen FL. Chicken skin mucosa surrounding small colorectal cancer could be an endoscopic predictive marker of submucosal invasion. *World J Gastrointest Oncol* 2023; 15(6): 1062-1072
URL: https://www.wjgnet.com/1948-5204/full/v15/i6/1062.htm
DOI: https://dx.doi.org/10.4251/wjgo.v15.i6.1062

INTRODUCTION

Abnormal colorectal adenomatous mucosa is widely used as an indication to screen for colorectal cancer early. Chicken skin mucosa (CSM) is a mucosal anomaly defined by a pale-yellow speckled pattern in the colon and rectum observed under conventional white light endoscopy. It was first reported in 1998 [1] and is characterized by fat accumulation in the lamina propria macrophages. Previous studies suggest that CSM is caused by colonic intestinal metaplasia, toxic factors from damaged intraluminal mucosa, or previous mild damage. Recent studies have observed that it may effectively predict colorectal adenoma and adenoma carcinogenesis[2,3]. However, its significance in intramucosal and submucosal cancers is unclear. Therefore, we retrospectively analyzed the endoscopic results of 233 patients with early colorectal cancer (ECC) (< 20 mm in diameter), including the tumor location, morphology, CSM features, and other conventional white light endoscopic findings, to improve endoscopists' understanding of the white light endoscopic features of invasive colorectal cancer (< 20 mm diameter) to prevent misdiagnosis and reduce non-curative resection, thereby improving patient outcomes.

MATERIALS AND METHODS

Clinical data

CSM is a common endoscopic finding during a colonoscopy screening; it is a mucosal anomaly characterized by a pale-yellow speckled pattern surrounding the colon and rectum polyps observed before or after injection under conventional white light endoscopy. Patients aged between 18 and 85 years who underwent screening, surveillance, or diagnostic colonoscopy at the Digestive Endoscopy Center of Chengdu Second People's Hospital between January 2021 and August 2022 were enrolled in this retrospective study. ECCs were screened based on the pathological results after endoscopic or surgical operation. These are cancers with an invasion depth limited to the mucosa and submucosa, regardless of lymph node metastasis.

Our study complied with the diagnostic criteria of the Japanese Colorectal Cancer Research Association[4]. Intramucosal carcinoma refers to cellular or structural atypia to a certain extent, and the lesions are limited to the mucosal layer, confining the focus to the mucosal layer. Submucosal carcinoma (SM-stage cancer) refers to lesions where atypical cells break through the muscularis mucosae and infiltrate the submucosa.

The inclusion criteria were as follows: (1) Receiving endoscopic or surgical treatment, including endoscopic mucosal resection (EMR), endoscopic submucosal dissection (ESD) or surgical treatment, and pathologically confirmed colorectal cancer; and (2) a lesion diameter < 2 cm.

The exclusion criteria were as follows: (1) A history of colorectal carcinoma (CRC) or inflammatory bowel disease; (2) familial adenomatous polyposis; (3) poor bowel preparation; and (4) a history of malignancy at other sites.

Study equipment

Standard colonoscopes were used throughout (CF H260AI, CF Q260AI, or CF Q290AI, Olympus Limited, Tokyo, Japan), and lesion size was measured *in vivo* using open biopsy forceps with a deployed diameter of 7 mm (QYQ-AXC2.3X2300, Changchun Huichun Medical Devices, China).

Research method

Endoscopic findings: The endoscopic imaging data of the patients were reviewed, and when the record was unclear or controversial, an experienced doctor reconfirmed. The lesion location and size, morphological classification under endoscopy, and morphological indexes for predicting ECC depth reported in previous literature were analyzed.

(1) Location: Tumors were either in the right (including the cecum, ascending colon, transverse colon, or splenic flexure) or left (including the descending colon, sigmoid colon, and rectum) colon; and (2) Morphology: According to the Paris classification[4], there were three types of tumors based on their endoscopic morphological characteristics, including protruded (0-I), flat (0-II), and depressed (0-III) types. According to whether the lesions had no pedicle, type 0-I polyp was classified into pedunculated and sessile lesions.

The following parameters[5-7] facilitated ECC depth prediction: CSM, fold convergency, loss of lobulation, surface fullness, a depressed area with a clear boundary, a deeper red mucosal color, erosion or ulcer bleeding, and stalk swelling[5-8]. The relationship between our results and ECC depth was determined using statistical analysis.

Cure criterion: Tumor invasion limited to the mucosal layer is referred to as mucosal carcinoma (M-stage cancer), and invasion into the submucosal layer without muscularis propria invasion is known as SM-stage cancer. With a boundary of the submucosal membrane (SM) of 1000 μm, the penetration depth to the inferior margin of the mucosal layer was defined as superficial submucosal membrane carcinoma (SM1), and that of > 1000 μm was defined as deep SM-stage cancer (SM2 and SM3).

All the cases in this study were adenocarcinomas, and the submucosal invasion depth was measured in SM-stage cancer specimens resected using ESD. The requirements for curative resection were as follows: (1) R0 resection; (2) an invasion depth of M- or SM-stage cancer of < 1 mm from the muscularis mucosa, or an invasion depth of pedunculated SM-stage cancer of < 3 mm from the Haggitt's level II; (3) no lymphatic or vascular vessel invasion; and (4) well- and moderately-differentiated adenocarcinoma. However, failure to meet any of the criteria above resulted in non-curative resection (Figure 1).

Statistical analysis

The statistical review of the study was performed by a biomedical statistician. Statistical analysis was performed using IBM SPSS Statistics, Version 23.0 (IBM Corp., Armonk, NY, United States) based on the pathological diagnosis. Continuous variables are expressed as mean ± SD. This study's primary outcome was to evaluate the different endoscopic findings among small M- and SM-stage cancers. Patients' baseline characteristics were analyzed using descriptive statistics. Furthermore, enumeration data are expressed as percentages or rates (%). Fisher's exact test, the χ^2 test, and Student's *t*-test were used to analyze the patients' basic characteristics, and the endoscopy revealed differences in CRC with different immersion depths. Statistical significance was considered at $P < 0.05$. Multivariate analysis was

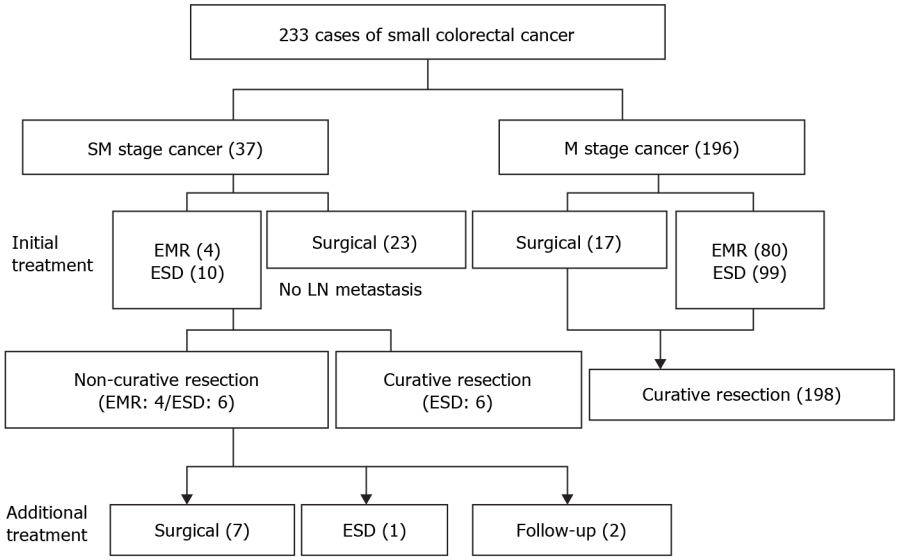

DOI: 10.4251/wjgo.v15.i6.1062 **Copyright** ©The Author(s) 2023.

Figure 1 Treatment of colorectal cancer. SM: Submucosal; ESD: Endoscopic submucosal dissection; EMR: Endoscopic mucosal resection; M: Mucosal; LN: Lymph node.

performed using logistic regressions. We included the data that had a level of significance at $P < 0.05$ or approximately 0.05 in the bivariate analysis as independent variables. This study's statistical methods were reviewed by Yang Y and Chen FL from the Department of Chengdu Medical College Statistics.

RESULTS

Prevalence of ECCs and CSM

Between January 2021 and August 2022, 233 ECC cases (198 patients) were diagnosed under endoscopy and pathologically confirmed at our hospital. There were 133 males and 65 females, with a male-to-female ratio of 2.05:1. The patients' ages were 29-85 years (median, 62.2 years). There were 196 and 37 cases of M- and SM-stage cancers, respectively, with a ratio of 5.3:1. M- and SM-stage cancers were commonly observed in the left colon. The diameter of M-stage cancer was 1.34 ± 0.46 cm, and that of SM-stage cancer was significantly larger (1.72 ± 0.41 cm). The diameters of all SM-stage cancers were > 1 cm, and a statistical difference was observed between the groups (Table 1).

The CSM prevalence in this study was 31.3% (73/233). The positive rates of CSM in flat, pedunculated, and sessile lesions were 18% (11/61), 30.6% (30/98), and 43.2% (32/74), respectively, with significant differences ($P = 0.007$). The positive rate of CSM in sessile lesions was the highest. However, the positive CSM rate in the left colon was higher than that in the right colon (36.07% *vs* 14%), with a significant difference ($P = 0.03$). Lesions > 1 cm were more likely to reveal CSM (34.39% *vs* 18.18%), and the difference was significant ($P = 0.037$) (Table 2).

Relationship between morphological characteristics and invasion depth under white light endoscopy

Based on the endoscopic morphological classification, elevated lesions (73.8%, 172/233) were more common than flat lesions (26.2%, 61/233). In this study, the proportions of flat and sessile lesions were higher than that of M-stage cancer; however, no significant difference was observed between the types at different depths of invasion. The number of laterally spreading tumors (LSTs) included in 0-IIA lesions and SM-stage cancer was low and could not be further stratified. In addition, the 0-IS + 0-IIC type was classified as 0-IS type, 0-IIA + 0-IIC type as 0-IIA type, and 0-IIC + 0-IIA type as IIc type (Table 3).

CSM is a depressed area with clear boundaries, erosion, or ulcer bleeding, and these features are more common in SM-stage cancers. In total, 59.5% (22/37) of cases had "chicken skin" changes in the basal mucosa around the SM-stage cancer lesion; however, the corresponding number in M-stage cancer was 26.2% (51/196), and the difference was significant ($P < 0.001$). In 45.9% (17/37) of SM-stage cancers, local depressions with clear boundaries were observed, whereas these were observed in 8.7% (17/196) of M-stage cancers, and the difference was significant ($P < 0.001$).

The proportion of local erosion or ulcer bleeding in M-stage cancer was 4.1% (8/196), whereas it was 27.3% (10/37) in SM-stage cancer, and the difference was significant ($P < 0.01$). There were 98 0-Ip and 0-Isp lesions, including 87 M- and 11 SM-stage tumors. Stalk swelling was observed in 13.8% (12/87) and 54.6% (6/11) of M- and SM-stage tumor cases, respectively. The *P* value of Fisher's exact probability

Table 1 Demographics of both groups [mean ± SD, *n* (%)]

		SM (37)	M (196)	*P* value
Age (mean ± SD, yr)		66.9 ± 9.6	61.24 ± 11.1	0.06
Sex	Male	25 (67.6)	110 (66.3)	0.879
	Female	12 (32.4)	56 (33.7)	
Size (mm)		17.2 ± 4.1	13.4 ± 4.6	< 0.001
Location	Right colon	5 (13.5)	45 (23)	0.199
	Left colon	32 (86.5)	151 (77)	

SM: Submucosal; M: Mucosal; SD: Standard deviation.

Table 2 Chicken skin mucosa prevalence in different morphological lesions, *n* (%)

		CSM (+) 73	CSM (-) 160	*P* value
M		51 (69.86)	145 (90.63)	< 0.001
SM		22 (30.14)	15 (9.37)	
Morphology	Flat (IIa, LST)	11 (15.07)	50 (31.25)	0.007
	Pedunculated (Isp, Ip)	30 (41.1)	68 (42.5)	
	Sessile (Is, Is + IIc)	32 (43.84)	42 (26.25)	
Location	Left colon	66 (90.41)	117 (73.13)	0.03
	Right colon	7 (9.59)	43 (26.88)	
Size	≥ 10 mm	65 (89.04)	124 (77.5)	0.037
	< 10 mm	8 (10.96)	36 (22.5)	

CSM: Chicken skin mucosa; SM: Submucosal; M: Mucosal; LST: Laterally spreading tumor.

Table 3 Comparison of different morphological tumor types and depth of invasion in early colorectal cancer, *n* (%)

	Total	SM	M	*P* value
Morphology	233	37	196	0.252
Flat	61 (26.18)	12 (32.43)	49 (25)	
Pedunculated	98 (42.06)	11 (29.73)	87 (44.39)	
Sessile	74 (31.76)	14 (37.84)	60 (30.61)	

SM: Submucosal; M: Mucosal.

analysis was 0.04. However, its significance should be further explored using data from a larger sample. Therefore, if "chicken skin" changes and local depressions with clear boundaries, local erosion, or ulcer bleeding are observed under white light endoscopy, possible lesion invasion of the submucosa should be considered. However, no significant difference was observed in the proportion of mucosal fold convergency, loss of lobulation, surface fullness, and deeper red mucosal color between M- and SM-stage cancers ($P > 0.05$) (Table 4). Logistic regression results showed that CSM, a depressed area with clear boundaries, erosion, or ulcer bleeding, and size (≥ 10 mm) were independent risk factors for submucosal invasion in ECC (Table 5).

Relationship between CSM prevalence and invasion depth of ECC

Further stratification based on the growth morphology of the lesions revealed that the positive rates of CSM in flat-type SM- and M-stage cancers were 41.64% (5/12) and 12.24% (6/49), respectively, with a significant difference ($P = 0.03$).

Table 4 Comparison of morphological characteristics and invasion depth of early colorectal cancer under white light endoscopy, *n* (%)

Endoscopic finding	SM (37)	M (196)	*P* value
(All) CSM	22 (59.5)	51 (26.2)	< 0.001
(All) Ulceration or errhysis	10 (27.3)	8 (4.1)	< 0.001
(All) Demarcated depressed area	17 (46)	17 (8.7)	< 0.001
(All) Deeper red mucosal color	26 (70.3)	130 (66.3)	0.354
(P, S) Loss of lobulation	5/15 (33.3)	30/145 (20.7)	0.323
(P) Stalk swelling	6/11 (54.6)	12/87 (13.8)	0.04
(F) Fold convergency	2/49 (4.1)	4/12 (33.3)	0.11
(P, S) Fullness	28/147 (19)	8/25 (32)	0.14

CSM: Chicken skin mucosa; SM: Submucosal; M: Mucosal.

Table 5 Logistic regression analyses of the risk factors for invasion depth of early colorectal cancer under white light endoscopy

Variable	OR (95%CI)	*P* value
Size (≥ 10 mm/10 mm)	3.89 (1.35-11.26)	0.01
CSM (+/-)	2.54 (1.14-5.95)	0.04
Ulceration or errhysis (+/-)	5.44 (1.64-17)	0.006
Demarcated depressed area (+/-)	5.82 (2.31-14.6)	0.01
Stalk swelling	1.03 (0.26-4.06)	0.97

CSM: Chicken skin mucosa; OR: Odds ratio; CI: Confidence interval.

The positive rates of CSM in protruded-type SM- and M-stage cancers were 63.64% (7/11) and 26.44% (23/87), respectively, with a significant difference (P = 0.03). Furthermore, the positive rates of CSM in sessile-type SM- and M-stage cancers were 71.43% (10/14) and 36.67% (23/87), respectively, with a statistical difference (P = 0.02) (Table 6). According to the results of logistic regressions, submucosal invasion, anatomical position (left colon), and growth morphology (pedunculated or sessile) were independent risk factors for CSM changes in ECCs (Table 7).

DISCUSSION

According to statistics, the incidence and mortality rates of CRC rank third and second in the incidence and death spectrums, respectively, of malignant tumors[9]. The CRC incidence and mortality rates also have an increasing trend in China. However, early diagnosis and intervention can considerably improve the quality of life and the 5-year survival rate of patients with CRC. Endoscopic treatment is feasible for colorectal precancerous lesions, M-stage cancer, and colorectal cancer confined to SM1. However, surgical treatment is necessary for patients with an invasion depth exceeding a third of the upper submucosa due to the high lymph node metastasis rate[10]. Therefore, an accurate judgment of tumor nature, size, and depth of invasion under endoscopy is a vital prerequisite for making tumor treatment choices. Combining narrowband imaging and magnifying endoscopy has been consistently recognized for identifying and diagnosing early tumors, with improved detection rates of early and advanced cancers[11]. However, many primary hospitals lack the conditions for routinely using magnifying endoscopy and can only screen using conventional white light endoscopy. Furthermore, the current understanding of such lesions is insufficient, particularly those with a diameter < 2 cm. Before the pathological tissue evaluation, it is challenging to judge the nature and invasion depth of lesions under conventional white light endoscopy, which may lead endoscopists to select inappropriate treatment; however, it cannot achieve curative resection. The definition of colorectal cancer differs between Western countries and Japan, and this study referred to the Japanese Society for Colon Cancer Research and Vienna classification criteria[4,12]. M-stage cancer refers to a certain degree of cellular or structural atypia where the lesion is confined to the mucosal layer. In contrast, SM-stage cancer refers to lesions where abnormal cells break through the muscularis mucosa and infiltrate the submucosa. In SM-stage

Table 6 Comparison of chicken skin mucosa prevalence and invasion depth in different lesion morphologies

	Total	SM	M	*P* value
Morphology	233	37	196	0.252
Flat	CSM (+)	5 (41.67)	6 (12.24)	0.03
	CSM (-)	7 (58.33)	43 (87.76)	
Protruded	CSM (+)	7 (63.64)	23 (26.44)	0.03
	CSM (-)	4 (36.36)	64 (73.56)	
Sessile	CSM (+)	10 (71.43)	22 (36.67)	0.02
	CSM (-)	4 (28.57)	38 (63.33)	

CSM: Chicken skin mucosa; SM: Submucosal; M: Mucosal.

Table 7 Logistic regression analyses of risk factors for the occurrence of chicken skin mucosa

Variable	OR (95%CI)	*P* value
SM/M	3.76 (1.7-8.3)	0.01
Location (left/right colon)	2.45 (1.03-5.82)	0.04
Size (≥ 10 mm/< 10 mm)	1.15 (0.59-1.41)	0.09
Morphology (flat/pedunculated/sessile)	1.54 (0.79-3.06)	
	1.66 (0.85-3.27)	0.03

CSM: Chicken skin mucosa; SM: Submucosal; M: Mucosal; OR: Odds ratio; CI: Confidence interval.

carcinoma, if the immersion depth exceeds 1000 μm of the submucosal layer, there is a metastasis risk of 6%-12%[13]. At this time, endoscopic resection cannot attain curative standards; therefore, it is unsuitable for treatment, and clinicians should pay more attention. Endoscopists frequently select treatment based on the location, shape, and endoscopic appearance of the lesion[14]. In this study, the most common sites of ECCs were the rectum and sigmoid colon, consistent with the common site of colorectal cancer in the left colon. Moreover, the lesion diameter affects the depth of ECCs invasion. The diameter of SM-stage cancers was significantly larger than that of M-stage cancers, and there was a significant difference between the groups. Furthermore, the SM-stage cancer diameter was > 1 cm, similar to the conclusion of a previous study[5]. According to the literature, the lesion morphology of ECC detected in Western countries is mainly the hump type (0-I type). Conversely, this study's results were similar to the protruded type (0-I type). The proportion of protruded type (0-I type) lesions was 73.82%, possibly because hump-type lesions are easier to detect than flat types during colonoscopy. In this study, the proportions of flat, pedunculated, and sessile lesions in ECCs with different depths of invasion were similar, without significant differences. Because of the few 0-IIa, 0-IIa + 0-IIc, 0-IIc + 0-IIa, and LST lesions, further detailed stratification and comparison were not performed.

According to the literature, CSM, fold convergency, loss of lobulation, surface fullness, a depressed area with a clear boundary, deeper red mucosal color, erosion, or ulcer bleeding, and stalk swelling under standard white light endoscopy are commonly used to analyze the depth of invasion of ECC. In this study, the sessile lesions, left hemicolons, and lesions > 1 cm had a higher positive rate of CSM, which is consistent with the results of previous studies[1-3].

CSM is an endoscopic finding with uniform yellow-white spots around the lesion base, and the corresponding pathological manifestation is fat accumulation in the lamina propria macrophages. It is similar to the endoscopic appearance of gastric xanthoma. CSM is not the same as white spots, which are associated with invasive cancer, and is effective in inhibiting the progression of lesions with high malignant potential[15]. The CSM was classified into two based on their characteristics in related research[3]. Type 1 CSM was obvious under a white light endoscope and could be confirmed before injection, which was similar to white spots. However, type 2 differed from white spots and was certainly difficult to detect under the routine white light endoscopy screening. Therefore, the submucosal injection (NS: Normal saline + methylene blue) was needed, and CSM was observed in the bulging mucosa and the blue background of the mucosa (Figure 2).

The histopathology revealed foam cells filled with lipids in the mucosa. Furthermore, it is regarded as a compensatory response to polyp growth[16]. However, a study in 2012 reported that the expression

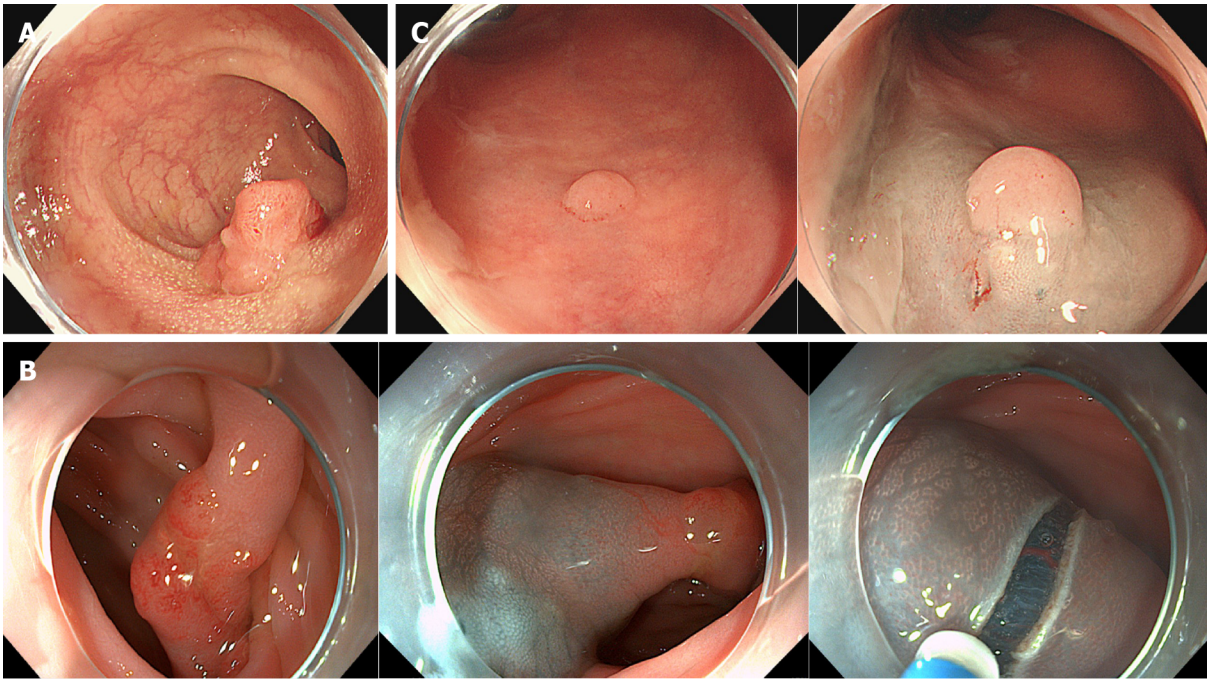

DOI: 10.4251/wjgo.v15.i6.1062

Figure 2 Endoscopic appearances of chicken skin mucosa. A: Type 1 chicken skin mucosa (CSM, confirmed before injection); B: Type 2 CSM (confirmed after injection); C: CSM not be observed.

levels of proliferation markers (ki-67, COX-2) were higher in adenocarcinomas and adenomas with CSM [17]. A recent study revealed that CSM is associated with carcinogenesis and its progression[18]. Macrophages are important immune cells vital to cancer pathophysiology progression. The stool is retained in the left colon for a longer time; therefore, because of the retaining stool, bacteria, and macrophages, more bowel inflammation is experienced. Therefore, the abnormal inflammation or increased expression of inflammatory genes may have resulted in tumorigenesis despite the lack of macrophages revealing CSM.

Currently, for the endoscopic resection of lesions without signs of submucosal invasion, cold snare polypectomy is recommended for lesions smaller than 10 mm; EMR is recommended for non-pedunculated lesions larger than 20 mm according to the European Society of Gastrointestinal Endoscopy clinical guidelines and the United States Multi-Society Task Force[19,20]. However, the optimal resection method of 10-20 mm (medium size) remains controversial, and whether hot or cold resection is preferable remains unclear. Recently, some studies have demonstrated that cold-snare EMR can be safely performed e*n bloc* for 10-14 mm colorectal adenomas without severe adverse events. However, the histological complete resection rate and submucosal layer found in the resected specimens were 63.8% and 25.0%, respectively[21]. For early-stage small colorectal cancer with submucosal invasion, this resection is non-curative. Therefore, it is crucial to determine whether the ECC has a submucosal invasion before the surgical choice of treatment and the prognosis of patients. Our study can be useful in this regard.

Previous studies have revealed that surface fullness is an important characteristic of ECC; however, this study's results reveal that it is not vital to determine whether the tumor invades the submucosa. The primary reason could be that the surface fullness mainly reflects tumor growth expansion. When it progresses to a certain stage, with tumor volume increase, particularly deep infiltration, the surface tumor cells may have different extents of necrosis, resulting in different degrees of well-defined surface depressions. Fold convergency and loss of lobulation showed no differences in ECCs with different depths of invasion, whereas the *P* value of the difference in the stalk swelling in ECCs with different depths of invasion was approximately 0.05, which may be due to the small sample size of this study, which requires further discussion.

This study had some limitations. First, we did not further measure the specific submucosal infiltration depth, distinguishing SM1, SM2, and SM3 for surgical resection and EMR resection of patients with submucosal infiltration. Therefore, this may have impacted the preoperative evaluation and treatment selection. Second, we did not define surveillance colonoscopy after EMR and ESD. The current European and United States guidelines recommended a 3-year surveillance colonoscopy for patients with adenoma larger than 10 mm; hence, the true complete resection rate and the necessity of additional treatment in this study require our regular review and further evaluation following the recommendations in the guidelines. Third, this study was a single-center, retrospective clinical analysis. In addition,

the sample size was limited, and the study's single-center nature may have caused bias. Therefore, using a larger sample size and multi-center clinical study is necessary to elucidate the relationship between endoscopic appearance and immersion depth from the perspective of fine cell segmentation.

CONCLUSION

CSM has a clinicopathological value for predicting deep immersion in early CRC in the left colon. It can enable endoscopists to better identify the submucosal infiltrates of ECC, thereby providing patients with more appropriate treatment options.

ARTICLE HIGHLIGHTS

Research background

Currently, endoscopists frequently decide the treatment of colorectal polyps according to the characteristics of white light endoscopy, and polyps smaller than 2 cm usually do not receive adequate attention, leading to their inappropriate treatment.

Research motivation

Chicken skin mucosa (CSM) surrounding colon polyps is a common endoscopic finding that could be an endoscopic predictive marker of submucosal invasion. Therefore, we should consider the lesions with such characteristics and adopt more appropriate treatment.

Research objectives

To explore potential markers of small colorectal cancer early invasion under white light endoscopy, We found that CSM was more common in early submucosal invasive carcinoma than intramucosal carcinoma. Therefore, a more aggressive treatment should be used rather than cold-snare polypectomy or cold-snare endoscopic mucosal resection.

Research methods

This retrospective cross-sectional study included 198 consecutive patients [233 early colorectal cancers (ECCs)] who underwent endoscopy or surgical procedures. Logistic regression analysis was used to examine the relationship between morphological characteristics, size, CSM prevalence, and invasion depth of ECC under white light endoscopy.

Research results

CSM, a depressed area with clear boundaries, erosion, or ulcer bleeding, and size (≥ 10 mm) were independent risk factors for submucosal invasion in ECC. We should consider the lesions with such characteristics and adopt more appropriate treatment.

Research conclusions

CSM has a clinicopathological value for predicting deep immersion in early colorectal carcinoma in the left colon.

Research perspectives

We will further expand our research to test our conclusions from various geographic, ethnic, and other factors.

FOOTNOTES

Author contributions: All authors contributed to the study's conception and design; Zhang YJ, Wen W, and Yuan MX performed the material preparation, data collection, and analysis; Zhang YJ wtote the first draft; all authors commented on the previous versions of the manuscript; all authors read and approved the final manuscript.

Institutional review board statement: The study was approved by the Ethics Committee of the Second People's Hospital (approval No: 2021018).

Informed consent statement: The requirement for informed consent was waived because our study does not involve personal privacy and has little risk to patients.

Conflict-of-interest statement: The authors declare no competing interests.

Data sharing statement: No additional data are available.

Country/Territory of origin: China

ORCID number: Ying-Jie Zhang 0000-0002-5033-1217; Wu Wen 0000-0001-6192-132X; Fan Li 0000-0003-0607-5903; Yi Jian 0000-0001-6770-6073; Chuan-Ming Zhang 0000-0002-9675-627X; Meng-Xia Yuan 0000-0002-8115-3695; Ye Yang 0000-0002-2434-1382; Feng-Lin Chen 0000-0002-1210-4523.

S-Editor: Yan JP
L-Editor: A
P-Editor: Yuan YY

REFERENCES

1 **Shatz BA**, Weinstock LB, Thyssen EP, Mujeeb I, DeSchryver K. Colonic chicken skin mucosa: an endoscopic and histological abnormality adjacent to colonic neoplasms. *Am J Gastroenterol* 1998; **93**: 623-627 [PMID: 9576459 DOI: 10.1111/j.1572-0241.1998.177_b.x]

2 **Chung EJ**, Lee JY, Choe J, Chang HS, Kim J, Yang DH, Ye BD, Byeon JS, Kim KJ, Yang SK, Kim JH, Myung SJ. Colonic Chicken Skin Mucosa is an Independent Endoscopic Predictor of Advanced Colorectal Adenoma. *Intest Res* 2015; **13**: 318-325 [PMID: 26576137 DOI: 10.5217/ir.2015.13.4.318]

3 **Lee YM**, Song KH, Koo HS, Lee CS, Ko I, Lee SH, Huh KC. Colonic Chicken Skin Mucosa Surrounding Colon Polyps Is an Endoscopic Predictive Marker for Colonic Neoplastic Polyps. *Gut Liver* 2022; **16**: 754-763 [PMID: 35000932 DOI: 10.5009/gnl210271]

4 **Watanabe T**, Itabashi M, Shimada Y, Tanaka S, Ito Y, Ajioka Y, Hamaguchi T, Hyodo I, Igarashi M, Ishida H, Ishiguro M, Kanemitsu Y, Kokudo N, Muro K, Ochiai A, Oguchi M, Ohkura Y, Saito Y, Sakai Y, Ueno H, Yoshino T, Fujimori T, Koinuma N, Morita T, Nishimura G, Sakata Y, Takahashi K, Takiuchi H, Tsuruta O, Yamaguchi T, Yoshida M, Yamaguchi N, Kotake K, Sugihara K; Japanese Society for Cancer of the Colon and Rectum. Japanese Society for Cancer of the Colon and Rectum (JSCCR) guidelines 2010 for the treatment of colorectal cancer. *Int J Clin Oncol* 2012; **17**: 1-29 [PMID: 22002491 DOI: 10.1007/s10147-011-0315-2]

5 **Park W**, Kim B, Park SJ, Cheon JH, Kim TI, Kim WH, Hong SP. Conventional endoscopic features are not sufficient to differentiate small, early colorectal cancer. *World J Gastroenterol* 2014; **20**: 6586-6593 [PMID: 24914381 DOI: 10.3748/wjg.v20.i21.6586]

6 **Li N**, Jin P, Yu DL, Yang L, Xie H, Kan Q, He YQ, Sheng JQ. The relationship between morphological characteristics of early colorectal cancer under the white light endoscopy and its infiltration depth. *Zhonghua Xiaohua Neijing Zazhi* 2016; **33**

7 **Wen CC**, Zhou S, Liu H, Wu DQ, Xu XR. Endoscopic findings combined with Ki67 for evaluating submucosal invasion of early colorectal cancer. *J Tongji Univ (Med Sci)* 2022; **43**

8 **Bugajski M**, Kaminski MF, Orlowska J, Mroz A, Pachlewski J, Rupinski M, Zagorowicz E, Rawa T, Regula J. Suspicious macroscopic features of small malignant colorectal polyps. *Scand J Gastroenterol* 2015; **50**: 1261-1267 [PMID: 25865832 DOI: 10.3109/00365521.2015.1024280]

9 **Sung H**, Ferlay J, Siegel RL, Laversanne M, Soerjomataram I, Jemal A, Bray F. Global Cancer Statistics 2020: GLOBOCAN Estimates of Incidence and Mortality Worldwide for 36 Cancers in 185 Countries. *CA Cancer J Clin* 2021; **71**: 209-249 [PMID: 33538338 DOI: 10.3322/caac.21660]

10 **Ikematsu H**, Yoda Y, Matsuda T, Yamaguchi Y, Hotta K, Kobayashi N, Fujii T, Oono Y, Sakamoto T, Nakajima T, Takao M, Shinohara T, Murakami Y, Fujimori T, Kaneko K, Saito Y. Long-term outcomes after resection for submucosal invasive colorectal cancers. *Gastroenterology* 2013; **144**: 551-9; quiz e14 [PMID: 23232297 DOI: 10.1053/j.gastro.2012.12.003]

11 **Gonai T**, Kawasaki K, Nakamura S, Yanai S, Akasaka R, Sato K, Toya Y, Asakura K, Urushikubo J, Fujita Y, Eizuka M, Uesugi N, Sugai T, Matsumoto T. Microvascular density under magnifying narrow-band imaging endoscopy in colorectal epithelial neoplasms. *Intest Res* 2020; **18**: 107-114 [PMID: 31671929 DOI: 10.5217/ir.2019.00061]

12 **Bray C**, Bell LN, Liang H, Collins D, Yale SH. Colorectal Cancer Screening. *WMJ* 2017; **116**: 27-33 [PMID: 29099566]

13 **Dumoulin FL**, Hildenbrand R. Endoscopic resection techniques for colorectal neoplasia: Current developments. *World J Gastroenterol* 2019; **25**: 300-307 [PMID: 30686899 DOI: 10.3748/wjg.v25.i3.300]

14 **Shaukat A**, Kaltenbach T, Dominitz JA, Robertson DJ, Anderson JC, Cruise M, Burke CA, Gupta S, Lieberman D, Syngal S, Rex DK. Endoscopic Recognition and Management Strategies for Malignant Colorectal Polyps: Recommendations of the US Multi-Society Task Force on Colorectal Cancer. *Gastroenterology* 2020; **159**: 1916-1934.e2 [PMID: 33159840 DOI: 10.1053/j.gastro.2020.08.050]

15 **Iwai T**, Imai K, Hotta K, Ito S, Yamaguchi Y, Kawata N, Tanaka M, Kakushima N, Takizawa K, Ishiwatari H, Matsubayashi H, Ono H. Endoscopic prediction of advanced histology in diminutive and small colorectal polyps. *J Gastroenterol Hepatol* 2019; **34**: 397-403 [PMID: 30070395 DOI: 10.1111/jgh.14409]

16 **Nowicki MJ**, Subramony C, Bishop PR, Parker PH. Colonic chicken skin mucosa: association with juvenile polyps in children. *Am J Gastroenterol* 2001; **96**: 788-792 [PMID: 11280552 DOI: 10.1111/j.1572-0241.2001.03623.x]

17 **Guan J**, Zhao R, Zhang X, Cheng Y, Guo Y, Wang L, Mi L, Liu F, Ma X, Li B. Chicken skin mucosa surrounding adult colorectal adenomas is a risk factor for carcinogenesis. *Am J Clin Oncol* 2012; **35**: 527-532 [PMID: 21654311 DOI: 10.1097/COC.0b013e31821dedf7]

18 **Yang M**, McKay D, Pollard JW, Lewis CE. Diverse Functions of Macrophages in Different Tumor Microenvironments. *Cancer Res* 2018; **78**: 5492-5503 [PMID: 30206177 DOI: 10.1158/0008-5472.CAN-18-1367]

19 **Ferlitsch M**, Moss A, Hassan C, Bhandari P, Dumonceau JM, Paspatis G, Jover R, Langner C, Bronzwaer M, Nalankilli K, Fockens P, Hazzan R, Gralnek IM, Gschwantler M, Waldmann E, Jeschek P, Penz D, Heresbach D, Moons L, Lemmers A, Paraskeva K, Pohl J, Ponchon T, Regula J, Repici A, Rutter MD, Burgess NG, Bourke MJ. Colorectal polypectomy and endoscopic mucosal resection (EMR): European Society of Gastrointestinal Endoscopy (ESGE) Clinical Guideline. *Endoscopy* 2017; **49**: 270-297 [PMID: 28212588 DOI: 10.1055/s-0043-102569]

20 **Kaltenbach T**, Anderson JC, Burke CA, Dominitz JA, Gupta S, Lieberman D, Robertson DJ, Shaukat A, Syngal S, Rex DK. Endoscopic Removal of Colorectal Lesions-Recommendations by the US Multi-Society Task Force on Colorectal Cancer. *Gastrointest Endosc* 2020; **91**: 486-519 [PMID: 32067745 DOI: 10.1016/j.gie.2020.01.029]

21 **Yabuuchi Y**, Imai K, Hotta K, Ito S, Kishida Y, Yoshida M, Kawata N, Kakushima N, Takizawa K, Ishiwatari H, Matsubayashi H, Aizawa D, Oishi T, Imai T, Ono H. Efficacy and safety of cold-snare endoscopic mucosal resection for colorectal adenomas 10 to 14 mm in size: a prospective observational study. *Gastrointest Endosc* 2020; **92**: 1239-1246 [PMID: 32464143 DOI: 10.1016/j.gie.2020.05.019]

World Journal of Gastrointestinal Oncology

Submit a Manuscript: https://www.f6publishing.com

World J Gastrointest Oncol 2023 June 15; 15(6): 1073-1085

DOI: 10.4251/wjgo.v15.i6.1073

ISSN 1948-5204 (online)

ORIGINAL ARTICLE

Retrospective Study

Relationship between multi-slice computed tomography features and pathological risk stratification assessment in gastric gastrointestinal stromal tumors

Tian-Tian Wang, Wei-Wei Liu, Xian-Hai Liu, Rong-Ji Gao, Chun-Yu Zhu, Qing Wang, Lu-Ping Zhao, Xiao-Ming Fan, Juan Li

Specialty type: Oncology

Provenance and peer review: Unsolicited article; Externally peer reviewed.

Peer-review model: Single blind

Peer-review report's scientific quality classification

Grade A (Excellent): 0
Grade B (Very good): B, B
Grade C (Good): C
Grade D (Fair): 0
Grade E (Poor): 0

P-Reviewer: Huh YM, South Korea; Ojima T, Japan; Terashima M, Japan

Received: March 9, 2023
Peer-review started: March 9, 2023
First decision: March 22, 2023
Revised: April 2, 2023
Accepted: April 25, 2023
Article in press: April 25, 2023
Published online: June 15, 2023

Tian-Tian Wang, Rong-Ji Gao, Chun-Yu Zhu, Xiao-Ming Fan, Juan Li, Department of Medical Imaging, The Second Affiliated Hospital of Shandong First Medical University, Taian 271000, Shandong Province, China

Wei-Wei Liu, Department of Rheumatology, The Second Affiliated Hospital of Shandong First Medical University, Taian 271000, Shandong Province, China

Xian-Hai Liu, Department of Network Information Center, The Second Affiliated Hospital of Shandong First Medical University, Taian 271000, Shandong Province, China

Qing Wang, Department of Ultrasound, The Second Affiliated Hospital of Shandong First Medical University, Taian 271000, Shandong Province, China

Lu-Ping Zhao, Department of Medical Imaging, The Affiliated Hospital of Ji'ning Medical University, Jining 272000, Shandong Province, China

Corresponding author: Juan Li, MM, Attending Doctor, Department of Medical Imaging, The Second Affiliated Hospital of Shandong First Medical University, No. 366 Taishan Street, Taian 271000, Shandong Province, China. 191962554@163.com

Abstract

BACKGROUND

Computed tomography (CT) imaging features are associated with risk stratification of gastric gastrointestinal stromal tumors (GISTs).

AIM

To determine the multi-slice CT imaging features for predicting risk stratification in patients with primary gastric GISTs.

METHODS

The clinicopathological and CT imaging data for 147 patients with histologically confirmed primary gastric GISTs were retrospectively analyzed. All patients had received dynamic contrast-enhanced CT (CECT) followed by surgical resection. According to the modified National Institutes of Health criteria, 147 lesions were classified into the low malignant potential group (very low and low risk; 101

lesions) and high malignant potential group (medium and high-risk; 46 lesions). The association between malignant potential and CT characteristic features (including tumor location, size, growth pattern, contour, ulceration, cystic degeneration or necrosis, calcification within the tumor, lymphadenopathy, enhancement patterns, unenhanced CT and CECT attenuation value, and enhancement degree) was analyzed using univariate analysis. Multivariate logistic regression analysis was performed to identify significant predictors of high malignant potential. The receiver operating curve (ROC) was used to evaluate the predictive value of tumor size and the multinomial logistic regression model for risk classification.

RESULTS

There were 46 patients with high malignant potential and 101 with low-malignant potential gastric GISTs. Univariate analysis showed no significant differences in age, gender, tumor location, calcification, unenhanced CT and CECT attenuation values, and enhancement degree between the two groups ($P > 0.05$). However, a significant difference was observed in tumor size (3.14 ± 0.94 *vs* 6.63 ± 3.26 cm, $P < 0.001$) between the low-grade and high-grade groups. The univariate analysis further revealed that CT imaging features, including tumor contours, lesion growth patterns, ulceration, cystic degeneration or necrosis, lymphadenopathy, and contrast enhancement patterns, were associated with risk stratification ($P < 0.05$). According to binary logistic regression analysis, tumor size [$P < 0.001$; odds ratio (OR) = 26.448; 95% confidence interval (CI): 4.854-144.099)], contours ($P = 0.028$; OR = 7.750; 95%CI: 1.253-47.955), and mixed growth pattern ($P = 0.046$; OR = 4.740; 95%CI: 1.029-21.828) were independent predictors for risk stratification of gastric GISTs. ROC curve analysis for the multinomial logistic regression model and tumor size to differentiate high-malignant potential from low-malignant potential GISTs achieved a maximum area under the curve of 0.919 (95%CI: 0.863-0.975) and 0.940 (95%CI: 0.893-0.986), respectively. The tumor size cutoff value between the low and high malignant potential groups was 4.05 cm, and the sensitivity and specificity were 93.5% and 84.2%, respectively.

CONCLUSION

CT features, including tumor size, growth patterns, and lesion contours, were predictors of malignant potential for primary gastric GISTs.

Key Words: Computed tomography; Gastrointestinal stromal tumor; Risk stratification, Stomach

Core Tip: Gastrointestinal stromal tumors (GISTs) are rare but are nevertheless the most common mesenchymal neoplasms of the gastrointestinal tract. GISTs are most frequently found in the stomach. Preoperative prediction of the malignant potential and prognosis of these GISTs is crucial for clinical decision-making. The present study identified the computed tomography (CT) imaging characteristics for predicting the malignancy risk stratification in 147 patients with primary gastric GISTs. We demonstrated that the qualitative and quantitative features of gastric GISTs on contrast-enhanced CT may be favorable for preoperative risk stratification. This may provide a simple yet effective tool for clinicians to make appropriate clinical decisions.

Citation: Wang TT, Liu WW, Liu XH, Gao RJ, Zhu CY, Wang Q, Zhao LP, Fan XM, Li J. Relationship between multi-slice computed tomography features and pathological risk stratification assessment in gastric gastrointestinal stromal tumors. *World J Gastrointest Oncol* 2023; 15(6): 1073-1085
URL: https://www.wjgnet.com/1948-5204/full/v15/i6/1073.htm
DOI: https://dx.doi.org/10.4251/wjgo.v15.i6.1073

INTRODUCTION

Gastrointestinal stromal tumors (GISTs) are the most common mesenchymal tumors originating in the digestive tract and are thought to be derived from the interstitial cells of Cajal[1,2]. GISTs can arise everywhere in the gastrointestinal tract, but they are predominantly located in the stomach (50%-60%), followed by the small bowel (30%-35%), colon and rectum (5%), and esophagus (< 5%)[3]. They also develop within the mesentery omentum, retroperitoneum, and pelvis. GISTs are classified as borderline tumors, and they range from essentially benign tumors to aggressive sarcomas, and they are physiologically diverse with varied malignant potential[4]. To evaluate the risk of recurrence following complete

resection of primary GISTs, a number of risk categorization techniques have been put forth. The most widely used classification systems for GISTs are the modified National Institutes of Health (NIH) criteria[5] and Armed Forces Institute of Pathology criteria[6], which divide GISTs into four risk categories (very low, low, intermediate, and high risk) based on tumor size, mitotic count, tumor site, and tumor rupture. The 10-year recurrence-free survival rates of patients with the very low-, low-, and intermediate-risk GISTs are 94.9%, 89.7%, and 86.9%, respectively, and are lower in patients with high-risk GISTs (36.2%)[3]. The biological features of GISTs play an essential role in prognosis and evolution, but evaluating their features is usually challenging unless the tumor is excised or has metastasized[7].

The preoperative prediction of the malignant potential and prognosis of these GISTs is crucial for clinical decision-making. Currently, preoperative contrast-enhanced computed tomography (CECT) is regarded as the fundamental imaging modality for the detection and evaluation of GISTs[8,9]. The correlation between CT image features and pathological risk grade of GISTs has been previously reported in some pieces of literature[10-13], revealing that CT imaging features such as tumor location, growth pattern, contour, tumor size, margin, cystic degeneration or necrosis, ulceration, presence of enlarged vessels feeding or draining the mass (EVFDM), contrast enhancement pattern, lymphadenopathy, and direct organ invasion were associated with risk stratification. However, only a few studies have attempted to correlate CT features with the histological grading or prediction of malignancy in the stomach. They have yielded conflicting results because of the limited number of cases[14]. Therefore, the purpose of the present study was to identify the CT imaging characteristics for predicting the malignancy risk stratification in 147 patients with primary gastric GISTs.

MATERIALS AND METHODS

Patients

We enrolled 147 patients with histologically confirmed primary gastric GISTs from the Second Affiliated Hospital of Shandong First Medical University from July 2013 to March 2022. This retrospective study was approved by the Institutional Ethics Committee of the Second Affiliated Hospital of Shandong First Medical University. The inclusion criteria were as follows: (1) Patients underwent curative surgery for primary gastric GISTs; (2) A standard CECT examination was performed within 15 d before surgery; (3) Complete CECT images and clinicopathological data were available; and (4) No distant metastasis at the time of diagnosis. The exclusion criteria were: (1) Patients received treatment before CT and surgery; and (2) Tumor rupture before or during surgery.

Clinical data were reviewed, including age, sex, clinical presentation, and operational styles. There were 74 men and 73 women, aged 31-82 years, with a mean of 61 years. The main symptoms were abdominal pain/discomfort (n = 48), melena (n = 28), and abdominal mass (n = 37). Twenty-five patients were asymptomatic, and the tumors were detected during a regular medical checkup. The remaining nine patients presented with acid reflux, hematemesis, poor appetite and other symptoms. All patients were treated with surgical resection including laparoscopic resection (n = 71), endoscopic resection (n = 46), or open surgery (n = 30). The tumor specimens were subsequently processed for histological examination.

The cases were further categorized according to the risk assessment table published by the modified NIH criteria in 2008[5]. The very low-and low-risk groups were classified into the low malignant potential group, and the intermediate-, high-risk groups were classified into the high malignant potential group. The cohorts were subsequently grouped into the low- and high-grade malignant potential groups.

CT imaging acquisition

All patients underwent abdominal standard CECT before surgery using Philips Brilliance iCT (Philips Medical Systems, Cleveland, OH, United States) and GE LightSpeed VCT (GE Healthcare, Princeton, NJ, United States). Before CT examinations, all patients were fasted for at least 8 h and were encouraged to consume 500-800 mL of water to maximize gastric distension. The scan range covered the upper or entire abdomen, including the pelvic cavity. The acquisition parameters were as follows: Tube voltage, 120 kV; tube current, 300 mAs; slice thickness, 5 mm; slice interval, 5 mm; pitch, 0.9; detector collimation, 64 mm × 0.5 mm; field of view, 350 mm × 350 mm; and matrix, 512 × 512. After the acquisition of unenhanced images, a nonionic iodinated intravenous contrast agent (2.5 mL/kg, 300 mL/mg) was injected intravenously at a rate of 3.0 mL/s. The arterial phase (AP) scan began 25-30 s after injection, while the portal venous phase (PVP) and delayed phase/equilibrium phase scan were started after 55-60 s and 180/120 s, respectively. The original imaging data were reconstructed with a 1.5-mm slice thickness. Axial, sagittal, and coronal multiplanar reconstruction images were obtained with a reconstruction thickness of 2-5 mm. The images were uploaded into the picture archiving and communication system for subsequent analysis.

Imaging analysis

The multi-slice CT scan data were independently reviewed by two radiologists with 13 and 9 years of experience in abdominal imaging, and a consensus was reached for the final interpretations. The pathological diagnosis of GISTs was recorded, but the radiologists were blinded to the pathological data. The CT imaging features were categorized as follows: Tumor size, lesion location (cardia-fundus, body, or antrum), contour (irregular or regular), calcification (presence or absence), cystic degeneration or necrosis (presence or absence), growth patterns (endoluminal, exophytic or mixed), enhancement pattern (heterogeneous or homogenous), degree of contrast enhancement (mild, moderate or marked), and lymphadenopathy (presence or absence). Tumor size was defined as the maximal diameter on the transverse, coronal or sagittal plane. The largest tumor diameter was classified as ≤ 5, 5-10 or > 10 cm. The regular contour was defined as round/ovoid, and irregular was lobulated. Ulceration was considered present when a focal mucosal defect/indentation filled with air or fluid or when contrast material was found on the endoluminal surface of the lesion[13]. Regional lymphadenopathy was considered present if the short-axis diameter of the lymph node was > 1 cm. On CECT scans, areas of cystic degeneration, necrosis, or relative enhancement > 10 HU in any phase were considered heterogeneous enhancement. Necrosis and cystic degeneration were further differentiated. Necrosis was characterized by an irregular low attenuation region without obvious enhancement (≤ 10 HU difference) with a CT attenuation value ≤ 20 HU in each contrast-enhanced phase. Cystic degeneration was characterized by a region with a clear and smooth border and near-water density (CT attenuation value 0-10 HU). The degrees of enhancement for GISTs included absolute and relative enhancement. Absolute enhancement was obtained as the measured CT values in AP, PVP and delayed phase. In contrast, relative enhancement was calculated by the differences in CT values between the unenhanced phase and each enhancement phase. The calculated average values were recorded as the final results. Mild enhancement degree was defined as relative enhancement CT value ≤ 20 HU, and moderate and significant enhancement degrees were 20-40 and > 40 HU, respectively. The CT values of lesions were measured with a 30-50 mm^2 region of interest, selecting the most intensely enhanced solid components of the tumors, excluding tumor vessels, calcification, hemorrhage, and necrotic and cystic regions. The locations of the regions of interest were kept consistent in each phase. Intratumoral necrosis, degree of enhancement, and patterns of enhancement were discerned by PVP CECT scan, and tumor calcification was identified by unenhanced CT.

Statistical analysis

Univariate and multivariate regression analyses were performed with Statistical Package for Social Sciences (SPSS) version 21.0 software packages (SPSS Inc, Chicago, IL, United States), with a two-sided $P < 0.05$ considered statistically significant. Shapiro-Wilk tests were conducted to verify the normality of all variables. Independent samples *t*-tests were conducted for continuous variables (including age, tumor size, attenuation value in noncontrast images, AP and PVP of gastric GISTs with different pathological risk categories. χ^2 tests or Fisher's exact tests were performed to compare the sex and the radiological variables between different risk stratifications (categorical variables). A binary logistic regression analysis was subsequently carried out to identify independent predictors for risk stratification of gastric GISTs. Radiological variables with a $P < 0.05$ in the univariate analysis were enrolled in the binary logistic regression analysis. Odds ratio (OR) with 95% confidence interval (CI) for each risk factor were used to represent the relative risk estimates. Two-sided $P < 0.05$ was considered statistically significant. The statistical chart was created using GraphPad Prism 9 software. The receiver operating curve (ROC) analysis of significant variables was performed, including the CT model from the binary logistic regression analysis. The area under the curve (AUC) was obtained, and the sensitivity, specificity and optimal cutoff values for distinguishing the high-malignant potential from the low-malignant potential group were calculated.

RESULTS

Clinicopathological characteristics of the patients

There were 46 patients with high-malignant potential gastric GISTs (including 27 intermediate grade and 19 high grade), and 101 patients with low-malignant potential gastric GISTs (including 11 very low and 90 low grades). Table 1 displays the characteristics of all the patients involved in this investigation. Age and sex did not significantly differ between the groups with low and high malignant potential, according to a univariate analysis ($P > 0.05$).

CT findings

All 147 patients with gastric GISTs had solitary tumors: 83 (low/high: 55/28) tumors were located in the fundus, 49 (35/14) in the body, and 15 (11/4) in the antrum. In 87 (69/18) patients, the growth patterns of GISTs were endoluminal, in 39 (24/15), exophytic, and in 21 (8/13) individuals, they were mixed types (Figures 1A and 1B).

Table 1 Quantitative features between low-grade and high-grade group

Variables	Low-grade group	High-grade group	χ^2/*Z*/*t* value	*P* value
	n = 101, 68.7%	*n* = 46, 31.3%		
Age (mean ± SD, yr)	60.59 ± 10.33	62.09 ± 11.19	-0.791	0.43
Sex (*n*, %)				
Male	47 (46.5)	26 (56.5)	1.261	0.261
Female	53 (53.5)	20 (43.5)		
Tumor size (mean ± SD), cm	3.14 ± 0.94	6.63 ± 3.26	-9.918	< 0.001
Unenhanced CT, Hu	34.26 ± 3.86	33.93 ± 4.80	0.434	0.665
Absolute enhancement				
AP, Hu	49.72 ± 8.63	47.15 ± 9.44	1.625	0.106
PVP, Hu	60.83 ± 11.07	59.11 ± 11.79	0.858	0.393
DP, Hu	64.68 ± 9.06	63.09 ± 9.12	0.988	0.325
Relative enhancement				
AP, Hu	15.47 ± 7.57	13.22 ± 9.40	1.544	0.125
PVP, Hu	26.57 ± 10.11	25.17 ± 11.69	0.745	0.457
DP, Hu	30.43 ± 7.66	29.15 ± 9.03	0.883	0.379

CT: Computed tomography; AP: Arterial phase; DP: Delayed phase; PVP: Portal venous phase.

The size (largest diameter) of the lesions ranged from 1.0 to 20.7 cm (mean 4.23 cm): 116 (low/high: 98/10) patients had tumor size ≤ 5 cm, and 23 (2/21) had tumor size 5-10 cm, while eight (1/7) had tumor size > 10 cm (Figure 1C). Lesions were irregular in 19 (3/16) patients and regular in 128 (98/30) (Figure 1D). Cystic degeneration or necrosis within lesions was found in 85 (45/40) patients but was absent in 62 (56/6). Ulceration was noted in 48 (25/23) patients but was absent in 99 (76/23). Tumor calcification was found in 22 (14/8) patients but was not seen in 125 (87/38) (Figures 1E and F). Lymphadenopathy was observed in 36 (19/17) patients but was absent in 111 (83/29). On the enhanced CT images, the lesions showed heterogeneous enhancement in 95 (51/44) patients, while homogeneous enhancement was observed in the other 52 (50/2). Primary lesions showed mild enhancement in 12 (6/6) patients, moderate enhancement in 113 (83/30), and marked enhancement in 22 (12/10) on CECT images.

Relationship between CT findings and different risk categories of gastric GISTs (univariate analysis)

Univariate analysis indicated a significant difference in tumor size (3.14 ± 0.94 cm *vs* 6.63 ± 3.26 cm, $P < 0.001$) between the low-grade and high-grade groups. Higher tumor risk was observed with larger tumor size (Figure 2). Tumors with irregular contours were observed more frequently in high-malignant potential GISTs ($P < 0.001$). High-malignant potential GISTs were more likely to exhibit mixed growth, whereas low-malignant potential GISTs predominantly involved endoluminal growth ($P < 0.05$). The presence of ulceration, cystic degeneration or necrosis, lymphadenopathy, and enhancement patterns were significantly different between the two groups ($P < 0.05$). However, there were no appreciable variations between the two groups in terms of any qualitative characteristics, including tumor location, calcification and enhancement degree ($P = 0.760$, 0.578 and 0.075, respectively). There was no significant difference in the risk categories between nonenhancement and each enhancement phase ($P > 0.05$). Table 2 shows the correlation between stomach GIST risk grades and CT findings.

Association of CT features and malignant potential of GISTs (binary logistic regression analysis)

The findings of the univariate analysis revealed that, with the exception of calcification, location, CT values on unenhanced CT and CECT images, and enhancement degree, all of the summary variables in gastric GISTs were linked with risk classes ($P < 0.05$). The CT features that differed significantly in univariate analysis were enrolled in the binary logistic regression analysis. Only tumor size ($P < 0.001$; OR = 26.448; 95%CI: 4.854-144.099), contour ($P = 0.028$; OR = 7.750; 95%CI: 1.253-47.955), and mixed growth ($P = 0.046$; OR = 4.740; 95%CI: 1.029-21.828) were identified as independent predictors for the risk stratification of gastric GISTs (Table 3). The forest plot (Figure 3) included the independent CT characteristics of gastric GISTs with high malignant potential that were obtained using binary logistic regression analysis.

Table 2 Association of computed tomography features and malignant potential in patients with gastric gastrointestinal stromal tumors

Factor	Low risk group (*n* = 101)	High risk group (*n* = 46)	χ^2	*P* value
Location			0.548	0.76
Fundus	55 (54.5)	28 (60.9)		
Body	35 (34.7)	14 (30.4)		
Antrum	11 (10.9)	4 (8.7)		
Tumor diameter (cm)[1]			64.928	< 0.001
> 10 cm	1 (1.0)	7 (15.2)		
5-10 cm	2 (2.0)	21 (45.7)		
≤ 5 cm	98 (97.0)	18 (39.1)		
Tumor contours			28.42	< 0.001
Irregular	3 (3.0)	16 (34.8)		
Regular	98 (97.0)	30 (65.2)		
Ulceration			9.161	0.002
Present	25 (24.8)	23 (50.0)		
Absent	76 (75.2)	23 (50.0)		
Cystic degeneration or necrosis			23.3	< 0.001
Present	45 (44.6)	40 (87.0)		
Absent	56 (55.4)	6 (13.0)		
Calcification			0.309	0.578
Present	14 (13.9)	8 (17.4)		
Absent	87 (86.1)	38 (82.6)		
Growth patterns			14.634	0.001
Mixed	8 (7.9)	13 (28.3)		
Endoluminal	69 (68.3)	18 (39.1)		
Exophytic	24 (23.8)	15 (32.6)		
Lymphadenopathy			5.627	0.018
Present	19 (18.8)	17 (37.0)		
Absent	82 (81.2)	29 (63.0)		
Enhancement pattern			28.192	< 0.001
Heterogeneous	51 (50.5)	44 (95.7)		
Homogenous	50 (49.5)	2 (4.3)		
Enhancement degree			5.188	0.075
Marked	12 (11.9)	10 (21.7)		
Moderate	83 (82.2)	30 (65.2)		
Mild	6 (5.9)	6 (13.0)		

[1]Fisher's exact tests were applied to compare the differences.
χ^2 tests were applied to all other variables.

ROC analysis

ROC analysis for the multinomial logistic regression model and tumor size to differentiate high-malignant potential from low-malignant potential GISTs is shown in Figure 4. The multinomial logistic regression model for gastric GISTs achieved a maximum AUC (0.919; 95%CI: 0.863-0.975), while that for tumor size achieved AUC (0.940; 95%CI: 0.893-0.986). The tumor size cutoff value between the low and high malignant potential groups was 4.05 cm. The sensitivity and specificity were 93.5% and 84.2%,

Table 3 Logistic regression analysis of significant computed tomography features for prediction of high malignant potential

CT feature	β	Odds ratio (95%CI)	*P* value
Size	3.275	26.448 (4.854-144.099)	< 0.001
Contour	2.048	7.750 (1.253-47.955)	0.028
Growth patterns	1.556	4.740 (1.029-21.828)	0.046

CI: Confidence interval; CT: Computed tomography.

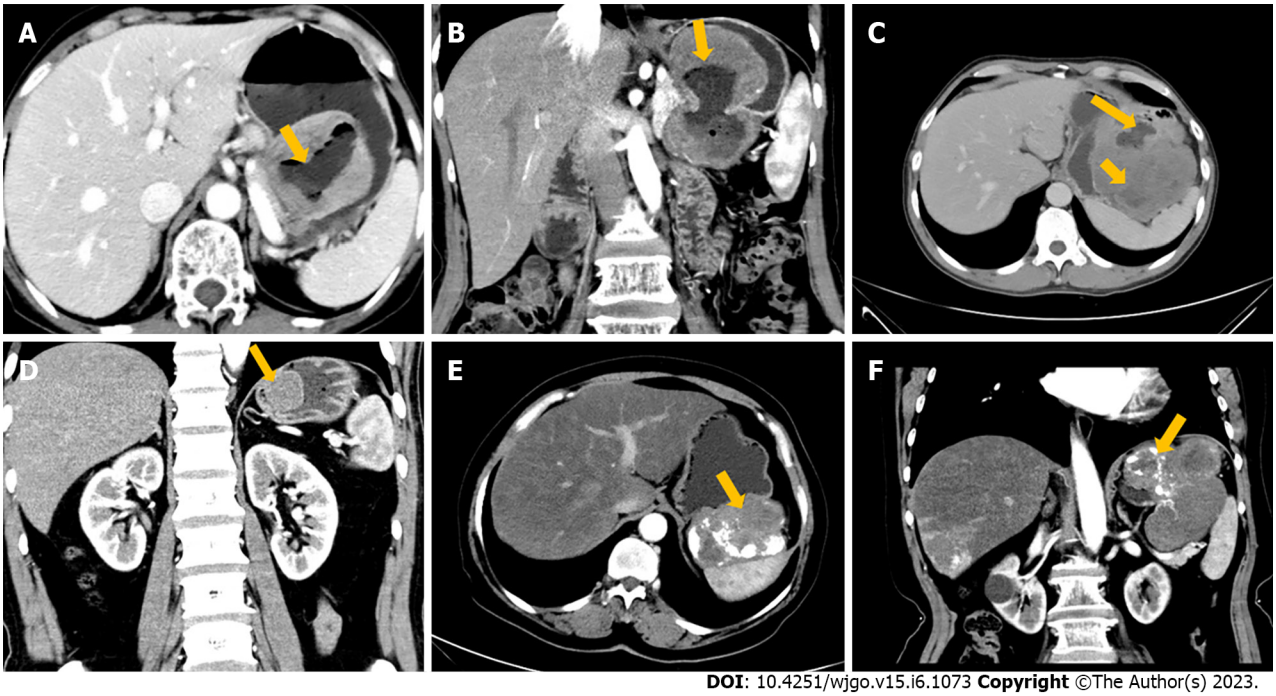

DOI: 10.4251/wjgo.v15.i6.1073 **Copyright** ©The Author(s) 2023.

Figure 1 Computed tomography findings. A and B: A 71-year-old woman with high-risk category gastric gastrointestinal stromal tumor (GIST). Axial (A) and coronal (B) in the arterial phase (AP) computed tomography (CT) images demonstrate an irregular, mixed growth pattern, heterogeneously enhanced tumor with prominent ulceration (arrow); C: A 54-year-old man with high-risk gastric GIST. Axial portal venous phase shows a lesion with a mixed growth pattern, 20-cm, irregular contour, heterogeneous pattern of contrast enhancement with necrotic areas inside (short arrows), and surface ulceration (long arrow); D: A 49-year-old man with low-risk category gastric GIST. Coronal AP shows a 3-cm mass with regular contours, well defined, and homogeneous pattern of contrast enhancement (homogeneous enhancement) (arrow); E and F: A 69-year-old woman with high-risk gastric GIST. Axial (E) and coronal (F) contrast-enhanced CT images in the AP show a lobular, well-defined tumor with exophytic growth pattern and heterogeneous pattern of contrast enhancement, with prominent calcification and necrotic areas inside (arrows).

respectively (Figure 4).

DISCUSSION

GISTs are rare but are nevertheless the most common mesenchymal neoplasms of the gastrointestinal tract. GISTs are most frequently found in the stomach. Numerous investigations have revealed a connection between the anatomical placement and the biological behavior of GISTs[5,6]. Tang *et al*[14] compared the CT features of gastric and small bowel GISTs to evaluate their association with risk grades and showed that small bowel and stomach GISTs had considerably different risk grades. Tumors originating in the stomach are less aggressive than tumors of intestinal origin[14].

For detection, qualitative diagnosis, staging, assessment of therapy response, follow-up after surgery, and forecasting of rupture and biologic aggressiveness, CT is the primary imaging modality[15-17]. The development of risk-segmented GISTs can be predicted using CECT, according to a number of studies [13,18,19], and many of them involved intestinal GISTs[16,20]. However, to our knowledge, only a few studies have focused on the association of gastric GIST CT findings and the degree of malignancy or mitotic rate and metastatic risk. There has been research on the correlation between CT findings and the degree of mitotic rate[20]. As NIH standards 2008 for GISTs risk stratifications are widely accepted, only

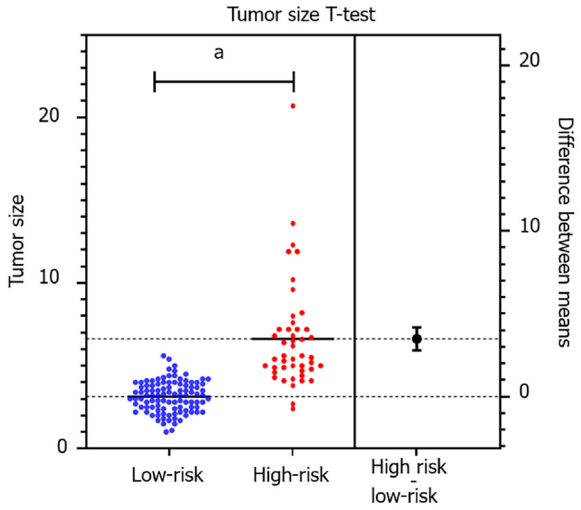

DOI: 10.4251/wjgo.v15.i6.1073 **Copyright** ©The Author(s) 2023.

Figure 2 Independent sample *t*-test estimation chart. [a]*P* < 0.0001.

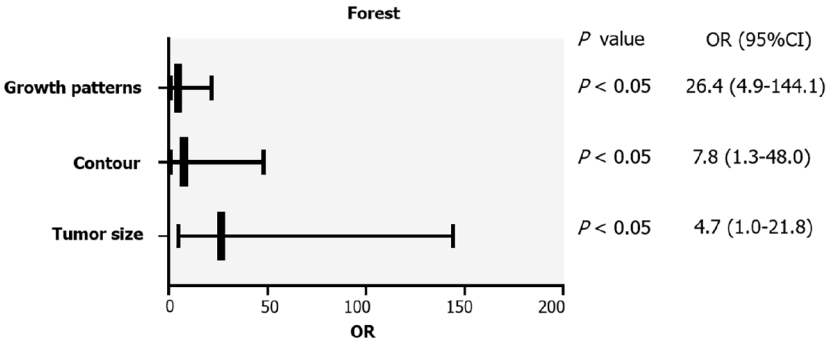

DOI: 10.4251/wjgo.v15.i6.1073 **Copyright** ©The Author(s) 2023.

Figure 3 Forest plot of the independent computed tomography features of gastric gastrointestinal stromal tumor with high malignant potential. OR: Odds ratio; CI: Confidence interval.

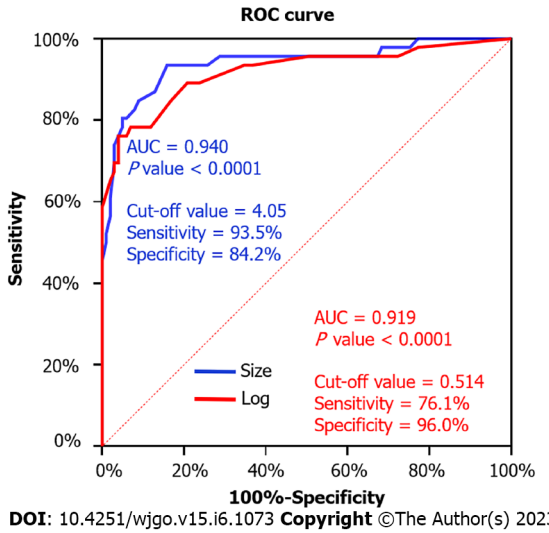

DOI: 10.4251/wjgo.v15.i6.1073 **Copyright** ©The Author(s) 2023.

Figure 4 Receiver operating curve for tumor size and the multinomial logistic regression model to differentiate high-malignant potential from low-malignant potential gastrointestinal stromal tumor. ROC: Receiver operating curve; AUC: Area under the curve.

a few studies[14,21,22] enrolled patients with gastric GIST to evaluate the predictive value of CT imaging features for risk stratification. However, the variation in results may be due to the different inclusion criteria and subjective assessment standards.

Numerous studies have shown that different CT imaging features, including as lesion margin, size, shape, necrosis, ulceration, growth patterns, enhancement pattern, EVFDM, direct organ invasion, and lymphadenopathy, are related to risk classification. However, logistic regression analysis only identified a few CT features of the primary tumor as independent risk stratification predictors.

Li *et al*[10] analyzed the CT features of gastric GISTs, including size, location (cardiac/pericardial region, fundus, body, or antrum), EVFDM, necrosis, ulceration, growth pattern, contour, mesenteric fat infiltration, and direct organ invasion. The results revealed that tumor size, cardia/pericardial origin, EVFDM, and mesenteric fat infiltration might be independent indicators of high malignant potential.

The study by Tang *et al*[14] reported that only tumor size, necrosis and the difference of CT values between AP and PVP were independent factors influencing the risk stratification of gastric GISTs. For small bowel GISTs, the independent predictors were tumor size and ulceration. In the study about GISTs, Zhou *et al*[12] reported that CT imaging features, including tumor margin, size, shape, tumor growth pattern, direct organ invasion, necrosis, EVFDM, lymphadenopathy, and contrast enhancement pattern, were associated with the risk stratifications. However, in multinomial logistic regression analysis, only lesion size, development pattern, and EVFDM were recognized as independent risk factors.

In this study, 147 cases of gastric GISTs were retrospectively analyzed and the CT features such as location, size, contour, necrosis or cystic degeneration, ulceration, growth pattern, lymphadenopathy and contrast enhancement were correlated with the risk and prognosis of malignancy. Both the low-malignant potential group (very low and low risk) and the high-malignant potential group (mid and high risk) were created from the 147 patients. Our research demonstrated that the tumor size, contour, presence of necrosis or cystic generation, ulceration and lymphadenopathy, tumor growth pattern and enhancement pattern were significant factors for risk stratification of GISTs. However, only tumor size (> 5 cm), irregular contours, and mixed growth pattern were independent predictors for high malignant potential in multivariate logistic regression analysis (OR = 26.448, 7.750 and 4.740, respectively). We transformed the above independent factors into the CT model for risk stratification of gastric GISTs. The AUC of the ordinal multinomial logistic regression model was 0.919, which shows that the risk stratifications may be reasonably predicted by the logistic regression model.

Rubin *et al*[23] reported that the risk of developing gastric GISTs was the same for both sexes, and although they occurred over a wide age distribution, about 75% were diagnosed in patients older than 50 years. Univariate analysis revealed that the prognosis of GISTs was independent of age and sex in the present study, and the mean age of the patients was 61 years, which is consistent with our research.

Gastric GISTs can occur anywhere but are more common in the fundus of the stomach. In this study, 56.46% (83/147) of tumors were located in the gastric fundus and 33.33% (49/147) in the gastric body, while the gastric antrum accounted for 10.20% (15/147). However, there was no significant difference between the location of the GISTs in the stomach and the risk stratification of the GISTs.

Tumor size is considered one of the most commonly used and reliable indicators for assessing GIST risk. The multivariate analysis in this study revealed that tumor size was an independent influencing factor for risk stratification of gastric GISTs, with a cut-off value of 4.05 cm. Tumor size is a component of the modified NIH criteria. A larger tumor size tends to suggest a more aggressive biological behavior. These results corroborate many earlier findings[23-25].

In terms of tumor contours, we demonstrated that gastric GISTs with a high-risk malignant potential were more likely to have an irregular tumor shape on CT. Our results are consistent with the study by Iannicelli *et al*[26], which found that irregular contours were the only CT feature that showed a linear correlation with risk. As the risk increases, the likelihood of detecting irregular margins of the gastric GISTs also increases. With higher tumor risk, higher tumor volume, disordered mitotic phase, invasive mesenchyma, and irregular contours are usually observed. Many studies have found that large stromal tumors were irregular and lobulated[27,28]. Wei *et al*[29] investigated the relationship between risk stratification and the shape of GISTs and reported that the method for quantifying tumor shape predicted the risk level and mitotic value of GISTs.

In our study, mixed growth patterns were independent predictors for high malignant potential. Endoluminal growth was detected in 59.18% (87/147) cases, exophytic growth in 26.53% (39/147) cases, and 21 patients showed mixed growth patterns, including 13 in the high-risk potential group, accounting for 61.90%. Our research revealed that compared to primary lesions with an endoluminal development pattern, those with mixed growth patterns were more likely to have greater GIST risk stratification. However, there is inconsistency in the literature on whether different GIST growth patterns are beneficial for judging the risk of GIST[10,12,22]. Therefore, further research is required in the future.

Peng *et al*[22] demonstrated that high-risk gastric GISTs were likely to present with necrosis even though it was not an independent predictor, which is consistent with our study. However, the studies by Liu *et al*[30] and Tang *et al*[14] demonstrated that tumor necrosis was an independent predictor of unfavorable disease-free survival in gastric GISTs. One possible explanation for the discrepancy may be that tumor necrosis is more common in the high-malignant potential group and is sometimes difficult to

be identified with the naked eye. However, these results suggested that tumor necrosis was a significant factor in classifying the malignancy of gastric GISTs. Even though necrosis was not an independent predictor, the research by Peng *et al*[22] showed that high-risk gastric GISTs were likely to present with it, which is consistent with our analysis. Tumor necrosis was found to be an independent predictor of poor disease-free survival in gastric GISTs, according to research by Liu *et al*[30] and Tang *et al*[14]. Tumor necrosis, which can be challenging to detect with the unaided eye sometimes, is more prevalent in the group of patients with high-malignant potential, which may be one reason for the discrepancy. These findings, however, revealed that tumor necrosis had a substantial role in determining the degree of malignancy of gastric GISTs.

The consistency between pathology and CT in identifying tumor necrosis should be validated. In our study, necrosis or cystic lesions and ulcers were also found to be important factors in the risk stratification of GISTs. In contrast, we found no significant difference between calcification and risk category, which was similar to previous studies[13,14].

The heterogeneous pattern of contrast enhancement was mainly observed in high-risk gastric GISTs. In contrast, tumors belonging to the low-risk classes mostly appeared with a homogeneous pattern of contrast enhancement. The result is consistent with the study of Iannicelli *et al*[26]. A high degree of contrast enhancement is usually considered a characteristic of tumor biological activity, but was not associated with the risk stratification in our research, which was in accordance with previous studies[13,26]. However, the enhancement degree plays an important role in distinguishing GISTs from other tumors such as leiomyomas[31].

Hong *et al*[32] reported that lymph node metastases are extremely rare, but a recent study by Zhou *et al*[12] of > 120 patients with histologically confirmed primary GISTs reported that lymphadenopathy was associated with risk stratification. In this study, a significant difference in lymphadenopathy was found between the low malignant potential and high malignant potential groups (18.81% *vs* 36.96%, respectively). We believe that lymphadenopathy around the lesion is more likely to occur in tumors with high malignant potential. However, among the 36 lymph nodes reported, only one had a short diameter > 1 cm. Therefore, the clinical significance of lymphadenopathy should be further studied.

The present investigation included some restrictions. First of all, because it was a retrospective study conducted by just one institution, there may have been selection bias. Secondly, signs such as hemorrhage, EVFDM, tumor margin, peripheral fat infiltration, and other organ invasion were not evaluated.

CONCLUSION

Tumor size, contours and growth pattern were significant independent predictors for identifying high-risk patients, while primary GIST > 5 cm, irregular contours, or mixed growth patterns indicate a potentially high-risk tumor. In addition, tumor necrosis or cystic degeneration, ulceration, enhancement patterns and lymphadenopathy on dynamic CECT could improve the prognostic accuracy of patients with gastric GISTs. As a result, our study showed that preoperative risk stratification may benefit from the qualitative and quantitative characteristics of stomach GISTs on CECT. Clinicians may be given a straightforward yet useful tool to use in order to choose the best surgical method and administer preoperative neoadjuvant therapy.

Future prospective and multicenter studies will be required to confirm our early findings. Magnetic resonance imaging and positron emission tomography combined with CT may predict the malignant potential of gastric GISTs, and dual-energy CT may be used in the assessment. These aspects should be further studied. In addition, artificial intelligence should be applied in future research to assess the prognosis of GISTs.

ARTICLE HIGHLIGHTS

Research background

Clinical decision-making depends on preoperative assessment of the likelihood of malignancy and prognosis of these gastrointestinal stromal tumors (GISTs). Correlation between computed tomography (CT) image features of GIST and pathological risk grade has been previously reported in several publications. However, only a few studies have attempted to correlate CT features with histologic grading or prediction of gastric malignancy.

Research motivation

The research is to explore the multi-slice CT imaging features for predicting risk stratification in patients with primary gastric GISTs, and to give clinicians a straightforward yet useful tool to use in choosing the best surgical approach and preoperative neoadjuvant therapy.

Research objectives
The purpose of this study was to identify the CT imaging characteristics for predicting risk stratifications in patients with primary gastric GISTs.

Research methods
This retrospective analysis of clinicopathological and CT imaging data for 147 patients with gastric GISTs. The association between malignant potential and CT features was analyzed using univariate analysis and multivariate logistic regression analysis, receiver operating curve was used to evaluate the predictive value of tumor size, and the multinomial logistic regression model for risk classification.

Research results
Tumor size, tumor contours, lesion growth patterns, ulceration, cystic degeneration or necrosis, lymphadenopathy, and contrast enhancement patterns, were associated with the risk stratification; tumor size, contours and growth pattern were independent predictors for risk stratification of gastric GISTs.

Research conclusions
CT features, including tumor size, growth patterns, and lesion contours, were predictors of malignant potential for primary gastric GISTs.

Research perspectives
The CT characteristics could offer clinicians a straightforward yet useful tool for making smart clinical judgments.

FOOTNOTES

Author contributions: Wang TT designed and performed the research and wrote the paper; Li J designed the research and supervised the report; Liu XH designed the research and contributed to the analysis; Liu WW, Gao RJ, Zhu CY, and Wang Q provided clinical advice; Zhao LP and Fan XM supervised the report.

Supported by the Roentgen Imaging Research Project of Beijing Kangmeng Charitable Foundation, No. SD-202008-017.

Institutional review board statement: This study was approved by the Institutional Ethics Committee of the Second Affiliated Hospital of Shandong First Medical University (2022-016).

Informed consent statement: This is retrospective study that used anonymous clinical data. According to institutional policies, informed consent was not required from patients in this study.

Conflict-of-interest statement: All the authors report no relevant conflicts of interest for this article.

Data sharing statement: The data for this study can be obtained from the corresponding author upon request.

Country/Territory of origin: China

ORCID number: Tian-Tian Wang 0000-0003-3872-1949; Wei-Wei Liu 0000-0001-8606-5777; Xian-Hai Liu 0000-0001-9706-7196; Rong-Ji Gao 0000-0002-7385-6438; Chun-Yu Zhu 0000-0002-3622-2073; Qing Wang 0000-0001-9430-1442; Lu-Ping Zhao 0000-0002-4945-2820; Xiao-Ming Fan 0000-0002-1555-225X; Juan Li 0000-0003-1254-5748.

S-Editor: Wang JJ
L-Editor: A
P-Editor: Yu HG

REFERENCES

1 **Fletcher CD**, Berman JJ, Corless C, Gorstein F, Lasota J, Longley BJ, Miettinen M, O'Leary TJ, Remotti H, Rubin BP, Shmookler B, Sobin LH, Weiss SW. Diagnosis of gastrointestinal stromal tumors: a consensus approach. *Int J Surg Pathol*

2002; **10**: 81-89 [PMID: 12075401 DOI: 10.1177/106689690201000201]
2 **Cola D**, Bahoura L, Copelan A, Shirkhoda A, Sokhandon F. Getting the GIST: a pictorial review of the various patterns of presentation of gastrointestinal stromal tumors on imaging. *Abdom Radiol (NY)* 2017; 1350-1364 [DOI: 10.1007/s00261-016-1025-z]
3 **Joensuu H**, Hohenberger P, Corless CL. Gastrointestinal stromal tumour. *Lancet* 2013; **382**: 973-983 [PMID: 23623056 DOI: 10.1016/S0140-6736(13)60106-3]
4 **von Mehren M**, Joensuu H. Gastrointestinal Stromal Tumors. *J Clin Oncol* 2018; **36**: 136-143 [PMID: 29220298 DOI: 10.1200/JCO.2017.74.9705]
5 **Joensuu H**. Risk stratification of patients diagnosed with gastrointestinal stromal tumor. *Hum Pathol* 2008; **39**: 1411-1419 [PMID: 18774375 DOI: 10.1016/j.humpath.2008.06.025]
6 **Miettinen M**, Lasota J. Gastrointestinal stromal tumors: pathology and prognosis at different sites. *Semin Diagn Pathol* 2006; **23**: 70-83 [PMID: 17193820 DOI: 10.1053/j.semdp.2006.09.001]
7 **Wang Y**, Wang Y, Ren J, Jia L, Ma L, Yin X, Yang F, Gao BL. Malignancy risk of gastrointestinal stromal tumors evaluated with noninvasive radiomics: A multi-center study. *Front Oncol* 2022; **12**: 966743 [PMID: 36052224 DOI: 10.3389/fonc.2022.966743]
8 **Theiss L**, Contreras CM. Gastrointestinal Stromal Tumors of the Stomach and Esophagus. *Surg Clin North Am* 2019; **99**: 543-553 [PMID: 31047041 DOI: 10.1016/j.suc.2019.02.012]
9 **Ma X**, Ling W, Xia F, Zhang Y, Zhu C, He J. Application of Contrast-Enhanced Ultrasound (CEUS) in Lymphomatous Lymph Nodes: A Comparison between PET/CT and Contrast-Enhanced CT. *Contrast Media Mol Imaging* 2019; **2019**: 5709698 [PMID: 30809108 DOI: 10.1155/2019/5709698]
10 **Li C**, Fu W, Huang L, Chen Y, Xiang P, Guan J, Sun C. A CT-based nomogram for predicting the malignant potential of primary gastric gastrointestinal stromal tumors preoperatively. *Abdom Radiol (NY)* 2021; **46**: 3075-3085 [PMID: 33713161 DOI: 10.1007/s00261-021-03026-7]
11 **Danti G**, Addeo G, Cozzi D, Maggialetti N, Lanzetta MM, Frezzetti G, Masserelli A, Pradella S, Giovagnoni A, Miele V. Relationship between diagnostic imaging features and prognostic outcomes in gastrointestinal stromal tumors (GIST). *Acta Biomed* 2019; **90**: 9-19 [PMID: 31085970 DOI: 10.23750/abm.v90i5-S.8343]
12 **Zhou C**, Duan X, Zhang X, Hu H, Wang D, Shen J. Predictive features of CT for risk stratifications in patients with primary gastrointestinal stromal tumour. *Eur Radiol* 2016; **26**: 3086-3093 [PMID: 26699371 DOI: 10.1007/s00330-015-4172-7]
13 **Li H**, Ren G, Cai R, Chen J, Wu X, Zhao J. A correlation research of Ki67 index, CT features, and risk stratification in gastrointestinal stromal tumor. *Cancer Med* 2018; **7**: 4467-4474 [PMID: 30123969 DOI: 10.1002/cam4.1737]
14 **Tang B**, Feng QX, Liu XS. Comparison of Computed Tomography Features of Gastric and Small Bowel Gastrointestinal Stromal Tumors With Different Risk Grades. *J Comput Assist Tomogr* 2022; **46**: 175-182 [PMID: 35297574 DOI: 10.1097/RCT.0000000000001262]
15 **Kim JS**, Kim HJ, Park SH, Lee JS, Kim AY, Ha HK. Computed tomography features and predictive findings of ruptured gastrointestinal stromal tumours. *Eur Radiol* 2017; **27**: 2583-2590 [PMID: 27761711 DOI: 10.1007/s00330-016-4515-z]
16 **Maldonado FJ**, Sheedy SP, Iyer VR, Hansel SL, Bruining DH, McCollough CH, Harmsen WS, Barlow JM, Fletcher JG. Reproducible imaging features of biologically aggressive gastrointestinal stromal tumors of the small bowel. *Abdom Radiol (NY)* 2018; **43**: 1567-1574 [PMID: 29110055 DOI: 10.1007/s00261-017-1370-6]
17 **Inoue A**, Ota S, Nitta N, Murata K, Shimizu T, Sonoda H, Tani M, Ban H, Inatomi O, Ando A, Kushima R, Watanabe Y. Difference of computed tomographic characteristic findings between gastric and intestinal gastrointestinal stromal tumors. *Jpn J Radiol* 2020; **38**: 771-781 [PMID: 32246352 DOI: 10.1007/s11604-020-00962-0]
18 **Zhang X**, Bai L, Wang D, Huang X, Wei J, Zhang W, Zhang Z, Zhou J. Gastrointestinal stromal tumor risk classification: spectral CT quantitative parameters. *Abdom Radiol (NY)* 2019; **44**: 2329-2336 [PMID: 30980116 DOI: 10.1007/s00261-019-01973-w]
19 **Mazzei MA**, Cioffi Squitieri N, Vindigni C, Guerrini S, Gentili F, Sadotti G, Mercuri P, Righi L, Lucii G, Mazzei FG, Marrelli D, Volterrani L. Gastrointestinal stromal tumors (GIST): a proposal of a "CT-based predictive model of Miettinen index" in predicting the risk of malignancy. *Abdom Radiol (NY)* 2020; **45**: 2989-2996 [PMID: 31506758 DOI: 10.1007/s00261-019-02209-7]
20 **Su Q**, Wang Q, Zhang H, Yu D, Wang Y, Liu Z, Zhang X. Computed tomography findings of small bowel gastrointestinal stromal tumors with different histologic risks of progression. *Abdom Radiol (NY)* 2018; **43**: 2651-2658 [PMID: 29492604 DOI: 10.1007/s00261-018-1511-6]
21 **Chen Z**, Yang J, Sun J, Wang P. Gastric gastrointestinal stromal tumours (2-5 cm): Correlation of CT features with malignancy and differential diagnosis. *Eur J Radiol* 2020; **123**: 108783 [PMID: 31841880 DOI: 10.1016/j.ejrad.2019.108783]
22 **Peng G**, Huang B, Yang X, Pang M, Li N. Preoperative CT feature of incomplete overlying enhancing mucosa as a high-risk predictor in gastrointestinal stromal tumors of the stomach. *Eur Radiol* 2021; **31**: 3276-3285 [PMID: 33125563 DOI: 10.1007/s00330-020-07377-5]
23 **Rubin BP**, Heinrich MC, Corless CL. Gastrointestinal stromal tumour. *Lancet* 2007; **369**: 1731-1741 [PMID: 17512858 DOI: 10.1016/S0140-6736(07)60780-6]
24 **Xu D**, Si GY, He QZ. Correlation analysis of multi-slice computed tomography (MSCT) findings, clinicopathological factors, and prognosis of gastric gastrointestinal stromal tumors. *Transl Cancer Res* 2020; **9**: 1787-1794 [PMID: 35117526 DOI: 10.21037/tcr.2020.02.26]
25 **Cho JW**; Korean ESD Study Group. Current Guidelines in the Management of Upper Gastrointestinal Subepithelial Tumors. *Clin Endosc* 2016; **49**: 235-240 [PMID: 26898512 DOI: 10.5946/ce.2015.096]
26 **Iannicelli E**, Carbonetti F, Federici GF, Martini I, Caterino S, Pilozzi E, Panzuto F, Briani C, David V. Evaluation of the Relationships Between Computed Tomography Features, Pathological Findings, and Prognostic Risk Assessment in Gastrointestinal Stromal Tumors. *J Comput Assist Tomogr* 2017; **41**: 271-278 [PMID: 27753723 DOI: 10.1097/RCT.0000000000000499]

27 **Wang M**, Feng Z, Zhou L, Zhang L, Hao X, Zhai J. Computed-Tomography-Based Radiomics Model for Predicting the Malignant Potential of Gastrointestinal Stromal Tumors Preoperatively: A Multi-Classifier and Multicenter Study. *Front Oncol* 2021; **11**: 582847 [PMID: 33968714 DOI: 10.3389/fonc.2021.582847]

28 **Chen T**, Xu L, Dong X, Li Y, Yu J, Xiong W, Li G. The roles of CT and EUS in the preoperative evaluation of gastric gastrointestinal stromal tumors larger than 2 cm. *Eur Radiol* 2019; **29**: 2481-2489 [PMID: 30617491 DOI: 10.1007/s00330-018-5945-6]

29 **Wei SC**, Xu L, Li WH, Li Y, Guo SF, Sun XR, Li WW. Risk stratification in GIST: shape quantification with CT is a predictive factor. *Eur Radiol* 2020; **30**: 1856-1865 [PMID: 31900704 DOI: 10.1007/s00330-019-06561-6]

30 **Liu X**, Qiu H, Zhang P, Feng X, Chen T, Li Y, Tao K, Li G, Sun X, Zhou Z; China Gastrointestinal Stromal Tumor Study Group (CN-GIST). Prognostic role of tumor necrosis in patients undergoing curative resection for gastric gastrointestinal stromal tumor: a multicenter analysis of 740 cases in China. *Cancer Med* 2017; **6**: 2796-2803 [PMID: 29058376 DOI: 10.1002/cam4.1229]

31 **Yang HK**, Kim YH, Lee YJ, Park JH, Kim JY, Lee KH, Lee HS. Leiomyomas in the gastric cardia: CT findings and differentiation from gastrointestinal stromal tumors. *Eur J Radiol* 2015; **84**: 1694-1700 [PMID: 26051977 DOI: 10.1016/j.ejrad.2015.05.022]

32 **Hong X**, Choi H, Loyer EM, Benjamin RS, Trent JC, Charnsangavej C. Gastrointestinal stromal tumor: role of CT in diagnosis and in response evaluation and surveillance after treatment with imatinib. *Radiographics* 2006; **26**: 481-495 [PMID: 16549611 DOI: 10.1148/rg.262055097]

World Journal of Gastrointestinal Oncology

Submit a Manuscript: https://www.f6publishing.com

World J Gastrointest Oncol 2023 June 15; 15(6): 1086-1095

DOI: 10.4251/wjgo.v15.i6.1086

ISSN 1948-5204 (online)

ORIGINAL ARTICLE

Observational Study

Diagnostic value of circular free DNA for colorectal cancer detection

Yao Cui, Lu-Jin Zhang, Jian Li, Yu-Jie Xu, Ming-Yue Liu

Specialty type: Gastroenterology and hepatology

Provenance and peer review: Unsolicited article; Externally peer reviewed.

Peer-review model: Single blind

Peer-review report's scientific quality classification

Grade A (Excellent): 0
Grade B (Very good): B, B
Grade C (Good): 0
Grade D (Fair): 0
Grade E (Poor): 0

P-Reviewer: Bianciardi E, Italy; Quaresima S, Italy

Received: March 13, 2023
Peer-review started: March 13, 2023
First decision: March 28, 2023
Revised: March 29, 2023
Accepted: May 17, 2023
Article in press: May 17, 2023
Published online: June 15, 2023

Yao Cui, Lu-Jin Zhang, Yu-Jie Xu, Ming-Yue Liu, Department of Oncology, Henan Provincial People's Hospital, People's Hospital of Zhengzhou University, Henan University People's Hospital, Zhengzhou 450003, Henan Province, China

Jian Li, Department of General Surgery, Henan Tumor Hospital, The Affiliated Tumor Hospital of Zhengzhou University, Zhengzhou 450000, Henan Province, China

Corresponding author: Ming-Yue Liu, MD, Doctor, Department of Oncology, Henan Provincial People's Hospital, People's Hospital of Zhengzhou University, Henan University People's Hospital, No. 7 Weiwu Road, Zhengzhou 450003, Henan Province, China.
liumingyuezz@163.com

Abstract

BACKGROUND

Minimally invasive or noninvasive, sensitive and accurate detection of colorectal cancer (CRC) is urgently needed in clinical practice.

AIM

To identify a noninvasive, sensitive and accurate circular free DNA marker detected by digital polymerase chain reaction (dPCR) for the early diagnosis of clinical CRC.

METHODS

A total of 195 healthy control (HC) individuals and 101 CRC patients (38 in the early CRC group and 63 in the advanced CRC group) were enrolled to establish the diagnostic model. In addition, 100 HC individuals and 62 patients with CRC (30 early CRC and 32 advanced CRC groups) were included separately to validate the model. CAMK1D was dPCR. Binary logistic regression analysis was used to establish a diagnostic model including CAMK1D and CEA.

RESULTS

To differentiate between the 195 HCs and 101 CRC patients (38 early CRC and 63 advanced CRC patients), the common biomarkers CEA and CAMK1D were used alone or in combination to evaluate their diagnostic value. The area under the curves (AUCs) of CEA and CAMK1D were 0.773 (0.711, 0.834) and 0.935 (0.907, 0.964), respectively. When CEA and CAMK1D were analyzed together, the AUC was 0.964 (0.945, 0.982). In differentiating between the HC and early CRC groups, the AUC was 0.978 (0.960, 0.995), and the sensitivity and specificity were 88.90% and 90.80%, respectively. In differentiating between the HC and advanced CRC groups, the AUC was 0.956 (0.930, 0.981), and the sensitivity and specificity were

81.30% and 95.90%, respectively. After building the diagnostic model containing CEA and CAMK1D, the AUC of the CEA and CAMK1D joint model was 0.906 (0.858, 0.954) for the validation group. In differentiating between the HC and early CRC groups, the AUC was 0.909 (0.844, 0.973), and the sensitivity and specificity were 93.00% and 83.30%, respectively. In differentiating between the HC and advanced CRC groups, the AUC was 0.904 (0.849, 0.959), and the sensitivity and specificity were 93.00% and 75.00%, respectively.

CONCLUSION

We built a diagnostic model including CEA and CAMK1D for differentiating between HC individuals and CRC patients. Compared with the common biomarker CEA alone, the diagnostic model exhibited significant improvement.

Key Words: Healthy control; Colorectal cancer; Circular free DNA; Biomarker

Core Tip: Minimally invasive or noninvasive, sensitive and accurate detection of colorectal cancer (CRC) is urgently needed in clinical practice. We aimed to build a joint diagnostic model based on circular free DNA for detection of colorectal cancer. We evaluated the diagnostic value of circular free CAMK1D DNA for differentiating between HC individuals and CRC patients and demonstrated that CAMK1D may represent a potential diagnostic biomarker for CRC detection. Further analysis should use the colorectal polyp group to validate the diagnostic model in future studies.

Citation: Cui Y, Zhang LJ, Li J, Xu YJ, Liu MY. Diagnostic value of circular free DNA for colorectal cancer detection. *World J Gastrointest Oncol* 2023; 15(6): 1086-1095
URL: https://www.wjgnet.com/1948-5204/full/v15/i6/1086.htm
DOI: https://dx.doi.org/10.4251/wjgo.v15.i6.1086

INTRODUCTION

Colorectal cancer (CRC) is a common malignant tumor in China. The 5-year survival rate for early CRC patients after effective treatment is more than 90%. Approximately 25% of patients have local or distant metastasis at the time of initial diagnosis, and the 5-year survival rate is only 12%. Early detection, diagnosis and treatment are currently recognized methods that can effectively improve the treatment of CRC. At present, the common clinical screening tests include fecal occult blood tests and blood marker tests, but the sensitivity and specificity remain insufficient[1]. Imaging examination can effectively evaluate the scope of the lesion and the stage of the tumor, but it is of limited value in the diagnosis of early lesions. Endoscopy combined with tissue biopsy is the gold standard for the early diagnosis of CRC at present, but there are some disadvantages, such as cumbersome operation, poor compliance and the invasive nature of testing. Thus, the commonly used methods for the early diagnosis of CRC remain insufficient[2]. The identification of a minimally invasive or noninvasive, sensitive and accurate early diagnostic test is urgently needed.

Liquid biopsy technology has gained increasing interest because it is noninvasive and comprehensive and permits real-time and repeated monitoring[3]. Liquid biopsy technology primarily uses human peripheral blood, saliva, urine and other body fluid components to identify tumor heterogeneity and genetic information for the early diagnosis and individualized treatment of CRC. With the advent of precision medicine, liquid biopsy has become increasingly important. Circulating tumor cells (CTCs), circulating tumor DNA (ctDNA) and secreted proteins are the primary targets of liquid biopsy at present[4-6]. Compared with CTCs and exosomes, ctDNA is now the most widely used marker in clinical practice. A variety of tests based on ctDNA have been used in clinical practice; however, due to clearance by macrophages, the amount of circulating free DNA in body fluid is extremely low. Furthermore, ctDNA accounts for only a small portion of circulating free DNA and therefore requires high sensitivity detection equipment.

Single-stranded or double-stranded DNA is traditionally the form of ctDNA that is detected. With the development of high-throughput sequencing technology and single-cell gene amplification technology, a new type of circular free DNA has been identified[7]: Extrachromosomal circular DNA. This is a closed, circular single- or double-stranded form of DNA located in the chromatin body that can be detected in many eukaryotes, including humans[8]. Compared with free linear DNA, extrachromosomal circular DNA is not easily degraded by nucleases, and its structure is more stable[9]. Studies have also detected circular DNA in the plasma of pregnant women. Detection of the level and type of circular

DNA in human plasma is expected to permit ultra-early prediction, prognosis evaluation and even targeted treatment of tumors or other physiological and pathological conditions[10,11].

Currently, detection of ctDNA is primarily achieved through polymerase chain reaction (PCR) technology and second-generation sequencing[12]. ctDNA detection based on PCR includes: (1) Amplification-refractory mutation system PCR (ARMS-PCR) technology; (2) high resolution melting curve technology (HRM); (3) digital PCR (dPCR)[13]; and (4) BEAMING technology. Compared with other PCR detection methods, dPCR has a strong reaction solution segmentation ability and has advantages of high sensitivity, high accuracy, high tolerance and absolute quantification[14]. For plasma-free DNA, the screening strategy based on second-generation sequencing technology and the sensitive detection of dPCR can realize the accurate detection of trace plasma ctDNA[15].

In our study, we aimed to provide a noninvasive, sensitive and accurate diagnostic marker detected by dPCR for the early diagnosis of CRC.

MATERIALS AND METHODS

Study samples

All individuals enrolled in our study provided informed consent. Our study was approved by the ethics committee. From April 2019 to July 2022, a total of 295 healthy control (HC) individuals and 163 CRC patients were enrolled in our study. The project included a colorectal polyp (CRP) group, an early CRC group and an advanced CRC group. The staging of CRC was performed in accordance with the tumor node metastasis (TNM) staging of CRC of the United States Joint Commission on Cancer and the guidelines for screening and endoscopic diagnosis and treatment of early colorectal cancer in China: (1) The inclusion criteria of the CRP group were colonoscopic diagnosis and postoperative pathological confirmation of villous/tubular adenoma, with or without mild to moderate atypical hyperplasia, or local high-grade neoplasia of villous tubular adenoma confirmed by pathology and immunohistochemistry. To be included in this group, no abnormalities could be detected on any biochemical or auxiliary examinations, patients could have no chief complaint of gastrointestinal discomfort, patients could have no clinical signs of tumor, and the adenoma (villous adenoma, mixed adenoma, or adenoma with moderate or severe dysplasia) could not exceed 1 cm in diameter; (2) To be included in the early CRC group, adenocarcinoma of the intestinal wall had to be localized in the mucosa or submucosa, and no lymphatic metastasis could be detected (*i.e.*, stage 0-T1 tumors). Pathologically confirmed local high-grade villous tubular adenomas or adenocarcinoma of the intestinal wall localized to the mucosa or submucosa were eligible for inclusion. Patients had not received treatment by surgery, chemotherapy, radiotherapy, or other modalities prior to sample collection, and patients had not received blood transfusions in the last 3 mo; and (3) The advanced CRC group was diagnosed based on the TNM CRC staging of the United States Joint Commission on Cancer, and T2-IV stage was defined as intermediate and advanced CRC. All diagnoses were based on pathologically confirmed CRC. Patients had not undergone treatment with surgery, chemotherapy, radiotherapy, or other modalities prior to sample collection, and patients had not received any blood transfusions in the last 3 mo. CRC tissue samples and corresponding clinical examination data were available for all patients included in the study. None of the patients received chemotherapy, radiotherapy or immunotherapy before sample collection, and patients with other tumors and gastrointestinal diseases detected during the admission examination were excluded.

A BD Vacutainer PPT plasma preparation tube was used to collect peripheral blood samples from patients. Within 2 h of collection, samples were centrifuged at 2000 × g for 10 minutes, and the supernatant was then divided into several aliquots. All plasma samples were kept at -80 °C until use.

dPCR detection

Free DNA was extracted from plasma samples using a QIAamp DNA Blood Kit. ATP-dependent DNase was added to the free DNA and digested at 37 °C for 1.5 h until the final concentration was 0.4 U/μL. Linear double-stranded DNA was removed and incubated at 70 °C for 30 min to inactivate ATP-dependent DNase. The primers were designed according to the eccDNA sequence. The primer probe was designed using Primer3 software and synthesized by Invitrogen after a homologous search with BLAST. The primer and probe were diluted with deionized water, and the storage concentration was 200 μmol/L with a working concentration of 10 μmol/L. The total PCR volume was 20 μL: 10 μL 2 × ddPCR™Super mixture, 1.8 μL forward and reverse primers (final concentration 900 nmol/L), 0.5 μL probe (final concentration of 250 nmol/L), 4 μg template DNA, and ddH_2O to a final volume of 20 μL. Then, a 20 μL reaction volume was added to the droplet generation card. All generated microdroplets were transferred to a 96-well plate for PCR amplification. The PCR conditions were as follows: 95 °C/10 min, followed by 40 cycles of 94 °C/30 s 60 °C/1 min and 98 °C/10 min. Quanta Soft 1.6 software was used to analyze the results. The system was flushed before each experiment. The sample for the 96-well plate was input, and the sample droplets were analyzed.

Statistical analysis

SPSS 22.0 was used for statistical analysis. Normally distributed data were compared using independent sample *t* tests. Nonnormally distributed data were compared using the rank sum test. The area under the curve (AUC), sensitivity and specificity were used to assess the diagnostic value of the indicators. $P < 0.05$ represents a statistically significant difference. The binary logistic regression model, which used the forward conditional method, was used to combine the indicators. The Z score test was used to compare the AUC values.

RESULTS

General clinical characteristics of study subjects

As shown in Table 1, 195 HC individuals and 101 CRC patients (38 in the early CRC group and 63 in the advanced CRC group) were enrolled for model establishment. In addition, 100 HC individuals and 62 patients with CRC (30 early CRC and 32 late CRC) were included separately to validate the model. The CRC stage was in accordance with the TNM CRC stage of the United States Joint Commission on Cancer and the guidelines for screening and endoscopic diagnosis and treatment of early CRC in China. T1 and T2 were defined as early CRC, and T3 and T4 were defined as advanced CRC. The age and sex of the patients in the model generation group and the validation group were matched. In the model generation group, 21 tumors were located in the ascending colon, 15 were located in the descending colon, 3 were located in the transverse colon, 59 were located in the sigmoid colon and 3 were located in the rectum. Twenty-one tumors were well differentiated, 57 exhibited intermediate differentiation, and 23 were poorly differentiated.

Concentrations of the indicators in the HC and CRC groups

As shown in Table 2, the levels of NDUFB7, CAMK1D, PIK3CD and PSEN2 were compared between the 195 HCs and 101 CRC patients. First, homogeneity of variance was tested. CAMK1D, PIK3CD and PSEN2 exhibited nonhomogeneity of variance; NDUFB7 exhibited homogeneity of variance. Three of the four indicators, CAMK1D, PIK3CD and PSEN2, exhibited statistically significant differences between the HC and CRC groups ($P < 0.05$). NDUFB7 exhibited no significant differences.

Evaluation of the diagnostic value of CAMK1D, PIK3CD and PSEN2

Based on the significant differences between the HC and CRC groups, three indicators, CAMK1D, PIK3CD and PSEN2, were used for AUC analysis. As shown in Table 3, the AUCs of CAMK1D and PIK3CD exhibited statistically significant differences ($P < 0.01$) between the HCs and CRC patients when the ROC curve was used to evaluate the diagnostic value. Therefore, CAMK1D and PIK3CD were selected for subsequent multiparameter diagnostic model analysis.

Univariate and multivariate logistic regression analysis

Based on the significant differences between the HC and CRC groups and ROC curves, univariate logistic regression was performed. As shown in Tables 4 and 5, CAMK1D and PIK3CD differed significantly between the two groups ($P < 0.01$). Next, multivariate logistic regression analysis was performed for CAMK1D and PIK3CD, and only CAMK1D remained statistically significant ($P < 0.01$).

Diagnostic value evaluation of the indicator for differentiating HC and CRC

CAMK1D and the common biomarker CEA were used alone or in combination to evaluate their ability to differentiate between 195 HC individuals and 101 CRC patients (38 early CRC patients and 63 advanced CRC patients). As shown in Figure 1A, the AUCs of CEA and CAMK1D were 0.773 (0.711, 0.834) and 0.935 (0.907, 0.964), respectively. As shown in Figure 1B, the use of both CEA and CAMK1D produced an AUC of 0.964 (0.945, 0.982) by binary logistic regression analysis. Next, the diagnostic value of the CEA and CAMK1D model in the differentiation of 195 HC individuals and 38 early CRC patients was evaluated. As shown in Figure 1C, the AUC was 0.978 (0.960, 0.995), and the sensitivity and specificity were 88.90% and 90.80%, respectively. As shown in Figure 1D, when applying the model to differentiate between the 195 HC individuals and 63 advanced CRC patients, the AUC was 0.956 (0.930, 0.981), and the sensitivity and specificity were 81.30% and 95.90%, respectively.

Validation of the diagnostic model for differentiating between HCs and CRC

After building the diagnostic model containing CEA and CAMK1D, 100 HC individuals and 62 patients with CRC (30 early CRC patients and 32 advanced CRC patients) were enrolled to validate the model. As shown in Figure 2A, the AUC of the CEA and CAMK1D joint model was 0.906 (0.858, 0.954). Next, the diagnostic value of the CEA and CAMK1D model in the differentiation of 100 HC individuals and 32 early CRC patients was evaluated. As shown in Figure 2B, the AUC was 0.909 (0.844, 0.973), and the sensitivity and specificity were 93.00% and 83.30%, respectively. As shown in Figure 2C, the AUC for the differentiation of the 100 HC individuals and 32 advanced CRC patients was 0.904 (0.849, 0.959), and

Table 1 General clinical characteristics of the subjects

Characteristics	CRC (training)	HC (training)	CRC (validation)	HC (validation)
Number	101	195	62	100
Age, yr				
Mean	58	53	57	55
Range	29-81	33-57	33-74	34-67
Sex				
Male	60	116	37	64
Female	41	79	25	36
TNM stage				
T1	11		11	
T2	27		21	
T3	44		7	
T4	19		23	

CRC: Colorectal cancer; HC: Healthy control; TNM: Tumor node metastasis.

Table 2 Comparison of the four markers between the healthy control group and colorectal cancer group

Indicator	HC (*n* = 195)	CRC (*n* = 101)	F	Sig	*P* value
NDUFB7	1.54 (0.94, 2.31)	2.10 (1.29, 3.08)	0.15	0.70	0.60
CAMK1D	9.71 (6.38, 18.25)	70.39 (35.26, 155.57)	34.24	< 0.01	< 0.01
PIK3CD	297.11 (232.76, 374.69)	333.22 (259.40, 417.90)	10.47	< 0.01	0.03
PSEN2	5.48 (4.04, 7.21)	8.69 (6.00, 11.67)	5.89	0.02	< 0.01

CRC: Colorectal cancer; HC: Healthy control.

Table 3 Evaluation of the diagnostic value of three markers exhibiting statically significant differences between the healthy control group and colorectal cancer group

Indicator	AUC	SD	*P* value	95%CI	
				Lower	Upper
CAMK1D	0.935	0.015	< 0.001	0.907	0.964
PSEN2	0.740	0.031	< 0.001	0.678	0.801
PIK3CD	0.582	0.036	0.021	0.511	0.653

AUC: Area under the curve.

Table 4 Univariate and multivariate logistic regression of CAMK1D and PSEN2

Indicator	B	SE	Wals	*P* value	Exp (B)	95%CI	
						Lower	Upper
CAMK1D	0.560	0.137	16.781	< 0.001	1.751	1.339	2.289
PIK3CD	0.071	0.011	41.382	< 0.001	1.074	1.051	1.097

Table 5 Multivariate logistic regression of CAMK1D and PSEN2

Indicator	B	SE	Wals	*P* value	Exp (B)	95%CI	
						Lower	Upper
CAMK1D	0.125	0.039	10.400	0.001	1.133	1.050	1.222
PIK3CD	-0.002	0.004	0.208	0.648	0.998	0.990	1.006

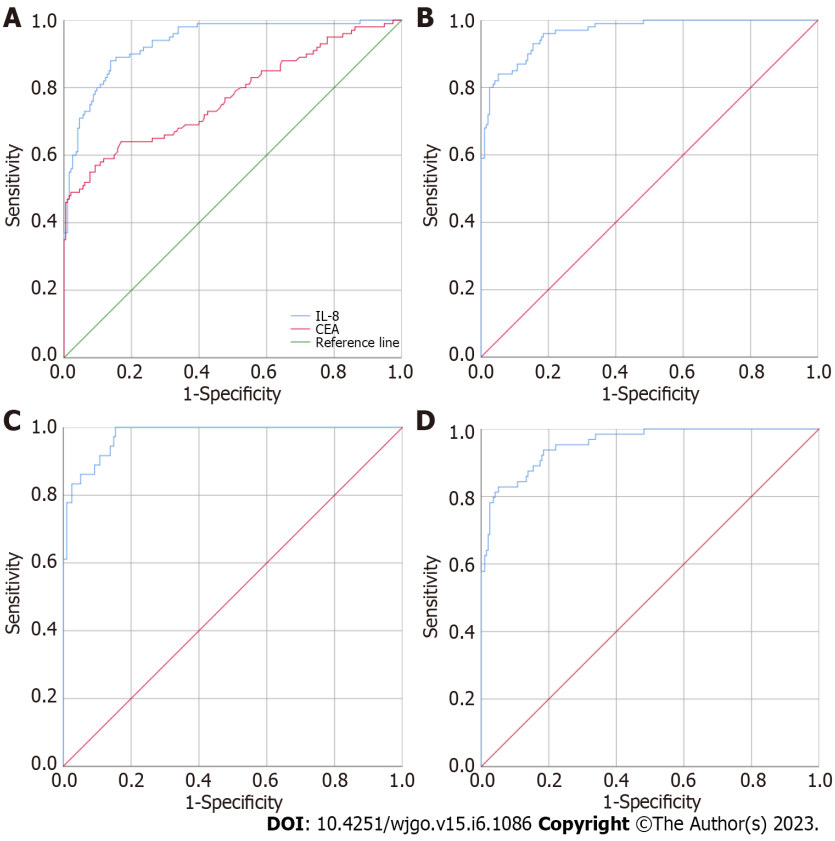

DOI: 10.4251/wjgo.v15.i6.1086 **Copyright** ©The Author(s) 2023.

Figure 1 Diagnostic value evaluation of the indicator for differentiation between the healthy control group and colorectal cancer group. A: CEA and CAMK1D used alone to differentiate between the 195 healthy controls and 101 colorectal cancer patients; B: CEA and CAMK1D joint model for the differentiation of the 195 healthy controls and 101 colorectal cancer patients; C: CEA and CAMK1D joint model for the differentiation of the 195 healthy controls and 38 early colorectal cancer patients; D: CEA and CAMK1D joint model for the differentiation of the 195 healthy controls and 63 advanced colorectal cancer patients.

the sensitivity and specificity were 93.00% and 75.00%, respectively.

DISCUSSION

There have been many studies exploring the use of circulating free DNA as a diagnostic and prognostic tumor biomarker[16]. Because the molecular weight of circulating free DNA is relatively large, optical microscopy can use common DNA dyes to observe extracellular DNA in M-phase cells[17]. Ultrahigh-resolution microscopy technology has been developed in recent years to aid in imaging[18]. Superresolution three-dimensional structured illumination microscopy can also be used for imaging analysis. Due to the resolution limitations of optical microscopy, it is difficult to observe and analyze fine circular DNA structures. Therefore, researchers turned to electron microscopy to solve this problem[19]. Electron microscopy has made significant contributions to structural studies. Both scanning electron microscopy and transmission electron microscopy can be used for imaging. However, due to the large sample size required and low abundance of ctDNA, this method is not commonly used at present. Transposase-accessible chromatin visualization analysis is a transposase-mediated imaging technology. This technology uses direct *in situ* imaging, cell sorting and depth sequencing of accessible genomes to reveal the identity of imaging elements. Single-molecule real-time sequencing technology has addressed many of the previous technological limitations. ctDNA is typically large and may contain sequences from multiple chromatin sources[20]. Therefore, it is difficult to use high-throughput sequencing to

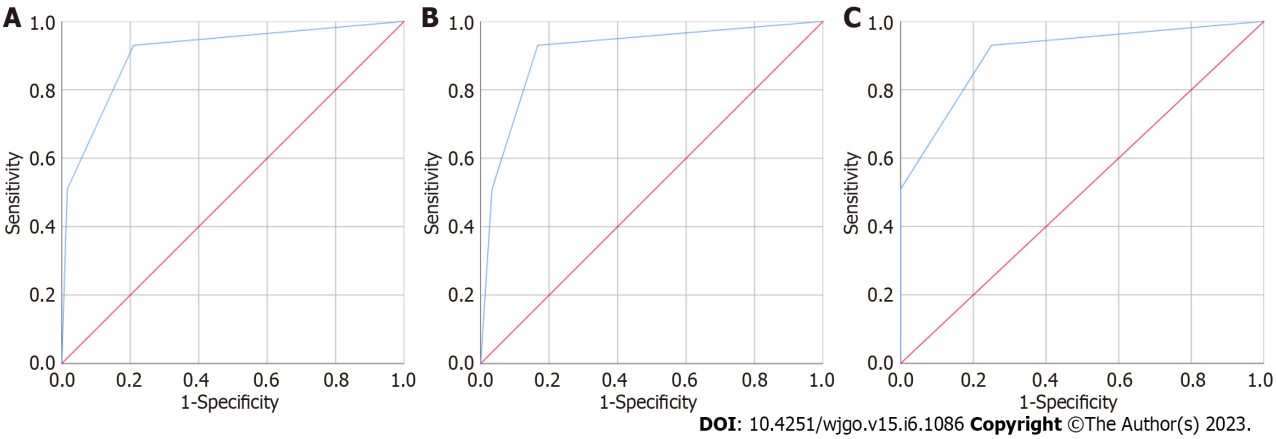

DOI: 10.4251/wjgo.v15.i6.1086

Figure 2 Diagnostic value evaluation of the indicator for the differentiation between the healthy controls and colorectal cancer patients in the validation group. A: CEA and CAMK1D joint model for the differentiation of 100 healthy controls and 62 patients with colorectal cancer; B: CEA and CAMK1D joint model for the differentiation of 100 healthy controls and 30 patients with early colorectal cancer; C: CEA and CAMK1D joint model for the differentiation of 100 healthy controls and 32 patients with advanced colorectal cancer.

completely reconstruct the full-length sequence. ATAC-seq and DNA transposase technology were first proposed as a means of chromatin accessibility analysis in 2013[21,22]. DNA transposase can randomly insert sequences into the genome. The identification of ctDNA in plasma and serum prompted the demand for a novel detection method in plasma[14,23,24].

dPCR can precisely quantify target nucleic acids in a sample and overcomes the shortcomings of qPCR. In dPCR, the sample is first divided into many independent PCR subreactions so that each part contains either a few target sequences or no target sequences[13]. After PCR, the score of the amplification positive zone was used to quantify the concentration of the target sequence, and Poisson statistics were used to statistically define the accuracy. In addition, this approach exhibits higher tolerance for the presence of inhibitors in the sample. Each subreaction acts as a separate PCR microreactor, and the subreaction containing the amplified target sequence is detected by fluorescence. The ratio of the positive distribution to the total number of sequences can be used to determine the concentration of the target in the sample. The primary difference between dPCR and qPCR is the method of measuring the number of target sequences. Unlike qPCR, dPCR does not rely on a calibration curve for sample quantification. Therefore, dPCR avoids the limitations related to the change in reaction efficiency. dPCR is theoretically superior to qPCR because it provides an effective method to perform sample allocation and single-molecule target amplification[25]. In practice, due to its higher sensitivity, qPCR can outperform dPCR in specific applications. Calcium/calmodulin-dependent protein kinases (CAMKs) are involved in a wide range of cancer-related functions in multiple tumor types. CAMK1 may have potential prognostic value in pancreatic cancer, suggesting that CAMK1 may have a distinct role in pancreatic cancer progression[26]. In addition, CAMK1D may also be involved in immune resistance by T-cell recognition, which rapidly inhibits the terminal apoptotic cascade[27]. Other regulatory molecules, such as miRNAs and lncRNAs, may also regulate CAMK1D to participate in cancer progression. In our study, the overexpression of circular CAMK1D may also have a potential function in CRC progression[28-30].

There are still some limitations in our study. First, we only assessed the diagnostic value of our model in distinguishing between HC individuals and CRC patients; the utility of the model in the CRP group was not evaluated. Second, we only evaluated the common biomarker CEA, and other biomarkers may also possess diagnostic value. Third, the experimental protocol may affect the results.

CONCLUSION

We evaluated the diagnostic value of circular free CAMK1D in differentiating between HC individuals and CRC patients and demonstrated that CAMK1D may represent a diagnostic biomarker for CRC detection.

ARTICLE HIGHLIGHTS

Research background

Endoscopy combined with tissue biopsy is currently the gold standard for the early diagnosis of colorectal cancer (CRC), but there are some disadvantages, including cumbersome operation, poor compliance and the invasive nature of testing. The commonly available methods for the early diagnosis of CRC remain insufficient.

Research motivation

The identification of a minimally invasive or noninvasive, sensitive and accurate early diagnostic marker for the clinical detection of CRC is urgently needed. Common biomarkers and circular free DNA may exhibit potential diagnostic value for CRC.

Research objectives

To evaluate the diagnostic value of circular free DNA in CRC.

Research methods

A total of 195 healthy control (HC) individuals and 101 CRC patients (38 in the early CRC group and 63 in the advanced CRC group) were enrolled to generate the model. One hundred HC individuals and 62 patients with CRC (30 early CRC and 32 advanced CRC patients) were included separately to validate the model. CAMK1D was detected by digital PCR. Binary logistic regression analysis was used to establish a joint CAMK1D and CEA diagnostic model for CRC.

Research results

Inclusion of both CEA and CAMK1D in the model produced an area under the curve (AUC) of 0.964 (0.945, 0.982). For the differentiation between the HC group and early CRC group, the AUC was 0.978 (0.960, 0.995), and the sensitivity and specificity were 88.90% and 90.80%, respectively. For the differentiation between the HC group and advanced CRC group, the AUC was 0.956 (0.930, 0.981), and the sensitivity and specificity were 81.30% and 95.90%, respectively. In the validation group, the AUC of the CEA and CAMK1D joint model was 0.906 (0.858, 0.954). For differentiating between the HC group and early CRC group, the AUC was 0.909 (0.844, 0.973), and the sensitivity and specificity were 93.00% and 83.30%, respectively. For differentiating between the HC group and the advanced CRC group, the AUC was 0.904 (0.849, 0.959), and the sensitivity and specificity were 93.00% and 75.00%, respectively.

Research conclusions

We evaluated the diagnostic value of circular free CAMK1D DNA for differentiating between HC individuals and CRC patients and demonstrated that CAMK1D may represent a potential diagnostic biomarker for CRC detection.

Research perspectives

Further analysis should use the colorectal polyp group to validate the diagnostic model in future studies.

FOOTNOTES

Author contributions: Cui Y and Liu MY designed the study; Zhang LJ, Li J and Xu YJ performed the research; Cui Y and Li J analyzed the data; Cui Y wrote the manuscript; Cui Y and Liu MY revised the manuscript for final submission; Liu MY is the corresponding author.

Supported by the Henan Medical Science and Technology Research Program, No. LHGJ20210045.

Institutional review board statement: The study was reviewed and approved by the Henan Provincial People's Hospital, People's Hospital of Zhengzhou University, Henan University People's Hospital.

Informed consent statement: All study participants, or their legal guardian, provided informed written consent prior to study enrollment.

Conflict-of-interest statement: We declare that we have no financial or personal relationships with other individuals or organizations that can inappropriately influence our work and that there is no professional or other personal interest of any nature in any product, service and/or company that could be construed as influencing the position presented in or the review of the manuscript.

Data sharing statement: We have no data to share.

STROBE statement: The authors have read the STROBE Statement—checklist of items, and the manuscript was prepared and revised according to the STROBE Statement—checklist of items.

Country/Territory of origin: China

ORCID number: Yao Cui 0000-0003-0273-9178; Lu-Jin Zhang 0000-0003-1264-9571; Jian Li 0000-0002-2168-4240; Yu-Jie Xu 0000-0003-1833-6541; Ming-Yue Liu 0000-0002-5896-5011.

S-Editor: Yan JP
L-Editor: A
P-Editor: Yan JP

REFERENCES

1 **Kuipers EJ**, Grady WM, Lieberman D, Seufferlein T, Sung JJ, Boelens PG, van de Velde CJ, Watanabe T. Colorectal cancer. *Nat Rev Dis Primers* 2015; **1**: 15065 [PMID: 27189416 DOI: 10.1038/nrdp.2015.65]
2 **Goldstein MJ**, Mitchell EP. Carcinoembryonic antigen in the staging and follow-up of patients with colorectal cancer. *Cancer Invest* 2005; **23**: 338-351 [PMID: 16100946 DOI: 10.1081/cnv-58878]
3 **Polakis P**. Wnt signaling and cancer. *Genes Dev* 2000; **14**: 1837-1851 [PMID: 10921899]
4 **Alix-Panabières C**, Pantel K. Liquid Biopsy: From Discovery to Clinical Application. *Cancer Discov* 2021; **11**: 858-873 [PMID: 33811121 DOI: 10.1158/2159-8290.CD-20-1311]
5 **Junqueira-Neto S**, Batista IA, Costa JL, Melo SA. Liquid Biopsy beyond Circulating Tumor Cells and Cell-Free DNA. *Acta Cytol* 2019; **63**: 479-488 [PMID: 30783027 DOI: 10.1159/000493969]
6 **Chen M**, Zhao H. Next-generation sequencing in liquid biopsy: cancer screening and early detection. *Hum Genomics* 2019; **13**: 34 [PMID: 31370908 DOI: 10.1186/s40246-019-0220-8]
7 **Wang M**, Chen X, Yu F, Ding H, Zhang Y, Wang K. Extrachromosomal Circular DNAs: Origin, formation and emerging function in Cancer. *Int J Biol Sci* 2021; **17**: 1010-1025 [PMID: 33867825 DOI: 10.7150/ijbs.54614]
8 **Sun Z**, Ji N, Zhao R, Liang J, Jiang J, Tian H. Extrachromosomal circular DNAs are common and functional in esophageal squamous cell carcinoma. *Ann Transl Med* 2021; **9**: 1464 [PMID: 34734016 DOI: 10.21037/atm-21-4372]
9 **Zuo S**, Yi Y, Wang C, Li X, Zhou M, Peng Q, Zhou J, Yang Y, He Q. Extrachromosomal Circular DNA (eccDNA): From Chaos to Function. *Front Cell Dev Biol* 2021; **9**: 792555 [PMID: 35083218 DOI: 10.3389/fcell.2021.792555]
10 **Wang T**, Zhang H, Zhou Y, Shi J. Extrachromosomal circular DNA: a new potential role in cancer progression. *J Transl Med* 2021; **19**: 257 [PMID: 34112178 DOI: 10.1186/s12967-021-02927-x]
11 **Yu W**, Hurley J, Roberts D, Chakrabortty SK, Enderle D, Noerholm M, Breakefield XO, Skog JK. Exosome-based liquid biopsies in cancer: opportunities and challenges. *Ann Oncol* 2021; **32**: 466-477 [PMID: 33548389 DOI: 10.1016/j.annonc.2021.01.074]
12 **Zhu H**, Zhang H, Xu Y, Laššáková S, Korabečná M, Neužil P. PCR past, present and future. *Biotechniques* 2020; **69**: 317-325 [PMID: 32815744 DOI: 10.2144/btn-2020-0057]
13 **Váňová B**, Malicherova B, Burjanivová T, Liskova A, Janikova K, Jasek K, Lasabová Z, Tatár M, Plank L. Droplet digital PCR as a novel dia-gnostic tool. *Klin Onkol* 2021; **34**: 33-39 [PMID: 33657817 DOI: 10.48095/ccko202133]
14 **Feng Z**, Shu Y. An Overview of Digital PCR. *Bing Du Xue Bao* 2017; **33**: 103-107 [PMID: 30702829]
15 **Lin J**, Su G, Su W, Zhou C. [Progress in digital PCR technology and application]. *Sheng Wu Gong Cheng Xue Bao* 2017; **33**: 170-177 [PMID: 28956373 DOI: 10.13345/j.cjb.160269]
16 **Wu S**, Turner KM, Nguyen N, Raviram R, Erb M, Santini J, Luebeck J, Rajkumar U, Diao Y, Li B, Zhang W, Jameson N, Corces MR, Granja JM, Chen X, Coruh C, Abnousi A, Houston J, Ye Z, Hu R, Yu M, Kim H, Law JA, Verhaak RGW, Hu M, Furnari FB, Chang HY, Ren B, Bafna V, Mischel PS. Circular ecDNA promotes accessible chromatin and high oncogene expression. *Nature* 2019; **575**: 699-703 [PMID: 31748743 DOI: 10.1038/s41586-019-1763-5]
17 **Paulsen T**, Shibata Y, Kumar P, Dillon L, Dutta A. Small extrachromosomal circular DNAs, microDNA, produce short regulatory RNAs that suppress gene expression independent of canonical promoters. *Nucleic Acids Res* 2019; **47**: 4586-4596 [PMID: 30828735 DOI: 10.1093/nar/gkz155]
18 **Paulsen T**, Kumar P, Koseoglu MM, Dutta A. Discoveries of Extrachromosomal Circles of DNA in Normal and Tumor Cells. *Trends Genet* 2018; **34**: 270-278 [PMID: 29329720 DOI: 10.1016/j.tig.2017.12.010]
19 **Hull RM**, Houseley J. The adaptive potential of circular DNA accumulation in ageing cells. *Curr Genet* 2020; **66**: 889-894 [PMID: 32296868 DOI: 10.1007/s00294-020-01069-9]
20 **Zhu J**, Zhang F, Du M, Zhang P, Fu S, Wang L. Molecular characterization of cell-free eccDNAs in human plasma. *Sci Rep* 2017; **7**: 10968 [PMID: 28887493 DOI: 10.1038/s41598-017-11368-w]
21 **Kumar P**, Kiran S, Saha S, Su Z, Paulsen T, Chatrath A, Shibata Y, Shibata E, Dutta A. ATAC-seq identifies thousands of extrachromosomal circular DNA in cancer and cell lines. *Sci Adv* 2020; **6**: eaba2489 [PMID: 32440553 DOI: 10.1126/sciadv.aba2489]

22 **Su Z**, Saha S, Paulsen T, Kumar P, Dutta A. ATAC-Seq-based Identification of Extrachromosomal Circular DNA in Mammalian Cells and Its Validation Using Inverse PCR and FISH. *Bio Protoc* 2021; **11**: e4003 [PMID: 34124304 DOI: 10.21769/BioProtoc.4003]

23 **Feng XJ**, Yi HM, Ren XX, Ren JL, Ge JR, Wang FG. [Digital PCR and its application in biological detection]. *Yi Chuan* 2020; **42**: 363-373 [PMID: 32312705 DOI: 10.16288/j.yczz.19-351]

24 **Mann L**, Seibt KM, Weber B, Heitkam T. ECCsplorer: a pipeline to detect extrachromosomal circular DNA (eccDNA) from next-generation sequencing data. *BMC Bioinformatics* 2022; **23**: 40 [PMID: 35030991 DOI: 10.1186/s12859-021-04545-2]

25 **Quan PL**, Sauzade M, Brouzes E. dPCR: A Technology Review. *Sensors (Basel)* 2018; **18** [PMID: 29677144 DOI: 10.3390/s18041271]

26 **Lei Y**, Yu T, Li C, Li J, Liang Y, Wang X, Chen Y. Expression of CAMK1 and its association with clinicopathologic characteristics in pancreatic cancer. *J Cell Mol Med* 2021; **25**: 1198-1206 [PMID: 33342045 DOI: 10.1111/jcmm.16188]

27 **Volpin V**, Michels T, Sorrentino A, Menevse AN, Knoll G, Ditz M, Milenkovic VM, Chen CY, Rathinasamy A, Griewank K, Boutros M, Haferkamp S, Berneburg M, Wetzel CH, Seckinger A, Hose D, Goldschmidt H, Ehrenschwender M, Witzens-Harig M, Szoor A, Vereb G, Khandelwal N, Beckhove P. CAMK1D Triggers Immune Resistance of Human Tumor Cells Refractory to Anti-PD-L1 Treatment. *Cancer Immunol Res* 2020; **8**: 1163-1179 [PMID: 32665263 DOI: 10.1158/2326-6066.CIR-19-0608]

28 **Dimitrova N**, Gocheva V, Bhutkar A, Resnick R, Jong RM, Miller KM, Bendor J, Jacks T. Stromal Expression of miR-143/145 Promotes Neoangiogenesis in Lung Cancer Development. *Cancer Discov* 2016; **6**: 188-201 [PMID: 26586766 DOI: 10.1158/2159-8290.CD-15-0854]

29 **Sui MH**, Zhang WW, Geng DM, Sun DJ. CircPRKCI regulates proliferation, migration and cycle of lung adenocarcinoma cells by targeting miR-219a-5p-regulated CAMK1D. *Eur Rev Med Pharmacol Sci* 2021; **25**: 1899-1909 [PMID: 33660800 DOI: 10.26355/eurrev_202102_25085]

30 **Wang L**, Lin Y, Meng H, Liu C, Xue J, Zhang Q, Li C, Zhang P, Cui F, Chen W, Jiang A. Long non-coding RNA LOC283070 mediates the transition of LNCaP cells into androgen-independent cells possibly *via* CAMK1D. *Am J Transl Res* 2016; **8**: 5219-5234 [PMID: 28077997]

World Journal of Gastrointestinal Oncology

Submit a Manuscript: https://www.f6publishing.com

World J Gastrointest Oncol 2023 June 15; 15(6): 1096-1104

DOI: 10.4251/wjgo.v15.i6.1096

ISSN 1948-5204 (online)

CASE REPORT

Advanced gastric cancer achieving major pathologic regression after chemoimmunotherapy combined with hypofractionated radiotherapy: A case report

Meng-Long Zhou, Ruo-Ne Xu, Cong Tan, Zhen Zhang, Jue-Feng Wan

Specialty type: Oncology

Provenance and peer review: Unsolicited article; Externally peer reviewed.

Peer-review model: Single blind

Peer-review report's scientific quality classification

Grade A (Excellent): A, A
Grade B (Very good): 0
Grade C (Good): C
Grade D (Fair): 0
Grade E (Poor): 0

P-Reviewer: Kotelevets SM, Russia; Taghizadeh-Hesary F, Iran

Received: February 19, 2023
Peer-review started: February 19, 2023
First decision: March 22, 2023
Revised: April 9, 2023
Accepted: April 23, 2023
Article in press: April 23, 2023
Published online: June 15, 2023

Meng-Long Zhou, Ruo-Ne Xu, Zhen Zhang, Jue-Feng Wan, Department of Radiation Oncology, Fudan University Shanghai Cancer Center, Shanghai 200032, China

Meng-Long Zhou, Ruo-Ne Xu, Cong Tan, Zhen Zhang, Jue-Feng Wan, Department of Oncology, Shanghai Medical College, Fudan University, Shanghai 200032, China

Meng-Long Zhou, Ruo-Ne Xu, Zhen Zhang, Jue-Feng Wan, Shanghai Key Laboratory of Radiation Oncology, Fudan University, Shanghai 200032, China

Cong Tan, Department of Pathology, Fudan University Shanghai Cancer Center, Shanghai 200032, China

Corresponding author: Jue-Feng Wan, MD, Assistant Professor, Department of Radiation Oncology, Fudan University Shanghai Cancer Center, No. 270 Dong' an Road, Shanghai 200032, China. wjf62313172@163.com

Abstract

BACKGROUND

Currently, chemotherapy combined with immunotherapy is the established first-line standard treatment for advanced gastric cancer (GC). In addition, the combination of radiotherapy and immunotherapy is considered a promising treatment strategy.

CASE SUMMARY

In this report, we present a case of achieving nearly complete remission of highly advanced GC with comprehensive therapies. A 67-year-old male patient was referred to the hospital because he presented with dyspepsia and melena for several days. Based on fluorodeoxyglucose positron emission tomography/computed tomography (FDG PET/CT), endoscopic examination and abdominal CT, he was diagnosed with GC with a massive lesion and two distant metastatic lesions. The patient received mFOLFOX6 regimen chemotherapy, nivolumab and a short course of hypofractionated radiotherapy (4 Gy × 6 fractions) targeting the primary lesion. After the completion of these therapies, the tumor and the metastatic lesions showed a partial response. After having this case discussed by a multidisciplinary team, the patient underwent surgery, including total gastrectomy and D2 lymph node dissection. Postoperative pathology showed that major pathological regression of the primary lesion was achieved. Chemoimmuno-

therapy started four weeks after surgery, and examination was performed every three months. Since surgery, the patient has been stable and healthy with no evidence of recurrence.

CONCLUSION
The combination of radiotherapy and immunotherapy for GC is worthy of further exploration.

Key Words: Gastric cancer; Oligometastasis; Immunotherapy; Hypofractionated radiotherapy; Gastrectomy; Case report

Core Tip: This case report describes a patient with unresectable advanced gastric cancer who received comprehensive treatment including chemoimmunotherapy and hypofractionated radiotherapy that was applied to treat the primary lesion; satisfactory efficacy was achieved. The combination of radiotherapy and immunotherapy is worthy of further exploration, and the dose division of radiotherapy is an important factor. Hypofractionated radiotherapy, compared to conventional fractionated radiotherapy, may better coordinate with immunotherapy.

Citation: Zhou ML, Xu RN, Tan C, Zhang Z, Wan JF. Advanced gastric cancer achieving major pathologic regression after chemoimmunotherapy combined with hypofractionated radiotherapy: A case report. *World J Gastrointest Oncol* 2023; 15(6): 1096-1104
URL: https://www.wjgnet.com/1948-5204/full/v15/i6/1096.htm
DOI: https://dx.doi.org/10.4251/wjgo.v15.i6.1096

INTRODUCTION

According to GLOBOCAN 2020, gastric cancer (GC) ranks fifth and fourth in terms of the estimated number of new cases and the number of deaths worldwide, respectively[1]. Of note, the majority of worldwide GC cases and deaths occur annually in China, accounting for 43.9% of the worldwide cases and 48.6% of the worldwide deaths[1]. The median overall survival of patients with advanced GC is only 1 year[1,2]. Such disappointing survival outcomes are mainly the result of the inherent biological aggressiveness of GC and the relatively poor response to currently available therapies.

Cancer immunotherapy has opened a new era of cancer treatment. In 2020, two clinical studies based on KEYNOTE-059 and ATTRACTION-02 established the status of pembrolizumab and nivolumab as third-line treatments for advanced GC[3,4]. While moving from being a third-line treatment to a first-line treatment, immunotherapy for GC has encountered many difficulties and failures. Currently, chemotherapy combined with immunotherapy is the established first-line standard treatment for advanced GC[5].

At present, the focus of tumor immunotherapy has shifted from single-drug therapy to combined immunotherapy, as the combination could potentially lead to increased therapeutic efficacy. Radiotherapy can destroy tumor cells, promote the release of tumor antigens, and promote the infiltration of immune cells, thus changing the tumor microenvironment[6]. Therefore, the combination of radiotherapy and immunotherapy is considered a promising treatment strategy[6].

This report presents the case of a patient who was initially diagnosed with unresectable advanced GC and successfully treated with comprehensive therapies including chemotherapy, immunotherapy, and hypofractionated radiotherapy (HFRT). The tumor showed significant regression, and surgery was performed. Eventually, the patient achieved major pathologic regression.

CASE PRESENTATION

Chief complaints

A 67-year-old male patient presenting with dyspepsia and melena for several days was admitted to the Fudan University Shanghai Cancer Center (FUSCC, Shanghai, China) on May 12, 2022.

History of present illness

The patient developed dizziness, poor appetite, epigastrium fullness and discomfort, occasional dull pain, defecation, and no relief after taking omeprazole capsules for five days. Then the patient went to hospital accordingly.

History of past illness

The patient had no significant history of past illness.

Personal and family history

The patient had a past history of smoking and alcohol consumption for more than 30 years and had already quit smoking for 2 years. The patient had no significant family history.

Physical examination

Physical examination showed a pale face, indicating anemia (hemoglobin, 97 g/L). An enlarged lymph node was palpated in the left supraclavicular area. No positive signs were observed in abdominal and digital rectal examinations.

Laboratory examinations

The serum levels of carcinoembryonic antigen, alpha-fetoprotein, carbohydrate antigen (CA) 19–9, CA125, CA72-4, CA50, and CA242 were all in the normal ranges.

Imaging examinations

Enhanced computed tomography (CT) scan of the stomach showed thickening of the wall of the gastric body and the antrum with enhancement, and multiple enlarged lymph nodes were detected around the stomach, hepatogastric space, hilar region, and retroperitoneum (Figure 1A). Gastroscopy indicated Borrmann type 3 GC, and pathology examination of gastroscopic biopsy suggested poorly differentiated adenocarcinoma with a proportion of signet ring cell carcinoma and the mixed type according to Lauren's classification. Immunohistochemistry of biopsy tissue showed proficient mismatch repair (pMMR), HER2 2+ and EBER negativity. Fluorescence in situ hybridization (FISH) showed no HER2 amplification. Next-generation sequencing showed that the tumor mutation burden (TMB) was 5.98 muts/MB. Whole-body fluorodeoxyglucose positron emission tomography/CT (FDG PET/CT) showed the following findings: (1) Diffuse thickening of the gastric wall in the antrum and body with FDG hypermetabolism; (2) perigastric mesenteric turbidity; (3) metastatic lymph nodes visible around the stomach, hepatogastric space, hilar region, retroperitoneum, and left supraclavicular area; (4) left acetabular metastasis; and (5) a small amount of pelvic effusion (Figure 2).

FINAL DIAGNOSIS

The patient was diagnosed with metastatic GC (cT4N3M1, stage IV) according to the 8th edition of the Union for International Cancer Control TNM classification for GC.

TREATMENT

First-line standard treatment was performed, including the mFOLFOX6 regimen and a programmed death-1 (PD-1) inhibitor. The mFOLFOX6 regimen was applied as follows: oxaliplatin (85 mg/m^2) was injected intravenously within 2 h on day 1; leucovorin (400 mg/m^2) was injected intraveneously within 2 h on day 1; 5-fluorouracil (400 mg/m^2) was injected intraveneously and then was continuously infused (2400 mg/m^2) within 46 h; chemotherapy was repeated every two weeks. Nivolumab 240 mg was administered every two weeks. Considering that the patient was bleeding from gastric lesions and that the distal gastric tumor induced incomplete obstruction, we decided, after detailed communication with the patient and his family, to add radiotherapy for the primary lesion. After two cycles of chemoimmunotherapy, HFRT targeted to the primary lesion and lymphatic drainage area was performed with a total dose of 24 Gy split into 6 fractions. Then, another four cycles of chemoimmunotherapy were performed.

OUTCOME AND FOLLOW-UP

One month after these treatments, whole-body FDG PET/CT and enhanced abdominal CT were performed to evaluate the treatment effect. The adverse events (AEs) of the treatment were assessed according to the National Cancer Institute Common Terminology Criteria for AEs (CTCAE) version 4.0. AEs included grade 1 gastrointestinal discomfort and grade 2 leukocytopenia. These side effects were resolved after symptomatic treatment, and leukocytopenia was relieved by using granulocyte colony-stimulating factor (G-CSF). The patient's dyspepsia and melena were relieved remarkably. His tumor markers were still in the normal ranges. Enhanced CT scan of the stomach showed a decrease in the thickness of the gastric wall and the size of the perigastric lymph nodes (Figure 1B). There was an obvious reduction of the gastric lesions and metastatic lymph nodes with a lowered FDG metabolism.

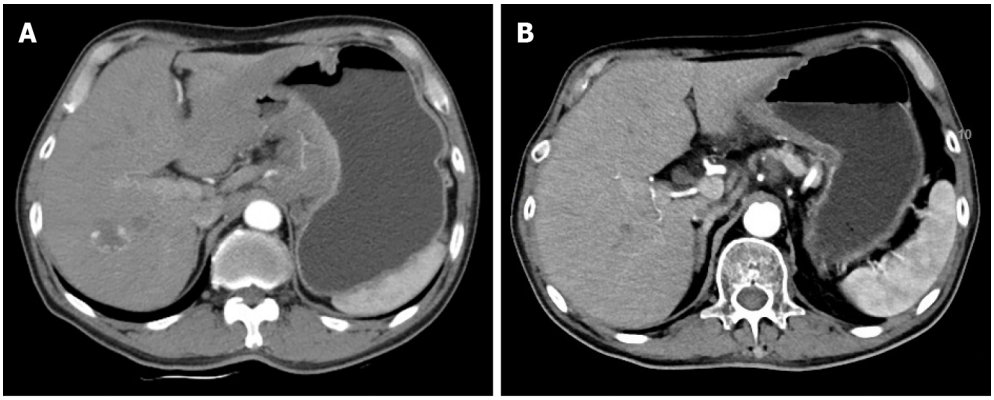

DOI: 10.4251/wjgo.v15.i6.1096

Figure 1 Enhanced computed tomography images prior to and after combined treatment. A: Enhanced computed tomography (CT) before any treatment showed a lesion in the gastric wall; B: Enhanced CT after combined treatment revealed that the lesion was apparently decreased in size.

The FDG metabolism of the left acetabular metastasis and left supraclavicular lymph nodes tended to be normal (Figure 2). The clinical response was classified as partial response according to the Response Evaluation Criteria in Solid Tumors version 1.1.

Afterward, the case was submitted for multidisciplinary team discussion of GC in FUSCC, and surgery was cautiously recommended. Surgery was performed on October 20, 2022. Laparoscopic exploration found neither ascites nor peritoneal seeding. Therefore, laparoscopic surgery was converted to an open approach, and total gastrectomy with Roux-en-Y reconstruction and D2 lymph node dissection was performed. The histological change was classified as TRG grade 1, according to the National Comprehensive Cancer Network clinical practice guidelines in oncology for GC. Postoperative pathology showed that the tumor bed had ulceration with interstitial fibrosis and inflammatory cell infiltration, which was consistent with the changes after treatment. Combined with the immunohistochemical results, a small number of epithelioid cells, AE1/AE3^{+}, were found within the mucosa, tending to be poorly differentiated adenocarcinoma with changes after treatment. Twenty-six lymph nodes were harvested without tumor metastasis. Thus, the postoperative staging was ypT1aN0Mx. There were no postoperative complications observed. The postoperative treatment plan involved the continuous use of the original regimen and then maintenance with nivolumab until one year after surgery. Chemoimmunotherapy started four weeks after surgery and examinations were performed every three months.

DISCUSSION

This study describes a patient with oligometastatic GC who received comprehensive treatment, including chemotherapy, radiotherapy, immunotherapy, and surgery. Pronounced remission of the primary lesion was achieved, as shown by FDG PET/CT and validated by postoperative pathology. Meanwhile, the metabolism of bone metastasis and left supraclavicular lymph nodes was also significantly reduced. In contrast to standard treatment, along with chemotherapy and immunotherapy, the primary lesion was also treated with HFRT due to bleeding and incomplete obstruction.

There is a special group of patients with stage IV disease, termed oligometastatic disease, who are in a relatively early and stable state without the tendency of metastasis spreading throughout the body. The number and location of metastatic lesions are limited, and it is believed that long-term survival can be achieved through systemic treatment with local treatment[7,8]. In gastroesophageal (GEJ) tumors, surgery, as a local treatment, is included in systemic treatment and brings survival benefits to patients with oligometastasis, which has been confirmed in the AIO-FLOT3 study[9]. Moreover, a subsequent AIO-FLOT5 study is in progress[10].

With the wide application of immunotherapy, radiotherapy combined with immunotherapy is considered a promising strategy due to its effect on immune activation and tumor microenvironment remodeling. Besides, enhanced mitochondrial metabolism plays an important role in the better treatment response to anti-PD1 agents[11] and radiotherapy[12]. The combination of immunotherapy and radiotherapy can cure patients with oligometastatic tumors, which has been proven in non-small cell lung cancer[13,14], prostate cancer[15], and other tumors[16]. However, the options of radiotherapy, including the sequence, dose, fractionation, and irradiated sites, that exert the best synergies need to be explored and optimized.

The conventional radiotherapy fraction mode is routinely used in GC. Selected studies have attempted HFRT for palliative treatment, especially for curing hemostasis, and several retrospective studies have indicated its good efficacy and safety[17-21]. However, the application of HFRT in GC is

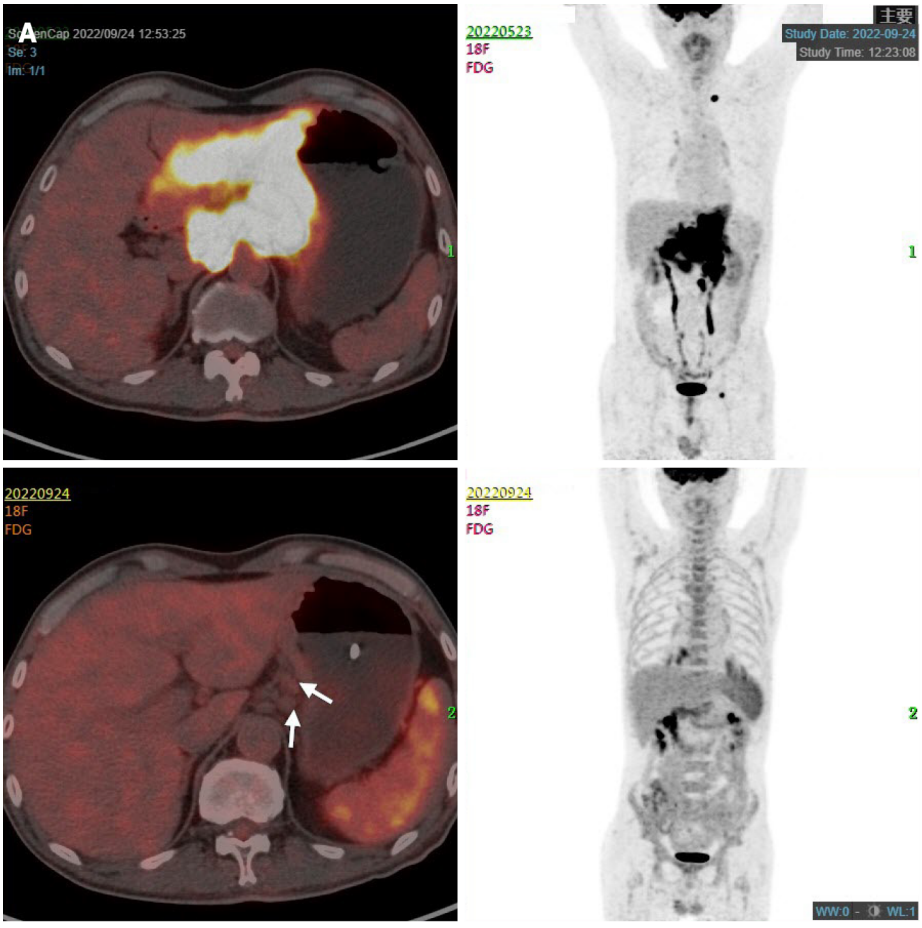
A
20220523
18F
FDG
Study Date: 2022-09-24
Study Time: 12:23:08
20220924
18F
FDG
WW:0 - WL:1

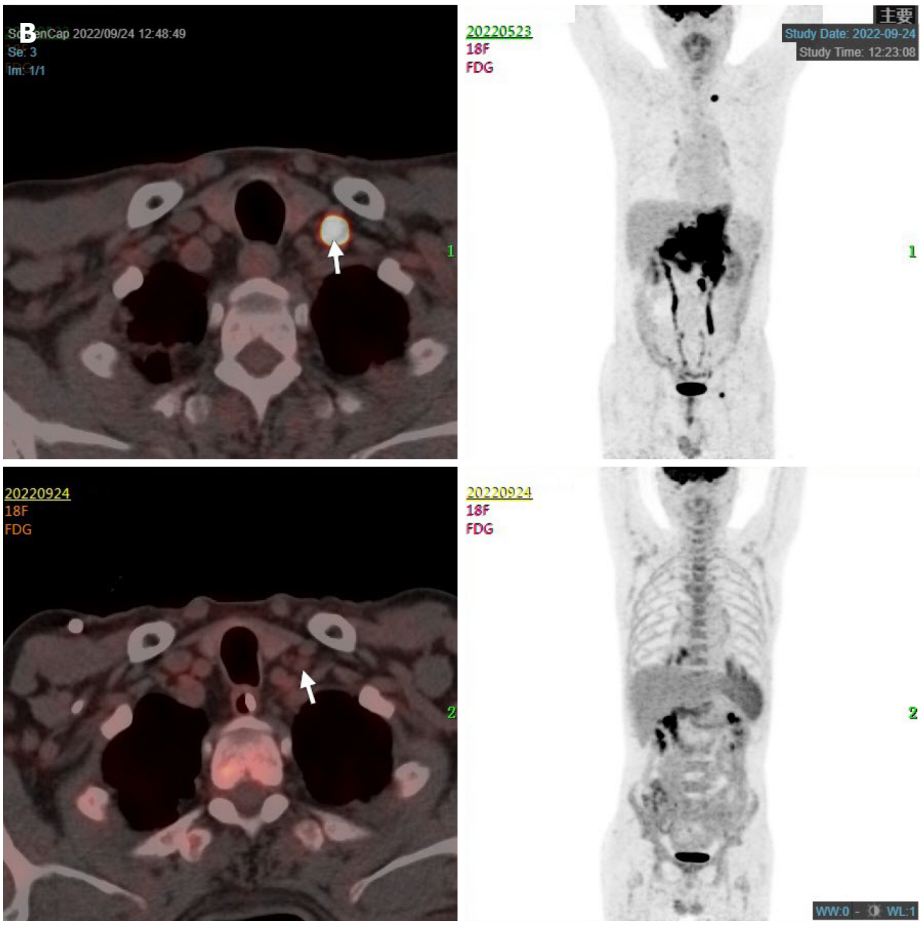
B
20220523
18F
FDG
Study Date: 2022-09-24
Study Time: 12:23:08
20220924
18F
FDG
WW:0 - WL:1

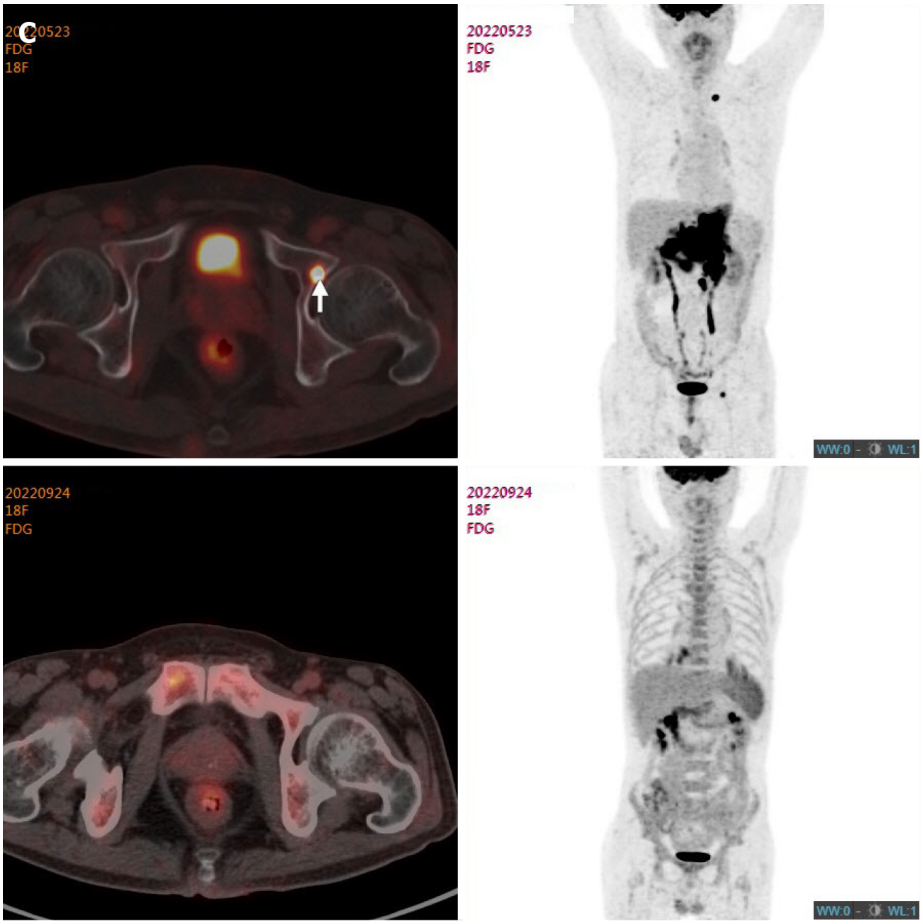

DOI: 10.4251/wjgo.v15.i6.1096 **Copyright** ©The Author(s) 2023.

Figure 2 Fluorodeoxyglucose positron emission tomography/computed tomography images prior to and after combined treatment. A: Fluorodeoxyglucose positron emission tomography/computed tomography (FDG PET/CT) prior to any treatment showed a large gastric mass with hypermetabolism, and the lesion was clearly decreased in size and metabolism after combined treatment; B: FDG PET/CT prior to any treatment showed hypermetabolism in the left supraclavicular area, and the lesion was clearly decreased in size and metabolism after combined treatment; C: FDG PET/CT prior to any treatment showed hypermetabolism in the left acetabular area, and the lesion was clearly decreased in size and metabolism after combined treatment.

still limited.

Li *et al*[22] reported a prospective phase I study (ClinicalTrials.gov identifier: NCT03427684) of HFRT for the neoadjuvant treatment of GC. This was a dose-escalating study that included three levels of radiotherapy doses: 40.0 Gy/2.5 Gy/16 fractions, 95% isodose line covering the planning target volume (PTV); 95% PTV 41.6 Gy/2.6 Gy/16 fractions; and 95% PTV 43.2 Gy/2.7 Gy/16 fractions. Ultimately, 40.0 Gy/2.5 Gy was determined to be the maximum tolerated dose. Another single-arm prospective study (ClinicalTrials.gov identifier: NCT04162665) from the University of Washington in the United States adopted a short course of HFRT, sequential consolidation chemotherapy, and surgery for locally advanced GC. HFRT adopted a 5 Gy × 5 model with magnetic resonance guidance. The primary endpoint of this study was the pathologic complete regression rate. A single-arm prospective Phase Ib study (ClinicalTrials.gov identifier: NCT04523818) from MD Anderson Cancer Center in the United States explored the efficacy of short-course radiotherapy, sequential consolidation chemotherapy, and surgery in patients with resectable GC. The short course of radiotherapy in this study was divided into 10 fractions and completed within 2 wk. The primary endpoint was the incidence of AEs.

In preclinical models, HFRT has been proven to have better immune activation and less impact on lymphocytes[23,24]. In clinical practice, it seems that HFRT may show advances in certain cancers, and the combination of cancer immunotherapy and HFRT may have more potential[25]. Moreover, HFRT has the advantage of shortening the total treatment duration and saving medical resources. All these findings indicate that HFRT is a direction worth exploring in GC not only in the palliative setting but also in perioperative or treatment for oligometastatic patients.

Based on the aforementioned background, a Phase II clinical trial is being carried out in our center. This study targets patients with gastric/GEJ adenocarcinoma with limited liver metastases or paraaortic lymph node metastases. On the basis of systemic chemotherapy and immunotherapy, combined with HFRT of primary and metastatic lesions, the patients whose lesions can be surgically resected after treatment will receive surgery for primary and metastatic lesions when possible. The primary end point of the study was overall survival.

CONCLUSION

This study describes a patient with unresectable advanced GC who received comprehensive treatment; satisfactory efficacy was achieved. HFRT was applied to treat the primary lesion. The combination of radiotherapy and immunotherapy is worthy of further exploration. At the same time, the dose division, radiation range, choice of chemotherapy drugs, and arrangement of treatment sequence of radiotherapy need to be explored to better coordinate with immunotherapy.

FOOTNOTES

Author contributions: Zhou ML and Xu RN collected the pathological, biological, and clinical data; Zhou ML drafted the initial manuscript; Tan C reviewed the pathological results; Wan JF and Zhang Z reviewed or revised the manuscript and approved the final version; Wan JF had full access to all data and had final responsibility for the decision to submit for publication; and all authors contributed to the article and approved the submitted version.

Supported by the National Natural Science Foundation of China (General Program), No. 81773357.

Informed consent statement: Written informed consent was obtained from the patient for the publication of this manuscript and all accompanying images.

Conflict-of-interest statement: There is no potential conflicts of interest were disclosed.

CARE Checklist (2016) statement: The authors have read the CARE Checklist (2016), and the manuscript was prepared and revised according to the CARE Checklist (2016).

Country/Territory of origin: China

ORCID number: Meng-Long Zhou 0000-0002-8130-5812; Cong Tan 0000-0001-6912-4579; Zhen Zhang 0000-0001-7825-2679; Jue-Feng Wan 0000-0001-5361-1663.

S-Editor: Chen YL
L-Editor: A
P-Editor: Yuan YY

REFERENCES

1 **Sung H**, Ferlay J, Siegel RL, Laversanne M, Soerjomataram I, Jemal A, Bray F. Global Cancer Statistics 2020: GLOBOCAN Estimates of Incidence and Mortality Worldwide for 36 Cancers in 185 Countries. *CA Cancer J Clin* 2021; **71**: 209-249 [PMID: 33538338 DOI: 10.3322/caac.21660]

2 **Sitarz R**, Skierucha M, Mielko J, Offerhaus GJA, Maciejewski R, Polkowski WP. Gastric cancer: epidemiology, prevention, classification, and treatment. *Cancer Manag Res* 2018; **10**: 239-248 [PMID: 29445300 DOI: 10.2147/CMAR.S149619]

3 **Kang YK**, Boku N, Satoh T, Ryu MH, Chao Y, Kato K, Chung HC, Chen JS, Muro K, Kang WK, Yeh KH, Yoshikawa T, Oh SC, Bai LY, Tamura T, Lee KW, Hamamoto Y, Kim JG, Chin K, Oh DY, Minashi K, Cho JY, Tsuda M, Chen LT. Nivolumab in patients with advanced gastric or gastro-oesophageal junction cancer refractory to, or intolerant of, at least two previous chemotherapy regimens (ONO-4538-12, ATTRACTION-2): a randomised, double-blind, placebo-controlled, phase 3 trial. *Lancet* 2017; **390**: 2461-2471 [PMID: 28993052 DOI: 10.1016/S0140-6736(17)31827-5]

4 **Fuchs CS**, Doi T, Jang RW, Muro K, Satoh T, Machado M, Sun W, Jalal SI, Shah MA, Metges JP, Garrido M, Golan T, Mandala M, Wainberg ZA, Catenacci DV, Ohtsu A, Shitara K, Geva R, Bleeker J, Ko AH, Ku G, Philip P, Enzinger PC, Bang YJ, Levitan D, Wang J, Rosales M, Dalal RP, Yoon HH. Safety and Efficacy of Pembrolizumab Monotherapy in Patients With Previously Treated Advanced Gastric and Gastroesophageal Junction Cancer: Phase 2 Clinical KEYNOTE-059 Trial. *JAMA Oncol* 2018; **4**: e180013 [PMID: 29543932 DOI: 10.1001/jamaoncol.2018.0013]

5 **Moehler M**, Shitara K, Garrido M, Salman P, Shen L, Wyrwicz L, Yamaguchi K, Skoczylas T, Campos Bragagnoli A, Liu T, Schenker M, Yanez P, Tehfe M, Poulart V, Cullen D, Lei M, Kondo K, Li M, Ajani JA, Janjigian YY. LBA6_PR Nivolumab (nivo) plus chemotherapy (chemo) *vs* chemo as first-line (1L) treatment for advanced gastric cancer/gastroesophageal junction cancer (GC/GEJC)/esophageal adenocarcinoma (EAC): First results of the CheckMate 649 study. *Ann Oncol* 2020; **31**: S1191 [DOI: 10.1016/j.annonc.2020.08.2296]

6 **Kim TK**, Vandsemb EN, Herbst RS, Chen L. Adaptive immune resistance at the tumour site: mechanisms and therapeutic opportunities. *Nat Rev Drug Discov* 2022; **21**: 529-540 [PMID: 35701637 DOI: 10.1038/s41573-022-00493-5]

7 **Katipally RR**, Pitroda SP, Juloori A, Chmura SJ, Weichselbaum RR. The oligometastatic spectrum in the era of improved detection and modern systemic therapy. *Nat Rev Clin Oncol* 2022; **19**: 585-599 [PMID: 35831494 DOI: 10.1038/s41571-022-00655-9]

8 **Palma DA**, Olson R, Harrow S, Gaede S, Louie AV, Haasbeek C, Mulroy L, Lock M, Rodrigues GB, Yaremko BP, Schellenberg D, Ahmad B, Griffioen G, Senthi S, Swaminath A, Kopek N, Liu M, Moore K, Currie S, Bauman GS, Warner A, Senan S. Stereotactic ablative radiotherapy *vs* standard of care palliative treatment in patients with oligometastatic cancers (SABR-COMET): a randomised, phase 2, open-label trial. *Lancet* 2019; **393**: 2051-2058 [PMID: 30982687 DOI: 10.1016/s0140-6736(18)32487-5]

9 **Al-Batran SE**, Homann N, Pauligk C, Illerhaus G, Martens UM, Stoehlmacher J, Schmalenberg H, Luley KB, Prasnikar N, Egger M, Probst S, Messmann H, Moehler M, Fischbach W, Hartmann JT, Mayer F, Höffkes HG, Koenigsmann M, Arnold D, Kraus TW, Grimm K, Berkhoff S, Post S, Jäger E, Bechstein W, Ronellenfitsch U, Mönig S, Hofheinz RD. Effect of Neoadjuvant Chemotherapy Followed by Surgical Resection on Survival in Patients With Limited Metastatic Gastric or Gastroesophageal Junction Cancer: The AIO-FLOT3 Trial. *JAMA Oncol* 2017; **3**: 1237-1244 [PMID: 28448662 DOI: 10.1001/jamaoncol.2017.0515]

10 **Al-Batran SE**, Goetze TO, Mueller DW, Vogel A, Winkler M, Lorenzen S, Novotny A, Pauligk C, Homann N, Jungbluth T, Reissfelder C, Caca K, Retter S, Horndasch E, Gumpp J, Bolling C, Fuchs KH, Blau W, Padberg W, Pohl M, Wunsch A, Michl P, Mannes F, Schwarzbach M, Schmalenberg H, Hohaus M, Scholz C, Benckert C, Knorrenschild JR, Kanngießer V, Zander T, Alakus H, Hofheinz RD, Roedel C, Shah MA, Sasako M, Lorenz D, Izbicki J, Bechstein WO, Lang H, Moenig SP. The RENAISSANCE (AIO-FLOT5) trial: effect of chemotherapy alone vs. chemotherapy followed by surgical resection on survival and quality of life in patients with limited-metastatic adenocarcinoma of the stomach or esophagogastric junction - a phase III trial of the German AIO/CAO-V/CAOGI. *BMC Cancer* 2017; **17**: 893 [PMID: 29282088 DOI: 10.1186/s12885-017-3918-9]

11 **Houshyari M**, Taghizadeh-Hesary F. Is Mitochondrial Metabolism a New Predictive Biomarker for Antiprogrammed Cell Death Protein-1 Immunotherapy? *JCO Oncol Pract* 2023; **19**: 123-124 [PMID: 36469835 DOI: 10.1200/OP.22.00733]

12 **Taghizadeh-Hesary F**, Houshyari M, Farhadi M. Mitochondrial metabolism: a predictive biomarker of radiotherapy efficacy and toxicity. *J Cancer Res Clin Oncol* 2023 [PMID: 36719474 DOI: 10.1007/s00432-023-04592-7]

13 **Antonia SJ**, Villegas A, Daniel D, Vicente D, Murakami S, Hui R, Yokoi T, Chiappori A, Lee KH, de Wit M, Cho BC, Bourhaba M, Quantin X, Tokito T, Mekhail T, Planchard D, Kim YC, Karapetis CS, Hiret S, Ostoros G, Kubota K, Gray JE, Paz-Ares L, de Castro Carpeño J, Wadsworth C, Melillo G, Jiang H, Huang Y, Dennis PA, Özgüroğlu M; PACIFIC Investigators. Durvalumab after Chemoradiotherapy in Stage III Non-Small-Cell Lung Cancer. *N Engl J Med* 2017; **377**: 1919-1929 [PMID: 28885881 DOI: 10.1056/NEJMoa1709937]

14 **Theelen WSME**, Peulen HMU, Lalezari F, van der Noort V, de Vries JF, Aerts JGJV, Dumoulin DW, Bahce I, Niemeijer AN, de Langen AJ, Monkhorst K, Baas P. Effect of Pembrolizumab After Stereotactic Body Radiotherapy *vs* Pembrolizumab Alone on Tumor Response in Patients With Advanced Non-Small Cell Lung Cancer: Results of the PEMBRO-RT Phase 2 Randomized Clinical Trial. *JAMA Oncol* 2019; **5**: 1276-1282 [PMID: 31294749 DOI: 10.1001/jamaoncol.2019.1478]

15 **Kwon ED**, Drake CG, Scher HI, Fizazi K, Bossi A, van den Eertwegh AJ, Krainer M, Houede N, Santos R, Mahammedi H, Ng S, Maio M, Franke FA, Sundar S, Agarwal N, Bergman AM, Ciuleanu TE, Korbenfeld E, Sengeløv L, Hansen S, Logothetis C, Beer TM, McHenry MB, Gagnier P, Liu D, Gerritsen WR; CA184-043 Investigators. Ipilimumab *vs* placebo after radiotherapy in patients with metastatic castration-resistant prostate cancer that had progressed after docetaxel chemotherapy (CA184-043): a multicentre, randomised, double-blind, phase 3 trial. *Lancet Oncol* 2014; **15**: 700-712 [PMID: 24831977 DOI: 10.1016/S1470-2045(14)70189-5]

16 **Postow MA**, Callahan MK, Barker CA, Yamada Y, Yuan J, Kitano S, Mu Z, Rasalan T, Adamow M, Ritter E, Sedrak C, Jungbluth AA, Chua R, Yang AS, Roman RA, Rosner S, Benson B, Allison JP, Lesokhin AM, Gnjatic S, Wolchok JD. Immunologic correlates of the abscopal effect in a patient with melanoma. *N Engl J Med* 2012; **366**: 925-931 [PMID: 22397654 DOI: 10.1056/NEJMoa1112824]

17 **Kim MM**, Rana V, Janjan NA, Das P, Phan AT, Delclos ME, Mansfield PF, Ajani JA, Crane CH, Krishnan S. Clinical benefit of palliative radiation therapy in advanced gastric cancer. *Acta Oncol* 2008; **47**: 421-427 [PMID: 17899453 DOI: 10.1080/02841860701621233]

18 **Hashimoto K**, Mayahara H, Takashima A, Nakajima TE, Kato K, Hamaguchi T, Ito Y, Yamada Y, Kagami Y, Itami J, Shimada Y. Palliative radiation therapy for hemorrhage of unresectable gastric cancer: a single institute experience. *J Cancer Res Clin Oncol* 2009; **135**: 1117-1123 [PMID: 19205735 DOI: 10.1007/s00432-009-0553-0]

19 **Asakura H**, Hashimoto T, Harada H, Mizumoto M, Furutani K, Hasuike N, Matsuoka M, Ono H, Boku N, Nishimura T. Palliative radiotherapy for bleeding from advanced gastric cancer: is a schedule of 30 Gy in 10 fractions adequate? *J Cancer Res Clin Oncol* 2011; **137**: 125-130 [PMID: 20336314 DOI: 10.1007/s00432-010-0866-z]

20 **Chaw CL**, Niblock PG, Chaw CS, Adamson DJ. The role of palliative radiotherapy for haemostasis in unresectable gastric cancer: a single-institution experience. *Ecancermedicalscience* 2014; **8**: 384 [PMID: 24482669 DOI: 10.3332/ecancer.2014.384]

21 **Tey J**, Choo BA, Leong CN, Loy EY, Wong LC, Lim K, Lu JJ, Koh WY. Clinical outcome of palliative radiotherapy for locally advanced symptomatic gastric cancer in the modern era. *Medicine (Baltimore)* 2014; **93**: e118 [PMID: 25396330 DOI: 10.1097/MD.0000000000000118]

22 **Li N**, Wang X, Tang Y, Zhao D, Chi Y, Yang L, Jiang L, Jiang J, Liu W, Fang H, Liu Y, Song Y, Wang S, Jin J, Li Y. A prospective phase I study of hypo-fractionated neoadjuvant radiotherapy for locally advanced gastric cancer. *BMC Cancer* 2018; **18**: 803 [PMID: 30089457 DOI: 10.1186/s12885-018-4707-9]

23 **Lan J**, Li R, Yin LM, Deng L, Gui J, Chen BQ, Zhou L, Meng MB, Huang QR, Mo XM, Wei YQ, Lu B, Dicker A, Xue JX, Lu Y. Targeting Myeloid-derived Suppressor Cells and Programmed Death Ligand 1 Confers Therapeutic Advantage of Ablative Hypofractionated Radiation Therapy Compared With Conventional Fractionated Radiation Therapy. *Int J Radiat Oncol Biol Phys* 2018; **101**: 74-87 [PMID: 29619980 DOI: 10.1016/j.ijrobp.2018.01.071]

24 **Marciscano AE**, Ghasemzadeh A, Nirschl TR, Theodros D, Kochel CM, Francica BJ, Muroyama Y, Anders RA, Sharabi

AB, Velarde E, Mao W, Chaudhary KR, Chaimowitz MG, Wong J, Selby MJ, Thudium KB, Korman AJ, Ulmert D, Thorek DLJ, DeWeese TL, Drake CG. Elective Nodal Irradiation Attenuates the Combinatorial Efficacy of Stereotactic Radiation Therapy and Immunotherapy. *Clin Cancer Res* 2018; **24**: 5058-5071 [PMID: 29898992 DOI: 10.1158/1078-0432.CCR-17-3427]

25 **Zhang Z**, Liu X, Chen D, Yu J. Radiotherapy combined with immunotherapy: the dawn of cancer treatment. *Signal Transduct Target Ther* 2022; **7**: 258 [PMID: 35906199 DOI: 10.1038/s41392-022-01102-y]

Published by **Baishideng Publishing Group Inc**
7041 Koll Center Parkway, Suite 160, Pleasanton, CA 94566, USA
Telephone: +1-925-3991568
E-mail: bpgoffice@wjgnet.com
Help Desk: https://www.f6publishing.com/helpdesk
https://www.wjgnet.com